FOSSIL ENERGY

NIPER-669
CONF-930217
(DE93000154)

PROCEEDINGS

FIELD APPLICATION OF FOAMS FOR OIL PRODUCTION SYMPOSIUM

February 11-12, 1993
Red Lion Inn
Bakersfield, California

Compiled by
David K. Olsen
Partha S. Sarathi

July 1993

IIT Research Institute
National Institute for Petroleum and Energy Research
Bartlesville, Oklahoma

Bartlesville Project Office
U. S. DEPARTMENT OF ENERGY
Bartlesville, Oklahoma

DISCLAIMER

This report was prepared as an account of work sponsored by an agency of the United States Government. Neither the United States Government nor any agency thereof, nor any of their employees, makes any warranty, express or implied, or assumes any legal liability or responsibility for the accuracy, completeness, or usefulness of any information, apparatus, product, or process disclosed, or represents that its use would not infringe privately owned rights. Reference herein to any specific commercial product, process, or service by trade name, trademark, manufacturer, or otherwise does not necessarily constitute or imply its endorsement, recommendation, or favoring by the United States Government or any agency thereof. The views and opinions of authors expressed herein do not necessarily state or reflect those of the United States Government or any agency thereof.

This report has been reproduced directly from the best available copy.

Available to DOE and DOE contractors from the Office of Scientific and Technical Information, P.O. Box 62, Oak Ridge, TN 37831; prices available from (615)576-8401, FTS 626-8401.

Available to the public from the National Technical Information Service, U.S. Department of Commerce, 5285 Port Royal Rd., Springfield, VA 22161.

NIPER-669
CONF-930217
Distribution Category UC-122

PROCEEDINGS

FIELD APPLICATION OF FOAMS FOR OIL PRODUCTION SYMPOSIUM

February 11-12, 1993
Bakersfield, California

Compiled by
David K. Olsen
Partha S. Sarathi

July 1993

Performed Under Cooperative Agreement No. FC22-83FE60149

Prepared for
U.S. Department of Energy
Assistant Secretary for Fossil Energy

Thomas B. Reid, Project Manager
Bartlesville Project Office
P. O. Box 1398
Bartlesville, OK 74005

Prepared by
IIT Research Institute
National Institute for Petroleum and Energy Research
P.O. Box 2128
Bartlesville, OK 74005

TABLE OF CONTENTS

Page

Preface vi
Introduction 1
Acknowledgments 1

Morning Technical Session
February 11, 1993

Welcome: Jerry Casteel, U.S. DOE, and Arden Strycker, NIPER

Session Co-Chairmen: Shane Mohammadi, UNOCAL Science & Technology; George Bain, Chevron Chemical

FS1 *Field Optimization of Steam Foam Diversion in Cyclic Steaming*, R. W. Cooke and R. L. Eson, Enhanced Petroleum Technology, Bakersfield, California 3

FS2 *Critique of a Steam Foam Field Pilot,* W. E. Brigham and L. M. Castanier, Stanford University Petroleum Research Institute (SUPRI), Stanford, California 11

FS3 *Cyclic Steam-Foam Injection in a Carbonate Reservoir*, J. Ivory, G. van der Voet, D. A. Best, E. E. Isaacs, and W. D. Gunter, Alberta Research Council, Edmonton, Alberta, Canada 23

FS4 *Steam Foam Mechanistic Field Trial in the Midway-Sunset Field*, M. E. Smith, F. Friedmann, and W. R. Guice, Chevron Oil Field Research Company, La Habra, California; and J. M. Gump and D. G. Nelson, Chevron USA, Bakersfield, California 37

FS5 *Key Factors Influencing the Success of Steam Foam Applications*, V. T. Hoang and E. A. Waninger, Chevron Chemical Co., San Ramon, California 53

FS6 *Cyclic Steam Injection with Foam: Interpretation of Field Test Results*, J. M. Alvarez, E. Escobar, Z. Mendez, P. Colonomos, and E. Campos, INTEVEP, S.A., Caracas, Venezuela 61

Thermal Foam Application Session—Discussion (Questions and Answers) 75

Afternoon Panel Discussion
February 11, 1993

Session Chairman/Moderator: Rod Eson, Enhanced Petroleum Technology

Panel Members	**Affiliation**
Eric Waninger	Chevron Chemical Co.
John Heller	NM Petroleum Recovery Research Center
Ralph Cooke	Enhanced Petroleum Technology
Laurier Schramm	Petroleum Recovery Institute
Shane Mohammadi	UNOCAL Science & Technology

TABLE OF CONTENTS—Continued

Page

Summary of Panel Presentation and Discussion (Questions and Answers)..... 85

Evening Poster Session — Chairman: John Prieditis, Texaco
February 11, 1993

Abstract or Extended Abstract

FSP1 *Oil Interaction with Foams at Static and Flowing Conditions in Porous Media*, M. Dalland and J. E. Hanssen, Rogaland Research, Stavanger, Norway; and T. S. Kristiansen, Iku Petroleum Research, Trondheim, Norway..... 99

FSP2 *Foam Diversion in Matrix Acidization of Sandstones*, W. R. Rossen and Z. H. Zhou, University of Texas at Austin, Austin, Texas.....111

FSP3 *Laboratory Evaluation of Surfactants as Steam Diverters*, S. M. Mahmood, P. S. Sarathi, D. K. Olsen, and E. B. Ramzel, IITRI/National Institute for Petroleum and Energy Research, Bartlesville, Oklahoma.....113

FSP4 *Foam Treatment of Producing Wells to Increase Oil Production at Prudhoe Bay*, R. E. Krause and R. H. Lane, ARCO Alaska Inc., Anchorage, Alaska; D. L. Kuehne, Chevron Research & Technology, Richmond, California; and G. F. Bain, Chevron Chemical Co., Bakersfield, California.....127

FSP5 *Surfactant Selection for Gas Foam Application*, D. L. Kuehne and J. Cantor, Chevron Research and Technology, Richmond, California.....137

FSP6 *The Influence of Disjoining Pressure on Foam Stability and Flow in Porous Media*, A. S. Aronson, V. Bergeron, M. E. Fagan, and C. J. Radke, University of California at Berkeley, Berkeley, California.....151

FSP7 *Foam Flow Through Porous Media in the Presence of Residual Oil: The Role of Thin-Film Forces*, V. Bergeron, M. E. Fagan, and C. J. Radke, University of California at Berkeley, Berkeley, California.....153

FSP8 *Selection of Oil-Tolerant Foams for Hydrocarbon Miscible Gas Flooding*, L. L. Schramm, K. Mannhardt, and J. J. Novosad, Petroleum Recovery Institute, Calgary, Alberta, Canada.....155

Morning Session: February 12, 1993

Session Co-Chairmen: Jerry Casteel, U.S. DOE, and Mark Hoeffner, Mobil R&D

FS7 *Design Considerations for Foam Diversion of Acid Stimulation Treatments*, R. Gdanski, Halliburton Services, Duncan, Oklahoma.....163

FS8 *Implications of the "Limiting Capillary Pressure" for Field Application of Foams*, W. R. Rossen and Z. H. Zhou, University of Texas at Austin, Austin, Texas.....173

TABLE OF CONTENTS—Continued

Page

FS9 *A Comprehensive Description of Transient Foam Flow in Porous Media,* A. R. Kovscek and C. J. Radke, University of California at Berkeley, Berkeley, California 185

FS10 *CO_2 Foam Field Verification Pilot at EVGSAU: Phase II - Foam Injection Design and Operating Plan,* J. E. Stevens, Phillips Petroleum Co., Midland, Texas; K. J. Harpole and D. R. Zornes, Phillips Petroleum Co., Bartlesville, Oklahoma; and F. D. Martin, New Mexico Petroleum Recovery Research Center, Socorro, New Mexico 201

FS11 *Well Treatment Against Gas Coning Must Exploit Gravity Effects*, S. Ekrann and J. E. Hanssen, Rogaland Research, Stavanger, Norway 217

FS12 *CO_2 Foam Field Trial at North Ward-Estes*, S. I. Chou, S. L. Vasecek, and D. L. Pisio, Chevron Oil Field Research Co., La Habra, California; and D. E. Jasek and J. A. Goodgame, Chevron USA Inc., Midland, Texas 231

FS13 *Two Field Tests of CO_2-Foam*, J. P. Heller, New Mexico Petroleum Recovery Research Center; and R. J. Watts, U.S. DOE, Morgantown, West Virginia 243

Gas Foam Application Session—Discussion (Questions and Answers) 257

Appendix: List of Symposium Attendees 263

PREFACE

For the past 15 years, foam has been increasingly used in the United States, Canada, Venezuela and other parts of the world to improve oil recovery from existing fields. During this period, considerable effort has been expended by industry, academia, and service companies in understanding the mechanism of foam flow in porous media and in improving and fine tuning field application techniques. Even though the technology has been shown to be both technically and economically viable, the technology is still in its infancy.

As part of its technology transfer mission, the U.S. Department of Energy periodically sponsors symposia on various aspects of oil recovery technologies. The basic objective of this DOE-sponsored foam symposium was to determine the state-of-the-art in field application of foam for oil recovery by providing a medium for information exchange among specialists in the technology. By encouraging the foremost experts on this subject matter to exchange their experiences and findings, their successes and failures, and their expectations of the projects, it was hoped that the technology could be further advanced and the risk of failures lowered.

The success of this symposium was due to a large number of people whose efforts we wish to acknowledge. In particular, we wish to recognize Dr. David K. Olsen of NIPER for his dedication and enthusiasm in attending to the details and making the symposium a success. We also thank the authors and symposium attendees for exchanging their experiences and voicing their views.

Thomas B. Reid, U.S. DOE

Arden R. Strycker, NIPER, Co-Chairmen

INTRODUCTION

By Partha S. Sarathi and David K. Olsen

The contents of this volume represent the collective presentation, entitled "Field Application of Foams for Oil Production," which was held in Bakersfield, California, February 11-12, 1993. This symposium was sponsored by the U.S. Department of Energy (DOE) as part of its technology transfer mission and was organized by the National Institute for Petroleum and Energy Research (NIPER).

The symposium was organized into two technical sessions devoted to "Thermal Foam Application" and "Gas Foam Application" and a panel session devoted to the assessment of the current state of the technology. In addition to the panel and technical sessions, a poster session devoted broadly to laboratory research on foams was held on the evening of February 11, 1993. A total of 73 participants from seven countries attended the conference and the evening poster and social hour session and made the symposium an overwhelming success. A list of attendees is appended at the end of the proceedings.

A total of 13 technical papers and 8 poster abstracts were presented at the symposium and are included in these conference proceedings. These proceedings also include a summary of the panel presentation and discussions. For convenience, the proceedings are assembled into four parts, each containing related materials. The first part includes the six papers presented at the "Thermal Foam Application" session, followed by the paper discussion section. The second part includes a summary of panel presentations and discussion. The third part includes the extended abstracts of the papers presented at the poster session. The final part includes the seven papers and summary discussion presented during the "Gas Foam Application" session. The papers are included in the order in which they were presented, and the discussion section includes selected questions posed by the audience to the authors and their response.

ACKNOWLEDGMENTS

We thank the Technical Program Committee for undertaking the difficult task of selecting abstracts of papers that reflect the current state of the foam technology, the session chairmen for coordinating and conducting their section of the meeting, the authors for their willingness to share their experiences and findings, and the organizations that financed their work and permitted them to present their findings. The technical papers together with their discussion included in these proceedings provide up-to-date information vital to an understanding of this technology.

We also wish to thank the panel members and registrants for making the panel discussion session a success and for providing DOE with feedback on the current state of foam technology. The editors also wish to thank Rod Eson for assembling and moderating the panel discussion, panel members for their assessment of the technology, Annalea Kerr of NIPER for compiling this

volume, Syed Mahmood of NIPER for recording the meeting discussion, Bill Linville of NIPER for his guidance in organizing the symposium, and Yesh Tyagi, a DOE summer intern at NIPER for designing the cover.

This symposium was sponsored by the U.S. Department of Energy under cooperative agreement DE-FC22-83FE60149 as project SGP63. On behalf of the participants, the editors wish to thank Thomas B. Reid, Herb Tiedemann and Fred Burtch of U.S. DOE, Bartlesville Project Office, for supporting this symposium.

Field Optimization of Steam Foam Diversion in Cyclic Steaming

by R. W. Cooke and R. L. Eson, Enhanced Petroleum Technology, Bakersfield, California

Originally presented as Society of Petroleum Engineers paper No. 21531 at the SPE International Thermal Operations Symposium held in Bakersfield, California, February 7-8, 1991. Copyrighted by Society of Petroleum Engineers, Inc., 1991.

This paper was prepared for presentation at the DOE/NIPER, Symposium on Field Application of Foams for Oil Production held in Bakersfield, California, February 11-12, 1993.

This paper was selected for presentation by a Program Committee following review of in formation contained in an abstract submitted by the author(s). Contents of the paper, as presented, have not been reviewed and are subject to correction by the author(s). The material, as presented, does not necessarily reflect any position of the U.S. Department of Energy or the National Institute for Petroleum and Energy Research.

ABSTRACT

Steam foam diverters have been utilized to improve oil production in cyclic steaming applications since 1973. As reservoirs have aged and changed due to substantial oil production from both cyclic steaming and steam drive operations, the development of effective steam foam diversion treatment programs has become more complex.

This paper deals with the development of field application methods to optimize the effectiveness of cyclic steam foam diverters. Actual field results of the applications are described. Various foam diversion treatment methods are outline. Several steam foam diversion agents representing different types of chemical structures were utilized. The oil production responses are reported and the effects of changes in foam diverter type, quantity and method of application are correlated. The economic impact of various application methods, different materials and quantities are reported.

INTRODUCTION

Thermal Recovery Methods

Various thermal oil recovery methods were identified and summarized by Prats.(1) Of the various methods identified, steam drive utilizing continuous steam injection and cyclic steam injection, some times called huff and puff, are the two most widely utilized in the United States. Steam drive and cyclic steam injection account for majority of the approximately 500,000 barrels of oil per day of heavy oil production. Most of the heavy oil production in the United States occurs in Kern County, near Bakersfield California. It has been estimated by Cooke,(2) that in the United States, approximately 75 percent of all oil produced by enhanced oil recovery (EOR) methods comes from steam drive and cyclic projects.

Problems Encountered with Thermal EOR

The primary problem encountered with thermal recovery is poor volumetric sweep efficiency,

with volumetric sweep efficiency being defined as vertical sweep efficiency times areal sweep efficiency. A number of the primary factors determining sweep efficiency are: reservoir heterogeneity, permeability variation, relative permeability, well spacing, steam quality and fluid mobility ratios.

In cyclic steam stimulation, the steam from the initial steam cycle often seeks the area of highest permeability. During subsequent steam cycles, it is believed the steam tends to enlarge the oil depleted zone established in the first cycle. Unless gravity re-saturation, or some other mechanism replaces the oil swept from the areas contacted in the initial cycle or cycles, a substantial reduction in oil production may occur by the third steam cycle. The water to oil ratio may also increase rapidly.

In order to correct the apparent steam distribution problems in cyclic stimulation, surfactants (steam foam diverters) may be utilized to generate in-situ foams within the reservoir. This should help redirect the steam from the initial steam channels or areas of gravity override, into portions of the reservoir containing greater oil saturation.

Steam foam diverters were first utilized in actual field operations in 1973.(3) Over the next 17 years steam foam diverters have been utilized in more than 4,000 cyclic steam stimulations.

Initial Foam Diversion Treatment Methods

Initial cyclic foam diverter treatment methods were very simple. A typical treatment would have been the injection of 110 to 220 gallons of a foam diverter containing 30-40% active surfactant. The foam diverter would have been injected in one or two slug injections of 55 to 110 gallons over a 20-45 minute period for each injection. The injection period would have been during the first half of the steam cycle. Generally, there was one injection during a four to six day cycle and two injections during seven to fourteen day steam cycles.

Initial Oil Production Responses

Oil production responses shown in table 1 are from 286 treatments during the period of 1980 through 1984 in the Midway Sunset field from the Potter Sand.(3) The average incremental barrels of oil produced, ranged from 3,040 to 4,390 depending on the foam diverter utilized. No attempt was made to identify up-dip and down-dip wells. The average number of steam cycles per well was five. The data was received from various operators, both majors and independents.

In all cases the incremental oil production is estimated by establishing the production decline from cycle to cycle and estimating the expected production for subsequent steam cycles. The incremental oil was assumed to be the oil produced in excess of the projected amount, this data was then compared to those wells that had been cyclicly stimulated without the application of a foam diverter. Where substantial changes had been made in steam rates, qualities or surrounding steam drive activity, those wells were dropped from the evaluation. Individual well responses to cyclic stimulation can vary over a wide range, but when a large sampling of wells is evaluated, definite trends can be determined with substantial accuracy.

STEAM FOAM DIVERTER APPLICATION OPTIMIZATION

Production Response Observations

From 1985 through 1988 it was observed that oil production response per steam cycle was declining and the amount of foam diverter and the number of treatments required per cycle was increasing. The average incremental barrels of oil produced, ranged from 464 to 1,460, depending on the foam diverter utilized. Various steam foam diverting agents were evaluated. It was noted that the average number of times the wells had been cycled had risen to 9. The data is shown in table 2. Again the data was received from various major and independent operators.

During 1989 and 1990 various foam diverter injection programs were evaluated, increased amounts of foam diverters were utilized using a larger number of injection slugs. At the same time application by semi-continuous injection, where foam diverter was injected from 6 to 24 hours per day for up to 8 days of the steam cycle was expanded and the results evaluated. The average incremental barrels of oil produced per steam cycle increased to 1,710 for steam diverter number 2. A new diverter, number 5 was evaluated for semi-continuous injection as a replacement for diverter number 4. The average number of cycles for each producer evaluated in 1989 and 1990 was 11. Data obtained in 1989 and 1990 was from both major and large independent oil operators. The data is shown in table 3.

During 1990, the slug injection application method of steam foam diverter number 2, was optimized with respect to both diverter quantity and the number of injection periods. By increasing the average foam diverter injection quantity to 440 gallons and increasing the average number of injection slugs to four, the incremental oil produced per cycle was increased to 2,194 barrels. The data obtained by this optimization is listed in table 4.

Semi-continuous application of foam diverter number 2 was also investigated in 1990. The semi-continuous application of both foam diverters number 2 and 5 were optimized resulting in substantial increases in incremental production per steam cycle for both products. The optimization resulted in increasing the average incremental oil produced per cycle by diverter number 2, to 2,683 barrels. This data is presented in table 5.

Two other factors were investigated in an attempt to optimize the application of cyclic steam foam diverters. The response to steam foam diversion by up-dip and down-dip wells was compared, this data is shown in table 6. Based on the data obtained, those cyclic wells that were down-dip responded substantially better to foam diversion than those located up-dip structurally. It was also noted that the producers treated prior to 1985 responded better than those treated after 1985.

Also evaluated was the production response to foam diversion, by producers that had been cycled 7 or less times and producers that had been cycled 8 or more times. In some cases the producers had been cycled up to 15 times. This data is presented in table 7. It was observed from the data that producers generally respond much better in the early cycles, such as cycles 3 through 7. As the number of steam cycles increases, the response to steam foam diversion tends to diminish.

OPTIMIZATION EXAMPLE

Four producers were selected in the Midway-Sunset field, Potter sand, that had similar cyclic steam applications and responses. The four producers were treated with cyclic foam diversion agent #2. The treatment method and surfactant quantity were varied for each producer.

Specific examples are reported in figures 1 through 4 and table 8. In this set of examples, the more foam diverter utilized in both slug and semi-continuous applications, the greater the oil production when compared to the untreated steam cycles.

CONCLUSIONS

1.) Kern County heavy oil reservoirs are aging. The number of steam stimulation cycles has increased dramatically over the past ten years. The response of these wells to cyclic steam foam diversion is declining.

2.) Larger and more complex steam foam diverter treatments are being required to bring about substantial increases in oil production.

3.) Steam foam diverter treatment optimization is required to determine the most cost effective method of foam diversion.

4.) Down-dip producers tend to respond better to steam foam diversion treatment programs.

5.) Cyclic producers respond to foam diversion treatment programs better during early steam cycles.

6.) As reservoirs age, various steam foam diversion treatment methods, materials and programs need to be evaluated to determine the most cost effective treatment.

REFERENCES

1.) Prats, M. "Thermal Recovery". Society of Petroleum Engineers Monograph 7, 1982.

2.) Cooke, R. "Areal Sweep Efficiency Determination in Steam-Drive Projects Utilizing Chemical Tracers". SPE Paper 11805

3.) Eson, R. L. "Field Results of Steam Diversion Agents in Cyclic Steam Applications". Presented at the 1985 United Nations Conference on Heavy Oil and Tar Sands, Long Beach CA.

TABLE 1.

INCREMENTAL OIL PRODUCTION, SLUG INJECTION 1980-1984

	Number of Wells/Cycles	Average Gallons Foamer	# Of Injections	Average Incremental BBL Oil Production Due to Foam Diverter
Steam with Diverter #1	62	165	1.5	3,041
Steam with Diverter #2	184	165	1.5	4,394

TABLE 2.

INCREMENTAL OIL PRODUCTION, SLUG INJECTION 1985-1988

	Number of Wells/Cycles	Average Gallons Foamer	# Of Injections	Average Incremental BBL Oil Production Due to Foam Diverter
Steam with Diverter #1	86	220	2.0	943
Steam with Diverter #2	341	220	2.0	1,460
Steam with Diverter #3	72	220	2.0	870
Steam with Diverter #4	7	1,200	Continuous	464
Steam with Diverter #4	29	400	Semi-Continuous	381

TABLE 3.

INCREMENTAL OIL PRODUCTION, SLUG INJECTION 1989-1990

	Number of Wells/Cycles	Average Gallons Foamer	# Of Injections	Average Incremental BBL Oil Production Due to Foam Diverter
Steam with Diverter #2	112	275	3.0	1,710
Steam with Diverter #5	36	400	Semi-Continuous	611

TABLE 4.

INCREMENTAL OIL PRODUCTION, SLUG INJECTION 1990

	Number of Wells/Cycles	Average Gallons Foamer	# Of Injections	Average Incremental BBL Oil Production Due to Foam Diverter
Steam with Diverter #2	63	440	4.0	2,194

TABLE 5.

INCREMENTAL OIL PRODUCTION, SEMI-CONTINUOUS INJECTION 1990

	Number of Wells/Cycles	Average Gallons Foamer	# Of Injection Periods	Average Incremental BBL Oil Production Due to Foam Diverter
Steam with Diverter #2	48	500	4.0	2,583
Steam with Diverter #5	11	500	4.5	844

TABLE 6.

INCREMENTAL OIL PRODUCTION OF UP-DIP AND DOWN-DIP PRODUCERS AFTER APPLICATION OF STEAM FOAM DIVERTER NUMBER 2.

	Number of Wells/Cycles	Average Incremental BBL Oil Production Due to Foam Diverter
Up-Dip Producers Prior to 1985	42	2,232
Down-Dip Producers Prior to 1985	105	4,861
Up-Dip Producers After 1985	118	1,126
Down-Dip Producers After 1985	251	2,277

TABLE 7.

INCREMENTAL OIL PRODUCTION BASED ON NUMBER OF STEAM CYCLES AFTER APPLICATION OF STEAM FOAM DIVERTER NUMBER 2.

	Number of Wells/Cycles	Average Incremental BBL Oil Production Due to Foam Diverter
Producers Cycled 7 Times or Less	323	3,211
Producers Cycled More Than 7 Times	361	1,680

TABLE 8.

OIL PRODUCTION: LEASE A, WELL'S 1 THROUGH 4

Well Number	Figure Number	Cycle Number	Oil Production	
1	1	1	11,970	
1	1	2	8,900	
1	1	3	6,540	
1	1	4	9,690	Foam Diverted
1	1	5	4,170	(Small Slug)
2	2	1	8,640	
2	2	2	9,510	
2	2	3	9,570	
2	2	4	8,700	
2	2	5	12,840	Foam Diverter (Large Slug)
3	3	1	12,600	
3	3	2	10,140	
3	3	3	8,970	
3	3	4	6,570	
3	3	5	9,210	Foam Diverter (S. Semi-Cont)
4	4	1	13,440	
4	4	2	8,610	
4	4	3	8,910	
4	4	4	6,570	
4	4	5	9,210	Foam Diverter (L. Semi-Cont)

Three 100 Gallon Slugs of Diverter #2
11,300 BBL of Steam, 17 Day Steam Cycle

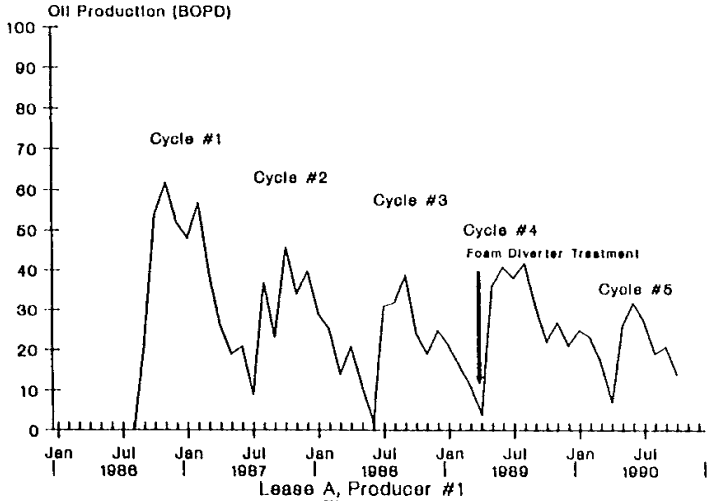

Lease A, Producer #1
Figure 1.

Five 100 Gallon Slugs of Diverter #2
10,780 BBL of Steam, 19 Day Steam Cycle

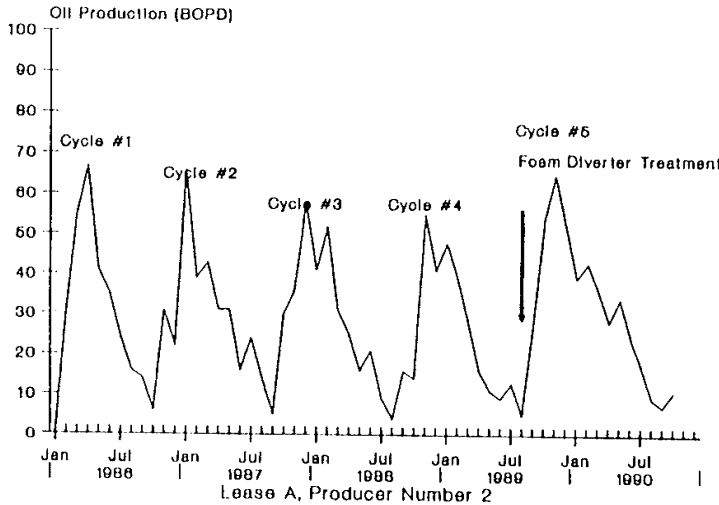

Lease A, Producer Number 2
Figure 2.

300 Gallons Semi-Continous, Diverter #2
3 Injections of 100 Gallons In 12 Hours
10,200 BBL of Steam, 16 Day Steam Cycle

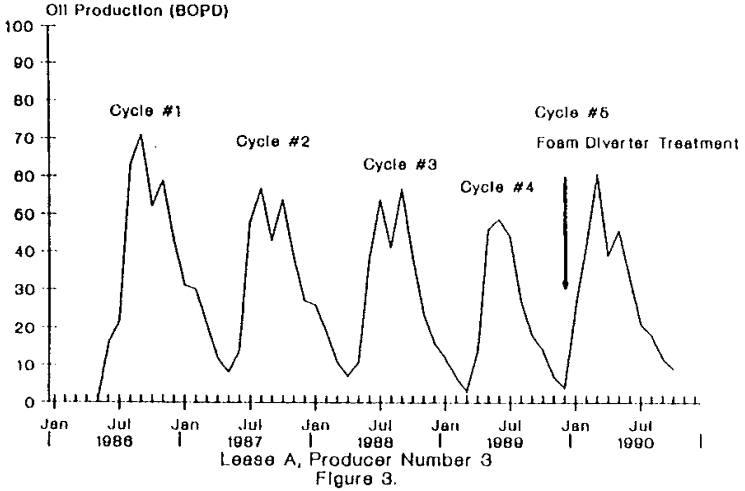

Lease A, Producer Number 3
Figure 3.

540 Gallons Semi-Continous, Diverter #2
Six Injections of 90 Gallons Each
11,080 BBL of Steam, 19 Day Steam Cycle

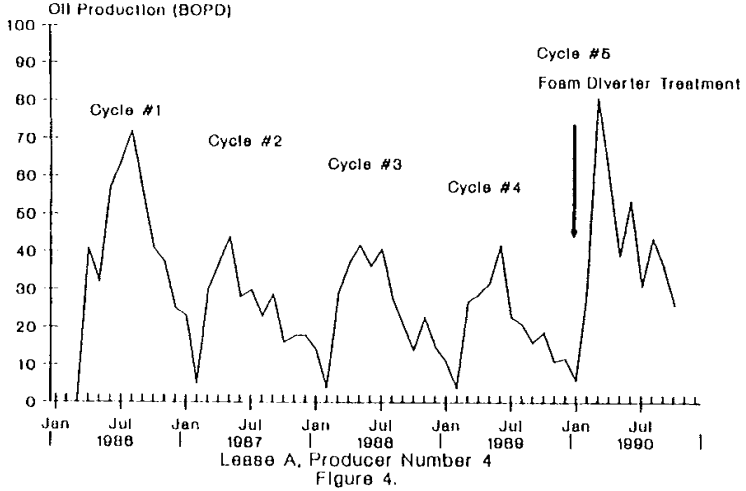

Lease A, Producer Number 4
Figure 4.

No. FS2

DOE/NIPER

Critique of a Steam Foam Field Pilot

by W. E. Brigham and L. M. Castanier, Stanford University Petroleum Research Institute (SUPRI), Stanford, California

Author(s) are solely responsible for copyright and contents.

This paper was prepared for presentation at the DOE/NIPER, Symposium on Field Application of Foams for Oil Production held in Bakersfield, California, February 11-12, 1993.

This paper was selected for presentation by a Program Committee following review of information contained in an abstract submitted by the author(s). Contents of the paper, as presented, have not been reviewed and are subject to correction by the author(s). The material, as presented, does not necessarily reflect any position of the U.S. Department of Energy or the National Institute for Petroleum and Energy Research.

ABSTRACT

From 1981 to 1983, the Stanford University Petroleum Research Institute (SUPRI) performed a field test of steam with foaming additives in the MacManus lease of the Kern River field. The test was operated by CORCO on a Petrolewis lease. The goal of this communication is to review the monitoring techniques and injection procedures used during this test in light of the advances in technology that have been made in the past ten years. We hope to draw on a successful but imperfect experiment to provide information that can be used by field operators who wish to run similar pilots.

The discussion will start with the choice of a surfactant as foaming agent for a specific field and will point to the importance of laboratory screening. Injection mode (continuous or multiple slugs) and the effect of noncondensable gases will be evaluated. Evaluation of production results and problems experienced during this evaluation will be described in detail. A new method to accurately measure oil production was developed during the project and we will comment on its applicability.

We will show how the logging program that was implemented during the SUPRI test could be improved by better temperature and neutron logging. Tracer tests, pressure transient tests and injection profile determination methods all showed some limitations during the pilot. We shall discuss the gap between the information available in theory from those methods and what was really achieved in the field. We shall also make suggestions for improve-ment in designing and interpreting such formation evaluation methods.

The goal of a pilot is to provide information on the application of a process to a reservoir. The best monitoring methods should be used to ensure that this objective is met. Examination of past results can be an excellent way to improve current and future projects.

INTRODUCTION

Steam/foam has been used as a way to improve the efficiency of steam injection for over 15 years. In a typical steam/foam project, aqueous solutions of surfactants are injected, often with a small amount of noncondensable gas, to generate a foam when mixed with the steam. The foam in turn increases local pressure gradients, improving the sweep efficiency of the steam.

A Department of Energy contract for a field pilot was initiated in October, 1980. The field work lasted from 1981 to 1983. The test was preceded by extensive laboratory studies performed at Stanford University. The goals were to obtain field scale data unobtainable in the laboratory and to test the effectiveness of the steam/foam process. This project was concluded at the end of 1983. The results were presented in Refs. 1 and 2. The purpose of this communication is to review the results of this test, to constructively criticize the methods and operational procedures used in view of recent progress of technology, and to provide recommendations for the design and operation of future tests of the steam/foam process.

LABORATORY STUDIES AND FOAMER SELECTION

The SUPRI pilot was initiated after a comprehensive laboratory evaluation of various surfactants.[3,4] Selection

of a proper product involves screening for thermal stability, adsorption, and partitioning into the oil phase. Cost of the surfactants should also be considered. The number of suitable thermally stable surfactants has greatly increased in the last ten years, thus allowing more flexibility in the search for the optimum product.

We feel that the laboratory screening program implemented prior to the test was adequate. The adsorption measurements were only performed at static conditions while dynamic adsorption data would be more realistic. However, collection of dynamic adsorption data is costly and usually such data can be inferred from static adsorption measurements. These experiments should be performed with cores, brines and crudes from the pilot area at steam injection temperatures and pressures. Core selection for the laboratory studies are now easier than at the time of the pilot through proper use of CT scanners and better description of mineralogy.

An interesting technique to select the best surfactant for a given reservoir was suggested by Mohammadi and McCollum,[5] to supplement laboratory studies. In the field, a small slug of foamer was injected with the steam and the pressure increase in the well treated was monitored with time. This procedure was repeated in different injection wells for three of the foamers preselected from laboratory studies. The criteria for the choice of the best product were pressure response and speed of pressure buildup. This approach is probably more suitable to full scale field applications than for pilot studies, but it allows at least partial confirmation of the validity of the laboratory work at low cost to the operator. It also allows a small scale rehearsal of the injection procedure that could warn of future operational problems during the main injection period.

SITE SELECTION

The MacManus lease, operated at the time by Petrolewis was chosen as the test site. The choice was based on the need for a mature steam drive project where there would be adequate production and injection facilities. Chemical Oil Recovery Corporation (CORCO) was selected as the field manager because of their experience in steam/foam operations.

The oil in the lease is heavy (12° API) and the water slightly brackish. This last point is important because the chosen foamer would have been adversely affected if any divalent ions had been present in the MacManus water. The reservoir is shallow (180 to 500 ft) and parts of it had been under steam drive for several years prior to the project. The reservoir pressure was low (50 psig in the test pattern) ensuring moderate steam injection temperatures and pressures.

A geological model of the field site was developed and two confined inverted 5 Spot patterns (2.25 acres) were chosen, one for a test pattern where steam/foam would be used, and the other a control pattern where steam only would be used (Fig. 1).

One of the problems experienced was the differing stages of exploitation of those two patterns. While the test pattern (centered on Well 208) had been under steam drive for several years, the control pattern (centered on Well 214) was not even drilled. Because of changes of operators on the lease prior to the start of the pilot, it was not possible to obtain details of the production data for all wells before 1980. This made direct comparisons between the two patterns impossible.

Another problem was the lack of time between site selection and the start of the project. A baseline production curve for the test pattern could not be generated from existing data on the pattern itself. It had to be inferred from only three months of good data prior to the test and from lease-wide decline curves obtained from the California Department of Oil and Gas database. Ideally a pilot test site should be well monitored by the pilot operator for several months before the start of a project. It is difficult to distinguish between the production increase due to the EOR process being tested and the increase caused by better monitoring and more efficient operational practices during the project. These two factors need to be decoupled to evaluate the effectiveness of the process. The best way to obtain that evaluation is to have the same personnel operate the pilot site for some time before the test.

DRILLING AND OBSERVATION WELLS

The two observation wells were drilled in August, 1981 in the 208 and 214 patterns. As direct comparison of the test pattern and control pattern was impossible, it would have been better in retrospect to drill two observation wells in the test pattern at various distances from the injector to better follow foam propagation in the reservoir.

Core recovery was poor because of the presence of large boulders and the unconsolidated nature of the formation. Advances have been made in coring techniques in the intervening ten years. Of particular importance is the preservation of cores for use in the laboratory screening process. Changes in core wettability can greatly affect the results of laboratory tests and can give erroneous information about steam/foam feasibility. We were lucky that our pilot test results confirmed the laboratory data, for the core material we received in the laboratory had been damaged by exposure to air and desaturation.

The observation wells were cased to total depth after an extensive suite of open hole logs had been run by several companies. Observation wells were not perforated during the project thus loosing sampling opportunities for surfactant and or tracers. A possible further improvement would have been nonmetallic casing in these wells. This would have allowed modern

monitoring methods such as electromagnetic or acoustic logging and tomography to locate the steam invaded region and its changes with the use of steam foam. It also would have allowed the use of some open hole logs that are not normally of use through metallic casing.

INJECTION PROGRAM

The SUPRI pilot project was a demonstration project designed to show the feasibility of the steam foam process. As a result, only a very crude attempt was made to optimize the surfactant injection process.

Preliminary Injectivity Tests

Two preliminary injection tests gave useful information. The first test was the injection of 2,300 gallons of 15% active surfactant without nitrogen. It was a failure because of a faulty batch of surfactant. This showed the need for better coordination with the supplier and on site quality control. No further problems with surfactant quality were experienced during the project. The second preliminary test consisted of injection of 1,400 gallons of 15% active surfactant with no nitrogen, followed by another 1,100 gallons with nitrogen. The resulting pressure data showed the importance of adding a noncondensable gas to improve the foam stability. It was decided to inject nitrogen at about 5% of the mole fraction of the steam. During these tests, the injection equipment performed as planned.

Main Injection Program

Three main slugs of surfactant were coinjected with steam and nitrogen. The same amount of surfactant (about 22,000 gallons of 15% active solution) was injected in each slug but the concentration was halved for the second slug and halved again for the third. As a result the second slug injection lasted twice as long as the first while the third lasted four times as long. The laboratory data showed the need for a concentration of 0.25% or above for optimum results, this number being the critical micelle concentration of the Suntech IV surfactant. The design concentrations for each slug were 4%, 2% and 1%, respectively. This was a deliberate overkill to take into account possible surfactant losses due to adsorption or phase partitioning.

No effect of the decreases in surfactant concentration were seen in the pressure responses at the injector, showing that indeed the surfactant concentration had been higher than needed. The longer duration of the second and third slugs caused injectivity profile effects for a longer time and greater response at the producers.

Since the SUPRI pilot, many attempts have been made to optimize surfactant use in a steam foam project.[6,7] It appears that injection of small slugs of surfactant for a short time can be effective. Continuous injection to generate a large foam bank is probably not economical.[8] Preflush of the near wellbore region by alkali or by a liquid slug of surfactant could improve the economics of the process.[9] As no predictive model yet exists for steam foam applications, the best optimization method to date is to monitor injection pressure and injectivity profiles. Experience gained from small pilot tests can help in planning injection programs for fieldwide operations. Economic optimization should be the ultimate objective of the engineer.

LOGGING PROGRAM

The logging program was comprehensive. Table 1 lists the logs run in the observation wells. Qualitative analysis of the logs allowed geological description of the layers present in the test and control patterns. Figure 2 shows a cross-section between the test injector (Well 208) and the updip producer (Well 114). Four major slices can be identified. Steam channeling was detected using one or more of the following: (1) gamma ray spikes, (2) high electrical conductivity in shales, (3) high core porosity indicating possible high permeability streaks, and (4) high temperature. Porosity and saturations were estimated from logs and cores and appeared to give reasonable values.

It was hoped that C/O logs could be used to follow oil saturation changes in the observation wells. These logs were run every three months but the accuracy was not sufficient to distinguish saturation changes. Temperature and neutron logs have been shown by others[10,11] to be a good combination to follow the growth of the steam invaded zone at observation wells.

Production logging, particularly periodic temperature surveys should also prove useful as a tool to follow the effect of steam/foam on sweep efficiency near the producers. In the SUPRI project, marked decreases were observed in the producers' temperatures in the test pattern, especially at the updip producer (Well 14), while no similar decrease was seen in the control pattern. Although the data were scattered and difficult to analyze, this temperature decrease was interpreted as further evidence of steam diversion.

New tools, now under development by the service companies, allow flow measurements at any given interval of a producer. Such data would be valuable , for rate and temperature data from each of the producing layers could provide evidence of steam diversion.

PRESSURE TRANSIENT TESTING

Pressure fall-off surveys were performed on Wells 208 and 214. The testing equipment consisted of a capillary tube filled with helium, a helium purge system, a downhole pressure chamber, a recorder, and a quartz-crystal pressure gauge. All components performed well during three surveys made at four month intervals: October '81, February '82 and May '82. The setup

provides pressure change readings accurate to 0.01 psi under ideal conditions.

The goal of such tests is to provide an estimate of the volume of the steam zone.[12] Analysis of the data obtained in Well 214 which had been under steam injection only since October 1981, gave reasonable estimates for the steam zone volume. The data from Well 208, however, could not be analyzed. This well had been under steam injection for over three years prior to the first survey. Breakthrough of steam at the producers was probably the cause of the problem. Fall-off pressure transient data are difficult to analyze.[13] New developments in the analysis of such tests were published by Ambastha and Ramey,[14] and computer aided well test analysis can also allow better test interpretation.[15] It is certain that the results of these tests are more reliable for wells that have received steam for a short period of time than they are for mature injectors. In summary, the data obtained during the pilot were of good quality but interpretation techniques needed improvement.

INJECTION PRESSURE DATA

Monitoring of the injection pressure was continuous. The reservoir pressure was about 50 psig. Injection pressure increased to 80 psig under 500 bbl/day CWE steam injection at about 80% quality. Addition of surfactant and nitrogen increased the injection pressure to 150 psig. This level was maintained during the injection of surfactant, then reverted slowly to 80 psig in about thirty days after completion of each surfactant slug. This increase in injection pressure is far too large to be explained by the additional fluids injected. Most of the increase can be attributed to foam generation blocking the steam. In shallow reservoirs, care must be taken not to exceed fracturing pressure. An optimum pressure increase should exist for each pattern and could be approached by changing the concentration or rate of foamer injected, depending on the pressure response at the injector.

TRACER TESTING

Tracer testing can be a useful technique to define reservoir heterogeneity (well-to-well) or to study flow behavior near a given injector (injectivity profiles). This section deals with SUPRI experience with tracers during the pilot test.

Well-to-Well Radioactive Tracers

A radioactive tracer survey was conducted in November, 1981. The objective of this survey was to define the reservoir. A technique for the analysis of tracer breakthrough curves has been developed by Abbaszadeh and Brigham.[16] Although this method is only valid for a mobility ratio equal to one, it was hoped that the data from the survey would be amenable to a similar analysis. Tritium, krypton 85, sulfur hexafluoride and Freon 14 were injected into Well 208 and tritium and krypton 85 were injected into Well 214. As an experiment, gamma ray logging of the observation wells was attempted to try to detect the radioactive tracers--to no avail. No tracer response was seen. Nor were Tritium or Freon 14 detected in any of the producers. Krypton 85 and sulfur hexafluoride were observed in Well 120 (see Fig. 1) and a smaller amount was seen in Well 119. The data from these wells could not be analyzed using the technique of Ref. 16.

No samples were taken from Well 114, the most updip producer in the test pattern. This was unfortunate. The results of the inorganic tracer tests (discussed later) and the temperature surveys showed that most of the steam injected into Well 208 moved towards Well 114. The oversight in not sampling this well probably cost access to valuable data.

Timing was faulty on the sampling program. As shown by the inorganic tracer results, described in the next section, steam traveled from Well 208 to Well 114 in less than half an hour, much faster than expected. As a result we may have missed most of the tracer responses by sampling too late. One other reason for the failure of the radioactive tracer program lays in the small amounts of tracers that can be injected under California law. Present restrictions are even more stringent, thus it is difficult to design a good radioactive well-to-well tracer testing program in California.

Nitrogen was injected as a noncondensable gas to improve the efficiency of the steam/foam test. It would have been useful to use nitrogen as a tracer and obtain information in that manner. No sampling facilities for nitrogen were available at the time.

Inorganic Well-to-Well Tracers

Due to the poor results of the radioactive tracer survey, an attempt was made to use sodium bromide and sodium nitrate as tracers. These salts are water soluble, are supposed to be nonvolatile and their transport properties in steam/water systems are not understood. Even though the inorganic tracers are nonvolatile, a strong tracer response was observed in the most updip wells in less than half an hour. This can only be explained by some transport of the tracers by the steam. Since no theory exists for this behavior, quantitative analysis of the breakthrough curves is impossible. It was possible, however, to qualitatively compare surveys performed before the steam/foam test (Fig. 3a) and during injection of foam (Fig. 3b). Evidence of steam diversion from Well 120 to Wells 113b and 119 can be inferred from the changes in relative amounts of tracers recovered at the producers.

Inorganic tracer surveys are inexpensive. They can provide useful qualitative data; but, as no interpretation method exists to extract quantitative reservoir information from such tests, they should be used only as a supplement to other monitoring methods.

Injectivity Profiles

Injectivity profiles are used in wells where spinner surveys are not accurate enough to provide information on the amount of fluids entering a given interval of the formation. That happens when rates of injection are too low or when two phase flow effects perturb the measurements. Spinner surveys have been successfully used[17,18] in Venezuela and should be preferred when possible. The SUPRI test was in a lease operated at conditions where the spinner surveys are not reliable. We decided to use injectivity profiling instead.

Injectivity profiles are obtained by injecting a water soluble radioactive tracer with the steam and making repeated passes over the perforated interval with a detector. The procedure is repeated for the gas phase, this time using a gas soluble tracer. The amount of fluid entering a given interval of the formation is calculated from the intensity and the rate of decay of the radioactivity detected. Interpretation procedures of these tests vary for different service companies, and no sound theory seems to be available to analyze them. We feel, consequently, that quantitative analysis of these tests should be used with caution.

Profiles were taken in Well 208 before, during and after every surfactant slug injection. They provided useful qualitative information. The same profile patterns with time were obtained for each of the three main slugs. Before the slug, injectivity profiles in our test pattern were atypical; for instead of normal steam override most of the fluids went into the bottom of the well in the fourth layer. We found later that there had been additional unreported perforations in that interval. During the treatment, injectivity into this zone was reduced and Slices 1 to 3, previously poorly swept, were contacted by the steam (Fig. 4). The profiles reverted to the original values a few days after completion of each surfactant slug injection.

In the SUPRI test, we planned a deliberate overkill in the amount of surfactant injected. As a result, the steam diversion was not perfect during injection of the first slug. The profiles showed improvement at the beginning with steam being diverted from Slice 4 to Slices 1 to 3; then they reverted to the original profiles as surfactant injection continued. We feel that the excess foam reduced the injectivity of Slices 1 to 3 after a few days and that the steam then swept back into the higher permeability desaturated layer, Slice 4. When the surfactant concentration was reduced during injection of the two later slugs, this problem disappeared and better vertical sweep was achieved throughout the injection sequence.

In theory, one would like to compare spinner surveys and injectivity profiles from radioactive tracers. Both techniques are useful in detecting injectivity changes near the wellbore caused by the additives, and in qualitatively monitoring the near wellbore vertical sweep efficiency.

SAMPLING AND PRODUCED FLUIDS ANALYSIS

Sampling could have been attempted in the observation well located in the test pattern. Designing a sampling program should be done carefully for it can complicate later logging operations. However, it is worth the effort, for knowledge of surfactant transport through the reservoir can lead to better modeling of foam propagation for a given site and offer some predictive tools for management decisions. A good example of such an approach was presented by Patzek and Myhill[8]. Detection of surfactant, and/or degradation by-products, could have provided insight on the validity of the laboratory studies. Surfactant transport is an important problem, as noted by Lau and Borchardt,[9] and Liu et al.,[19] for transport properties can directly affect the economics of the steam foam process.

Produced fluids were sampled during the SUPRI pilot. The water samples did not show either surfactant or products resulting from possible surfactant degradation. Other projects[6-8] have found surfactant transported to the producers.

The fact that surfactant can be transported to the producers has led to fear of emulsion problems. The surfactants used in steam/foam projects are not designed to reduce oil/water interfacial tension. In the laboratory, the lowest IFT measured by SUPRI in oil/foamer systems was several dynes/cm. This is probably the reason why no emulsion problems have been attributed to the surfactants in published steam/foam projects.

PRODUCTION RESULTS

Two sets of production data were obtained during the field experiment. One set was provided by the lease operator and proved to be radically different from the second set collected by CORCO, the operator of the pilot test. A testing procedure was designed to evaluate the production data.

Both sets of data were obtained by testmeters where total production of oil and water was measured using turbine flowmeters and the water cut was determined by sampling. Such meters require careful handling and calibration. To check the accuracy of the production measurements, 500 bbl tanks were installed on site and the production from individual wells was tested periodically in these tanks. To obtain the exact cut of oil in the tanks a new sampling device was constructed,[1,2] Fig. 5. This device was needed because of the problem of separating oil and water in the tanks. The CORCO set of

data was found to be the more reliable by comparison with the tank measurements.

Unfortunately these test measurements were not available during the entire pilot test, so there is some doubt about the accuracy of the production data. We recommend the use of tanks for individual wells whenever possible.

Oil production estimates from the test pattern are shown in Fig. 6. A pronounced upward trend was observed within days of the start of each of the slugs. These increases are remarkable in light of the general decline of about 16% per year observed on the lease as a whole as can be seen from the dashed lines on Fig. 6 and as discussed earlier. The baseline production trend is not accurately known, but an increase in rate is clear. The increase can be attributed to the steam foam treatments because no significant operational changes were made in the test pattern during the life of the project. Economic projections performed on a leasewide basis[20] show the process to be economic. This conclusion was later confirmed by others.[6]

Measuring produced fluids in heavy oil reservoirs is not simple. Even if a correct baseline or decline curve for the test area has been established, care has to be taken to assess individual wells' oil and water rates. Use of individual tanks with proper determination of the oil cut is one of the best methods. Overall lease data should be viewed with caution because of normal variations between individual wells and sometimes insufficient operating personnel or equipment. As oil production is the main indicator of economic success of a process, every effort should be made to obtain accurate data.

CONCLUSIONS

Even in a carefully designed research pilot, we have seen that significant improvements could have been made in the design and operation of the SUPRI project. The goal of a pilot test is to obtain information. This information is valuable for it allows understanding of a process behavior in a given reservoir. In the search for accurate field data, redundant monitoring methods can and should be used to forestall unexpected problems or equipment failures. The reservoir is not often going to behave as expected. It is important to understand the reservoir physics prior to the application of any enhanced oil recovery process. Time and money spent on reservoir characterization and proper monitoring methods are a wise investment.

ACKNOWLEDGMENTS

The authors gratefully acknowledge the technical contributions of numerous Stanford students and staff. In addition, the financial support of US DOE/FG22-90BC14600 and the financial and technical advice by the SUPRI-A industrial associates are acknowledged.

REFERENCES

1. Brigham, W. E., Marcou, J. A., Sanyal S. K.,, Malito, O. P. and Castanier, L. M. "A Field Experiment of Improved Steam Drive With In-Situ Foaming" SPE 12784, paper presented at the California Regional Meeting, Long Beach (April 11-13, 1984); also SPERE 4, No. 1 (1989) 239-248.

2. Brigham, W. E., "A Field Experiment of Improved Steam Drive with In--Situ Foaming," DOE Final Report (1984) [DE-AC03-80AF11564].

3. Owete, O., Al-Khafaji, A., Sanyal, S. K., Castanier, L. M. and Brigham, W. E., " Foam as a Mobility Control Agent In Steam Injection Processes" SPE 8912-B, paper presented at the California Regional Meeting, Los Angeles (April 9-11, 1980).

4. Al-Khafaji A., Wang P. F., Castanier, L. M. and Brigham, W. E, "Steam Surfactant Systems at Reservoir Conditions," SPE 10777, paper presented at the California Regional Meeting, San Francisco (March 24-26, 1982).

5. Mohammadi, S. S. and McCollum, T. J., "Steam-Foam Pilot in Guadalupe Field, SPE 15054, paper presented at the California Regional Meeting, Oakland (April 2-4, 1986).

6. Eson, R. L. and Cooke, W. W., "A Compre-hensive Analysis of Steam Foam Diverters and Application Methods", SPE 18785, paper presented at the California Regional Meeting, Bakersfield (April 2-4, 1989).

7. Castanier, L. M. and Brigham, W. E., "Steam With Additives: Field Projects of the Eighties," Jour. of Pet. Science and Tech. 2 (April 1989) 192-206.

8. Patzek, T. W. and Myhill, N. A. "Simulation of a Bishop Steam Foam Pilot," SPE 18786, paper presented at the California Regional Meeting, Bakersfield (April 2-4, 1989).

9. Lau, H. C. and Borchardt, J. K., "Improved Steam Foam Formulations: Concepts and Laboratory Results" SPE 18783, paper presented at the California Regional Meeting, Bakersfield (April 1989).

10. Hirasaki, G., Shell Development, Personal Communication (1984).

11. Mohammadi, S. S., Van Slyke, D. C., and Ganong, B. L., "Steam-Foam Pilot Project in Dome Tumbador, Midway Sunset Field" SPE 16736, paper presented at the Annual Technical Conference and Exhibition, Dallas (September 27-30, 1987).

12. Walsh, J. W., Ramey, H. J., Jr. and Brigham,, W. E., "Thermal Injection Well Fall-off Testing" SPE 10227, presented at the Technical Conference and Exhibition, San Antonio (October 5-7, 1981).

13. Messner, G. L. and Williams, R. L., "Applications of Pressure Transient Analysis in Steam Injection Wells," SPE 10781 paper presented at the California Regional Meeting, San Francisco (March 24-26, 1982).

14. Ambastha, A. K. and Ramey, H. J., Jr., "Thermal Recovery Well Test Design and Interpretation," SPE 16746 paper presented at the Annual Technical Conference and Exhibition, Dallas (September 27-30, 1987).

15. Horne, R. N.: "Modern Well Test Analysis: A Computer-Aided Approach," Petroway, Inc., Palo Alto (1990).

16. Abbaszadeh, M. and Brigham, W. E., "Analysis of Well-to-Well Tracer Flow to Determine Reservoir Layering," J. Pet. Tech. 36, No. 11 (October 1984) 1753-1762.

17. Keijzer, P. P. M., Muijs, H. H., Jansen-Van Rosmallen, R., Teeuw, D., Pino, H., Avila, J. and Rondon, C., "Application of Steam Foam in the Tia Juana Field, Venezuela" SPE 16305, paper presented at the 5th Symposium on Enhanced oil Recovery, Tulsa (April 2-4, 1986).

18. D'orazio, F., Zirritt, J. L., Rondon L., Rivas, O.,Paz, F. and Paez, E., "Prueba Piloto de Injection Alternada de Vapor Con Surfactantes," Proceedings 2nd International Symposium on Heavy Oils, Maracaibo, Venezuela, (February 24-27, 1987).

19. Liu, D., Castanier, L. M. and Brigham, W. E., "Displacement by Foam in Porous Media," SPE Conference and Exhibition, Washington, D. C. 24664, paper presented at the Annual Technical (October 4-7, 1992).

20. Strom, J. and Brigham, W. E., "An Engineering Economic Analysis of a Steamflood Plus Surfactant Field Project, DOE (1984) [DE-AC03-80SF11445].

TABLE 1
LOGGING PROGRAM IN THE OBSERVATION WELLS

OPEN-HOLE LOGS	COMPANY
FDC-CNL Gamma Ray	Schlumberger
Nuclear Magnetic Log	Schlumberger
Electromagnetic Propagation Tool	Schlumberger
Dual Induction-SFL	Schlumberger
Cyberlook	Schlumberger
Spectralog	Dresser-Atlas
Dielectric Constant	Gearhart Industries
CASED-HOLE LOGS	**COMPANY**
Dual Spacing Thermal Neutron Decay Time	Schlumberger
Cement Bond	Schlumberger
Gamma Ray Spectroscopy (in Well 214M only)	Schlumberger
Carbon/Oxygen	Dresser-Atlas
Temperature	USGS
COMPUTER-PROCESSED LOGS	**COMPANY**
VOLAN	Schlumberger
Production Management	Schlumberger

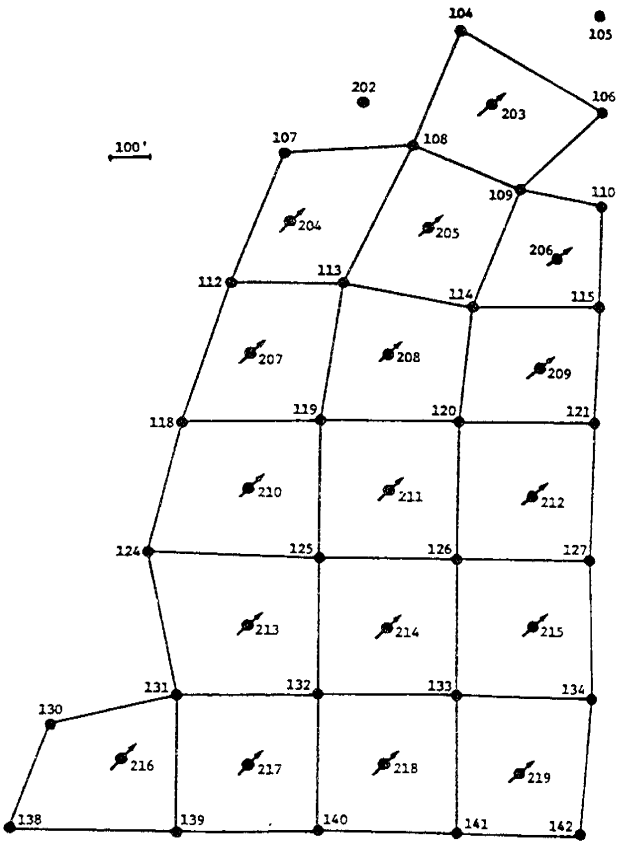

Figure 1. MacManus lease test and control pattern location.

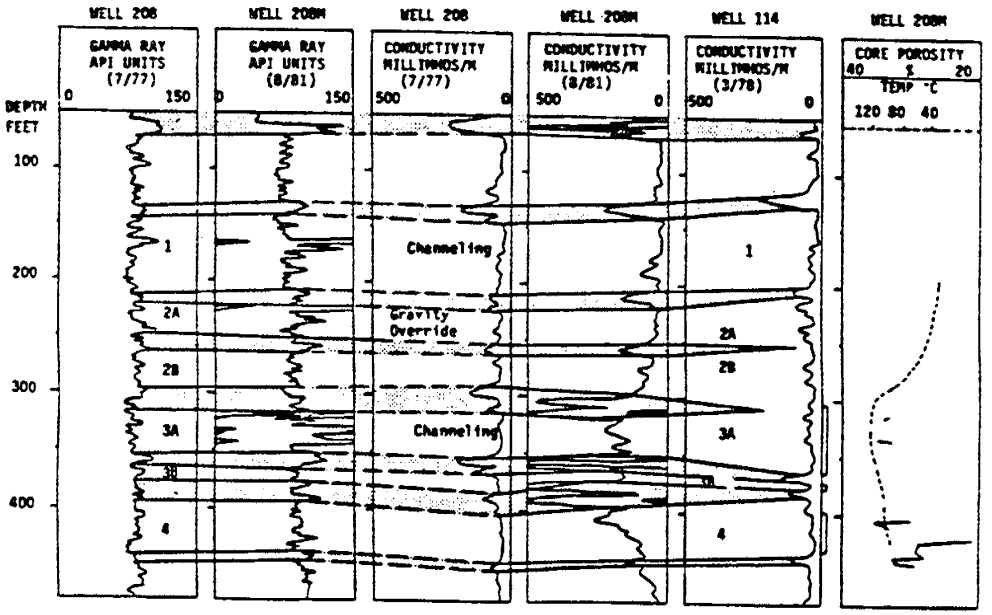

Figure 2. Cross section test pattern.

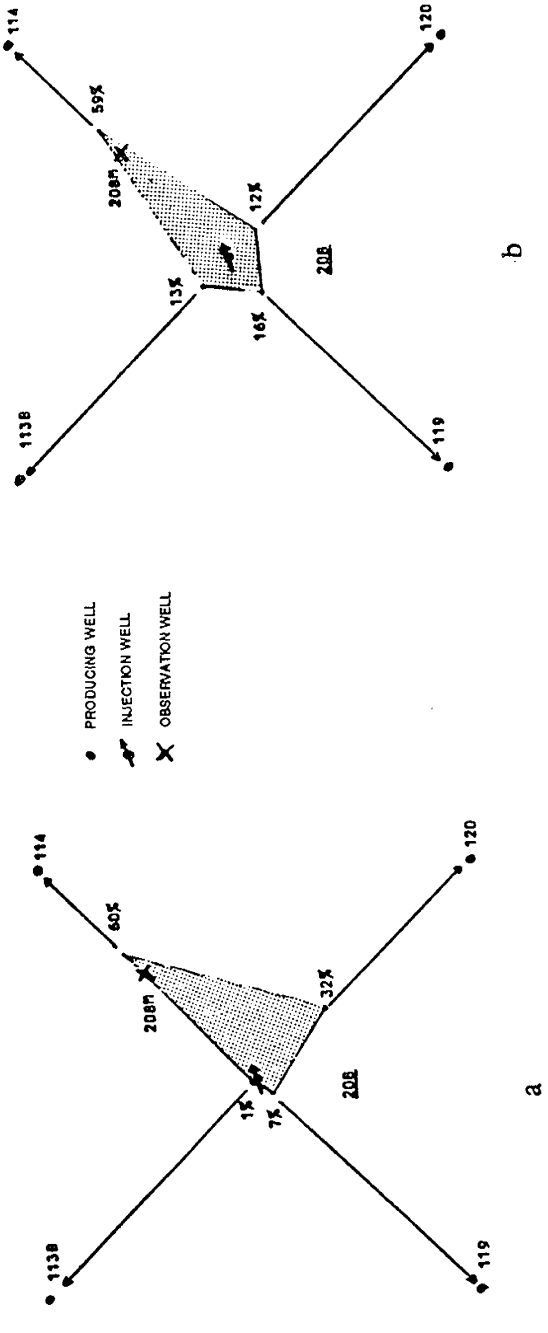

Figure 3a. Tracer response before and after second slug injection.

Figure 3b. Tracer response during second slug injection.

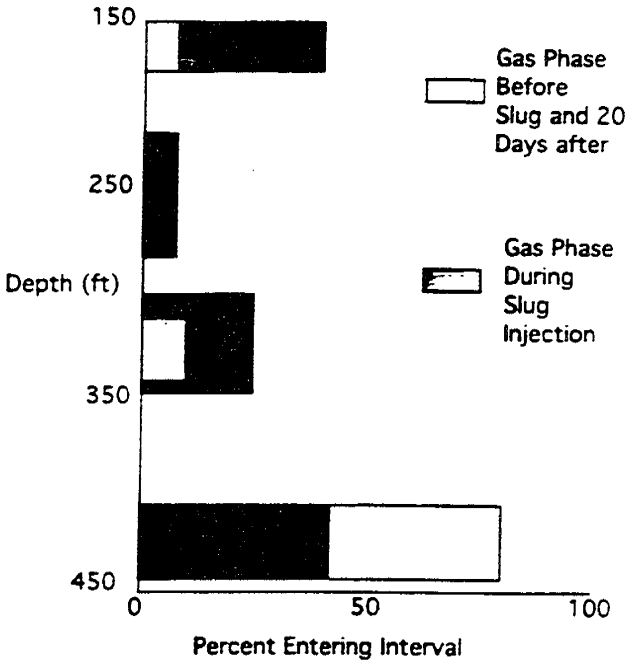

Figure 4. Injection profiles during first slug injection.

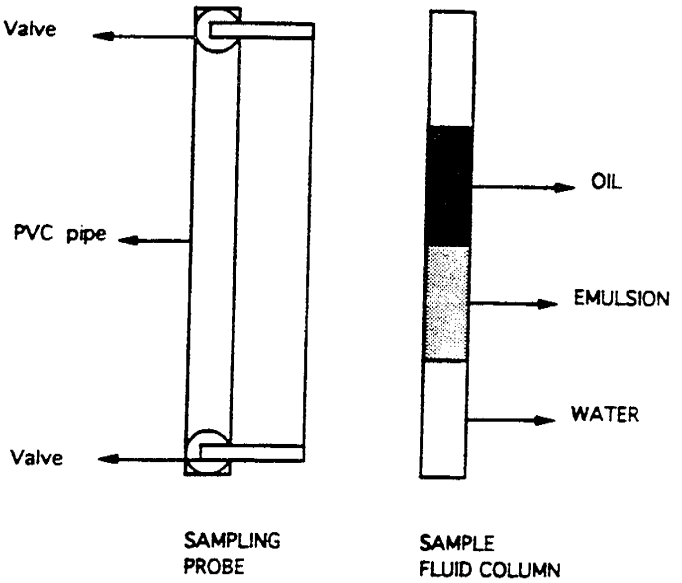

Figure 5. Sampling probe assembly.

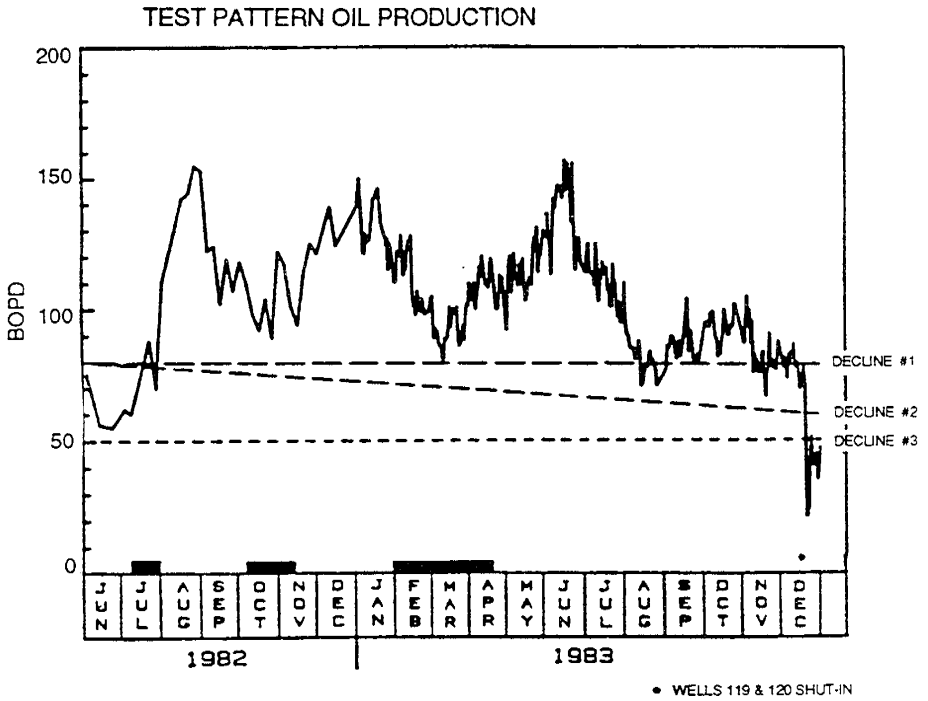

Figure 6. Test pattern oil production.

No. FS3

DOE/NIPER

Cyclic Steam-Foam Injection in a Carbonate Reservoir

by J. Ivory, G. van der Voet, D. A. Best, E. E. Isaacs and W. D. Gunter, Alberta Research Council, Edmonton, Alberta, Canada

Author(s) are solely responsible for copyright and contents.

This paper was prepared for presentation at the DOE/NIPER, Symposium on Field Application of Foams for Oil Production held in Bakersfield, California, February 11-12, 1993.

This paper was selected for presentation by a Program Committee following review of information contained in an abstract submitted by the author(s). Contents of the paper, as presented, have not been reviewed and are subject to correction by the author(s). The material, as presented, does not necessarily reflect any position of the U.S. Department of Energy or the National Institute for Petroleum and Energy Research.

ABSTRACT

A single well cyclic steam foam test was performed at well C13 in the Upper Devonian Grosmont carbonates in Northern Alberta, Canada. This well had previously been subjected to eight steam injection cycles. Being a typical Grosmont producer, bitumen cuts after a few weeks' production were of the order of five percent. The primary purpose of the test was to determine if the injection of foam in a cyclic process would ultimately improve bitumen recovery as a result of steam diversion.

The results indicated that foam did succeed in diverting steam. Radioactive tracer velocity shot surveys, pressure buildup and falloff tests, and injectivity pressure data all showed that flow patterns close to the wellbore and fluid transmissibility in the reservoir were altered by foam injection. Over the first 24 days, cumulative bitumen production was significantly higher in the foam cycle 9 and the post-foam cycle 10 as compared to pre-foam cycles 7 and 8. Foam increased the bitumen concentration of the produced liquid. This was especially apparent in the post-foam cycle 10 where the average bitumen concentration in the produced liquid over the first 24 days of production was 19.7% as compared to 3.6%, 5.9%, and 8.2% in cycles 7, 8, and 9.

Chevron Chaser SD1000 surfactant was used. The active surfactant concentrations in the produced water indicated that somewhat less than 25% of the surfactant was lost by (1) adsorption on the reservoir rock, (2) absorption into the bitumen, and (3) thermal degradation.

INTRODUCTION

Geological Description

The Grosmont carbonate formation represents an extensive 7°API bitumen resource (50 billion m^3)[1] which has not yet been commercially produced. It is approximately 160 km wide and 500 km long[1] (Figure 1). The Grosmont formation is underlain by and laterally joins the Ireton formation (Figure 2)[2]. The Grosmont overlies the Leduc formation to which it is stratigraphically equivalent. It is overlain by the Nisku formation. The average Grosmont thickness is about 150 m. The formation is divided into four sub-units by thin shale layers, which, in ascending order, are identified as Lower Grosmont, Upper Grosmont 1, 2, and 3 (Figure 3). Dolomite accounts for 98% of the rock[3]. The remainder is composed of minerals such as quartz, diopside, kaolinite, feldspar, illite, pyrite, and mixed-layer clay. All of the pilot testing has been carried out in the Upper Grosmont 2.

In the Grosmont formation bitumen saturations frequently exceed 70 - 80%[2]. It is a very

heterogeneous formation with a large variance in the type and distribution of porosity. The four common pore types are: (1) moldic - from leaching of skeletal fragments, (2) fractures - usually short and sub-vertical, (3) dissolution vugs - irregular, both microscopic and macroscopic, and (4) intercrystalline (sucrosic) - resulting from dolomite formation.

Despite its viscosity of 1,600,000 mPa.s at native reservoir conditions, bitumen production rates as high as 80 m^3/d have been reported from steam stimulation of a single well in a carbonate formation[4]. However, fracture systems and karsts have been found to greatly affect the production behaviour of steam-cycled wells. By reducing the steam mobility, foam has the potential to reduce the flow of steam through the fractures and karst fill sediments.

Steam Foam Concept

A cyclic steam foam test was performed in 1986. The purpose of this test was to determine if the injection of foam into the Grosmont 2 carbonate formation would ultimately improve bitumen recovery. To understand how foam can improve the performance of a well in the Grosmont formation one should be aware that it is essentially a dual porosity system. High permeability fractures and vugs connect low permeability (0.1 darcy) matrix regions which contain much of the bitumen. Injected steam essentially flows through the fracture system and heats up the matrix regions by conduction.

Steam preferentially moves through those fractures which offer the least resistance to flow. Consequently, bitumen is primarily produced from those fractures and from the matrix sections adjacent to them. During injection, foam has the potential to perform two major functions:

- It may divert some of the steam flow from previously preferred flow paths (fractures) to other fractures which are in contact with less depleted regions of the formation.

- It may decrease the mobility of the steam by an order of magnitude so that the pressure drop across the fractures is increased. As a result more steam is forced into the matrix and more bitumen is displaced into the fractures and recovered.

As a result of gas expansion and water flashing, foam can be regenerated during the production period. A laboratory investigation[5] demonstrated that foam formation due to surfactant was apparent mainly in the low pressure phase at the end of a drawdown. Overall, this is a positive effect as it provides a resistance to water flow. A negative effect would be if foam formation hinders bitumen flow. However, a foam generated by SD1000 collapses readily in the presence of oil[6].

Foam has been shown to increase both oil recovery and injection pressures as a result of steam diversion in sand reservoirs[7 - 10]. The present pilot study was performed to determine if similar results could be obtained in a carbonate reservoir. This was considered a more stringent test of the ability of foam to divert steam. The collapsing and regeneration which occurs as a foam flows through a sand reservoir may only occur to a limited degree in the fracture system of a carbonate reservoir as the foam may flow predominantly through the high permeability fracture network rather than through pore throats.

SELECTION OF TEST WELL, SURFACTANT, AND STABILIZING GAS

The test was performed at a pilot site pattern which had seven cyclic wells and four observation wells (Figure 4). A well (C13) was selected which had sufficient history (8 cycles) and was not too depleted. Although bitumen cuts of 12% had occurred during cycles 7 and 8, those cuts had decreased to less than 5% after a few weeks production. Well C13 was one of the poorer wells at the pilot site. Thus, the selection of C13 was seen as a stringent test of the foam process. A well schematic is shown in Figure 5.

Preliminary lab testing had identified a few surfactants that were commercially available and had good foam forming characteristics under steam injection conditions. Chevron Chaser SD1000 was selected for the pilot test mainly because:

- It had a high active concentration (40%) which minimized the costs of transporting the surfactant to the isolated pilot site.

- The foam formed readily collapsed in the presence of oil.

The properties of SD1000 are summarized in Table 1.

Prior to the field test a laboratory study was carried out to determine if surfactant losses from adsorption on the carbonate rock and absorption into the bitumen would be significant. The experiments were performed at the

Alberta Research Council. They showed that about 20% of SD1000 was lost by partitioning into the bitumen phase. However, this was a smaller percentage than would be obtained with a surfactant which is not as strongly hydrophillic as SD1000. Other experimental results indicated that SD1000 had a higher adsorption on carbonate than on silica sand (50% versus 20%) in the absence of bitumen. However, in a bitumen saturated carbonate the surfactant losses were only 15%. The bitumen likely provided a barrier to the adhesion of the surfactant molecules to the carbonate.

It should also be noted that the laboratory study involved static steady state experiments and these tend to produce higher adsorption values than do dynamic measurements. This is because in static experiments the surfactant has time to diffuse to all the available surface sites. In contrast, in a dynamic situation (experiment or field), as a result of channelling, the surfactant will not contact every available adsorption site. In addition, in a dynamic reservoir situation, the desorption of surfactant from the rock may have a beneficial effect.

Natural gas was selected as the noncondensible gas because it was readily available. The natural gas contained 97.3 vol.% CH_4 and 2.2% CO_2. In addition to stabilizing the foam, the natural gas may also have helped bitumen recovery as a result of dissolution in the bitumen thereby reducing the bitumen viscosity and contributing to a gas drive during the production phase.

EXECUTION OF THE TEST

Foam Injection System

A flow diagram of the foam injection system is given in Figure 6. Air actuated chemical injection pumps were used to inject the surfactant into the steam injection line. The surfactant injection rate was obtained by monitoring the liquid level in the surfactant drum. The natural gas flow rate was measured with an orifice meter.

Monitoring the Effects of Foam

Prior to the test, it was expected that if the foam succeeded in diverting steam then an increase in bottomhole pressure (BHP) would be observed. In order to monitor this increase in pressure it was decided to establish a relatively stable BHP by injecting steam at a rate of 150 m^3/d (CWE) for 20 days. A number of other measurements were made during the injection phase of the cycle to determine how effectively the foam was diverting the steam. They included frequent temperature surveys and BHP measurements at surrounding wells.

A radioactive velocity shot survey was performed during the 45th day of the injection period. This survey involved the injection of cold water at the surface and the injection of a water based iodine 131 tracer downhole. From the time it took the tracer to travel between two detectors, which were 0.96 m apart, it was possible to estimate the perforation depths at which the water preferentially entered the formation. Above the perforations, the tracer travelled quickly between the detectors as it was carried by the full water flow. As the tool was moved down below the top perforations there was less water available to transport the iodine as some of it had passed through the perforations into the reservoir. Thus, the time for the iodine to move between the detectors was increased. The measured times at different levels were used to determine the flow rates at these levels.

Pressure falloff and buildup tests were also performed to determine the effect of foam on steam zone transmissibility.

Injection Strategy

Steam was injected for 50 days at approximately 150 m^3/d as shown in Figure 7. Gas was injected with the steam for 4 days (day 8 - day 11) prior to foam injection to determine if the gas itself would have an effect on the injection pressure. The surfactant and natural gas concentrations in the injected fluid are provided in Figure 8. They are based on an assumed steam quality of 70%. Initially surfactant was injected at a high rate (1.2 wt.% in liquid phase) so as to generate a foam in the reservoir. Then, in order to reduce costs, the surfactant concentration was reduced to 0.15 wt.%. The total mass of active SD1000 injected was 3818 kg. The natural gas concentration was about 0.8 mole% before being reduced to 0.5 mole% on day 40 because of compressor problems. The total volume of natural gas injected was 26,285 m^3 (ST).

RESULTS

Injection Pressure

The BHP response to foam injection as shown in Figure 9 is hardly noticeable. However, a Bourdet[11] plot of injection data (Figure 10) suggests foam addition did raise steam injection pressures. The pressure derivative starts to increase at the beginning of foam injection. This increase can be interpreted as a

decrease in fluid transmissibility.

Temperature

Temperature surveys at well C13 indicated that, during steam injection, the temperature increased to more than 190°C over most of the Grosmont section. Figure 11 shows that temperatures were much lower over the lowermost portion of the interval, which was perforated between 279 and 289 m, indicating that most of the steam was entering the top perforations. There was no observable change in temperature at observation wells which was attributable to foam injection. Figure 11 also shows that the temperatures in well C13 declined during the production cycle as bitumen and water flowed from colder areas of the reservoir.

Radioactive Tracer Velocity Shot Survey

On the 45th day of injection, a radioactive tracer velocity shot survey (using water injection) was performed. The results (Table 2) were compared to those from a previous survey which was performed prior to the foam test. The initial survey indicated that 63% of the flow entered through 4.5 m of perforations (279.5 - 284 mKB) with the remainder entering below 285 mKB. There was no flow through the 1 m interval 284 - 285 m. The post-foam survey showed that all of the water flowed through the top 5 m of perforations i.e. foam blocked flow into the interval below 285 m where previously 37% of the water had gone. It is reasonable to assume that much of the surfactant initially moved, with the water phase of the injected fluid, to the bottom of the perforations and built up a high surfactant concentration there. Alternatively, bitumen may have drained into the region around the bottom of the well, thereby impeding steam flow.

Pressure Falloff Test

The 43 hour pressure falloff test (Figure 12) on well C13 at the end of the cycle 9 injection period indicated that the transmissibility was 920 $(\mu m)^2$. m/mPa.s in cycle 9 as compared to 1138, 1195, and 1757 $(\mu m)^2$. m/mPa.s for cycles 5, 6, and 7 where previous falloff tests had been performed. This indicates that the injection of foam in cycle 9 reduced the steam zone transmissibility by about 30% as compared to previous cycles.

Pressure Buildup Test

After 24 days, production was terminated and a 142 hour pressure buildup test was initiated. From the slopes of the straight line regions in the Horner plot (Figure 13), it was determined that the transmissibility following cycle 9 was four times that following cycle 7 (8 $(\mu m)^2$. m/mPa.s versus 2 $(\mu m)^2$. m/mPa.s). The increase in the transmissibility which resulted from cycles 8 and 9 was probably due to cleaning out of new flow paths by diverted steam. The transmissibility (permeability x height/viscosity) values in the buildup tests are low because they primarily represent the flow of bitumen and water. In contrast, the falloff transmissibility values are one to two orders of magnitude higher because they are dominated by gas flow in the steam zone.

Bitumen Production

Foam injection did not cause any production problems such as foaming or tight emulsions. This was probably because the foam which was injected collapsed in the presence of oil. The bitumen production data in Figures 14 and 15 are normalized. Figures 14-16 show that initial bitumen production rates and bitumen cuts in cycles 9 and 10 were significantly better than cycles 7 and 8. Although the cycle 9 bitumen production tapered off after about 15 days, cycle 10 continued to produce bitumen at a relatively high rate until the cycle was ended. This indicates that the foam did indeed succeed in diverting steam either into the matrix or into different fracture paths. It is unlikely that the extra bitumen resulted from cleaning out the depleted zone as SD1000 is not a good emulsifier. Also, at steam temperatures the surfactant has little impact on the interfacial tension[6].

Economics

The cost of the surfactant SD1000 at the pilot site was about $2.50/kg of surfactant solution (including trucking charges and taxes). This is equivalent to $6.25/kg of active surfactant. At a natural gas price of $0.1/$m^3$ (ST), the extra cost of surfactant and gas for the tests was about $26,500. The incremental bitumen production was 0.02 m^3/ kg active surfactant in cycle 9 and 0.06 m^3/kg active surfactant in cycle 10. The cost of the incremental bitumen recovery for cycles 9 and 10 combined was $84/$m^3$. As part of another test, cycle 8 had a packer in the well which restricted steam injection to the bottom half of the perforations. Thus, cycle 8 is not directly comparable to cycles 7, 9, and 10 which did not have the packer.

Surfactant Losses

The C13 field results indicated that surfactant adsorption was not a major factor in the foam test.

From analysis of surfactant concentration in the produced aqueous phase, it was estimated that less than 25% of the injected surfactant was lost by (1) adsorption on the reservoir rock, (2) absorption into the oil, and (3) thermal degradation.

CONCLUSIONS

- Foam succeeded in diverting the flow of steam in the Grosmont carbonate as indicated by the radioactive tracer velocity shot survey, the injection pressure data, the pressure falloff and buildup tests, and the bitumen recovery profile.

- The incremental bitumen recovery during the foam cycle 9 was 0.02 m^3/kg active surfactant and in the post-foam cycle was 0.06 m^3/kg active surfactant. The cost of this incremental recovery was \$84/m^3 of bitumen.

- The surfactant losses in the reservoir due to adsorption, absorption, and thermal degradation were less than 25%.

- There were no production problems associated with the injection of SD1000.

REFERENCES

1. Energy Resources Conservation Board "Atlas of Alberta's Crude Bitumen Reserves", Energy Resources Conservation Board Report 82-38, 1981.

2. Harrison, R. "Exploration for Heavy Crude Oil and Bitumen", AAPG Research Conf. Proc., Santa Maria, Oct. 29 - Nov.2 (1984).

3. Bizon, A.E., Boon, J.A., and Kubacki, W. "Mineral Transformations During In Situ Recovery of Bitumen from Carbonate Rock, A Statistical Experimental Study", I Simposio Internacional sobre Recuperacion Majerda de Crudos, Petroleos de Venezuela, Inpeluz, Maracaibo, Feb. 19-22, 1985.

4. Cordell, G.M. "Reservoir Simulation of a Grosmont Carbonate Pilot", AOSTRA conference on "Advances in Petroleum Upgrading and Technology", June 9 - 11, 1982.

5. Green, M.K., Isaacs, E.E., and Non Chomm, K. "Laboratory Study of the Use of Foam in Cyclic Steam Injection", Paper No. 89-40-34, 40th Annual Technical Meeting of the Petroleum Society of CIM, Banff, May 28 - 31, 1989.

6. Isaacs, E.E., Jian, L., Green, M.K., McCarthy, C., and Maunder, D. "Use of Foam-Forming Surfactants to Enhance the Recovery of Heavy Oils", AOSTRA Journal of Research, 4, pp 267 - 276, 1988.

7. Keijzer, P.P.M., Muijs, H., Janssen-van Rosmalen, R., Teeuw, D., Pino, H., Avila, J., and Rondon, L. "Application of Steam Foam in the Tia Juana Field, Venezuela; Laboratory Tests and Field Results", SPE and USDOE 5th Joint Conf. on EOR, April 20 - 23, 1986, Tulsa, Oklahoma.

8. Chevron Bulletin, Chevron Chemical Company, 576 Market Street, San Francisco, California 94105.

9. Eson, R.L. and Cooke, R.W. "Field Results of Steam Diversion Agents in Cyclic Steam Applications", 3rd Intl. Conf. on Heavy Crude and Tar Sands, UNITAR/UNDP Information Centre for Heavy Crude and Tar Sands, Long Beach, July 22 - 31, 1985.

10. Fitch, J.P. and Minter, R.B. "Chemical Diversion of Heat Will Improve Thermal Oil Recovery", 51st Ann. Fall Tech. Conf. and Exhibition of SPE, New Orleans, Oct 3 - 6, 1976.

11. Bourdet, D., Ayoub, J.A., Whittle, T.M., Pirard, Y.M., and Knlazeff, V. "Interpreting Well Tests in Fractured Reservoirs", WORLD OIL, pp 77 - 87, October 1983.

ACKNOWLEDGEMENTS

The authors wish to thank the Alberta Oil Sands Technology and Research Authority and Mobil Oil Ltd. for permission to publish this paper.

TABLE 1

Typical Properties of Chevron Chaser SD1000

TYPE: Dimerized alpha olefin sulfonate	
APPEARANCE: Clear amber liquid	
COMPOSITION (wt.%):	
Active	40
Oil	1
Inorganic Salts	1
Excess Caustic	0.1
Pour Point (°C)	2
Viscosity at 21°C (mPa.s)	64
Density at 21°C (g/cm^3)	1.07
Specific Heat (J/g/°C)	3.1
Mass of SD1000/drum (kg)	222.0
Mass of Active Ingredient/drum	88.8

TABLE 2

Radioactive Tracer Velocity Shot Results

Perforation Interval (mKB)	Percentage of Flow Pre-Foam	Post-Foam
279 - 280	2.5	14.9
280 - 281	15.0	5.5
281 - 282	10.9	30.2
282 - 283	21.6	25.0
283 - 284	12.6	24.3
284 - 285	0.0	0.0
285 - 286	1.4	0.0
286 - 287	9.3	0.0
287 - 288	14.2	0.0
288 - 289	12.6	0.0

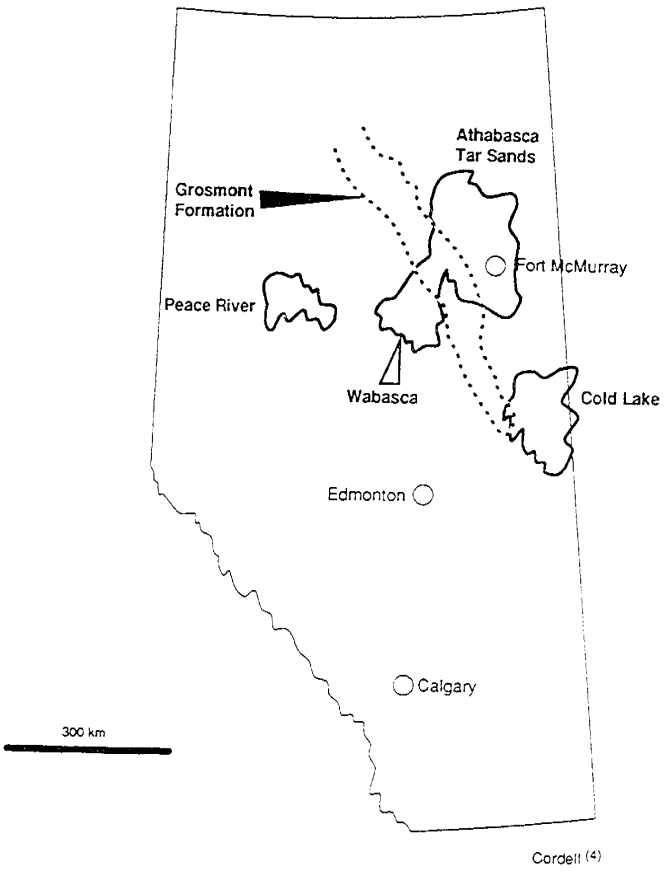

Figure 1. Alberta bitumen and heavy oil deposits.

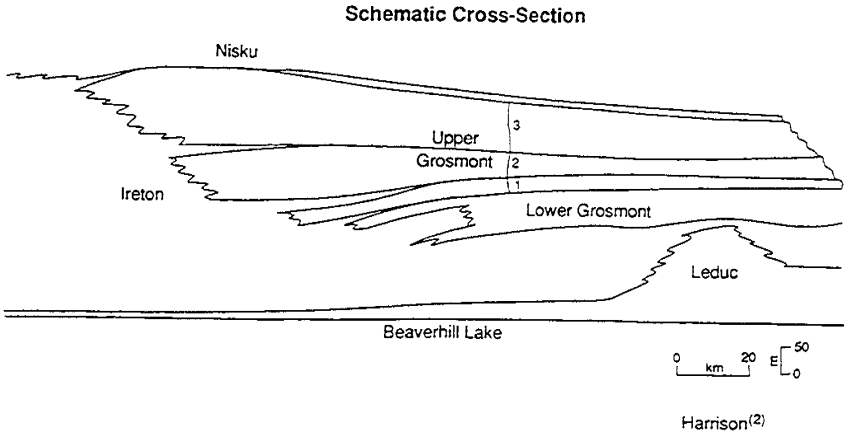

Figure 2. Stratigraphy of Grosmont Formation.

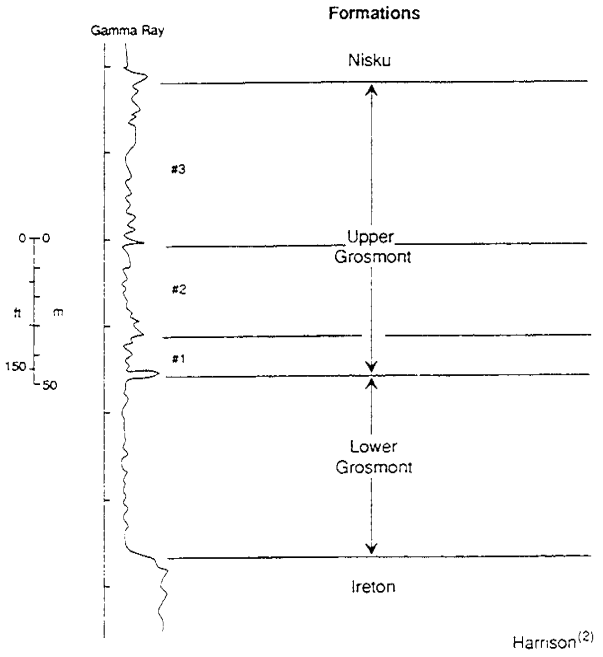

Figure 3. Grosmont units.

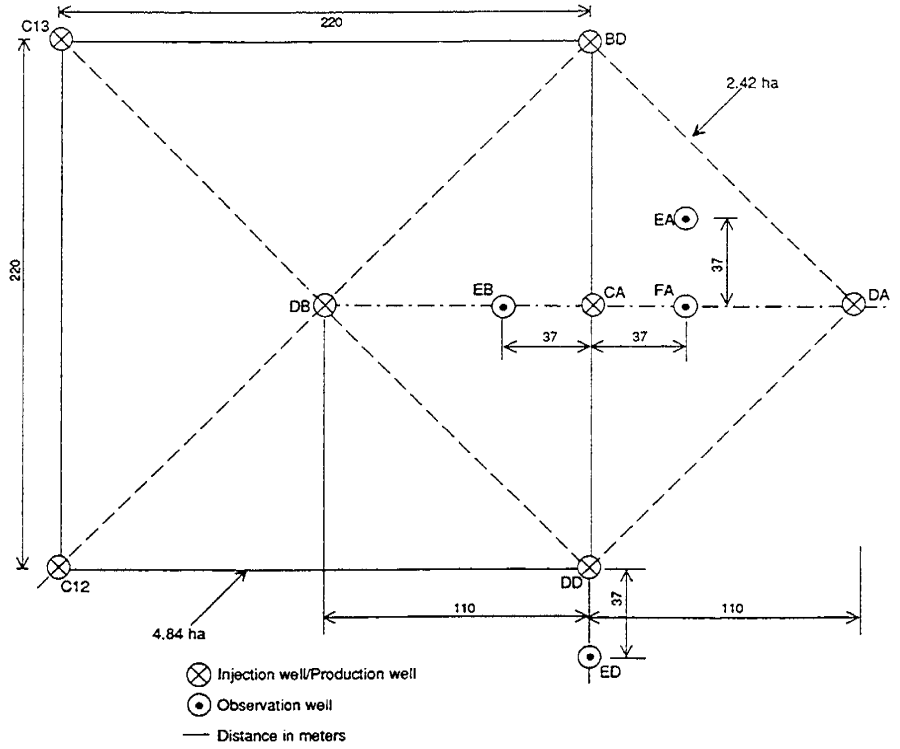

Figure 4. Pilot pattern.

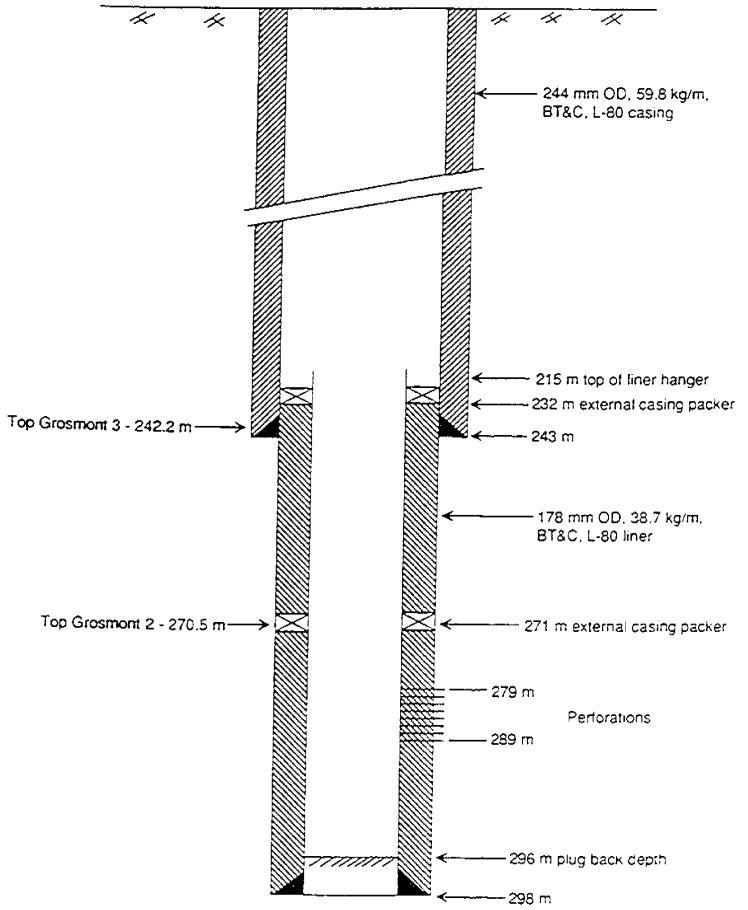

Figure 5. Test well C13.

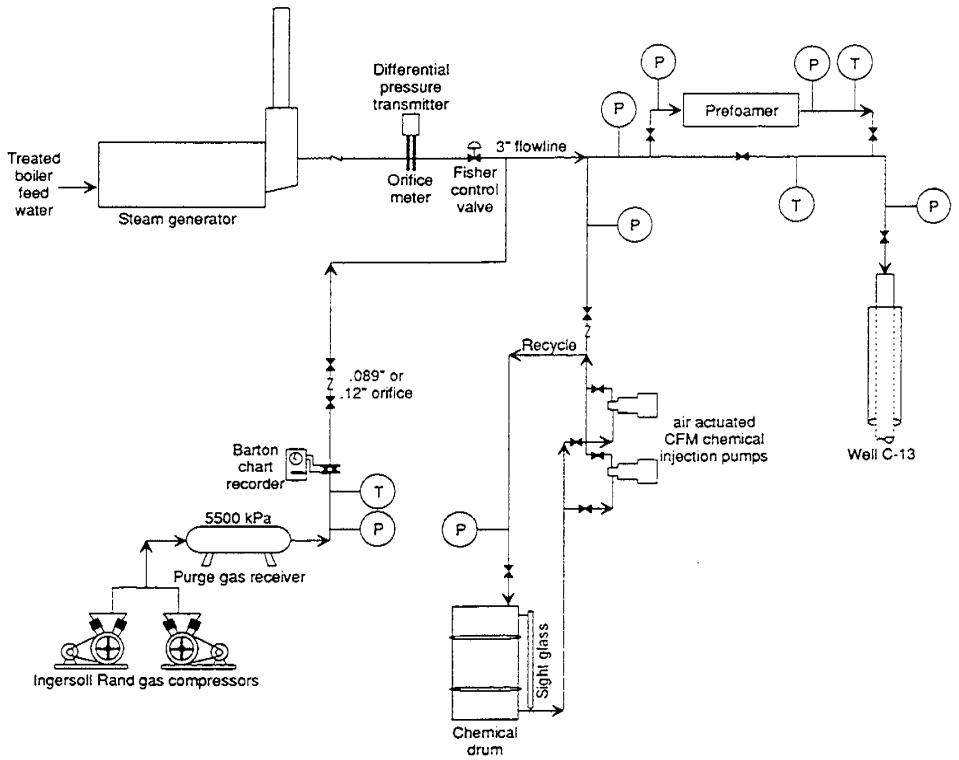

Figure 6. Schematic of foam injection system.

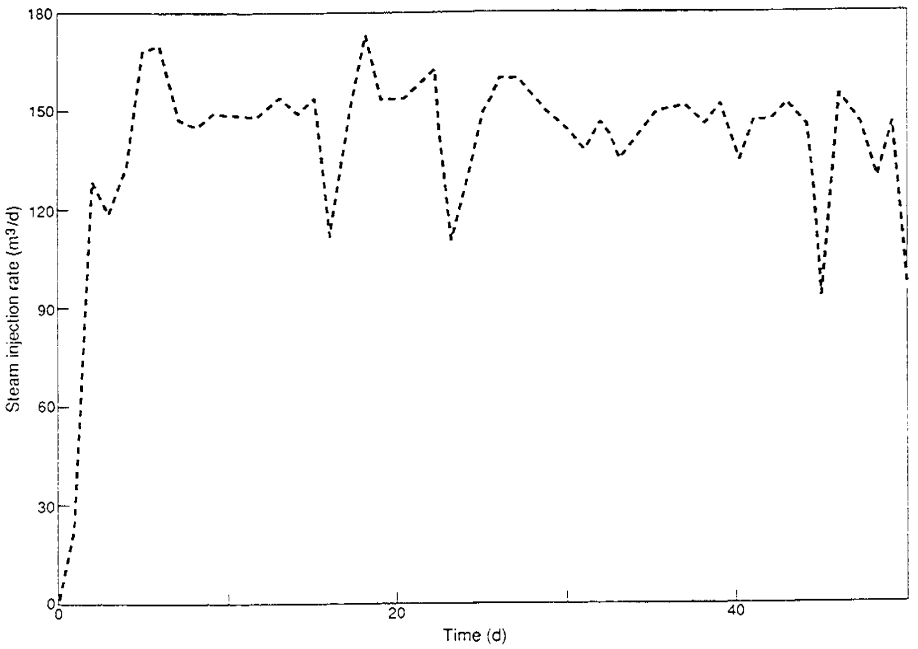

Figure 7. Steam injection rate for C13 Cycle 9.

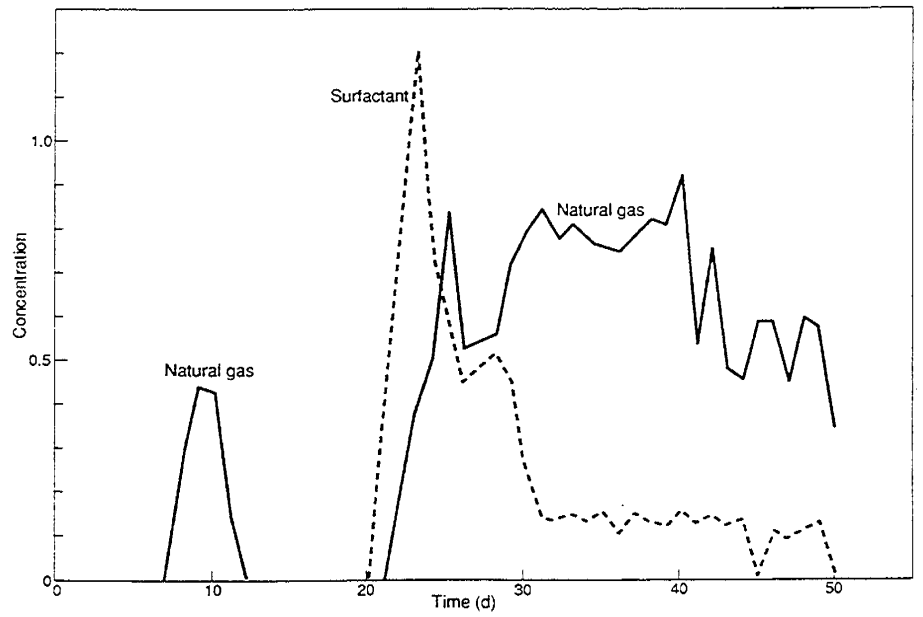

Figure 8. Concentration of surfactant (wt.% in liquid phase) and natural gas (Mole % in gas phase) in injection fluid.

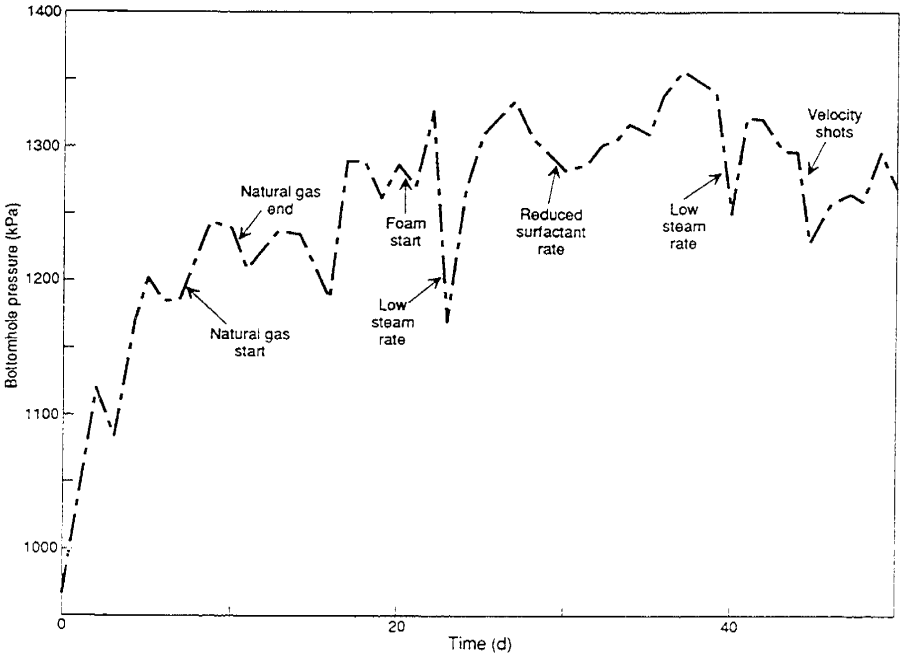

Figure 9. C13 bottomhole pressure for Cycle 9 injection.

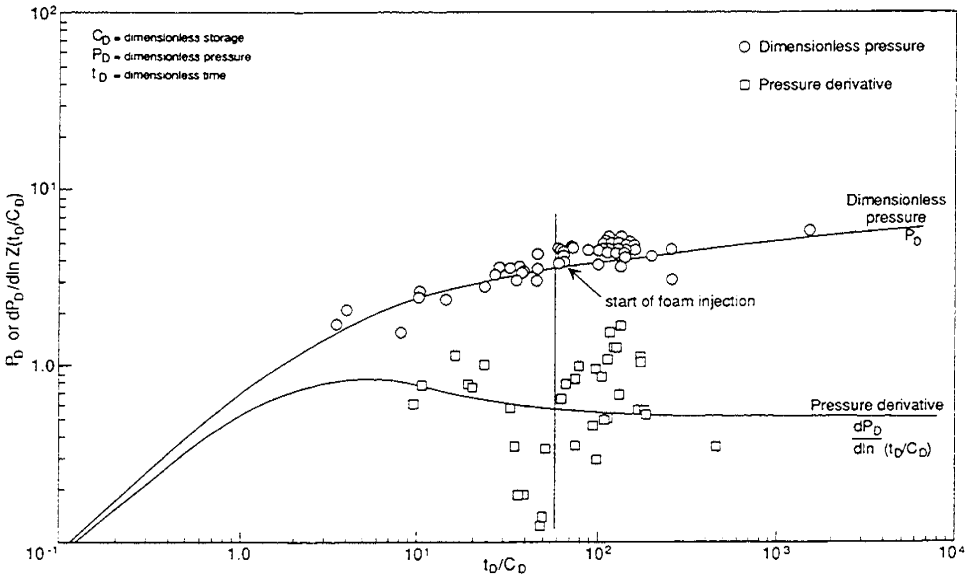

Figure 10. Bourdet normalized pressure drawdown plot.

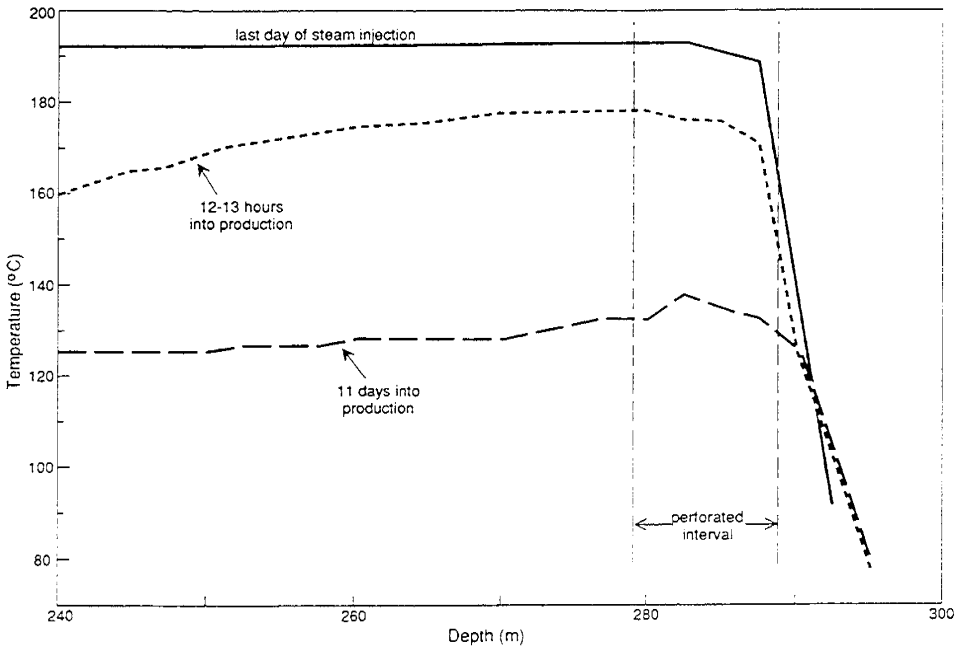

Figure 11. C13 temperature surveys during injection and production.

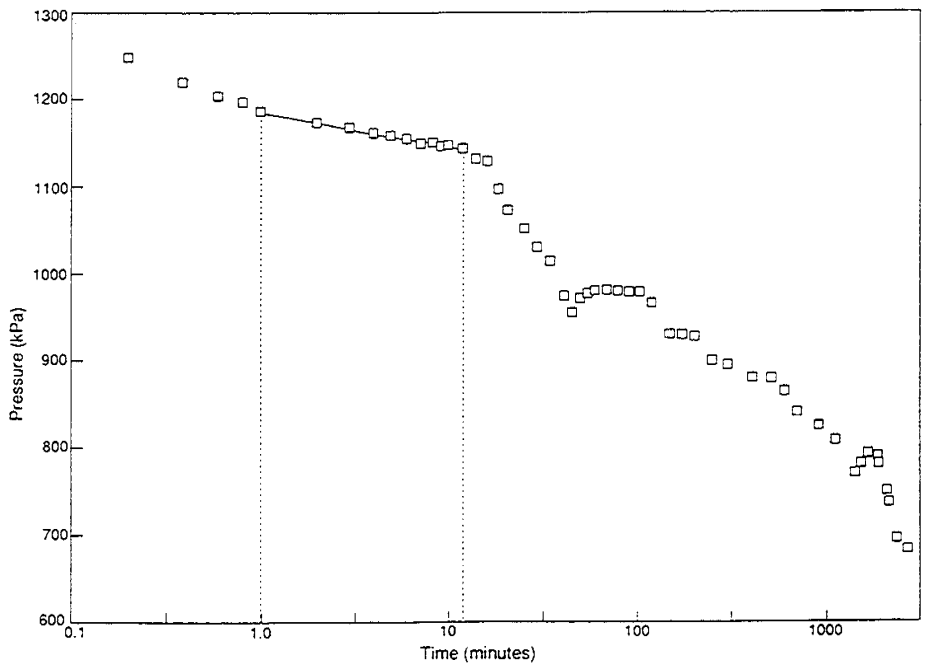

Figure 12. MDH plot of falloff test results for C13 Cycle 9.

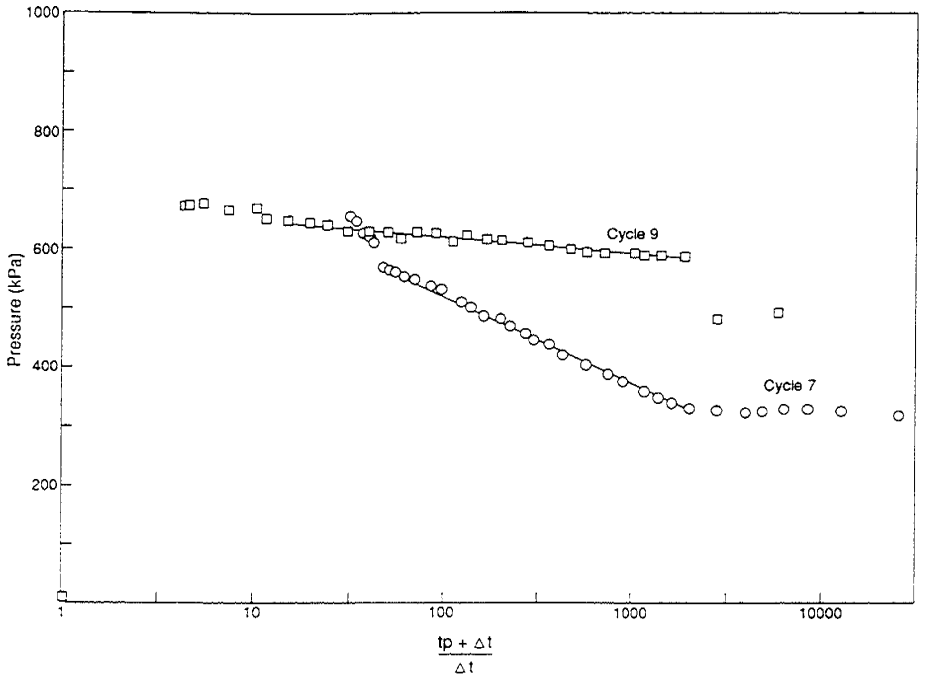

Figure 13. Horner plot of buildup test results for Cycles 7 and 9.

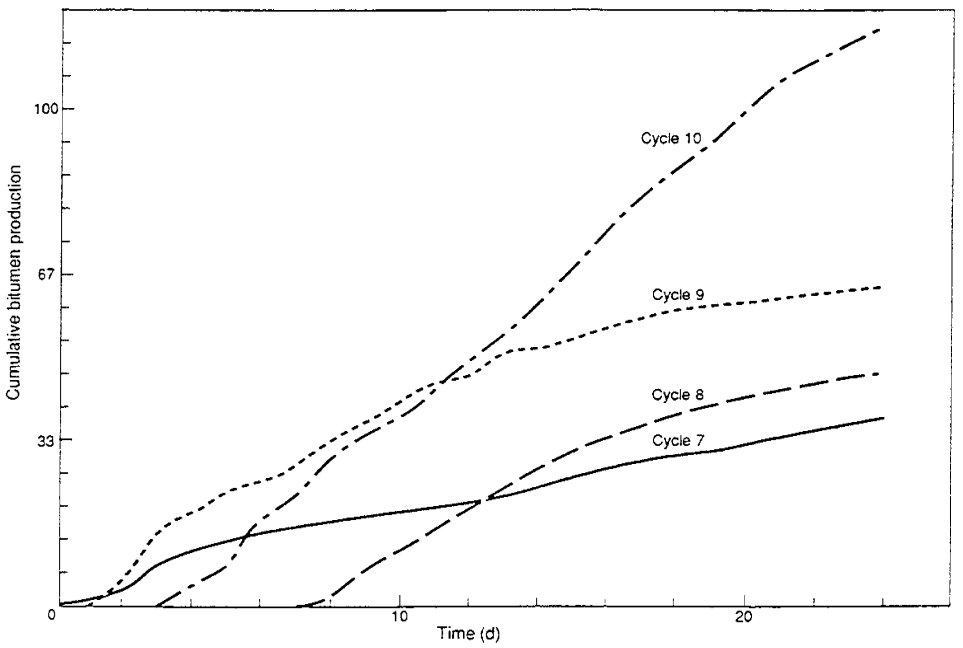

Figure 14. Cumulative bitumen production versus time for Cycles 7-10.

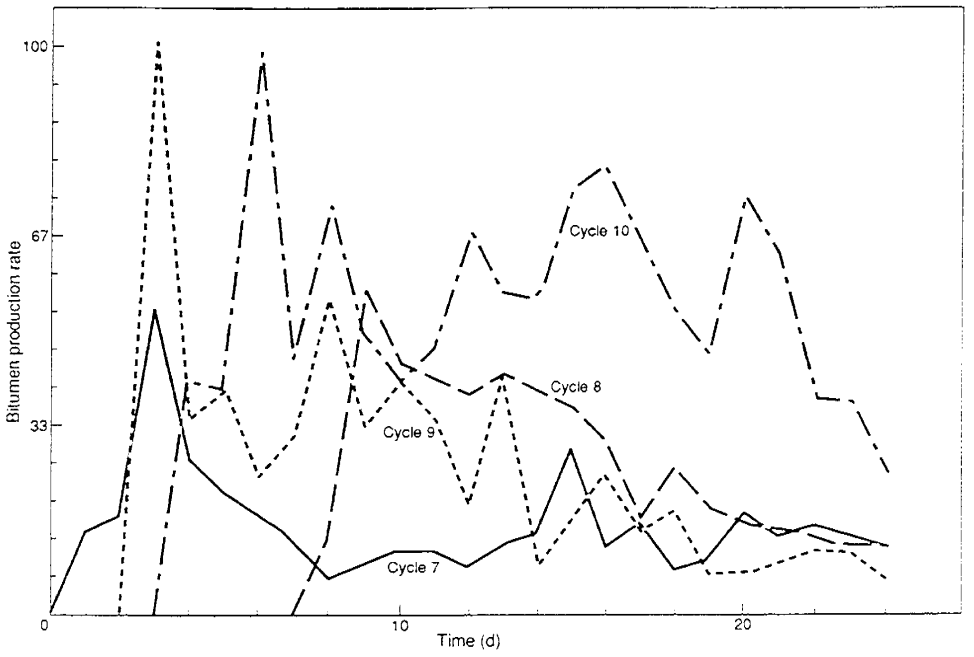

Figure 15. Bitumen production rate versus time for Cycles 7-10.

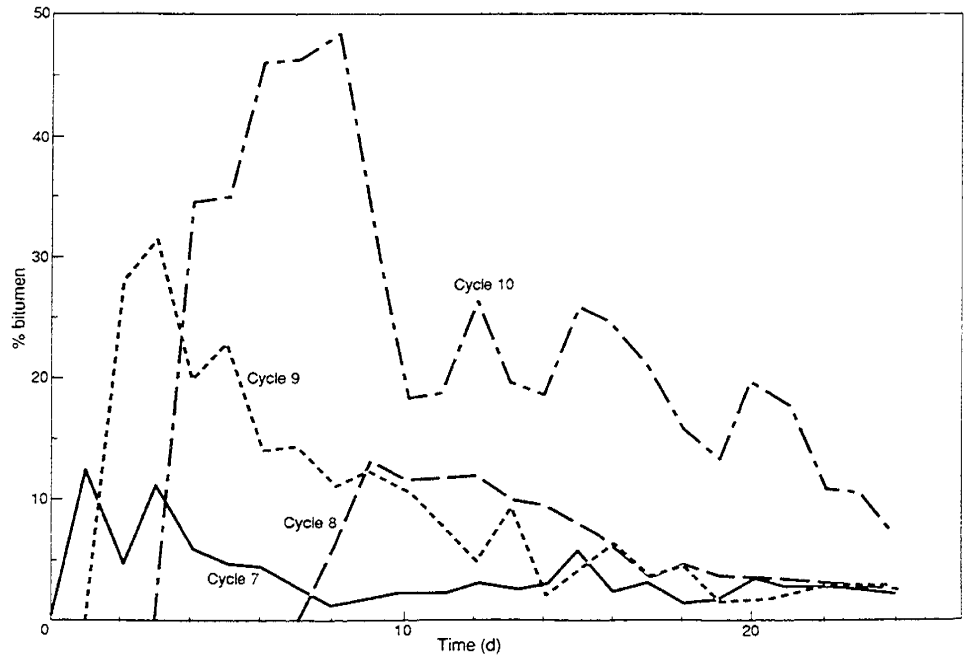

Figure 16. Bitumen in produced liquid versus time for Cycles 7-10.

Steam Foam Mechanistic Field Trial in the Midway-Sunset Field

by M. E. Smith, F. Friedmann and W. R. Guice,* Chevron Oil Field Research Company, La Habra, California, and J. M. Gump and D. G. Nelson, Chevron USA, Bakersfield, California

Originally presented as Society of Petroleum Engineers paper No. 21780 at the SPE Western Regional Meeting held in Long Beach, California, March 20-22, 1991. Copyrighted by Society of Petroleum Engineers, Inc., 1991.

This paper was prepared for presentation at the DOE/NIPER, Symposium on Field Application of Foams for Oil Production held in Bakersfield, California, February 11-12, 1993.

This paper was selected for presentation by a Program Committee following review of information contained in an abstract submitted by the author(s). Contents of the paper, as presented, have not been reviewed and are subject to correction by the author(s). The material, as presented, does not necessarily reflect any position of the U.S. Department of Energy or the National Institute for Petroleum and Energy Research.

ABSTRACT

A one pattern, steam-foam mechanistic field trial was conducted in Section 26C of the Midway-Sunset field (upper Monarch sand). The test objectives were: 1) to understand the mechanisms of steam diversion due to foam under reservoir conditions, 2) to establish if foam can exist in-depth away from the injection well, and 3) to measure incremental oil that can be attributed to foam.

Chevron Chaser™ SD1020 surfactant was continuously injected with steam and nitrogen for approximately 16 months. Bottomhole injection pressure increased from 100 psig to 300 psig, indicating good foam generation. Better steam distribution across the injector's perforations occurred when foam was generated. Improvements in both vertical and areal sweep efficiency of steam were observed.

Substantial temperature and gas saturation increases coincided with surfactant breakthrough and local reservoir pressure increases at observation wells located 42 ft from the injector. Complementary laboratory corefloods showed that foam generation could occur at low-pressure gradients,which are typical of in-depth conditions. Both laboratory and field data were interpreted as evidence that the presence of foam in-depth was due to local generation wherever surfactant, steam, and nitrogen were present, rather than the propagation of a foam bank generated near the injector. Some oil-production increase was also observed during the test. However, an accurate quantitative estimate of the incremental oil due to foam was difficult to establish.

*Now with Rendova Oil Company

References and illustrations at end of paper.

INTRODUCTION

Foam can be used to reduce injected gas mobility in both non-condensible gas and steam drives if early gas breakthrough occurs at producing wells due to either gravity override or viscous fingering. Mechanisms of gas mobility reduction with foam have been studied both theoretically and experimentally by various investigators. Specifically, events such as lamella generation,[1] coalescence,[2,3] and bubble trapping, which establish local foam texture and hence mobility, have been observed and understood in porous media under flow conditions. A critical pressure gradient, which must be exceeded for the onset of foam generation, has been measured in sandstone rocks.[4] Foam displacement experiments under radial conditions have suggested that an individual lamella cannot propagate a long distance in reservoir rocks.[5] These studies, although rigorous, are not sufficient to understand fully the impact of foam on gas mobility under reservoir conditions.

Foam technology has been field-tested by many operators with varying degrees of success. Many of these projects were conducted in steam drives to establish the impact of foam on both the steam-swept pore volume and on ultimate oil recovery.[6,7,8] In the most successful tests, surfactant was injected either continuously or semicontinuously with steam and nitrogen for at least a year to ensure in-depth penetration of the surfactant bank. In these cases, increases of the steam chest attributed to foam were observed using strategically located observation wells. However, neither direct evidence of an in-depth foam bank nor a mechanistic model of steam mobility reduction with foam could be inferred from these tests.

The amount of incremental oil due to foam varied widely between field tests, with a surfactant requirement from about 1 lb / incremental barrel in the most successful case[8] to

more than 10 lbs/incremental barrel in Shell's Kern River tests.[7]

In order to understand foam behavior under reservoir conditions better, Chevron has conducted a steam-foam mechanistic field trial in the Midway-Sunset field. The test's objectives were to establish whether and how foam propagated away from the injecting well, the impact of foam on the steam-swept pore volume, and whether any incremental oil was produced.

PREFOAM STUDY

Preparatory work was completed prior to foam injection. This included site selection to meet the test's objectives, geological study, drilling and completion of three observation wells, surface equipment design, acquisition of baseline temperature, gas saturation and oil production data, and surfactant selection in the laboratory.

Pattern Selection

A multidisciplinary team of engineers, development geologists, formation evaluation specialists, production engineers, and researchers determined the optimum pattern location and monitored pilot performance. All fields operated by Chevron USA in the San Joaquin Valley were considered. The following four qualitative criteria were used to select the location:

1. A minimum of reservoir heterogeneity to ensure that foam had a chance to alter steam paths in the reservoir and not be limited by permeability barriers or pinchouts.
2. The most bypassed oil reserves, ensuring that enough oil was still available for an incremental production response to occur if foam altered steam flow.
3. A steady producing baseline to prove that any production response was due to foam and not to some injection or facility change. In addition, it was felt that if injection and production parameters had been constant for a long time prior to the field trial, then reservoir conditions would also be more stable.
4. The lowest consistent steam quality to provide the highest water saturation near the injector for easy foam generation and propagation.

Section 26C (T32S.R23E M.D.B.M.) of the Midway-Sunset field was selected (Figure 1). Within Section 26C, the southern portion was selected because it had been on continuous steamdrive at a consistent generator quality of 40-50% for approximately five years.

Of all the patterns that were considered, the team determined that the 68BW pattern was the best for the following reasons:

1. Reservoir heterogeneity was least severe and most similar to a foam pilot that had been conducted previously.[9] More semicontinuous diatomite streaks were present in other patterns which might confine steam to specific channels. Oil desaturation in these channels may be significant.
2. Estimated remaining oil reserves were highest. Reserves had been at least partially replaced by gravity drainage into the pattern.
3. Even though 68BW's wellhead steam quality was higher than other patterns, it was still within acceptable ranges.
4. The 68BW production baseline was steadily declining, an indication of reservoir stability.

Geology

The main producing zone in the pilot area is the Miocene age Monarch Sand. It is an extremely heterogeneous sand-rich reservoir, ranging from silt to very coarse sands with pebbles and cobbles. Individual beds range from a few inches to a few feet and can show excellent fining sequences or massive deposition. Diatomite interbeds are usually less than one foot thick but do appear to be good barriers to steam on a localized basis. The structure in the area is controlled by an anticline and syncline whose axes trend northwest to southeast and plunge to the southeast.

The lower portion of the Monarch Sand is approximately 350 feet thick in the field trial area. This interval, between the G and H markers, is predominantly amalgamated beds of coarse-grained, massive sandstone and conglomerate. The interval between the H marker and the base of the Monarch consists of complexly interbedded coarse- to very fine-grained sandstone, conglomerate, siltstone, and mudstone. Figure 2 gives the correlation of the G and H markers and the base of the Monarch. However, more detailed bed to bed correlations are questionable. Even correlation of the H marker becomes difficult outside of this small area.

Figure 3 shows the perforated injection intervals for 68BW. The upper four perforated intervals are in the massive, coarse-grained interval. The lower nine perforated intervals are in the complexly interbedded interval.

Interwell Tracer Studies

Table 1 summarizes the results of the pre-foam, tritiated water tracer study, which was conducted from July 1987 to April 1988. Tritiated water partitions into both vapor and liquid and therefore, is an effective steam tracer.[10] Although the tritiated water tracer study showed most tracer was breaking through at 68F, an earlier interpretation of the tracer data suggested more tracer was breaking through at 68Z. Based on that interpretation, it was decided to drill OW1 between 68BW and 68Z to ensure the observation wells were located in a significant steam channel.

In May 1988, following the tritiated water tracer study, the steam vapor annular production rates from the casings of 58V, 68F, and 68Z into the casing collection system were measured. 68F showed about 40 bpd-cwe; 68Z about 32 bpd-cwe; and 58V had no flow. Because only flowline samples were obtained during the tritiated water tracer study, it is possible that the tritiated water associated with direct breakthrough of steam in layers containing continuous vapor phase steam was produced but not observed. Perhaps if the casing collection lines were sampled during the tracer study, earlier tracer breakthrough and greater tracer recoveries would have been observed.

As a supplement to the prefoam tritiated water-tracer study, a prefoam SF_6 tracer study was conducted in December 1988. SF_6 is a gas, detectable at concentrations as low as one part per trillion. [11] The results are summarized in Table 1. The SF_6 partitions only into the vapor phase, and results of the study indicated that direct vapor-phase steam breakthrough occurred in some wells. Backflow from the casing collection system gathering station to some cold wells may have

occurred and caused some erroneous results. However, it is likely that the one-day SF_6 breakthrough observed in the hot wells indicates one or more layers of direct vapor-phase communication.

Observation Wells

In 1988 three observation wells were directionally drilled in the 68BW pattern with bottomhole locations shown in Figure 4. The injection well, 68BW, is about 40 feet from the closest observation well, OW1, and 70 feet from observation well OW4. OW3 is a twin well to OW1, located the same distance from 68BW. OW1 was perforated and completed with a rod pump and pumping unit to allow periodic fluid sampling for detection of the surfactant front and to allow pressure monitoring. Fluids were sampled every two weeks. OW3 and OW4 were not perforated and were intended for temperature and neutron logging. Schlumberger's TDT-P log was run periodically in OW3 and OW4 to allow calculation of changes in steam vapor saturation based on change in Sigma response.

Well OW3 was cored, and routine core analysis completed on one-inch diameter plugs taken at one foot intervals. Seven steam zones appear in OW3 at depths shown in Figure 5. Steam zone 1 is 104 feet thick, and underlying zones are thin in comparison. This massive, coarse-grained interval has an average porosity of 25% and an average permeability of 1000 md. Oil saturations in the swept zone are less than 20%. Notice that the upper three perforated intervals from Figure 3 merge into a single swept zone due to the massive, coarse grained lithology.

The complexly interbedded interval reacted much differently to the effects of steamflooding. Steam zones 2, 3, 4, 6, and 7 are coincident with local high-permeability streaks, suggesting that permeability is an important control on steam occurrence. However, there is poor correlation between permeability and steam (as indicated by logs), between oil saturation and steam (as indicated by logs), and between permeability and oil saturation. Steam zone number 4 partly coincides with the highest permeabilities in the entire well. This zone correlates to steam in OW1, OW4, 68Z, 68F, and 58V and also to maximum temperatures in 68F and 68Z. Zone 4, therefore, appears to be a high-permeability streak that exerts a major influence on steam pathways in the 68BW pattern. A zone at 1522-1520 ft is the second-most permeable reservoir unit in OW3, but it is neither occupied by steam nor effectively depleted. This is a classic example of bypassed or uncontacted oil due to inappropriate perforation depths in injector 68BW, to reservoir characteristics, or to steam override.

Baseline Data

Efforts to identify baseline reservoir and producing trends and characterize the reservoir consisted of four projects: base logging, a tritiated water tracer survey, analyses of producing trends, and development of structural cross sections.

Nuclear, contact temperature, injection fluid exit, and gyro surveys were run in pattern wells 58F, 58K, 58V, 68B, 68BW, 68C, 68F, 68G, 68J, 68Z, OW1,and OW3 in cased or open hole as appropriate. Cross sections, such as that shown in Figure 2, were developed to evaluate the continuity of major facies from well to well within the pilot area.

Surfactant Selection

Two Chevron Chemical surfactants, Chaser™ SD1000 and Chaser™ SD1020, were tested in the laboratory as candidates for the field trial. Specifically, the minimum pressure gradient for the onset of foam generation was measured in both 1-ft long Berea sandstone (k=1d) and Well OW3 cores. A schematic of the experimental equipment is given elsewhere.[12] These experiments were conducted by coinjecting brine (with or without surfactant) and nitrogen at a constant liquid volume fraction (0.05), while controlling a constant pressure drop across the core. By comparing flow rates of the base flood (no surfactant in the brine) with the foam flood for the same pressure drop, a Mobility Reduction Factor (MRF) can be calculated. Strong foam generation is arbitrarily chosen to occur when MRF is greater than 10. The corresponding pressure gradient is the critical pressure gradient for the onset of foam generation $(\nabla P)_c$. Figure 6 shows the effect of pressure gradient on MRF for 0.3% solutions of both surfactants at 330 °F in Berea sandstone. Foam generation occurs at substantially lower pressure gradients with Chaser™ SD1020 than with Chaser™ SD1000 (1 vs. 30 psi/ft).

Table 2 lists the prefoam average pressure gradients between injector well 68BW and observation wells OW3 and OW4. These were based on the temperatures at the wells assuming the steam was at saturation pressure. Clearly, in-depth foam generation can only occur if Chaser™ SD1020 is used. It was, therefore, selected for the field test. Figure 7 gives the effect of Chaser™ SD1020 concentration on $(\nabla P)_c$. A target concentration of 0.3% was selected for the test. Finally, $(\nabla P)_c$ was measured for a sequence of well OW3 cores of increasing permeability (Figure 8). The critical pressure gradient for the onset of foam generation increases sharply as permeability decreases. In the field, foam should generate easier in the higher permeability strata that have been preferentially swept by steam.

SURFACE EQUIPMENT

Figure 9 is a schematic of the surface equipment for the foam pilot. Steam is obtained from the 26C cogeneration plant. A fixed orifice choke at the well controls the steam injection rate. Thermocouples upstream and downstream of the choke are used to determine steam temperature drop across the choke (and hence pressure drop), and the injection rate is then estimated via the Thornhill-Craver equation. The surface line at the 68BW wellhead was modified for addition of surfactant, nitrogen, and make-up water. Additionally, fittings were added for periodic connection of a portable test separator to accurately measure steam quality and rate.

Water was added to the injected steam to increase the liquid volume fraction for improved foam generation. An electrically powered positive displacement pump was set to deliver approximately 40 BWPD.

Surfactant was injected with a positive displacement pump with a maximum output capacity of 35 gph at 1000 psi. Initially, the pressure increase due to foam was too large and resulted in significant reduction of the steam injection rate. Consequently, pressure sensors were installed to stop the surfactant injection pump automatically if the wellhead

pressure increased above 500 psi or the pressure upstream of the choke decreased drastically due to interruptions at the cogeneration plant. The surfactant pump automatically restarted when the pressure dropped below 450 psi. The total cycle length was approximately three minutes with a surfactant on-time of approximately two minutes.

Surfactant was stored in a polyethylene tank. A circulating pump and inline heater were used to keep the surfactant mixed at 110 °F and prevent buildup of viscosity. Bulk trucks delivered 5000-gallon loads directly to the tank to refill as required.

Nitrogen was provided by a membrane extraction unit that separated nitrogen from air. Resulting oxygen levels within the injection stream were reduced to less than 1%. The unit included a compressor, mass flowmeter, and a run time clock. The nitrogen was injected through a flow regulator, which was set to maintain a rate of approximately 30 SCFM. The nitrogen plant injected continuously and did not stop or start in response to pressure changes at the injection line sensors. It was electrically powered and had little down time.

Capillary tubing run to 1445 feet through the tubing in 68BW and to 1500 feet in the annulus of OW1 allowed measurements of bottomhole pressures. Four transducers, including one on each capillary tubing string and one on each of the casings, were attached to a digital data logger that recorded pressures at programmed intervals.

FOAM INJECTION RESULTS

Injector Response

Continuous foam injection commenced into 68BW on May 15, 1989. Originally, 35 gallons per hour of Chaser™ SD1020, mixed with 30 SCFM of Nitrogen, were injected. Figure 10 shows the initial injection pressure response to foam injection. Bottomhole pressure increased from approximately 100 psig to 255 psig within 75 hours. Surface pressure rose from 250 psig to 470 psig during the same time interval. Later, the surface pressure increased, eliminating critical flow through the surface choke. Therefore, it was decided to cycle the surfactant injection, based on surface injection pressure as discussed earlier. Thereafter, surfactant injection averaged .27 weight % of the steam liquid phase.

Figure 11 shows the bottomhole pressure response during the foam trial. During steam and foam injection, bottomhole pressure averaged approximately 300 psig, compared to 100 psig without foam. The fluctuation in bottomhole pressure was caused by instabilities in the steam generation facilities. In addition, the well was shut in October 1989, March 1990, and October 1990 to replace the injection packer.

A series of injection profile surveys were conducted using krypton gas and sodium iodide (NaI) as vapor and liquid tracers, respectively, after four months of foam injection. Figure 12 is a plot of the injection profile in 68BW before, during, and after foam injection. Steam did not enter the upper and lower intervals prior to foam injection. During foam injection, the profile was much more uniform. We conducted a test of the longevity of profile improvement. The foam injection was shut off for three days, at which time another profile survey was run. Figure 12 shows that the profile regressed rapidly toward its prefoam shape indicating that foam was washed away by steam near the injector.

Foam injection was shut off on November 6, 1990. A total of 115,000 pounds of active surfactant was injected during the test. The nitrogen injection was shut in on November 10, 1990.

Observation Well Response

Temperature and gas saturation started to increase in well OW3 by the beginning of August 1989 (Figure13), well before surfactant breakthrough at well OW1. A large incremental increase in temperature occurred by early January 1990 (Figure 13A) coinciding with surfactant breakthrough (Table 3) and a sharp increase in reservoir pressure in well OW1. An increase in the steam saturation also occurred at that time, based on TDT-P log (Figure 13B). This indicated that a foam front had reached the well. The TDT-P logs show substantial improvement in the vertical sweep (Figure 13B) with the steam zone growing downward with time. Since then, additional temperature increases were observed toward the top (1350 ft.) and the bottom of the sand (1460-1480 ft.) while temperature stayed constant in the remaining sand lobes (Figure 13A).

Changes in the temperature profile of well OW4 (70 ft away from the injector) started by early spring 1990. A sharp increase in temperature was observed in May 1990 between 1360 and 1460 ft., which intensified in June 1990 (Figure 14A). This indicated that a foam front was progressing from OW3 towards OW4. No additional changes in the temperature profile were measured in July 1990. Since no surfactant sampling well was coupled with well OW4, surfactant concentration history was not obtained at that location. However, modelling of surfactant propagation rate, based on laboratory measurement of adsorptive losses on well OW3 cores, predicted breakthrough to occur by the end of August 1990. In all probability, the foam front had reached its maximum penetration somewhere between OW3 and OW4. Improvement in the vertical sweep by steam was also observed based on the TDT-P logs for this well (Figure 14B).

Production Response

The producers in the 68BW pattern were averaging 350 BOPD (unallocated production) prior to foam injection. During the period of foam injection the pattern producers averaged 422 BOPD (Figure 15). The production changes during the foam trial were assessed on an individual well basis in order to quantify the amount of incremental oil.

The ten 68BW pattern producers were reviewed for changes in operational characteristics in order to find any evidence of incremental oil production. These characteristics consisted of oil rate, water rate, steam (casing effluent) rate, and flowline temperature. Any oil production increases attributable to well pulling operations were not considered incremental. The results of the review showed that three of the ten wells produced incremental oil as a result of foam injection; five wells remained unchanged; and two wells had oil production increases resulting from normal well pulling operations.

Wells 68A, 68B, 68C, 68G, and 68Z showed no significant change in oil production that could be attributed to foam

injection. It should be noted that well 68Z did show a decrease in overall produced heat (produced heat = BTU_{oil} + BTU_{water} + $BTU_{produced\ steam}$) during foam injection. This decrease in heat production is attributed to the diversion of steam from the existing steam channel.

Wells 58F (Figure 16) and 58K showed oil production increases during foam injection, but these increases are thought to be the result of pump changes and liner jet washes. Therefore, these wells were not used to estimate the volume of incremental oil associated with foam injection.

Wells 58V, 68D and 68F (Figures 17-19) demonstrated oil production increases that were independent of well pulling. Wells 58V and 68D are located in infill positions, and both wells exhibited significant increases in flowline temperature and gross fluid production during foam injection. These increases are thought to be the result of improved areal steam distribution in the pattern. The foam injection appears to have diverted the steam from wells 68F and 68Z towards wells 68D and 58V.

Well 68F benefitted from foam injection in a manner different from wells 58V and 68D. Prior to foam injection, well 68F was producing approximately 40 BPD of 100% quality steam into the casing collection system. This high annular steam rate created a back pressure between 10 and 20 psi on the casing. During foam injection, the annular steam flow rate in well 68F decreased to less than 5 BPD of steam, the casing pressure decreased to below 5 psi, and the total heat production decreased substantially (Figure 20). The increase in oil production in well 68F can be attributed to two changes: the decrease in casing back pressure and the improved vertical sweep in the steam channel.

During foam injection, wells 58V, 68D, and 68F combined to produce 27,300 barrels of incremental oil. Improved vertical and areal steam distribution in the 68BW pattern generated this volume of incremental oil, which was calculated using the average production for each well one year prior to foam injection as the baseline. Exponential declines, six-month production averages, and two-year production averages were also considered as baselines. The one-year production interval yielded the most conservative estimation of incremental oil. This one-year interval also represents the period of least operation change in the surrounding patterns.

MECHANISMS OF FOAM PROPAGATION

Wells OW3 and OW4 data clearly indicated that foam was present more than 42 ft. from well 68BW. Both field and laboratory data must be used to explain the existence of foam indepth.

Foam propagation cannot be visually observed in naturally occurring porous media. This can be explained by using laboratory data to complement the observation well data. Consequently, several plausible pictures of foam propagation have emerged. Two of these are moving-lamellae and in-situ regeneration. In the former, foam lamellae generated in the high-pressure gradient zone near the injector may move from pore to pore over large distances without breaking. In the latter, lamellae break shortly after generation if they move, but new lamellae can be regenerated as long as surfactant and gas are present and the local pressure gradient exceeds the critical gradient for foam generation. In this case, the foam front would propagate at the same rate as the surfactant front.

Foam creation and bubble transport were investigated in a cone-shaped Ottawa sandpack with a ratio of injection-face to exit-face diameter of 1.25:5.00 (Figure 21). Such a system mimics radial flow conditions encountered in the reservoir; the frontal advance rate is monotonically decreasing as the diameter is increasing along the core. Nitrogen and brine with or without 0.3 wt.% Chaser™ SD1020 were injected into the pack at a constant frontal advance rate of 250 cm/min, which is representative of a steam injection well. The injected liquid volume fraction was kept constant at a value (0.013) that simulated well 68BW.

Figure 21 gives a history of MRF measured in six zones along the pack. Under such flow conditions, foam generated at the injector (region of highest rates) started to deteriorate in zone 5 and did not propagate into the exit zone (Figure 21) by the moving-lamellae mechanism. Since in-depth generation did not occur in zone 6 conditions, a foam bank could not exist in the outer region of the core.

Based on these laboratory results, it is unlikely that lamella propagation could occur over large distances under reservoir conditions. The sharp temperature and gas saturation increases at well OW3 in January 1990, which coincided with surfactant breakthrough and reservoir pressure increases, indicated that foam lamellae were generated in-situ. Moreover, the local pressure gradient (Table 2) was about the critical pressure gradient for foam generation with Chaser™ SD1020 (Figure 6). It is likely that the local reservoir pressure gradient decreased below $(\nabla P)_c$ somewhere between wells OW3 and OW4. Therefore, foam could not propagate beyond this point while surfactant transport continued.

POSTFOAM BEHAVIOR

Steam delivery problems followed by mechanical problems in the injector occurred during August and part of September 1990, resulting in partial cooling at wells OW3 and OW4. Surfactant injection was terminated on November 6, 1990, while nitrogen injection continued until November 10, 1990.

Bottomhole injection pressure decreased rapidly from 300 psig to about 200 psig and then gradually toward the prefoam base value of 100 psig (Figure 22). The surfactant was rapidly washed away in the zones that were preferentially swept by steam prior to foam (between 1400 ft. and 1500 ft., Figure 12), resulting in the initial pressure decline. The second slower decline was due to a gradual dilution of the surfactant in the other zones where foam occurred. The sharp pressure decline (20 psig) after discontinuing N_2 injection (Figure 22) could indicate that a noncondensible gas enhanced foam stability.

Well 68BW was shut in for three weeks in October 1990 due to a packer failure. Reservoir temperature decreased somewhat due to this long interruption in steam injection. This explains the lower temperatures in well OW3 (Figure 23, 11/5/90 profile) compared to previous profiles (Figure 13A). However, one month after discontinuing foam injection, no further substantial decrease in well OW3 temperature profile was observed. The injected liquid steam phase had not yet sufficiently diluted the surfactant slug ahead of it to break the foam at well OW3 (Figure 23). Temperature profiles are still taken once a month at wells OW3 and OW4. Eventually, dilution of the surfactant occupied pore volume with the injected steam should result in foam collapse.

CONCLUSIONS

A field trial was conducted to understand the mechanisms of steam diversion due to foam in steam drives. The following conclusions can be drawn:

1. Foam was generated near the injection well, resulting in a substantial injection pressure increase and a more even steam distribution across the injector's perforations. However, these effects dissipated rapidly after discontinuing surfactant injection.
2. Foam was generated in-depth resulting in the presence of a foam front more than 40 ft. away from the injector. The foam front moved at the same rate as the surfactant front.
3. Substantial improvements in both the vertical and areal sweep of the reservoir with steam were observed, which can be directly attributed to the presence of foam indepth.
4. About 27,000 barrels of incremental oil has been produced at this time. Most of the response occurred in producers that were offset from the main steam channel prior to the test.

ACKNOWLEDGEMENTS

The authors would like to recognize the contributions of the multidisciplinary team, especially the efforts of Henry Duran, Tom Kelly, Don Shay, Dave White, and Nick Zana, without whose help this project could not be completed. We also thank Chevron Oil Field Research Company and Chevron USA for the opportunity to publish the results of this project.

REFERENCES

1. Ransohoff, T. C., and Radke, C .J., "Mechanisms of Foam Generation in Glass Bead Packs," SPERE (May 1988) 573-585.
2. Kathib, Z. I., Hirasaki, G. J., and Falls, A. H.,"Effects of Capillary Pressure on Coalescence and Phase Mobilities in Foams Flowing in Porous Media," paper SPE 15442 presented at the 1986 SPE Annual Technical Conference, New Orleans, Oct.5-8, 1986.
3. Gauglitz, P. A., "Coalescence during Division: A Mechanism of Lamella Rupture in Porous Media," Paper 164G presented at AICHE 1990 Annual Meeting, Chicago, Ill., Nov. 11-16, 1990.
4. Rossen, W. R., and Gauglitz, P. A., "Percolation Theory of Creation and Mobilization of Foams in Porous Media," AICHEJ., Vol 36, 8, (1990), 1176-1188.
5. Gauglitz, P. A., Private Communication.
6. Mohammadi, S. S., Slyke, D. C., and Ganong, B., "Steam-Foam Project in Dome-Tumbador, Midway-Sunset Field," SPERE, (February 1989), 7-16.
7. Patzek, T. W., and Koinis, M. T., "Kern River Steam Foam Pilots," JPT, (April 1990), 1137-1146.
8. Djabbarah, N. F., Weber, S. L., and Freeman, D. C., "Laboratory Design and Field Demonstration of Steam Diversion with Foam," SPE 20067 Presented at the 1990 SPE California Regional Meeting, Ventura, CA, April 4-6,1990.
9. Ploeg, J. F. and Duerksen, J. H., "Two Successful Steam-Foam Field Tests, Sections 15A and 26C, Midway-Sunset Field," SPE 13609 presented at the 1985 SPE California Regional Meeting, Bakersfield, CA, March 27-29, 1985.
10. Wagner, O. R., "The Use of Tracers in Diagnosing Interwell Reservoir Heterogeneities - Field Results," JPT (November 1977) 1410-1416.
11. Tang, J. S., and Harker, B. C., "Interwell Tracer Test to Determine Residual Oil Saturation in a Gas-Saturated Reservoir Part II: Field Application," paper CIM/SPE 90-130 presented at the International Technical Meeting jointly hosted by Petroleum Society of CIM and the SPE, Calgary, June 10-13, 1990.
12. Friedmann, F., Chen, W. H., and Gauglitz, P. A., "Experimental and Simulation Study of High-Temperature Foam Displacement in Porous Media," to be published in SPERE, (February 1991).

Table 1
Comparison of Prefoam Tracer Studies

Well	Tracer Breakthrough Time: Tritiated H_2O	Tracer Breakthrough Time: SF_6	Tracer Response: Total Tritiated H_2O Produced*	Tracer Response: SF_6 Concentration at Day 4, ppb	Flowline Temperature (°F)
58F	NA	NA	NA	0	188
58K	NA	<3 days	NA	0.55	165
58V	80 days	<1 day	0.4%	2.6	152
68A	NA	<1 day	NA	62.4	236
68B	60 days	<1 day	0.7%	39.7	210
68C	NA	NA	NA	9.3	206
68D	NA	NA	NA	14.3	117
68F	30 days	<1 day	19.4%	96.6	238
68G	NA	NA	NA	3.6	154
68Z	30 days	<1 day	2.5%	29.6	212

* Percent of injected amount through April 1988

Table 2
Average Prefoam Pressure Gradients at 1400 Feet
Between Wells 68BW, OW3, and OW4

Wells	Pressure Gradient, psi/ft
68BW - OW3	0.9
OW3 - OW4	0.3

Table 3
Well OW1 Surfactant and Pressure Responses

Date	Surfactant Concentration, ppm	Pressure, psi
6/8/89	3	69
8/9/89	7	72
9/20/89	4	-
11/15/89	20	68
1/5/90	1100	89
2/8/90	2200	92
4/24/90	2392	90
5/23/90	3307	-
8/22/90	2670	92

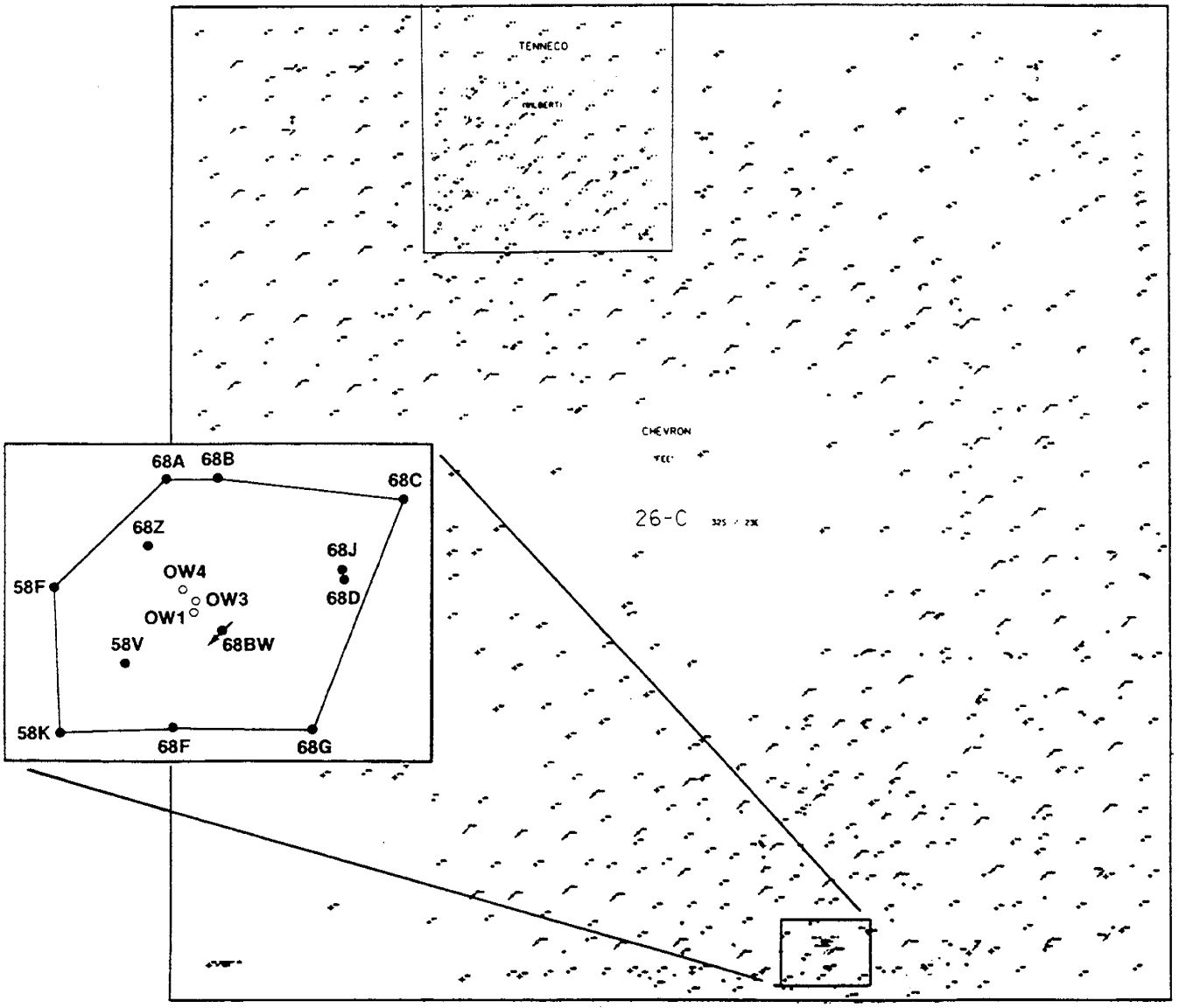

Figure 1

Section 26C, Midway-Sunset Field

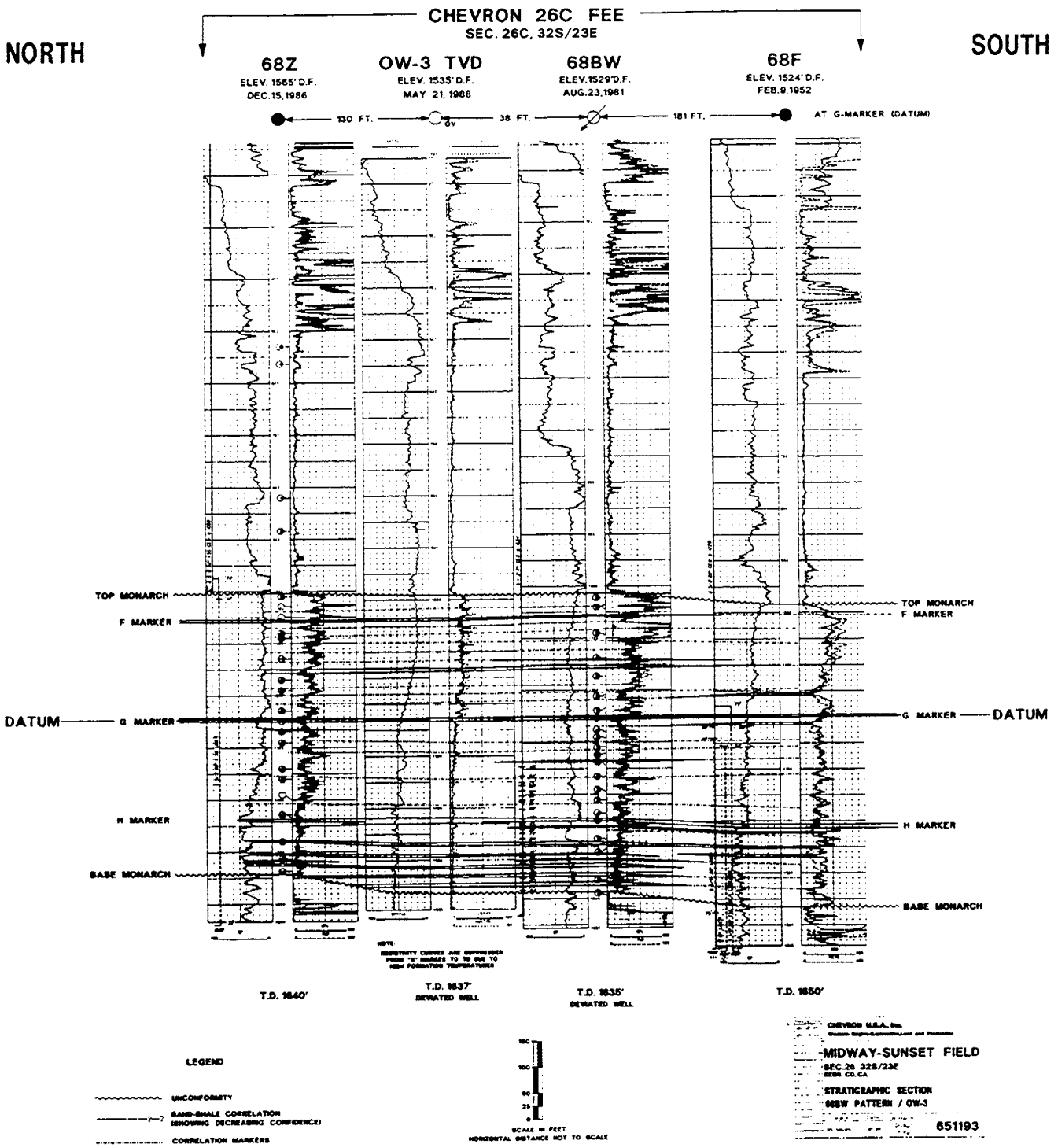

Figure 2

Cross-Section Through Pilot Area

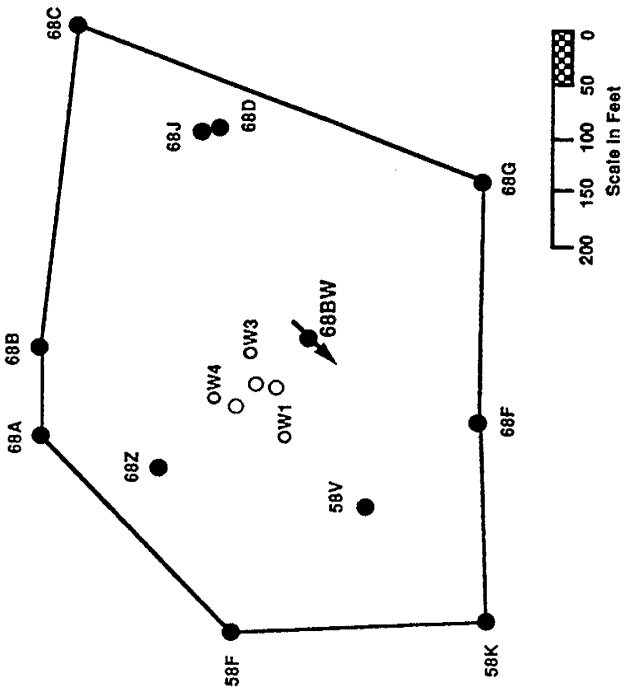

Figure 4
Pilot Pattern Well Bottomhole Locations

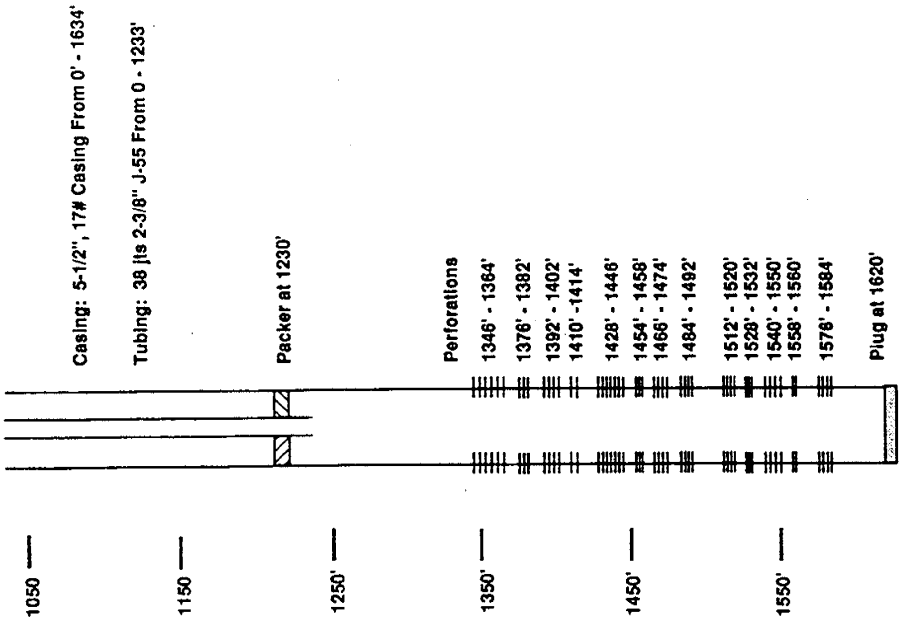

Figure 3
Well 68BW Wellbore Schematic

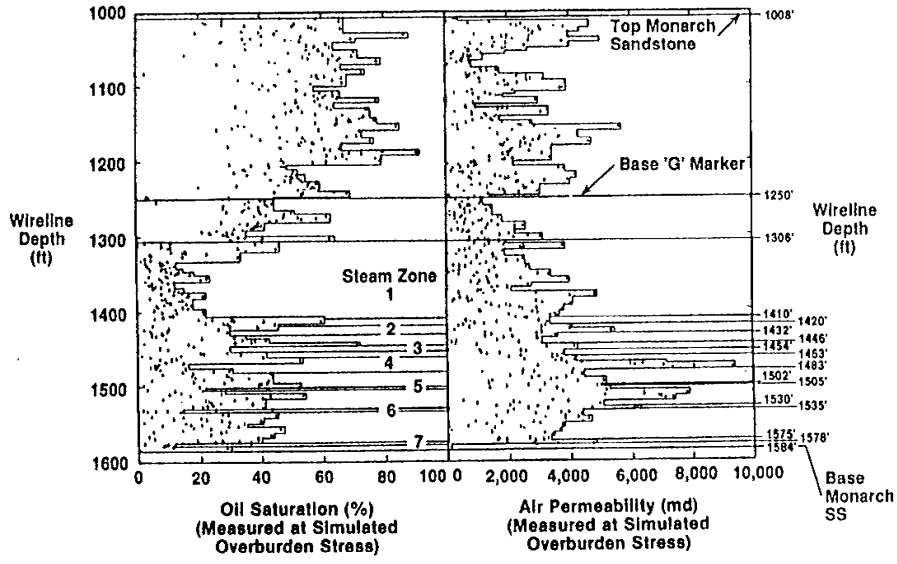

Figure 5

OW3 Core Analysis Showing Steam Zones

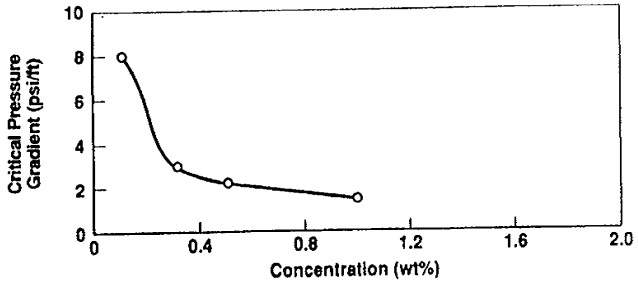

Figure 7

Effect of Surfactant Concentration on $(\nabla P)_c$ for Chaser SD 1020 in Berea Sandstone

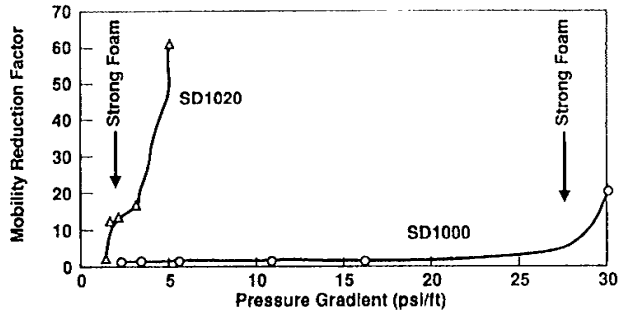

Figure 6

Experimental Determination of $(\nabla P)_c$ in Berea Sandstone Cores for Both Chaser SD 1000 and Chaser SD 1020 Surfactants

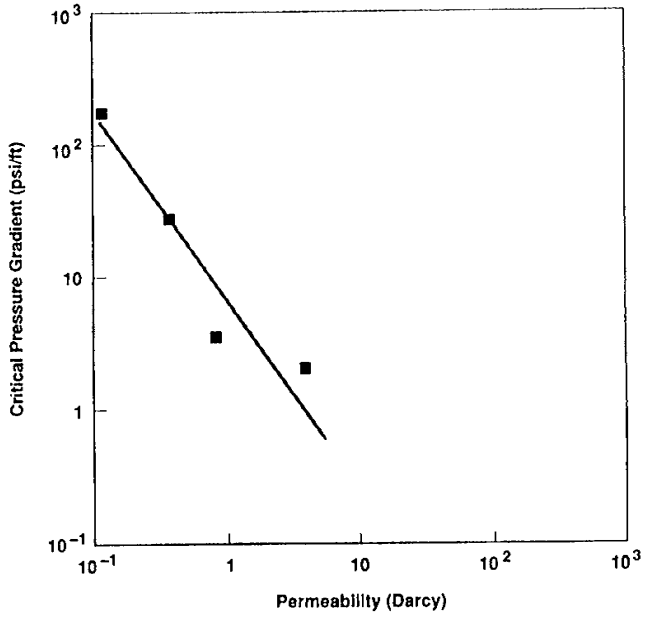

Figure 8

Effect of Rock Permeability (Well OW3 Cores) on $(\nabla P)_c$ for Chaser SD 1020

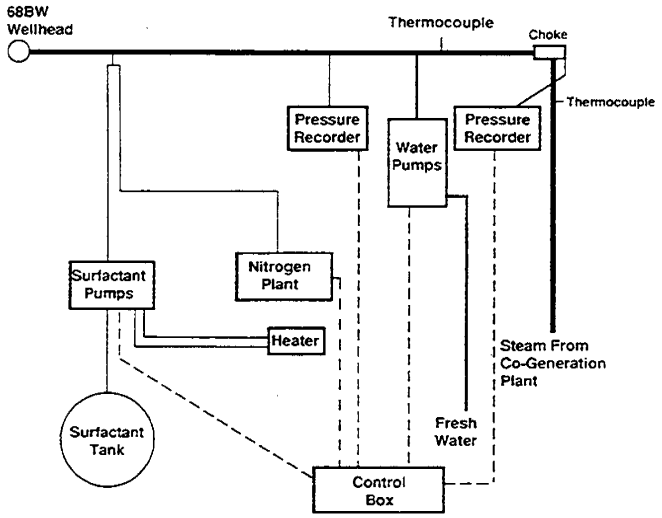

Figure 9

Foam Injection Surface Facilities

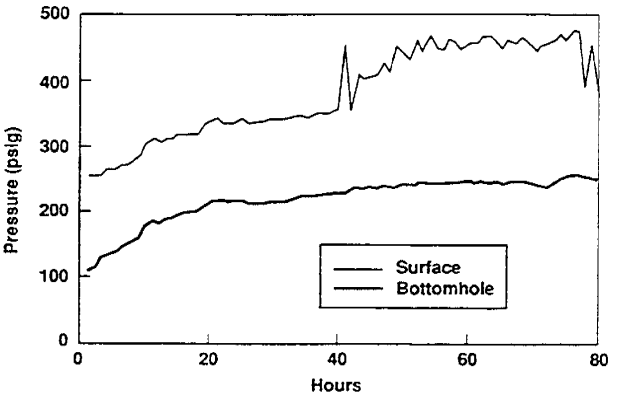

Figure 10

Initial Pressure Response to Foam Injection

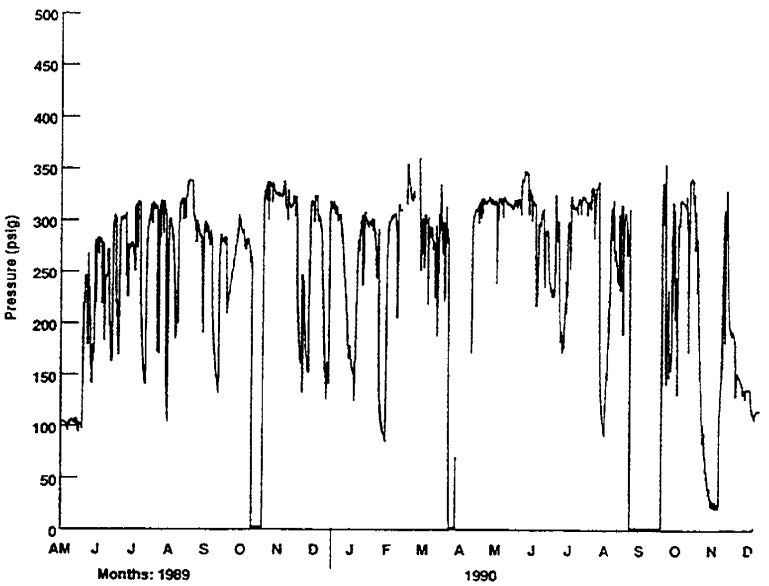

Figure 11

Overall Pressure Response to Foam Injection

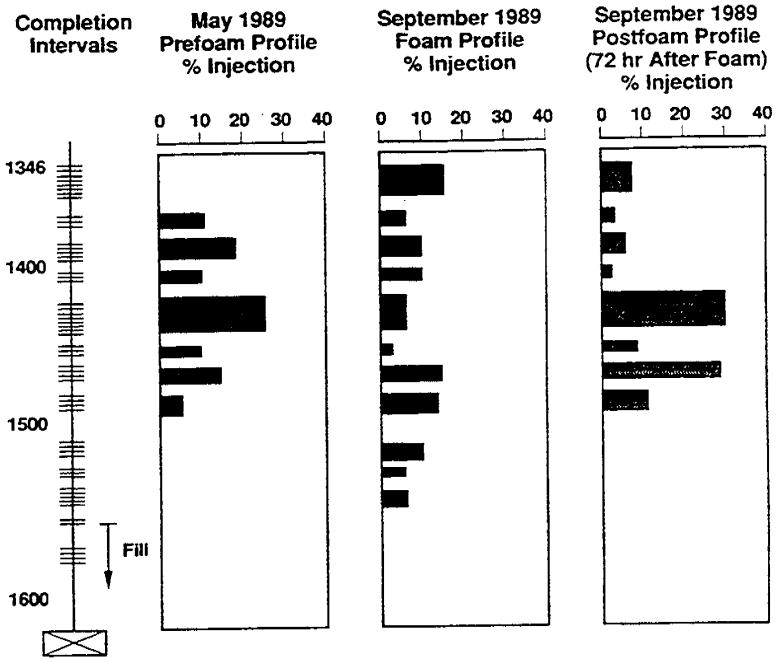

Figure 12

Changes in Steam Injection Profiles Due to Foam in Well 68BW, Midway Sunset Section 26C

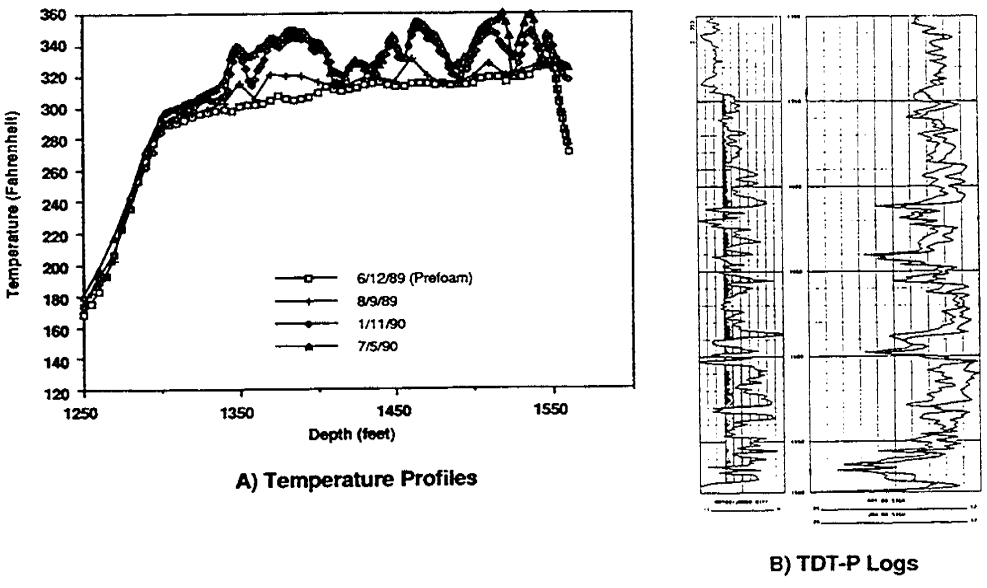

A) Temperature Profiles

B) TDT-P Logs

Figure 13

Changes in Temperature and Steam Saturation in Observation Well OW3, Midway Sunset Section 26C

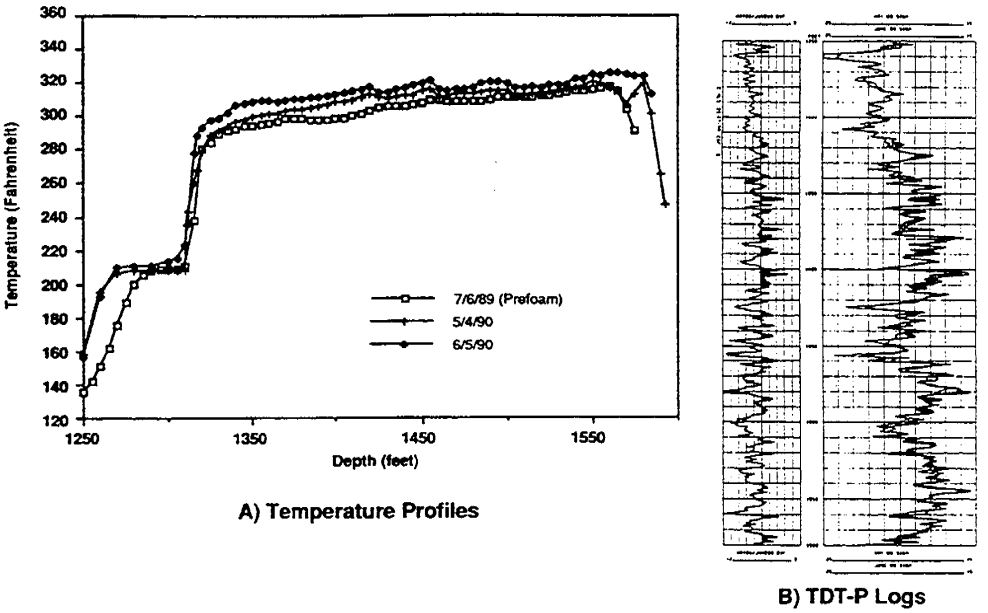

Figure 14

Changes in Temperature and Steam Saturation in Observation Well OW4, Midway Sunset Section 26C

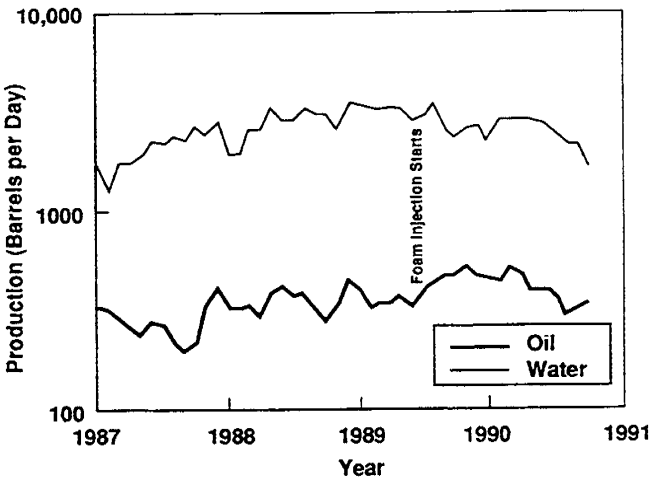

Figure 15

Total Pattern Production Response

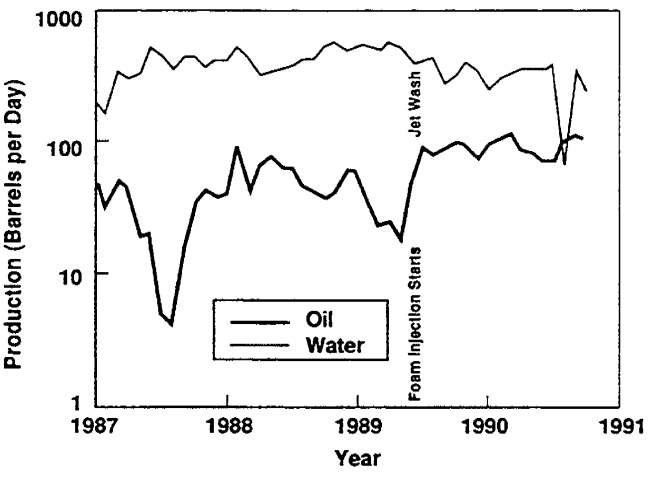

Figure 16

Well 58F Production Response to Wellwork

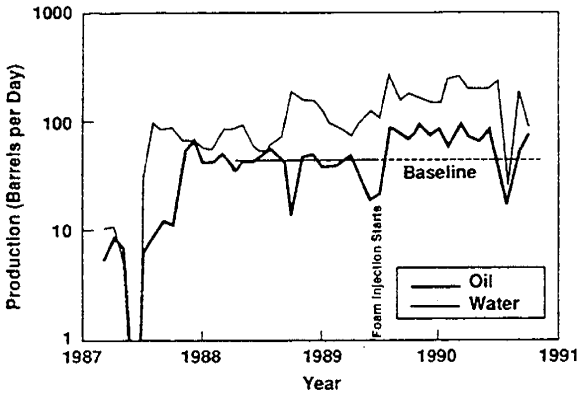

Figure 17

Well 58V Production Response to Foam Injection

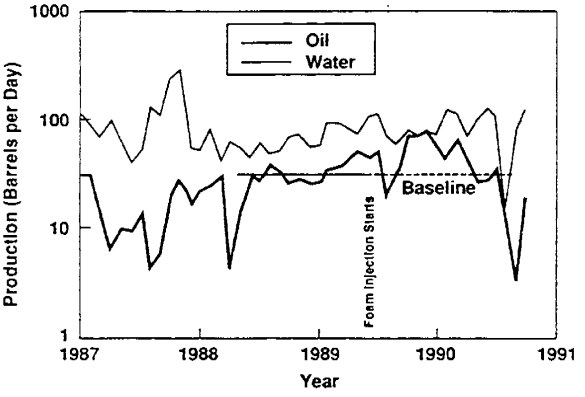

Figure 18

Well 68D Response to Foam Injection

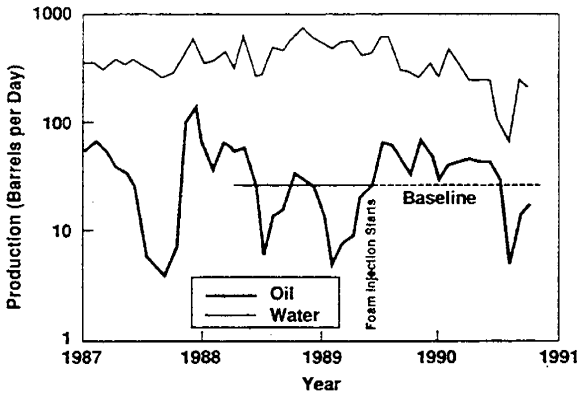

Figure 19

Well 68F Response to Foam Injection

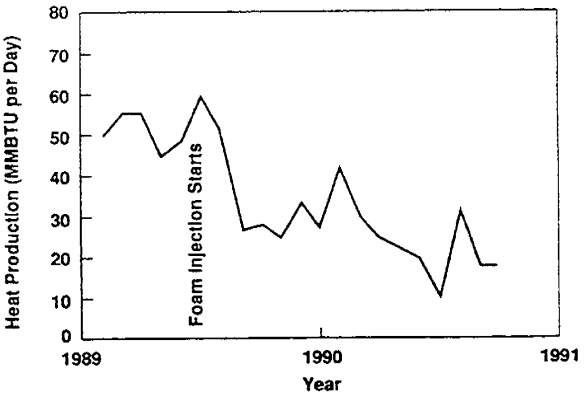

Figure 20

Well 68F Heat Production Response to Foam Injection

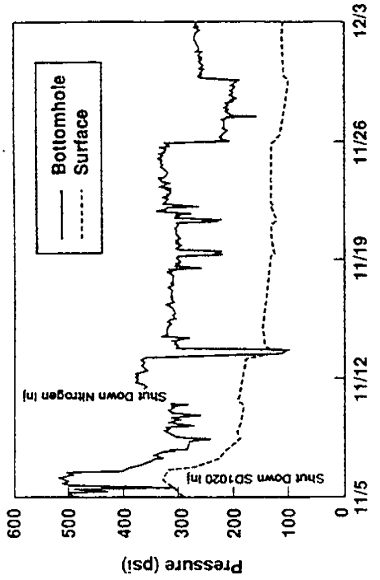

Figure 22

Injection Pressure After Discontinuing Foam Injection

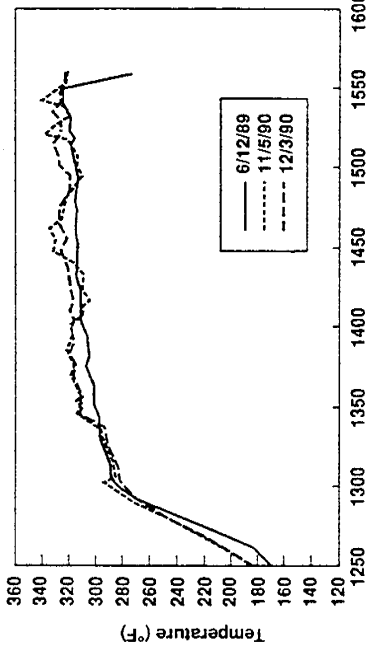

Figure 23

Well OW3 Temperature Profiles: Prefoam, End-of-Foam, Post-Foam

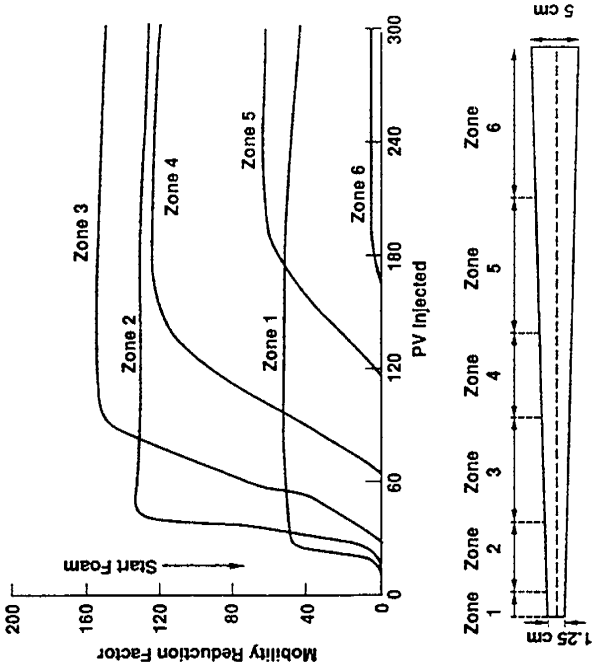

Figure 21

Foam Propagation Experiment in Cone-Shaped Ottawa Sandpack (60-140 Mesh) Using Chaser SD 1020 Surfactant

Key Factors Influencing the Success of Steam Foam Applications

by V. T. Hoang and E. A. Waninger, Chevron Chemical Company, San Ramon, California

Author(s) are solely responsible for copyright and contents.

This paper was prepared for presentation at the DOE/NIPER, Symposium on Field Application of Foams for Oil Production held in Bakersfield, California, February 11-12, 1993.

This paper was selected for presentation by a Program Committee following review of information contained in an abstract submitted by the author(s). Contents of the paper, as presented, have not been reviewed and are subject to correction by the author(s). The material, as presented, does not necessarily reflect any position of the U.S. Department of Energy or the National Institute for Petroleum and Energy Research.

Abstract

This paper discusses screening criteria which can be used to maximize the technical and economic success of steam foam applications. These screening criteria are based on laboratory work and published field tests. The screening process includes 1) evaluating pertinent reservoir and well data to select proper candidates and 2) performing laboratory tests to select a suitable surfactant. The discussion addresses the two most common uses of foam, injection profile improvement and in-depth mobility control. The paper also discusses some options for optimizing foam applications.

Introduction

In recent years, foam has been applied effectively to improve the sweep efficiency of projects experiencing gravity override or steam channeling[1-4]. These successful projects are the results of better understanding the foam process, improved application techniques, and developments in surfactant formulations.

References and illustrations at end of paper.

In most field applications, sweep improvement was achieved by either propagating foam in-depth or by modifying the injection profile. Correcting the injection profile with near wellbore foam generation will improve the vertical sweep in a multi-zone reservoir with little or no vertical communication. To improve the sweep efficiency in reservoirs having gravity override or steam channeling with crossflow, in-depth foam propagation is required[1]. Modifying the injection profile in this case is usually not sufficient for reservoir sweep improvement because vertical communication allows steam to redistribute in the reservoir. In-depth mobility control can also increase the sweep efficiency in reservoirs experiencing uneven areal heat distribution or early steam breakthrough due to preferential flow.

Effective application of foam depends strongly on the understanding of reservoir characteristics, the nature of the problem, and proper surfactant selection. A data evaluation process involving reservoir and well data screening, surfactant selection, and process parameter design is generally required to assess the steam foam application. Screening data for in-depth mobility control requires a more extensive review than does injection profile modification. This paper discusses screening criteria for steam foam applications and options to optimize

foam generation based on laboratory data and published field results.

RESERVOIR AND WELL SCREENING

One of the most important steps to ensure effective foam application is proper candidate selection. Selecting candidates involves screening reservoir and well data to identify problems and the design of an appropriate treatment program. Candidates for injection profile improvement can be selected from wells exhibiting poor injection or temperature profiles. Indications of poor areal sweep efficiency due to adverse mobility ratios or gravity override include uneven steam zone temperature and fluid saturation distributions, uneven production flowline temperature distributions, excessive steam production from production wells, and low oil recovery. Having identified the nature of the problem, additional evaluation of reservoir data are necessary to insure a successful foam application.

Oil Target

The primary objective of a foam application is to improve oil recovery through sweep efficiency improvements. This is feasible only if sufficient recoverable oil is present in the reservoir. Generally, projects with higher mobile oil saturations yield better economics. This is true for both profile modification and in-depth mobility control processes. Production increases due to foam can be attributed to improved vertical and areal sweep improvements and production well productivity increases. Production wells experiencing steam breakthrough often experience restricted production capacity due to high casing pressures or high pump placement. Elevated casing pressure reduces the effective pressure drop between the formation and wellbore and, in turn, the productivity of the well. Pump efficiency can also be reduced by steam flashing in producers[1]. Foam can mitigate steam breakthrough thus allowing the pump to be operated at a higher efficiency. Field data from Midway-Sunset by Friedmann et al[3] and Mohammadi and McCollum[5] shows considerable production increase after steam breakthrough was mitigated.

Thermal Maturity

A significant volume of foam is normally required to divert steam to oil saturated zones in reservoirs with gravity override problems. For mature steamfloods, large steam zones can result in oil response delays which increases the cost of the application. To improve economics, foam projects should be implemented in non-mature steamfloods where the steam volume is still relatively small and the oil target is high.

Geology

The oil production improvement of a foam project depends strongly on the connectivity between the injector and the producers in the foam pattern. Reservoirs with pinch-out or lenticular sands may prevent foam from diverting the steam to oil saturated sands or to the production wells. Cross sections, interference testing, etc., can be utilized to verify connectivity between the injectors and producers.

In a dipping reservoir, the location of the project can play an important role in the success of the foam application. Injecting foam near structure tops or aquifers can result in a poor oil response due to surfactant loss and low oil saturation. Steamfloods with downdip steam breakthrough on the other hand, can be good candidates for foam application as the surfactant tends to stay with the downward migrating liquid phase of the injected steam. Gravity drainage also assists recovery as additional reserves are heated by the diverted steam. A foam pilot at the Cymric Field successfully mitigated downdip steam migration and quickly increased oil production[6].

Reservoir Rock Mineralogy

Surfactant adsorption on reservoir rocks significantly affects the economics of the steam-foam applications, especially for in-depth mobility control. Many projects produced considerable incremental oil but failed economically due to high adsorption rates[5,7,8].

In general, surfactant adsorption varies with the formulation and chemical structure of the surfactant, reservoir temperature, clay content and clay composition[1]. Clays with high smectite, illite or chlorite contents exhibit high cation exchange capacities which greatly affect surfactant adsorption. Formations containing these clay minerals can pose serious problems for the steam foam application. Table 1 shows the properties of clay minerals commonly found in the San Joaquin Valley, California[9]. In certain cases, adding salt or sequestering agents can reduce surfactant absorption[7]. These options, however, are generally expensive, hence, steam foam applications will be more favorable in reservoirs possessing low clay contents and low cation exchange capacities.

Permeability

Experimental data suggest that the mobility reduction factor (MRF) and oil recovery vary proportionally with rock permeability[2,5,10]. Friedmann et al[3] and Isaacs et al[11] also showed that the critical velocity/pressure gradient for foam generation decreases sharply with increasing permeability. These findings indicate a high permeability formation is more favorable for foam generation and propagation than a low permeability. The data also suggests that wells with poor injection profiles caused by large permeability contrasts can be good candidates for foam injection.

Fracture Pressure

Foam generation will reduce the steam mobility which will raise the injection pressure. In many shallow reservoirs, the maximum injection pressure is limited by the formation fracture pressure. Thus, the pressure increase due to foam injection that the formation can safely withstand may limit the maximum obtainable MRF and subsequently, the effectiveness of the foam application.

SURFACTANT SCREENING

Three types of screening tests are normally conducted to evaluate the ability of a surfactant to generate strong foam near the wellbore. The first test is to ensure that the surfactant is thermally stable at the operating temperatures. At these temperatures, typically in the range of 300°-500°F, many surfactants degrade quickly and loose their ability to foam. In the last few years, formulations have been developed to improve the thermal stability of surfactants which extended the steam foam applications in the temperature environment higher than 500°F[2,13,14], Figure 1.

Brine Compatibility

The water used for steam generation should be compatible with the surfactant. Water with high TDS or divalent ion concentration can cause precipitation which significantly reduces the foaming ability of the surfactant. In many cases, adding softened blend water, sequestering agents, or switching to a different water source can reduce or eliminate these adverse effects.

Mobility Reduction Factor (MRF)

Surfactant effectiveness in controlling steam mobility is determined using corefloods and is usually expressed in terms of MRF. MRF is defined as the ratio of the pressure drop during steam injection with foam injection to the pressure drop during steam injection alone, at constant flow rate. Surfactants which generate high resistance factors are more effective in improving sweep efficiency. One factor affecting the ability of surfactants to generate high MRF's is the operating temperature of the steam drive. Surfactants often exhibit an optimal temperature or temperature range as shown in Figure 2. Muijs et al[13] and Mendez and Campos[14] observed that the chemical structure and molecular weight have a significant effect on a surfactants foaming ability at high temperatures. This information suggests that in order to maximize the MRF, surfactant selection should be based on project operating conditions. Due to the sensitivity of the mobility reduction factor to these parameters, laboratory corefloods should be performed using reservoir rock at conditions similar to actual operating conditions[15].

Adsorption

For in-depth mobility control, additional tests need to be performed to ensure the compatibility of the surfactant with reservoir brine and to identify reservoir adsorption characteristics. As mentioned above, the measurement of reservoir adsorption is a crucial test for this type of application since surfactant adsorption strongly affects the rate of foam propagation and the cost of the treatment. High adsorption of surfactant on reservoir rocks can negatively effect project economics despite oil production increases[7].

Critical Velocity for Foam Generation

Sweep efficiency improvement depends on the extent of foam propagation in the reservoir. Typical pressure gradients existing deep in the reservoir may not be sufficient for lamellae propagation,[3,16] hence, the extent of foam propagation depends strongly on in-situ reservoir pressure gradients. Friedmann[4] also showed that the critical velocity varies strongly with surfactant formulation, temperature, surfactant concentration, and liquid volume fraction (LVF)[17]. Figure 3 shows the effects of temperature and LVF on the critical velocity. Hence, for a given steamflood, the surfactant that can generate foam at lower steam velocity or pressure gradient should propagate foam deeper in the reservoir and provide better sweep improvement. The maximum distance a foam can propagate in a reservoir can be estimated by comparing the reservoir pressure gradients with the surfactant critical pressure gradient as illustrated in Figure 4.

Oil Saturation Sensitivity

Surfactants exhibit a wide range of sensitivity to oil saturation. Some surfactants cannot generate strong foam until the oil saturation becomes very low. Figure 5 shows the effects of oil saturation on various surfactants. The presence of oil appears to delay foam formation. Data obtained by other authors indicates similar results[2,13,18].

For in-depth mobility control, surfactants should be able to generate foam in the presence of oil at a saturation considerably higher than the residual value measured near the injector.

PROCESS PARAMETERS DESIGN

In addition to selecting good candidates and proper surfactants, an appropriate liquid volume fraction (LVF), surfactant concentration, and steam velocity will create favorable conditions for foam generation and maximize the benefits of foam applications. Although corefloods can be used to determine the effects of these parameters, field tests usually provide a better means to delineate and optimize these relationships.

Liquid Volume Fraction

Experimental and field data indicate the onset of steam foam generation is very sensitive to the LVF of the injected steam. LVF is defined as the ratio of the liquid volume to the total saturated steam volume. LVF is a function of both the steam quality and saturated steam temperature (or pressure). It is easier to generate strong foam with high LVF's than with low ones[19] (Figure 3). For a given set of operating conditions, foam may not be generated until a certain minimum value of LVF is reached. Field data in several areas indicate that, for most steam foam applications, an LVF of 0.01 is necessary for foam generation[3,4,20]. The minimum LVF can vary with surfactant type, concentration, temperature and velocity. A few options are available to increase the injected steam LVF if its value falls below the desired level. One common method is the addition of make up water into the steam line. Another option is to reduce the steam quality coming from the steam generator. Field practices, facility installations and operating conditions often predicate the available options. In certain cases, once foam is generated, the LVF can be reduced without adversely affecting the resistance factor. Reducing the LVF also lowers the chemical rate which reduces project costs.

Surfactant Concentration

The effectiveness of steam foam depends strongly on the surfactant concentration. The MRF, however, does not vary lineary with the concentration and there usually exists an optimum concentration beyond which little additional steam mobility reduction is obtained[3,13,21]. This optimum concentration appears to vary with temperature and LVF and its value needs to be established for each project to optimize the economics.

For profile modification, surfactant injection can be reduced by using either a non-continuous injection mode or a concentration-reduction injection schedule. Pressure switches and timers have been used effectively in the fields to initiate non-continuous injection. Pressure switches allow the injection pump to operate in a preset range of pressure; the pump will stop when pressure reaches a maximum value and will restart when the pressure falls to a minimum level. For slug or non-continuous injection, a timer can be used to control and regulate the chemical injection pumps.

Implementing a concentration-reduction injection scheme has proven to be beneficial in certain cases. It can reduce the cost of application significantly while maintaining the resistance generated by the initial high concentration. Figure 6 shows that a gradual reduction of the concentration from 0.5 wt% to 0.10% decreases the resistance factor only slightly. A series of injection profiles taken in San Joaquin Valley indicated a gradual reduction in the surfactant concentration, from 0.5 wt% to 0.2wt%, produced no noticeable effects on the injection profile after it had been modified (Figure 7). In this case, foam apparently created a long lasting effect on the injection profile.

Steam Injection Velocity

Foam generation appears to be sensitive to the steam velocity exiting the perforations. For a given steam injection rate, the steam velocity at the sand face can vary over a wide range dependent upon the completion style of the injector. Wells completed with limited entry style completions can have velocities hundreds of times higher than that of high density perforated completions. Figures 8A and 8B show the wellhead pressure response of two wells with comparable steam rates, steam quality, LVF, and surfactant injection rates. The well with the limited entry completion showed a quick pressure increase with surfactant injection, while the well with high density perforations did not respond initially. After the LVF of the high density perforated well was increased a good pressure response was observed. These data collaborated the experimental results which indicate that a critical velocity or pressure gradient is necessary for foam generation[3,11,20].

Non-Condensible Gas

In many previous field trials a small amount of non-condensible gas, about 1 to 5% mole fraction of the gas phase, was injected with surfactant to impede the collapse of foam bubbles due to steam condensation in the reservoir[22]. Nitrogen or hydrocarbon gas is usually used as a non-condensible gas source in steam foam applications. The use of a non-condensible gas will promote faster and stronger foam generation. Figure 9 shows the increase in wellhead pressure after nitrogen was added to the steam and surfactant. As mentioned by Gauglitz et al,[19] an increase in surfactant concentration and/or LVF may provide the same result hence, the relative cost of these options needs to be considered when electing an appropriate action to promote foam generation.

CONCLUSIONS

Steam foam can be applied effectively and economically when appropriate reservoir evaluation and screening is performed. Pertinent reservoir data reviewed includes oil saturation, thermal maturity, reservoir structure, and rock permeability and mineralogy. Data reviewed for surfactant performance include thermal stability, fluid compatibility, adsorption, mobility reduction, and critical velocity for foam generation. Varying the LVF, concentration, or adding a non-condensible gas during foam injection, can create favorable conditions for foam generation and optimize the use

of surfactant. Field data also shows that improved surfactant formulations can extend steam foam applications to a higher temperature range and provide deeper foam propagation.

ACKNOWLEDGEMENT

We thank W. Loh, W. F. Beumer and M. I. Holtzclaw for providing some of the experimental and field data. We thank Chevron Chemical for the permission to publish this paper.

REFERENCES

1. Hirasaki, G. J.: "The Steam-Foam Process," JPT, pp. 449-456, May 1989

2. Djabbarah, N. F. et al.: "Laboratory Design and Field Demonstration of Steam Diversion with Foam," SPE 20067, presented at the 60th California Regional Meeting, Ventura, CA, April 4-6, 1990

3. Friedmann, F. et al.: "Steam Foam Mechanistic Field Trial in the Midway-Sunset Field," SPE 21780, presented at the Western Regional Meeting, Long Beach, CA, March 20-21, 1991

4. Sander, P. R., Clark, G. J., and Lau, E. C.: "Steam-Foam Diversion Process Developed to Overcome Steam Override in Athabasca," SPE 22630, presented at the 66th Annual Technical Conference and Exhibition, Dallas, TX, October 6-9, 1991

5. Mohammadi, S. S. and McCollum, T. J.: "Steam-Foam Pilot Project in Guadalupe Field, California," SPERE, pp. 17-23, Feb. 1989

6. Bautista, L. S. and Waninger, E. A.: "The Effects of Steam Foam Injection in a Steamflood Experiencing Downdip Steam Migration," SPE 25783, to be presented at the 2nd International Symposium on Thermal Operations, Bakersfield, CA, February 8-10, 1993

7. Patzek, T. W. and Koinis, M. T.: "Kern River Steam-Foam Pilots," JPT, pp. 496-503, April 8. Mohammadi, S. S. et al.: "Steam-Foam Pilot Project in Dome-Tumbador, Midway-Sunset Field," SPERE, pp. 7-16, Feb. 1989

8. Reed, M. G.: "Fluid-Rock Interactions Affecting Petroleum Production," Chevron Internal Notes

9. Chou, S. I. et al.: "CO_2 Foam Field Trial at North Ward-Estes," SPE 24643, presented at the 67th Annual Conference and Exhibition, Washington, D.C., October 4-7, 1992

10. Isaacs, E. E. et al.: "Investigation of Foam Stability in Porous Media at Elevated Temperatures," SPERE, pp. 565-572, May 1988

11. Muijs, H. M. et al.: "Surfactants for Mobility Control in High-Temperature Steam-Foam Applications," SPE 17361, presented at SPE/DOE Enhanced Oil Recovery Symposium, Tulsa, OK, April 17-20, 1988

12. Mendez, Z. and Campos, E.: "Experimental Evaluation of the Efficiency of Foaming Agents in Steamflood Processes," paper presented at the 5th UNITAR International Conference on Heavy Oil and Tar Sands, Caracas, Venezuela, 1991

13. Mohammadi, S. S. et al.: "Test of Steam-Foam Process for Mobility Control in S. Casper Creek Reservoir," paper No. CIM and AOSTRA 91-77, presented at Petroleum Society of CIM and AOSTRA Meeting, 1991

14. Kuehne, D. L. et al.: "Evaluation of Surfactants for CO_2 Mobility Control in Dolomite Reservoirs," SPE 24177, presented at the SPE/DOE 8th Symposium on Enhanced Oil Recovery, Tulsa, OK, April 22-24, 1992

15. Rosen, W. R. and Gauglitz, P. A.: "Percolation Theory of Mobilization of Foams in Porous Media," AIChEJ. 36, 1176, 1990

16. Gauglitz, P. A. and Friedmann, F.: "Foam Creation in Porous Media," to be published in AIChEJ.

17. Jensen, J. A. and Francois, F.: "Physical and Chemical Effects of an Oil Phase on the Propagation of Foam in Porous Media," SPE 16375, presented at the 57th California Regional Meeting, Ventura, CA, April 8-10, 1987

18. Gauglitz, P. A. et al.: "Field Optimization of Steam-Foam for Profile Control: Midway-Sunset 26C," to be presented at the 2nd International Symposium on Thermal Operations, Bakersfield, CA, February 8-10, 1993

19. Friedmann, F., Chen, W. H., Gauglitz, P. A.: "Experimental and Simulation Study of High-Temperature Foam Displacement in Porous Media," SPE 17357, presented at the SPE/DOE Enhanced Oil Recovery Symposium, Tulsa, OK, April 17-19, 1988

20. Kular, G. S. et al.: "Foam Application in an Oil Sands Steamflood Process," SPE 19690, presented at the 64th Annual Technical and Exhibition, San Antonio, TX, October 8-11, 1989

21. Falls, A. H. et al.: "The Role of Non-Condensable Gas in Steam Foams," JPT, pp. 95-104, Jan. 1988

No. FS6

DOE/NIPER

Cyclic Steam Injection with Foam: Interpretation of Field Test Results

by J. M. Alvarez, E. Escobar, Z. Mendez, P. Colonomos and E. Campos, INTEVEP, S.A., Caracas, Venezuela

Author(s) are solely responsible for copyright and contents.

This paper was prepared for presentation at the DOE/NIPER, Symposium on Field Application of Foams for Oil Production held in Bakersfield, California, February 11-12, 1993.

This paper was selected for presentation by a Program Committee following review of information contained in an abstract submitted by the author(s). Contents of the paper, as presented, have not been reviewed and are subject to correction by the author(s). The material, as presented, does not necessarily reflect any position of the U.S. Department of Energy or the National Institute for Petroleum and Energy Research.

ABSTRACT

During the 1980's decade, cyclic steam injection with two different commercial foaming agents (LTS and BBS) was tested in 16 heavy oil (11° API) producer wells located at west of Venezuela. These additives were selected after laboratory experiments using concentrations between 0.5 and 2 % v/v.

In this work, the incremental oil recovery associated to each test, additives blocking efficiency and vertical steam distribution changes due to foam formation at the porous medium are presented.

Test results indicated a production increment of 4500-42000 STB for a two-years cycle, a significative improvement of the vertical steam distribution with increments of the steam contacted intervals up to 68 ft. On the other hand, the incremental oil production obtained from wells treated with LTS is due mainly to an improvement of the injection profile, while in the wells injected with BBS the production was favored by two mechanisms, a better injection profile and a decrease in the water-oil interfacial tension.

In general, the tests results indicated that under certain operational conditions this process can be applied with high possibility of success.

INTRODUCTION

At present, the heavy and extraheavy crude oil reserves in Venezuela are about 59,000 millions of barrels. It represents the second largest in the world after the Canadian reserves of this type of crude. To this date, most of the heavy oil reservoirs have been underwent cyclic steam injection and recoveries around 20 % of the O.O.I.P have been reported. In spite of these results, the efficiency of this process is frequently affected by the preferential steam flow toward determined zones as a consequence of gravity override and steam channelling through high permeability regions.

One of the available techniques to minimize the above mentioned phenomena is the co-injection of foaming agents with steam. Since Fried proposition (1961)[1] to control the reservoir fluid mobility using foam in secondary recovery projects, numerous laboratory and field studies have been undertaken to investigate the mechanisms associated to this process and determine the best foaming agents performance ruling parameters.

References and illustrations at end of paper.

Between 1984 and 1986, cyclic steam-foam co-injection tests were carried out in 16 wells located at Maracaibo Lake Eastern Coast. After laboratory evaluation at the same average injection conditions prevailing in the pilot tests area, two different foaming agents were selected for these tests.

The main focus of this work is to present certain factors to evaluate steam-foam injection process, and also to determine the influence of some injection parameters on the process performance.

WELLS CHARACTERISTICS

The cyclic steam/foam injection tests were performed in Lagunillas, Tía Juana, and Bachaquero fields. Figure 1 shows geographical location of the pilot tests. These wells belonging to Miocene age reservoirs, and they are characterized by the presence of deposited channels in a fluvial environment, with differentiation of two unconsolidated sands packs separated by a clayish interval. These sands present high vertical and horizontal heterogeneities and as the injection cycles progress, gravity override and/or steam flow channeling phenomena occur. It affects the steam efficiency, because, a non-uniform sand drainage is produced, and great formation zones are not contacted by steam, remaining with a high oil saturation.

ADDITIVES CHARACTERISTICS

Due to the temperature conditions associated to the steam injection processes, the additives have to accomplish the following characteristics: foaming properties, thermal stability and plugging capacity. Laboratory tests have shown that sulphonated anionic surfactants undergo lower thermal degradation than other structures, therefore they are the most recommended for processes at high temperatures. The field tests were carried out with two sulphonated additives previously evaluated at the laboratory. A linear alkyl toluene sulphonate (LTS) with 15% weight of active material and branched alkyl bencene sulphonate (BBS) with 56% of active material [2,3].

WELLS SELECTION PREMISES

The wells tested were selected according to the following premises [4].

a. Wells injected in a conventional way with no possibility of selective injection of each sand individually.

b. Presence of severe gravity override and/or steam channelling.

c. Wells were representatives of several depletion stages.

d. Wells with good mechanical conditions.

e. Existence of facilities for steam injection.

INJECTION PARAMETERS

Tables 1 and 2 show the injection parameter values for each field test. Since the prevailing field operating conditions for steam with/without additives injection are difficult to be controlled. Then, it was necessary to evaluate the influence of some parameters in the steam/foam injection process on the production behavior. As a consequence, tests were performed with variation of the following parameters:

Injection pressure.

Injection cycle.

Steam quality.

Additive concentration.

It is remarkable that, the schedule started with steam injection for 3-7 days. At the end of this period a flowmeter (spinner log register) was run to know the vertical steam profile, to be used as reference, for evaluating the additives efficiency. Then, steam was injected together with surfactant and several flowmeter were carried out in order to observe changes in the vertical

steam distribution. Finally, only steam was injected.

PARAMETERS EVALUATION

In this work, the surfactant capacity to block steam high permeability zones and divert steam to new sand intervals, and also, the incremental oil production obtained by steam/foam injection, were evaluated. The following are the tool and factors used to determine the performance of steam/foam pilot tests.

Flowmeter Surveys

The flowmeter is one of the available tools to analysis the steam/foam co-injection tests. By this mean, it is possible to know the steam vertical distribution profile and the contacted or stimulated zones by steam. The graph obtained during a flowmeter run gives a qualitative information about the steam distribution in the producing sands (see Fig. 2). In a cyclic steam/foam injection test whose purpose is to block the previously steam contacted zones, is very important to run the flowmeter before and after the additive injection. Because, any modification in these profiles should be attributed to foam generation into the reservoir. Also, flowmeter results can be used to establish the relationship between injection conditions and the foaming agent performance.

Based on the flowmeter results, two factors were used in order to obtain a quantitative determination of the steam diversion toward non-contacted zones as well as the foam blocking efficiency.

Blocking Factor (E_b)

The main objective of foaming additives application is to block those zones where the steam flows preferentially, therefore it was necessary to define a factor to evaluate fundamentally the additive blocking capacity, using the flowmeter registers before and after foam injection [5].

The mathematical equation developed was:

$$E_b = \frac{\sum_{i=1}^{n} (P_{aj} * F_{bj})}{P_{at}} \qquad (1)$$

where

$$F_{bj} = 1 - \frac{V_{fj}}{V_{ij}} \qquad (2)$$

Equation (1) takes into account the following limit cases (see nomenclature at the end of paper):

If F_{bj} ----> 0, V_{ij} is equal to V_{fj}, which indicates that no blockage occurred, since the zone where steam channelled continues taking the same amount after surfactant addition.

If F_{bj} ----> 1, V_{fj} is equal to zero, i.e. the surfactant totally blocked the zone that was initially taking steam.

Fig. 3 presents those blocking efficiency values for the LTS and BBS injected wells. As observed, the results are somewhat different for each well. In the LTS case, four of the wells injected present blocking efficiency values above 50%, and the maximum efficiency is approximately 90%.

For BBS surfactant only two out of the seven wells show values above 50%, and the maximum value is approximately 75%. At a glance, one could think that LTS surfactant blocks better than BBS.

Steam Diversion Factor (SDF)

Through this factor developed by Rivas[6], in 1989 it is possible to determine the steam distribution changes produced by the additive application.

The evaluation model compares the distribution profiles through this factor, which is mathematically calculated for each survey. This factor considers the intervals receiving steam with respect to the total sand thickness. The proposed mathematical expressions is:

$$SDF = \frac{\bar{h} - \bar{h}_b}{H - \bar{h}_b} \qquad (3)$$

$$SDF = \frac{\text{actual contacted sand incremented}}{\text{max. expected contacted sand incremented}}$$

A positive value of SDF is an indication that steam distribution was improved, while a negative value indicates that steam profile deteriorates with the new operating conditions.

Fig. 3 shows the values of SDF for each injected well and both additives. For the BBS, the variation range for this factor is between -0.2 y +0.2, which is lower than the obtained with the surfactant LTS ranging between -0.3 to +0.35. This SDF variations can be attributed to the injection conditions and the petrophysical characteristics of each well.

For LTS, in general, the values are positive and the maximum is around 0.35. Only one well shows a negative value indicating that the new contacted interval is smaller than the original one, perhaps due to reservoir heterogeneities. In the case of BBS two wells present negative values.

Even though it is expected a greater steam diversion for those cases with higher blocking efficiency, in general, a direct correlation between both factors is not observed. Wells with high blocking efficiency showed positives and negatives SDF values, which indicates that this factor not only depends on the surfactant blocking capacity but also on the heterogeneity of the medium. This effect is most important in the case of SDF due to the fact that the comparison between steam profiles before and after foam injection is made in different sand intervals with probably different petrophysical properties. In the case of E_b factor the evaluation is made in the same sand interval, so the effect of this variable is not as important as in the SDF case.

OIL PRODUCTION BEHAVIOR

Another important factor already mentioned, for the additive efficiency evaluation is the production increment result from the additive incorporation in the process. Once this increment is known, the process profitability can be determined and therefore, the economic feasibility. Nevertheless, at present, there is no numerical tool for predicting in a reliable manner, the incremental recovery magnitude. It became necessary, to develop an analytical methodology, which based on the previous cycle production with no surfactant addition, would allow to estimate the production obtained if only steam was injected in this new cycle. This value subtracted from the actual production of the new cycle in which the foaming agent was injected, gives the incremental production value.

The methodology [7] followed to estimate the additional production consists in obtaining for each well and each injection cycle the function that better fits the monthly production rate behavior with respect to time. This type of function should be the same for all cycles in the same well, in order to extrapolate the constants defining the function and obtain those describing the production to be reached in a conventional cycle, i.e. without adding surfactant to steam.

Fig. 4 shows a scheme of the method used. It is noteworthy that this methodology excludes those wells (total = 3) where surfactant was injected in a second cycle (see Tables 3 and 4).

Fig. 5 shows the additional production thus obtained. Notice that only two wells showed no incremental production.

Fig. 6 shows the additional oil production behavior with respect to blocking efficiency and steam diversion factor. In the case of LTS, exists a direct relationship, i.e. the higher the blocking efficiency and steam diversion factor, the greater the incremental recovery. This implies that the blocking mechanism is rather important for this additive and, therefore, the operational parameters affecting the blocking efficiency should be controlled in order to improve the process. However, BBS showed a different behavior since there is no relation at all between

additional production, blocking efficiency, and steam diversion factor. This seems to indicate the existence of an additional mechanism which is likely to be the modification of the interfacial properties favoring a larger crude production.

Finally, the conclusions reached in the following analysis will provide valuable information for designing future pilot tests, in terms of operational ranges and critical variables to be controlled.

INJECTION VARIABLES INFLUENCE

Due to the surfactant blocking capacity depends on variables such as steam quality, reservoir pressure, injection cycle and additive accumulation and also, this factor is not as affected by vertical changes in the petrophysical properties as SDF factor, then the influence of injection parameters on the process performance was evaluated through the blocking efficiency.

Given the variability of the efficiencies obtained, it became necessary to carry out an analysis for determining the most important process parameters. The ideal procedure would be to relate efficiencies with the operational conditions, and perform a multivariable analysis. However, since the well population is not large enough, each parameter to be evaluated will be individually studied.

Steam Quality Influence

This parameter seems to have a major impact on the blocking efficiency. Fig. 7 shows, there is a direct relationship between steam quality and blocking efficiency for both surfactants. However, in the case of LTS, the highest blocking efficiency values are obtained at steam quality ranges greater than 83%. In the case of BBS, the maximum values corresponds to steam qualities over 90%.

Injection Pressure Influence

Blocking efficiency values as a function of injection pressure, for each well, are shown in Fig. 8. It illustrates that there is an unfavorable tendency as pressure increases for LTS additive injected wells. The lowest efficiency values are obtained at pressures above 500 psi, which probably indicates that above these values the additive starts undergoing thermal degradation reactions due to the high saturation temperatures associated with injection pressures.

The small pressure range at which BBS was assessed (344-543 psi) does not allow the observation of any efficiency trend with regard to this parameter. However, it is noteworthy that variation in efficiency values for this parameter was not influenced by injection pressure.

Injection Cycle Influence

Fig. 9 presents the efficiency variation with respect to this parameter. It may be concluded that the additive injected cycle does not influence the blocking power thereof. This is important, because, if the well has enough production energy, it indicates the feasibility of using foam in any cycle.

Surfactant Accumulation Effect

The blocking efficiency variation for wells 2705 and 1335 as a function of the additive concentration in the steam aqueous phase is presented in Fig. 10. Flowmeter were effected in both wells for each concentration evaluated. At the beginning, well 2705 was injected with additive 0.25%, then the concentration was increased to 2%. It was observed that the blocking efficiency goes up as concentration increases and that, according to this separate analysis, the higher the additive concentration, the better the results. Nevertheless, when studying well 1335 behavior (2% initial concentration then reduced to 0.5%), it is observed that efficiency increases as concentration diminishes. Similar results were obtained when other LTS and BBS treated wells were analyzed.

The above behavior indicates that a certain amount of surfactant should be accumulated in the zones to be blocked, before starting obtaining the desired effects. As a result, at the beginning of these tests, it is advisable to inject a foaming agent at concentrations lower than the one recommended in the

laboratory tests. Concentrations should be increased as an increase in the blocking efficiency is indicated in the flowmeter evaluation.

CONCLUSIONS

The steam diversion factor and the blocking efficiency are useful parameters for evaluating the cyclic steam injection field tests with foaming agents.

High steam qualities favor the blocking efficiency and the additional crude oil production.

Each surfactant shows a different behavior: BBS seems to have an additional mechanism other than the blocking one, which improves the cyclic steam injection process efficiency.

The additive-related blockage in high permeability zones and steam diversion to other zones are not immediately observed. Therefore, it is necessary to inject a certain amount of surfactant to the medium in order to have the saturation conditions required for an stable foam.

Under the appropriate conditions, the cyclic steam injection with foaming agents is a recommendable method for increasing heavy oil production in Bolívar Coast.

NOMENCLATURE

F_{bj}= blocking factor in the interval j.

$\overline{h}$ = effective thickness of steam/foam contacted sand.

$\overline{h}_b$ = effective thickness of steam contacted sand.

H = total sand thickness.

O.O.I.P. = original oil in place.

P_{aj} = thickness of blocked sand interval.

P_{at} = total blocked thickness.

V_{ij} = initial steam taken by the interval j, %.

V_{fj} = steam taken by the interval after foam injection, %.

ACKNOWLEDGEMENTS

The authors wish to thank Maraven, S.A. for facilitating access to the field data presented in this paper. They also thank Petróleos de Venezuela, S.A., and INTEVEP, S.A. for authorizing the publication of this work.

REFERENCES

1. Fried, A. N., "The Foam-Drive Process for Increasing the Recovery of Oil", USBM 5866, 1961.

2. Ziritt, J. L., Rancel, C., and Paz, F., "Inyección de Vapor con Agentes Espumantes," Presented at the I Simposio Internacional de Recuperación Mejorada de Crudos, Maracaibo, Venezuela, 1985.

3. Méndez, Z., and Campos, E., "Experimental Evaluation of the Efficiency of Foaming Agents in Steamflood Processes," Presented at the 5th Unitar International Conference on Heavy Oil and Tarsand, Caracas Venezuela, 1991.

4. D'Orazio, F., Ziritt, J. L., Rubio, R., Páez, E., Rivas, O., and Paz, F., "Pruebas Piloto de Inyección Alterna de Vapor con Surfactantes," Presented at the II Simposio de Recuperación Mejorada de Crudos, Maracaibo, Venezuela, 1987.

5. Méndez, Z., Alvarez, J. M., Escobar, E., Colonomos, P., and Campos, E., " Cyclic Steam Injection with Additives Laboratory and Field Test Results of Steam/Foam and Steam/Solvent Processes" Paper SPE 24632 Presented at the 67 th Annual Technical Conference of the Society of Petroleum Engineers, Washington, 1992.

6. Rivas, O., "Interpretación Cuantitativa de Registros de Flujo en Pruebas Piloto de Inyección de Vapor con Espuma" Presented at the II Simposio Internacional de Recuperación Mejorada de Crudos, Maracaibo,Venezuela, 1987.

7. Alvarez, J. M., "Estudio Técnico Económico para un Proyecto de Inyección de Vapor con Surfactantes a Nivel Comercial" Industrial Engineering Thesis, Universidad Politécnica Experimental L. C. Mejias, Caracas, 1991.

TABLE 1 TEST DATA OF WELLS INJECTED WITH LTS

Well		Cycle	Injection Pressure (psig)	Steam Quality (%)	Steam Injected (Tn)	Surfactant Injected (Tn)	Brine Injected (Tn)
TIA JUANA EAST FIELD							
LSE - 2705	(L1)	IV	450	85	5650	40.8	1.65
LSE - 2282	(L2)	III	320	92	6017	21.5	3.52
LSE - 3782	(L3)	II	480	83	6104	45.0	-
LSE - 1335	(L4)	IV	400	90	6322	36.1	-
LSE - 1317	(L5)	IV	430	75	7125	40.6	-
LAGUNILLAS FIELD							
LS - 3670	(L6)	II	780	70	6323	54.2	-
LS - 2687	(L7)	IV	560	50	6104	61.4	-
LS - 2093	(L8)	IV	800	50	6105	63.4	-
BACHAQUERO FIELD							
LB - 1908	(L9)	II	760	50	5755	47.8	-

TABLE 2 TEST DATA OF WELLS INJECTED WITH BBS

Well		Cycle	Inj. Pres. (psig)	Steam Quality (%)	Steam Injected (Tn)	Surfactant Injected (Tn)	Gas Injected (MSCF)
LSE -3116	(B1)	IV	533	85	5245	29	-
LSE -1831	(B2)	I	383	75	5960	39	-
LSE -3547	(B3)	III	344	75	5169	20	-
LSE -1609	(B4)	IV	550	70-95	5468	41	-
LSE -1693	(B5)	III	440	90	5297	18	1200
LSE -1452	(B6)	IV	420	90	5598	46	274
LSE -1549	(B7)	IV	410	98	6426	49	-

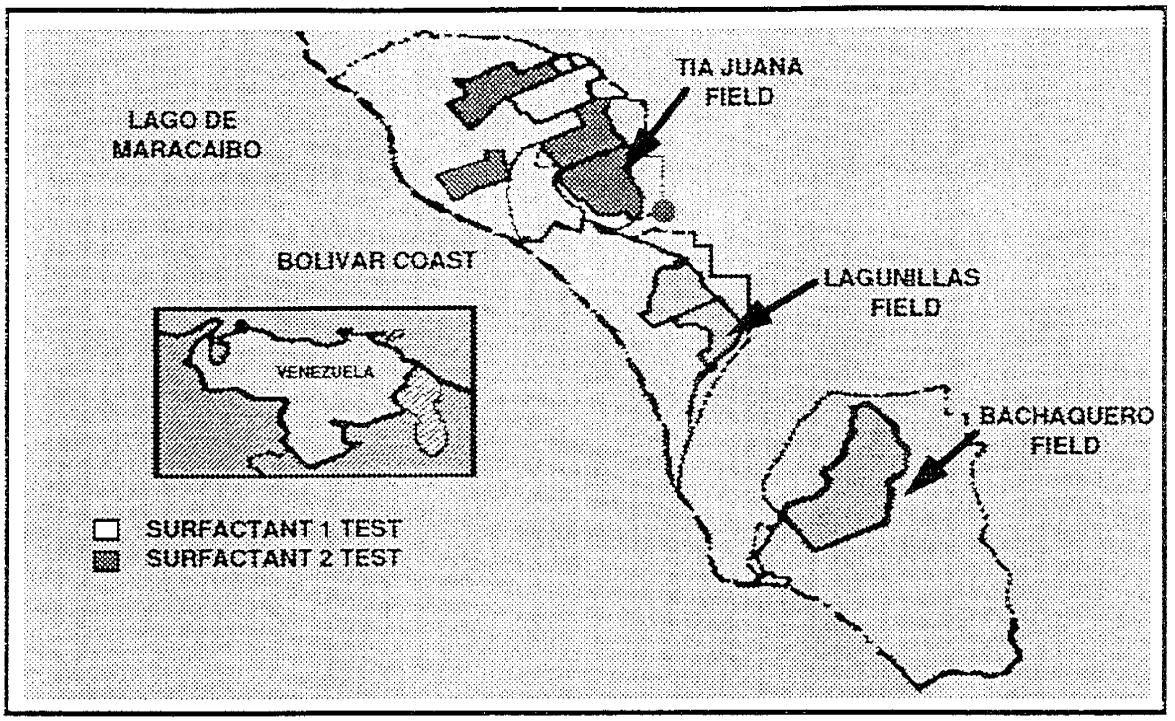

Fig. 1 GEOGRAPHICAL LOCATION OF FOAM PILOT TESTS

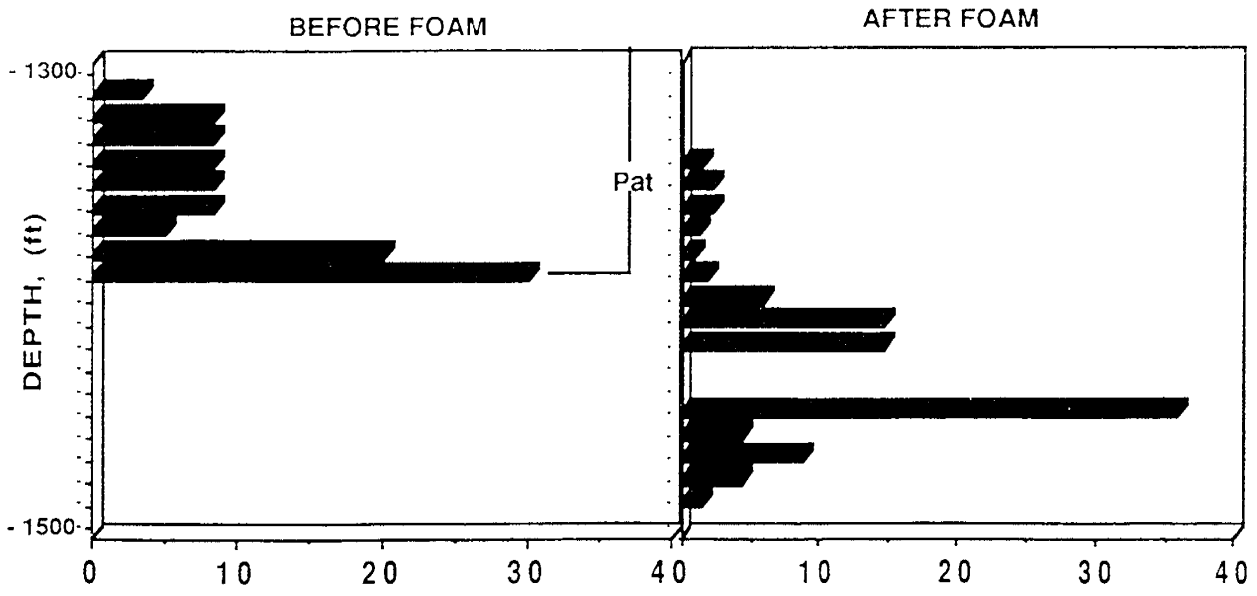

Fig. 2 FLOWMETER RESULTS

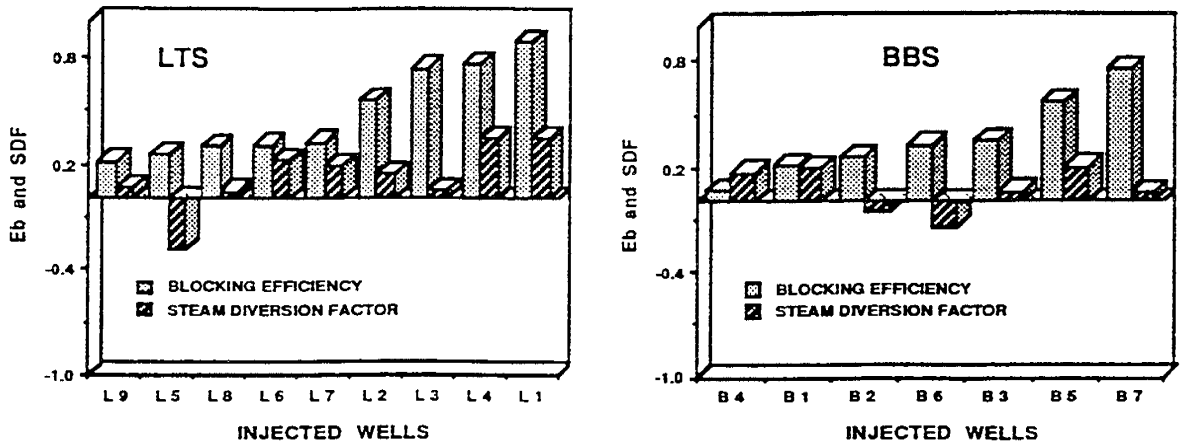

Fig. 3 BLOCKING FACTOR AND STEAM DIVERSION FACTOR

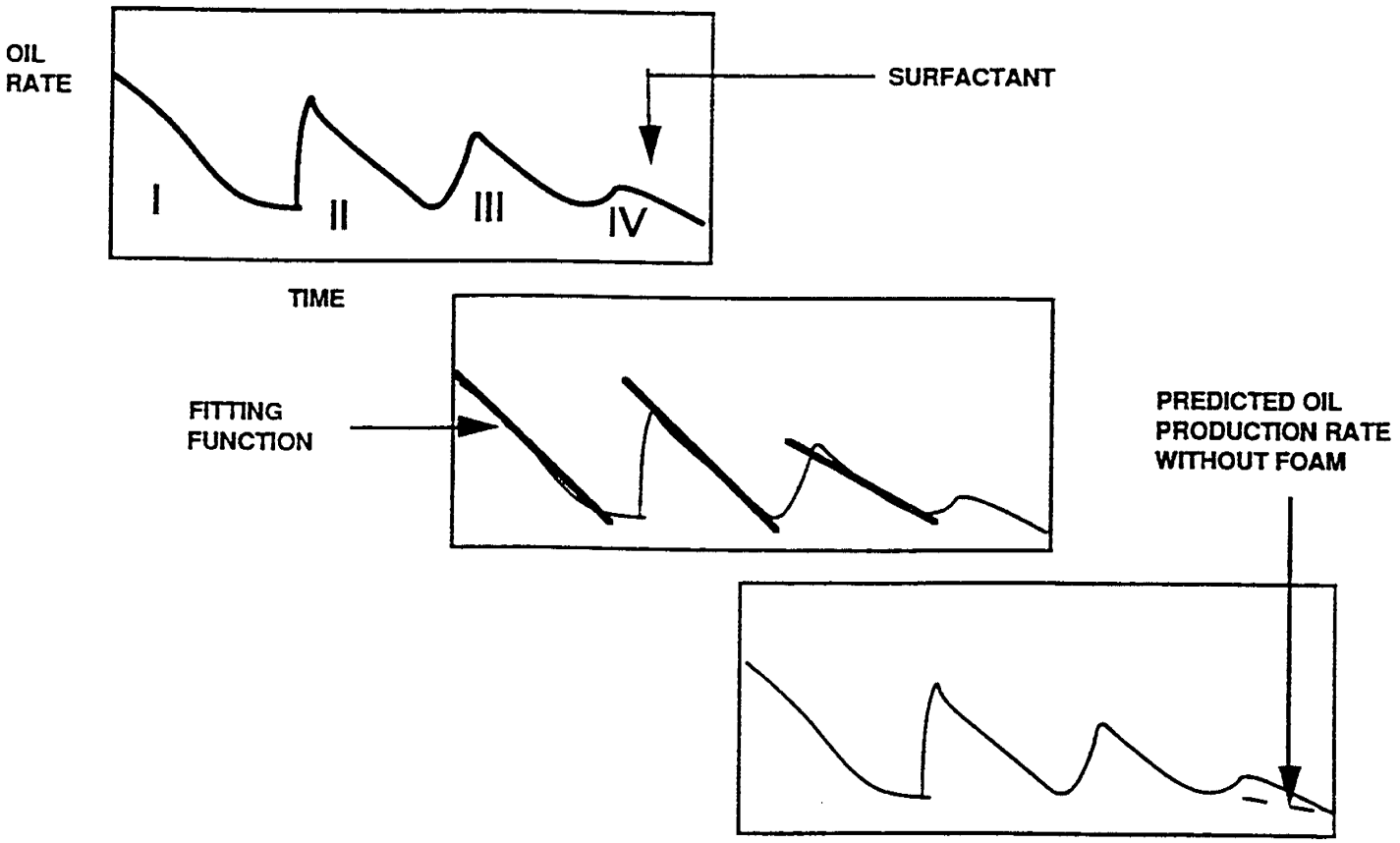

Fig. 4 METHOD TO DETERMINE INCREMENTAL OIL RECOVERY

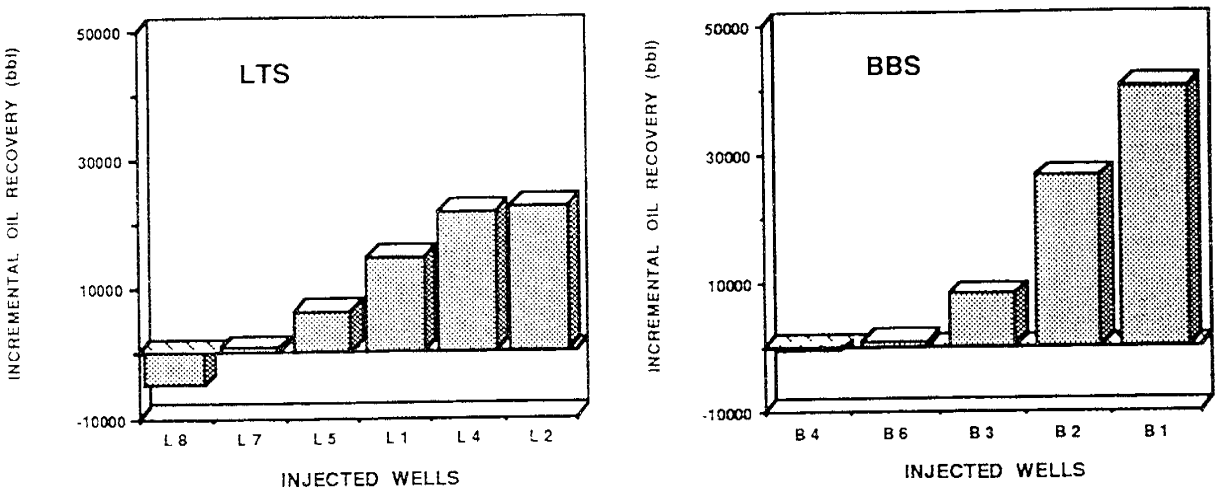

Fig. 5 ADDITIONAL PRODUCTION

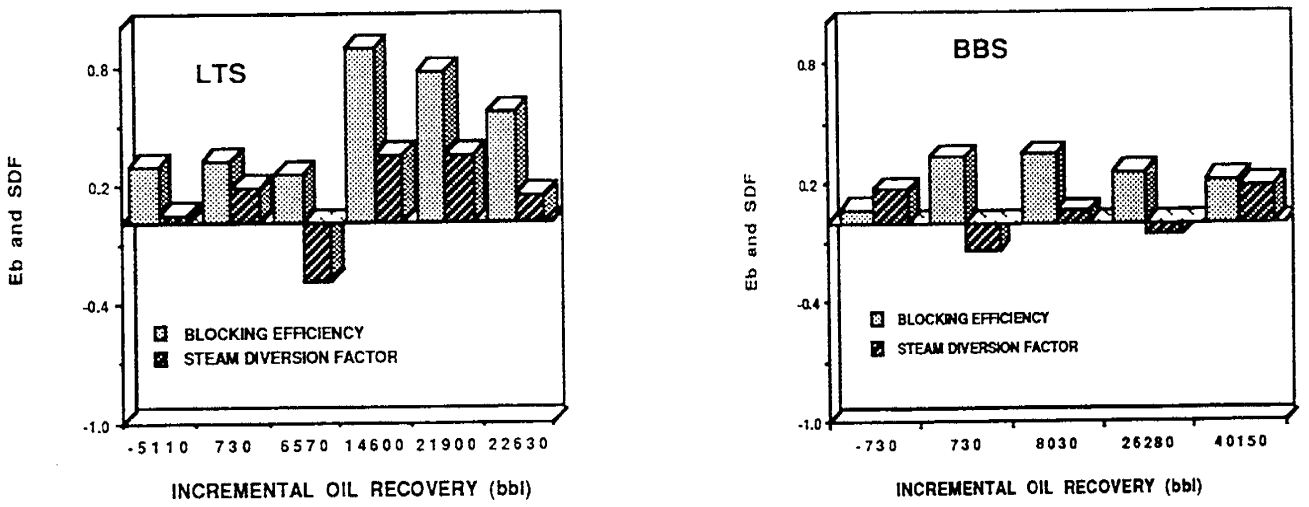

Fig. 6 EVALUATION FACTORS VS INCREMENTAL OIL RECOVERY

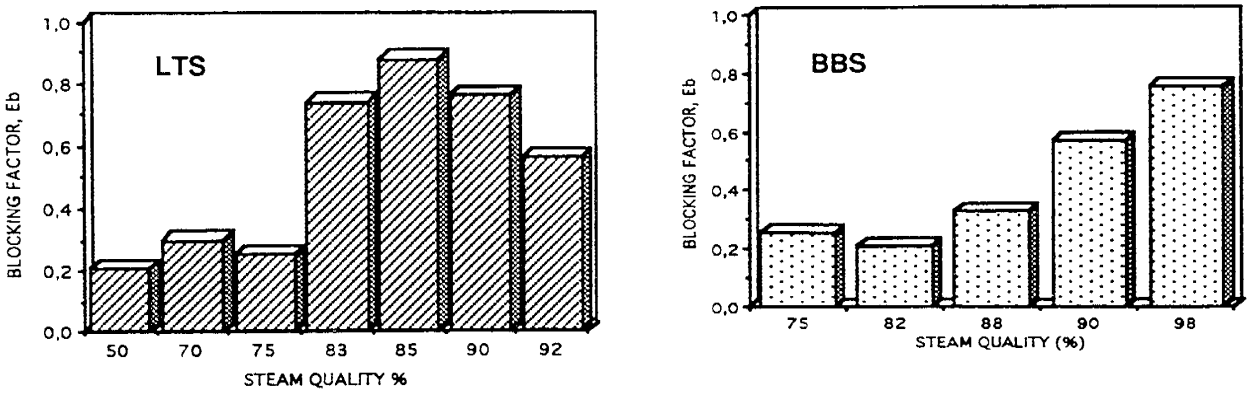

Fig. 7 BLOCKING FACTOR VS STEAM QUALITY

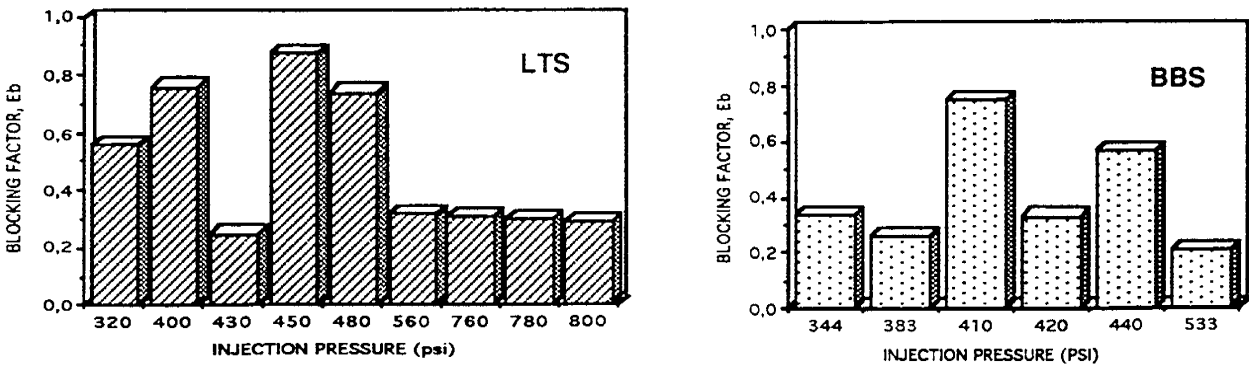

Fig. 8 BLOCKING FACTOR VS INJECTION PRESSURE

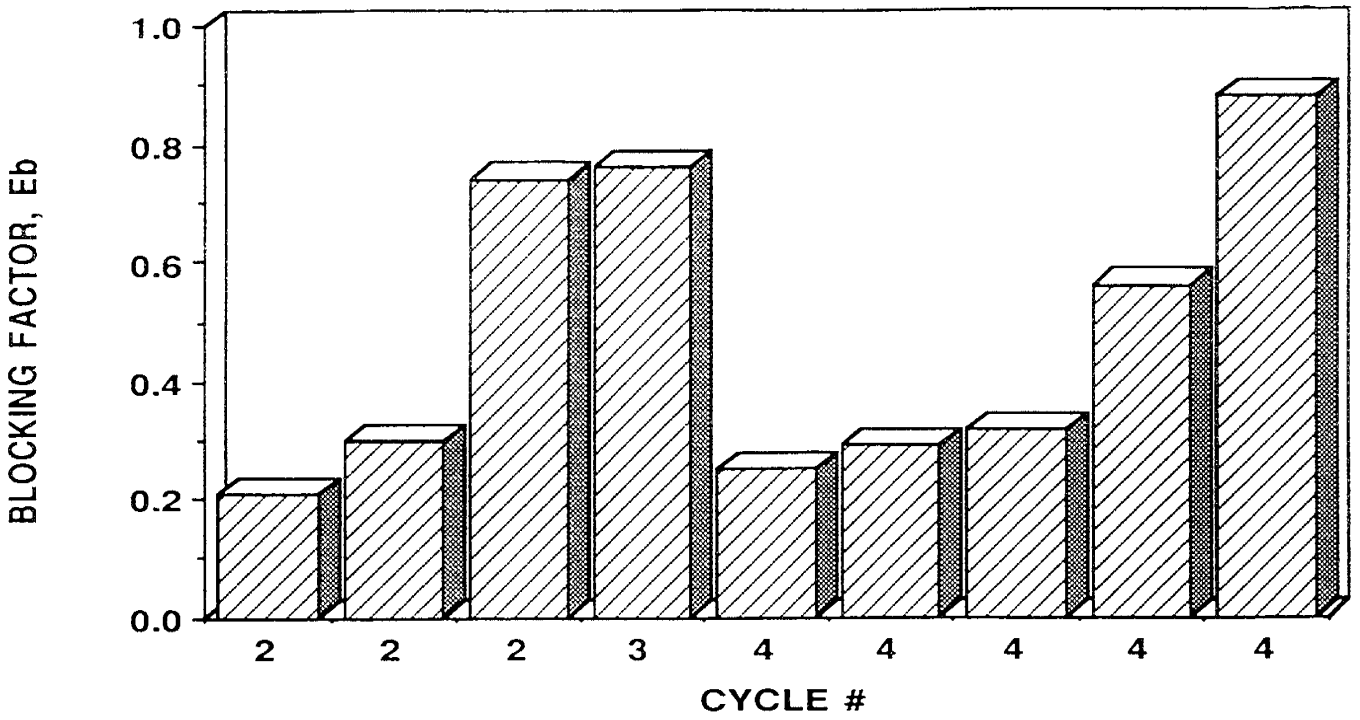

Fig. 9 CYCLE INFLUENCE

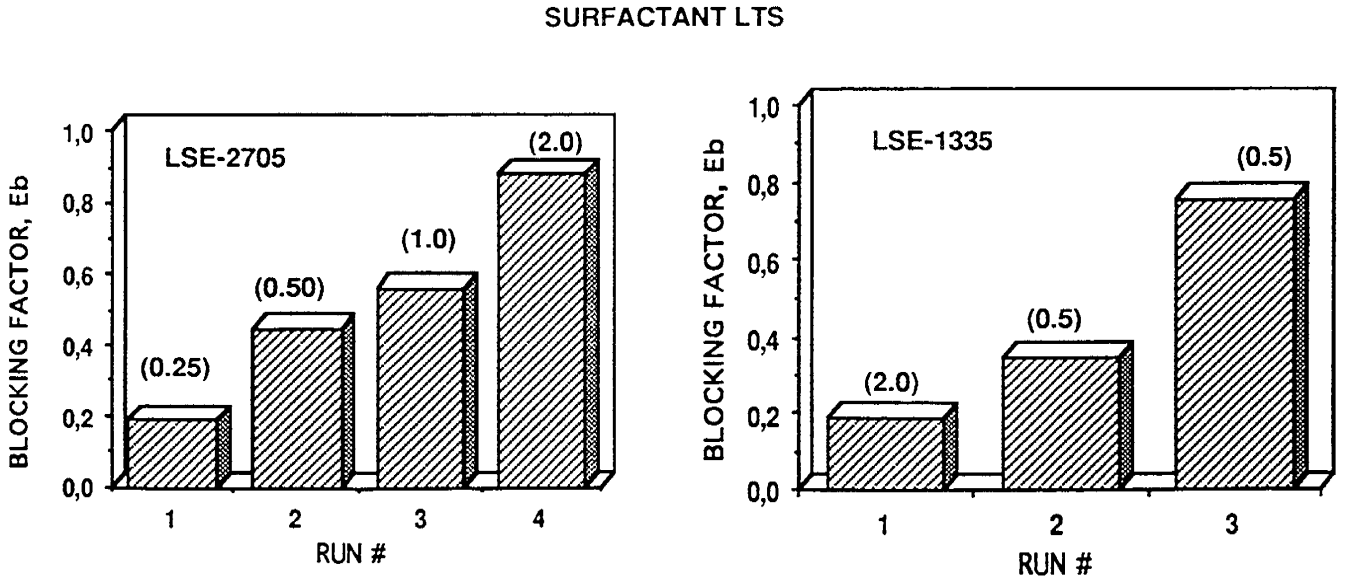

Fig. 10 ACUMULATIVE EFFECT

THERMAL FOAM APPLICATION SESSION
DISCUSSION

Co-Chairmen: Shane Mohammadi, UNOCAL Science & Technology
George Bain, Chevron Chemical Company

Speakers: Ralph Cooke, Enhanced Petroleum Technology
Bill Brigham, Stanford University
Eddy Isaacs, Alberta Research Council, Canada
Mike Smith, Chevron Oilfield Research Company
Eric Waninger, Chevron Chemical Company
Zaleyka Mendez, INTEVEP S.A., Venezuela

Paper FS1—Field Optimization of Steam Foam Diversion in Cyclic Steaming

Question for Ralph Cooke from Terry Osterloh, Texaco

You mentioned about two low-cost foam treatment programs that have high chances of success on specific reservoirs. Would you briefly describe what those treatments are?

Response by Ralph Cooke

Currently we are using two different products in our steam-foam diverter application in cyclic wells. One is a low-cost product which is essentially a flash former and were effective right at the wellbores. These are inexpensive materials and are used in slug injection, each slug consists of 50 to 100 gallons of 30 to 40% active surfactant. We typically inject two slugs per treatment. These treatments generally cost between $1,000 to $2,000, depending upon the volume of the slugs injected. The other is a more sophisticated product that is more expensive. The expensive product is used in smaller amounts on specific semi-continuous programs. Specific conditions must be met before this product produces a good foam. Though expensive, in the proper situation, it gives the best return on investment in many reservoirs. The semi-continuous treatments costs generally range between $6,000 to $8,000 per well.

Question for Ralph Cooke from Terry Osterloh, Texaco

In steam-foam treatments, often times field personnel quote indices like so many pounds of surfactants have been used to produce an incremental barrel of oil. Can you give me a range?

Response by Ralph Cooke

We usually evaluate a treatment project from the standpoint of cost per incremental barrel of oil produced. From this perspective, the cost varies from less than a dollar per barrel to several dollars per barrel of incremental oil. If you used wrong material and/or wrong program, it can cost up to $10/bbl. In most cases though the treatment cost generally ranges from $1 to $3/bbl of additional oil produced. Since the treatment costs vary with the reservoir and process conditions and type of materials to be used, we cannot give a definitive number to the operator.

Question for Ralph Cooke from Maura Puerto, Exxon Production Research

Did you experience any emulsion problem? If so, how much did it cost to break the emulsion?

Response by Ralph Cooke

Virtually all steam injection operation in heavy oil reservoirs results in emulsion production, irrespective of any chemical usage. Use of surfactants in cyclic wells does not pose any unusual difficulty in breaking emulsions. The cost of breaking the emulsion is no greater than the cost of breaking the emulsion produced without the foamer. I cannot say for certain that the foaming agents will not aggravate the emulsion problem. In our 20+ years of steam-foam treatment experience, we have not encountered a project where the operation has to be suspended due to an emulsion problem.

Comment by Shane Mohammadi

I would like to make a comment about emulsion problems in cyclic wells subjected to steam-foam treatment. Emulsion should not be a major problem in cyclic diversion application. The reason I am saying this is because at any given time in a field only a small fraction of the cyclic wells are subjected to foam treatment and the amount of surfactants produced back from these wells are usually small and so well diluted that they pose no threat to the treatment plant operation. However, when a large number of wells in a given location are treated at the same time, there is a cause for concern. In 1986, UNOCAL implemented a large foam treatment program in cyclic wells and at one point in time approximately 20% of the wells within the field were subjected to foam treatment. This resulted in a serious and rather expensive emulsion problem in our dehydration plants. The problem disappeared when the treatment program was revamped. I think this is something that you have to deal with if you plan to implement a large scale foam diversion program in a specific lease or field.

Comment by Ralph Cooke

Thanks for clarifying the issue. If you are treating a dozen cyclic wells out of say 150 wells in a given month, then the chances are that you will have no treatment plant upsets due to produced chemicals. Normally, one should not encounter costly emulsion treatment problems in cyclic foam treatment projects unless the majority of the wells in a given area are treated simultaneously.

Question for Ralph Cooke from Louis Castanier, Stanford University

When is the appropriate time to initiate a steam-foam treatment in cyclic steam wells?

Response by Ralph Cooke

We recommend foam treatment after the third cycle or when the steam injection cycle productivity begins to drop. In our experience, steam diversion treatments are most effective when

the wells are treated early rather than late in the life of cyclic operations. One reason for that is because the oil saturation is usually high early in the life of the project and this tends to lower the treatment costs per barrel of incremental oil produced. However, there are exceptions to this rule of thumb. We have also seen wells with 20 or 25 steam cycles on it respond quite well to foam treatment.

Paper FS2—Critique of a Steam Foam Field Pilot

Question for Bill Brigham from Lyman Handy, University of Southern California

How does your surfactant slug concentration compare with the present day practices?

Response by Bill Brigham

We used a much higher surfactant concentration in our slugs than one would normally use today.

Question for Bill Brigham from Eric Waninger, Chevron Chemical Company

What do you attribute your production improvement to? Is it due to an improvement in areal conformance or is it simply because you are producing from multiple sands?

Response by Bill Brigham

I think it is both, but I cannot say for sure. Our tracer surveys showed an improvement in areal conformance. If there had been a marked improvement in areal conformance then I think we would have seen a drastic improvement in production from individual wells. I do not think that was the case.

Paper FS3—Cyclic Steam-Foam Injection in a Carbonate Reservoir

Question for Eddy Isaacs from Tad Patzek, University of California, Berkeley

I am trying to understand the production mechanism in your reservoir. In a fractured system the oil is produced by flowing through the fracture network. However, when you inject foam into such a system, it is very likely to occupy the fracture than the matrix and plug the flow channel for the oil. This situation seems to me as self-defeating. Could you explain the production mechanism?

Response by Eddy Isaacs

We deliberately selected an oil-sensitive foamer for use in this project. The foam collapses in the presence of oil. Hence, it is unlikely that the surfactant-foam will block the flow of oil through the fracture network. Since the reservoir is very vuggular, the foam is more likely to occupy these big holes and divert the steam into the matrix and cause oil to drain into the fracture. Because of

the presence of these vugs, we did not see any rise in injection pressure, but saw an increase in oil production. This is a very simplistic explanation.

Question for Eddy Isaacs from Terry Osterloh, Texaco

Do you have any evidence that some of your production increase might have been caused by a wettability reversal due to the surfactant injection?

Response by Eddy Isaacs

No, we did not look into that aspect. I do not think some of the increased production could be attributed to wettability reversal phenomena because the surfactant concentration used was very low.

Question for Eddy Isaacs from Maura Puerto, Exxon Production Research

Did you measure the interfacial tension for this system? Do you think a lowering of interfacial tension between oil and water might have been responsible for some of the production increase?

Response by Eddy Isaacs

We did not measure the interfacial tension between this oil and surfactant solution. I do not expect the interfacial tension to be a contributing factor to oil production increase because this surfactant does not significantly reduce the interfacial tension.

Question for Eddy Isaacs from Lyman Handy, University of Southern California

Did you use this surfactant in any other field? If so, did you see similar increase in production?

Response by Eddy Isaacs

This is the only field where this surfactant was used.

Question for Eddy Isaacs from Shane Mohammadi, UNOCAL

Would you or anyone in the audience care to comment on the transport of foam in a fracture-vuggular system?

Response by Eddy Isaacs

We did not study the mechanism of foam transport in a fractured reservoir. Most of the work we carried out in the laboratory has been in a simpler system. I am not sure whether the foam is transported as lamella or moves as bulk foam in the fracture. Perhaps someone in the audience would like to comment.

Comment by Clay Radke, University of California, Berkeley

Sometime ago we briefly looked into the flow of foam in a single fracture system. In a fracture system, the foam appeared to be transported as bulk foam rather than lamella. The flow characteristic is dependent upon the fractional flow. This suggests that in a vuggular system the foam is likely to be transported as bulk foam. Any opinion?

Response by Eddy Isaacs

The lateral continuity of vugs is critical to the flow of foam in a vuggy system. I am not sure vugs are present everywhere in the reservoir. If such is the case, I am not sure how the nature of the foam flow changes upon exiting the vugs. The only thing we are sure about is that the injection of foam resulted in increased oil production. This and some other data suggests that foam did manage to create some diversion.

Question for Eddy Isaacs from Tad Patzek, University of California, Berkeley

Why is the cycle No. 11 so productive, while the earlier ones are not?

Response by Eddy Isaacs

I cannot speculate on that question at this time. This work shows that sometimes perseverance pays off.

Paper FS4—Steam Foam Mechanistic Field Trial in the Midway-Sunset Field

Question for Mike Smith, Chevron Oilfield Research, from Eddy Isaacs, Alberta Research Council

You mentioned that the foam front and the liquid surfactant front arrived at the observation well at the same time. Other people have reported that in real reservoirs foam front propagate much more slowly than the surfactant front. Do you have an explanation for that?

Response by Mike Smith

I do not have an explanation for that. Our conclusion was based upon the arrival time of injection pressure waves and surfactant front at the observation well. We monitored the pressure pulse at the observation well continuously and analyzed the observation well fluids periodically for the presence of surfactant. We did see the arrival of surfactant front at the observation well coincide with an increase in the observation well bottomhole pressure.

Comment by Shane Mohammadi, UNOCAL

I want to make a comment on the arrival time of surfactant and foam front at the observation well. I want to caution people who monitor the surfactant and pressure pulse movement in the reservoir and trying to correlate these two movements. In laboratory coreflood experiments you may be able to correlate the arrival time of pressure pulses and surfactant front accurately because

of the 1-D flow characteristics. In real reservoirs, the foam propagates in three dimensions and the foam flow is affected by the tendency of aqueous based surfactant to underrun (i.e., remain at the bottom of the reservoir). This underrunning of surfactant may result in reduced surfactant concentration in gas regions of the reservoir which in turn results in a reduced rate of foam growth and propagation. Thus, foam propagation is much more complex in the field and one cannot accurately correlate the time of arrival of surfactant front and pressure pulses in the reservoir. In our pilot projects we were less than successful in correlating the arrival time of foam front and surfactant front at the observation well. In my experience, foam simulators do a much better job in providing the answer. By inputting detailed reservoir and process specific information into the simulator we can come up with a better explanation as to what is the correlation between the time of arrival of surfactant and foam front.

Question for Mike Smith from Eric Waninger, Chevron Chemical Company

Your production plot showed a fast production response to foam injection. What do you attribute that to?

Response by Mike Smith

Yes, the reservoir responded more quickly to surfactant injection than we anticipated. The plot I showed was for well 68F. I would attribute this quick production response to the reduction in steam channeling, because observation well data indicated diversion of steam to the lower zone. We believe the shutting off of the thief zone by foam rather than the increased sweep is the major reason for the faster production response.

Paper FS5—Key Factors Influencing the Success of Steam Foam Applications

Question for Eric Waninger from Tad Patzek, University of California, Berkeley

How many steam-foam field projects is Chevron currently involved with and how many projects does Chevron plan to implement in the near future?

Response by Eric Waninger

Currently, Chevron Chemicals is associated with 6 foam projects. We are very active, both in North and South America. Hopefully, in the future we will do a lot more projects.

Question for Eric Waninger from Yanis Yortsos, University of Southern California

Can you tell us a little bit about the effect of perforation on foam generation? Why is it important?

Response by Eric Waninger

The reason I think it is important is because we use perforation velocity as the controlling factor for the ability of surfactant to generate foam. In the laboratory, we measure the foaming ability of a surfactant based on the velocity through the core rather than the pressure drop across the core. We then correlate this velocity to the perforation velocity. In going through the perforation, the surfactant must attain a minimum or critical velocity to be able to generate a strong foam. The magnitude of this velocity, however, depends upon the type of completion.

Question to Eric Waninger from Bill Rossen, University of Texas

If the emphasis is not to generate foam near wellbore, but out in the formation, how important is the velocity at the perforation to the generation of foam?

Response by Eric Waninger

In that case it is not very critical. If your object is to improve sweep efficiency, then you want to get the surfactant into the formation before generating the foam. In such cases, the velocity at the perforation is not that critically important. If the objective of the project is to correct injection profile near wellbore, foam must be generated at the wellbore and the perforation velocity becomes critical.

Question for Eric Waninger from Eddy Isaacs, Alberta Research Council

In one of your slides you compared the thermal stability of your product (Chevron SD-1020) with that from your competitor (Shell LTS-18) and inferred that your product is superior, but you failed to quote the pH of the two surfactants. Products must be compared at the same pH, because the acid concentration affects the thermal stability of a surfactant. Can you tell us what the pH of the two products are?

Response by Eric Waninger

We did not measure the pH. The pH of SD-1020 was its natural state pH, which is 9 to 11. The LTS-18 data was taken from a Shell publication.

Paper FS6—Cyclic Steam Injection with Foam: Interpretation of Field Test Results

Question for Zaleyka Mendez from Maura Puerto, Exxon Production Research

What is the molecular weight of BBS (Alkyl Benzene Sulfonate) and LTS (Linear Alkyl Toluene Sulfonate)?

Response by Zaleyka Mendez

The molecular weight of BBS is 300 to 400. We do not have the information on LTS.

Question for Zaleyka Mendez from Shane Mohammadi, UNOCAL

It is well known that the temperature affects the foaming ability of a surfactant and each surfactant performs best over a particular temperature range. Did you take this into consideration when interpreting the performance of BBS and LTS surfactants?

Response by Zaleyka Mendez

Surfactant stability with temperature was not evaluated.

Comment by Shane Mohammadi, UNOCAL

It is well known that there exists an optimal temperature range over which a surfactant performs best. When comparing the performance of two surfactants, it is very important that we are comparing their optimal behavior. What this means is that we should not compare the performance of two surfactants at the same temperature. When comparing the performance of different surfactants in the field at different temperatures and field conditions, you must somehow account for the fact that these surfactants may not be behaving at their optimal condition. Otherwise, the comparisons tend to become biased.

Question for Shane Mohammadi from Jim Stevens, Phillips Petroleum Company

Does that really mater?

Response by Shane Mohammadi

Yes, it definitely does.

Question for Shane Mohammadi from Jim Stevens, Phillips Petroleum Company

No matter what surfactant you plan to use, they all have to work under the same reservoir temperature. Why should temperature matter?

Response by Shane Mohammadi

I presume you are talking about CO_2-foam application. However, in steam-foam application, the reservoir temperature varies with time, and temperature significantly influences the surfactant's foaming ability.

Comment by Ralph Cooke, Enhanced Petroleum Technology

You are presenting a post-mortem analysis of data that is at least 8 years old. In the 1980s, steam-foam projects were conducted differently than today because at that time we had very little control over many factors that can influence the project performance. For example, the steam quality which affects the surfactant's foaming ability was not accurately known then. In the 1990s, we can control many of these factors due to the availability of better monitoring tools. If you are to do this project today with the same surfactants, your analysis is likely to be different.

Question for Zaleyka Mendez from Bill Rossen, University of Texas

Your presentation introduced the concept of blocking factor. Blocking factor of 1 for a given zone would be 100% blockage. The ideal situation then would be to block all steam thief zones. My question—is that the best way to do it or is it better to look at what the optimum injection profile is likely to be and how close you can achieve it based on the injected chemical?

Response by Zaleyka Mendez

I do not know the answer for that question and I would appreciate an audience comment.

Comment by Shane Mohammadi, UNOCAL

The way Ms. Mendez defined the blocking factor, to me it is a description of the surfactant's diversion behavior. I think this definition is sufficient for this analysis. As I understand, your question refers to an extreme case and may not be relevant to the steam injection condition.

In a typical steam injection project, foam is used to divert steam from one zone to another. Consider the case where you have all the steam going to the top zone and you want 50% of it going to the top zone and 50% to the bottom zone. For such a case, I would define the optimal blocking factor as the one that would give me a 50-50 split across the zone.

SUMMARY OF PANEL PRESENTATION AND DISCUSSION

As part of the foam symposium, a six-member panel with expertise in various aspects of field foam application was convened to discuss the current state of foam technology and to assess the future of field foam applications. To garner varied viewpoints on the status of foam technology, members were drawn from diverse interest groups. These included majors, chemical suppliers, service companies, academia, and not-for-profit research institutes.

Panel Moderator: Rod Eson, Enhanced Petroleum Technology

Panel Members: Eric Waninger, Chevron Chemical Company
Shane Mohammadi, UNOCAL
Ralph Cooke, Enhanced Petroleum Technology Inc.
John Heller, New Mexico Petroleum Recovery Research Center
Laurier Schramm, Petroleum Recovery Institute

The panel presentation and discussion, which lasted for 2 1/2 hours, was divided into three subtopics to allow discussion on the different facets of foam technology and to cater the varied interest of the audience. The topics discussed included the following:

Subtopic No. 1

What characteristics make a good foaming agent?

How do you test these characteristics?

What reservoir and/or co-injection property beneficially or adversely affects the foam and whether the oil recovered is residual oil, incremental oil, or accelerated oil?

Subtopic No. 2

Foam simulation: Its importance or lack of it.

Subtopic No. 3

Field projects and how do you handle them?

Subtopic 1 was addressed by three members from the perspective of hydrocarbon-foam (Laurier Schramm), CO_2-foam (John Heller), and steam-foam (Eric Waninger). Shane Mohammadi of UNOCAL discussed the pros and cons of foam simulation (subtopic No. 2) and Ralph Cooke discussed the field implementation aspects of foam technology (subtopic No. 3).

The panel members presentation are summarized in the following paragraphs.

SUMMARY OF PRESENTATION BY LAURIER SCHRAMM

Dr. Laurier Schramm, who represented the Petroleum Recovery Institute (PRI) of Calgary, Canada, addressed the use of foam to control mobility in western Canadian hydrocarbon miscible floods. Some western Canadian basin reservoirs are characterized by the presence of connate waters that are high in hardness (25,000 ppm or higher as $CaCO_3$) and salinity (greater than

290,000 ppm NaCl). These values can be quite variable since many pools have been flooded with fresh water.

The characteristics of the surfactant that makes a good foaming agent for these environments are quite different from those used in steam-foam and CO_2-foam applications. A typical surfactant for use in hydrocarbon gas flooding of the harsh Canadian environments is one that is extremely hydrophilic, can tolerate the presence of high monovalent and divalent ion concentrations, possesses low rock adsorption characteristics, and exhibits good foaming ability in the presence of crude oil. High-temperature stability is desirable, but it need not be as high temperatures as are employed in steam-foam applications. Since very few of the commercially available surfactants were able to satisfy all of the above criteria, attempts were made to formulate surfactants to satisfy the requirements of specific reservoir environments. This proved to be an extremely difficult task. The requirement of low adsorption on reservoir rock was difficult to attain. The degree of adsorption was found to depend on surfactant structure, rock mineralogy, solution pH, salinity and hardness, temperature, residual oil saturation, and rock wettability. The foaming ability of the surfactant was found to depend on the nature of the crude oil present and on such foam lamella characteristics as surface elasticity, surface viscosity, and disjointing pressure. Many times a surfactant that exhibited good bulk foaming ability failed to perform well in ""standard" porous media (e.g., Berea sandstone). Furthermore, in some cases a surfactant that exhibited good foaming performance in Berea sandstone (or Indiana limestone) failed to perform as well in reservoir rock samples flooded at reservoir conditions. Dr. Schramm also pointed out that assessment of gas mobility reduction itself is beset with problems. The mobility reduction factors depend on not only the surfactant but also on the nature of the brine and porous medium, on foam quality and texture, and on the residual oil saturation and the nature of the crude oil. Thus, it can be extremely difficult to design a good and effective foaming surfactant for use in harsh western Canadian reservoir environments. However, when such a foam is found and applied, coreflood studies have shown it should not only improve reservoir sweep efficiency but also be effective in recovering incremental oil in the range of 2 to 10% beyond the waterflood residual oil recovery.

SUMMARY OF PRESENTATION BY JOHN HELLER

Dr. John Heller, a Senior Scientist at the New Mexico Petroleum Recovery Research Center, outlined the surfactant requirements for CO_2 foam use. These, in many respects, are similar to those for surfactants used in the hydrocarbon foam application. Briefly, the surfactant (a) must be compatible with the chemical and thermal environment of the reservoir; (b) must exhibit low adsorption characteristics on the reservoir rock; (c) should exhibit minimal solubility in the oil or in dense CO_2; and (d) must produce relatively long-lasting foam in the presence of the crude oil. Surfactants formulated to satisfy these requirements are currently being field tested for their

effectiveness in lowering the mobility of CO_2; to reduce the flow of CO_2 in high-permeability regions of the reservoir, and to produce incremental oil.

SUMMARY OF PRESENTATION BY ERIC WANINGER

Eric Waninger of Chevron Chemical Co. detailed the requirements of a good foaming surfactant from the steam-foam application perspective. These requirements were as follows:

1. The surfactant must be inexpensive and compatible with the reservoir environment.
2. The injected surfactant must be able to sustain its foaming ability over a wide temperature range. In steamflood application, the temperature will likely vary from about 250° F for a very low-pressure steaming operation to about 550° F for high-pressure operation.
3. The surfactant must be compatible with the liquid volumes that they are likely to encounter in the reservoir. The surfactant concentration may range from 0.3 to 2%, depending upon the quality of steam injected.
4. Since the foaming ability of the surfactant and the foam stability depend upon crude oil composition, laboratory tests must be performed to assure foamability and estimate the desirable surfactant concentration.
5. Although injection of foaming surfactant into the reservoir results in additional oil production, quantification of this additional production into residual, incremental or accelerated oil is not possible.

SUMMARY OF PRESENTATION BY SHANE MOHAMMADI

Dr. Shane Mohammadi, a senior scientist at UNOCAL, addressed the issues associated with the simulation of steam-foam processes. In particular, he discussed the following topics: (1) validity and reliability of steam-foam simulation studies; (2) primary factors controlling the propagation of foam in the reservoir and can the simulator be used to predict the effect of these parameters on process behavior; and (3) can the pilot steam-foam history match results be used to predict the field-wide steam-foam performance?

Simulators are reservoir management tools that can be used to improve the understanding of foam flow behavior in the reservoir and increase the odds for successful completion of a steam-foam project. Simulators have been used since the mid-80s with some success to capture certain features of successful steam-foam pilots. The currently available commercial steam-foam simulator employs semi-empirical correlations to model surfactant propagation in porous media and to simulate the dynamics of foam generation and decay. The empirical nature of the model usually precludes accurate history match, and engineering judgment is critical in the interpretation of results and in future performance prediction. Nevertheless, the simulator has been used successfully to confirm the field observations in a Midway-Sunset (CA) steam-foam pilot. Because of the incomplete understanding of foam transport mechanism in the porous media and the complex

nature of the steam-foam drive process, empiricism in steam-foam simulation practice is likely to be continued for the foreseeable future.

The primary factors controlling the rate of foam stability and propagation include surfactant type and concentration, surfactant loss mechanism (adsorption into rock, partition into oil and precipitation), reservoir salinity, matrix permeability and capillary effects. Simulation studies indicate that steam-foam simulators can predict qualitatively the effect of these factors on the process behavior.

Recently, existing steam-foam simulators have been validated using simplified reservoir prototypes and limited field pilot data. Validation at a more complex level (i.e., multi-pattern simulation) has not been attempted. Multi-pattern steam-foam recovery is a slow and complicated process and under today's economic climate, it is difficult to justify any significant effort to perform this task. Once validation at more complex levels has been completed, the simulator can be used for process optimization. For example, improved formulation of surfactants can be studied and evaluated on various techniques for surfactant injection.

SUMMARY OF PRESENTATION BY RALPH COOKE

Ralph Cooke of Enhanced Petroleum Technology Inc. discussed the techniques used in the field to evaluate the effectiveness of steam-foam treatment and their shortcomings.

Steam-foam treatment is a low-cost chemical heat diverter technique, principally employed in cyclic steam stimulation wells to correct apparent steam distribution (poor injection profile) problems. Steam-distribution problems arise in cyclic operations conducted in massive unconsolidated heavy oil-bearing sands (such as the Potter sand of Midway-Sunset field) where gravity drainage is the major producing mechanism.

Steaming operations in such reservoirs results in localized depletion of oil from the upper portions of the sand. During subsequent cycles, steam tends to seek oil-depleted zones, resulting in poor production. Steam-distribution problems in cyclic stimulation are corrected by injecting an aqueous solution of a high-temperature foaming surfactant. The surfactant converts to a stable foam on contact with steam in the depleted zones and helps redirect steam from areas of gravity override into portions of the reservoir containing greater oil saturation. As the reservoir (steam) temperature drops below 200° F, the foam converts back to a liquid and is produced with the reservoir fluids.

Some of the signs watched for in the field to confirm the success of a steam-foam treatment are: (1) increase in the tubing pressure over the average pressure prior to the treatment; (2) an increase in oil production in comparison to the expected production without the treatment; and (3) temperature-tracer surveys before and after treatment to confirm the diversion of steam into a zone that had not been contacted before.

While an increase in the flow line (tubing) and casing pressures are indicators of diverter success, pressure increase does not necessarily confirm diverter success. The results from several individual wells treated with foam diverters indicate large pressure increases without corresponding increases in oil production. In fact, some of these wells showed a decline in production. Similarly, there are cases of steam-foam treatment projects that have shown substantial increases in oil production without any increase in wellhead (tubing) pressure.

Further, production of incremental oil in wells treated with foam diverters does not necessarily confirm the diverter success. In many cases, changes made in steam rates, steam qualities, production interference from the stimulation of adjacent wells, etc., can cause production to increase. It is imperative that the effect of these factors be discounted from the determination of incremental oil due to foam treatment.

In assessing the success of a foam treatment, all of the aforementioned "watched for signs" must be considered. If one or more of these signs are not present, changes must be made to the treatment methods. These may include lowering the steam quality, changes in surfactant concentration, changes in the mode of application (for example, switching from continuous to semicontinuous application), changes in the frequency of application, etc. Thus, careful monitoring of steam-foam diversion treatment is critical to the economic success of the program.

PANEL DISCUSSION

Following the panel presentation, the session was opened for discussion. Selected questions from the symposium participants and the panel members responses are summarized in this section.

Question for Audience from Rod Eson

One of the panel members (Laurier Schramm) expressed his inability to relate laboratory tests of foam conducted on clean porous media results with those obtained using reservoir rock. Everyone I know do tests in the laboratory with Berea sandstone. Is there any real value in this kind of test? Why work with them if they do not relate to the field?

Comment by Louis Castanier, Stanford University

In the steam injection process study, all work was done in clean sand and good laboratory work under controlled conditions is good and should not be ridiculed. Most of the initial screening of surfactants for steam-foam application was done on clean sand and porous media and most of the observations are still valid, even though not necessarily correlated with field results. Good laboratory work under controlled conditions can provide us with useful information for the design of field projects.

Comment by John Heller, New Mexico Petroleum Research Center

Using a well characterized system, you can test and determine how foam forms and how it propagates in porous media. Laboratory tests shed light on the physics of foam formation and propagation in porous media and this information is critical to the development of foam simulators.

Question for Shane Mohammadi, UNOCAL, from Laurier Schramm, Petroleum Recovery Institute

What is the validity of steam-foam history matching when you do not have a very good scientific understanding of what is going on in the reservoir?

Response by Shane Mohammadi

I did not cover in-depth the current state of the steam-foam simulation. On a small laboratory scale, simulators are available that account for population balance of lamellae and address other mechanistic issues. But due to the complexity of computation and because on a field scale we are not sure what happens to these foam lamellae, the industry has adopted a different modeling approach to the development of field-type simulators. The approach that UNOCAL, as well as others in the industry have taken, is the semi-empirical approach. Because of this, the steam-foam simulation (for that matter any field level simulation) must be performed by a knowledgeable person. When you try to simulate any type of process, you really have to know the process and do some experiments to assist in history match. Also, I want to address the criticism that anyone can history match production by fiddling with parameters and call it a solution. Anyone in the audience who has significant simulation experience, whether it is black oil, compositional or any other process, knows that the history matching process is a frustrating and tedious chore. You cannot fudge one or more parameters such as the relative permeability to obtain a match and call it a solution. To history match you have to know your field and be able to zoom in on the actual solution to your problem for the time period you are interested in. No, history match is not an open field where every knob is available to you to turn. A knowledgeable person who is able to history match 30 years of production by judiciously adjusting selected parameters and then make a production prediction for the next 10 years, has done a pretty good job. My point is that steam-foam history match has validity if done properly by a person who knows the process.

Comment by Tad Patzek, University of California, Berkeley

Reservoir simulation is nonunique. This stems from the basic fact that the pressure equation that you are trying to solve is a diffusion equation, which means there is no unique solution. For example, Shell in their earlier approach to foam simulation employed the population balance technique to understand the basic physics of foam flow in the porous media. Though it has a theoretical foundation, it is very difficult to describe mathematically and solutions cannot be found except for very simple ideal cases. On the other hand, to simulate the Bishop steam-foam pilot, we

(Shell) restored to empiricism because we do not understand the physics in 3-dimension. All we did to simulate the pilot was to maintain the mass balance on the surfactant. We then looked at the foam propagation in the field pilot and adjusted the rate of propagation of surfactant in the simulator so as to match the average rate of propagation of foam in the field. The surfactant propagation rate in the simulator was varied by adjusting the surfactant partition coefficient. Thus, we have only one knob to play with. This then reflected all the first-order characteristics of the system. We were able to do a reasonable job in matching everything else by adjusting this one knob. I am very weary of multiple knob models in which people who do not know how to perform a simulation, blindly turn several knobs, come up with a solution, publish it, and call it a history match. There is one more point I want to make. Under the present economic climate, I do not anticipate industry to spend (certainly not Shell) any money in the research and development of a basic foam model. So the second best solution as pointed out by Shane is the use of semi-empirical models to describe foam propagation. I think it is the only practical solution, and I do not foresee anything else.

Question for Shane Mohammadi, UNOCAL

How much faith do you have in your simulation results and how well can you match field data when you do not know how far into the reservoir the foam moves and the characteristics of the reservoir?

Response by Shane Mohammadi

I think your question applies to simulation as a whole, regardless of whether it is foam simulation or thermal simulation or any other type of simulation. To the extent that industry has accepted the role of simulation in the decision-making process and believe me we are putting platforms out in the ocean based on the outcome of these simulation results, I think I can say confidently that industry has faith in simulation. Having accepted that, I say let us see whether we can push it one step further and apply it to predict foam pilot test outcome. This is essentially testing its validity. You are absolutely right in your comment regarding whether simulator results are valid. I think the industry has pretty much accepted them as a reservoir management tool, and I personally have accepted them. As an example, we have made significant progress in 3-D seismic data processing, and the industry is in the process of including 3-D seismic data into the simulator to better describe the reservoir. How soon we can do this and how successful we can be is not known at this time. Until then you have to exercise caution and use engineering judgment in the interpretation of foam simulation results.

Question for Shane Mohammadi from Rod Eson

In your presentation you said that you satisfactorily history matched your 9-day mini steam-foam pilot test (S. Casper Creek, WY, Mini-Foam Test) and used the results to predict reservoir

response to a 6-month-long foam injection project. Making such a long-term projection based on the results of a short-duration test involves a certain leap of faith. In simulation, the result is only as good as your input data. In the 9-day mini test all you did was to lower the steam injection rate and raise the wellhead pressure. The duration of the test is too short to confirm the oil production response changes. Given such minimal project information, my question is can you confidently predict long-term reservoir response based on short-duration results?

Response by Shane Mohammadi

You are absolutely right. In 9 days all you are doing is pressuring up the well, indicating that foam had been formed near the wellbore. It was argued that if steam is diverted away from the observation well, then the concentration of total dissolved solids in the produced water from the observation well should increase and approach that of the formation water. We observed this trend, verifying that steam diversion had occurred. The point I am trying to make is that if I can history match satisfactorily the short-duration test observations, then to me it is an indication that the simulator is capable of describing the foam propagation effect in the reservoir, and the predicted results are going to be close to what I will actually observe had I prolonged the test for 6 months. I cannot vouch for it. The next step should be the history match of our 3-year steam-foam project in Dome-Tumbardor. I understand DOE is sponsoring a project at NIPER to do this. That will then make it clear whether the simulator can do the job and predict steam-foam performance. As a designer, I have faith in the simulator, and I believe it will work. Somebody has to prove it.

Question for Eric Waninger, Chevron Chemical

When you do a steam-foam project in the field, how do you determine that the foam is working?

Response by Eric Waninger

In all the successful projects (economically successful projects) I am associated with, we have seen an increase in wellhead pressure. That is the first thing I look for.

Comment by Louis Castanier, Stanford University

Pressure increase is not necessarily an indication of success. There are documented case histories that showed substantial increases in oil production (over 1,000 bbl/d) but did not show any increase in wellhead pressure. Some other mechanism is at work. Pressure increase does not necessarily translate to economic success. There are also cases where substantial wellhead pressure increase was observed, but no significant increase in the total oil recovery.

Comment by Shane Mohammadi, UNOCAL

Let me comment on Louis' observation. In the past, back in the mid-80s, there was a tendency on the part of the chemical suppliers to come up with a multicomponent type foaming

agent designed to cause wellbore pressure increase. For example, it combines linear toluene sulfonate with some caustic in order to raise the pH and make they foam better. We tested some of these formulations. A particular formulation that comes to mind, is called "Suntech IV-FA." This particular surfactant, when tested in the field, showed phenomenal wellhead pressure increase. Soon after, when the test was completed, we saw no increase in oil recovery. In fact, the oil production went down. When we analyzed the data, we realized that the caustic in the surfactant was consumed by the reservoir rock. The surfactant by itself was not an effective foamer. One should make sure that the foamer used is compatible with the reservoir rock.

Comment by Eric Waninger, Chevron Chemical

I concede that increase in wellhead pressure does not mean success, but in all the projects I am associated with I saw at least a minimal increase in wellhead pressure. Increase in the wellhead pressure is not the only sign I look for. In steam-foam drives, often another fairly immediate thing we look for is the reduction in casing effluent production. In successful steam-foam projects, steam production at your production well goes down. That is an indication that foam blocks the high-permeability channels. When you notice a very abrupt change in casing heat production (and this happens quickly, often within a month of injecting the surfactant), it is an initial indication that the foam is doing what you wanted it to do. Another thing you can do is to run an injection profile test. After a few days of surfactant injection, run a krypton or other radioactive tracer survey, and you should notice the change. If you do not see any change, a redesign of the project may be recommended.

Comment by Todd Reppert, Exxon Production Research

I disagree. A reduction in casing heat production does not mean foam is blocking a thief zone or a channel. Foam blocks anything it can block near the injector, not necessarily a particular channel. What happens is as you increase the injection pressure for a while, the injected steam moves into the reservoir where it encounters a colder formation, so it condenses. This decreases your inflow of steam to your producer and increases the pumping efficiency. You see a decrease in casing heat production and increase in oil production due to increased pumping efficiency.

Question for Eric Waninger, Chevron Chemical

How do you know where the foam is in the reservoir and its effect on the flood?

Response by Eric Waninger

No one can tell where in the reservoir the foam is located. Perhaps a simulation study would provide the best answer. Through simulation I have seen excellent matches of field observation. Since we know the adsorption characteristics of surfactant and rock, we can estimate the surfactant loss due to adsorption and have an idea of how far the surfactant can propagate. If you have temperature observation wells, and if you see the well temperature goes up and many times these

wells also produce surfactant; this is an indication of the location of a foam bank in the reservoir. An increase in oil production hopefully is also an indication of the effectiveness of foam.

Question for Eric Waninger, Chevron Chemical

What corrective action will you implement if you do not see any visible sign indicating that the foam is working?

Response by Eric Waninger

There are several things one can do if foam is not doing what we think it ought to do. If you see no pressure response upon injecting foam forming surfactants into a well, inject surfactant at a higher rate or increase the surfactant concentration. If you still see no pressure response, increase the liquid volume fraction by lowering either the steam quality or adding water into the steam line at the wellhead. More than likely you will see a pressure response. Our experience in the laboratory and in the field indicates that the ability of a surfactant to form foam is more sensitive to liquid volume fraction than to surfactant concentration.

Question from Terry Osterloh, Texaco

Throughout the day I got the impression that it is better to get the foam out as far into the reservoir as you possibly can, but in terms of optimizing the economics of the process that is not necessarily true. Has anyone looked into that?

Response by Eric Waninger, Chevron Chemical

Yes, it has been looked at pretty thoroughly by the industry. If you have a stratified reservoir with well defined shale-sand sequence and you want to correct the injection profile problem in that reservoir, it can be accomplished cost-effectively by injecting slugs of low concentration foaming chemicals. When you inject low concentration chemicals, it will alter the injection profile near wellbore, but the foam will not move very far away from the wellbore due to adsorption into the rock. For foam to propagate out into the reservoir you have to inject large volumes of chemical.

Question from Terry Osterloh, Texaco

You modified the vertical profile for a number of layers and stopped. Is that an economical optimum thing to do?

Response by Eric Waninger, Chevron Chemical

That depends on a lot of things. If you have a well that has been completed in a certain way and cannot change it, then you may be correct. What is optimum in one case may not even be a solution to another case. You have to ask what your alternatives are and seek the best solution. The best solution is not necessarily an optimum.

Question from Terry Osterloh, Texaco

But in terms of gravity override, can you afford to put enough surfactant in the reservoir to solve that problem?

Response by Shane Mohammadi, UNOCAL

I would like to comment on the question whether you can afford to stop gravity override by injecting foam. Between the year 1986 to middle of 1989, UNOCAL injected foam continuously into four injectors in Midway-Sunset field. Now I can furnish some dollar amounts on that project. To the best of my recollection, UNOCAL spent something close to 2 million dollars on that project. This included cost of chemicals, surface facilities, and other operations expenses. During that time, the heavy oil was selling at about $18/bbl, and gradually falling. Early on in the project, we were able to recover a lot of the so-called accelerated oil and cash-in on high oil price. We made a profit on that project. Toward the end of the project, when incremental oil production was low, the oil was selling at about $11/bbl. That is when we decided to terminate the project. For the whole project, I think we made about $3.2 million. For an income like that, the project was well worth it. We were able to mitigate the gravity override problem by injecting large quantities of surfactant. But at today's oil price, the project may not be economical. If the price of the oil is say $20/bbl or more, we will consider implementing the project again. The bottom line is that if the price is right you can afford to inject surfactant to solve gravity override or any other problem associated with steamdrive.

Question by Eric Waninger, Chevron Chemical

What effect do the cheaper chemicals have on decision making?

Response by Shane Mohammadi, UNOCAL

The problem right now, especially in the San Joaquin Valley steaming operations, is that you can barely make any money. If you can barely make money out of your steam operation, it is impossible to go to management and propose a project that has a front end cost of the order of about $400,000 for surface facilities and additional half a million dollars worth of chemical. Irrespective of whether the chemical is cheap or expensive, it will be a hard sell under the current economic climate.

Comment by Jerry Casteel, DOE

I would like to make a comment here. I am Jerry Casteel from U.S. DOE and we are currently funding a project in New Mexico on profile modification with gel. This may find an application in a steamdrive reservoir, if we can design a temperature insensitive gel. One of the things we found was profile modification may sometimes do more harm than good. Simply injecting a profile modification chemical into the well and allowing it to go where it wants to go may not be the best thing to do. Monitoring the project is critical to confirm the diverting character

of the chemical and then taking corrective action, if needed. You may inject a gel and get a pressure response and think the well is responding properly, when in fact you may be getting crossflow and everything else in the reservoir. Unless you do a zonal isolation to ensure that the chemical is going where you wanted it to go, you may be out of luck.

Question by Rod Eson, Enhanced Petroleum Technology

To wrap up this panel discussion session, I want to throw in one final question to the participants and panel members. The question is though foam technology is proven to be both technically and economically viable, why aren't more people doing this in the field? I would like your personal opinion, not your company's position. I would like the audience to answer first, and then the panel members. Keep your comments brief please.

Comment by Tad Patzek, University of California, Berkeley

I contributed to steam-foam research at Shell and no doubt my work contributed to the success of Shell's steam-foam pilot. I can tell you the reason why many steam-foam projects are not being implemented. There is no such thing as a generic steam-foam process. Every steam-foam project is unique and must be tailored to a particular reservoir. Each company or corporation inventories its portfolio of reservoirs and seeks processes that are applicable to those reservoirs. In the case of Shell, it is steam. Since Shell has started steam projects much earlier than other operators, its thermal projects are nearing their economic limit. The projected recovery from Shell's steam projects are very high on the order of 70% or more of OOIP. Therefore, at the moment you are proposing a steam-foam project in a matured reservoir where steamflood proved to be very efficient. You are trying to compete against a very efficient and cheap process and going after an oil that is very difficult to recover. Even though we have shown that steam-foam processes can economically recover incremental oil, it was disregarded because the rate of return from steam-foam projects from Shell's point of view does not meet its corporate objectives.

Comment by Rod Eson, Enhanced Petroleum Technology

It is a catch-22 situation and is true for any EOR process. If you start early, you can make money, but convincing management to start the project early is nearly impossible.

Question by Eric Waninger, Chevron Chemical

Is the price of surfactant derailing the project economics?

Response by David Hutchison, Shell Western E&P

That is correct. In Shell's case, the operating personnel were going after continuous surfactant injection. This increased the cost of steam-foam pilot. Most of the steam-foam projects are only marginally economical. The incremental profit over and above the well-conceived and

well-run steamdrive projects were less than acceptable to management, and under such situations it is difficult to convince management to commit funds for additional projects.

Comment by Nizar Djabbarah, Mobil

Under today's economic climate, you cannot afford to inject surfactant continuously to produce incremental oil. You have to balance the value of surfactant injected to the value of oil produced. Mobil had very good success in recovering oil with steam-foam in the Tulare. The reason for that is we have a very good understanding of surfactant, rock interaction and the losses due to adsorption were more favorable than in other formations. The geology of Tulare is such that there is connectivity between flow channels and the foam is able to block thief channels. Surfactant that works best in one area may not work in another area. You have to take your time and evaluate the surfactants for that specific reservoir and specific injection and well completion scheme. You must base your economics on surfactant type, steam quality, steam injection rate, and expected additional recovery. If you keep your surfactant injection rate constant or surfactant, concentration same throughout the life of a project, it probably is not going to be economical. Since steam quality and injection rate varies from day-to-day, keeping surfactant injection rate or surfactant concentration constant is not going to be beneficial. You have to have a good understanding of potential surfactant losses and the effect of steam quality on the surfactant formability to do an effective job. You have to do your homework well ahead and move cautiously. If you do that, chances are the project will succeed. Coming to the main question, will Mobil continue steam-foam projects, I will say no. Steam-foam projects are manpower intensive and involve a lot of leg work. and the current economic conditions do not justify that.

Comment by Shane Mohammadi, UNOCAL

I would like to offer an explanation for why I think the management of many oil companies are not supporting this type of work to the extent they should be and also offer a suggestion as to how you can get around that.

In my opinion, foam technology, whether it is applied to steam, CO_2 or hydrocarbon miscible drive, is truly a tertiary recovery process. The object of the foam process is to recover the oil left behind by steam or CO_2 or what not. The management and operational personnel of most oil companies are very comfortable with primary production and somewhat comfortable with secondary recovery operations, but skeptical with tertiary recovery. Part of the skepticism arose from the failure of tertiary recovery processes such as the chemical flooding of the 1970s. Foam is a truly tertiary process, and there are risks involved in implementing it. When I started my career in foam, I was under the impression that here is a substance that is primarily gas and I am only using very little chemical to generate large volumes of foam and arrest mobility. In reservoirs, we are dealing with huge pore volumes, and foam is the only substance that can cost-effectively plug

the depleted zone and improve volumetric conformance. I am still convinced foam technology has a much better chance of acceptance than some other exotic techniques we have developed over the years.

Now, let me explain how we can convince management to go along with doing a project like this. First, identify the problem areas in the field, wherever that may be. Then at a very low level, say at the engineering supervisory level, propose some sort of small duration test. The cost of the project must be very minimal. At the same time, make sure what you are proposing is likely to succeed and you have a good understanding of it. For example, we proposed and implemented a 9-day mini steam-foam test and demonstrated to the management, the viability of the project. Once you have established the viability of your mini project, go ahead and propose a short-duration expansion, say a 6-month project. Keep your fingers crossed and hope that towards the end of 6 months you have some positive results. If you do, then you can expand your expansion. This is exactly what we did with one of our major steam-foam project. The original project was designed to be a 6-month experimental project, but we continued it on for 3 1/2 years. We were able to do that because we showed positive results at the end of each year and the management was willing to funnel additional money into the project. The project was highly profitable to the company. Thus, the key to a successful project is to start small and expand as you go along. In my opinion, this is the only way to overcome management's skepticism on tertiary recovery projects.

Comment by Rod Eson, Enhanced Petroleum Technology

Let me offer my views before bringing today's session to a close. I have been associated with steam-foam technology for almost 20 years, the last 13 of which was in sales, design, and implementation of the process. In my opinion, none of the explanations offered by previous speakers satisfactorily answer the question. The technical and economic viability of steam-foam technology have been well established. As Nizar (Djabbarah) pointed out, economic success can be assured by careful design. Politics, more than economics, is the primary reason why we are not seeing many steam-foam projects. Because of low oil prices, oil companies have slashed their staffs and moved people around. Engineers, who have escaped the ax, are under pressure to show profit. Their bonus depends upon keeping the operation in the black. So, the engineers are less willing to take a risk. If we do succeed in getting a project approved and by the time we complete the design and are ready to implement it, the engineer who approved it is not around. I can name dozens of projects where we have gone through this—when a new engineer who is responsible for implementing the project comes along, they are reluctant to spend the money. If he implements the project and by the time the project bears the fruit he is not going to be around to collect his bonus. So there is no incentive for him to spend the money.

No. FSP1

DOE/NIPER

Oil Interaction with Foams at Static and Flowing Conditions in Porous Media

by M. Dalland and J. E. Hanssen, Rogaland Research, Stavanger, Norway, and T. S. Kristiansen, IKU Petroleum Research a.s., Tondheim, Norway

Author(s) are solely responsible for copyright and contents.

This poster/paper was prepared for presentation at the DOE/NIPER, Symposium on Field Application of Foams for Oil Production held in Bakersfield, California, February 11-12, 1993.

This paper was selected for presentation by a Program Committee following review of information contained in an abstract submitted by the author(s). Contents of the paper, as presented, have not been reviewed and are subject to correction by the author(s). The material, as presented, does not necessarily reflect any position of the U.S. Department of Energy or the National Institute for Petroleum and Energy Research.

Introduction

Because of its dispersed nature, foam can have a profound influence on the fluid flow patterns in a reservoir. A properly designed foam can reduce gas mobility by several orders of magnitude [1]. Foam selectively reduces gas flow, leaving the relative permeability of its liquid phase unchanged [2].

Foam confined inside a pore network on the scale of that in most reservoir rocks has a different morphology from that of bulk foams [3, 4], as illustrated by Figure 1. A confined foam lacks the complex three-dimensional structure of bulk foam and is made up of single gas bubbles separated by liquid lamellae. Its flow behavior is largely dominated by lamella/pore wall interaction [5]. Bulk foam properties should therefore be applied to confined foams with caution. Nevertheless, successful correlation of foam stability measured in various bulk foam tests with porous-medium foam performance has been reported [6-8].

In our previous work, we have studied foam with different reservoir applications in mind, *viz.* in injection wells to reduce the overall mobility of injected gas [9-12], or in production wells to reduce the gas/oil ratio [13-17]. For efficient gas blockage, foam must be oil tolerant, while for mobility reduction, some oil sensitivity may be acceptable or even beneficial under some circumstances [18]. A proper characterization of foam/oil interaction, ideally resulting in a screening criterion based on measurement only on bulk foams or bulk solutions, is equally required in both cases. This motivates the present work.

A recent paper provides some guidance on our current phenomenological understanding of how foams influence reservoir flow, referencing key works in the literature [19]. In the present context, our main interest is the interaction between aqueous foam and oil at elevated temperatures in porous media. High temperature is known to be detrimental to foam stability in the bulk as well as in porous media. Oil is also detrimental, but its interaction mechanisms with foam in porous media are complex and remain unclear despite much research. However, to the extent that film stability phenomena are controlling both cases, general conclusions on the somewhat better described effects of foam inhibitors on foams in general should apply and are chosen as our starting point.

Robinson and Woods [20] noted that for a droplet of potential defoamer (such as oil) to affect the stability of a foam film, it must first be able to wet the aqueous/gas interface. This process of penetrating, or entering, the interface is thermodynamically favorable if the sign of the *entering coefficient* is positive:

$$E_{ow} = \sigma_{wg} - \sigma_{og} + \sigma_{wo} \qquad \text{(eq. 1)}$$

Equivalently, one might consider the aqueous phase *not* to spread around an engulfed oil droplet, or *dewetting* the oil. Of the 54 systems investigated by Robinson and Woods, all 14 cases where E_{ow} was negative (or zero) gave foam films unaffected by the presence of "oil". 40 cases had $E_{ow} > 0$, of which 37 showed foam inhibition [20].

The coefficient for *spreading* of oil on an aqueous/gas interface, due to Harkins [21]:

$$S_{ow} = \sigma_{wg} - \sigma_{og} - \sigma_{wo} \qquad \text{(eq. 2)}$$

was proposed by Ross as an additional stability criterion [22], noting that $S_{ow} > 0$ implies $E_{ow} > 0$. When a defoamer is applied to bulk foam, foam lamellae will rupture when oil is dewetted on both sides [23]. The intermediate configuration of oil entering but not spreading on the aqueous/gas interface is not well described.

Aqueous foams in reservoir rock may contain films separating gas from oil in addition to foam films. Such *asymmetric films* have been much studied on bulk liquids [24], and are often

referred to as *pseudoemulsion* films by analogy with bulk emulsions [25]. Wasan, Nikolov *et al.* [26] defined stability criteria for such films based on interferometric and visual film studies. They commented that spreading and entering parameters should be calculated from actual values of the various tensions operating in the pseudoemulsion film, which may be different from those measured on bulk phases. In a micromodel study, Radke and Manlowe observed that the rupture of pseudoemulsion films initiated rupture also of surrounding foam films [27].

It is well known in defoamer formulation that reduction of the particle or droplet size to approximately the thickness of a foam lamella is a requirement for its effectiveness as a foam inhibitor [22, 23]. Similarly, a parameter called the *lamella number* has been defined to characterize the emulsification of oil droplets into foam lamellae moving through a water wet porous medium:

$$L = \frac{\sigma_{wg}}{\sigma_{wo}} \cdot \frac{r_o}{r_p} \qquad \text{(eq. 3)}$$

Here, r_o is the radius of an oil droplet engulfed by water, and r_p is the radius of curvature at the Plateau border of the aqueous foam film. The reader is referred to the original work of Schramm *et al.* [28-30] for the microvisual observations which formed the basis for this definition and a discussion of the physical phenomena considered. In this paper, we merely want to test the lamella number as an empirical correlating parameter for our data, on a par with entering and spreading coefficients. In the lamella number model, the value of L determines whether oil can get into the thin foam lamellae. If it can, then S_{ow} and E_{ow} become relevant [28]. A value of $L > 1$ would favor emulsification of oil and thus be a first step towards destabilization of the foam.

Experimental

All porous medium experiments reported here were performed at back pressures of order 10 bar. The flowing foam experiments were conducted at 80 °C and the static, or gas-blocking, foam experiments at 70 °C. The flowing foam experiments were performed on 500 md Berea sandstone with lengths of approximately 0.4 m according to experimental procedures described elsewhere [11, 12]. The gas blockage experiments with foam were performed on 2 m long packed columns of 8 darcy permeability as previously described and validated against sandstone-core data [15, 17].

Gas blockage tests are considered to represent the persistent state of static foam required for an effective production well treatment.

Bulk foam stability was measured by the gas sparging method using large test columns to minimize wall and end effects. Surfactant solution and oil were equilibrated in the test apparatus at test temperature for 48 hours. Gas was bubbled through a sinter with pores the same order of magnitude as those in the bead packs (25 μm) into glass columns 100 cm tall, 2.0 cm in diameter, and containing 10 ml surfactant solution equilibrated with 2 ml of oil. Gas was fed at an optimum velocity selected for steady foam growth, low rate sensitivity and good repeatability until foam reached a constant level or the top of the column. Foam volume was measured from the time when gas flow was switched off, correcting for heterogeneities in the decaying foam. Drainage of oil and aqueous phase was measured separately, if possible. Qualitative observations of foam texture were made.

For gas blockage tests and bulk foam measurements, a Norwegian naphthenic crude oil of density 0.877 g/cm^3 (30 °API) was used, denoted Crude 1. In the flowing foam experiments, four different oils were used: Crude 2, a Norwegian paraffinic crude of density 0.820 g/cm^3 (41 °API), tetralin, acetophenone and a (70 vol% : 30 vol%) nonane : xylene blend. The aqueous phase was synthetic sea water in the gas blockage tests and a synthetic brine with 32.2 g/l NaCl and 2.8 g/l $CaCl_2$ in the flowing-foam tests. Surfactants used are listed in Table 1. Surfactant concentrations are expressed as weight per cent active material. Nitrogen was used as the gas phase.

Interfacial tensions were measured at 70 °C or 80 °C and atmospheric pressure using the pendant drop, spinning drop or ring tensiometer methods as appropriate for each system.

Results and Discussion

Gas-blocking foams

Conventional surfactants

Results of static foam gas-blockage tests for a set of foaming agents with conventional (hydrocarbon) hydrophobic chains are shown on Figure 2. The data were obtained for foams generated *in situ* by gas displacing surfactant solution from a pack containing residual oil, at a differential pressure of order 1 bar. In cases

favorable to formation of gas-blocking foam, this results in establishment of a persistent state characterized by constant saturation and gas flowing through the essentially static foam at greatly reduced mobility. If the applied pressure drop ΔP is increased, successive gas-blocking states may be reached, and an apparent gas permeability k_{gf} and relative gas mobility, k_{gf}/k calculated for each ΔP. The phenomenon is described more closely in two other papers [31, 32]. For now, we state that good performance is exemplified by the data in the lower right of the figure. At 70 °C and in the presence of oil, however, it is seen that this group of surfactants, which includes most common types of foamer and many excellent gas blocking agents for oil-free porous media, cannot reduce gas mobility sufficiently to be of interest for field use. Most of them do not even reach a gas blocking state, but instead display a continuously increasing flow rate of foam and gas. Based on these performance data, they are all cathegorized as oil sensitive foams. The destabilizing effect of oil is greater than that of temperature.

Fluorinated surfactants

The use of fluorinated surfactants for generating foam in oil reservoirs was suggested by Robin [33], who noted the marked oil tolerance of one such foam. Little has been published about the relative merits of the various classes of fluorosurfactants as foaming agents. Some investigators have compared one fluorosurfactant with a set of conventional surfactants and tried to derive general conclusions on differences in properties [30, 34]. We wanted to study a range of fluorosurfactants. The general structure of eight fluorosurfactants studied are given in Table 1.

Figure 3 shows results of gas-blockage tests in porous media, corresponding to those in Figure 2. Four of the eight fluorosurfactant foams are categorized as gas-blocking. They reduce gas permeability by two to four orders of magnitude even at higher differential pressures. The remaining four fluorosurfactant foams give significantly poorer performance, two actually being inferior to a conventional surfactant.

Surfactant structure might be expected to give some clue, in that three of the four fluoroalkyl ethoxy alcohols included produce oil tolerant foams. But this hardly qualifies as a selection criterion; further, the fourth oil tolerant system identified (FC 751) is a perfluoroalkyl sulfobetaïne, an analog of which (Hoe S 3172) gives an oil sensitive foam.

Assuming all the aqueous phase to be in the foam, foam qualities , Γ, in these tests range from 0.79 to 0.98 and S_{or} was approx. 0.12 (average S_{orw} in the preceding waterflood for 27 tests; little oil was mobilized by foam). Note that foam quality is a resultant variable, not a set parameter, in a gas-blockage test.

Bulk foam stability

To evaluate any great number of products for field application, a quick "pre-screening" test would save time and effort. As mentioned, bulk foam stability has been widely used for this purpose, but our introductory studies gave no correlation between gas blockage performance and bulk foam stability as measured by a simple shake test [35]. However, following the advice of investigators who did obtain correspondence between bulk and porous-medium foam data [34], we put some effort into designing a better bulk test. Our main aims were to ensure good repeatability and close mechanistic similarity between the two kinds of experiment. See *Experimental* for details.

The eight fluorosurfactants produced bulk foams of widely differing stability in the presence of oil, with foam volume half-lives ranging from a few minutes to several hours. On Figure 4, we have selected one point in time which quite well captures the main trends found. There are three quite stable bulk foams: Zonyl FSC, Hoe S 3172 and Fluowet CL. Fluowet OTN, Zonyl FSO and Zonyl FSN are especially poor performers. These trends are repeated in half-lives and when comparing liquid drainage and texture observations: Zonyl FSC foam drains slowly and has very fine bubbles with little spread in size; Fluowet OTN produces heterogeneous, coarse foam.

Thus, a ranking appears which is completely different from that based on gas-blockage performance, as summarized by the cross-plot in Figure 5, obtained by extracting single point data for both performance evaluation methods. A positive correlation here should place the effective gas-blocking foams in the lower left corner. We consider this firm evidence that, for aqueous foam in the presence of oil, bulk foam stability — even when measured by this carefully designed test — **cannot** predict the suitability of any particular system for use as a gas-blocking foam in a porous medium.

Flowing foams

On the pore level, the phenomena that govern foam/oil interaction should be the same in a flowing foam experiment and a static foam

experiment, although it has been suggested that flowing oil-sensitive foams may be "dynamically metastable" if moving lamellae and oil are in contact only for limited periods [27]. To facilitate comparison with the gas blockage data, results at comparable foam quality (*i.e.*, probably similar saturations) were selected. Figure 6 shows measured apparent viscosities as a function of interstitial velocity for foams of C_{14} AOS surfactant in contact with four different oils; nonane/xylene blend, Crude 2, acetophenone, and tetralin, at foam quality of 0.94. Clearly, a given surfactant can be made to produce oil sensitive or oil tolerant foams by changing the oil.

The properties of flowing foam are expressed by apparent viscosity, μ_{app}, calculated by Darcy's law:

$$\mu_{app} = \frac{k \cdot A \cdot \Delta P}{q \cdot l} \qquad \text{(eq. 4)}$$

Interfacial properties

As bulk foam stability was found not to correlate with porous medium behavior, we searched for a set of physico-chemical properties that might explain the variation in foam oil tolerance observed and thus be useful in pre-screening. Also, we hoped to learn something about the phenomena controlling oil tolerance in foams. In the present paper, we would like to focus on the measured interfacial tensions at high temperature, listed in Table 2. Table 3 presents the values obtained for the proposed correlating parameters S_{ow}, E_{ow}, and a simplified form of L (explained below).

Spreading and entering coefficients may be calculated from IFT's for non-equilibrated or equilibrated phases (σ° or σ in Tables 2 and 3, respectively), giving initial or final values. There are significant differences between equilibrated and non-equilibrated systems for some surfactants. The water/gas IFT is slightly affected by equilibration with oil. A previous study [14] found that the change in σ_{wg} due to equilibration with oil correlated surprisingly well with foam gas-blockage performance for a set of model oils and surfactants at room temperature. A corresponding trend is not repeated in the crude oil/high temperature data. However, since the changes measured for the model systems were slight (between -1 and +4 mN/m), trends may be overshadowed by the greater measurement errors in the present systems. The oil/gas IFT was somewhat more influenced by equilibration than was the water/gas IFT. Most of these predominantly water-soluble surfactants are thus to some degree surface-active also on the oil phase. This has been shown before for some fluorosurfactants [36], but is not always considered for other systems.

If foam or foaming agent solution is flowing through a porous medium containing oil, the aqueous phase will quickly become saturated in oil. Whether oil becomes saturated in surfactant depends on whether the oil has been contacted by foam or surfactant solution. To the extent that foaming agent solution and oil are equilibrated in the porous medium, equilibrated rather than initial IFT's should therefore be used in correlating foam properties. For our AOS systems, only initial values of σ_{wg} and σ_{og} were available. However, equilibrated IFT's for the same oils with a different AOS have recently been measured by Fagan [37] and are close to initial values for this system. It is therefore unlikely that replacing initial with final values will change the signs of E_{ow} or S_{ow} The only possible sign change is for S_{ow} in AOS/tetralin, but even if this happened, it would only produce one more case of $E_{ow} > 0$ and $S_{ow} < 0$ and thus not contradict any of our conclusions (see below).

For the fluorosurfactants, only final values can be used in correlating because otherwise, all systems would have $E_{ow} < 0$ and thus be predicted to create oil tolerant foams.

In the static foam data, all systems have negative spreading coefficients, but only four were found to make oil tolerant foams. The only data with positive oil-spreading coefficients are the two oil sensitive flowing foams. The criterion about spreading as an indicator of oil tolerance [38] is therefore not sufficient: a spreading oil does give an oil sensitive system but the reverse is not true.

Entering coefficients for the systems studied have positive as well as negative values. Four systems have negative E_{ow} and S_{ow} (including one with $E_{ow} = 0$ within experimental error) and all create oil tolerant foams, both in the static foam experiments and flowing foam experiments. The two systems with $S_{ow} > 0$,are seen to be oil sensitive. The configuration with a positive entering coefficient and a negative spreading coefficient accounts for 7 of 13 systems studied. This group includes both oil sensitive and oil tolerant foams, and there is no correlation between the value of the coefficients and the measured oil sensitivity of the foam.

Schramm's definition of the lamella number includes the ratio of the oil droplet radius r_o and

the radius of curvature at the Plateau border r_p. These cannot be measured in our porous media. Schramm [29] measured the ratio r_o/r_p for his systems in a micromodel and found it to be a constant equal to 0.15. We thus choose to exclude the ratio and use a *pseudo* lamella number:

$$L' = \frac{L}{(ro / rp)} = \frac{\sigma_{w/g}}{\sigma_{w/o}} \qquad \text{(eq. 5)}$$

By the original definition, $L < 1$ would favor oil tolerant foams. If we follow Schramm in assuming $r_o/r_p = 0.15$, the corresponding value of L' should be ≈7. In any case, the chances of finding an oil tolerant foam should be greatest at low values of L. However, in our data, we find oil tolerant foams with L' values from 1 to 65 and oil sensitive foams with L' from 2 to 37. As Figure 7 confirms, there is no correspondence between the pseudo lamella number and the oil sensitivity of the foam. One of the reasons for this could be that we take the radius ratio to be constant. In a realistic porous medium, it is difficult to predict this ratio, although it might be expected to be a constant for media of identical pore size distribution, saturation, and wettability as is likely the case within each of our data sets on beadpacks and sandstone cores. However, Schramm also observed foams that were quite stable to oil in the micromodel (and hence had low lamella numbers) to produce low mobilities in corefloods [28]. To the extent that such a trend would be captured also by the pseudo lamella number, a similar correlation is absent in our data.

With the lamella number unsuccessful, and the E and S coefficients merely predicting the majority of our systems to be unpredictable, the outlook for finding a simple physico-chemical correlating parameter for our foam oil tolerance data appears disappointing. We feel the apparent lack of understanding of the "entered, but not spread oil" configuration, and its wide occurrence in our data, justifies some speculation. Figure 8 is a simplistic attempt to illustrate the spreading conditions possible. Surfactant-stabilized aqueous films on oil are well known and correspond to water spreading on oil. Since $S_{wo} = -E_{ow}$, this is nonentering oil as in the left beaker. The middle beaker shows the entering, nonspreading case: oil has entered the aqueous/gas interface, breaking the film and leaving submerged aqueous lense on the oil surface. In the right beaker, oil spreads on water.

The condition of entering oil cannot, therefore, be associated with the presence of a stable pseudoemulsion film. If gas is introduced to a system of oil engulfed in water, and these conditions prevail, water will retract from the oil drop and oil will achieve direct contact with the gas. Returning to our picture of foam and oil in pores (Fig. 1), no coherent gas bubble could exist in the pore body bordering an oil droplet unless the oil droplet was on all sides surrounded by stable aqueous films. This requires oil to be non-entering. Thus, $E_{ow} > 0$ must be a necessary *and sufficient* condition for unstable foam, as originally stated by Robinson and Woods, and the reason we observe oil tolerant foams at this configuration *must be that our values of E_{ow} are not representative for the conditions in the pores*. Notably, the capillary pressure in porous media may be significant while E_{ow} is calculated from IFT's measured at zero P_c. We speculate that, if a suitable method were available to measure entering coefficients at the relevant capillary pressure for a given porous medium and set of conditions, it would indeed predict the oil tolerance of a foam.

Such a method may be available. E_{ow} is the integral of disjoining pressure π with respect to the film thickness h [39, 40] and can therefore be measured by thin film techniques and interpreted by DLVO theory [41]. Recently, trends in measured π *vs.* h (film thickness) isotherms for pseudoemulsion films [40] have shown good correlation with flowing foam mobility in the presence of oil [37]. Only positive portions of the π (h) curve can be measured. However, the value of E_{ow} at the thinnest film where $\pi = 0$ corresponds to the E_{ow} obtainable from ordinary IFT measurements at zero capillary pressure. Consequently, measuring the positive values of π from this point to the appropriate level of P_c, or to the maximum P_c that the film can withstand, should give the additional negative contribution to the actual entering coefficient for the porous medium system.

Conclusions

New data for the oil tolerance of foams in porous media has been obtained through the apparent foam viscosity at steady state foam flow, and the degree of gas permeability reduction at gas blockage, for a wide range of systems including a set of fluorinated surfactants. In both modes of experiment, oil tolerant and oil sensitive behavior can be clearly and consistently distinguished.

At gas blocking conditions, a set of conventional surfactants created only oil sensitive foams with the crude oil selected. The fluorosurfactant foams showed all ranges of oil tolerance from being as strongly gas blocking as the best foams known in oil-free systems, to

foams even more oil sensitive than those created by typical conventional surfactants. Four of eight fluorosurfactants were categorized as creating oil tolerant foams. At flowing foam conditions, the same conventional surfactant was found to give oil tolerant or oil sensitive foams as a result of varying the oil.

A negative oil entering coefficient without exception predicted correctly the formation of an oil tolerant foam in the porous medium tests, and a positive oil spreading coefficient conversely predicted an oil sensitive foam. For systems with positive entering, but negative spreading coefficients, both types of behavior were observed. Bulk foam stability and a simplified lamella number did not correlate the data. The predictions found were of equal strength for flowing and gas-blocking foams, for conventional and fluorinated surfactants, in cores and beadpacks, and in the presence of several oils.

We cannot visualize the presence of a stable pseudoemulsion film in a system with entered but non-spread oil, and thus expect all such systems to create unstable foams. We therefore speculate that systems of this configuration in reality are subject to non-entering conditions in the porous medium, and that if E could be measured at the prevailing capillary pressure, it would correctly predict the observed oil tolerance of the foam.

Acknowledgments

We are very much indebted to Vance Bergeron for the last paragraphs of the discussion in particular. Any oversimplifications on the basis of his results and their implications are our own responsibility. The expert laboratory work of Paul Goonewardene is acknowledged. Financial support for parts of the work reported was given by Norske Shell and Statoil under the program *Foam as a gas-blocking barrier* and by the State program for improved recovery research, SPOR. Additional financing for preparation of the paper was given by the newly initiated RUTH program as a part of its Foam subprogram, co-sponsored by NTNF, Norsk Hydro, Norske Shell, and Amoco Norway.

Nomenclature

S_{ow} = Spreading coefficient of oil on water
E_{ow} = Entering coefficient of oil through water
L = Lamella number
IFT = Interfacial tension
σ_{wg} = Interfacial tension between water and gas for equilibrated systems
σ_{og} = Interfacial tension between oil and gas for equilibrated systems
σ_{wo} = Interfacial tension between water and oil for equilibrated systems
σ°_{wg} = IFT between water and gas for non-equilibrated systems
σ°_{og} = IFT between oil and gas for non-equilibrated systems
r_o = Radius of an oil droplet engulfed by water
r_p = Radius of curvature at the Plateau border of an aqueous film
k = Absolute permeability of a porous medium
k_{gf} = Gas permeability through foam
ΔP = Differential pressure
Γ = Foam quality, gas volume fraction
S_{or} = Irreducible oil saturation
S_{orw} = Irreducible oil saturation to water
μ_{app} = Apparent viscosity
A = Area [m^2]
q = Flow rate [cm^3/s]
l = Length [m]
π = Disjoining pressure
MRF = Mobility reduction factor

References

1. L.W. Holm and G.G Bernard: "Effect of Foam on Permeability of Porous Media to Gas". *Society of Petroleum Engineers Journal*, September, 1964, 267-274.
2. L.W. Holm: "Mechanism of Gas and Liquid Flow through Porous Media in the Presence of Foam". *Society of Petroleum Engineers Journal*, **8:** June, 1968, 359-369.
3. J. J. Bikerman: *Foams*. Springer-Verlag: Berlin 1973.
4. S. Ross and I. D. Morrison: *Colloidal Systems and Interfaces*. Wiley-Interscience: New York 1988.
5. G.J. Hirasaki and J.B. Lawson: "Mechanisms of Foam Flow in Porous Media: Apparent Viscosity in Smooth Capillaries". *Society of Petroleum Engineers Journal*, **25:** February, 1985, 176-190.
6. A.R. Strycker, M.P. Madden, and A.P. Sarathi: "Effectiveness of screening tests as predictive method for steamflood additives". *SPE Resv. Eng.*, **2:** 4 (November), 1987

7. J. Borchardt, *et al.*: "Surfactants for CO_2 foam flooding". Paper *SPE 14394* presented at the *60th Annual SPE Technical Conference and Exhibition*, Las Vegas 1985.
8. F.E. Suffridge, K.T. Raterman, and G.C. Russell: "Foam Performance under Reservoir Conditions". Paper *SPE 19691* presented at the *64th SPE Annual Technical Conference and Exhibition*, San Antonio 1989.
9. T. Holt and T.S. Kristiansen: "Foam flooding using alpha olefin sulfonates". Paper presented at the *5th European Symposium on Enhanced Oil Recovery*, Budapest 1989.
10. T. Holt and T.S. Kristiansen: "Improved sweep efficiency during gas injection—mobility control". Paper presented at the *SPOR Seminar*, Stavanger 1990.
11. T. Strøm Kristiansen and T. Holt: "Properties of flowing foam in porous media containing oil". Paper presented at the *IEA collaborative project on EOR, workshop and symposium*, Bath, UK 1991.
12. T. Strøm Kristiansen and T. Holt: "Properties of flowing foam in porous media containing oil". Paper *SPE/DOE 24182* presented at the *8th SPE/DOE Symposium on Enhanced Oil Recovery*, Tulsa 1992.
13. S. Ekrann and J.E. Hanssen: "Method for Establishing Effective Barriers to Production of Undesired Fluids in the Recovery of Oil". *U.S. Patent no . 4 903 771* (1990).
14. J.E. Hanssen and T. Meling: "Gas-blocking foams in porous media: Effects of oil and surfactant hydrophobe carbon number". *Progr. Coll. Polym. Sci.*, **82:** 1990, 140-154.
15. J.E. Hanssen and M. Dalland: "Foams for Effective Gas Blockage in the Presence of Crude Oil at Reservoir Temperature". Paper *SPE/DOE 20193* presented at the *7th SPE/DOE Symposium on Enhanced Oil Recovery*, Tulsa 1990.
16. J.E. Hanssen and P. Haugum: "Gas Blockage with Non-Aqueous Foams". Paper *SPE 21002* presented at the *SPE International Symposium on Oil-Field Chemistry*, Anaheim, CA 1991.
17. J.E. Hanssen and M. Dalland: "Foam barriers for thin oil rims: Gas blockage at reservoir conditions". Paper presented at the *6th European Symposium on Improved Oil Recovery*, Stavanger 1991.
18. L.W. Holm: "Use of Surfactant to Reduce CO_2 Mobility in Oil Displacement". *Society of Petroleum Engineers Journal*, **20:** August, 1980, 281-292.
19. J. E. Hanssen: "Use of foams in gas flooding", in *Recent advances in Improved Oil Recovery Methods for North Sea Sandstone Reservoirs* (S. M: Skjæveland and J. Kleppe, Editors) Norwegian Petroleum Directorate, Stavanger 1992.
20. J.V. Robinson and W.W. Woods: "A method of selecting foam inhibitors". *J. Soc. Chem. Ind. (London)*, **67:** 1948, 361-365.
21. W.D. Harkins: "A general thermodynamic theory of the spreading of liquids to form duplex films and of liquids or solids to form monolayers". *J. Chem. Phys.*, **9:** 1941, 552-568.
22. S. Ross: "Inhibition of foaming II. A mechanism for the rupture of liquid films by antifoaming agents." *J. Chem. Phys.*, **54:** 1950, 429-436.
23. S. Ross: "Ch. IVB: Foams", in *Colloidal Systems and Interfaces*, Wiley-Interscience: New York 1988, 294-326.
24. P. M. Kruglyakov: "Equilibrium properties of free films and stability of foams and emulsions", in *Thin Liquid Films*, I.B. Ivanov, Editor. Surfactant Science series, 29. Marcel Dekker, Inc.: New York and Basel 1988.
25. D.T. Wasan, *et al.*: "Effect of Oil on Foam Stability: Mechanisms and Implications for Oil Displacement by Foam in Porous Media". Paper *SPE 15443* presented at the *61st SPE Annual Technical Conference and Exhibition*, New Orleans, LA 1986.
26. D.T. Wasan, *et al.*: "Foam stability: Effects of oil and film stratification", in *Surfactant-Based Mobility Control*, D.H. Smith, Editor. ACS Symposium Series, 373. American Chemical Society: Washington, DC 1988, 136-162.
27. C.J. Radke and D.J. Manlowe: "A Pore-Level Investigation of Foam-Oil Interactions in Porous Media". *SPE Reservoir Engineering*, **5:** November, 1990, 495-502.
28. L. L. Schramm, A. T. Turta, and J. J. Novosad: "Microvisual and coreflood studies of foam interactions with a light crude oil". Paper *SPE/DOE 20197* presented at the *SPE/DOE 7th Symposium on Enhanced Oil Recovery*, Tulsa, OK 1990.
29. L. L. Schramm and J. J. Novosad: "Micro-visualization of foam interactions with a crude oil". *Coll. Surf.*, **46:** 1990, 21-43.
30. L. L. Schramm and J. J. Novosad: "The destabilization of foams for improved oil recovery by crude oils: Effect of the nature of the oil". *J. Petr. Sci. Eng.*, **7:** 1992, 77-90.
31. J.E. Hanssen: "Gas-blocking foams in porous media I: Experimental observations and parametric study." Submitted for journal publication, 1992.
32. J.E. Hanssen: "Gas-blocking foams in porous media II: Mechanisms of gas blockage." Submitted for journal publication, 1992.
33. M. Robin: "Utilisation d´agents moussants pour ameliorer l´efficacitè de l´injection de vapeur". Paper presented at the *3rd European Symposium on Improved Oil Recovery*, Rome 1985.
34. K. Raterman: "An Investigation of Oil Destabilization of Nitrogen Foam in Porous Media". Paper *SPE 19692* presented at the *64th SPE Annual Technical Conference and Exhibition*, San Antonio, 1989.
35. J.E. Hanssen: "A new method for testing of gas-blocking foams". Paper *SPE/DOE 17362* presented at the *6th SPE/DOE Symposium on Enhanced Oil Recovery*, Tulsa, Oklahoma 1988.
36. A. R. Katritzky, *et al.*: "Design and synthesis of novel fluorinated surfactants for hydrocarbon subphases". *Langmuir*, 4: 1988, 732-735.
37. M. E. Fagan: "The stability of foam and pseudoemulsion films and foam flow through

glass bead packs". *MS Thesis*, University of California, Berkeley, CA 1992.
38. H.C. Lau and S.M. O'Brien: "Effects of Spreading and Nonspreading Oils on Foam Propagation through Porous Media". *SPE Reservoir Engineering*, 3: August, 1988, 893-896.
39. G. J. Hirasaki: "Thermodynamics of thin films and three-phase contact regions", in *Interfacial Phenomena in Petroleum Recovery*, N.R. Morrow, Editor. Surfactant Science series, 36. Marcel Dekker, Inc.: New York and Basel 1991, 23-76.
40. V. Bergeron: "Forces and structure in thin liquid films". *PhD Thesis*, University of California, Berkeley, CA. In preparation.
41. I.B. Ivanov, Editor: *Thin Liquid Films: Fundamentals and Applications*. Surfactant Science series, Vol. 29. Marcel Dekker, Inc.: New York and Basel 1988. 1120 pp.

Table 1. Surfactants studied (conventional foams in Figure 2 not listed).

Trade name	Structural description	Cosolvent	Maker
OMC 376	alkyl sulfobetaïne	none	Henkel
C_{14} AOS	alpha olefin sulfonate		
FC 751	perfluoroalkyl sulfobetaïne	diglyme	3M
FC 760	perfluoroalkyl ethoxylated alcohol	none	3M
Fluowet OTN	fluoroalkyl ethoxylated alcohol	none	Hoechst
Fluowet CL	fluorinated acid derivative	ethylene glycol	Hoechst
Hoe S 3172	fluoroalkyl sulfobetaïne		Hoechst
Zonyl FSO	perfluoroalkyl ethoxylated alcohol	ethylene glycol	DuPont
Zonyl FSN	perfluoroalkyl ethoxylated alcohol	isopropanol	DuPont
Zonyl FSC	difluoroalkylthioethyl dimethyl ammonium sulfate	isopropanol	DuPont

Table 2. Measured interfacial tensions in mN/m. Systems classified as oil tolerant from porous-medium foam performance are in bold.

Surfactant + Oil	wt %	°C	σ°_{wg}	σ_{wg}	σ°_{og}	σ_{og}	σ_{wo}
OMC 376 + crude 1	2.0	70	24.9	16.4	25.0	17.2	2.7
AOS + crude 2	0.25	80	25.8		18.9		0.7
AOS + non/xyl	0.25	80	25.8		18.7		0.8
AOS + tetralin	**0.25**	**80**	**25.8**		**27.4**		**1.0**
AOS + acetophenon	**0.25**	**80**	**25.8**		**32.0**		**0.4**
FC 760 + crude1	0.5	70	18.0	15.9	25.0	17.8	> 4
Hoe S 3172 + crude1	0.5	70	15.8	13.8	25.0	18.8	6.9
Fluowet CL + crude1	0.5	70	16.0	13.6	25.0	15.7	3.4
Zonyl FSC + crude1	0.5	70	13.4	15.0	25.0	13.8	2.4
Zonyl FSO + crude 1	**0.5**	**70**	**15.3**	**13.2**	**25.0**	**16.8**	**9.8**
Fluowet OTN +crude 1	**0.5**	**70**	**16.2**	**17.4**	**25.0**	**19.2**	**10.0**
FC 751 + crude 1	**0.5**	**70**	**16.0**	**17.2**	**25.0**	**20.0**	**2.7**
Zonyl FSN + crude1	**0.5**	**70**	**16.8**	**15.4**	**25.0**	**23.2**	**2.5**

Table 3. Proposed correlating parameters calculated from data in Table 2. Systems classified as oil tolerant from porous-medium foam performance are in bold.

Surfactant + Oil	wt %	°C	S_{ow}	E_{ow}	$\frac{L}{r_o/r_p}$
OMC 376 + crude 1	2.0	70	-4	+2	9
AOS + crude 2	0.25	80	+6	+8	37
AOS + non/xyl	0.25	80	+6	+8	32
AOS + tetralin	**0.25**	**80**	**-3**	**-1**	**26**
AOS + acetophenon	**0.25**	**80**	**-7**	**-6**	**65**
FC 760 + crude1	0.5	70	≤ -6	≥ +2	<4
Hoe S 3172 + crude1	0.5	70	-12	+2	2
Fluowet CL + crude1	0.5	70	-6	+1	4
Zonyl FSC + crude1	0.5	70	-1	+4	6
Zonyl FSO + crude 1	**0.5**	**70**	**-13**	**+6**	**1**
Fluowet OTN + crude 1	**0.5**	**70**	**-12**	**+8**	**2**
FC 751 + crude 1	**0.5**	**70**	**-6**	**0**	**6**
Zonyl FSN + crude 1	**0.5**	**70**	**-10**	**-5**	**6**

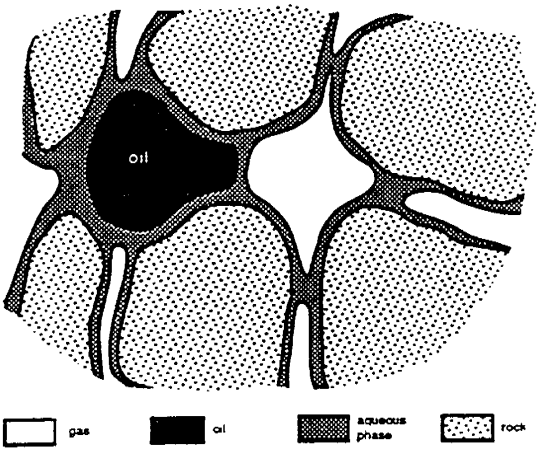

Figure 1. Aqueous foam and residual oil in typical water-wet sandstone pores.

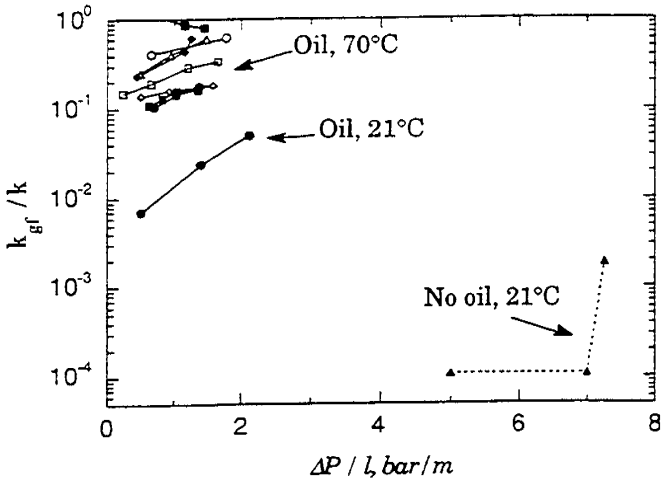

Figure 2. Gas-blockage performance of conventional-surfactant foams. See text and Ref. [15] for details. Oil is Crude 1 at S_{or}.

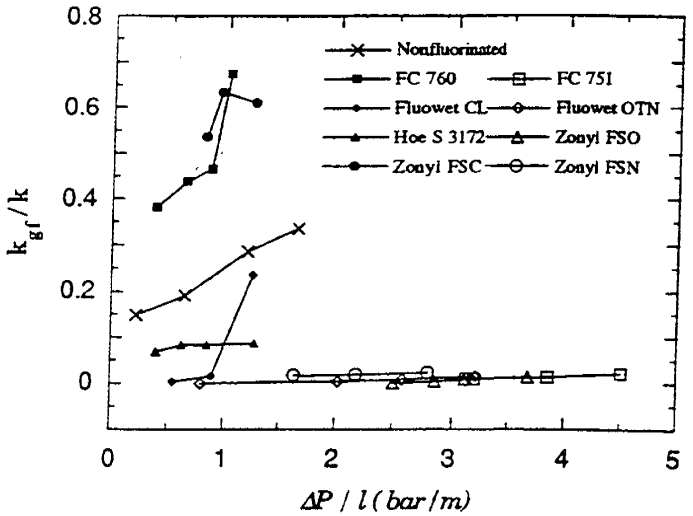

Figure 3. *Gas-blockage test performance of foams from fluorinated surfactants and OMC 376 in the presence of residual saturations of Crude 1 at 70 °C.*

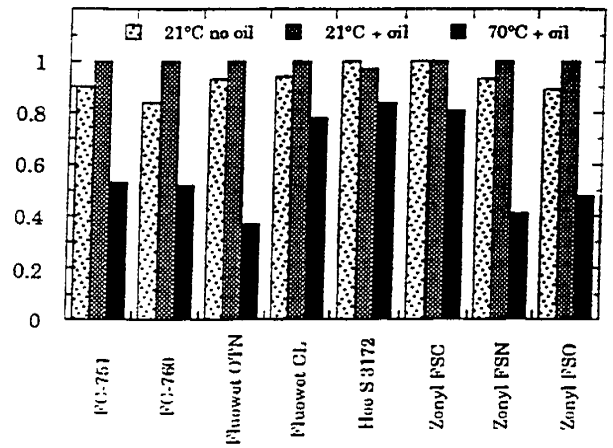

Figure 4. *Bulk stability of fluorosurfactant foams in the presence of Crude 1, expressed as the fraction of foam volume remaining after 20 minutes.*

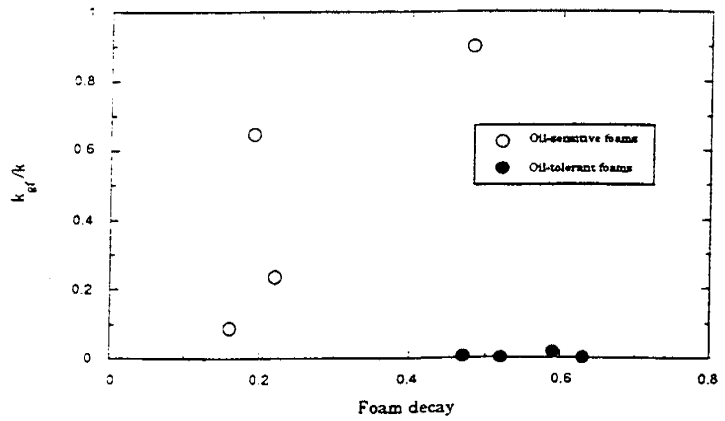

Figure 5. *Bulk stability (volume fraction lost in 20 minutes) and porous medium performance of fluorosurfactant foams (relative mobility at $\Delta P/l \approx 1.25$ bar/m in gas blockage tests.) Indicated oil tolerance refers to gas-blockage tests.*

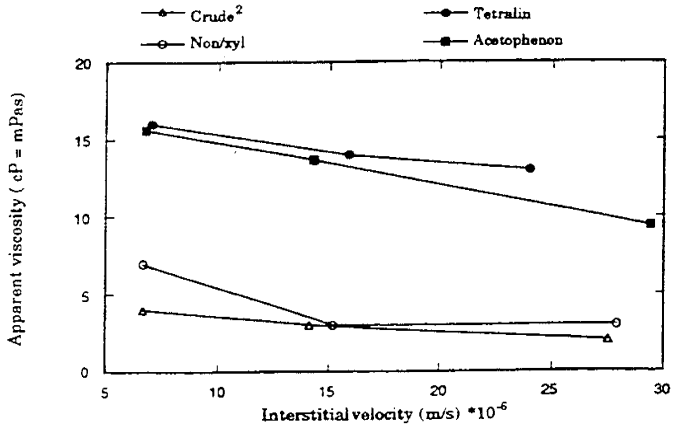

Figure 6. Measured steady state apparent viscosities for foams of C_{14} AOS. Flowing-foam quality, taken as njected gas volume fraction, is 0.94.

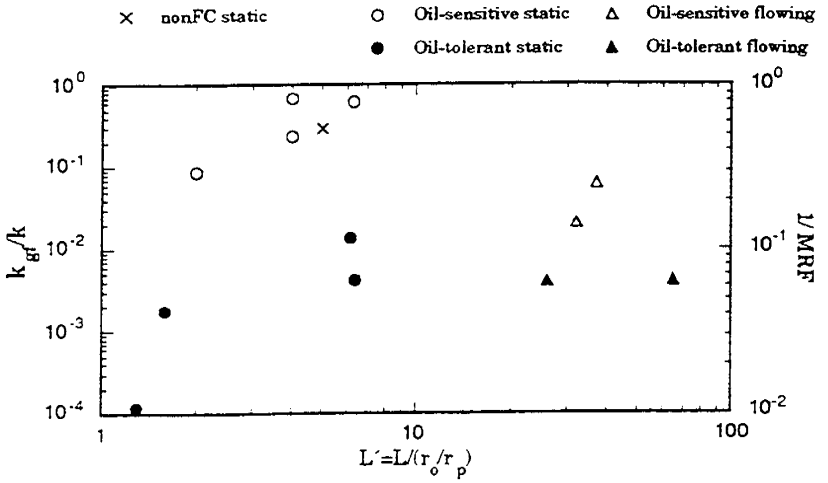

Figure 7. Calculated L´ and measured mobility reduction in flowing and static foams. Values of k_{gf}/k at 1.25 bar/m and of MRF at 10^{-5} m/s.

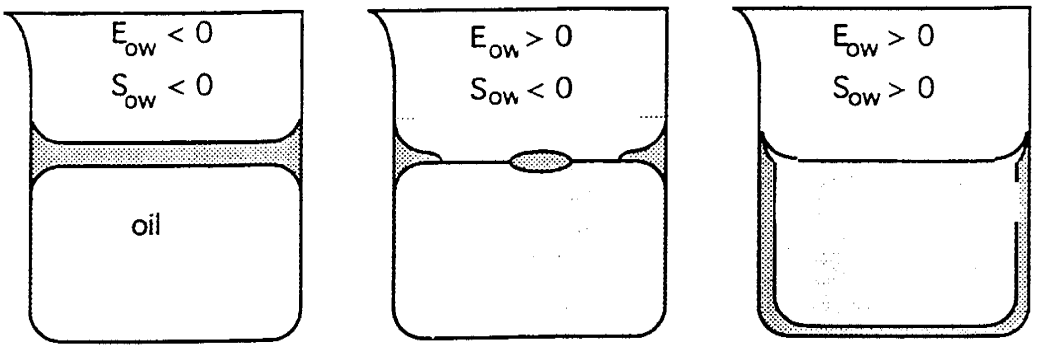

Figure 8. Entering/spreading configurations for aqueous surfactant film on bulk oil. Thickness of aqueous film grossly exaggerated.

No. FSP2

DOE/NIPER

Foam Diversion in Matrix Acidization of Sandstones

by W. R. Rossen and Z. H. Zhou, Department of Petroleum Engineering, The University of Texas at Austin, Texas

Author(s) are solely responsible for copyright and contents.

This poster/paper was prepared for presentation at the DOE/NIPER, Symposium on Field Application of Foams for Oil Production held in Bakersfield, California, February 11-12, 1993.

This paper was selected for presentation by a Program Committee following review of information contained in an abstract submitted by the author(s). Contents of the paper, as presented, have not been reviewed and are subject to correction by the author(s). The material, as presented, does not necessarily reflect any position of the U.S. Department of Energy or the National Institute for Petroleum and Energy Research.

ABSTRACT

Fractional-flow theory presents a simple, approximate way to predict foam diversion in matrix acidization of sandstones. We present such a model based on foam-coreflood data and the "limiting capillary pressure" concept. This model predicts that foams can efficiently divert acid injection into low-permeability layers because capillary pressure makes foam less stable in these layers. The greatest diversion is obtained when foam is preceded by a surfactant preflush and followed by an acid slug that is compatible with the foam. The key to the success of such a process is the ability of surfactant solution to immobilize the gas in previously injected foam. The benefit of a shut-in period after foam injection depends on whether foam collapses, or gas remains trapped, as gas expands in the various layers. In the ideal case, foam collapses in low-permeability layers due to high capillary pressure but remains trapped as it expands in high-permeability layers, further reducing liquid mobility there. A process in which acid is injected continuously with foam can also achieve effective diversion. However, our model suggests that better performance is obtained by separating the foam and foam-compatible-acid slugs, and preceding the foam with a surfactant preflush.

There are several factors that must be explored further before fractional-flow theory can be applied in a quantitative, predictive way to these treatments.

INTRODUCTION

Since at least the 1960's[1] foams have been used to divert acid into less-permeable and oil-saturated strata in matrix acidization treatments.[2-6] Foams used in this way differ fundamentally from several other foam applications in the oil industry: well cleanout,[7] fracturing[8] (including acid fracturing), drilling,[9] and cementing.[10] In those applications, the flow geometry (e.g., wellbore or hydraulic fracture) is relatively simple and the bubbles in the foam are much smaller than the flow geometry. Therefore for these applications foam can be treated as a homogeneous (albeit complex), single-phase fluid.[11] Moreover, for these applications the liquid in the foam is frequently modified with complex viscosifiers that dominate the rheology of the foam. Foams for matrix acidization have in common with foams for enhanced oil recovery (EOR)[12] that, once the bubbles enter the rock, they are as large as or larger than the flow geometry (pore throat). Therefore the foam no longer acts as a single phase; moreover, the surface forces on liquid films, or lamellae, that separate the foam bubbles dominates the apparent rheology of the foam.

There are relatively few published studies of foams for diversion in matrix acidization. Several studies demonstrate that foam can divert acid into low-permeability media in corefloods or in the field.[2,3,5] Bernardiner et al.[4] and Thompson and Gdanski[6] studied the effect of foam on acidization patterns in limestones. In these processes, formation of wormholes dominates the acidization process, and it appears that the retention of bulk foam in these voids is a key to foam diversion.

For sandstones, Zerhboub et al.[5] report the effect of several variables on foam diversion. No acid was present in their coreflood experiments. They found that foam diverted liquid flow to low-permeability cores and was shear-thinning, and that a shut-in period increased foam effectiveness. Unfortunately, too few experimental details are given in this paper to interpret the laboratory data fully. Most important, the extent of gas expansion along the core during foam injection and shut-in is unclear, which makes it difficult to interpret the reported foam qualities and the role of the shut-in period.

In contrast to the scant literature on foams for matrix acidization, there is a wide literature on foams for EOR (see the reviews by Hirasaki[13,14] and Rossen[12] and volume by Smith[15]). In most respects, foams for acidization are similar to foams for EOR: for instance, they use similar surfactant concentrations in the liquid phase and similar qualities (injected gas volume fractions). There are differences: foams for acidization are followed by liquid injection rather than gas injection, for instance; treated volumes are much smaller; and the acid slug injected after foam may contain chemical components detrimental to foam. These differences are matters of design and application, however, not at the heart of the physics of foam processes. The key role played by rock dissolution and formation of large voids in limestone acidization[4,6] is fundamentally different from any mechanisms in foam EOR, though, and may make the mechanisms of foam/acid processes in limestones distinctly different from those of foam EOR. For sandstones, however, we expect that the mechanisms controlling EOR foams and foams for matrix acidization are similar. The poster summarized here applies the findings of the EOR foam literature to the interpretation of foam acidization processes in sandstones and proposes a simple model for analysis of these processes.

Details can be found in paper SPE 24660, presented at the 1992 Annual Meeting of the Society of Petroleum Engineers.[16] The

References at end of paper.

approach is similar to that in the paper, "Implications of the 'Limiting Capillary Pressure' for Field Application of Foams," in this volume. The conclusions of this study are as follows:

1. A fractional-flow model for foam diversion in matrix acidization of sandstones can be derived from laboratory foam coreflood data. We have derived such a model based on laboratory data of Persoff et al.[17,18] for EOR foams and the "limiting capillary pressure" model. A fractional-flow model could be tailored for specific acid/foam processes as additional laboratory data become available.

The following conclusions are derived from our fractional-flow model based on Persoff et al.'s EOR foam data:

2. Diversion of flow during foam injection is not the same as diversion of acid following foam injection. The key to diversion of acid following foam is trapping as much of the gas in the foam as possible with the acid. For this purpose a foam-compatible acid is needed. Otherwise the foam quickly disappears due to adsorption, and diversion dissipates rapidly. This advantage may be less pronounced in later slugs of a multi-slug process, as the surfactant-adsorption capacity of the rock near the well is satisfied.
3. Foams can be extremely effective in diverting acid if the acid slug is compatible with foam and efficiently traps foam in place. Then diversion can last as long as foam-compatible acid is injected.
4. Preceding foam injection with a surfactant preflush helps place a larger foam slug in the high-permeability zones and thereby improves diversion over a process with no preflush.
5. The benefit from a shut-in period after foam injection depends on whether foam collapses or gas remains trapped as pressure declines. In the ideal case, foam collapses in low-permeability layers due to high capillary pressure but remains trapped as it expands in high-permeability layers, further reducing liquid mobility there.
6. A process in which acid is injected with foam can also achieve effective diversion to low-permeability strata. However, our model suggests that diversion is more complete and is achieved more quickly with a surfactant preflush followed by a slug of foam and then foam-compatible acid.

Our fractional-flow model indicates that foam can be extremely effective in diverting acid in matrix acidization treatments in sandstones. Our model is based on plausible extrapolations of the data of Persoff et al.[17,18] for foams without acid in oil-free and water-wet Boise sandstone. Therefore our quantitative results are undoubtedly optimistic for field application. Further data are needed to verify or revise these assumptions for foams, rock types and permeability ranges typical of matrix acidizing processes. Key issues to be settled are (1) whether foams made compatible with acid can achieve the same low mobilities and trap gas as effectively in reservoir rock as assumed here, (2) the shape of the fractional-flow curves for these foams, (3) the effect of permeability on the fractional-flow curves, and (4) whether gas remains trapped as it expands during a shut-in period.

Experimental data required to calibrate this model for quantitative application to foam/acid treatments include the following, as a function of permeability or other geological parameters:

- surfactant-free gas/water relative-permeability curves
- total mobility and water saturation during foam injection
- rate of foam propagation during foam injection, and whether this is controlled by surfactant adsorption or bubble breakage at the foam front (i.e., whether surfactant breakthrough substantially precedes foam breakthrough)
- any foam-induced skin effect at the rock surface during foam injection
- effect of oil and wettability on foam
- mobility and gas saturation in the acid slug following foam.

With such data the velocities and mobilities of the various slugs in each layer could be determined and the fractional-flow analysis applied in a quantitative manner.

ACKNOWLEDGMENTS

This work was supported by a consortium on Stimulation, Logging and Formation Damage at The University of Texas at Austin.

REFERENCES

1. C. L. Smith, J. L. Anderson and P. G. Roberts, SPE 2751, presented at the Ann. Mtg. of the Soc. Petr. Eng., San Francisco, 1969.
2. J. W. Burman and B. E. Hall, SPE 15575, presented at the Ann. Mtg. of the Soc. Petr. Eng., New Orleans, 1986.
3. D. K. Kennedy, F. W. Kitziger and B. E. Hall, SPE 20621, presented at the Ann. Mtg. of the Soc. Petr. Eng., New Orleans, 1990.
4. M. G. Bernadiner, K. E. Thompson and H. S. Fogler, SPE 21035, presented at the Symposium on Oilfield Chem. of the Soc. Petr. Eng., Anaheim, 1991.
5. M. Zerhboub, E. Touboul and K. Ben-Naceur, SPE 22854, presented at the Ann. Mtg. of the Soc. Petr. Eng., Dallas, 1991.
6. K. Thompson and R. D. Gdanski, SPE 23436, presented at the Eastern Regional Mtg. of the Soc. Petr. Eng., Lexington, KY, Oct. 22-25, 1991.
7. T. O. Allen and A. P. Roberts, Production Operations, Vol. 1, Oil & Gas Consultants, Intl., Tulsa, 1982.
8. P. C. Harris, D. E. Kelbenow and D. P. Kundert, SPE Prod. Eng. 6:15 (1991).
9. G. V. Chilingarian and P. Vorabutr, Drilling and Drilling Fluids, Elsevier, Amsterdam, 1981.
10. J. de Rozieres and R. Ferriere, SPE Prod. Eng. 6: 297 (1991).
11. P. C. Harris, SPE 14257, presented at the Ann. Mtg. of the Soc. Petr. Eng., Las Vegas, 1985.
12. W. R. Rossen, in Foams: Theory, Measurements and Applications (R. K. Prud'homme and S. Khan, ed.), Marcel Dekker, Inc., New York, in press.
13. G. J. Hirasaki, J. Petr. Technol. 41:449 (1989).
14. G. J. Hirasaki, SPE 19518, Soc. Petr. Eng., Richardson, TX, 1989.
15. D. H. Smith, in Surfactant-Based Mobility Control: Progress in Miscible-Flood Enhanced Oil Recovery (D. H. Smith, ed.), ACS Symposium Ser. no. 373, Am. Chem. Soc., Washington, 1988, p. 429.
16. Z. H. Zhou and W. R. Rossen, SPE 24660, presented at the Ann. Mtg. of the Soc. Petr. Eng., Washington, 1985.
17. P. Persoff, C. J. Radke, K. Pruess, S. M. Benson and P. A. Witherspoon, SPE Reserv. Eng. 6:365 (1991).
18. P. Persoff, K. Pruess, S. M. Benson, Y. S. Wu, C. J. Radke and P. A. Witherspoon, Proc. Intl. Gas Res. Conf., Tokyo, 1989.

No. FSP3

DOE/NIPER

Laboratory Evaluation of Surfactants as Steam Diverters

by S. M. Mahmood, P. S. Sarathi, D. K. Olsen and E. B. Ramzel, IITRI/National Institute for Petroleum and Energy Research

Author(s) are solely responsible for copyright and contents.

This poster/paper was prepared for presentation at the DOE/NIPER, Symposium on Field Application of Foams for Oil Production held in Bakersfield, California, February 11-12, 1993.

This paper was selected for presentation by a Program Committee following review of in formation contained in an abstract submitted by the author(s). Contents of the paper, as presented, have not been reviewed and are subject to correction by the author(s). The material, as presented, does not necessarily reflect any position of the U.S. Department of Energy or the National Institute for Petroleum and Energy Research.

ABSTRACT

Laboratory tests have been undertaken to evaluate the effectiveness of surfactants with nitrogen for steam diversion for possible application in the light oil steamfloods at Naval Petroleum Reserve fields in California (NPR-1) and Wyoming (NPR-3), and in two heavy oil steamfloods in California. Each reservoir is a quite different environment with the steamfloods at NPR fields experiencing early steam breakthrough.

Steamflood displacement tests (with and without surfactant) were performed in both linear (1-D) and rectangular sandpacks (2-D physical models with single or multiple layers of permeability) at high temperature and pressures with reservoir crude oil. The effect of steam on oil displacement in steamfloods, and of surfactants for steam diversion where commercial surfactants, surfactant concentrations, injection rates, injection strategies, and vapor-to-liquid ratios on steam-foam performance were studied.

The studies showed the ability of 2-D laboratory models to qualitatively predict scaling and reduction of permeability in the steamflood at NPR-1, problems that were encountered in the field. No satisfactory surfactant was found to perform adequately in the steamflood environment at NPR-1. Multiple surfactants were found capable of maintaining foam integrity at NPR-3, Round Mountain and Kern River steamflood conditions.

Linear sandpacks yielded a high steamflood oil recovery even without any additives because of the homogeneous permeability distribution and piston-like displacement. The surfactants' performance (pressure buildup rate, maximum pressure, and rate of decline) varied with operating conditions and crude oil; hence, proper formulation/injection design is important for a successful steam-foam treatment.

Rectangular sandpacks, however, simulated gravity override and channeling problems typically encountered in reservoirs. In 2-D models, foam was able to divert steam to previously unswept layers; consequently, additional oil was produced from unswept zones. Thus, 2-D models are a valuable tool for determining the effectiveness of foam in improving steamfront profile conformance to increase oil production.

INTRODUCTION

Three light oil steamfloods have been conducted in Naval Petroleum Reserve (NPR) fields in the last decade. The tests have been in NPR-2, Buena Vista Hills field, California; NPR-1, Elk Hills field, California; and NPR-3, Teapot Dome field, Wyoming. The first pilot was at NPR-2 conducted by Chevron from May 1985 to May 1986 and has been described by Ziegler.[1] Simulation studies by Hong,[2] field analysis,[3] and laboratory studies of the interaction of steam with the carbonate-rich reservoir sand were described by Cathles, Schoell and Simon.[4] At NPR-1 the light oil (27° API) steamflood tested the 2,200-ft-deep Shallow Oil Zone (SOZ) which is the same-age sand as that of the Buena Vista Hills steamflood.[5] The NPR-1 steamflood operation has been described by Gangle et al.[6] Steam broke through early in both pilots, significant off-pattern production was observed, and hot producing

References and illustrations at end of paper.

wells with scaling problems lead to uneconomic prospects for conversion to a commercial scale operation (Weyland[7] and Hong et al.[8]).

The steamflood at NPR-3 (32° API) is being conducted in a shallow (450-ft-deep), tight (63 md) highly fractured Shannon sandstone. The steamflood has expanded beyond the initial pilot as described by Chapelle et al.[9] and now uses five 50 MMBtu/hr steam generators to flood 150 acres. Commercial steamflood operations have been described by Olsen et al.[10]

Due to lower viscosity and density contrast in light oil steamfloods, they are less prone to gravity override and fingering than heavy oil steamfloods. Nevertheless, the tendency for gravity override and fingering is clearly observed in laboratory tests such as those performed using NIPER's two-dimensional (2-D) laboratory steamflood model shown in Fig. 1. This model and its operation have been previously described by Sarathi et al.[11] This 27-in.-long 6-1/2-in.-tall 1-1/2-in-thick physical model was packed with sand to form a single layer (Fig. 1) or to form multiple layers of different permeability. In Fig. 1 and all subsequent 2-D figures, the steam entered the model along the bottom half of right-hand side and was produced from the entire left-hand side. Steam overrides the oil and breaks through, producing little oil thereafter except as a result of steam stripping and convective heating of the model. The 2-D model has been used to evaluate the effectiveness of foams to divert steam in both homogenous and heterogeneous (multi-permeability) sandpacks as an aid in selection of surfactants for steam diversion.

NIPER briefly evaluated some commercial surfactants for their potential as steam diverters in the NPR light oil steamfloods, and some of the results are reported herein. These light oil steamfloods (NPR-1 and 2, NPR-3) were conducted in quite different environments. Preliminary surfactant screening tests are described, followed by results of 2-D steamflood model tests with light oils and a heavy oil (Kern River, California, 13° API gravity crude).

Preliminary Screening Tests

Many of the surfactants used in the 1-D and 2-D flow tests had been screened using a high temperature-pressure foamability (HTPF) test (Strycker et al., 1987).[12] This bulk foamability test generates foam at elevated temperature and pressure (reservoir temperature and pressure conditions) and can be used to evaluate surfactant foamability at various salinity, temperature, and pH as a function of surfactant concentration. Surfactants that show the best foaming characteristics are then evaluated by dynamic mobility control tests using linear (1-D) sandpacks filled with either clean quartz sand or reservoir sand, and/or reservoir oil at steamflood residual oil saturation.

One-Dimensional Steam Diverter (Foam) Experiments

A series of commercial surfactants were screened for possible use as steam diverters in NPR reservoirs using the screening technique that has been previously described.[13] The tests were performed in a linear 1-D steamflood model packed first with quartz sand and later with SOZ sand for tests under NPR-1 conditions or crushed Shannon sandstone for tests under NPR-3 conditions. Chevron Chemical Co.'s Chaser SD-1020, Chaser SD-1025 and Shell Chemical Co.'s LTS 18-20 were evaluated for potential application. Foam was successfully generated using these surfactants in clean quartz-sand over a wide variety of flow rates, surfactant concentrations, and liquid-to-vapor ratios, e.g., as shown in Fig. 2.[13] Foam or emulsion could be generated even when the quartz sand had been saturated with either of the three oils. However, with residual oil saturation, higher pore volumes of surfactant were required for the same differential pressure to develop as in an initially water saturated sandpack (Fig. 3). This suggests that the oil saturation must be even lower than residual oil saturation for effective foaming. Even though good foaming was evident in linear sandpack tests with SOZ oil (NPR-1) and clean quartz sand, attempts to generate a pressure drop indicative of foam or emulsion that can cause steam diversion were unsuccessful in tests containing reservoir sand (SOZ, NPR-1). Foaming was inhibited by the high divalent ion concentration in the calcium-rich SOZ sand.

The response of 1% by weight surfactant solution (Chevron Chaser SD-1020) with three oils (Kern River: 13° API, Shannon oil from Teapot Dome: 32° API, and SOZ oil from Elk Hills: 27° API) are compared in Fig. 4. In each of these 1-D tests, the Quartz sandpack was oil saturated and then steamed to residual oil saturation at which time the surfactant solution was injected. The response to the injected surfactant and nitrogen shows a time lag before a differential pressure across the 4-foot sandpack is noted. The peak foaming performance (maximum pressure drop) in each of the three tests is about the same under the same flow rates, surfactant concentrations, and liquid to vapor ratios (LVR). As the maximum pressure drop is attained, the system approaches the steam saturation pressure and steam condenses within the sandpack. Similarly, the rate of pressure declined at the termination of surfactant injection was about the same in each test. However, the onset of foaming and the rate of pressure rise were different for each oil (due to different degree of emulsification as discussed later). The microscopic displacement efficiencies for various oils may also vary because of the variable distillation rates, which could also influence the foaming onset. The higher the degree of emulsification, the earlier the pressure kick and the slower the rate of pressure rise.[13]

The characteristics of various phases of emulsions were visually observed by microscopic examination in some tests. These effluent observations were used only in conjunction with the pressure response histories since the presence of foam-like dispersions in the effluent does not necessarily imply their existence in the sandpack. Positive identification of the existence of in situ foam or emulsion were not undertaken. Any emulsion in the effluent was presumed to have originated in the sandpack because of a more favorable environment inside the porous medium. Microscopic examination of the effluent revealed that the light tan emulsions were composed of small oil-in-water emulsions with a narrow size distribution: median size ≈4 μ, majority ≈2-8 μ, and rarely above 12 μ. Darker emulsions were also oil-in-water, but had a broader size distribution: median size ≈ 10 μ, majority ≈ 4-16 μ, and rarely above 20 μ.

Figure 5 describes qualitatively the oil desaturation during a steam-foam tests of a 1-D sandpack where the sandpack was steamflooded to about 20% oil saturation before the same surfactant and gas were injected (same rate and liquid to vapor ratio). Oil saturation were obtained from analysis of the effluent and are not anticipated to be uniformly distributed along the core. The history of the physical appearance of effluents during the two steam-foam tests using two different oils (the heavy oil is 13° API gravity Kern River crude and the light oil is 32° API gravity Shannon crude from NPR-3). The pressure response at above 10% oil saturation coincides with the beginning of oil/water emulsion production. By about 8% oil saturation, visible foam was observed in the effluent from the steam-foam test with the heavy crude oil, whereas the oil saturation was <2% when similar foam quality was observed with the light oil. A strong foam was produced near the maximum pressure drop (at 5% oil saturation with the heavy crude) but only a tan emulsion was observed at this 5% oil saturation for the light oil. Both experiments reached the same pressure drop across the core (within five pounds). The onset of emulsification (as evidenced by microscopic observation of effluents) preceded the onset of foaming (as evidenced by a sudden rise in pressure).

Several 1-D (quartz sandpack) pressure buildup and pressure falloff tests were performed to determine an optimum injection strategy, the required LVR and surfactant concentration necessary for steam-foam generation for NPR-3 and Kern River reservoirs. A pressure response history of one test at NPR-3 conditions is shown in Fig. 6 where the time frame has been greatly compressed for presentation as a single figure. Each peak was measured when the pressure had stabilized for >20 minutes. The backpressure was set at 150 psi and thus steam alone generates a pressure of between 155 and 180 psi depending on the flow rate. This figure shows that significant pressure loss occurs within a short time after surfactant injection was suspended. The pressure is maintained only during continuous injection or frequent injection of small slugs. The figure also indicates that changes to the liquid to vapor ratio influences the rate of pressure buildup and the maximum pressure that can be obtained. The effect of nitrogen injection on the LVR is shown in the pressure buildup. The cumulative effect of surfactant injection on quartz sandpacks are not sufficient information to calculate adsorption. Data from adsorption experiments is required to estimate surfactant loss for designing a steam-foam process. Each of the numbers in Fig. 6 corresponds with the change in operating condition listed in Table 1. A more comprehensive analysis has been described in reference 13. An equilibrium (steady pressure for >20 minutes) was achieved at each operating condition before the operating conditions were changed. These tests were performed in oil-free conditions, but it is believed that the results are applicable to low-oil saturation conditions as well, since the foaming performance in oil-free and low-oil saturation conditions are similar (Fig. 3).

Figure 7 shows that the onset of foaming and the maximum pressure drop are both influenced by steam injection rate, an important design parameter for field applications. This figure also suggests that a minimum rate is required for foam formation and maximum pressure generation i.e., optimum surfactant performance. Finding a suitable noncondensable gas fraction is also important for an optimum field application, as shown in Fig. 8 for a series of pressure buildup (surfactant injection) and pressure falloff tests (no surfactant is injected and nitrogen remains at the same flow rate).

Two-Dimensional Steam Displacement Experiments

(A) Steamfloods Only—No Surfactant Tests

NIPER has conducted several two-dimensional (2-D) laboratory steamfloods using reservoir oil and sand. Most of the tests were aimed at finding the potential of foam as steam diverters; however, some tests were performed with steam only for comparative purposes. A variety of oils and corresponding reservoir sands were tested, including Shallow Oil Zone (SOZ) of Naval Petroleum Reserve No. 1, Elk Hills field, California, New London, Round Mountain, and Kern River crude oil. These laboratory experiments often showed production characteristics and problems similar to those encountered in respective fields. These experiments used friable core/sand from the respective field. Larger pieces of core material were crushed before being packed into the 2-D steamflood model.

A set of three 2-D steamfloods were conducted using the SOZ crude and sand.[14] One was a steam only test, whereas the other two were steamfloods after a waterflood. The model was saturated with the simulated formation brine. Permeability in 2-D experiments ranged between 482 and 581 millidarcies. Initial oil saturation was

typically 51 to 61%. The backpressure on the 2-D model was set to 150 psi corresponding to a steam saturation temperature of 355° F. Oil saturation in these tests was typically reduced from 61 to 27%.

The following observations in these three runs are interesting to note: (1) Under the conditions of these laboratory tests, i.e. scale deposition and clay swelling occurred,[14] and a linear model may not have been as effective as a 2-D model in diagnosing this field problem that occurred in steamflooding the SOZ.[3,7,8] The reason is that the slug-type displacement in linear models may unjustifiably delay the first appearance of a problem; e.g. the dilution of in situ brine by the water condensed from the steam appears at the production end only after the preceding oil bank has been produced, thus masking its effects on productivity during the useful life of the flood. It is quite possible—as it is a common practice—that the operators might have performed linear steamflood susceptibility tests and not seen any potential problems. (2) The first steamflood required multiple (decreasing) pump adjustments to maintain a relatively stable flow rate and pressure across the model perhaps because the initial clay swelling and scaling were already occurring. (3) Neither of the remaining two runs had significant pressure buildup nor production problems until after introduction of steam. (4) The total amount of oil produced in the third run was almost identical to the large front end production in steamflood only test (run 1), as well as identical to the front end production waterflood segment of waterflood followed by steam test (run 2). In these tests steam created production problems, but did not significantly improve oil production over an extended waterflood.

(B) Steamfloods Followed by Surfactants

Frontal behaviors with several surfactants and injection strategies are shown in Figs. 9 through 12. These photographs were taken at the end of the flood by exposing one of the sides of the sandpack. These photographs help qualitatively in depicting the history of fluid movement. When coupled with quantitative tools—such as determination of oil saturation by Dean Stark analysis of the sand for oil concentration (Fig. 13) and temperature mappings as shown in Fig. 14. Photographs can assist in visualizing complex steam-foam frontal behavior.

A variety of steam-foam frontal behavior has been observed. In a 5-Darcy, 35% porosity single-layer sandpack (Fig. 9) saturated with 15° API Round Mountain crude at 91% initial saturation, an almost piston-like displacement was observed and 87% OOIP was recovered with 5% SD-1020, 1% NaCl, and N_2 injection during a steam-foam flood, showing the potential of foam for improving front profiles. Simultaneous injection of foam and steam drastically altered the severe steam gravity override of oil observed in previous experimental runs in a homogeneous sandpack.

On the other hand (Fig. 10), 13° API gravity Kern River crude was produced from a bi-layer (separated by a clay barrier) sandpack composed of an upper layer of 26-Darcy permeability and a lower layer of 10 Darcies (43% porosity, $S_{oi} \approx 51\%$). The flood showed the steamflood and steam-foam recovered most of the oil from the high permeability layer. Injection of slugs of foam or emulsion produced little additional oil. Slugs of emulsified oil, produced by the reaction of sodium hydroxide and reservoir oil were externally mixed to create an emulsion, were tested in an attempt to divert steam.

A 15° API Round Mountain crude test ($S_{oi} \approx 86\%$) in a bi-sandpack (Fig. 11) with an upper layer of 56-Darcy permeability and a lower layer of 19 Darcies (36% porosity) showed from the oil production curve and temperature profile, that steam was producing oil (<35% of OOIP) from the high-permeability layer. When the water/oil ratio reached 200 a steam-foam was injected and the top layer started to cool while the bottom layer near the injector (right side) increased in temperature. The model began to produce additional oil resulting in recovery of 60% of the OOIP. The photograph of the sand after completion of the steam-foam test shows significant gravity override at the producing end of the model (left side). Dean Stark analysis of the sand showed an oil saturation in the dark portion of the picture as >45% whereas the lighter portions were <3% for most of the upper layer and <7% for most of the low-permeability, lower layer.

Another test with the same crude ($S_{oi} \approx 89\%$) in a bi-layer sandpack (Fig. 12) with an upper layer of 76-Darcy permeability and a lower layer of 15 Darcies (36% porosity) recovered 85% of OOIP. The photograph shows where steam has swept the upper portion of the top layer and was overriding the lower portion of the upper layer. However, Dean Stark analysis of the darker oil stained sand showed that the difference between light colored sand at the top ($S_o \approx 4\%$) and the darker sand (average $S_o \approx 9\%$) was not dramatic as the oil stain, from visual observation of the photograph indicates. The combination of post flood sand analysis for oil saturation (Fig. 13), temperature data acquired during the steamflood (Fig. 14), history of pressure and effluent analysis are not adequate to describe the steam-foam process. Dynamic saturation changes such as those obtained from X-ray CT of the displacement experiment[15,16] can yield additional information on dynamic changes in saturation and is the direction that NIPER's steamflood laboratory is proceeding in an effort to gain a better understanding steam diversion with foam.

CONCLUSIONS

Several conclusions can be drawn from the results presented. First, the study shows the importance of conducting steamflood experiments under field conditions of field core, reservoir fluids (water and oil) at simulated reservoir conditions. Problems revealed in the laboratory steamflood, such as scaling of the producer and swelling of clays causing production problems were seen concurrently in the lab and the steamflood at NPR-1. Laboratory evaluation of surfactants or steam diverters must be conducted at field conditions, i.e., use of field core (sand), formation fluids (oil and water), at flow rates calculated based on steam injection rate, steam quality, and gas injection rate.

Second, the high divalent ion concentration and 550° F operating temperature of the steamflood at NPR-1 were not amenable to steamflooding or foam generation for steam diversion using the surfactants studied. However, surfactants (Chaser SD-1020 or LTS 18-20) were shown to produce significant mobility reduction for steam diversion under the conditions of the steamfloods at NPR-3, Round Mountain, or from those operating at Kern River conditions. Generation of the pressure differential, either from emulsification of oil or foam, varied with operating conditions and occurred at oil saturations of <10%. Therefore, surfactant selection, formulation and injection strategy are needed for a successful steam-foam treatment.

Third, two-dimensional models provide an opportunity to observe gravity override and fingering more than 1-D models. Use of 2-D models with multipermeability allow observation of what is perceived to occur in the field. Foam has been shown to divert steam to previously unswept lower temperature areas resulting in increased oil production.

Fourth, bulk foam tests, tests at temperatures other than field operating conditions, tests in clean quartz sands, or oils other than formation oil may yield misinterpreted results leading to the recommendation of inappropriate surfactants as steam diverters.

Fifth, although not described in this paper, effluent analysis is critical to determining loss of surfactant via adsorption and partitioning into the oil phase or decomposition of the surfactant in the presence of divalent and trivalent ions in the reservoir at high temperature.

ACKNOWLEDGMENTS

This work was sponsored by the U.S. Department of Energy under cooperative agreement DE-FC22-83FE60149. The author wishes to thank S. D. Roark, W. I. Johnson, Arden Strycker and M. K. Tham of NIPER; the staff of F. D. Services, and the U.S. DOE staff at NPR No. 3; and Bechtel Petroleum Operations, Inc., Chevron U.S.A., and the U.S. DOE staff at NPR No. 1 for their assistance and permission to publish the results of the research. The authors thank Chevron Chemical, Shell Chemical, Witco Chemical, Stepan Chemical, and Huls America for supplying surfactant samples for steam foam studies.

REFERENCES

1. Ziegler, W. M. Injection Well Testing in a Light Oil Steamflood, Buena Vista Hills Field, California. Pres. at the 63rd Annual Technical Conf. and Exhib., Houston, TX, Oct. 2-5, 1988, pp. 333-337. SPE paper 18140 .

2. Hong, K. C. Numerical Simulation of Light Oil Steamflooding in the Buena Vista Hills Field, California. Pres. at SPE International Conference on Petroleum Engineering, Beijing, China, 1986. SPE paper 14104.

3. Grant, C. W., and A. A. Reed. The Effects of Steam Injection in a Sandstone Reservoir (Etchegoin Formation), Buena Vista field, California. AAPG Bulletin, v. 75, No. 3, March 1991, pp. 585-587.

4. Cathles, L. M., M. Schoell and R. Simon. CO_2 Generation During Steamflooding: A Geologically Based Kinetic Theory That Includes Carbon Isotope Effects and Application to High-Temperature Steamfloods. Pres. at SPE International Symposium on Oilfield Chemistry, San Antonio, TX, Feb. 4-6, 1987, pp. 255-270. SPE paper 16267.

5. Maher, J. C., R. D. Carter and R. J. Lantz. Petroleum Geology of Naval Petroleum Reserve No. 1, Elk Hills, Kern County, California. U.S. Geological Survey Professional Paper 912, 1975, p. 109.

6. Gangle, F. J., G. V. Weyland, J. P. Lassiter and E. J. Veith. Light Oil Steamdrive Pilot Test at NPR-1, Elk Hills, California. Proceedings of the 60th SPE California Regional Meeting, Bakersfield, Apr. 5-7, 1990, pp. 177-185. SPE paper 20032.

7. Weyland, H. V. Light Oil Steamflood Pilot Test at NPR-1, Elk Hills, California, in Structure, Stratigraphy and Hydrocarbon Occurrences of the San Joaquin Basin, California. Published by The Pacific Sections of the Society of Economic Paleontologists and Mineralogists and the American Association of Petroleum Geologists, Bakersfield, California, June 1, 1990, pp. 173-179.

8. Hong, K. C., J. H. Blunschi, C. C. Cease and D. L. Madison. Reservoir Management of Light Oil Steamflood Pilot in the SOZ Fault Block, Elk Hills Field. Pres. at SPE Western Regional Meeting, Bakersfield, CA, Mar. 30-Apr. 1, 1992. SPE paper 24037.

9. Chappelle, H. H., G. P. Emsurak Jr., and S. L. Obernyer, S. L. Screening and Evaluation of Enhanced Oil Recovery at Teapot Dome in the Shannon Sandstone, A Shallow Heterogeneous Light Oil Reservoir. Pres. at the SPE/DOE Fifth Symposium on Enhanced Oil Recovery, Tulsa, OK, Apr. 20-23, 1986. SPE/DOE paper 14918.

10. Olsen, D. K., P. S. Sarathi, M. L. Hendricks, R. K. Schulte and L. A. Giangiacomo. Case History of Steam Injection Operations at Naval Petroleum Reserve No. 3, Teapot Dome Field, Wyoming: A Shallow Heterogeneous Light-Oil Reservoir. Pres. at the International Thermal Operations Symposium, Bakersfield, CA, Feb. 8-10, 1993. SPE paper 25786

11. Sarathi, P. S., S. D. Roark and A. R. Strycker: Light-Oil Steamflooding: A Laboratory Study. SPE Reservoir Eng., May 1990, pp. 177-184.

12. Strycker, A. R., M. P. Madden and P. Sarathi. Effectiveness of Screening Tests as Predictive Models for Steamflood Additives. SPE Res. Eng., November 1987, pp. 543-548.

13. Mahmood, S. M., D. K. Olsen and E. B. Ramzel: Evaluation of Surfactants as Steam Diverters/Mobility Control Agents in Light Oil Steamfloods: Effects of Oil Composition, Rates and Experimental Conditions. U.S. DOE report NIPER-554, December 1991.

14. Olsen, D. K., P. S. Sarathi, S. M. Mahmood, E. B. Ramzel and S. D. Roark. Results of Task 52 Research on Light Oil Steamflooding, Report No. NIPER-605, July 1992.

15. Demiral, B. M. R., L. M. Castanier and W. E. Brigham: CT Imaging of Steam/Foam Laboratory Experiments. Proceedings of the 66th Annual SPE Technical Conf., Dallas, TX, Oct. 6-9, 1991, pp. 337-382. SPE paper 22631.

16. Demiral, B. M. R., P. A. Pettit, L. M. Castanier and W. R. Brigham: A Three-Dimensional Laboratory Steam Injection Model Allowing In-Situ Saturation Measurements. U.S. DOE report SUPRI TR-83, DOE/BC/141600-33, August 1992.

SI Metric Conversion Factors

acres x 4.046 873	E-01	=	ha
ft x 3.048*	E-01	-	m
°F (°F-32)/1.8		=	°C
in. x 2.54*	E+00	=	cm
mD x 9.869 233	E-04	=	μm^2
psi x 6.894 757	E+00	=	kPa

*Conversion factor is exact.

TABLE 1. - Injection Protocol for Figure 6

No. in Fig. 6	Description	Steam rate mL/min (CWE)	N_2 rate mL/min (STP)	Foamer rate mL/min
1	No Steam	0	200	5.52
2	Continuous Foamer Inj.	9.42	200	3.33
3	Continuous Foamer Inj.	9.42	100	3.33
4	No Foamer Inj.	9.42	100	0
5	1st 200 cc Foamer Slug Inj.	9.42	100	5.52
6	No Foamer Inj.	9.42	100	0
7	2nd 200 cc Foamer Slug Inj.	9.42	200	5.52
8	1st 100 cc Foamer Slug Inj.	9.42	0	5.52
9	No Foamer Inj.	9.42	100	0
10	2nd 100 cc Foamer Slug Inj.	9.42	0	5.52
11	No Foamer Inj.	9.42	100	0
12	3rd 100 cc Foamer Slug Inj.	9.42	0	5.52
13	No Foamer Inj.	9.42	200	0
14	No Foamer Inj.	9.42	100	0
15	No Foamer Inj.	9.42	200	0
16	4th 100 cc Foamer Slug Inj.	9.42	0	5.52
17	No Foamer Inj.	9.42	200	0
18	No Foamer Inj.	9.42	100	0
19	No Foamer Inj.	9.42	150	0
20	No Foamer Inj.	9.42	200	0
21	1st 50 cc Foamer Slug Inj.	9.42	0	5.52
22	No Foamer Inj.	9.42	100	0
23	2nd 50 cc Foamer Slug Inj.	9.42	0	6.1
24	No Foamer Inj.	9.42	100	0
25	3rd 50 cc Foamer Slug Inj.	9.42	0	6.1
26	Continuous Foamer Inj.	9.42	100	5.25
27	Continuous Foamer Inj.	9.42	0	5.25

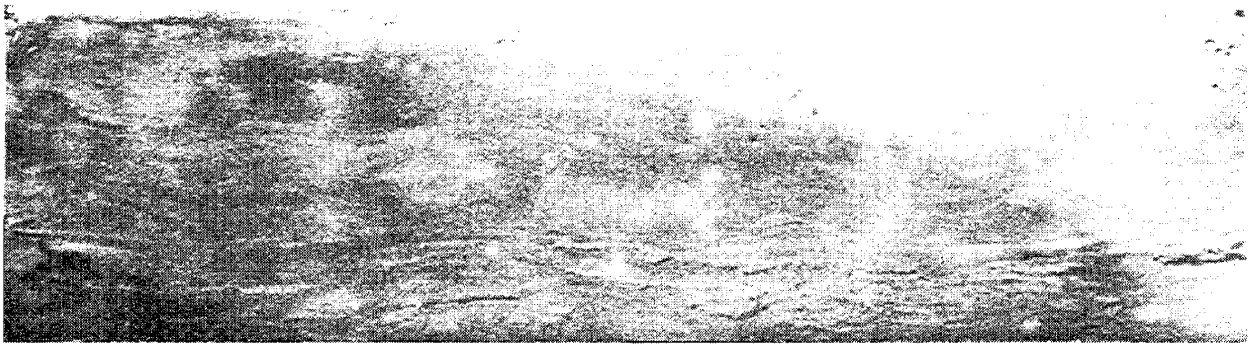

34° API NEW LONDON CRUDE
k ≈ 3.5 Darcies, Ø ≈ 37.5%, S_{oi} ≈ 78%
Ultimate Recovery ≈ 81% of OOIP

No Surfactant, Steam Only

FIGURE 1. - A steamflood test of a light oil (34° API gravity) without any additives in a 2-D model. This picture, taken at the end of the flood by exposing one of the sides of the sandpack, qualitatively shows a gravity override problem.

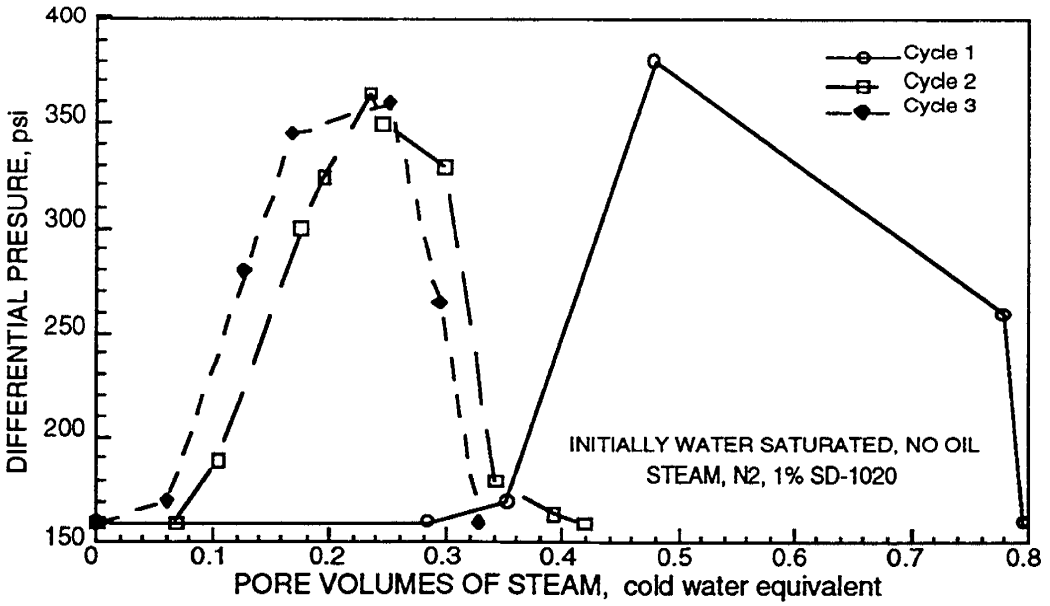

FIGURE 2 - The influence of surfactant losses on rock upon foaming. The first cycle did not show any response until 35% PV of steam injection.

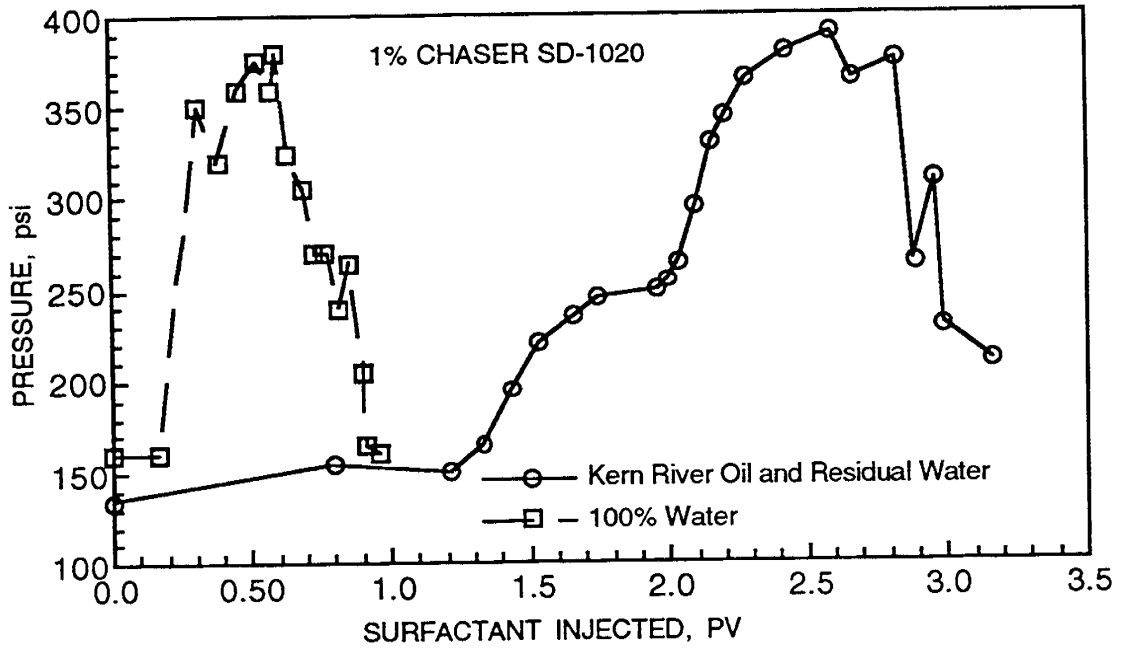

FIGURE 3. - Pressure responses during concurrent steam, N_2, and surfactant solution (1% SD-1020) injection into a preheated sandpack in the presence and absence of 13° API gravity Kern River oil.

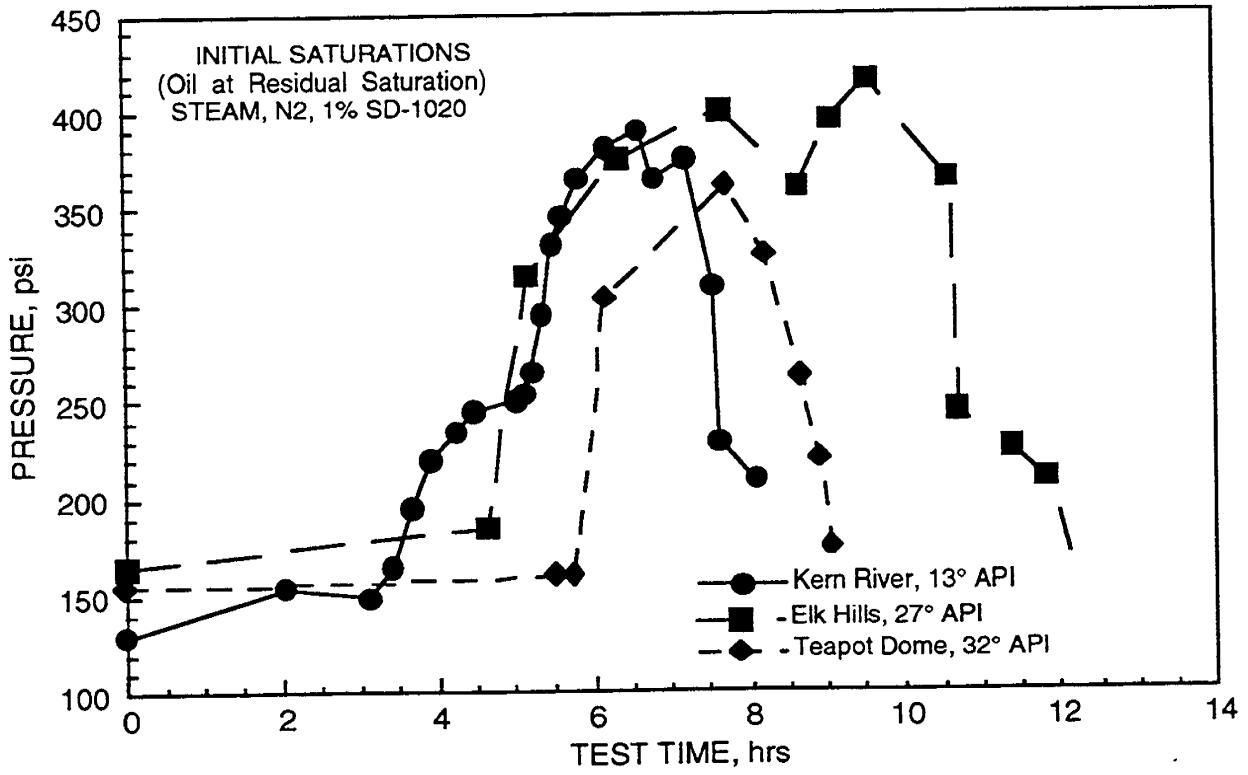

FIGURE 4. - Performance of three (13°, 27° and 32° API gravity) oils showing the effect of oil composition on foam generation in a heated linear 1-D quartz sandpack with 150 psi backpressure.

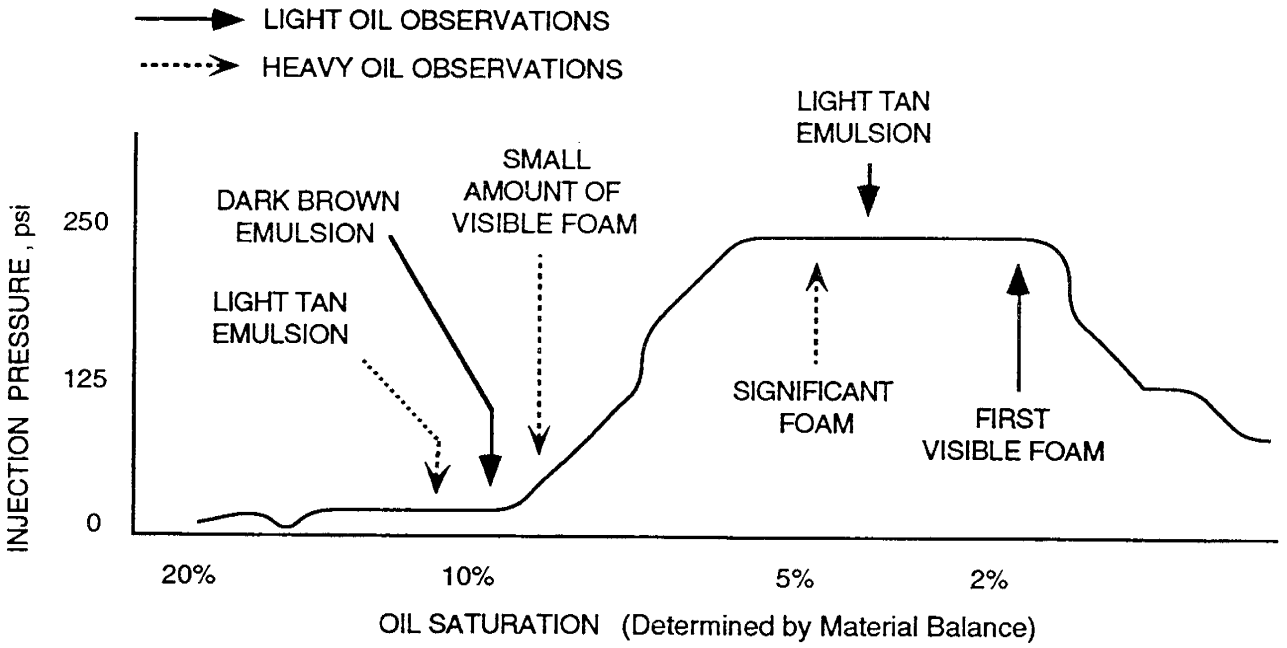

FIGURE 5. - Effluent appearance with concurrent injection of steam, N_2, and 1% SD-1020 into a partially oil-saturated linear sandpack. Initial oil saturation has been reduced to about 20% before the start of surfactant and N_2 injection. The non-linear scale shows that emulsion being produced prior to foam in the effluent.

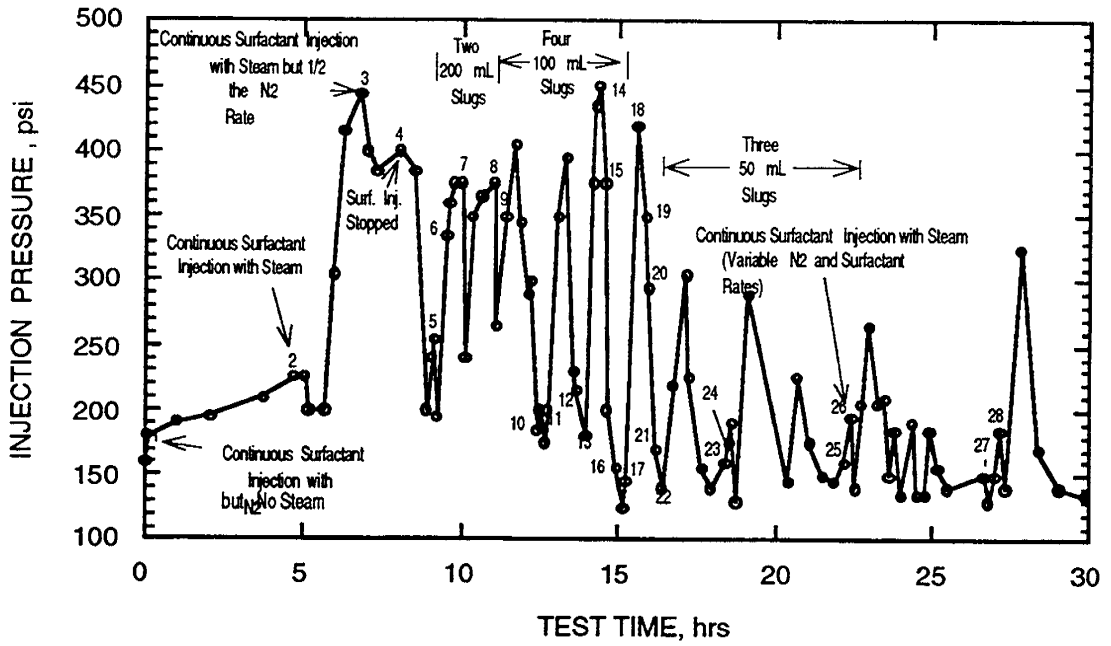

FIGURE 6. - Pressure response history from a variety of injection strategies beginning with a continuous injection strategy. Steam, N_2 and surfactant solution (1% SD-1020) were injected into a preheated sandpack initially saturated with water. The injection protocol is given in Table 1.

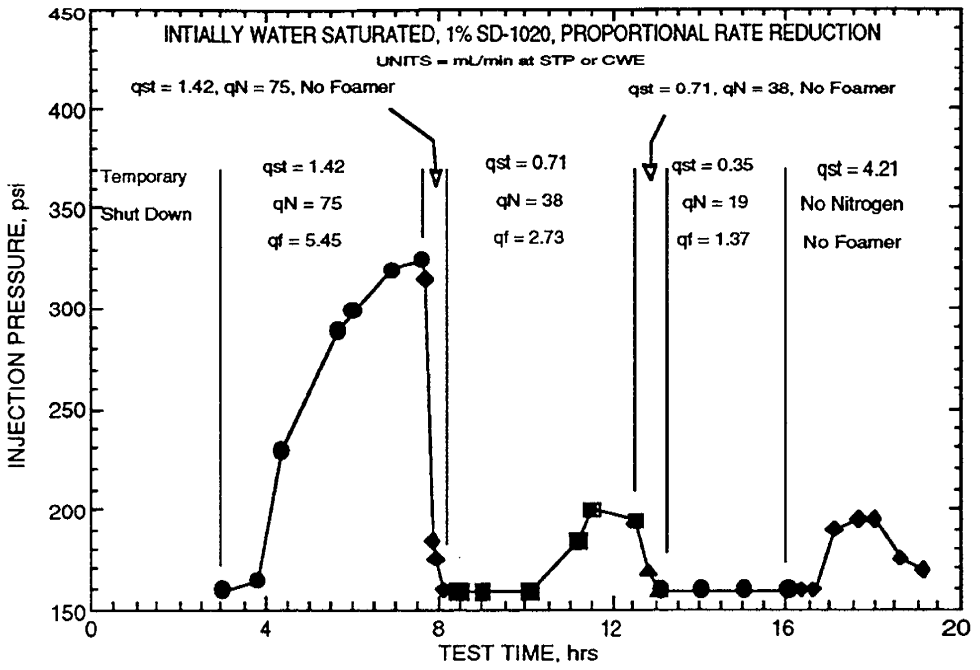

FIGURE 7. - Effect of steam injection rate on foaming behavior. The data suggest that both the onset of foaming and the peak pressure drop are influenced by rate and that a minimum rate is required (perhaps to overcome heat losses) for optimum performance of the foam.

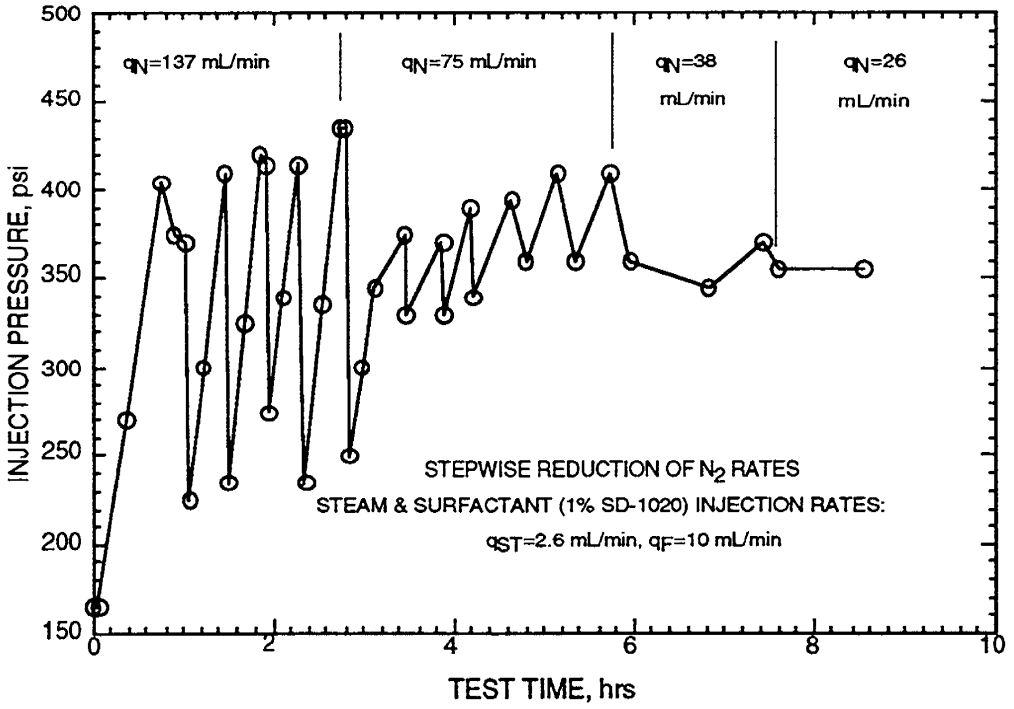

FIGURE 8. - The role of a noncondensable gas on foam performance in a series of pressure buildup (surfactant injected) and pressure falloff tests (no surfactant is injected but at the same nitrogen flow rate). Higher N_2 fractions are seen to cause higher peak pressure.

15° API ROUND MOUNTAIN CRUDE
k ≈ 4.6 Darcies Quartz Sandpack, Ø ≈ 34.7%, S_{oi} ≈ 71%
Ultimate Recovery ≈ 87% of OOIP

Incremental Recovery After Surfactant+N_2 ≈ 8% of OOIP
Steam Injection Started at 0 Hrs.
5% SD-1020 + 1% NaCl at 15 Hrs.
N_2 10cc/min at 16.5 Hrs.

FIGURE 9. - Example of a good sweep efficiency in 2-D model. Surfactant/salt slug followed by N_2 were injected after steamflood. This picture qualitatively shows the potential of foam for improving front profiles.

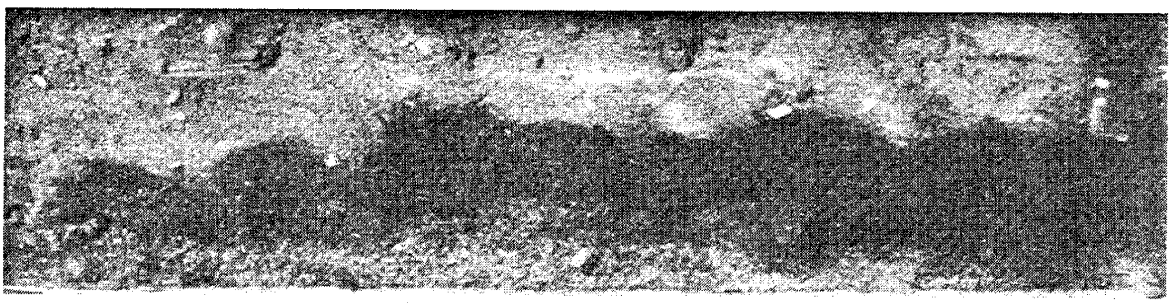

13° API KERN RIVER CRUDE
k_{top} ≈ 26 Darcies, k_{middle} ≈ clay, k_{bottom} ≈ 10 Darcies,
Ø ≈ 43%, S_{oi} ≈ 61% (average),
Ultimate Recovery≈ 86% of OOIP (average)

Incremental Recovery After Surfactant & Emulsion ≈ 3+2% ≈ 5% of OOIP
Steam Injection Started at 0 Hrs.
1st Slug 0.05 PV of 1% SD-1000 + N_2 4cc/min at 23 Hrs.
2nd Slug 0.10 PV of 1% SD-1000 + N_2 4cc/min at 25.5 Hrs.
3rd Slug 0.10 PV of 1% SD-1000 + N_2 4cc/min at 26.2 Hrs.
N_2 + Steam at 26.5 Hrs.
4th Slug Alkaline Emulsion 0.35 PV at 28.75 Hrs.
Highly Emulsified Oil Produced Starting at 31 Hrs.

FIGURE 10. - Example of fingering in 2-D model. This was a steamflood test displacing a heavy oil (13° API gravity). Multiple surfactant slugs, N_2, and alkaline emulsion slugs were injected to improve the profile.

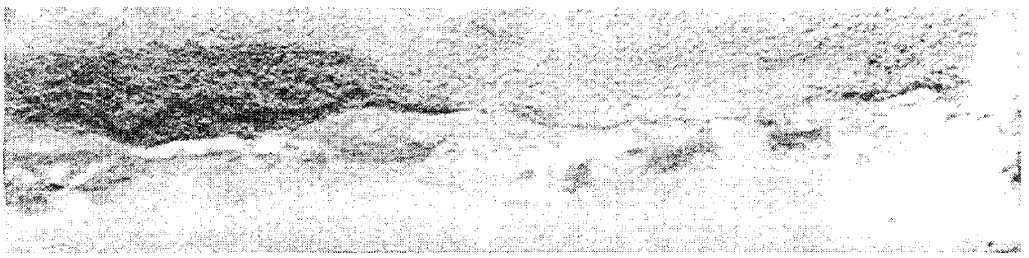

15° API ROUND MOUNTAIN CRUDE
k_{top} ≈ 56 Darcies, k_{bottom} ≈ 19 Darcies,
Ø ≈ 36%, S_{oi} ≈ 76%
Ultimate Recovery ≈ 60% of OOIP

Incremental Recovery After Surfactant+N_2 ≈ 25% of OOIP
Steam Injection Started at 0 Hrs.
5% SD-1020 + 0.1% brine at 13 Hrs.
N_2 3cc/min at 15.5 Hrs.

FIGURE 11. - Example frontal profile in layered 2-D model where foam diverted steam from the upper layer that had been steam swept to the lower layer resulting in additional oil production.

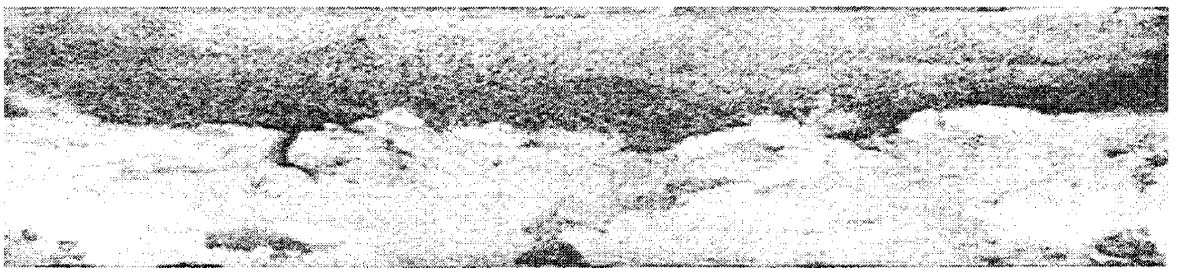

15° API ROUND MOUNTAIN CRUDE
k_{top} ≈ 76 Darcies, k_{bottom} ≈ 15 Darcies,
Ø ≈ 33%, S_{oi} ≈ 79%
Ultimate Recovery ≈ 85% of OOIP

Ultimate Recovery ≈ 85% of OOIP
Incremental Recovery After Surfactant+N_2 ≈ 8% of OOIP
Steam Injection Started at 0 Hrs.
Steam + 5% SD-1020 - 1cc/min at 18 Hrs.
N_2 + Steam + 5% SD1020 at 19.5 Hrs.

FIGURE 12. - Example of moderate profile improvement in layered 2-D model during a steamflood of a relatively heavier oil. Surfactant (and later N2 also) was continuously added with steam after the steamflood. There is no interlayer gravity segregation and no crossflow between the layers.

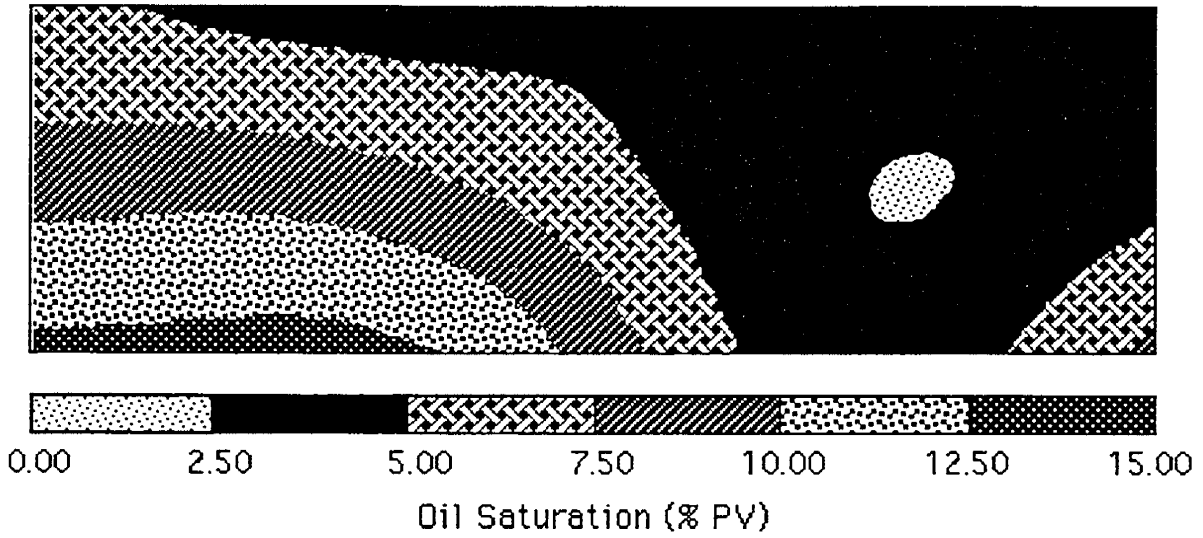

FIGURE 13. - Example of residual oil saturation mapping based on Dean Stark analysis of sand after a steamflood in 2-D experiments. This oil-wet quartz sandpack containing New London crude oil (32° API gravity) was steamflooded after a waterflood. This saturation map supports visual postflood observation of gravity override as shown in Fig. 1.

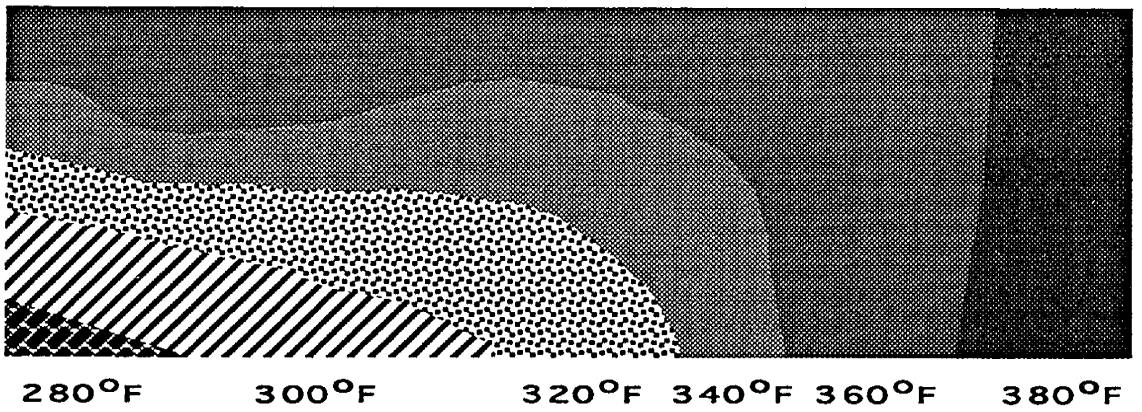

FIGURE 14. - Example of temperature profile obtained from thermocouples during the course of a 2-D steamflood. This oil-wet quartz sandpack containing New London crude oil (32° API gravity) was steamflooded after a waterflood. Steam injection temperature is 395° F. This temperature map supports visual postflood observation of gravity override as shown in Fig. 1.

Foam Treatment of Producing Wells To Increase Oil Production at Prudhoe Bay

by R. E. Krause and R. H. Lane, ARCO Alaska Inc.; D. L. Kuehne, Chevron Research & Technology Co.; and G. F. Bain, Chevron Chemical Co.

Originally presented as Society of Petroleum Engineers paper No. 24191 at the SPE/DOE Eighth Symposium on Enhanced Oil Recovery held in Tulsa, Oklahoma, April 22-24, 1992. Copyrighted by Society of Petroleum Engineers, Inc., 1992.

This poster/paper was prepared for presentation at the DOE/NIPER, Symposium on Field Application of Foams for Oil Production held in Bakersfield, California, February 11-12, 1993.

This paper was selected for presentation by a Program Committee following review of information contained in an abstract submitted by the author(s). Contents of the paper, as presented, have not been reviewed and are subject to correction by the author(s). The material, as presented, does not necessarily reflect any position of the U.S. Department of Energy or the National Institute for Petroleum and Energy Research.

Abstract

Since May of 1989, the Prudhoe Bay oil field has been on decline. No longer limited by the capacity of the TransAlaska Pipeline or state offtake restrictions, daily oil production is now restricted primarily by the amount of gas reinjection capability that currently exists at the North Slope.

This paper describes the results of several Prudhoe Bay field trials performed in 1991 in the Eastern Operating Area (EOA) by ARCO Alaska, Inc. The objective of these field trials was to assess the effectiveness of foamable EOR surfactants in preferentially reducing the gas production through direct treatment of high gas/oil ratio (GOR) producing wells. Three different methods of delivering the surfactant into the producing interval were tried. One method, the injection of foam, preformed at the surface using nitrogen, caused a significant GOR reduction which translated into an increase in oil production in the target well for a period of several weeks.

Work is ongoing in this area to determine the effectiveness and economic potential of these foam treatments.

References and illustrations at end of paper.

Introduction

Prudhoe Bay is the United States' largest producing oil field. As previously mentioned, oil production is constrained by the amount of gas reinjection capability. Therefore, oil production from any given well is prorated based on that well's measured gas/oil ratio or GOR. Under normal operating conditions, wells with higher GORs are choked back more than wells with lower GORs. Therefore, if a well's GOR can effectively be lowered while maintaining its oil rate, more oil can be produced from that well.

Since most of these wells produce at rates of 1000 bbl/D or greater, even a temporary drop in a well's GOR is economically significant. Because of this, certain wells at Prudhoe are shut-in and produced on a cyclical basis, if their GORs are known to drop after a shut-in period.

High GOR wells that do not respond to cycling are shut-in most of the time. Which wells are shut-in is determined by the field marginal GOR in current use. All wells with GORs higher than the marginal GOR are normally shut-in. Wells with GORs lower than marginal are produced. The rate at which they produce is primarily dependent on the magnitude of their GOR, as well as other considerations. This

system works to minimize gas production and maximize oil production in the field.

We noticed as early as 1985 at Prudhoe that occasionally a well's GOR was temporarily lowered after a corrosion inhibitor pumpdown in which the damaging inhibitor was inadvertently displaced into the formation. Because gas production was not the pivotal criteria for determining whether a well was produced or not at that time, no further attention was given to this particular phenomenon. However, it did suggest the possibility of temporarily controlling gas production by performing near wellbore chemical treatments. If a corrosion inhibitor could slow down gas production, why not try a foamable surfactant?

The use of foamable surfactants to reduce injected gas/steam "fingering" or gravity override between EOR injectors and producers has been under evaluation since the 1960s.[1-5] In the last decade, synthesized surfactants were developed which form stable foams in high temperature, high salinity environments in the presence of crude oil.[6,7] Because surfactants are able to control gas mobility via foam formation, we proposed that foamable surfactants be used on high GOR producing wells at Prudhoe.

We hypothesized that by backflushing a high GOR producing well with a foamable surfactant, a reduction in gas mobility would occur which would allow the well to produce at a lower GOR. How long this lower GOR would persist was a major concern. Because the cost of most surfactants was relatively inexpensive, we thought that potential existed at Prudhoe to periodically treat a well to lower its GOR, thereby increasing its net oil production. First, though, it was necessary to find a suitable surfactant.

Surfactant Selection

In early 1990, a literature search was undertaken to find a suitable surfactant to use in a field trial. Due to adsorption considerations in a sandstone reservoir like Prudhoe, only anionic surfactants were considered.[8]

The literature search identified several promising surfactant structures: alpha-olefin sulfonates,[6,9,10] alcohol ethoxy-ethyl sulfonates,[11] and alcohol ethoxy-glyceryl sulfonates.[8]

Much of the published data concerning foam stability was oriented around high temperature steam flood applications or low temperature, ambient pressure applications.[11-13] Until recently, relatively little work was done testing surfactants in the presence of crude oil.

A proprietary foam surfactant developed by Chevron Chemical (CHASER™ GR1080) was chosen for use at Prudhoe based on a pilot test with a similar surfactant in Chevron's Painter Reservoir in Wyoming.[14] The temperature, pressure, and salinity of the Painter reservoir were similar to Prudhoe Bay's (see Table 1). Prudhoe's porosity and permeability are higher, but according to most work done with foam to date, higher porosity and permeability should be more favorable to foam generation. The surfactant is a mixture consisting primarily of alpha-olefin sulfonates and is thermally stable at Prudhoe reservoir temperatures.

The attempt to control nitrogen mobility between the injection and production intervals of a dual well in the Painter field trial was largely unsuccessful and the nitrogen cut continued to increase as oil production continued to decrease. However, "pressure transient analysis showed that the effects of foam were limited to the near-wellbore region of the injector and diminished gradually over several months".[14] This indicated that the generated foam was most effective in the near wellbore region which is where it was proposed for use in the Prudhoe Bay producing wells.

Pressure transient analysis on the treated Painter Reservoir injector indicated that the injectivity index for nitrogen was 19.6 MSCF/D/psi on 10-10-86, prior to the foam treatment, and was 1.92 MSCF/D/psi on 12-22-86, immediately after the treatment. The injectivity index increased slowly to 5.82 MSCF/D/psi by 2-18-87 and to 10.5 MSCF/D/psi by 4-29-87. This data suggests that the foam treatment caused a pronounced nitrogen injectivity drop that lasted at least six months.

After choosing the surfactant, there still remained a concern that an oil-surfactant emulsion might form and cause separation or foaming problems in the surface facilities. To anticipate this, room temperature blender tests were done using

representative Prudhoe Bay crude oil and the Chevron surfactant. Test results showed that no emulsions were formed during any of the simulated conditions likely to be encountered in Prudhoe Bay wells.

Prudhoe Field Trials

Three different high GOR wells were chosen in the upstructure area of the Prudhoe Sadlerochit formation, near the gas cap. The GORs of these three wells all showed a steady upward trend and no evidence of cyclic GOR behavior after being shut-in for an extended period of time. Three different surfactant treatments were performed on these wells. The three different treatment methods chosen varied in complexity and expense.

An effective concentration of 0.5 wt% active surfactant was chosen for all three of the well treatments. Adsorption of the anionic surfactant by the Prudhoe Sadlerochit sandstone was not expected to be significant. The surfactant was trucked up to the North Slope as a 40 wt% active concentrate and diluted to 0.5 wt% using Beaufort seawater from the Seawater Treatment Plant. The seawater salinity was comparable to Prudhoe Sadlerochit formation water salinity of 21,100 mg/l TDS.

The first treatment simply entailed pumping a 1000 bbl slug of liquid surfactant down Well 2-12 followed by a 280 bbl seawater overflush with a 200 bbl diesel cap. When the well was brought back on production, we hoped that the gas approaching the wellbore would generate foam as it jetted through pore throats and contacted surfactant.

The second treatment design consisted of pumping a 500 bbl slug of liquid surfactant followed by a 200 MSCF slug of nitrogen into Well 7-4. This sequence was repeated once. We thought that the foam would be generated in the formation by chasing the surfactant with nitrogen. The sequence was repeated because two different intervals in Well 7-4 may have been responsible for the well's high GOR.

Results from both of these treatments were disappointing. In the case of the Well 2-12 treatment, we hoped that a measurable loss in injectivity could be observed during the job due to foam formation when gas invaded the surfactant-saturated region. Particularly in the case of Well 7-4, foam formation and a measurable surface injectivity loss were expected when the nitrogen contacted the surfactant solution in the reservoir. However, no loss in injectivity was observed during either job.

Neither treatment showed any post treatment GOR decline. In addition, test separator data showed that early production from both wells was primarily water. Both of these wells produced no water prior to the treatments. Instead of forming foam in-situ, as had been expected, the test separator data indicated that most of the surfactant had simply flowed out of the formation at about the same rate that the surfactant had been pumped into it.

One positive aspect of these two treatments was that no facility upsets were noted in conjunction with these large volumes of surfactant flowing back. This confirmed the earlier lab work suggesting that oil-surfactant emulsions would not be a problem.

Preformed Foam Treatment Design

The third treatment was performed on Well 15-15, in which there were two sets of leaking squeeze perforations above the rest of the perforated interval (see wellbore schematic diagram in Figure 1). These leaking squeeze perforations produced most of the well's gas and a substantial portion of its oil. A production profile run on Well 15-15 in September 1990 showed 75% of the total flow, primarily gas, was coming from the upper interval. The GOR of Well 15-15 was only 6700 SCF/bbl and the oil rate was 2291 BOPD at this time. Prior to the foam treatment in March 1991, the GOR of Well 15-15 had increased to 9600 SCF/bbl and was shut-in almost all of the time. Based on the previous profile, it was likely that the increased gas production was coming from the uppermost interval.

The first step in the Well 15-15 foam treatment was to pump a 400 bbl slug of liquid surfactant into the formation. This liquid surfactant bank would satisfy adsorption and would foam when contacted with formation gas. The rest of the treatment design was modeled after the process used during Chevron's Painter Field trial. A nitrogen foam of approximately 65% quality would be created on the surface and then injected downhole until the surface pressure became too high for reasonable rates of injection. A total of 2 MMSCF of nitrogen was committed for the treatment. Approximately 600

bbl of liquid surfactant would be allocated for this purpose, but more could be made up, if necessary.

Because of lingering oil/surfactant emulsion concerns, only the upper interval in Well 15-15 was treated, as it was believed to be the interval producing the most gas. Additionally, we thought that introducing foam into the lower interval might reduce the flow of oil from that interval. Prior to the foam treatment, a retrievable inflatable packer was set on electric line to isolate the uppermost leaking squeeze perforations.

Sizing the job was difficult because we did not know how much foam the interval would take before the injectivity dropped too low to continue pumping. Therefore, no particular target radius of treatment was chosen prior to the job. In addition, the total height of the high GOR interval was not known exactly. Based on a hypothetical 10' height of producing interval and 600 bbl of surfactant injected at a 65% foam quality, the estimated treatment radius would be approximately 40'.

Using the wellbore geometry of Well 15-15, a plot of maximum surface pressure as a function of injected foam quality was generated by Chevron personnel prior to the job using an in-house program[15,16] (Figure 2). Use of this plot by ARCO Alaska personnel on location would insure that the pressure at the formation face would not exceed hydraulic fracture pressure. In addition, plots of both surface and downhole foam quality versus surface pressure for various surfactant/nitrogen ratios were also generated (Figures 3 & 4). These plots provided field guidelines and operational flexibility while performing the treatment on location.

Well 15-15 Foam Treatment Execution

The foam treatment on Well 15-15 was performed on 4/6-7/91. A schematic of the onsite equipment used to perform the preformed foam injection is shown in Figure 5. It consisted of a liquid nitrogen pumping unit and a surfactant pump feeding into a common injection line where gaseous nitrogen and liquid surfactant mixed. The surfactant pump was connected to a surfactant tanker. Downstream of both the pump and nitrogen unit was a skid-mounted choke unit. A 100-200 psi pressure drop maintained across the choke caused the foam to form prior to being injected downhole.

Approximately 400 bbl of liquid surfactant were injected prior to the foam injection. Preformed foam injection was then initiated at 10.5 gal/min of surfactant and 500 SCF/min of nitrogen (Figures 6 and 7). As can be seen in Figure 6, the surface pressure started out at 1600 psi and steadily increased until foam was estimated to be at the formation face. At this point, the injection rate dropped off and the surface pressure increased sharply up to the maximum recommended pressure of 3250 psig.

Because of the high surface pressure and low injection rate, foamed surfactant injection was discontinued. Approximately 120 bbls of surfactant and 250 MSCF of nitrogen had been pumped. An additional 340 MSCF of nitrogen was then slowly pumped below the formation fracture pressure to displace the foam into the formation. The entire job lasted 36 hours. Based on the same hypothetical 10' interval, the estimated treatment radius was approximately 18'.

Well 15-15 Foam Treatment Results

The well was shut-in for approximately one week and then the bridge plug was pulled by a Coiled Tubing Unit. Two production tests performed immediately afterwards were indecipherable due to the large amount of nitrogen and liquid surfactant flowback that occurred. Well 15-15 was then tested on 4/14/91 at a 2150 SCF/bbl GOR on a 37° choke and on 4/15/91 at a 466 SCF/bbl GOR on a 40° choke. The choke was maintained at 40° and on 4/17/91 the well next tested at 1022 BOPD and a 3410 SCF/bbl GOR with no water cut (see Table 2 for a complete well test history for Well 15-15). At this point, the total gas production of the well seemed to stabilize at approximately 4 MMSCF/D (see Figure 8 for a complete post treatment statistics plot).

Well 15-15 was confined to a somewhat restricted choke setting at first. The reasons for this were twofold. First, as had been seen in laboratory tests by Chevron, once this foam was placed in an interval at a certain differential pressure, the foam would have low mobility unless subjected to a much greater differential pressure. A restricted choke setting would ensure a low differential pressure across the producing interval. Secondly, the change in GOR over time would be easier to see without constant choke changes.

The well continued to produce a consistent amount of gas, in the 4-5 MMSCF/D range, but the oil rate started to fall off due to the restrictive choke setting. Twenty six days after the well was brought on, the oil rate dropped down below 500 BOPD. Well 15-15 was shut-in because its 9547 SCF/bbl GOR exceeded the current marginal GOR for the field, approximately 8000 SCF/bbl. The average rate for this one month post-treatment period was 825 BOPD at a 4750 SCF/bbl.

The well was opened back up again one week later, this time at a higher choke setting. The choke was opened up to 44° and the well tested at 1500 BOPD, 5500 SCF/bbl GOR with no water cut (see Table 2 or Figure 8). The choke was opened up to 50° and the GOR continued to climb an average of 340 SCF/bbl/day until the well had to be shut-in on 6/1/91. On that date, the well tested at 8900 SCF/bbl which was higher than the field marginal GOR of 8000 SCF/bbl. The average rate for the 13 days the well was on production was 1675 BOPD at a GOR of 7072 SCF/bbl.

The average "net oil benefit" during the first post-treatment period of one month was 340 BOPD and for the second post-treatment period of 13 days was 94 BOPD. The "net oil benefit" concept was developed to better quantify and normalize production benefits for wellwork that lowers a well's GOR. Wellwork that reduces a well's GOR below the current marginal GOR essentially creates more oil in the gas-constrained production environment at Prudhoe Bay. How much more oil is created depends on the oil and gas rates before and after the treatment, as well as the field's marginal GOR, in this case--8000 SCF/bbl, at the time of treatment.

For the foam treatment, this means that its net benefit to Prudhoe was equivalent to bringing on a new well for 39 days with a production rate of 265 BOPD and no associated gas. A plot of the actual "net oil benefit" as calculated for each post-foam treatment well test is shown in Figure 8. The equation used to calculate "net oil benefit" is presented in Appendix A along with an example calculation.

A post-foam treatment production profile in Well 15-15 indicated that only 43% of the well's total production (primarily gas) was coming from the upper interval compared to 75% before. This production profile was run after the well's GOR had already risen significantly, so the actual percentage of gas temporarily shut-off from the upper interval may have been even higher, initially.

Foam Treatment Economic Considerations

Two major costs were associated with the foam treatment on Well 15-15. The first was the cost of the 617 MSCF of nitrogen used and associated pumping charges. Nitrogen costs are approximately an order of magnitude higher on the North Slope than what is normally encountered in the continental U.S. Secondly, a much smaller but still significant cost is associated with the placement and pulling of the inflatable bridge plug which provided zonal isolation.

Nitrogen costs will continue to be the major factor in foam treatment economics. If foam treatments should become standard practice, then expectations are that the nitrogen cost would decrease substantially with the increase in volume. Until that time, however, the economics of performing foam treatments will not be as competitive as they could be.

Another source of high pressure gas is available on the North Slope. Miscible gas used for EOR injection would be an adequate foaming agent for use in future attempts at foam treatment of producing wells. It would have the additional advantage of relatively low cost of operation in the situation where a foam treatment takes several days to perform due to low injectivity of the target well. For instance, the use of miscible gas to treat Well 15-15 may have afforded a much longer period of foam injection. It is not, however, available at all Prudhoe drillsites, including drillsite 15. The expense and logistics of using miscible gas for use in foamable surfactant treatments are currently under investigation.

Conclusions

1) By treating a producing well at Prudhoe Bay with a foamable EOR surfactant, the Gas-Oil Ratio of that well can be temporarily lowered.

2) Of the three foam treatment methods tested, preforming the foam on the surface prior to injection was the only method that produced a significant GOR reduction.

3) The primary economic constraint for preformed foam treatments at Prudhoe is the cost of the nitrogen used to foam the surfactant.

4) More work remains to be done on the optimization of numerous treatment parameters: foam quality, effective treatment radius, surfactant chemistry, well flowback rates, etc.

Acknowledgements

The authors thank the management of ARCO Alaska, Inc. and its partners in the Prudhoe Bay Unit for supporting the publication of this paper. The Wells Group on the Slope is acknowledged for professionally supervising each well treatment. This program has also benefited from support of the ARCO Alaska, Inc. library staff in Anchorage.

The techniques and/or conclusions described in this paper are those of the authors and are not necessarily shared by the Prudhoe Bay Unit working interest owners.

References

1. Bond, D.C. and Holbrook, O.C.: "Gas Drive Recovery Process," U.S. Patent No. 2,866,507 (1958).

2. Bernard, G.G. and Holm, L.W.: "Effect of Foam on Permeability of Porous Media to Gas," Soc. Pet. Eng. J. (Sept. 1964) 267-274.

3. Bernard, G.G. and Holm, L.W., and Jacobs, W.L.: "Effect of Foam on Trapped Gas Saturation and on Permeability of Porous Media to Water," Soc. Pet. Eng. J. (Dec. 1965) 295-300.

4. Holbrook, O.C. and Bernard, G.G.: "Use of Foam for Plugging Gas Producing Strata," U.S. Patent No. 3,207,218 (1965).

5. Holm, L.W.: "The Mechanism of Gas and Liquid Flow Through Porous Media in the Presence of Foam," Soc. Pet. Eng. J. (Dec. 1968) 359-369.

6. Dilgren, R.E., Deemer, A.R., and Owens, K.B.: "The Laboratory Development and Field Testing of Steam/Noncondensible Gas Foams for Mobility Control in Heavy Oil Recovery," SPE 10774 presented at the California Regional Meeting, San Francisco, March 24-26, 1982.

7. Duerksen, J.H.: "Laboratory Study of Foaming Surfactants as Stream-Diverting Additives," SPE 12785 presented at the California Regional Meeting, Long Beach, April 11-13, 1984.

8. Wellington, S.L. and Vinegar, H.J.: "CT Studies of Surfactant-Induced CO_2 Mobility Control," paper SPE - 14393, presented at the 60th Annual Technical Conference and Exhibition of the SPE, held in Las Vegas, NV, September 22-25, 1985.

9. Wilson, T.D. and Marsden, S.S.: "The Effectiveness of Foam as a Blocking Agent at Elevated Temperatures Over Extended Periods of Time," Stanford University Petroleum Research Institute, TR-14, DOE Contract DE-AC03-76ET12056, July, 1981.

10. Hu, P.C., Tuvell, M.E., and Bonner, G.A.: "Evaluation of alpha-Olefin Sulfonates for Steam Diversion," SPE 12660, presented at the SPE/DOE Fourth Symposium on Enhanced Oil Recovery, Tulsa, OK, April 15-18, 1984

11. Borchardt, D.B., Bright, D.B., Dickson, M.K., and Wellington, S. L.: "Surfactants for CO_2 Foam Flooding," SPE 14394, presented at the 1985 SPE Annual Technical Conference and Exhibition, Las Vegas, NV, Sept. 22-25, 1985.

12. Maini, B.B. and Ma, V.: "Relationship Between Foam Stability Measured in Static Tests and Flow Behavior of Foams in Porous Media," SPE 13073 presented at the 59th Annual Technical Conference, Houston, Sept. 16-19, 1984.

13. Maini, B.B. and Ma, V.: "Measurements of Foam Stability at Elevated Temperatures and Pressures," J. Canad. Pet. Tech. (Nov./Dec. 1986) 65.

14. Kuehne, D.L., Ehman, D.I., Emanuel, A.S., and Magnani, C.F.: "Design and Evaluation of a Nitrogen-Foam Field Trial," SPE/DOE - 17381, presented at the SPE/DOE Enhanced Oil Recovery Symposium, held in Tulsa, Oklahoma, April 17-20, 1988.

15. Beyer, A.H., Millhone, R.S., and Foote, R.W.: "Flow Behavior of Foam as a Well Circulating Fluid," SPE 3986 presented at the SPE Annual Meeting, San Antonio, Oct. 8-11, 1972.

16. Millhone, R.S., Haskin, C.A., and Beyer, A.H.: "Factors Affecting Foam Circulation in Oil Wells," SPE 4001 presented at the SPE Annual Meeting, San Antonio, Oct. 8-11, 1972.

SI METRIC CONVERSION FACTORS

Customary Unit	(•)	Conversion Factor	(=)	Metric Unit
ft		3.048 E-01		m
inch		2.540 E+01		mm
°F		(°F-32)/1.8		°C
gal (US)		3.785 E-03		m^3
bbl		1.590 E-01		m^3
psi		6.895 E-03		MPa
lbm/bbl		2.853 E-00		kg/m^3
lbm/U.S. gal		1.198 E-05		g/m^3

Appendix A

Net Oil Benefit Calculation

$$NOB = [(AO)(1 - ASI)] - [(BO)(1 - BSI)] + \frac{[(1-BSI)(BO)(BG)-(1-ASI)(AO)(AG)]}{MG}$$

where

NOB = Net Oil Benefit
AO = post treatment oil rate (BOPD)
AG = post treatment GOR (SCF/bbl)
ASI = fraction of time well is shut-in after treatment
BO = pre treatment oil rate (BOPD)
BG = pre treatment GOR (SCF/bbl)
BSI = fraction of time well is shut-in before treatment
MG= current marginal GOR (SCF/bbl) = 8000 SCF/bbl

An example calculation using data from Table 2 for a well test before the foam treatment on 3/29/91 and from a well test after the foam treatment on 4/15/91 is shown below:

$$NOB = [(970)(1)] - [(2391)(0)] + \frac{[(0)(2391)(9646) - (1)(970)(466)]}{8000}$$

$$NOB = 913 \text{ BOPD}$$

Assumptions:

Due to a GOR greater than the marginal GOR, the well is not produced before the foam treatment: BSI = 1

Due to a GOR less than the marginal GOR, the well is back on production after the foam treatment: ASI = 0

Table 1

Prudhoe Bay Reservoir Properties

Temperature (°F)	185-225	
Pressure (psia)		3500-3800
*Porosity (%)		20
*Permeability (md)	300-700	
Oil Gravity (°API)		27
**GOR (SCF/STB)	600-800	
Produced Water TDS (mg/L)		21,100

*Referenced to the zone of interest in this paper.

**Original solution gas/oil ratio

Table 2

Well 15-15 Test Results

Date (1991)	Choke Position (degrees)	Oil Rate (BOPD)	Water Rate (BWPD)	Gas Rate (MSCF/D)	GOR (SCF/bbl)
3-24	84	2838	0	23741	8365
3-29	60	2391	0	23064	9646
4-06	Foam Treatment				
4-14	37	510	387	1096	2149
4-15	40	970	74	452	466
4-17	40	1022	0	3485	3410
4-20	40	884	0	4033	4562
4-25	40	837	0	3946	4714
4-28	40	811	0	4783	5898
5-01	40	778	0	4856	6242
5-10	40	494	0	4716	9547
5-10	Well shut-in. GOR above marginal.				
5-17	Well brought back on production.				
5-21	44	1579	0	8614	5455
5-23	44	1457	0	9664	6633
5-25	50	1810	0	12090	6679
5-28	50	1752	0	12723	7262
5-31	50	1577	0	13983	8867
5-31	Well shut-in. GOR above marginal.				

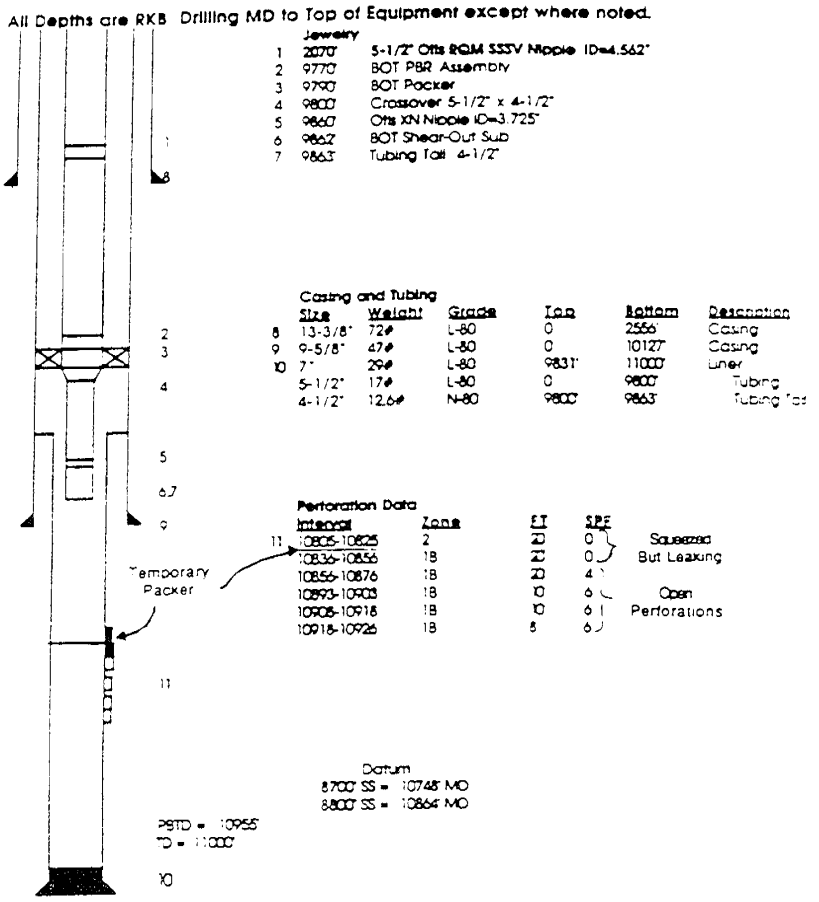

Figure 1. Wellbore Schematic for Well 15-15

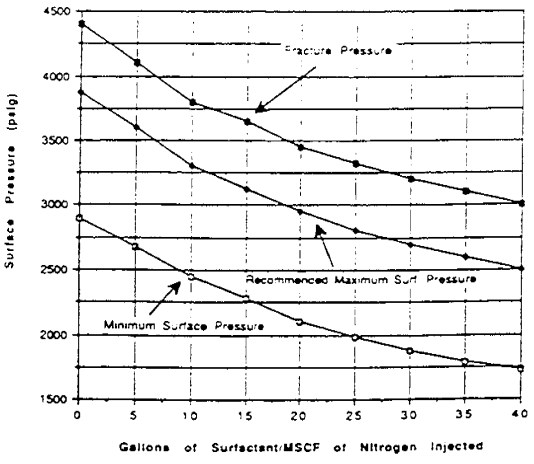

Figure 2. Surface Pressure Range for 15-15 Foam Treatment

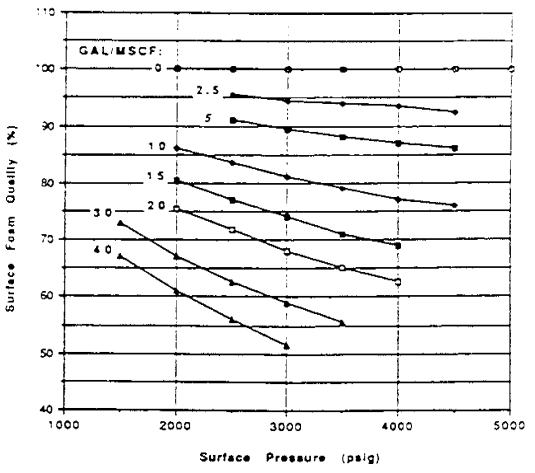

Figure 3. Relationship of Surface Foam Quality to Surface Pressure for Various Surfactant/Nitrogen Ratios

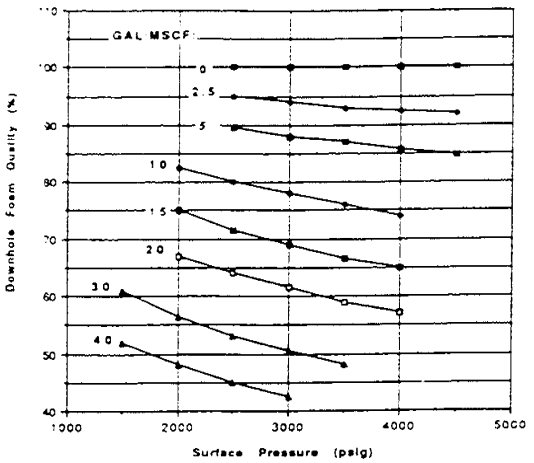

Figure 4. Relationship of Downhole Foam Quality to Surface Pressure for Various Surfactant/Nitrogen Ratios

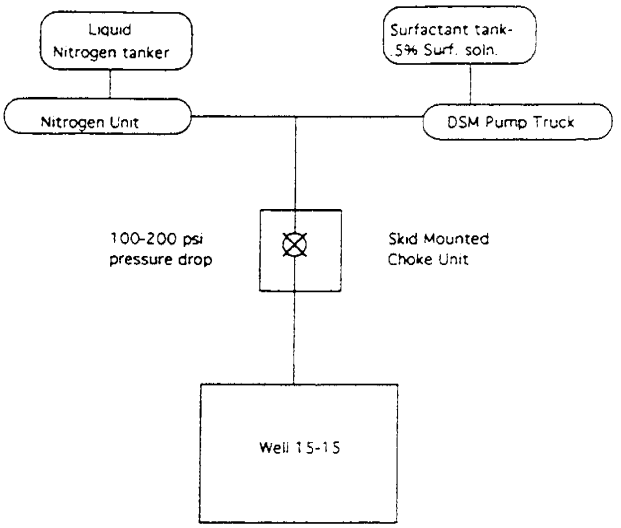

Figure 5. Foam Equipment Schematic Well 15-15

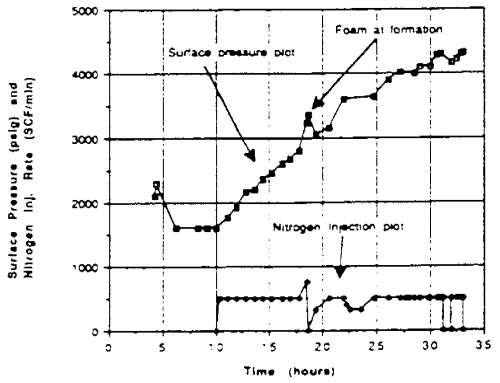

Figure 6. Plot of Surface Pressure and Nitrogen Injection Rate During Treatment

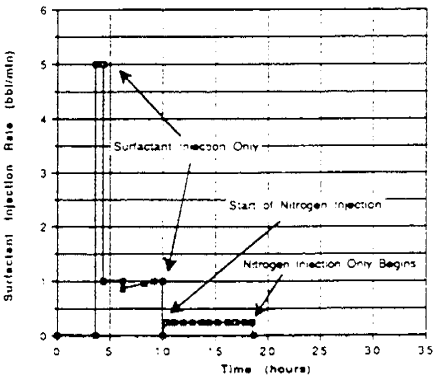

Figure 7. Surfactant Injection Rates during Foam Treatment

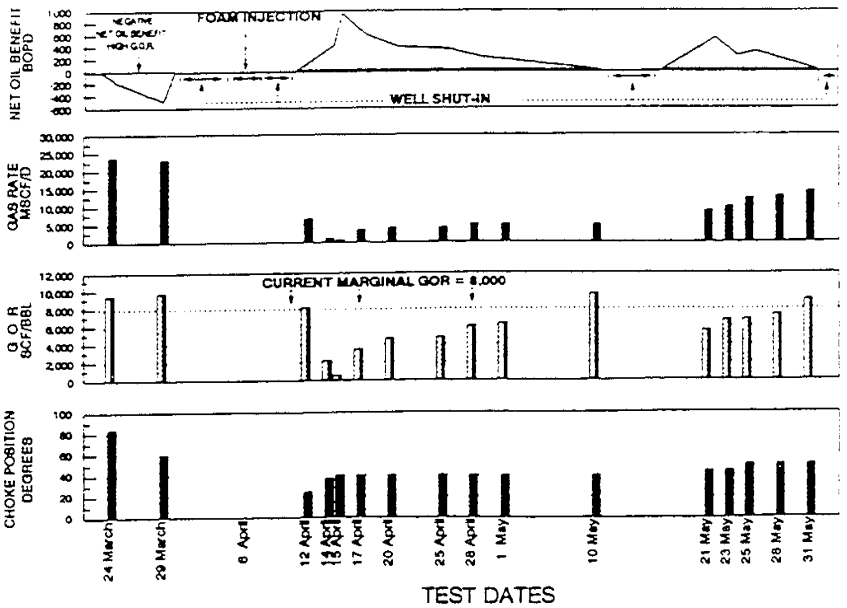

Figure 8. Post Foam Treatment Statistics Well 15-15 Prudhoe Bay

No. FSP5

DOE/NIPER

Surfactant Selection for Gas Foam Applications

by Donald L. Kuehne and Jeremy Cantor, Chevron Research and Technology Company

Author(s) are solely responsible for copyright and contents.

This poster/paper was prepared for presentation at the DOE/NIPER, Symposium on Field Application of Foams for Oil Production held in Bakersfield, California, February 11-12, 1993.

This paper was selected for presentation by a Program Committee following review of information contained in an abstract submitted by the author(s). Contents of the paper, as presented, have not been reviewed and are subject to correction by the author(s). The material, as presented, does not necessarily reflect any position of the U.S. Department of Energy or the National Institute for Petroleum and Energy Research.

ABSTRACT

This poster paper describes a laboratory methodology to test and evaluate foam-forming surfactants for specific reservoir applications. The same methodology can serve as a guide in the development of new or improved EOR products.

To find the best surfactant for a particular reservoir, surfactants are passed through a series of screening tests of increasing complexity to focus on the more attractive candidates. Relatively simple tests, such as brine compatibility and bench foam height, can be performed easily on a large number of samples. Surfactants which pass these tests are scrutinized further in core tests to measure adsorption and their effectiveness as mobility control agents. More accurate predictions of reservoir behavior are obtained when the corefloods are conducted at reservoir temperature and pressure using representative rock and fluid samples. Other surfactant properties such as viscosity, pour point, and freeze/thaw stability affect field handling and are also considered in the selection process.

This methodology is illustrated with laboratory data for a CO_2 foam project in a San Andres dolomite reservoir. Several conventional surfactants are compared with a new surfactant formulation that generates stronger, longer lasting foams in oil-wet dolomite cores.

INTRODUCTION

Foam-forming surfactants are used in miscible and immiscible gas flooding projects to improve sweep efficiency and increase oil production. This is accomplished by lowering the gas phase mobility and increasing the effective density so there is less tendency for channeling and gravity override. The results are delayed gas breakthrough, lower production gas-oil ratios, and a more efficient EOR process.

To reap the benefits of improved mobility control with foam, it is important to select the best surfactant for a particular reservoir application. Our laboratory methodology includes both simple and complex tests as illustrated by the inverted pyramid in Figure 1. The strategy here is to eliminate many of the surfactant candidates through the simpler screening tests, allowing more rigorous testing to be done on the better candidates.

While the methodology appears to be straightforward, our experience indicates that sometimes the tests may give misleading results. As we discuss each test below, we will point out some of the pitfalls and suggest ways to avoid them. Some of the data included in the examples came from an earlier evaluation of surfactants for San Andres dolomite reservoirs.[1] Table 1 lists the chemical type and source of the surfactant candidates, which included only a few of the more familiar commercial surfactants.

BRINE COMPATIBILITY TEST

The brine compatibility test shows whether or not a surfactant or mixture of surfactants would remain soluble under field conditions. Any tendency for a surfactant to form a precipitate or another phase is undesirable because this would inhibit propagation of the surfactant through the reservoir. In general, we prefer surfactants that have wide ranges of application with respect to total salinity, divalent ion

Tables and figures at end of paper.

concentration, and temperature. Figure 2 shows the range of application for three CHASER™ products.

Sometimes, the desired foam properties, such as brine or oil tolerance, cannot be obtained with a single-component surfactant. Then, formulations, or mixtures of surfactants, are evaluated to find ones that give improved performance. These experimental formulations must first pass the brine compatibility test, as illustrated in Figure 3. The test conditions included ranges for divalent ion concentration (1000-3000 ppm), total dissolved solids, TDS (1-5%), and temperature (72-200°F). The divalent cations Ca^{++} and Mg^{++} were present in equal concentrations by weight as the chloride salts. Of the three experimental formulations, only Formulation #2 remained clear under all conditions as determined by visual observation. For more quantitative results, clarity should be determined with a turbidimeter (HF Instruments, Model DRT 100B), which measures light scattered by suspended particles. Solutions which appear clear to the naked eye have a turbidity of less than about 10 NTU (Nephelometric Turbidity Units).

Our first brine compatibility tests were performed by aging surfactant solutions in glass vials or bottles. We found that in tests lasting several days or longer, silicates precipitated from some solutions, which interfered with our observations. We now use screw-capped plastic containers. Polysulfone, though having a slight yellow color, combines clarity, acid and base resistance, and resistance to alcohols (which makes them easy to clean). Polycarbonate, which is colorless, can also be used, but its chemical resistance is not as good as that of polysulfone.

BENCH FOAM TEST

The bench foam test determines how well a surfactant generates a bulk foam under ambient conditions with or without oil present. Because of its simplicity, this test was popular among early foam researchers to screen surfactants.[2,3] However, it is now well recognized that bench foam tests are inadequate for predicting foam behavior in porous media. The examples in this section are included for comparison with later tests that more closely approximate reservoir conditions.

Solutions of 0.5 wt% active surfactant were prepared with synthetic reservoir brine. For the bench foam test, 24 cm^3 of surfactant solution and 1 cm^3 of stock tank oil were added to a 100-cm^3 stoppered graduate cylinder and shaken vigorously. Foam height and liquid drainage volume were recorded at two-minute intervals for 16 min.

Results for four surfactants are listed in Table 2. Alipal CD-128 and NES-25 generated bulk foams that initially filled the graduate; whereas, CHASER™ CD1045 and CD1050 had smaller foam volumes. Most of the liquid drained out of all the foams very quickly. At the end of the test, Alipal CD-128 and NES-25 still had large foam volumes, but the lamellae were very thin and barely visible. CHASER™ CD1045 generated a much denser foam with finer texture. The difference in foam properties makes it difficult to choose the best surfactant. The selection would be different depending on whether foam height or foam density is considered more important.

LOW-PRESSURE FOAM TEST

The low-pressure foam unit (Figure 4) measures the flow resistance of foam in a core or other porous media. Typically, the test is run with reservoir rock and fluids at room temperature and 250-400 psig. This test is a vast improvement over the bench foam test because it models reservoir conditions more closely. Surfactant effectiveness in controlling gas mobility is characterized by the resistance factor, which is defined as the differential pressure across the core with foam divided by the differential pressure under simultaneous injection of gas and brine at the same flow rate. Preferably, foam is injected for multiple pore volumes until steady-state conditions are achieved. Figure 5 shows the superior performance of XP200 (a precursor to CHASER™ CD1045) in an oil-wet dolomite core, compared to five other surfactants. XP200 was specially formulated to foam in an oil-wet environment.

Simple construction and ease of operation are two important advantages of the low pressure foam unit. Brine, surfactant, and oil are injected into the unit with two HPLC pumps (Beckman 110B Solvent Delivery Module or equivalent). The gas is added just before the foam generator with a Brooks 5850E Series mass flow controller. Gas delivered to the mass flow controller should be at 200-300 psi above the set pressure of the back pressure regulator to allow for pressure build-up during foam generation. The foam generator consists of a 5 x 3/4 in. stainless steel tube packed with 70-100 mesh glass beads. The core, approximately 3 x 1 in., is set with epoxy in a 1 1/2 in. diameter aluminum tube and held between two end plates with o-ring seals. The end plate on the core inlet has a side port to allow flushing of the lines up to the core face. A Validyne differential pressure transducer connected to a data logger measures the pressure drop across the core. A sight glass (not shown) located at the core outlet allows visual observation of the foam.

The test procedure involves several preliminary steps to condition the core and collect baseline mobility data. These steps include an initial waterflood, oil flood, waterflood, gas flood, and gas/brine together (4:1 volume ratio). At this point, the core contains a relatively low residual oil saturation. Next, gas and 0.5 wt% active surfactant solution are injected

simultaneously (4:1 ratio) at an interstitial velocity of 100 ft/d, the same rate as gas/brine injection. The 4:1 ratio gives an 80% foam quality (volume ratio of gas to gas plus surfactant). As foam flows through the core, the differential pressure increases until a steady-state is reached. The resistance factor, as defined above, is plotted against pore volumes injected (Figure 5). Before testing another surfactant, the core is flushed with brine (> 100 PV) and then the preliminary steps are repeated.

ADSORPTION TEST

The adsorption of surfactant on reservoir rock is important because it affects the rate at which foam can be propagated through the reservoir. Low adsorption is preferred because the surfactant moves faster and contacts a larger portion of the reservoir. Other mechanisms that can reduce surfactant effectiveness include partitioning to the oil phase, entrapment in small pore throats, and precipitation with hardness ions. These mechanisms should be of minor importance compared to adsorption if the surfactant has good brine compatibility. Typically, adsorption is determined by the dynamic displacement method[4] or the recirculation method.[5] We prefer the dynamic displacement method because it is a better model of what happens in the reservoir and usually gives more accurate results. The adsorption rates for four surfactants in dolomite core (Table 3) are all below 0.2 mg/g of rock, which is considered acceptable for use in the field.

In the dynamic displacement method, a solution of surfactant and nonadsorbing tracer are pumped through a core at controlled temperature (Figure 6). After sufficient surfactant is injected to satisfy adsorption (inlet and outlet concentrations are equal), the core is flushed with brine. Effluent samples are collected and analyzed for surfactant and tracer by wet chemical or spectophotometric methods. Normalized concentrations of surfactant and tracer are plotted against time or pore volumes injected. Adsorption of surfactant on the rock is proportional to the area between the effluent concentration profiles for surfactant and tracer, as given by the following equation:

$$M_s = \frac{1000\ A\ PV\ \rho_w\ C}{\rho_r\ (V_t - PV)} \qquad (1)$$

Figure 6 shows one configuration of the adsorption apparatus that utilizes a differential refractometer for on-line monitoring of concentration changes in the core effluent. This type of detector makes it easier to measure the adsorption of multicomponent formulations such as CHASER™ CD1045. However, since the refractometer is nonselective with respect to different chemical species, tracer and surfactant must be run separately under identical conditions, and the effluent profiles superimposed later. The detector is also very sensitive to changes in salinity which may be caused by elution of minerals from the core. Before conducting an adsorption test, the core is flushed with a large volume of brine to reach steady-state conditions. During the test, effluent samples may be collected for wet chemical analysis to verify the refractometer results. For single-component surfactants, we prefer to add a nonadsorbing tracer, such as iodide, to the surfactant solution and measure the concentrations of both surfactant and tracer in the effluent samples. Then, the core effluent is sent directly to the fraction collector without passing through the differential refractometer.

The adsorption of CHASER™ CD1040 was measured on an unfired Berea core (1 x 6 in.) at 150°F. A 0.5 wt% active surfactant solution containing 0.05 wt% iodide was injected at 1 cm^3/min for approximately 5 PV. Then, the core was flushed with brine for another 5 PV. Effluent samples were analyzed for sulfur and iodine using an ion-coupled plasma spectrophotometer (ICP). The concentration of surfactant (alpha olefin sulfonate) was proportional to the amount of sulfur, since there were no other sulfur species in the brine. Normalized concentrations, relative to the injected concentrations, are plotted in Figure 7 against pore volumes injected. The small area between the curves from 1 to 2 PV is proportional to the amount of surfactant adsorbed, which is calculated to be 0.06 mg/g of rock from Equation (1) above. During the flushing step, most of the surfactant is desorbed from the rock surfaces, as evident from the other small area between 6 and 8 PV. Breakthrough of tracer does not occur at exactly 1.0 PV because the data were not corrected for line volume.

The adsorption of CHASER™ CD1045 was measured on a dolomite core (1 x 3 in.) at 100°F. First, 0.02 wt% iodide was injected for about 10 PV and then displaced with 20 PV of brine. Next, 0.2 wt% CD1045 was injected for over 20 PV and displaced with about 35 PV of brine. The concentrations of iodide and surfactant in the effluent were monitored continuously with a Waters Associates Model R401 Differential Refractometer. The normalized effluent concentration profiles were aligned and superimposed in Figure 8. In this case, the adsorption calculated from the area between the curves was somewhat higher, 0.18 mg/g of rock.

Certain precautions must be taken with a differential refractometer to obtain meaningful results. The detector is very sensitive to tiny variations in brine composition, so the entire experiment must be run with a single, large batch of brine. Brine is pumped continuously through both the reference and sample sides of the detector. This prevents plugging of the small diameter lines and gives a steadier baseline. The lines are flushed thoroughly with distilled water

at the end of the experiment before stopping the pumps. No back pressure is applied downstream of the refractometer because of the fragile glass cell. However, a smoother baseline can be obtained by elevating the exit lines from both sides of the detector. This applies a very small back pressure, which is usually sufficient to prevent bubble formation in the cell. The refractometer should be calibrated with known concentrations of tracer and surfactant. When possible, the results should be compared with those obtained by wet chemical analysis.

HIGH-PRESSURE COREFLOOD

In the high-pressure coreflood, surfactants are tested with reservoir rock and fluid samples under conditions that closely approximate those in the field. Our high-pressure coreflood unit is capable of operating over wide ranges of temperature and pressure (100-200°F and 1000-4000 psig). The unit is interfaced with a Hewlett Packard Series 300 computer and HP 3852A Data Acquisition/Control Unit. A menu-driven program developed in-house controls the pumps, switches valves, and collects and displays pressure data.

Figure 9 is a schematic diagram showing the key components of the unit. One dual-piston metering pump (Tracor Model 951) injects brine or surfactant directly. A second pump displaces oil and hydrocarbon gas from TEMCO floating piston accumulators with tap water. CO_2 is injected as a liquid with a dual-cylinder syringe pump (Applied Biosystems, MicroFeed Pump). One or two cores can be mounted inside the oven. If two cores are used, the first one serves as a foam generator, and foam properties are determined with the second core. The cores may be potted in stainless steel tubing or held under overburden pressure with a Hassler cell. System pressure is controlled with back pressure regulators (BPR's). Sometimes, flow is directed through a liquid-filled separator when precise pressure control is required. Then, there is only a single phase flowing through the BPR. Two sight glasses are included for observing foam properties. Liquid samples are collected with a Gilson Model 203 Micro Fraction Collector.

The typical injection sequence for high-pressure corefloods is similar to that described previously for the low-pressure foam test. In the first stage, baseline conditions are established by waterflooding, injecting oil, and then displacing the oil with brine and gas (Figure 10). The average differential pressures measured in Steps 4 and 5 are used to calculate resistance factors during foam injection. In subsequent stages, foam is generated by injecting surfactant solutions of different concentrations and then following with gas or simultaneously injecting surfactant and gas in a 4:1 ratio, corresponding to 80% quality foam. The example data are for CO_2 foam generation in an oil-wet dolomite core at 2100 psig and 100°F.

Figure 11 shows the differential pressure response for Alipal CD-128 at 0.2 wt% concentration. There is no pressure increase with CO_2 displacing surfactant. Under simultaneous injection of CO_2 and surfactant, a moderate pressure response is obtained, but the foam breaks down rapidly when only CO_2 is injected. In Figure 12, CHASER™ CD1045 generates a pressure response that is eight times larger than Alipal's under alternate injection and twice as large under simultaneous injection. The foam was stable under continuous CO_2 injection. The waterflood in Step 5 restored the core to its original permeability.

The relationship of resistance factor to surfactant concentration for CO_2 displacing surfactant (alternate injection mode) is illustrated in Figure 13. CHASER™ CD1045 generated much higher resistance factors than three other commercial surfactants at 0.2 wt% and above. The superior performance of CD1045 is clearly evident for the simultaneous injection mode also (Figure 14). The maximum resistance factor for CD1045 is twice as large as the resistance factors for the other surfactants.

HANDLING CHARACTERISTICS

The tests described above pertain primarily to how surfactants perform as foaming agents. For field applications, the physical properties which affect the handling characteristics are equally important. Concentrated, liquid products are preferred that have low viscosity for easy pumping. They should remain stable for long-term storage over a wide range of ambient temperatures and be unaffected by freeze/thaw cycles. The properties of two CHASER™ products which meet these requirements are listed in Table 4.

SUMMARY

1. The methodology outlined in this paper provides a sound basis for selecting surfactants for gas foam applications.

2. Bench foam tests are not reliable for predicting surfactant performance in porous media.

3. The high-pressure coreflood with reservoir rock and fluids is the most rigorous laboratory test of surfactant performance.

4. A new surfactant, CHASER™ CD1045, developed specifically for oil-wet dolomite reservoirs using this methodology is superior to other commercial surfactants.

NOMENCLATURE

A = Area between tracer and surfactant curves
C = Concentration of surfactant, mass fraction
M_s = Mass of adsorbed surfactant, mg/g of rock
PV = Pore volume of core, cm^3
V_t = Total volume of core, cm^3
ρ_r = Rock density, g/cm^3
ρ_w = Brine density, g/cm^3

REFERENCES

1. Kuehne, D.L., Frazier, R.H., Cantor, J., and Horn, W.: "Evaluation of Surfactants for CO_2 Mobility Control in Dolomite Reservoirs," SPE 24177 presented at the Eighth Symposium on Enhanced Oil Recovery, Tulsa, April 22-24, 1992.

2. Bernard, G.G., Holm, L.W., and Harvey, C.P.: "Use of Surfactant to Reduce CO_2 Mobility in Oil Displacement," Soc. Pet. Eng. J. (Aug. 1980) 281-292.

3. Borchardt, J.K., Bright, D.B., Dickson, M.K., and Wellington, S.L.: "Surfactants for CO_2 Foam Flooding," SPE 14394 presented at the 60th Annual Technical Conference, Las Vegas, Sept. 22-25, 1985.

4. Trogus, F.J., Sophany, T., Schechter, R.S., and Wade, W.H.: "Static and Dynamic Adsorption of Anionic and Nonionic Surfactants," Soc. Pet. Eng. J. (Oct. 1977) 337-344.

5. Bae, J.H. and Petrick, C.B.: "Adsorption/Retention of Petroleum Sulfonates in Berea Cores," Soc. Pet. Eng. J. (Oct. 1977) 353-357.

Table 1

Description of Commercial Surfactants

Product	Type	Source
XP200	proprietary	Chevron Chemical
CHASER™ CD1040	Alpha Olefin Sulfonate	Chevron Chemical
CHASER™ CD1045	proprietary	Chevron Chemical
CHASER™ CD1050	Alkyl Phenol Ethoxylate	Chevron Chemical
Alipal CD-128	Alcohol Ethoxysulfate	GAF
Avanel S-30	Alcohol Ethoxysulfonate	Mazur - PPG
Corexit 9444	Ethoxy Alcohol	Exxon Chemical
NES-25	Alcohol Ethoxy Sulfonate	Henkel

Table 2

Bench Foam Tests

TIME AFTER SHAKING (min.)	0.5% Alipal CD-128 BRINE VOLUME (mL)	0.5% Alipal CD-128 FOAM VOLUME (mL)	0.5% CD1045 BRINE VOLUME (mL)	0.5% CD1045 FOAM VOLUME (mL)
0	5.0	105.0	5.0	53.0
2	21.5	88.0	18.0	37.0
4	22.0	87.0	21.0	34.0
6	22.5	84.5	21.0	32.0
8	23.0	84.0	22.0	30.0
10	23.0	84.0	22.0	30.0
12	23.0	80.0	22.5	29.5
14	23.5	75.5	23.0	29.0
16	23.5	75.5*	23.0	28.0

TIME AFTER SHAKING (min.)	0.5% CD1050 BRINE VOLUME (mL)	0.5% CD1050 FOAM VOLUME (mL)	0.5% Henkel NES-25 BRINE VOLUME (mL)	0.5% Henkel NES-25 FOAM VOLUME (mL)
0	18.0	25.0	3.0	107.0
2	22.0	17.0	21.0	89.0
4	22.0	14.0	22.5	87.5
6	22.0	12.0	22.5	81.5
8	22.0	11.0	23.0	81.0
10	22.5	10.5	23.0	80.0
12	23.0	10.0	23.5	79.5
14	23.0	10.0	23.5	79.5
16	23.0	10.0	23.5	78.5§

* Extremely light foam
§ Light foam

Table 3

Surfactant Adsorption in Dolomite Core

Surfactant	Concentration (wt%)	Adsorption (mg/g of rock)
CD1045	0.2	0.18
NES-25	0.2	0.11
Alipal CD-128	0.1	0.06
CD1050	0.1	0.04

Table 4

Handling Characteristics of Selected Surfactants

	CD1045	CD1040
Composition	46.7% active in water	40% active in water
pH	8 - 10	8 - 10
Density	8.93 lb/gal	9.02 lb/gal
Viscosity	200 cp	50 cp
Flash point	136°F	nonflammable
Pour point	16°F	29°F
Appearance	clear amber liquid	clear amber liquid
Water solubility	100%	100%

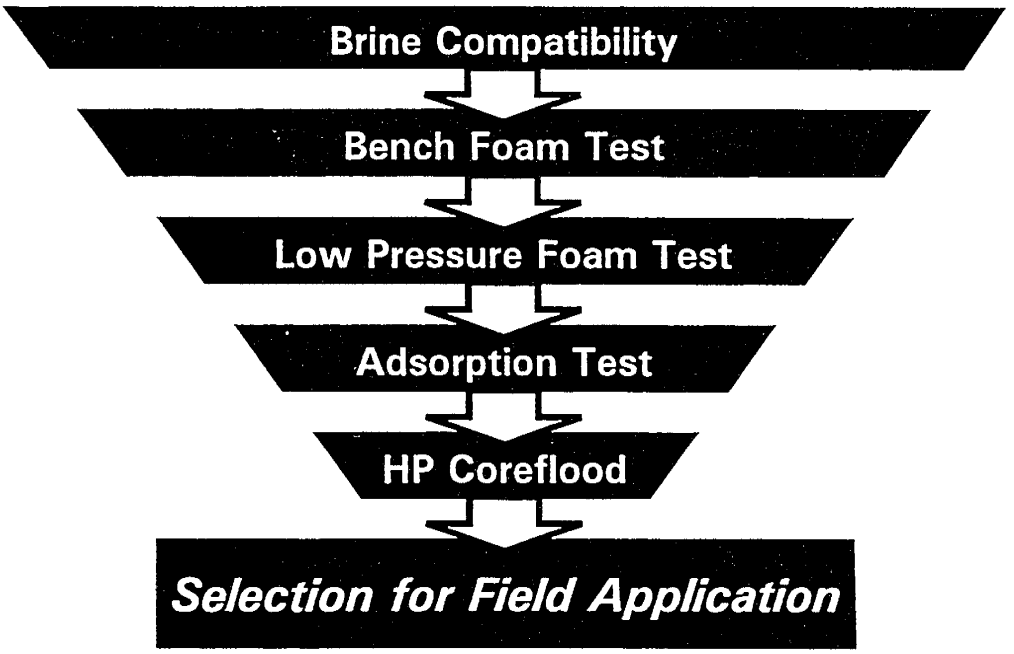

Figure 1
Strategy for Surfactant Evaluation

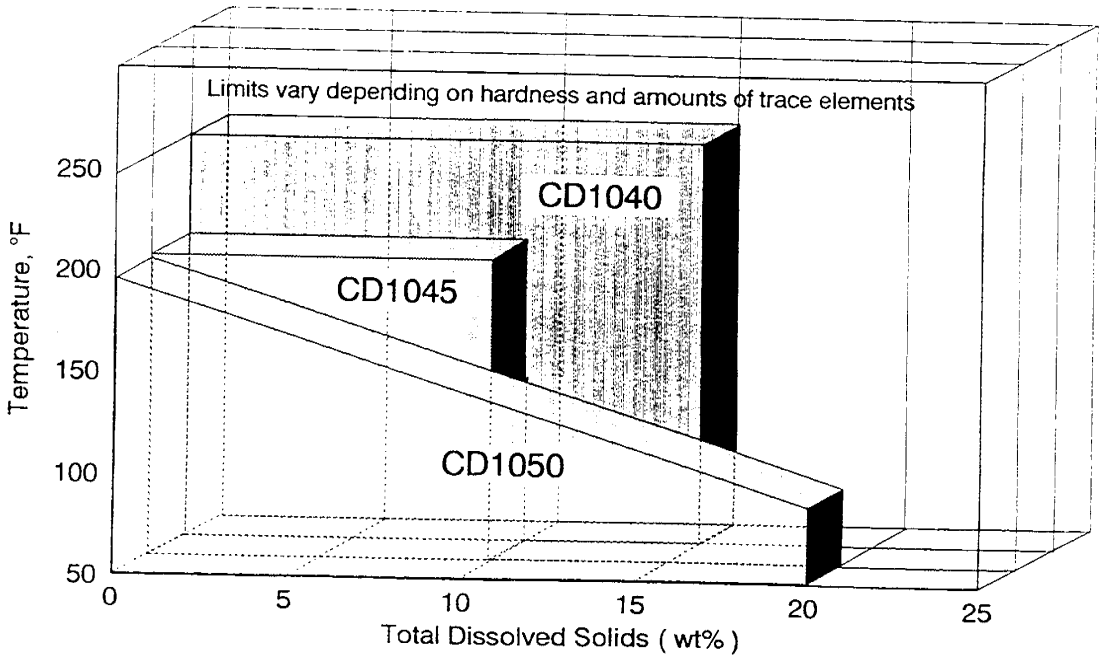

Figure 2
Range of Application
for Selected Surfactants

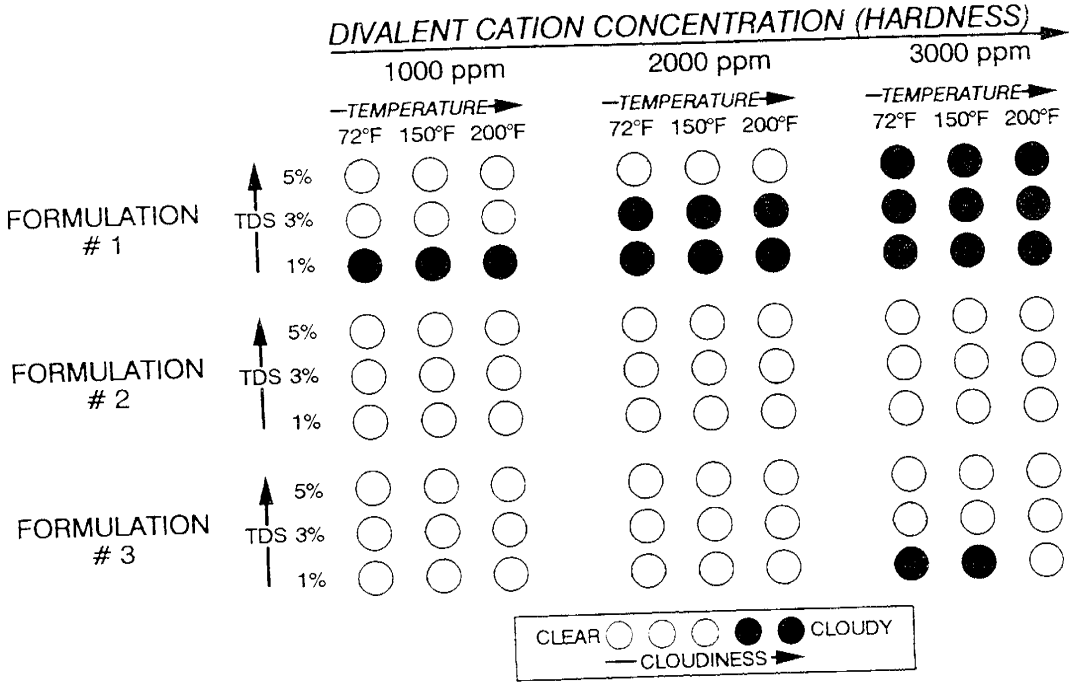

Figure 3
Brine and Temperature Tolerance
of Experimental Formulations

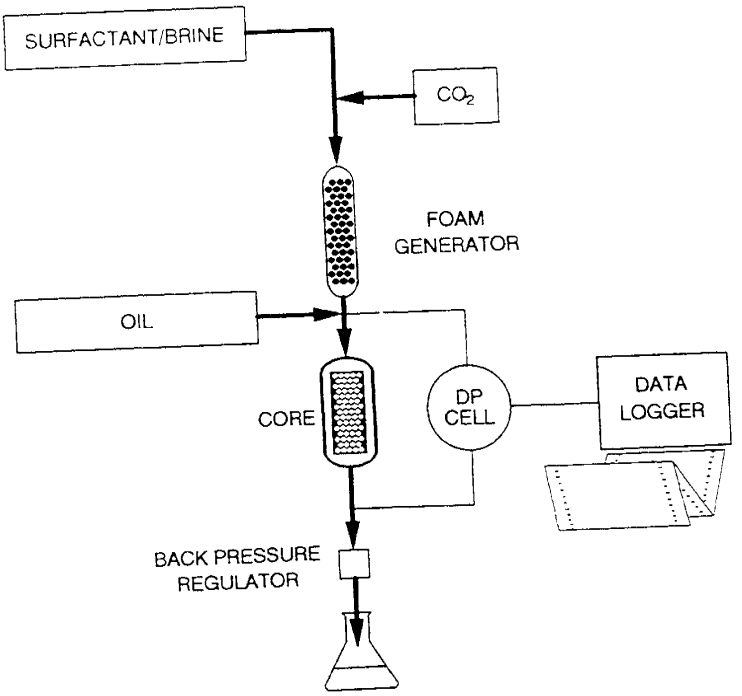

Figure 4
Low Pressure Foam Unit

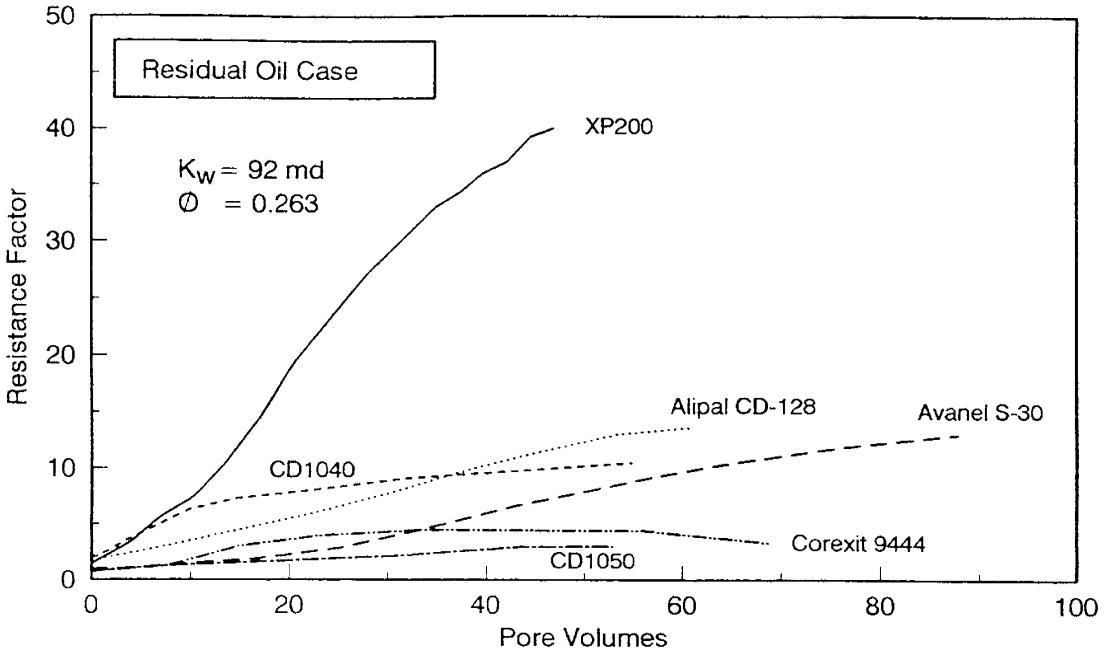

Figure 5
Surfactant Screening with Dolomite Core
in Low Pressure Foam Unit

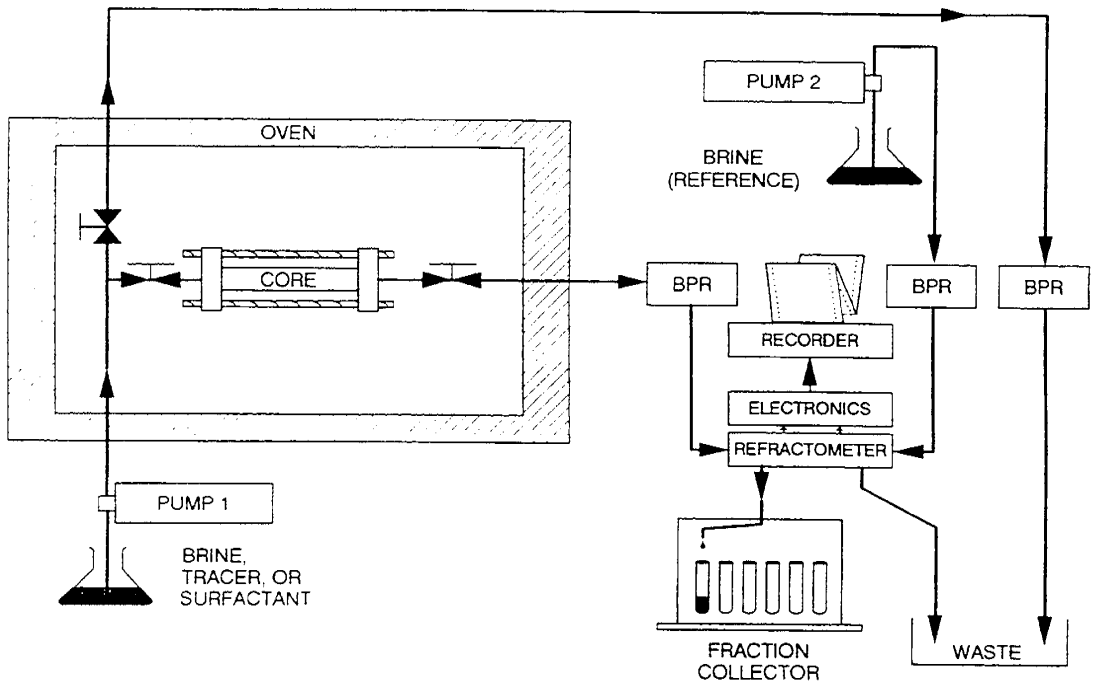

Figure 6
Apparatus for Measuring Surfactant Adsorption

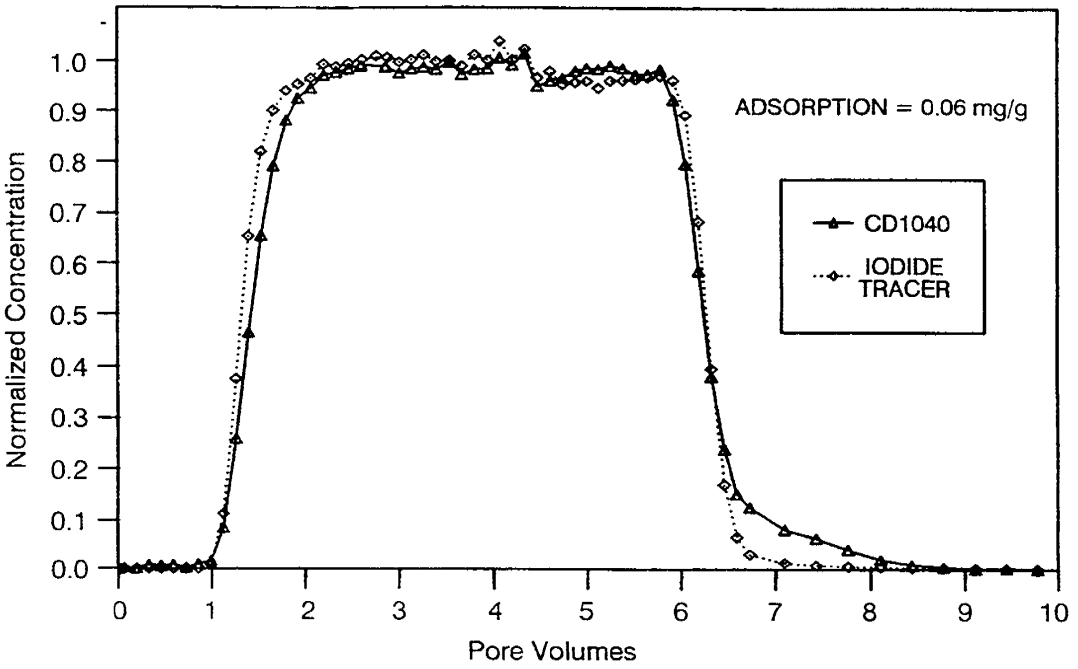

Figure 7
Adsorption of CHASER™ CD1040
on Unfired Berea at 150° F

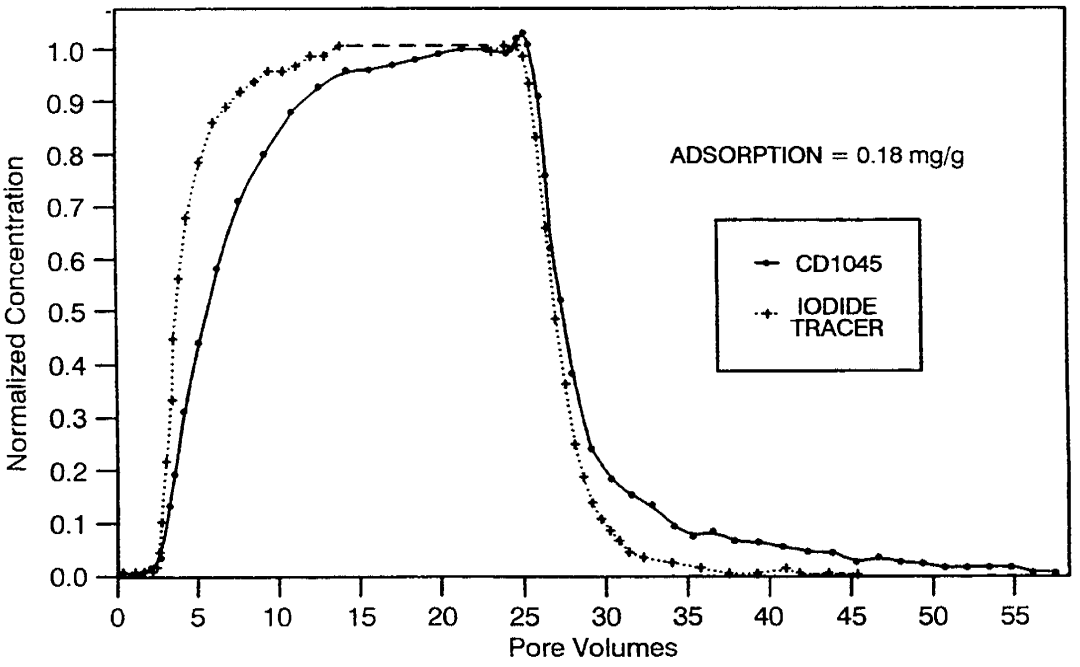

Figure 8
Adsorption of CHASER™ CD1045
on Dolomite at 100° F

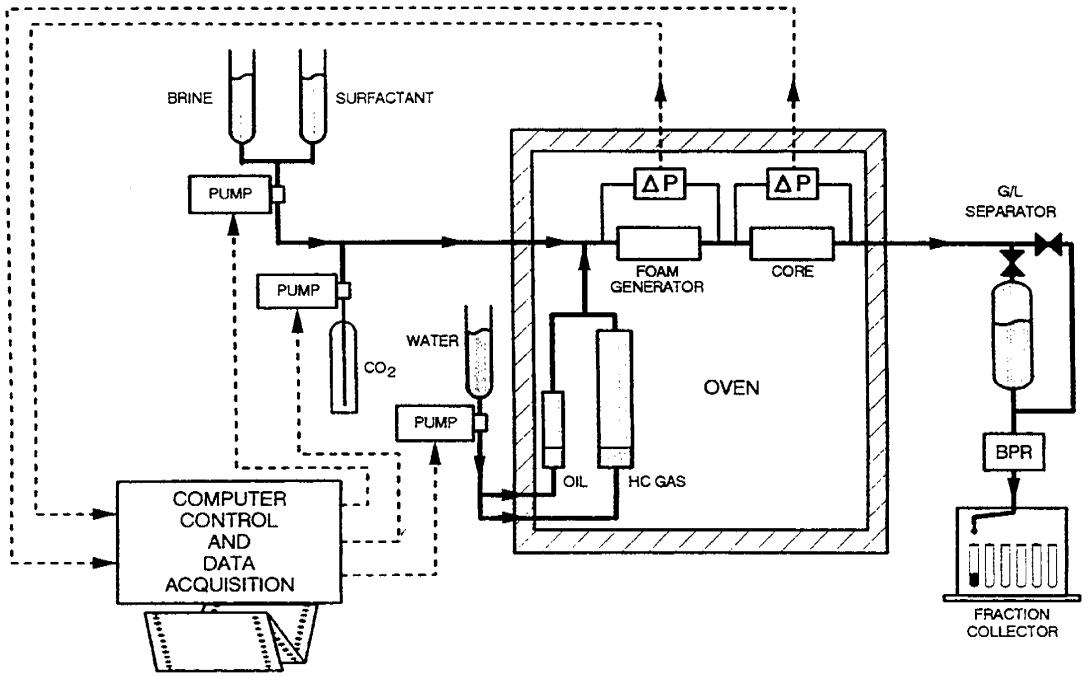

Figure 9
High Pressure Foam Unit

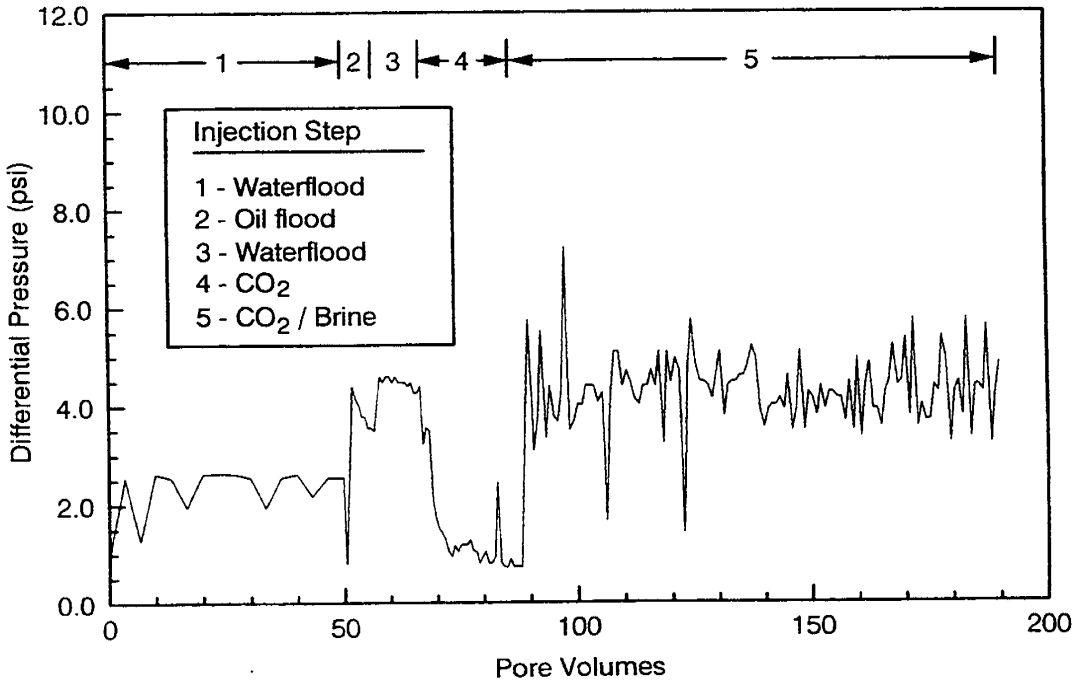

Figure 10
Preliminary Steps
for Foam Corefloods

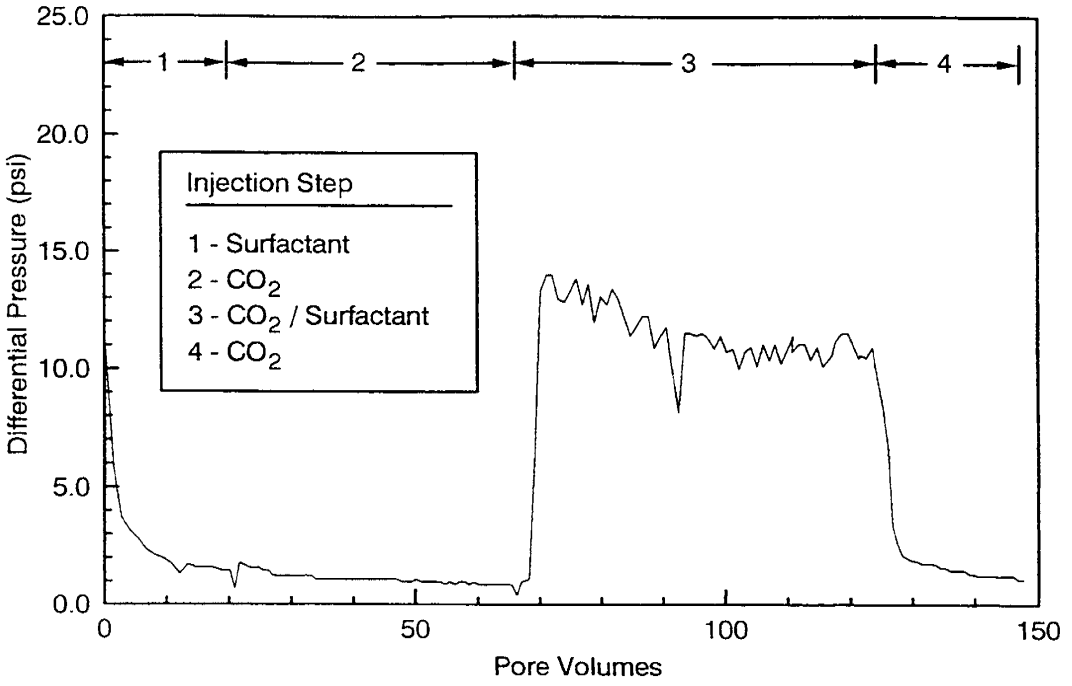

Figure 11
Coreflood with 0.2 wt% Alipal CD-128

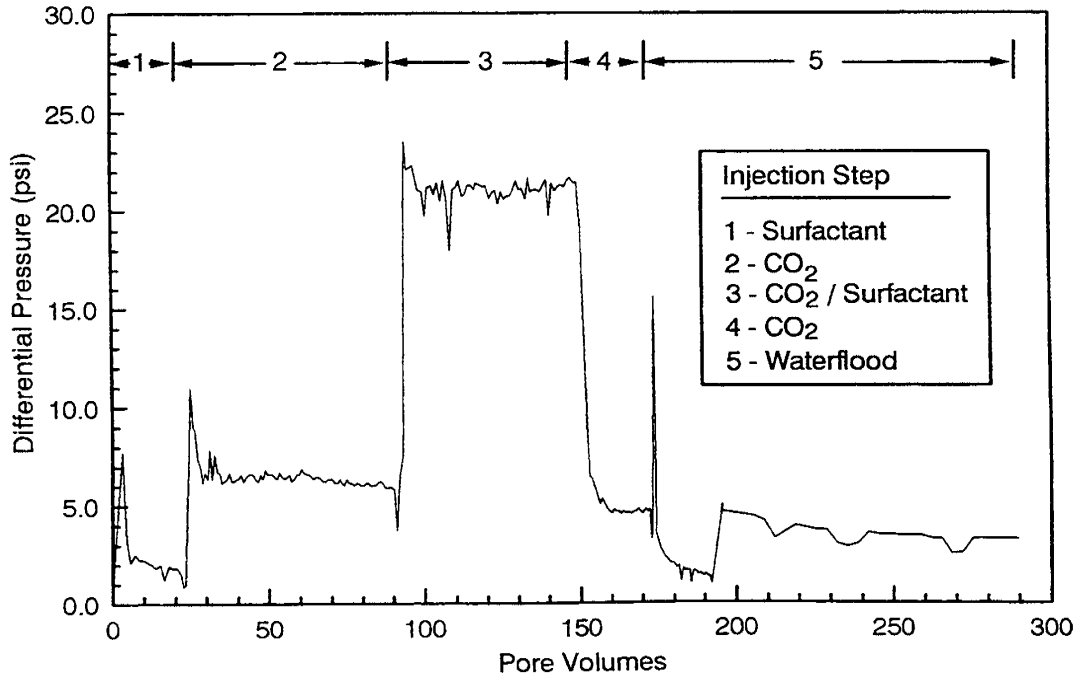

Figure 12
Coreflood with 0.2 wt% CHASER™ CD1045

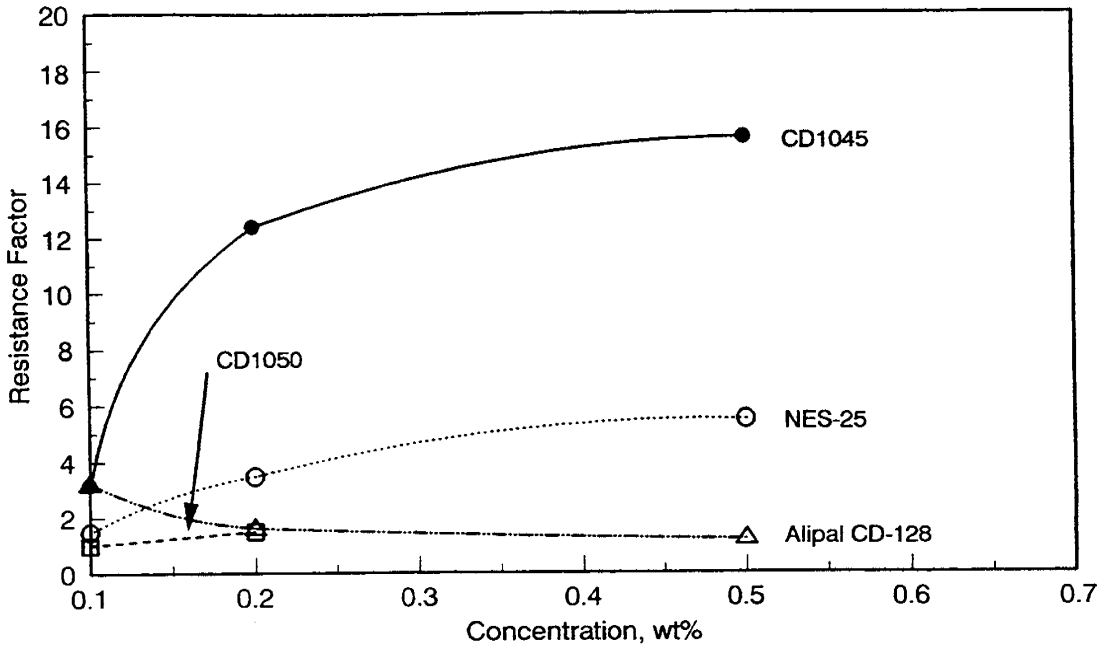

Figure 13
Resistance Factor
for CO_2 Displacing Surfactant

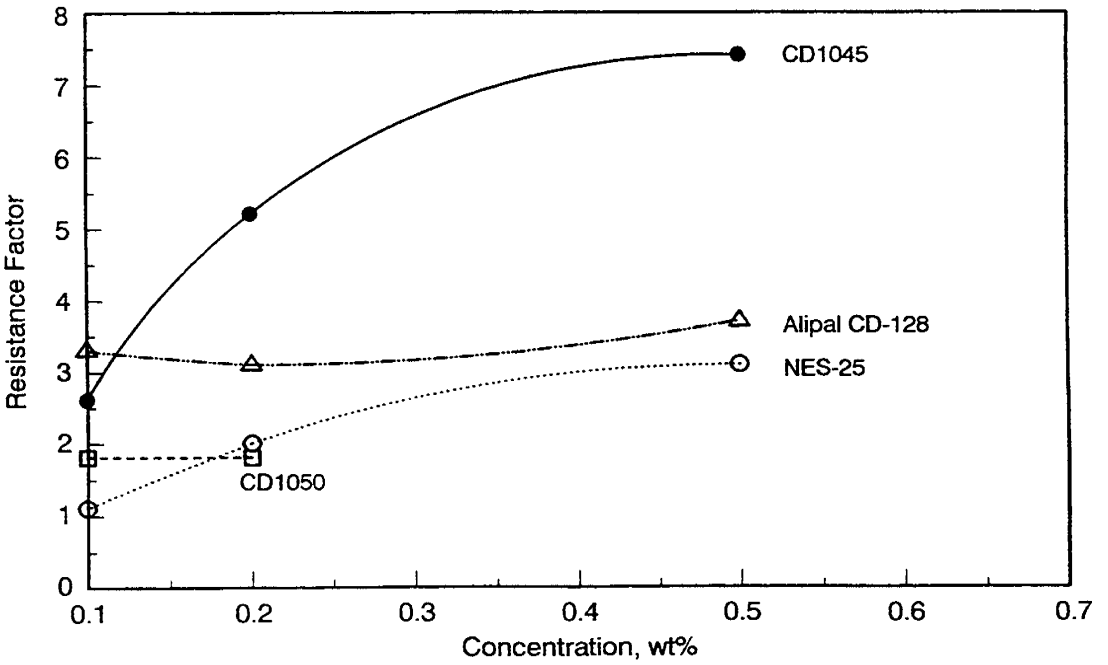

Figure 14
Resistance Factor
for Simultaneous Injection of CO_2 and Surfactant
4:1 Ratio

The Influence of Disjoining Pressure on Foam Stability and Flow in Porous Media

by A. S. Aronson, V. Bergeron, M. E. Fagan and C. J. Radke

Author(s) are solely responsible for copyright and contents.

This poster abstract was prepared for presentation at the DOE/NIPER, Symposium on Field Application of Foams for Oil Production held in Bakersfield, California, February 11-12, 1993.

This poster was selected for presentation by a Program Committee following review of information contained in an abstract submitted by the author(s). The poster, as presented, does not necessarily reflect any position of the U.S. Department of Energy or the National Institute for Petroleum and Energy Research.

ABSTRACT

Foam flowing in porous media can exhibit large flow resistance that make it an attractive fluid for improving underground oil recovery. To be an effective displacement fluid, however, the lamella, which discretize the gas into foam bubbles, must remain stable. This work studies how the stability of single foam films, as gauged by the magnitude of their disjoining pressures, influences the flow resistance of foam in porous media.

Steady-state pressure gradients of flowing foam in 2.3-μm^2 permeability glass beadpacks and disjoining pressure isotherms of single foam films are measured for 10^{-3} M and 0.017 M SDS solutions with and without NaCl. The constant-rate flow experiments show that the addition of salt to 10^{-3} M SDS increases the pressure gradient in the beadpacks from 0.1 to 4 MPa/m at 0.50 M NaCl. Surfactant solutions of 0.017 M SDS solutions exhibit pressure gradients of 22 MPa/m, quite independent of salt concentration. Likewise addition of salt to the 10^{-3} M SDS solutions dramatically influences the disjoining pressure isotherms by raising the rupture pressure from 0.5 to above 15 kPa at 0.50 M NaCl. The 0.017 M SDS solutions display rupture pressures above 30 kPa independent of salt concentration.

We conclude that high repulsive disjoining pressures in single foam films lead to strong foam in porous media with large flow resistance. Further, we find that the limiting capillary pressure for rapid foam coalescence in porous media is close to the rupture pressure of foam lamellae as obtained measured disjoining pressure isotherms.

[1] Earth Sciences Division of Lawrence Berkeley Laboratory &
Department of Chemical Engineering
University of California
Berkeley, California 94720

No. FSP7

DOE/NIPER

Foam Flow Through Porous Media in the Presence of Residual Oil: The Role of Thin-Film Forces

by V. Bergeron, M. E. Fagan and C. J. Radke

Author(s) are solely responsible for copyright and contents.

This poster abstract was prepared for presentation at the DOE/NIPER, Symposium on Field Application of Foams for Oil Production held in Bakersfield, California, February 11-12, 1993.

This poster was selected for presentation by a Program Committee following review of in formation contained in an abstract submitted by the author(s). The poster, as presented, does not necessarily reflect any position of the U.S. Department of Energy or the National Institute for Petroleum and Energy Research.

ABSTRACT

The unique mobility-control properties of foam in porous media make it an attractive choice as an injection fluid for enhanced oil recovery. Unfortunately, in many cases oil has a major destabilizing effect on foam. Therefore, it is important to understand how oil destabilizes foam and what surfactant properties lead to increased stability against oil. Here we utilize Frumkin-Deryaguin theory to generalize the ideas of spreading and entering behavior to explain the stability of foam in the presence of oil. This formulation exploits the inherent deficiencies in the classical spreading and entering coefficients used to attempt foam stability correlations. We find that oil tolerant foam can be produced by making the oil surface "water wet."

To test our theoretical ideas, we measure foam flow resistance through glass beadpacks, surface and interfacial tensions, and disjoining pressure isotherms for foam and pseudoemulsion films for a wide variety of systems. Most notably, we have measured pseudoemulsion-film disjoining pressure isotherms for the first time and have directly shown that the pseudoemulsion film stability controls the stability of the foam in the systems we tested.

[1] Earth Sciences Division of Lawrence Berkeley Laboratory &
Department of Chemical Engineering
University of California
Berkeley, California 94720

No. FSP8

DOE/NIPER

Selection of Oil-Tolerant Foams for Hydrocarbon Miscible Gas Flooding

by L. L. Schramm, K. Mannhardt and J. J. Novosad, Petroleum Recovery Institute, Calgary, Alberta, Canada

Author(s) are solely responsible for copyright and contents.

This paper was prepared for presentation at the DOE/NIPER, Symposium on Field Application of Foams for Oil Production held in Bakersfield, California, February 11-12, 1993.

This paper was selected for presentation by a Program Committee following review of information contained in an abstract submitted by the author(s). Contents of the paper, as presented, have not been reviewed and are subject to correction by the author(s). The material, as presented, does not necessarily reflect any position of the U.S. Department of Energy or the National Institute for Petroleum and Energy Research.

ABSTRACT

This paper addresses the selection of foam-forming surfactants for use in hydrocarbon gas miscible foam floods of high salinity and high hardness reservoirs such as are found in Alberta, Canada. The selection methods used are illustrated with an emphasis on the addition of crude oil tolerance to the list of screening criteria. For oil tolerance, an outline of predictive models, micro-visualization observations and coreflood measurements is given, and used to identify a framework for choosing surfactants that will create foams having the desired degree of oil tolerance.

INTRODUCTION

Major problems occur in gas flooding methods due to the displacing agent's high mobility and low density compared with that of reservoir fluids. Fingering (channelling) and gravity override reduce the sweep efficiency, contribute to early breakthrough of injected fluid, and thus reduce the amount of oil recovered.

Surfactant-stabilised foams may be used to counteract these kinds of problems. The use of foam is advantageous because the foam, which has an apparent viscosity greater than the displacing medium, lowers the gas mobility in the swept and/or higher permeability parts of the formation. This diverts at least some of the displacing medium into other parts of the formation that were previously unswept or underswept. It is from these latter areas that the additional oil is recovered. Since foam mobility tends to be reduced disproportionately more in higher permeability zones, improvement in both vertical and horizontal sweep efficiency can be achieved.

Many Canadian petroleum reservoirs currently undergoing hydrocarbon miscible flooding contain brines of extremely high salinity and hardness. We have been studying the properties of foam-forming surfactants for possible use in hydrocarbon miscible gas flooding in the Beaverhill Lake carbonate and Gilwood sand formations in Alberta, Canada. This region consists of some 46 producing pools containing light crude oil at temperatures in the range 40 to 127 °C, and is characterized by extremely high hardness and salinity formation brine. The salinities range from about 100,000 to 300,000 ppm total dissolved solids (TDS) while the hardness ranges from about 5,000 to 25,000 ppm calcium plus magnesium. Furthermore, waterflooding operations have caused large salinity variations within the fields.

INITIAL SELECTION CRITERIA

Suitable foam-forming surfactants for the kind of application just outlined must be soluble in the high salinity and hardness reservoir brines, and must exhibit long-term chemical stability. From an initial set of 157 commercially available foaming surfactants recommended by suppliers around the world, solubilities were determined [1] at different salinity, hardness, pH and temperature conditions (see Figure 1). It was found that only 62 were soluble in 21,000 ppm salinity at 130 °C and only 9 were soluble at 210,000 ppm salinity. The most salinity and hardness tolerant surfactants were mostly betaines and sulfobetaines. Chemical stability tests [1] indicated no significant changes for the soluble surfactants after ageing at 100 °C for 30 days.

References and illustrations at end of paper.

FOAMING CAPABILITY

We have generally found that the effectiveness of foams in porous media is not reliably predicted based on bulk foam measurements. Instead, we have found it more useful to study the foaming properties in porous media at various laboratory scales: micro, meso and macro.

Micro scale experiments involve the microscopic observation of flowing foams in etched-glass micromodels. Here the pore dimensions are typically on the order of hundreds of micrometers. Such experiments provide valuable and rapidly obtainable qualitative information about foam behaviour under a variety of experimental conditions. Figure 2 shows an example of the ranking of seven surfactants by bubble size distribution generated within a micromodel.

Meso scale experiments involve conducting foam floods in samples of porous rock, which may be reservoir core samples or quarried sandstones and carbonates, the quarried samples being more reproducible. The overall rock dimension here is of the order of 10 cm. These meso scale foam floods allow the determination of gas mobility reduction by foams under widely varying conditions of composition (surfactant and brine), flow rate, foam quality, rock type, temperature and pressure [1]. Figure 3 shows an example of the mobility reduction factors determined for a foam flowing at the same quality and flow rate in different rock samples. Mobility reduction factor is the ratio of pressure drops across the core resulting from the simultaneous flow of gas and liquid in the presence and absence of surfactant in the liquid phase.

Macro scale experiments involve a special apparatus that allows foam floods to be performed at reservoir conditions of temperature and pressure in an integral 2 meter length of rock sample, that is, in porous media samples one order of magnitude longer than the meso scale. In addition to being a first step in scale-up, this allows the study of dynamic foam behaviour that would be impossible in short core samples.

SURFACTANT RETENTION

The economics of foam flooding are determined to a large degree by the amount of surfactant required to generate and propagate a foam. Surfactant loss through adsorption on the rock surfaces cannot be completely eliminated, and is therefore an important (but undesirable) mechanism of surfactant loss. We have undertaken a systematic study of the adsorption properties of surfactants suitable for foam flooding at high salinity and hardness conditions [2-4].

Adsorption levels of salinity-tolerant, effective foam-forming surfactants were measured under a wide range of conditions in order to determine the factors responsible for high adsorption levels and to explore means by which the influence of these factors can be minimized. Foaming surfactants that are similarly effective in reducing gas mobility were found to exhibit adsorption levels from near zero up to extreme levels of 2.5 mg/g (Figure 4). These would lead to vastly different distances of foam propagation in a reservoir (Figure 5). Because many surfactants adsorb at levels too high to allow a foam to propagate deeply into the reservoir, selection of a surfactant with acceptable adsorption levels at the reservoir conditions of interest is crucial.

Temperature, brine salinity and hardness, rock type, wettability, and the presence of a residual oil phase were all found to influence adsorption of different surfactant types to different degrees. Perhaps of most interest was the effect of different rock types on surfactant adsorption, since hydrocarbon miscible floods are being conducted in both sandstone and carbonate reservoirs, and since the adsorption properties of EOR surfactants on carbonates have rarely been studied. We found that foam-forming surfactants with low to moderate adsorption levels can be selected for each type of reservoir [2].

Another promising approach to minimizing surfactant adsorption is the formulation of surfactant mixtures. If a surfactant mixture can be formulated such that at least one of the components (the more valuable one) is incorporated into micelles preferentially over the adsorbed phase, then the micelles prevent this surfactant from being adsorbed by keeping it in solution where it is needed for foam formation. The table below shows an example of the potential of surfactant mixtures. The amphoteric surfactant is a strong foamer and is tolerant of extremely high salinity and hardness, but adsorption losses on sandstone are high. The adsorption of the amphoteric surfactant can be reduced by almost an order of magnitude when mixed with a suitable anionic surfactant:

Adsorption on sandstone	From single-component solution (mg/g)	From mixture (mg/g)
Anionic surfactant	~0	~0
Amphoteric surfactant	1.7	0.2
Total	1.7	0.2

These studies show that surfactant adsorption, often blamed for poor economics of foam injection, can be brought to acceptable levels by properly designing the foaming surfactant. Surfactant adsorption can be minimized by properly matching the surfactant to the reservoir, or by formulating suitable surfactant mixtures.

IMPLICATIONS FROM AN EARLY FIELD TEST

Reference [5] describes an interesting example of field scale foam injection in an Alberta pool. Foam was injected to reduce the hydrocarbon gas requirements for voidage maintenance in an area where gas alone was breaking through too quickly. The initial field test involved a single-well foam (simultaneous gas and surfactant) injection, using a surfactant selected from the above screening study results, over a five day period. The foam injection produced a reduction in the rate of increase of gas/oil ratio and a significant increase in oil production (see Figure 6). The foam project illustrated the viability of small scale field foam applications, and the company continued the project for four years.

Results from the field test indicated that the foam achieved a lower gas mobility reduction than was anticipated based on the laboratory tests. This was attributed to either having injected an insufficient size slug or to the defoaming action of the residual crude oil phase. It was recommended that we investigate the possibility of using more oil tolerant foams. Based on this and other work [6] a series of investigations into the effects of crude oil on foam stability was initiated.

OIL TOLERANT FOAMS

There is a common impression that it is impossible to make foams that will be stable in the presence of crude oil. After all, crude oils have been successfully used as defoaming agents in various industrial processes. In order to test this paradigm we have observed foam - crude oil interactions in microvisual cells for a variety of different foams, brine salinities, and crude oils [7-9]. This work shows that foams exhibit a wide range of sensitivities to the presence of crude oils. In fact, three degrees of stability, ranging from completely oil resistant to extremely oil sensitive, have been distinguished which depend on the extent to which the oil can become imbibed into the foam, as illustrated in Figure 7. In coreflood tests, using sandstone at waterflood residual oil saturation, it was shown that the observed micromodel stabilities translate into foam effectiveness in realistic porous media [8]. A number of models have been advanced to explain the phenomena, with varying success [10]. Some examples are illustrated in Figure 8.

Temperature, brine salinity and hardness, and the nature of the crude oil phase were all found to influence the oil tolerance of a given foam. Perhaps of most interest was the effect of different crude oils on foam stability, since gas floods may be conducted in light through to heavy oil reservoirs. We found [9] that crude oils seem to behave quite differently from pure hydrocarbon oils. Among crude oils, it was observed that the foams were least tolerant of interaction with the lightest crude oils and most tolerant of interaction with the heaviest crude oils (Figure 9).

Some very important results have been derived from this work. First, it has been clearly shown that it is indeed possible to make foams that are oil resistant, or retain their native stability in the presence of crude oil. This holds true for crude oils of different gravity, from light through heavy crude oils [9]. These oil resistant foams may be made with relatively pure foaming agents (usually quite expensive), or else with specially formulated mixtures, which can be cost-competitive with traditional foaming agents that do not have the desired insensitivity to crude oil. An example [11] is the application of oil resistant foams made from formulations of a fluorocarbon surfactant mixed with either anionic or amphoteric hydrocarbon surfactant(s).

Secondly, it is possible to make foams that have a moderate sensitivity to the presence of crude oil but still retain sufficient stability to be used in an oil recovery process, and which have the additional property of being able to emulsify and imbibe oil into the foam, where it can be transported. This amounts to a new kind of microscopic oil displacement and means that foams can be used to increase oil recovery not only by improving sweep efficiency, but also by microscopic displacement and transport [12]. Figure 10 shows the incremental oil recovered by foam flowing in Berea sandstone cores at waterflood residual oil saturation. The recoveries shown are in excess of oil recoveries due to flooding with the foaming surfactant solution alone.

These are examples of foams which could be used where the residual oil saturation is not insignificant, relying on the ability to generate and propagate foams having reasonable degrees of stability in the presence of crude oil.

SUMMARY

Suitable foam-forming surfactants for use in hydrocarbon gas miscible foam floods of high salinity and high hardness reservoirs can be selected through an evaluation of the following properties: chemical stability and solubility, foaming capability in porous media, retention (adsorption) losses, and oil tolerance. These properties must be evaluated under realistic reservoir conditions of salinity, hardness, pH, temperature, crude oil type, and rock type.

We are currently investigating the effects on foam effectiveness of the wetting state of the porous medium (at residual oil saturation), and of the solvent composition and state (i.e., gas, supercritical fluid and liquid).

This summarizes much of what can be gained from laboratory testing in terms of surfactant selection. Subsequent steps in the evaluation of foam effectiveness include reservoir simulations and field tests.

REFERENCES

1. Novosad, J.J. and Ionescu, E.F.: "Foam Forming Surfactants for Beaverhill Lake Carbonates and Gilwood Sands Reservoirs," paper CIM 87-38-80 presented at the 1987 CIM Annual Technical Meeting, June 7-10.

2. Mannhardt, K., Schramm, L.L. and Novosad, J.J. "Adsorption of Anionic and Amphoteric Foam-Forming Surfactants on Different Rock Types," Colloids and Surfaces (1992) 68, 37-53.

3. Mannhardt, K. and Novosad, J.J. in **Foams, Fundamentals and Applications in the Petroleum Industry**, L.L. Schramm, Ed., Advances in Chemistry Series 242, American Chemical Society, Washington, Chapter 7, in press.

4. Novosad, J.J. in **Chemicals in the Oil Industry: Developments and Applications**, P.H. Ogden, Ed., Special Publication 97, Royal Society of Chemistry, Cambridge, 1991, pp. 159-173.

5. Chad, J., Matsalla, P. and Novosad, J.J. "Foam Forming Surfactants in Pembina Ostracod 'G' Pool," paper CIM 88-39-40 presented at the 1988 CIM Annual Technical Meeting, June 12-16.

6. Isaacs, E.E., Jian, L., Green, K., McCarthy, C. and Maunder, D. "Use of Foam-Forming Surfactants to Enhance the Recovery of Heavy Oils," AOSTRA J. Research (1988) 4, 267-276.

7. Schramm, L.L. and Novosad, J.J. "Micro-Visualization of Foam Interactions With a Crude Oil," Colloids and Surfaces (1990) 46, 21-43.

8. Schramm, L.L., Turta, A. and Novosad, J.J. "Micro-Visual and Coreflood Studies of Foam Interactions With a Light Crude Oil," paper SPE/DOE 20197 presented at the 1990 SPE/DOE Enhanced Oil Recovery Symposium, Tulsa, April 22-25.

9. Schramm, L.L. and Novosad, J.J. "The Destabilization of Foams for Improved Oil Recovery by Crude Oils: Effect of the Nature of the Oil," J. Petrol. Sci. & Eng. (1992) 7, 77-90.

10. Schramm, L.L. in **Foams, Fundamentals and Applications in the Petroleum Industry**, L.L. Schramm, Ed., Advances in Chemistry Series 242, American Chemical Society, Washington, Chapter 4, in press.

11. Rendall, W.A., Ayasse, C. and Novosad, J.J. "Surfactant-Stabilized Foams for Enhanced Oil Recovery," U.S. Patent 5,074,358, Dec. 24, 1991.

12. Schramm, L.L., Ayasse, C., Mannhardt, K. and Novosad, J.J. "Method for Improving Enhanced Oil Recovery of Oil Using Surfactant-Stabilized Foams," U.S. Patent 5,060,727, Oct. 29, 1991.

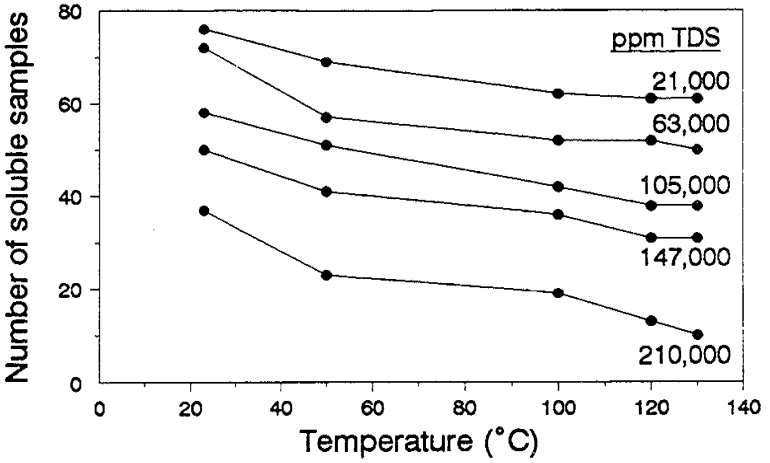

Figure 1.
Screening for surfactant solubility.
Adapted from reference [1].

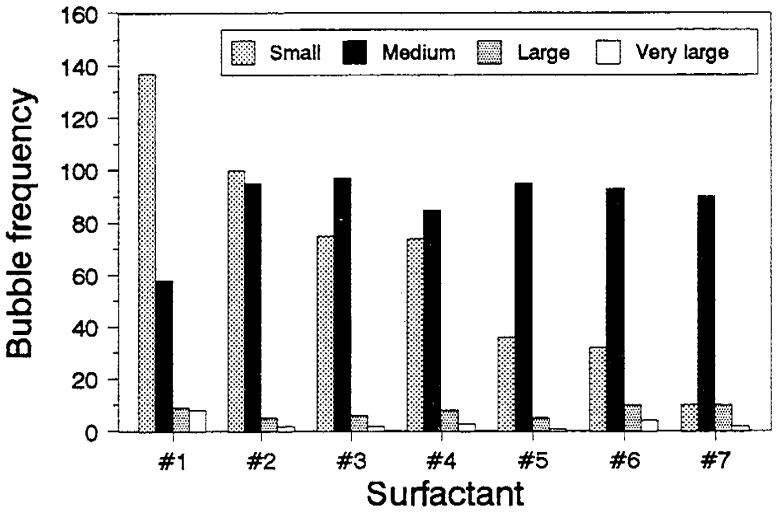

Figure 2.
Micromodel screening
for foaming potential.

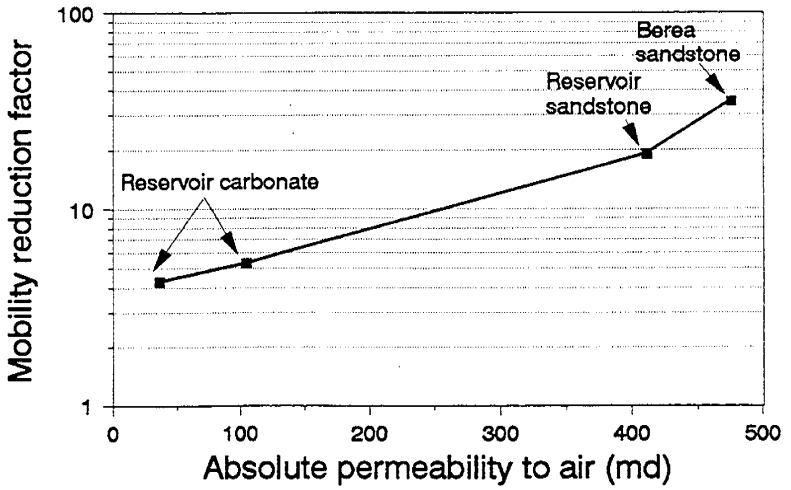

Figure 3.
MRF dependence on permeability.
Adapted from reference [3].

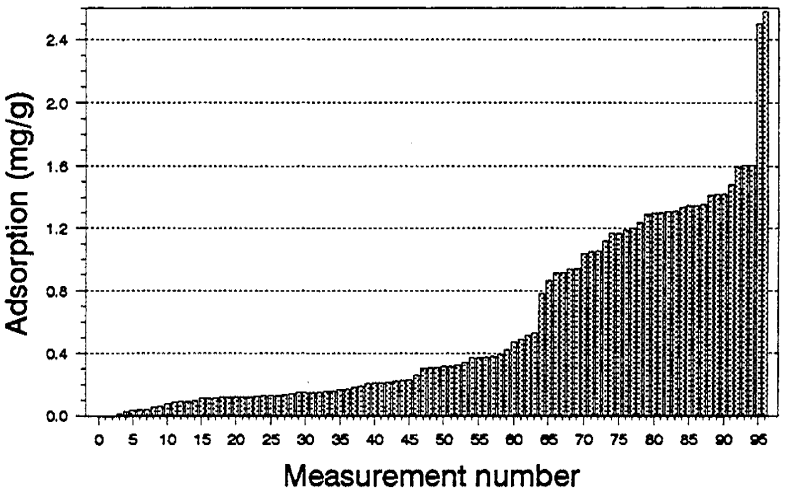

Figure 4.
Range of extents of adsorption for foaming surfactants.
Reproduced from reference [3].

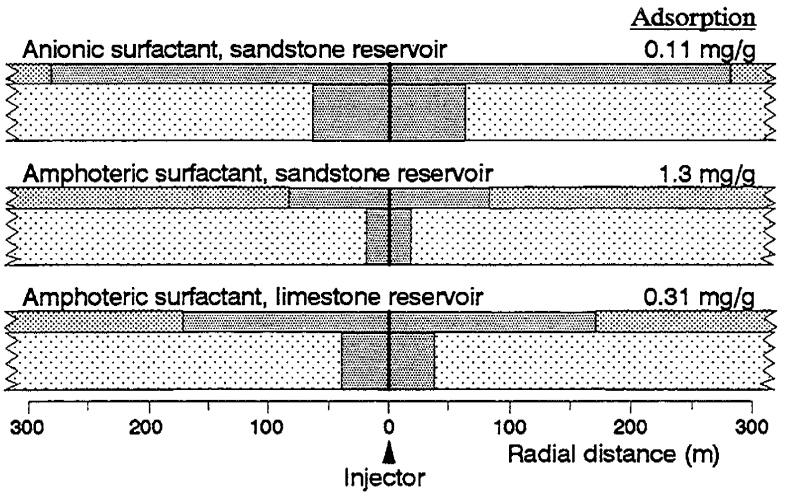

Figure 5.
Examples of surfactant propagation for different extents of adsorption in layered reservoirs.
Reproduced from reference [4].

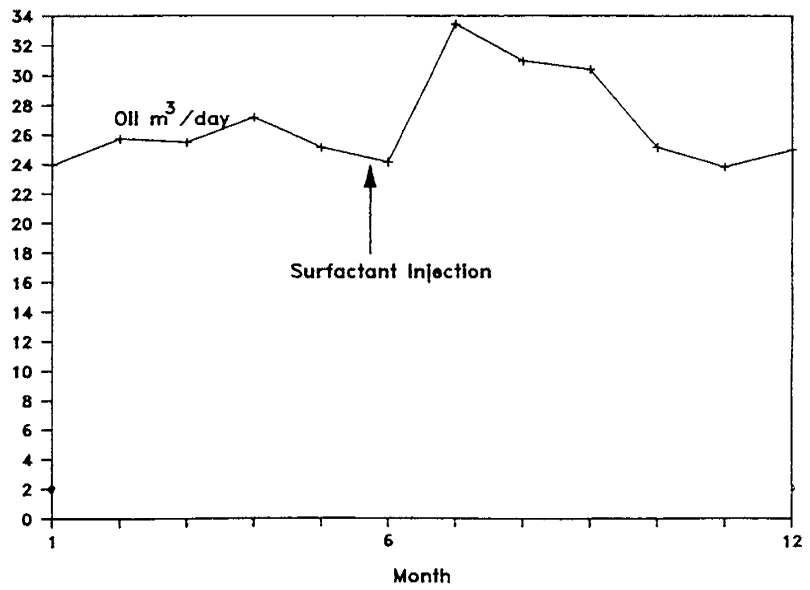

Figure 6.
Oil production increase due to 5-day foam field injection.
Adapted from reference [5].

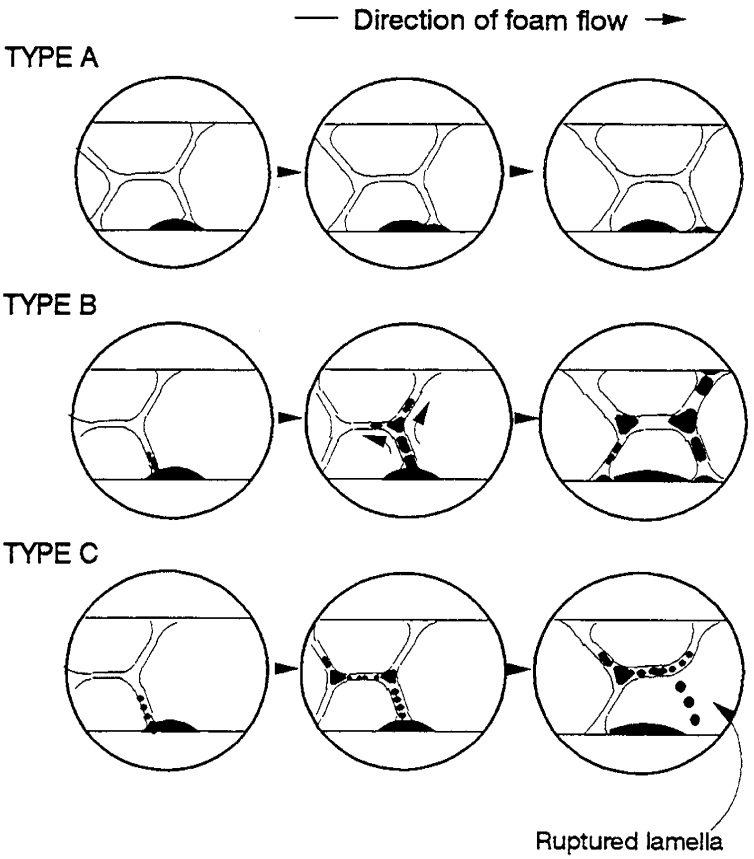

Figure 7.
Micromodel observations of foam-oil interaction.
Adapted from reference [7].

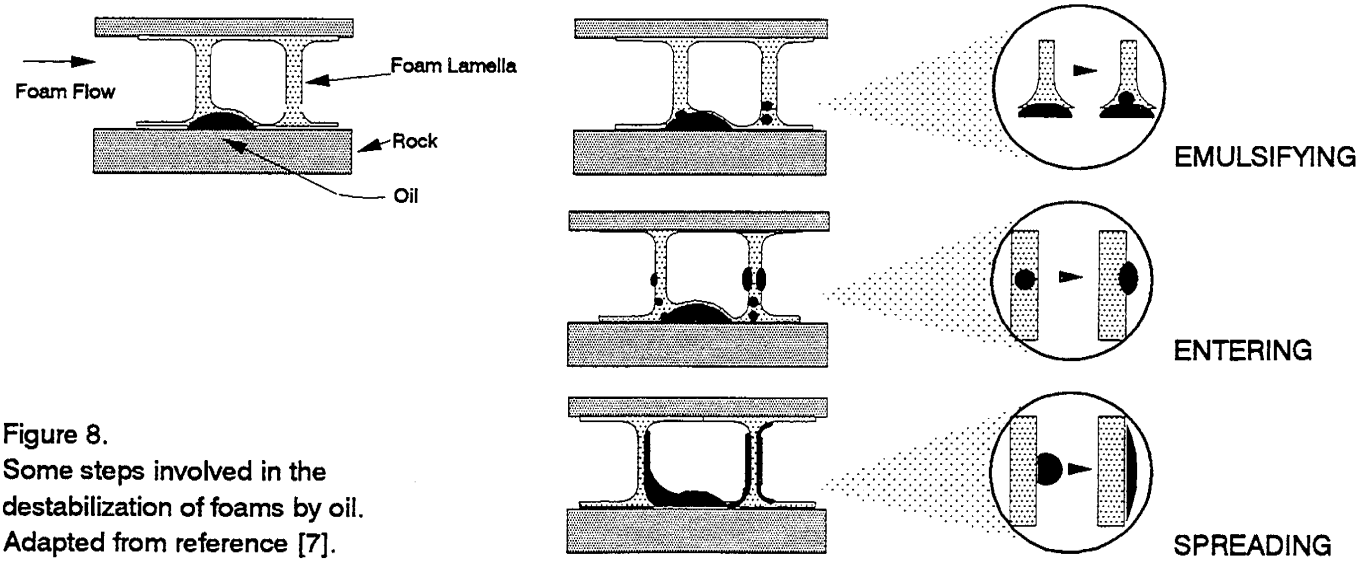

Figure 8.
Some steps involved in the destabilization of foams by oil.
Adapted from reference [7].

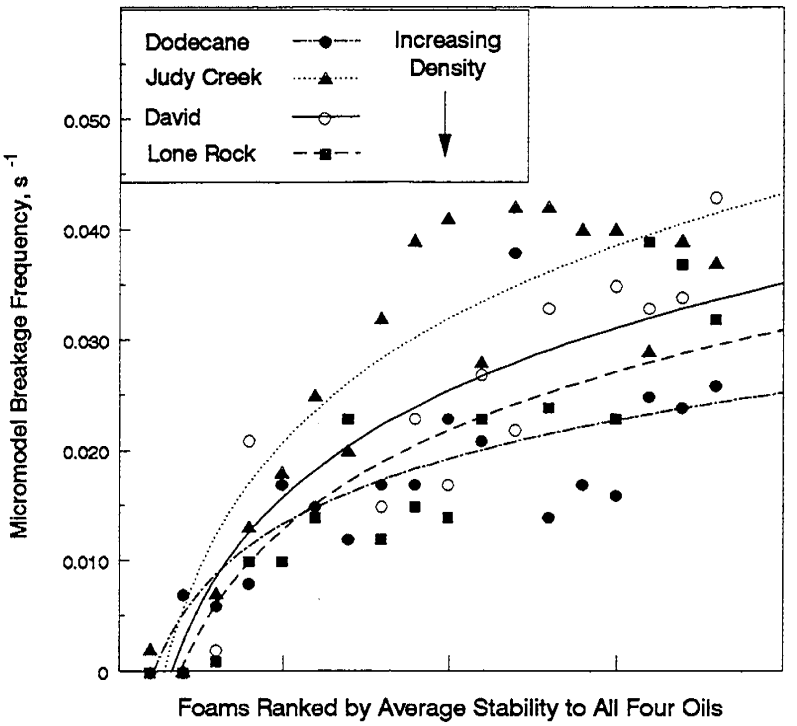

Figure 9.
Micromodel foam stability in the presence of different oils.
Adapted from reference [9].

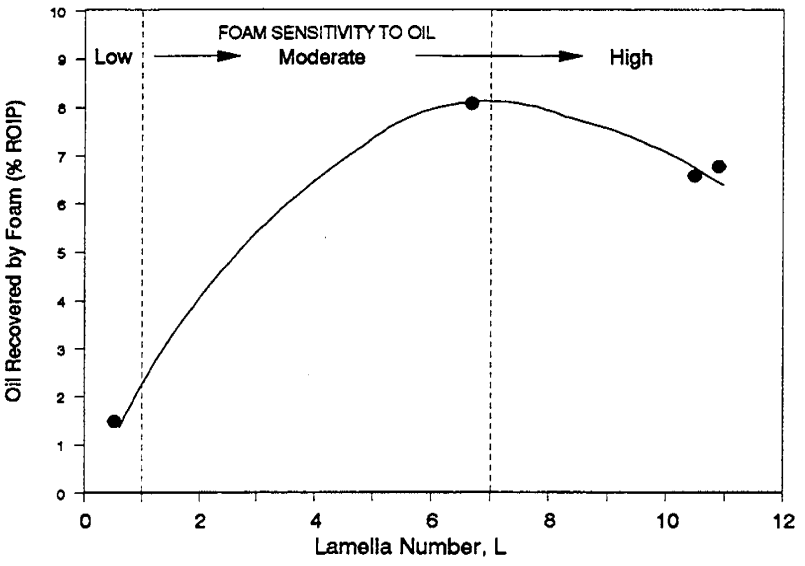

Figure 10.
Incremental oil recovery due to foam flooding versus model parameter L.
Adapted from reference [8].

No. FS7

DOE/NIPER

Design Considerations for Foam Diversion of Acid Stimulation Treatments

by Rick Gdanski and Rick Behenna, Halliburton Services, Duncan, Oklahoma

Author(s) are solely responsible for copyright and contents.

This paper was prepared for presentation at the DOE/NIPER, Symposium on Field Application of Foams for Oil Production held in Bakersfield, California, February 11-12, 1993.

This paper was selected for presentation by a Program Committee following review of information contained in an abstract submitted by the author(s). Contents of the paper, as presented, have not been reviewed and are subject to correction by the author(s). The material, as presented, does not necessarily reflect any position of the U.S. Department of Energy or the National Institute for Petroleum and Energy Research.

ABSTRACT

The use of foam for diversion of acid stimulation treatments has received increased interest with its success in offshore stimulation of relatively short intervals of gravel packed sandstone reservoirs.[1] Recent laboratory research has further studied foam diversion in limestone cores.[2,3] However, scaling of the successes from both the field and laboratory work to large scale stimulation treatments requires consideration of a number of factors including tubing size, treatment volumes, stage sizes, foam quality, formation composition, porosity and permeability, completion configuration, pumping rates, and interval length. This paper discusses how these many factors can affect the practical design of foam diversion for acid treatments ranging from 100 ft of vertical hole to 2000 ft of horizontal hole. Guidelines are presented for designing foam diverted acid stimulation treatments which will maximize the probability of successful acid diversion and hence damage removal and stimulation.

INTRODUCTION

The past 10 years have shown some remarkable success in the use of foamed fluids for diversion of stimulation treatments. The bulk of this work has been accomplished in areas where classical solids are deemed either undesirable or too expensive. The main area of work has been in the diversion of HF acid treatments in wells completed with gravel pack screens and where the formation thickness is less than about 50 ft (15 m). A second area has been in the diversion of HF acid treatments of very long intervals of sand and shale completed with gravel and slotted liners. These wells typically have formation thicknesses of about 1000 ft (300 m) and are drilled as vertical wells. In the first area, the trapping of oil soluble resins and benzoic acid is of concern if poor quality products are used or if the materials are used outside their recommended ranges. In the second area, the expense of the solids is a factor as well as a lack of confidence that the solids will do their intended job on such large intervals. As a result, foam diversion has been used to assist in accomplishing the goals of the stimulation treatment. The small intervals have relied heavily on slugs of foam to divert the stimulation fluid. The long intervals have primarily relied on continuous diversion with the entire stimulation treatment being foamed. Most of the designs were made without the help of experimental data. As a result, the design of the

treatments evolved to the state that they are today. In addition, most of the treatments have been pumped down either coiled tubing or small diameter production tubing such as 2 7/8 in. tubing.

The success of foam diversion has encouraged researchers to investigate the mechanisms of foam diversion so that improved designs may be contemplated. Much of the research in this area, however, has not been in stimulation but in conformance control where gas injection follows foam injection for enhanced oil recovery.[4] Some of the research has been directed toward stimulation and thus has led to improved insight into the diversion process under stimulation conditions.[2,3,5] The research by Rossen and co-workers has had as one of its goals the modeling of the foam diversion process on the same scale as stimulation treatments but in the absence of rock dissolution.[5] The work of Fogler and co-workers has focused on the impact of foam on dissolution properties in carbonates.[2,3]

Foam as a diverting tool also has international status and is being considered and used where other techniques have had the same problems as discussed earlier, namely, the undesirable nature of using solids and the uncertainties when treating large intervals. In addition, foam diversion has been considered in very long horizontal carbonate intervals as well as long intervals of vertical sandstones. These international wells also have tubing configurations not found in the earlier development of foam diversion treatments. One of the goals of this paper is to bring to light in one place some of the many considerations applicable to designing foam diverted stimulation treatments in the international arena.

SANDSTONE STIMULATION WITH HF ACID

General

The design of foam diverted treatments for HF acidization of sandstone formations must first recognize the nature of the dissolution patterns resulting from the HF acidizing fluids. Specifically, one can view HF acidizing as an interstitial process. That is, the fluids dissolve clay and silicate materials as they flow around and through the porous media. Wormholes are rarely generated though channeling undoubtedly occurs in some instances. In addition, the amount of rock dissolved is relatively small. For example, stimulation of a sandstone with 100 gallon per foot of 12% HCl - 3% HF results in the dissolution of only 18 lb of rock per foot of perforated interval. Thus, the 100 gallon per foot of HF increases the void space around the wellbore by less than 1 gallon per foot of perforated interval. Essentially all of the pumped stimulation fluid must occupy spaces within the unstimulated matrix. As a result, treating pressures usually remain high and the risk of fracturing can also be high. Fracturing of the formation during an HF treatment is considered by most to be catastrophic to the chances of a successful stimulation. Thus, precautions are taken to assure that fracturing of the formation does not occur. The use of foam diversion can lead to fracturing if the permeability is unable to accept the foam at acceptable rates. Indeed, foamed fluids have been found to be excellent for proppant fracturing due to their excellent fluid loss control. This leads to the first important guideline concerning the use of foam diversion. Foam is generally not considered in sandstone formations having permeabilities less than about 50 md. The permeability range of 50 to 150 md is one which requires careful design and caution in the event that the formation is treated with either too much foam or foam of a quality too high. Sandstone formations having permeabilities above 150 md seem to present little risk and are the best candidates for foam diversion of HF acid treatments.

Interval Length

The design of the treatments begins with the interval length. It is from this length that the volume of acid will be calculated. Classically accepted volumes for an HF treatment are 50 gallon per foot of HCl preflush, 150 gallon per foot of an HF acid stage, and 50 gallon per foot of an overflush. This gives volumes of 5000 gal of preflush, 15,000 gal of HF acid, and 5000 gal of

overflush for every 100 ft of interval. The first decision one must make is whether the entire perforated or open-hole interval will be taking fluid and/or producing fluid. In some cases it is known that 50% of the interval is impermeable shale and can be ignored. In other cases it is known that the entire interval is potentially productive. The total treatment volume should be based on the length of interval expected to take stimulation fluid.

The length of interval to be stimulated also plays an important role in determining the surface pumping rate for the treatment. A general starting point for pumping rates which should prevent fracturing is about 0.05 bbl/min per foot of zone or 5 bbl/min for every 100 ft of treated interval. For a 100 ft interval being treated down coiled tubing this rate would be too high due to excessively high friction pressures. Even through 3.5 in. tubing the rate could be too high because of formation damage. The maximum rate would likely be about 1 bbl/min. For a 500 ft interval being treated down 3.5 in. production tubing this would indicate about 25 bbl/min which might also be a little impractical from a logistics viewpoint as well as a formation damage viewpoint. A more practical pump rate would be about 10 bbl/min.

Tubing Size

Once the pump rate has been established, two times of interest can be calculated: (1) transit time from the surface to the first perforations, (2) total treatment time. Transit time is important for judging whether decisions about treatment design can be made real time and is calculated from the tubing size through which the treatment is pumped. For example, using coiled tubing having a capacity of 10 bbl and pumping at 1 bbl/min, a transit time of 10 min indicates that if a foam stage is providing too much resistance in the formation, the quality can be reduced or the size can be reduced. Additionally, one can calculate whether a break in treating pressure is from HCl on the formation or from HF on the formation. Such information can indicate the nature of the formation damage for future designs. In addition, if the first diverted stage of acid quickly goes on a vacuum, one might decide to increase the volume of foam diverter to improve the chances of a successful diversion. In large diameter production tubing this flexibility is lost due to long transit times and large fluid volumes. The total treatment time is also important for determining how long the initial foam stages must provide resistance. Treatments expected to last for over 5 hours should use foam volumes in subsequent stages sufficient to replace previous stages.

One of the most important considerations developed from the tubing size is the volume of the individual stages. With coiled tubing having a 10 bbl capacity, the volumes of the stages are rarely restricted by the tubing capacity. However, with large diameter tubing one must seriously consider the effects of mixing while in transit from the surface to the first perforations. For example, the capacity of 12,000 ft of 4.0 in. production tubing is about 140 bbl. For a 100 ft interval one might be tempted to use five diverted stages. Breaking the preflush HCl into 1000 gal (24 bbl) increments would result in the first stage occupying only 17% of the tubing. If the treatment was pumped at 3 bbl/min, the transit time would be about 45 min. It would seem unreasonable to expect the stage to be pumped to bottom without significant mixing between the separate stages. In fact, one might expect a mixing zone of about 10% of the tubing string to be reasonable when considering the long transit time, density difference with the following HF acid stage and thermally induced mixing effects in large diameter tubing. A minimum fluid stage volume of at least 30% and preferably about 50% of the tubing string seems reasonable. Considering the example again, the HCl preflush of 120 bbl could be split into two stages consisting of 50 bbl and 70 bbl. The first stage would occupy 36% of the tubing volume and the second stage would occupy 50%. To have broken the preflush into three stages would have resulted in either three equal stages of 40 bbl (29% of the tubing volume) or an initial stage significantly smaller. Thus, we conclude that the maximum number of sequences to be pumped without causing massive mixing of the various stages is two.

Diverting with Foam Slugs

Having established the number of diverted sequences for this example, we next turn to determination of the foam diverter stage. The two sequences will be separated by a single diverter stage. Assuming the ratio of the sequence volumes represents the ratio of the treated interval, one calculates a treated interval of about 40 ft for the first sequence. Though a little long, this is still a reasonable interval length over which one might expect the first stimulation sequence to enter the formation. As such, we will continue the design of the treatment using the foam slug technique. A general guideline that has been developed from field experience for determining the volume of a diverting foam slug is to use 1 bbl of foam for each foot of diverted interval. Thus, the diverter stage should be about 40 bbl of foam. However, one must also consider the volume occupied by the foam slug in the tubing. For the case of pumping through 12,000 ft of 4.0 in. production tubing we calculate the 40 bbl of foam to occupy 29% of the tubing. At this point we find that while the stage volume is probably large enough from our general guideline, the large difference in density between the foam slug and the stimulation fluids will likely be a major factor. The transit time of 45 min at 3 bbl/min will probably result in massive mixing of the foam slug due to the density gradients. Transit times of about 20 to 30 min are probably about the maximum that should be considered when using small diverting foam slugs in large diameter tubing. One must now decide whether to accept the mixing, pump the treatment through coiled tubing, pump at a faster rate, pump a larger foam slug or use the continuous diverting technique. Experience with the formation can give an indication as to which of these options to choose.

Continuous Diversion with Increasing Quality

Let us now consider the case of 500 ft of sandstone with a permeability of 100 to 300 md. Furthermore, we will assume the production tubing is 12,000 ft of 5 in. tubing and has a capacity of 225 bbl. From the length of the interval we will calculate a total acid preflush of 25,000 gal (600 bbl), an HF stage of 75,000 gal (1800 bbl) and an overflush of 25,000 gal (600 bbl). If we tried to design the diversion with foam slugs we might try to break the treatment into 10 stages covering 50 ft each. The 50 bbl stages of foam would occupy about 20% of the tubing volume and would not have much chance of making it to the perforations considering the large tubing volume.

A technique which utilizes continuous diversion with an increasing foam quality has been shown to provide several advantages in such cases. Field experience has shown that commingled nitrogen in HF acidizing fluids (40 to 50 quality) has little diverting effect. As such, we shall design the first sequence of preflush, HF and overflush to all be a 50 quality foam. It is also known that qualities above 70% can give too much resistance. Thus, we will design the last sequence to be at 70 quality. Next, we will assume that using 5% increments in quality will provide some increased resistance to matrix flow and thus diversion. This gives a total of 5 sequences having 50, 55, 60, 65, and 70 quality, respectively. The next step is to decide the percentage of the total treatment to assign to each quality sequence. It is reasonable to expect the initially treated intervals to be the higher permeability sections. These sections are also likely to require less stimulation or damage removal. Thus, we will design the first sequence to have a total of 10% of the treating volume and increase by 5% until the fluid is all accounted. This results in the five sequences having 10, 15, 20, 25, and 30% for a total of 100% of the treating volume.

Using these sequence volumes, we calculate that the first acid preflush will be 60 bbl, the first HF stage will be 180 bbl, and the first overflush will be 60 bbl. The 60 bbl of acid will then be foamed to 50 quality giving a total volume of 120 bbl. This will occupy 53% of the production tubing and is well within the guideline for a minimum stage volume discussed earlier. The second acid preflush will be 90 bbl of acid foamed to 55 quality to give a total volume of 200 bbl of foam. As this second stage of acid preflush

follows the first overflush, the higher quality foam keeps the acid from mixing as readily due to its lower density and higher bulk viscosity. Thus, the continuous diversion with increasing quality has a benefit which can reduce the mixing effects discussed earlier. In fact, one can see that the entire treating volume could have been cut in half and still stayed within the general guidelines for a particular stage volume.

Using the continuous diverting technique one can once again modify the treatment design based on well response. That is, the foam has increased the total pumped volume to the point that if a sequence is treating at too high of a pressure, then one can hold the quality on the next sequence or even reduce it slightly if necessary. Of course, if the treating pressure increases during the treatment above the designed pressure, then compression of the gas can result in a reduced downhole foam quality and easier formation entry. As a result, various treating parameters can help in providing an almost self adjusting foam quality based on well response.

CARBONATE STIMULATION WITH HYDROCHLORIC ACID

General

The design of foam diverted treatments for HCl acidization of limestone formations must first recognize the nature of the dissolution patterns resulting form the HCl acidizing fluids. Specifically, one can view carbonate acidizing as a process which generates wormholes and interconnects natural fractures and vugs. That is, the fluids dissolve the matrix itself leaving open voids. The volume of the void space is equal to the volume of the dissolved rock plus the porosity. When using 15% HCl, one calculates that 1000 gal will dissolve 10.9 ft^3 of limestone. If the porosity is 10% then the total void space will be about 12 ft^3. The 1000 gal occupied 134 ft^3 indicating that over 90% of the pumped fluid must leak off into the unacidized matrix. This leakoff process in all directions helps the acid to generate uncountable mini- and micro-wormholes. Research in this area has shown hairlike wormhole patterns branching off larger complex wormhole networks.[6] As a result, diversion in limestone matrix acidizing can be quite difficult to achieve. The most common methods utilize either ball sealers which plug perforations or 'block' which is a suspension of solids in a gelled carrier fluid. However, there are times when it is impractical or logistically difficult to use ball sealers or other solids. Such a case would be acidization of a horizontal well of great length.

One feature of matrix acidizing carbonates is that occasional fracturing after a diversion stage is quite acceptable. While it is generally not intended to treat the formation entirely above fracturing pressure, pressure increases from a diversion stage can fracture the damaged sections of the matrix thereby opening up flow passages. Since leakoff will still be massive, the treatment will quickly return to matrix acidizing and the treating pressure will fall below fracturing pressure. This feature minimizes the risks associated with using excessive foam diverting stages and allows enhanced flexibility in treatment design. In addition, recent research has indicated that foamed acid tends to produce less branched and longer, narrower wormholes than non-foamed acid.[3] This effect allows for deeper stimulation from the wellbore with smaller volumes of acid. It can also be a positive factor when acidizing chalks, which have minimal compressive strength to start with, since the matrix surrounding the wellbore receives deeper stimulation with less rock removal.

Permeability

In designing a foam diverted treatment in a carbonate, the first consideration will be the formation permeability. Carbonates with low permeabilities and low porosities will likely use small stages of foam to divert the acid. Such carbonates will have permeabilities of less than 1 md and porosities of less than 5%. In these cases the acid will need plenty of opportunity to penetrate the carbonate and develop the wormhole patterns. By the same token, they will be easily diverted with foam. Carbonates with medium permeabilities or which have moderate natural

fracturing can be diverted with either large stages of foam or with continuous foam techniques. Such carbonates will respond quickly to acid and thus will require more diverting resistance as the foam penetrates the natural fractures and matrix permeability. Carbonates with high permeabilities or high porosities generally will require continuous foam diversion. Carbonates in this category will have permeabilities above 50 md or will have porosities above 25%. Matrix invasion by the foam will be significant and thus diversion will require more resistance to flow. Indeed, while low permeability carbonates can be diverted with foamed acid, high permeability carbonates will require foamed brine or even foamed gelled brine to achieve a lasting diversion. Finally, some formations possess a thief zone of 'hyper' permeability. These zones will require the use of a temporary blocking system such as a delayed crosslinked, high viscosity gelled water stage as the initial step in the treatment. These temporary blocking systems can also contain internal breakers to provide a controlled break of the gelled system as well as contain large solids such as oil soluble resins, graded salt, or graded calcium carbonate to establish and strengthen the block. Once the temporary blocking system is in place, then continuous foam diversion techniques should be used to acidize the rest of the formation.

Interval Length

Interval length is once again used to start the treatment design. Typical treating volumes for matrix acidizing a carbonate range from about 25 gallon per foot for a small perforation wash to remove or dislodge damage up to about 250 gallon per foot for deeper penetration and stimulation. Economics and logistics can also play an important role in determining the volume of acid to use. Assuming 50 gallon per foot for a long interval, one calculates using 5000 gal for every 100 ft of treated interval.

Interval length is also used to estimate a reasonable treating rate. Recognizing that carbonates respond much more quickly to acid and that occasional fracturing is acceptable, a surface pumping rate of 0.1 bbl/min per foot of treated interval is a reasonable starting point. One must recognize that perhaps not all of the interval will take fluid at first. For example, in a 500 ft interval one might expect only 100 ft to take fluid at a time. The surface treating rate would be set at about 10 bbl/min. Low permeability carbonates might require lower rates while high permeability might tolerate higher rates. One would like to pump as fast as is reasonably possible without fracturing very often. Too much fracturing will render diversion unachievable as the foam will not divert a fracture.

Tubing and Casing Size

Design of the fluid stage size is easier when diverting in carbonates. The most obvious reason for this is the simplicity of the fluid sequences. Unlike HF acidizing which uses three fluid stages per sequence, carbonate acidizing uses simply one acid and perhaps a non-acid diverting fluid. Meeting the minimum of 30 to 50% of tubing volume is relatively straightforward to achieve using the procedures discussed earlier. Calculation of the transit time and total treatment time is still performed for judging effectiveness and duration of individual diverting stages.

Considering that many horizontal wells have been completed in carbonates, one must now recognize the dimensions of the casing or liner in the horizontal section. Up to this point it was assumed that once the foam diverting slugs exited the production tubing they would soon enter the formation. This was an adequate assumption for vertical wells and intervals shorter than a few hundred feet. However, in horizontal wells gravity induced overriding can be a serious problem. As such, one must estimate a reasonable diverting stage size that can be effectively transmitted long distances in large diameter pipe. For example, 100 ft of 7 in. casing has a capacity of about 4 bbl. While this would be a reasonable foam diverting stage if pumped through coiled tubing, it would not be reasonable to expect the 4 bbl of foam to travel through 1000 ft of horizontal hole without segregating and dispersing. Once again we return to the minimum volume of 30 to 50% of the travelled capacity. That is, one could

expect a 4 bbl stage of foam to travel about 200 to 350 ft and still remain fairly intact. However, as the following stages are diverted farther down the horizontal section one must use larger foam stages to maintain foam diverter integrity. For example, the final stages of a treatment for a 2000 ft horizontal well with a 7 in. liner should use a minimum of 25 to 40 bbl of foam diverter since the capacity of the horizontal section would be about 80 bbl.

Diverting with Foam Slugs

Determination of the size of a diverting foam slug is made relative to the acid stage pumped just before it, but taking into account the recommended minimum slug size and horizontal distance travelled. The determination begins by calculation of the amount of void space created by the preceding acid stage. Suppose the acid stage was 5000 gal (120 bbl) of 15% HCl and the formation porosity was 20%. Table 1 shows the amount of void space created depending upon acid concentration and porosity. From this table one can calculate that 120 bbl of 15% acid would create a void space of about 12 bbl. It will require a minimum of 12 bbl of foam (10% of the acid volume) just to fill the void. One could easily expect the leading 25 to 50% of the foam to enter the matrix beyond the created wormholes. In addition, the first portion of foam entering the matrix might be broken by residual oil, surfactant adsorption or other effects. Additional foam volume is used to take these factors into account. The amount of additional foam will depend on the significance of those factors. For example, in a low permeability carbonate which is expected to produce dry gas, 25% excess would probably be sufficient. However, in a high permeability or high porosity carbonate expected to produce oil, 100% excess would be quite reasonable. The foam diverting slug would therefore range from about 12 to 20% of the acid volume. This range would double if the acid were 28% HCl since it has twice the rock dissolving power as 15% HCl. Once again, considering that the preceding acid stage was 5000 gal (120 bbl) of 15% HCl and the formation porosity was 20%, one would probably use 100% excess for a total of 25 bbl of foam (21% of the acid volume). This volume would then be compared to the volume of the treating tubing and the volume of the travelled distance in the horizontal section. If these two minimum volumes require increasing the foam diverter stage then one should do so. If the minimum volume criterion requires increasing the diverter stage by more than 50%, then one should consider increasing the size of the preceding acid stage by a proportional amount.

It must also be considered that once the foam diverter has been placed it will continue to invade the matrix and that the foam will gradually break. Thus, the amount that each individual foam diversion stage breaks or is lost by penetration into the matrix during the remainder of the treatment should be taken into account. At this point there is very little information on this subject. However, the lost foam will likely be replaced first as the successive stages of foam diverter are pumped by the diverted interval. A reasonable estimate of this loss would be about 10 to 25% of the previous foam volume occupied in the created voids. The successive foam diverter stages should be increased to take this loss into account. For example, if the second stage of acid was also 5000 gal (120 bbl) of 15% HCl, one would again design 25 bbl of foam for the diverter stage. Since the first acid stage created a void of about 12 bbl, one would use an additional 1 to 3 bbl of foam in the second diverter stage bringing the total to 26 to 28 bbl.

To this point we have not discussed the composition of the foam diverting stage for the matrix carbonate treatments. Laboratory work has indicated that foamed acid can give excellent resistance and diversion.[2] Logistically this can be a benefit since it only requires increasing the nitrogen rate to achieve a high quality foam and not switching to a different fluid. Since 70 to 80 quality foams would be recommended for the foam diverting stage, 50 bbl of foamed acid would require only 15 to 10 bbl of acid, respectively, to create the foam diverter. The remainder of the acid could be commingled with nitrogen to about 40 quality to help prevent gas dispersion from the foam diverter stage. This approach works well in

low to medium permeability carbonates. In high permeability or high porosity carbonates one should primarily consider continuous foam diversion. However, logistics can dictate that the foam slug techniques must be used. In such cases the foamed diverter stage should be non-acid such as fresh water, a light brine or sea water. Non-acid diverter stages would also be recommended in high porosity chalks as well, regardless of the formation permeability. Laboratory studies using chalks have shown that foamed acid will still penetrate rapidly through a high porosity chalk resulting in minimal diversion.[2]

Tests conducted with foamed brine in the same chalks have shown large buildups in flow resistance which were largely retained even after non-foamed acid followed the foamed brine. The ineffectiveness of foamed acid in providing diversion in high porosity chalks was presumably due to the small amount of grain volume present in a given bulk volume of chalk as compared to an equivalent bulk volume of a low porosity limestone. In low porosity, medium permeability limestones the foamed acid generally gave adequate diversion. Additional stability can be achieved within the foam stage by the use of gelling agents.

Considering that the gelled foam will be displacing the acid from the wormhole network, it is not a requirement that the gelling agent be exceptionally stable in acid. Natural polymers such as xanthan, derivatized guar, and derivatized cellulose are quite acceptable. Gelled foam stages would be considered in high volume, low rate treatments such as those performed through coiled tubing into horizontal wells. Such treatments can last for many hours and require the additional foam stability provided by the gelled base fluid.

Continuous Diversion

Carbonates with high permeabilities should primarily be treated with continuous foamed acid. As in HF acidizing the quality can start low (50 quality) and can be gradually increased. However, in carbonates the foam quality can be increased to 80 quality if necessary. The goal of the continuous foam diversion is to provide sufficient resistance to matrix flow that all sections of the interval are exposed to acid. If the permeability is sufficiently high, one can start with 60 quality to provide quick diversion. One of the primary advantages of continuous foam diversion in carbonates is that calculation and control of stage size is no longer necessary.

Stages of foamed non-acid fluids can also be used to provide enhanced diverting effectiveness in continuous diversion treatments. In such cases, one must balance the benefits for the stimulation with the logistics of transporting additional fluid, etc. This approach would be used with constant quality foamed acid at about 60 to 70 quality with stages of foamed diverter designed using the foam slug technique. This technique would be the method of choice for diversion in high porosity chalks.

CONCLUSIONS

1. The design of acid stimulation treatments diverted with foam requires consideration of such things as the tubing volumes, transit times, treated interval length, permeability, and direction of the wellbore.

2. The minimum volume of any particular stage of acid or foam diverter should be 30 to 50% of the treating tubing volume.

3. The minimum stage volume can be the determining factor in designing the frequency of diversion.

4. Formation composition, permeability, and lithology strongly affect the choice of diversion technique.

5. Continuous diversion techniques have the advantage of increasing total pumped volume and thus increase the number of possible diverting stages.

6. In sandstone formations, the foam diverter slug technique utilizes about 1 bbl of foam

per foot of diverted interval for determining slug size.

7. In carbonate formations, the foam diverter slug technique utilizes the volume of acid created void space for determining slug size.

REFERENCES

1. Burman, J.W. and Hall, B. E.: "Foam as a Diverting Technique for Matrix Sandstone Stimulation," paper SPE 15575 presented at the 1986 SPE Annual Technical Conference and Exhibition, New Orleans, LA, Oct. 5-8.

2. Thompson, K. and Gdanski, R. D.: "Laboratory Study Provides Guidelines for Diverting Acid With Foam," paper SPE 23436 presented at the 1991 Eastern Regional Meeting, Lexington, KY, Oct. 22-25.

3. Bernadiner, M. G., Thompson, K.E. and Fogler, H.S.: "The Effect of Foams Used During Carbonate Acidizing," paper SPE 21035 presented at the International Symposium on Oilfield Chemistry, Anaheim, CA, Feb. 20-22, 1991.

4. Rossen, W. R. in Foams: Theory, Measurements and Applications (R. K. Prud'homme and S. Khan, ed.), Marcel Dekker, Inc., New York, in press.

5. Zhou, Z. H. and Rossen, W. R.: "Applying Fractional-Flow Theory to Foams for Diversion in Matrix Acidization," paper SPE 24660 presented at the 67th Annual Technical Conference and Exhibition, Washington, DC, Oct. 4-7, 1992.

6. Hoefner, M.L. and Fogler, H.S.: "Pore Evolution and Channel Formation During Flow and Reaction in Porous Media," *AIChE J.* (Jan. 1988) 45-54.

Table 1

Void Space Created With Hydrochloric Acid in Limestone

	Space (in bbl) Created by 100 bbl of Acid			
HCl (%)	ϕ = 0%	ϕ = 10%	ϕ = 20%	ϕ = 50%
28	16	18	20	32
20	11	12	14	22
15	8	9	10	16
5	3	3	3	5

No. FS8

DOE/NIPER

Implications of the "Limiting Capillary Pressure" for Field Applications of Foams

by W. R. Rossen and Z. H. Zhou, University of Texas at Austin, Austin, Texas

Author(s) are solely responsible for copyright and contents.

This paper was prepared for presentation at the DOE/NIPER, Symposium on Field Application of Foams for Oil Production held in Bakersfield, California, February 11-12, 1993.

This paper was selected for presentation by a Program Committee following review of information contained in an abstract submitted by the author(s). Contents of the paper, as presented, have not been reviewed and are subject to correction by the author(s). The material, as presented, does not necessarily reflect any position of the U.S. Department of Energy or the National Institute for Petroleum and Energy Research.

ABSTRACT

Predicting the field performance of foams for enhanced oil recovery has been a difficult task. Without a simple mathematical representation of the many processes that create and destroy foams, process prediction is unreliable. On the other hand, simultaneous mathematical representation these numerous processes appears to be impractical. Fortunately, many "strong" foams follow the "limiting capillary pressure" model, at least approximately. For these foams, simple yet powerful predictions about field performance are possible.

The "limiting capillary pressure" model indicates that foam collapses at a value of capillary pressure p_c^* that depends on surfactant formulation and rock type. The model explains why foams are strongest in high-permeability rock, a crucial property of foams intended to divert gas flow to unswept low-permeability reservoir layers. Further, it predicts that when reservoir layers are in capillary equilibrium, foam is ineffective at improving sweep. The model helps explain why foams that appear to be shear-thinning in the laboratory have been found to be shear-thickening in the field. It suggests that the simplest foam-simulation model, in which foam rheology is treated as roughly Newtonian, may be a reasonable approximation to true behavior. Finally, it suggests that design goals for WAG (water-alternating gas) foam processes differ fundamentally from those for continuous-injection foam processes. For continuous-injection processes, the ideal foamer would form a strong foam and drive capillary pressure to a high value, at which foam begins to collapse. For a WAG process, however, it is crucial that foam collapse, not at a single capillary pressure as in the p_c^* model, but over a range of capillary pressures.

INTRODUCTION

Foams can improve reservoir sweep in gas-injection enhanced-oil-recovery (EOR) projects.[1-3] A major attraction of foam is the prospect of spontaneously diverting flow from high-permeability to low-permeability layers.[4-9] This occurs because, under at least some conditions, stronger foams form in high-permeability media.

Unfortunately, foam EOR research is hampered by the complexities of the mechanisms controlling foam texture (bubble size), which in turn controls foam rheology.[10] The approach of most modeling to date had been either to treat each of these mechanisms separately,[11-14] which leads to models which are complete in principle but impractical to apply, or to abandon mechanistic modeling in favor of empirical curve-fitting and history-matching.[15-21]

Three facts on which there is wide agreement are (1) there is no such thing as a separate "foam" phase in rock; there is only the effect of foam on the separate mobilities of gas and water; (2) water mobility is the same function of water saturation with foam as without foam;[14,22-27] and (3) gas mobility in foam is controlled by foam texture.[10]

A much simpler mechanistic model based on the relation between capillary pressure and steady-state foam texture[28-30] is described Refs. (31) to (33) and, briefly, in the next section. Based on this hypothesis, surprisingly simple and powerful conclusions can be drawn for foam plugging and flow in homogeneous reservoirs in radial geometry and in heterogeneous reservoirs with layers either isolated or in capillary equilibrium. Moreover, unsteady-state foam behavior and resulting flow diversion in the absence of oil can be described approximately using this model and fractional-flow theory. We illustrate these possibilities using fractional-flow and mobility data from Persoff et al.[34-36]

In essence, this "limiting-capillary-pressure" model, which focuses on capillary pressure and foam coalescence, complements the model recently proposed by Friedmann et al.,[8] which focuses on foam generation. Each model isolates a portion of the overall foam population balance, in the hopes that the portion under study controls the remaining foam mechanisms.

Applying this model requires making substantial extrapolations from currently available data. Indeed, an important result of this work is the delineation of gaps in current data that must be filled to verify and expand the reliability of the fractional-flow model. The ultimate test of an approximate theory is whether it produces valuable insights. We believe the capillary pressure model presented here meets this test.

THE "LIMITING CAPILLARY PRESSURE"

Capillary pressure (p_c) governs foam texture. The higher the capillary pressure, the less stable are the liquid films (lamellae) that compose a foam.[28-30] Khatib et al.,[28] in sand- and bead-pack experiments, identified an abrupt transition from a strong foam to no foam (or weak foam) at a value of capillary pressure, p_c^*, which they called the "limiting capillary pressure." Because gas mobility depends on foam texture,[10] there is an abrupt change in gas mobility as well in the immediate vicinity of p_c^*. The nature of this change, and the magnitude of p_c at which it occurs, depends on surfactant type and concentration, rock type and other variables.

References and Illustrations at end of paper.

The abrupt change in gas mobility at p_c^* means that the system is maintained at p_c^* over a variety of water and gas flow rates.[12,28] Because S_w depends on p_c, and the function $k_{rw}(S_w)$ is unaffected by foam,[14,22-27] ∇p can be determined simply from Darcy's law applied to the water phase:

$$\nabla p = u_w \mu_w / [k\, k_{rw}(S_w^*)] \quad (1)$$

where u_w is the volumetric flux (Q/A) of water, μ_w is the viscosity of water, k is permeability, and $S_w^* \equiv S_w(p_c^*)$. In the absence of significant gradients of p_c, ∇p is the same in the water and gas phases. Therefore, for foams at p_c^*, one can calculate ∇p without knowing foam texture, if one knows the value of $k_{rw}(S_w^*)$.[28,34]

Equation (1) represents an enormous simplification over other mechanistic foam-modeling approaches.[10,11,13,14] The determination of the individual lamella generation, trapping and destruction mechanisms, as well as the determination of non-Newtonian gas mobility from foam texture and flow rates, are unnecessary for foams at their limiting capillary pressure. In essence, for foams at p_c^*, foam texture adjusts to whatever value is required to maintain p_c at p_c^*.

Some researchers have found that p_c^* (and therefore S_w^*) changes as gas or liquid flow rate changes.[27,28] Other indirect evidence supports this conclusion.[8,10,14,37,38] On the other hand, Persoff et al.[34] and Ettinger and Radke[12] conclude that S_w and $k_{rw}(S_w^*)$ (and by implication, p_c^*) did not change as both water or gas injection rates were changed substantially in their laboratory sandstone corefloods. Other indirect evidence agrees.[39,40] In the remainder of this report, we adopt as a working hypothesis that p_c^* is independent of gas and water flow rates. We call this model the "constant-p_c^*" model here, in contrast to the less-restrictive assumptions of the original p_c^* model proposed by Khatib et al.[28] In this case, for foams at the limiting capillary pressure, S_w^* in Eq. (1) is a constant, and Eq. (1) implies

$$\nabla p = \frac{u_w}{\lambda_w^*} \quad (2)$$

where

$$\lambda_w^* \equiv \frac{k\, k_{rw}(S_w^*)}{\mu_w} \quad (3)$$

is a constant independent of pressure gradient and gas and liquid flow rates. Gas mobility is then

$$\lambda_g = \lambda_w^* \frac{u_g}{u_w} = \lambda_w^* \frac{f_g}{f_w} = \lambda_w^* \left(\frac{1-f_w}{f_w}\right) \quad \text{for } S_w = S_w^* \quad (4)$$

where f_g and f_w are the fractional flows of gas and water, respectively. This equation means that gas mobility at p_c^* is a function of f_w (i.e, a function of foam quality $f_g = 1-f_w$) and S_w^* only.

A schematic steady-state fractional-flow curve for foam based on this hypothesis is shown in Figure 1. Values of $S_w < S_w^*$ correspond to $p_c > p_c^*$, i.e., no of foam. Values of $S_w > S_w^*$ correspond to $p_c < p_c^*$, i.e., strong foam. Therefore, due to the abrupt transition in gas mobility, water fractional flow rises from virtually zero, for $S_w < S_w^*$, to a much larger value for $S_w > S_w^*$. We present a fractional-flow curve based on laboratory data below.

The constant-p_c^* model applies directly to foams at steady state;[21] it may not apply to the period of foam generation[14,34,40,41] or at the leading edge of an advancing foam front.[14,18,36] If the period of foam generation is significant on a reservoir scale, i.e., if foam texture takes a significant period to reach its steady-state value under fixed conditions, then modeling foams using fractional-flow-theory would be invalid. Fractional-flow modeling can be modified to describe the retarded advance of a foam front, however, as described below.

Effect of Permeability on p_c^* and S_w^*

The effect of formation permeability on p_c^* determines the extent of flow diversion between layers. Figure 2 shows values of p_c^* taken from Khatib et al.'s[28] direct measurements as well as values inferred from other studies.[31] These estimates should be taken as only approximate, indicating a general trend. Figure 2 indicates that p_c^* increases as k decreases, but this increase in p_c^* is smaller than the increase expected in capillary entry pressure p_c^e and the entire $p_c(S_w)$ curve as k decreases.

Figure 3 explores the implications of these trends. This figure[32] is based on capillary-pressure data supplied by P. Persoff[36] for the same 1.3 d Boise core material used in the foam corefloods of Persoff et al.[34] The curves for other permeabilities assume that the same Leverett j function[42]

$$j(S_w) = \frac{p_c(S_w)}{\sigma} \left(\frac{k}{\phi}\right)^{1/2} \quad (5)$$

applies at all permeabilities. As k decreases, p_c^* increases (Figure 2); nevertheless, S_w^* increases as k decreases, as shown in Figure 3. Since k_{rw} depends on S_w, $k_{rw}(S_w^*)$ increases as k decreases as well.[31]

Figure 3 indicates that no foam can exist in a sufficiently low-permeability formation: that is, S_w^* approaches 1 as k approaches 0. Khatib et al.[28] make a similar point. The figure also indicates that foam can exist at almost all saturations, down to connate, in a sufficiently high-permeability medium. The specific numerical results should be taken as only approximate, given the assumptions made,[31] but indicate general trends we expect to apply broadly to formations where $p_c(S_w)$ increases as k decreases.

A FRACTIONAL-FLOW CURVE FOR FOAM

Because in the constant-p_c^* model p_c^* does not depend on flow rates or pressure gradient, one can construct a steady-state fractional-flow curve independent of flow rates and ∇p for foams at the limiting capillary pressure. Then the insights of fractional-flow theory can be applied to steady-state foam processes.

One can construct plausible fractional-flow curves for foam and for surfactant-free flow of gas and water from the data in Persoff et al.[34,35] Our goal is to derive fractional-flow curves based as closely on hard data as possible, but necessary assumptions and extrapolations make these curves somewhat speculative. We believe these curves are reasonable and indicate the general nature of behavior to be expected when more complete data are available and simplifying assumptions can be relaxed.

Fractional-Flow Curve Without Foam

The foam-free relative permeabilities of gas and water in a 1.3 d Boise sandstone core measured by Persoff et al.[34] are replotted and extended in Figure 4.[32] One can calculate $f_w^o(S_w)$ from relative permeabilities and viscosities as follows:

$$f_w^o(S_w) = \frac{k_{rw}(S_w)/\mu_w}{k_{rg}^o(S_w)/\mu_g^o + k_{rw}(S_w)/\mu_w} \quad (6)$$

where the superscript ^{o} indicates values in the absence of surfactant. We assume here that the values $\mu_g^o = 0.000018$ Pa·s for N_2[43] and $\mu_w = 0.0012$ Pa·s for surfactant solution[34] at atmospheric pressure are approximately correct at elevated pressures.

Fractional-Flow Curve in the Presence of Foam

Persoff et al.[34] found that, in the presence of foam, S_w and k_{rw} were virtually constant over a range of f_w^f from 0.004 to 0.29. (The superscript ^{f} indicates values in the presence of surfactant.) Small changes in S_w upon large changes in f_w^f have been observed also by Raza,[39] Chou,[41] and Osterloh and Jante.[38] The data from Persoff et al.'s Figure 13 are replotted as open circles on our Figure 5 along with the foam-free $k_{rw}(f_w^o)$ curve (AB'DE) computed using Eq. (6) and Figure 4. The corresponding curve in the presence of foam consists of three sections: (1) the strong-foam section ($S_w > S_w^*$, $p_c < p_c^*$, $f_w^f > 0.29$), (2) the section at p_c^* ($S_w = S_w^*$, $p_c = p_c^*$, $0.004 \le f_w^f \le 0.29$), and (3) the section with weak or broken foam ($S_w < S_w^*$, $p_c > p_c^*$, $f_w^f < 0.004$). Persoff et al. were able to measure data only in the middle section; extrapolations are necessary to complete the fractional-flow curve for foam.

The foam-free gas relative permeability at $S_w = S_w^* = 0.37$ is 0.68 (Figure 4), and the foam-free gas relative mobility is $\lambda_{rg}^o \equiv k_{rg}^o(S_w^*)/\mu_g^o = 37{,}800$ (Pa·s)$^{-1}$. At $S_w = S_w^* = 0.37$ and $f_w^f = 0.29$

(71% foam quality - the lowest foam quality employed by Persoff et al.), in the presence of foam, $\lambda_{rg}^f \equiv (\lambda_g^f / k) = [k_{rw}(S_w^*)/\mu_w] \cdot (0.71/0.29) = 2.0404$ $(Pa{\cdot}s)^{-1}$ (cf. Eq. (4)). In other words, to sustain a water fractional flow of 0.29 at this saturation as Persoff et al. observed, gas mobility must have been reduced by a factor of 18,500 below its foam-free value. Persoff et al. did not test any wetter foams; it is possible that S_w would be constant to yet-higher values of f_w^f, with greater reductions of gas mobility from the foam-free value. (For instance, in one sandpack, Raza[39] found S_w changed little as f_w^f varied from about 0.45 to almost 0.9.) Using similar calculations, one can show that for $f_w^f = 0.004$ (99.6% foam quality - the highest quality employed by Persoff et al.), the gas mobility was reduced by a factor of 182. It is possible that S_w would hold constant to yet-lower values of f_w^f, with smaller reductions in gas mobility. Thus $f_w^f = 0.004$ and 0.29 represent the boundaries of the confirmed limiting-capillary-pressure portion of the fractional-flow curve, shown in Figure 5 as the portion from B to C.

For $S_w = S_w^*$ ($0.004 \le f_w^f \le 0.29$), gas relative mobility with foam λ_{rg}^f is given by Eq. (4). To extend the fractional-flow curves beyond this range, we make the following assumptions: For $f_w^f > 0.29$, we assume that the same reduction in gas mobility, by a factor of 18,500, applies for $f_w^f > 0.29$ or $S_w > 0.37$

$$\lambda_{rg}^f = [k_{rg}^o(S_w)/\mu_g^o] / R \qquad (7)$$

$$R = 18{,}500 \quad \text{for} \quad S_w > S_w^* \quad . \qquad (8)$$

This assumption is plotted as the portion of the curve from A to B on Figure 5. For $S_w < S_w^* = 0.37$, we assume that foam breaks completely and that gas mobility returns to its foam-free values: i.e.,

$$R = 1 \quad \text{for} \quad S_w < S_w^* \quad . \qquad (9)$$

This assumption is represented by the horizontal line between points C and D on Figure 5. This "complete collapse" assumption cannot be confirmed by Persoff et al.'s data, which are also consistent with R as large as 182 for $S_w < S_w^*$. An alternate assumption is represented by the "weak foam" curve from C to E on Figure 5; this curve reflects an exponential decay of $R(S_w)$ with decreasing S_w, from a value of R = 182 at $S_w = 0.37$ to a value of R = 1 at $S_w = 0.27$. The distinction between the "complete collapse" and "weak foam" cases is significant for foam WAG (Water Alternating Gas) processes, where a large gas slug follows foam.[32] Finally, we ignore the small difference between the viscosity of water and of surfactant solution. The fractional-flow curve that results from these assumptions is shown along with the foam-free curve in Figure 6. The lettered points on this figure correspond to those on Figure 5. Except where noted, we assume below that f_w^f follows path ABCDE in both figures.

The fractional-flow curve ABCDE applies for foams with at least some injected gas. In a WAG, or in foam/acidization processes,[33] however, a slug of surfactant solution without gas ($f_w^f = 1$) may follow foam. When Persoff et al.[35] injected a large slug of surfactant solution at the same (relatively high) surfactant concentration as in the foam itself, however, they found identical k_{rw} and S_w during liquid injection as with the foam. In other words, subsequent surfactant injection trapped virtually all the gas in the foam in place, maintaining the low S_w and $k_{rw}(S_w)$ found in the foam itself. Bernard et al.[16] obtained roughly similar, though less striking, results, and found that low-concentration surfactant slugs were less effective at trapping gas (and maintaining low $k_{rw}(S_w)$) as they displaced foam than higher-concentration slugs. Here, in agreement with Persoff et al.,[33] we assume that surfactant solution injected following strong foam traps in place all the gas in the foam. This gives a third, "trapped-foam," fractional-flow curve, drawn vertically from the foam fractional-flow curve at a given injection point to the upper axis ($f_w = 1$) and then horizontally to the upper-right corner of the diagram (AFBCDE). The "trapped-foam" fractional-flow curve applies only to surfactant solution overtaking strong foam, not to surfactant solution entering a medium with gas and brine but no foam. For simplicity and to avoid clutter, in subsequent figures here we drop this fractional-flow curve, because we do not treat injection of surfactant slugs in this report.[32,33]

Figures 5 and 6 illustrate how a foam fractional-flow curve can be constructed using the data of Persoff et al.,[34,35] one of the most complete sets available. In fact, any of the empirical foam-simulation models for which gas and water mobility depend only on local saturations and compositions could be studied using fractional-flow theory. Fractional-flow theory would provide a simple, approximate tool of analyzing the implications of these models before introducing the additional complexities of large-scale simulation.

Effect of Permeability on Fractional-Flow Curves

Figure 3 shows how S_w^* is predicted to vary with rock permeability for similar Boise sandstones. To complete the specification of fractional-flow curves as a function of permeability, we add two further assumptions to those made above: First, we assume that the foam-free relative-permeability curves are independent of absolute permeability. This assumption is similar to the Leverett-j-function assumption made above. Second, we assume that the only effect of permeability on foam behavior is to shift the value of p_c^*. In other words, for all permeabilities, gas mobility is reduced by the same factor, 18,500, for $S_w > S_w^*$, and foam breaks completely for $S_w < S_w^*$.

Figure 7 shows the fractional-flow curves predicted for Boise sandstone of permeabilities of 13, 1.3, 0.43, 0.13, and 0.013 d, respectively. Each fractional-flow curve features a vertical line between the strong-foam (R = 18,500) and no-foam (R = 1) fractional-flow curves at the respective value of S_w^*. For example, if k = 0.13 d, there is no foam for $S_w < 0.75$. The same value of R for $S_w > S_w^*$ is assumed in all cases, but if the foam-free value of f_w^o is close to 0 or 1 the effect may not be visible on Figure 7.

From Figure 7, it can be seen that the lower the permeability, the smaller the range of S_w in which a strong foam can exist (section AB in Figures 5 and 6). For k = 0.013 d, the range in S_w in which strong foam can exist has shrunk to virtually zero. The opposite case is k = 13 d, for which strong foam can exist for S_w extending to connate water saturation.

Fractional-Flow Curve for Layers in Capillary Equilibrium

If two layers are in capillary equilibrium, fractional-flow curves in the presence or absence of surfactant are constructed from the corresponding curves for the two layers.[44] Figures 8 and 9 illustrate this construction for two layers of permeability 1.3 and 0.13 d, of equal thickness and porosity, in capillary equilibrium. For any p_c, the capillary-pressure curves determine S_{wi} in each layer i, as shown in Figure 8. The relation between p_c and S_w depends on surface tension, which depends on the presence or absence of surfactant; but if surfactant is either present or absent in both layers, the relation between S_{wi} in the two layers is that given in Figure 8. The value of S_{wi} determines the mobilities of both phases in the given layer, according to Figure 4 and, if surfactant is present, Eqs. (4) and (7) - (9). The total mobility of each layer i is the sum of the mobilities of the two phases

$$\lambda_{ti} = \lambda_{gi} + \lambda_{wi} \quad . \qquad (10)$$

For the two layers in p_c equilibrium, the overall water fractional flow f_{wt} is then the average of f_{wi} in the two layers, weighted according to the total mobilities of the layers

$$f_{wt} = (f_{w1}\,\lambda_{t1} + f_{w2}\,\lambda_{t2}) / (\lambda_{t1} + \lambda_{t2}) \quad . \qquad (11)$$

The overall S_{wt} is the average of S_{wi} in the two layers, weighted by their total pore volumes (assumed equal in this example)

$$S_{wt} = (S_{w1} + S_{w2}) / 2 \quad . \qquad (12)$$

The resulting fractional flow curves, for this example, with and without foam, are shown in Figure 9. The lettered points in Figures 8 and 9 are discussed below.

The relation between p_c and S_w can be complicated by the presence of surfactant: specifically, if foam is present, S_w can be less than predicted by the conventional capillary-pressure curve (corrected for lower surface tension with surfactant).[45] There is no distortion, of course, unless foam is present (i.e., $S_w > S_w^*$) in at least one layer. For the case shown in Figure 9, however, almost the entire fractional-flow curve with foam corresponds to $S_w \le S_w^*$ in the low-permeability layer and $S_w < S_w^*$ in the high-permeability layer.

Therefore the artifact is limited to extremely high f_w^f. The fractional-flow curve without surfactant is unaffected, of course.

Transient and Steady-State Flow

Khatib et al. observed that foam collapses abruptly as p_c rises to p_c^*.[28] The virtually instantaneous coarsening of a fine-textured foam upon entering rock[12] provides additional, indirect evidence for the immediate, catastrophic coarsening of a foam that exceeds p_c^*. However, foam generation, propagation and refinement of texture for $p_c<p_c^*$ can take time, whether initial foam generation takes place within the rock or foam is pre-generated and injected into the rock.[14,24,28,34] During this delay foam texture controls gas mobility and p_c, rather than the reverse, and gas mobility is not a unique function of p_c. For instance, plots of gas mobility in foam (usually reported as "relative permeability") as a function of S_w should show a nearly vertical rise of k_{rw}^f as Sw approaches S_w^*. Published plots do not show this.[24-26,37] We believe this reflects failure to reduce S_w to S_w^* in these tests, especially in the unsteady-state experiments. Therefore, we believe, the lowest measured value of S_w in such an experiment represents an upper limit to S_w^*.

Determining gas mobility during the transient build-up of foam texture requires a model for the refinement of foam texture, such as the population balance. Coreflood tests indicate that in the laboratory this transient period can be substantial. Whether a simpler model based on steady-state rheology at p_c^* would be adequate for reservoir simulation depends on how substantial the transient period is on the reservoir scale.[21]

IMPLICATIONS

Khatib et al.[28] cite three implications of the limiting-capillary-pressure concept. First, foaming surfactants could be ranked in effectiveness by comparing their values of p_c^* under identical conditions. According to Eq. (1), this is equivalent to the more-frequent practice of ranking surfactants according to ∇p built up in corefloods. Second, for a given formulation, p_c^* increases as k decreases, but not as sharply as the capillary entry pressure of gas p_c^e increases with declining k. Therefore there is in principle for any surfactant formulation some threshold permeability below which it cannot foam in rock. Third, foam may be unable to block an override zone if p_c is too high there due to water drainage to the bottom of the formation.

In this section we present some further implications.

Capillary End Effects

The capillary end effect in corefloods means that a region of low p_c may remain near the core outlet even after many pore volumes of gas injection. If the pressure difference across the core is small, this region may extend across much of the core. In this region foam remains strong. (During long-term gas injection, foam might slowly dry out and collapse due to transport of water dissolved in the gas phase.) The same would not be true in field application, where large gas slugs would push the region of low p_c and strong foam far from the injection point. Thus coreflood determinations of foam stability to subsequent injection of gas may be irrelevant to foam stability in the field, if the pressure difference across the core is comparable to p_c^*.

Steady Radial Flow of Foam

Consider the steady, 1-dimensional, radial flow of foam at its limiting capillary pressure in a homogeneous reservoir. We assume that foam quality is constant at the well and, initially, that the gas is incompressible. Equation (1) indicates that ∇p is proportional to u_w. Since p_c^* and S_w^* are uniform throughout the foam region, independent of radial position r, conservation of mass at steady state requires that u_w decline as 1/r as water flows from the well. As a result, ∇p declines as 1/r, just as in steady flow of a Newtonian fluid. Although foam rheology is strongly non-Newtonian and fixed texture,[10] foam texture degrades just fast enough, as foam flows from the well, to maintain p_c at p_c^*.

Patzek and Koinis[46] reported mobility reduction factors (MRF) inferred from a steam-foam field test at the Kern River field. Laboratory foam mobility data at fixed texture[10] suggest that MRF should increase as u_g decreases away from an injection well, reflecting the shear-thinning nature of foam at constant texture. Laboratory coreflood data measured at constant quality and unknown texture[14] also indicate a shear-thinning foam rheology. Both Khatib et al.'s[28] and de Vries and Wit's[27] data imply that p_c^* should increase as flow rates decline away from the well. This too indicates a shear-thinning rheology. Patzek and Koinis found instead, however, that MRF decreased steadily with increasing distance from the injection well, as shown in Figure 10. The prediction based on Eq. (1) is that MRF should be independent of radial position. This prediction is closer approximation to the field observation than an assumption of shear-thinning rheology, but is clearly not a complete explanation.

Accounting for gas compressibility does not change the p_c^* model's prediction of apparent Newtonian rheology in steady radial flow. For foam at p_c^*, ∇p depends on only u_w of the virtually incompressible water phase (Eq. (1)). Expanding gas volume as pressure declines away from an injection well raises u_g, but this merely affects the rate of foam coalescence required to maintain p_c constant at p_c^*; it does not change ∇p.

Thermal effects could alter the prediction of Newtonian rheology in Figure 10. Assuming adiabatic flow, some water must boil off to maintain constant enthalpy as pressure declines away from the well. The resulting faster decline in u_w would give the appearance of shear-thickening behavior, bringing the model prediction in Figure 10 a little closer to the field result.[32] Heat losses to overburden, however, would cause steam to condense, raising u_w and driving the model prediction further from the field result.

Friedmann et al.[9] propose a different explanation for the decreasing foam effectiveness away from the well illustrated in Figure 10. Based on laboratory and field results, they conclude that (1) foam generation occurs only near an injection well, where ∇p is high,[14,47] and (2) foam flow, which also requires a substantial ∇p,[10, 48-51] can likewise occur only relatively near the well; therefore there is an inherent limited range of penetration for foam. The constant-p_c^* model, however, imposes no limit to foam propagation, as discussed in the following section.

Foam Plugging

As we discuss above, foam of a given texture has a minimum pressure gradient, $(\nabla p)^{min}$, below which it does not flow in a given porous medium.[10,48-51] This threshold reflects the capillary resistance to the movement of individual liquid films through pore bodies and throats.

However, Eq. (1) implies that at steady state there can be no complete plugging of gas by foam at p_c^*. Were plugging to occur, water transport would continue and p_c would rise until, at p_c near p_c^*, foam texture had degraded sufficiently to allow gas flow to resume. The existence of a threshold $(\nabla p)^{min}$ for a given texture thus does not preclude foam flow at low ∇p; in effect it specifies how far foam must degrade in order to flow.

Complete gas blockage is possible temporarily until p_c rises sufficiently to degrade foam texture. The theory[48-51] of $(\nabla p)^{min}$ applies to such foams if foam texture is known as a function of time. For instance, a fine-textured foam flowing at steady state under an applied ∇p could plug a porous medium temporarily if ∇p were suddenly reduced below the value of $(\nabla p)^{min}$ for that texture. Eventually, however, continued water transport would dry out the foam, coarsening texture until gas flow could resume. If, as some suggest, stationary foam films are stable at higher p_c than moving films,[28,30] then p_c may have to rise temporarily above p_c^* to initiate foam coarsening and gas flow. The rate of change of p_c is determined by the rate of transport of water. If the water relative permeability is low at S_w^*, complete gas blockage could continue for an extended period of time. We assume here that water can continue to flow with finite relative permeability at all values of S_w; in other words, that there is no truly "irreducible" water saturation.[52]

Complete gas blockage is possible indefinitely if for some reason water transport is prevented. Possible causes include a zero ∇p in the water phase, as might occur in a coreflood due to the capillary end effect or in foam placed near a water/gas contact in a quiescent gas reservoir with an aquifer. In both cases there is a capillary pressure gradient but no ∇p in the water phase. Water transport might also be prevented by solidification of the water phase, e.g., by gel formation.

Diversion Between Isolated Layers

Consider the steady injection of water and gas into two layers, separated by an impermeable barrier, with equal fractional flow imposed at the injection point. This condition applies to parallel-core

corefloods and may apply to isolated layers in an injection well. Khatib et al.[28] point out that, at realistic permeabilities for oil reservoirs, p_c^* is higher in lower-permeability layers, but its increase is not as great as that of the ratio $\sqrt{k_2/k_1}$ that controls the capillary-pressure curves according to Eq. (5). This means that $S_w^* \equiv S_w(p_c^*)$ is higher in the low-permeability layer 1 than in the higher-permeability layer, as shown in Figures 3 and 7. We illustrate the resulting behavior using the fractional-flow curves for 1.3 d and 0.13 d Boise sandstone in Figure 7.

There are three possible outcomes for foam processes. (1) For $f_w^f < 0.00002$ (foam quality > 99.998%) there is no foam in either layer; both layers are at $p_c > p_c^*$ and $S_w < S_w^*$. Therefore there is no diversion of flow. (2) For $0.00002 < f_w^f < 0.046$ (foam qualities between 99.998% and 95.4%), the high-permeability layer is at p_c^* and S_w^*, but there is no foam in the low-permeability layer. At the upper limit of this range ($f_w^f = 0.046$), mobility is reduced in the high-permeability layer by a factor of 2200, and the ratio of mobilities in the two layers is 130:1 in favor of the low-permeability layer. (3) For $f_w^f > 0.046$, there is foam in both layers ($S_w > S_w^*$, $p_c < p_c^*$), but for reasonable values of f_w^f the foam is much stronger in the high-permeability layer. For instance, for $f_w^f = 0.2$, the ratio of injectivities is 15:1 in favor of the low-permeability layer, in spite of the adverse permeability ratio. In short, there is effective diversion from the high-permeability layer to the low-permeability layer, as long as the injected foam is wet enough to support foam in the high-permeability layer. This is the implication of Figure 10 of Khatib et al.,[28] who point out that at extremely high permeabilities (> 1,000 d) the effect may be reversed. This is, of course, the effect usually sought in foam applications.

This diversion is due to the much-lower value of S_w^* in the high-permeability layer (Figure 3). This results, in turn, not from the somewhat speculative increase in p_c^* with permeability shown by the few data in Figure 2, but in the much greater increase in the whole $p_c(S_w)$ curve with decreasing permeability (Eq. (5)). Unless the increase in p_c^* with decreasing k is much greater than that shown in Figure 2, the predicted diversion would take place.

Layers in Capillary Equilibrium

Consider the steady injection of water and gas into a pair of layers similar to the first pair, but in capillary equilibrium. In this case the condition imposed is not equal fractional flow in the two layers, but equal p_c. Because p_c^* is higher in the lower-permeability layer, p_c is lower in that layer, relative to p_c^*, than in the high-permeability layer.

Rossen et al.[31] point out that, according to the constant-p_c^* model, the ratio of injectivities with foam into layers in capillary equilibrium is worse than the ratio of permeabilities. However, the same is true of injection rates without foam, because S_w is higher and $k_{rw}(S_w)$ higher in the low-permeability layer than in the high-permeability layer. For instance, for $f_w^0 = 0.02$, in the absence of surfactant, the ratio of total injection rates into two layers with k = 1.3 and 0.13 d is 137:1 in favor of the high-permeability layer; moreover, virtually no gas enters the low-permeability layer ($f_w^f \sim 1$). The fractional flows and saturations in this case are shown as points A', A" and A in Figures 8 and 9.

Again, for foam injection, there are three cases, illustrated by layers of permeability 1.3 d and 0.13 d in Figures 8 and 9.

(1) With surfactant, for $f_{wt}^f < 0.00024$, there is no foam in either layer, and no diversion. (2) For $0.00038 > f_{wt}^f > 0.00024$ there is foam in the low-permeability layer but not in the high-permeability layer. (3) For $f_{wt}^f > 0.00038$, there is foam in both layers. For $f_{wt}^f = 0.02$, for instance, represented by points B', B", and B in Figures 8 and 9, there is foam in both layers, and the ratio of total injectivities into the two layers is 54:1 in favor of the high-permeability layer: i.e., worse than the ratio of permeabilities, but a little better than with no foam. There is still no gas injection into the low-permeability layer, where $f_w^f \sim 1$, however. In short, foam is ineffective at improving sweep of low-permeability layers in capillary equilibrium with higher-permeability layers, due to the increase in p_c^* observed with decreasing k in Figure 2.

A failure to divert gas flow into low-permeability layers need not mean failure of an EOR process. Layers in capillary equilibrium are expected to be relatively thin and interbedded. Conduction of heat and diffusion of CO_2 or other miscible gas into thin low-permeability layers could still accomplish process objectives in these layers in the absence of bulk flow of gas through them.

APPLYING FRACTIONAL-FLOW THEORY TO UNSTEADY FOAM FLOW

Fractional-flow theory has been used to model various oil-recovery processes since 1941.[53-60] In applying fractional-flow theory, we make the following assumptions, similar to those made by Walsh and Lake:[59]

1. The flow is one-dimensional, through an isothermal permeable medium. There are no phase changes.
2. The rock and fluid properties are independent of pressure. The gas is assumed to be incompressible.
3. The fluids do not react chemically with rock, except for surfactant adsorption.
4. The phases immediately take the steady-state mobilities dictated by their saturations, fractional flows and the presence or absence of surfactant.
5. Dispersion and viscous fingering can be ignored.
6. The initial conditions are uniform in the medium.
7. At most there are two phases:
   - a gas phase which contains only gas;
   - an aqueous phase, which contains water, or water and surfactant, only.
8. At most three components are present: water, gas, and surfactant.

In addition, we assume that the constant-p_c^* model described above applies to gas and water flow in the presence of surfactant.

Walsh and Lake[59] review the arguments for using fractional-flow modeling in spite of the simplifying assumptions involved. The assumption of gas incompressibility and no phase change are especially serious for foams in low-pressure steamfloods. Fisher et al.[12] review arguments for steady-state foam modeling on a field scale, as required by assumption (4). In the end, the utility of an approximate model rests on the usefulness of the insights it produces.

Fayers and Perrine[60] and Pope[57] describe how to incorporate surfactant adsorption into fractional-flow theory. One can account for propagation of foam slower than propagation of surfactant,[14,18,24] in violation of assumption (4), in an ad hoc way, by assuming an artificially high level of surfactant adsorption. We illustrate this approach with an example below. Patzek and Myhill[18] used this strategy to simulate slow foam propagation in their Kern River steam-foam test, and it is essentially equivalent to assuming trapping of lamellae as did Friedmann et al.[14] Friedmann et al.'s field data[9] suggest that foam propagates at the same velocity as surfactant. (As noted above, however, Friedmann et al.[9] also reached other conclusions from their field data that contradict the assumptions of our fractional-flow model.)

Solution of Fractional-Flow Equations

The equations relating the fractional-flow curve to wave velocities are described in the Refs. (32) and (59). Briefly, saturation waves move with velocities equal to the slope of the fractional-flow curve at that saturation. "Buckley-Leverett" shock fronts, discontinuities in saturation, occur where rearward waves overtake forward waves of lower velocity. With no dispersion, all liquid is at either zero or unit surfactant concentration. Mass balances on water and surfactant govern the "chemical" shock that separates regions of different surfactant concentration; graphically, for our cases, these conditions are equivalent to drawing a line from the origin of the $f_w(S_w)$ plot to the fractional flow curve.

We assume two layers of equal thickness and porosity differing in permeability by a factor of 10 (1.3 d and 0.13 d, respectively). We assume outward, radial flow through cylindrical disks with a ratio of inner to outer radii of 1:1000 (as for well and reservoir radii of 0.1 and 100 m). In all cases below the layers are assumed to be in capillary isolation; that is, the same fractional flow is imposed at the inlet face or well for both layers and there is no cross-flow.

The method of calculating relative injection rates into the two layers and total injectivity is given in the Ref. (32). We assume a constant total injection rate into the two layers

$$u_{t1} + u_{t2} = \text{constant} \qquad (15)$$

and we assume that the same Δp applies between inner and outer radii of both layers. Periods of low injectivity would be prolonged if a constant Δp were imposed instead of constant flow rates.

The positions of the various waves reflect the cumulative injection into both layers and in turn controls the respective injection rates. Some sort of numerical integration in time and space is required. We used a forward-difference finite-difference scheme in the results presented here.[32] There are small fluctuations in the results presented below, which indicates a grid of insufficient refinement in our finite-difference technique. We believe the trends shown accurately represent correct behavior, however.

In the plots of wave positions as a function of time, we plot the total relative mobility for each layer, defined as

$$\lambda_{rt} \equiv \frac{\lambda_g + \lambda_w}{k} \quad . \tag{16}$$

Thus the absolute mobilities in each layer are the product of the relative mobilities and permeability.

PREDICTIONS OF FRACTIONAL-FLOW THEORY FOR UNSTEADY FOAM PROCESSES

Initial Injection of Foam at Constant f_w^f

We present only two cases here. Further details are in Ref. (32).

Our first example is injection of foam at $f_w^f = 0.02$ (98% quality) into rock saturated with water and gas at $f_w^o = 0.02$. The fractional-flow curves, wave velocities, elution histories, saturation profiles and relative mobilities are indicated for the high-permeability layer (k = 1.3 d) in Figure 11 after the manner of Walsh and Lake.[59] Subsequent figures provide only the fractional-flow curves and time-distance diagrams, from which the other information can be derived. It is important to note that in each case dimensionless time is given in terms of pore volumes (PV) injected into that layer. Since the injection rates into the two layers vary during simultaneous injection, according to the mobilities in each layer, a given physical time may correspond to different dimensionless times in the two layers.

For the case of foam injected into rock saturated with surfactant-free water and gas, the concentration velocity is the slope of a line from the lower left corner ($f_w = 0$, $S_w = 0$) through the injection point J on the foam $f_w^f(S_w)$ curve as in Figure 11a. The point J is specified by the injected f_w^f (0.02). This line intersects the foam-free fractional-flow curve f_w^o at a point "WB," representing the water bank in front of the foam. Between initial-condition point "I" and "WB" is a Buckley-Leverett shock with velocity given by the slope of the line from I to WB. Thus there are three stationary states, I, WB and J, separated by shock fronts.

Foam propagates slowly in this case because the water saturation corresponding to the injected foam quality (point J) is much greater than the injected water fractional flow; in other words, it takes about 17.5 pore volumes of foam which is 2% surfactant solution by volume to fill 1 pore volume of rock with foam at $S_w^* = 37\%$ water saturation. Because water saturation behind the foam front is lower than that present initially, there is a water bank ahead of the foam.[61]

Total relative mobilities λ_{rt} are indicated in the three regions of Figure 11d. In this and subsequent figures, a box around the value means that the value applies throughout a region of the time-distance diagram; an unboxed value, with an arrow to a dotted line, means that the given value applies only to the indicated wave. Figure 11d indicates that mobility is reduced somewhat in the water bank relative to the initial state, but is reduced dramatically, by a factor of about 110 from the initial state, in the slowly advancing foam region.

In the low-permeability layer (Figure 12), no foam forms even in the presence of surfactant, because $p_c > p_c^*$ and $S_w < S_w^*$ at the injected f_w^f. Therefore the entire medium remains at its initial high mobility during foam injection. Thus once foam fills the high-permeability layer, the ratio of flow rates into the two layers is about 11:1 in favor of the low-permeability layer.

The results of simultaneous injection into two cylindrical layers are shown in Figure 13. The effect of foam is even more rapid, because foam quickly fills the crucial near-well region. The injection rates into the two layers cross over when only about 3 10^{-5} total PV foam has been injected, equivalent to the pore volume within only about 1/2 m of the well.[32] In fact, much less foam than this is actually in place, due to the slow propagation rate of foam (Figure 11d).

Figure 14 illustrates the effect of retarded foam propagation, due either to surfactant adsorption or to foam coalescence. To account for surfactant adsorption one draws the chemical shock, not from the origin ($f_w = 0$, $S_w = 0$) through point J as in Figure 11a but from a point to the left of the origin.[32,57,60] One can account for retarded foam propagation by assuming increased surfactant adsorption. In Figure 15, for illustration, we assume that same level of surfactant losses assumed by Patzek and Myhill[18,46] in simulating both adsorption and coalescence in a steam-foam field trial. They found that 1.5 bbl of surfactant solution was required for every 1 bbl of foam in place; this corresponds to a slope of the chemical shock of 0.0133 through the point J of the fractional-flow curve. The rate of foam propagation is four times slower than in Figure 11d, but diversion still occurs rapidly in radial flow, as shown in Figure 14.

For a continuous-injection foam process, the mobility at the injection condition J soon controls mobilities in the crucial near-well region. Therefore the greatest diversion is obtained with a surfactant that gives the lowest mobility at the injected foam quality. This is equivalent to obtaining the lowest k_{rw} (i.e., lowest S_w) at the injected f_w^f: or, as Khatib et al. state,[28] choosing the surfactant with the highest value of p_c^*. For effective diversion, the foamer should also be sensitive to differences in permeability in the injection interval. For foams that obey the p_c^* model, this sensitivity results automatically from the dependence of the $p_c(S_w)$ curve on k (Figure 3).

Figures 11-14 illustrate how the relation between limiting capillary pressure p_c^* and permeability k governs diversion between layers. In this case no foam forms at all in the low-permeability layer, due to the high value of S_w^* (Figures 3 and 7). Similar results obtain for higher values of f_w^f even though foam forms in both layers. For instance, for $f_w^f = 0.2$ (80% foam quality), foam forms in both layers, but the final ratio of injection rates is still 15:1 in favor of the low-permeability layer, due to higher $k_{rw}(S_w^*)$ in that layer. Foam propagates faster as well, due to greater slope of the chemical shock drawn through point J on the fractional-flow curve (cf. Figure 11a).

Gas Following Surfactant Solution in a WAG

Injection alternates between slugs of gas and surfactant solution in WAG foam processes. We assume for simplicity that, at the start of gas injection, surfactant solution saturates both layers, except for trapped gas from previous gas slugs. Thus the surfactant concentration is uniform in both layers, and the process in each layer is described by a single fractional-flow curve.

In the high-permeability layer (Figure 15) there is a Buckley-Leverett shock from the initial state I to the corner in the fractional-flow curve at S_w^*. There are a series of spreading waves at this corner, but all share the same mobility because they pivot on a single point. A wave of virtually zero velocity carries the final state J, with $f_w^f = 0$ and S_w at its irreducible value.

The relative mobility of the initial state I is relatively low (λ_{rt} = 292 $(Pa \cdot s)^{-1}$) due to the low relative permeability of water at trapped-gas saturation (Figure 4) and the high viscosity of water relative to gas. Although there is surfactant in the water at point I, and the gas mobility is assumed to be reduced by a factor R = 18,500 because $S_w > S_w^*$ (Eqs. (7) and (8)), this has no effect on λ_{rt} because gas mobility is zero at this saturation even in the absence of surfactant. Across the rapidly moving Buckley-Leverett shock, mobility increases by a factor of over 130. Ironically, there is no mobile foam anywhere in this layer: foam mobilization and collapse occurs in the narrow shock front between the initial state and S_w^*.

In the low-permeability layer (Figure 16) there is the same initial state and a similar (though faster-moving) shock. However, foam collapses at higher S_w^*, where a series of spreading waves have lower mobility than in the high-permeability layer. Gradually the mobility in this layer approaches that in the high-permeability layer at state J.

Figure 17 shows the results for simultaneous injection into cylindrical layers: virtually complete diversion of flow into the high-permeability layer! At the start, injection favors the high-permeability layer by a ratio of 10:1 due to permeability alone. As a result, the initial low-mobility state I is expelled from this layer faster than from the low-permeability layer in spite of the lower wave velocity suggested by Figures 15b and 16b. Once mobility rises 130-fold in the high-permeability layer, injection into the low-permeability layer virtually ceases. Injection into the low-permeability layer eventually rebounds slightly as the low-mobility initial state I is slowly pushed from the near-well region.

Persoff et al.'s data are also consistent with the "weak foam" model of Figure 5, in which foam collapses progressively over a range of water fractional flows less than $f_w^f = 0.004$. Allowing for a collapse of foam over a range of $f_w^f < 0.004$ as in curve ABCE of Figure 5 does not give an effective process, however.[32] The data of Persoff et al. are simply not consistent with an effective foam WAG process, according to fractional-flow theory.

The reason for the dismal performance of foam WAG predicted in Figure 17 is the nearly complete collapse of foam at a single low value of S_w^* in the high-permeability layer. The lower value of S_w^* (i.e., the higher the value of p_c^*), in fact, the higher the mobility behind the shock front. The trapped-gas saturation, gas-mobility reduction and fractional-flow curve for $S_w > S_w^*$ is of secondary importance, since the Buckley-Leverett shock bypasses this part of the curve. Indeed virtually the worst surfactant formulation possible for a WAG, according to this model, would be one that forms a strong foam at high S_w and collapses completely at a single low value of S_w^*. Such a foam would be ideal for a continuous-injection process, as noted above. Almost anything would perform better than such a foam in a WAG, however - even a foamer that collapsed completely at a higher S_w^* (as in the low-permeability layer in Figure 16), or no foam at all. The ideal surfactant would form a foam that degrades progressively over a wide range of S_w, producing spreading waves of low mobility.

Some have advocated using "weak" foams for CO_2 flooding because only a moderate mobility reduction is desired.[62,63] This is a separate issue from that we address here. The problem with using a foam that collapses at a single p_c^* in a WAG process is not that it reduces gas mobility too much, but that it gives no mobility reduction at all, except in a transition zone that, in fractional-flow theory, is compressed into a razor-thin shock front.

It is possible that these conclusions derive not from physical mechanisms of foam processes, but from the simplifying assumptions made in fractional-flow theory, such as no viscous fingering, gas incompressibility, lack of capillary-pressure gradients, or immediate attainment of equilibrium mobility at each location. In particular, it can take some time for foam to attain its steady-state mobility in laboratory WAG floods.[34,41] It is important to determine whether this period is significant on a reservoir scale. Another important issue is viscous fingering: the vanishingly thin foam zone predicted by fractional-flow theory would have extremely low mobility. It may be that fingering of high-mobility gas into this zone and subsequent mixing could explain the long foam lifetimes observed in the laboratory. Both laboratory and field data have found that foam is effective after substantial periods of gas injection in a WAG;[4,64,65] whether fractional-flow theory would have predicted this result for these particular formulations, or whether they obey the p_c^* model, is not clear.

NEED FOR FURTHER DATA

There are many gross simplifications in the constant-p_c^* model and in fractional-flow modeling of foam that need to be explored. The results presented here highlight the need for further study of the following topics:

- the range of conditions under which the constant-p_c^* model applies to steady-state foam flow. The evidence for and against the model are summarized above and in Ref. (31).
- the shape of the fractional-flow curve at the low values of f_w^f, which shapes behavior during injection of gas in a WAG process (Figures 15-17).
- the shape of the fractional-flow curve at the high values of f_w^f, which shapes behavior during injection of liquid in a WAG process.[34]
- the effect of permeability and other rock properties on p_c^* (Figure 2).
- any other effects of permeability on the fractional-flow curve for foam: for instance, whether permeability affects only p_c^*, as assumed here for simplicity, or also alters the gas mobility reduction with foam or the collapse of foam at $S_w < S_w^*$.
- whether fractional-flow modeling is relevant to field-scale foam processes: how the transient period of foam generation scales up to the field; the importance of other factors ignored by fractional-flow theory, such as phase changes, compressibility of gas, capillary-pressure gradients, viscous fingering and dispersion.
- the effect of oil. We have not considered oil here, but one could incorporate its effect into the constant-p_c^* model if, for instance, it merely altered the value of p_c^* or reduced the mobility reduction factor R in the presence of foam.

CONCLUSIONS

We have explored the implications of the limiting-capillary-pressure concept,[28] as extended by the findings of Persoff et al.[34] and Ettinger and Radke,[12] as a working hypothesis for strong foam at steady state. The implications of this hypothesis are striking in their simplicity and significance. These implications are as follows:

1. In steady, 1D radial flow without phase change in a homogeneous reservoir, foam at its limiting capillary pressure behaves like a Newtonian fluid, even though its rheology at constant texture is strongly non-Newtonian. Foam texture degrades just fast enough to give Newtonian behavior. Thermal effects could give foam somewhat non-Newtonian behavior.

2. Foam at p_c^* preferentially diverts flow from high- to low-permeability layers if the layers are isolated from each other. However, if the layers are in p_c equilibrium, foam is ineffective. Conduction of heat and diffusion of mass may still accomplish EOR process objectives in these layers, which are likely to be thin.

3. There can in general be no complete plugging of gas by injection of foam of a fixed quality. Were plugging to occur, liquid transport would continue until foam dried out and coarsened sufficiently to allow gas flow to resume. Temporary plugging is possible while this liquid transport occurs.

4. The capillary end effect can strongly affect foam corefloods with low imposed pressure differences across the core.

5. One can construct plausible fractional-flow curves for foam flow from conventional capillary pressure ($p_c(S_w)$) curves and data on foam-free relative permeabilities, foam mobilities at the limiting capillary pressure p_c^*, and the effect of permeability on p_c^*. These curves illustrate how capillary pressure governs steady-state foam mobility and diversion between layers either in isolation or in capillary equilibrium.

6. The construction of such curves from currently available data, and the application of fractional-flow theory to prediction of dynamic foam processes, requires numerous simplifying assumptions and extrapolations. More data are needed on the shape of the fractional-flow curves at very high and low foam qualities, the effect of permeability on the curves, and the effect of simplifying assumptions made in fractional-flow theory.

The following conclusions are based on a fractional-flow curve derived from the data of Persoff et al.[34,35] and assume layers in capillary isolation:

7. For continuous-injection foam processes, the best surfactant is one that drives water saturation to the lowest possible value at the injected foam quality but is sensitive to differences in permeability. If a surfactant creates a strong foam in the reservoir, diversion occurs quickly as the near-well region fills with foam, even if surfactant-retention and foam-propagation rates are slow.
8. Fractional-flow theory indicates that, in WAG processes employing surfactant formulations that obey the constant-p_c^* model, effective diversion does not occur. Instead, during gas injection, foam is mobilized and destroyed in a thin moving front. The theory suggests that the best foam for a WAG process is one that degrades progressively over a range of saturations, rather than at a single saturation as do formulations that obey the p_c^* model. However, factors not accounted for in fractional-flow theory, such as viscous fingering and slow foam-generation processes, may have biased this conclusion. It is critical to determine how such processes scale from laboratory to field.

NOMENCLATURE

f_g, f_w = fraction of total volumetric flux consisting of specified phase
$j(S_w)$ = Leverett j-Function
k = permeability of the porous medium
k_{rg}, k_{rw} = relative permeability to gas and water phase, respectively
p = pressure
p_c = capillary pressure
p_c^* = limiting capillary pressure
∇p = pressure gradient
Δp = pressure difference across layer
PV = pore volume of the rock
R = gas mobility-reduction factor due to foam (Eq. (7))
S_g, S_w = saturation of gas or water phase, respectively
t = time
u_g, u_w = volumetric flux of gas and water phases, respectively
λ_g, λ_w = mobility of gas and water phases, respectively
λ_{rg}, λ_{rw} = relative mobility of gas and water phases, respectively
λ_{rt} = total relative mobility of fluids
μ_g, μ_w = viscosity of gas and water, respectively
ϕ = porosity
σ = surface tension

superscripts:

^{o} applies to value in absence of surfactant
^{f} applies to value in presence of surfactant
* applies to value in presence of surfactant, at limiting capillary pressure

subscripts:

w, g water (aqueous) and gas phases, respectively
t as first subscript: total value summed for both phases
t as second subscript: value averaged over both layers (except as λ_{rt})
i, 1, 2 as second subscript: value in given layer

ACKNOWLEDGMENTS

This work was supported in part by consortia on Stimulation, Logging and Formation Damage and on Enhanced Oil and Gas Recovery Research at The University of Texas at Austin and by The Petroleum Research Fund, administered by the American Chemical Society. We thank Mr. P. Persoff for generously supplying p_c data from his experiments, used in Figures 2 and 3.

REFERENCES

1. Hirasaki, G. J.: "The Steam-Foam Process," *J. Petr. Technol.* (May 1989), 449-456.
2. Hirasaki, G. J.: "A Review of the Steam Foam Process Mechanisms," SPE 19518 (unsolicited), SPE, Richardson, TX, 1989.
3. Smith, D. H., ed., *Surfactant-Based Mobility Control: Progress in Miscible-Flood Enhanced Oil Recovery*, ACS Symp. Ser. no. 373, Am. Chem. Soc., Washington, 1988.
4. Bernard, G. G., and Holm, L. W.: "Effect of Foam on Permeability of Porous Media to Gas," *SPE J.* (Sept. 1964), 267-272.
5. Gall, J. W.: "Steam Diversion by Surfactants," SPE 14390, presented at 1985 SPE Ann. Mtg., Las Vegas, Sept. 22-25.
6. Yang, S. H., and Reed, R. L.: "Mobility Control Using CO_2 Foams," presented at 1989 SPE Ann. Mtg., San Antonio, Oct. 8-11.
7. Lee, H. O., and Heller, J. P.: "Laboratory Measurements of CO_2-Foam Mobility," *SPE Reser. Engr.* (May 1990), 193-197.
8. Lee, H. O., Heller, et al.: "Change in Apparent Viscosity of CO_2-Foam With Rock Permeability," SPE/DOE 20194, presented at 1990 SPE/DOE Symp. on EOR, Tulsa, Apr. 22-25.
9. Friedmann, F., et al.: "Steam-Foam Mechanistic Field Trial in the Midway-Sunset Field," SPE 21780, presented at 1991 SPE Western Regional Mtg., Long Beach, March 20-22.
10. Falls, A. H., et al.: "The Apparent Viscosity of Foams in Homogeneous Bead Packs," *SPE Reser. Engr.* (May. 1989), 155-164.
11. Falls, A. H., et al.: "Development of a Mechanistic Foam Simulator: The Population Balance and Generation by Snap-off," *SPE Reser. Engr.* (Aug. 1988), 884-892.
12. Ettinger, R. A., and Radke, C. J.: "The Influence of Texture on Steady Foam Flow in Berea Sandstone," SPE 19688, presented at 1989 SPE Ann. Mtg., San Antonio, Oct. 8-11.
13. Chang, S-H., et al.: "The Effect of Microscopic Heterogeneity on CO_2-Foam Mobility: Part 2 - Mechanistic Foam Simulation," SPE/DOE 20191, presented at 1990 SPE/DOE Symp. on EOR, Tulsa, Apr. 22-25.
14. Friedmann, F., et al.: "Experimental and Simulation Study of High-Temperature Foam Displacement in Porous Media," *SPE Reser. Engr.* (Feb. 1991), 37-45.
15. Mahmood, S. M., et al.: "A Model for Prediction of Recovery and Pressure History for 2-D Displacement of Oil Through Porous Media by Gas/Surfactant," SPE 15076, presented at 1986 SPE Calif. Regional Mtg., Oakland, Apr. 2-4.
16. Marfoe, C. H., et al.: "Numerical Simulation of Foam Flow in Porous Media," SPE 16709, presented at 1987 SPE Ann. Mtg., Dallas, Sept. 27-30.
17. Law, D. H, et al.: "Effect of Presence of Oil on Foam Performance: A Field Simulation Study," SPE 18421, presented at 1989 SPE Symp. on Reservoir Simulation, Houston, Feb. 6-8.
18. Patzek, T. W., and Myhill, N. A.: "Simulation of the Bishop Steam Foam Pilot," SPE 18786, presented at 1989 SPE Calif. Regional Mtg., Bakersfield, Apr. 5-7.
19. Kular, G. S., et al.: "Foam Application in an Oil Sands Steamflood Process," SPE 19690, presented at 1989 SPE Ann. Mtg., San Antonio, Oct. 8-11.
20. Islam, M. R., and Farouq Ali, S. M.: "Numerical Simulation of Foam Flow in Porous Media," *J. Can. Petr. Technol.* (July-Aug. 1990), 47-51.
21. Fisher, A. W., et al.: "Mathematical Modeling of Foam Flooding," SPE/DOE 20195, presented at 1990 SPE/DOE Symp. on EOR, Tulsa, Apr. 22-25.
22. Bernard, G. G., et al.: "Effect of Foam on Trapped Gas Saturation and on Permeability of Porous Media to Water," *SPE J.* (Dec. 1965), 195-300.
23. Holm, L. W.: "The Mechanisms of Gas and Liquid Flow Through Porous Media in the Presence of Foam," *SPE J.* (Dec. 1968), 359-69.
24. Friedmann, F., and Jensen, J. A.: "Some Parameters Influencing the Formation and Propagation of Foams in Porous Media," SPE 15087 presented at 1986 SPE Calif. Regional Mtg., Oakland, Apr. 2-4.
25. Sanchez, J. M., et al.: "The Effect of Trace Quantities of Surfactant on Nitrogen/Water Relative Permeabilities," SPE 15546, presented at the 1988 Annual Meeting of the SPE, New Orleans, Oct. 5-8.
26. Huh, D. G., and Handy, L. L.: "Comparison of Steady- and Unsteady-State Flow of Gas and Foaming Solution in Porous Media," *SPE Reser. Eng.* (Feb. 1989), 77-84.
27. de Vries, A. S., and Wit, K.: "Rheology of Gas/Water Foam in the Quality Range Relevant to Steam Foam," *SPE Reser. Engr.*, (May 1990), 185-192.
28. Khatib, Z. I, et al.: "Effects of Capillary Pressure on Coalescence and Phase Mobilities in Foams Flowing Through Porous Media," *SPE Reser. Engr.* (Aug. 1988), 919-926.
29. Gumerman, R. J., and Homsy, G. M.: "The Stability of Radially Bounded Thin Films," *Chem. Eng. Commun.* **2** (1975), 27-36.
30. Jimenez, A. I., and Radke, C. J.: "Dynamic Stability of Foam Lamellae Flowing Through a Periodically Constricted Pore," in *Oil-Field Chemistry: Enhanced Recovery and Production Stimulation* (J. K. Borchardt and T. F. Yen, ed.), ACS Symposium Ser. no. 396, Am. Chem. Soc., Washington, 1989.
31. Rossen, W. R., et al.: "Modeling Foam Mobility in Porous Media," SPE 22627, presented at SPE 1991 Ann. Mtg., Dallas, Oct. 6-9.
32. Zhou, Z. H., and Rossen, W. R.: "Applying Fractional-Flow Theory to Foam Processes at the 'Limiting Capillary Pressure," SPE 24180, presented at 1992 SPE/DOE Symp. on EOR, Tulsa, Apr. 22-24.
33. Zhou, Z. H., and Rossen, W. R.: "Applying Fractional-Flow Theory to Foams for Diversion in Matrix Acidization," SPE 24660, presented at 1992 SPE Ann. Mtg., Washington, Oct. 4-7.

34. Persoff, P., et al.: "A Laboratory Investigation of Foam Flow in Sandstone at Elevated Pressure," *SPE Reser. Engr.*, (Aug. 1991), 185-192.
35. Persoff, P., et al.: "Aqueous Foams for Control of Gas Migration and Water Coning in Aquifer Gas Storage," Proc. Intl. Gas Res. Conf., Tokyo, Nov. 6-9, 1989.
36. Persoff, P.: personal communication.
37. Liave, F. M., et al.: "Foams as Mobility Control Agents for Oil Recovery by Gas Displacement," SPE/DOE 20245, presented at 1990 SPE/DOE Symp., on EOR, Tulsa, Apr. 22-25.
38. Osterloh, W. T., and Jante, M. J., Jr.: "Effects of Gas and Liquid Velocity on Steady-State Foam Flow at High Temperature," SPE 24179, presented at 1992 SPE/DOE Symp. on EOR, Tulsa, Apr. 22-24.
39. Raza, S. H.: "Foam in Porous Media: Characteristics and Potential Applications," *SPE J.* (Dec. 1970), 328-336.
40. Baghdikian, S. Y., and Handy, L. L.: "Transient Behavior of Simultaneous Flow of Gas and Surfactant Solution in Consolidated Porous Media," in *Modifications of Chemical and Physical Factors in Steamflood to Increase Heavy Oil Recovery* (Y. C. Yortsos, ed.), DOE report DOE/BC/14126, 1990.
41. Chou, S. I.: "Conditions for Generating Foam in Porous Media," SPE 22628, presented at 1991 SPE Ann. Mtg., Dallas, Oct. 6-9.
42. Leverett, M. C.: "Capillary Behavior in Porous Solids," *Trans. A.I.M.E.* (1941), 152-169.
43. Weast, R. C., ed.: *CRC Handbook of Chemistry and Physics,* CRC Press Inc., Boca Raton, Florida, 1981.
44. Yokoyama, Y., and Lake, L. W.: "The Effects of Capillary Pressure on Immiscible Displacements in Stratified Porous Media," SPE 10109, presented at 1981 SPE Ann. Mtg., San Antonio, Oct. 5-7.
45. Chen, H.-L., et al.: "Experimental Studies of Capillary Pressure Effects of Foams in Porous Media," SPE 20069, presented at 1990 SPE Calif. Regional Mtg., Ventura, Apr. 4-6.
46. Patzek, T. W., and Koinis, M. T.: "Kern River Steam-Foam Pilots," *J. Petr. Technol.* (Apr. 1990), 496-503.
47. Rossen, W. R., and Gauglitz, P. A.: "Percolation Theory of Mobilization of Foams in Porous Media," *AIChE J.* **36**, 1176 (1990).
48. Rossen, W. R.: "Theory of Mobilization Pressure Gradient of Flowing Foams in Porous Media: I. Incompressible Foam," *J. Colloid Interface Sci.* **136**, 1-16 (1990).
49. Rossen, W. R.: "Theory of Mobilization Pressure Gradient of Flowing Foams in Porous Media: II. Effect of Compressibility," *J. Colloid Interface Sci.* **136**, 17-37 (1990).
50. Rossen, W. R.: "Theory of Mobilization Pressure Gradient of Flowing Foams in Porous Media: III. Asymmetric Lamella Shapes," *J. Colloid Interface Sci.* **136**, 38-53 (1990).
51. Rossen, W. R.: "Minimum Pressure Gradient for Foam Flow in Porous Media: Effect of Interactions with Stationary Lamellae," *J. Colloid Interface Sci.*, **139**, 457-68 (1990).
52. Melrose, J. C.: "Valid Capillary Pressure Data at Low Wetting-Phase Saturations," *SPE Reser. Eng.* (Feb. 1990), 95-99.
53. Buckley, S. E., and Leverett, M. C.: "Mechanism of Fluid Displacement in Sands," *Trans. AIME* **146** (1941), 107-116.
54. Welge, H. J.: "A simplified Method for Computing Oil Recovery by Gas or Water Drive," *Trans. AIME*, **195** (1952), 91-98.
55. Helfferich, F. G., and Klein, G.: *Multicomponent Chromatography*, Marcel Dekker, New York, 1970.
56. Helfferich, F. G.: "Theory of Multicomponent, Multiphase Displacement in Porous Media," *SPE J.* (Feb. 1981), 51-62.
57. Pope, G. A.: "The Application of Fractional Flow Theory to Enhanced Oil Recovery," *SPE J.* (June 1980), 191-205.
58. Lake, L.: *Enhanced Oil Recovery*, Prentice Hall, Englewood Cliffs, NJ, 1989.
59. Walsh, M. P., and Lake, L. W.: "Applying Fractional Flow Theory to Solvent Flooding and Chase Fluid," *J. Petr. Sci. Engr.* **2** (1989), 281-303.
60. Fayers, F. J., and Perrine, R. L.: "Mathematical Description of Detergent Flooding in Oil Reservoirs," *Petr. Trans. AIME* **216** (1959), 277-283.
61. Wellington, S. L., and Vinegar, H. J.: "X-Ray Computerized Tomography," *J. Petr. Technol.* (Aug. 1987), 885-898.
62. M. I. Kuhlman, et al.: "Carbon Dioxide Foam With Surfactants Used Below Their Critical Micelle Concentrations," SPE 20192, presented at 1990 SPE/DOE Symp. on EOR, Tulsa, Apr. 22-25.
63. Yang, S. H., and Reed, R. L.: "Mobility Control Using CO_2 Foams," SPE 19689, presented at 1989 SPE Ann. Mtg., San Antonio.
64. Holm. L. W.: "Foam Injection Test in the Siggins Field, Illinois," *J Petr. Technol.* (Dec. 1970), 1499-1506.
65. Holm, L. W., and Garrison, W. H.: "CO_2 Diversion With Foam in an Immiscible CO_2 Field Project," *SPE Reser. Engr.* (Feb. 1988), 112-118.

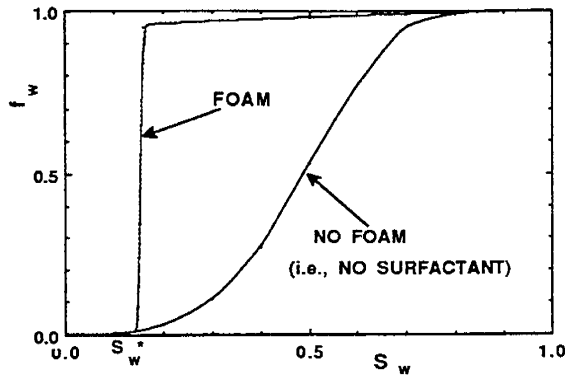

Fig. 1. Schematic fractional flow curves.

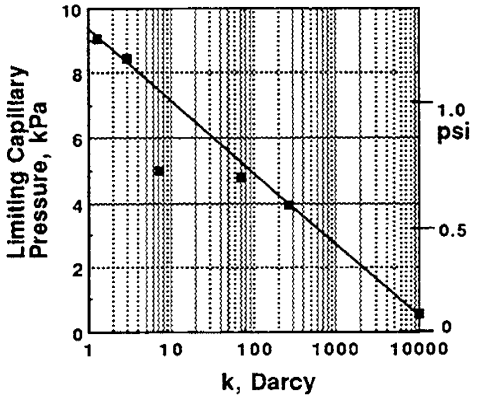

Fig. 2. Limiting capillary pressure vs. permeability, after Ref. (28).

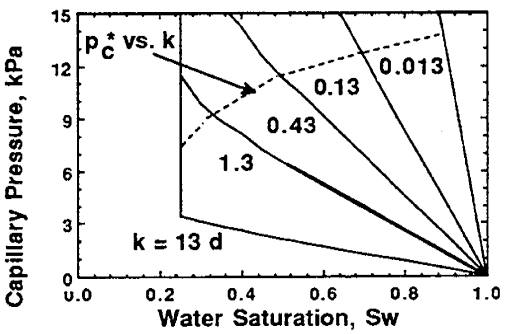

Fig. 3. Capillary-pressure curves for Boise Sandstone of different k, extrapolated from data supplied by Persoff for k = 1.3 d.

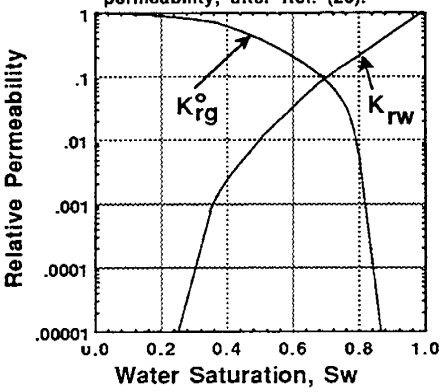

Fig. 4. Foam-free relative permeabilities of 1.3 d Boise Sandstone, after Ref. (34).

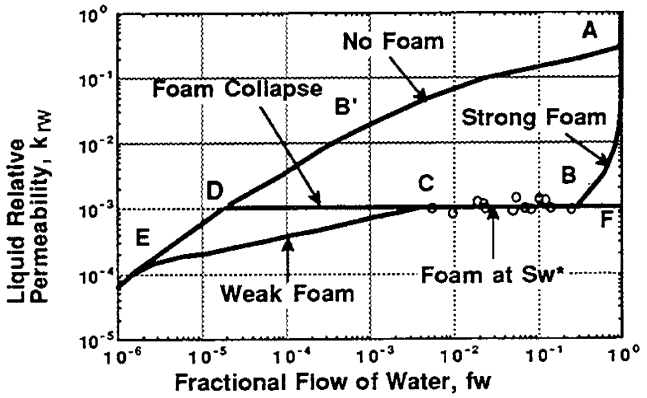

Fig. 5. Plot of krw vs. fw based on data of Persoff et al. (Refs. (34), (35)) for 1.3 d Boise Sandstone.

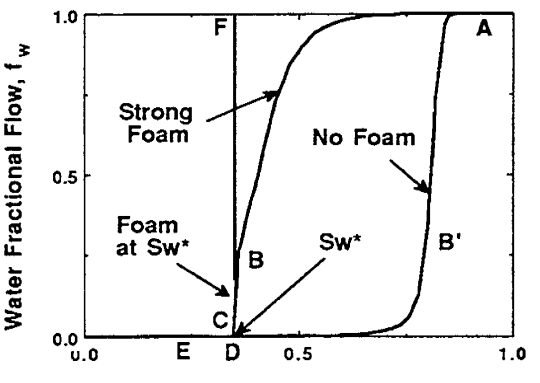

Fig. 6. Fractional-flow curves based on data of Persoff et al. (Refs. (34), (35)) for 1.3 d Boise Sandstone.

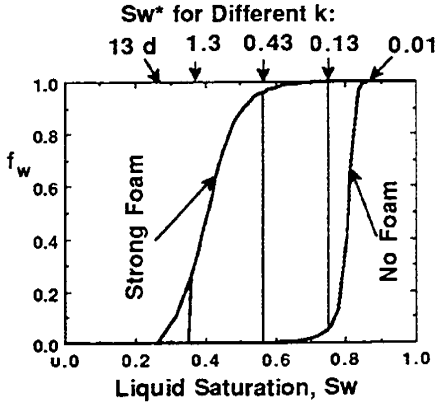

Fig. 7. Fractional-flow curves as a function of permeability.

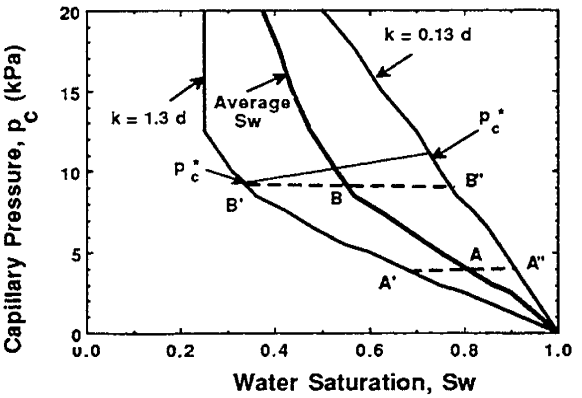

Fig. 8. Capillary-pressure curves for two layers in capillary equilibrium.

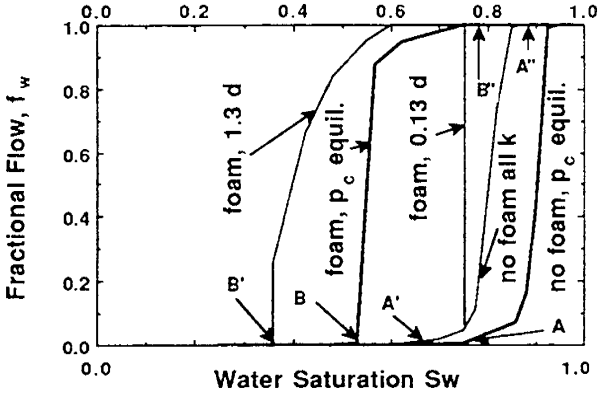

Fig. 9. Fractional-flow curves for two layers in capillary equilibrium.

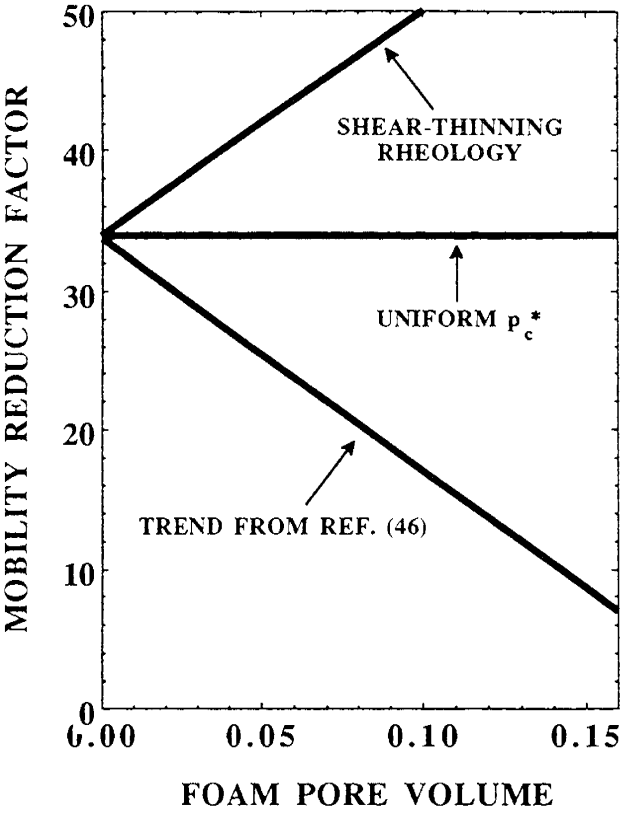

Figure 10. Foam Mobility in Steady, Radial Flow.

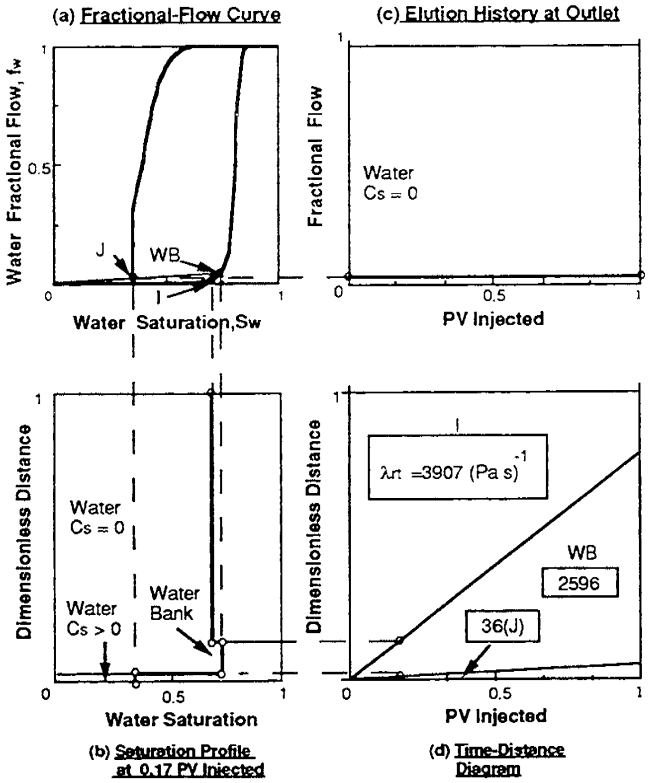

Fig. 11. Foam follows water and gas with the same fw = 0.02, k = 1.3 d.

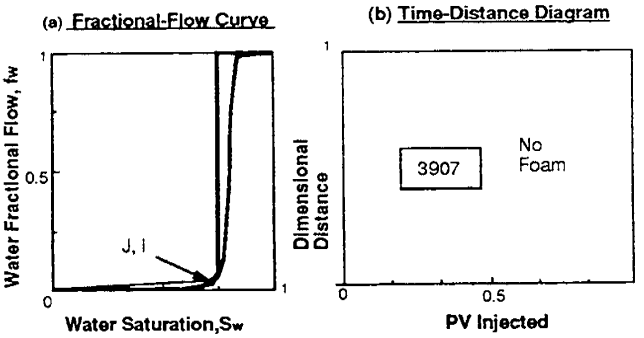

Fig. 12. Foam follows water and gas with the same fw = 0.02, k = 0.13 d.

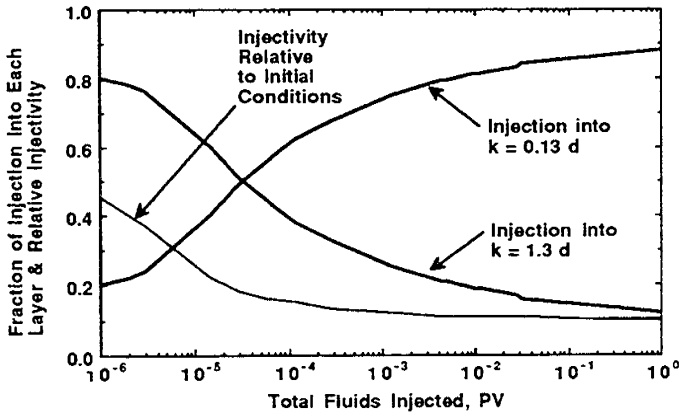

Fig. 13. Foam follows water and gas with the same fw = 0.02 in two isolated cylindrical layers.

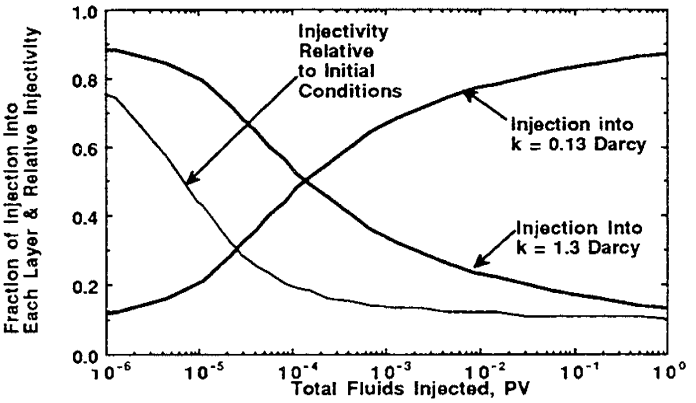

Fig. 14. Foam follows water and gas with the same fw = 0.02, in two isolated cylindrical layers, with retarded foam propagation.

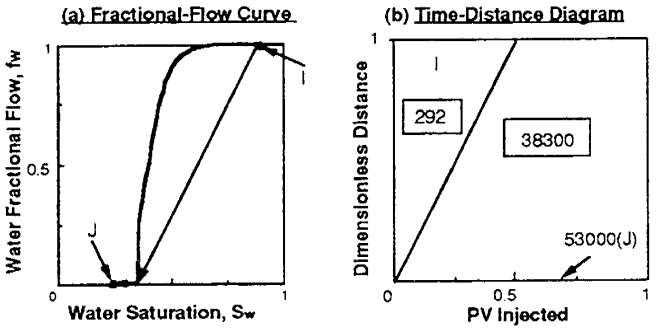

Fig. 15. Gas follows surfactant solution, k = 1.3 d.

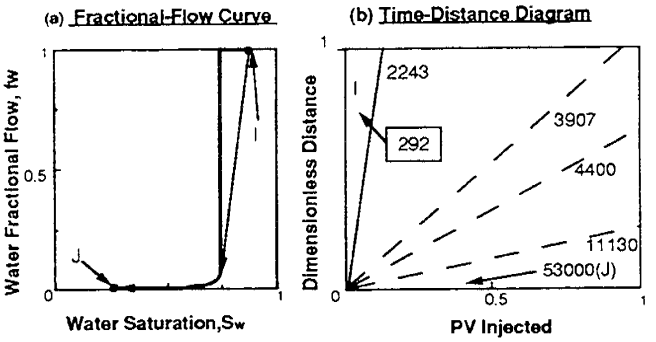

Fig. 16. Gas follows surfactant solution, k = 0.13 d.

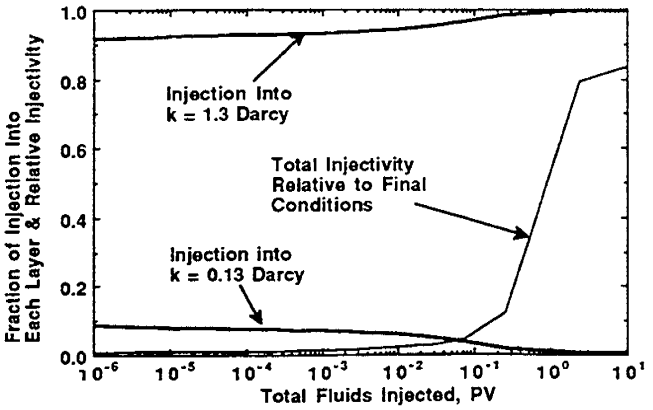

Fig. 17. Gas follows surfactant solution in two isolated cylindrical layers.

No. FS9

DOE/NIPER

A Comprehensive Description of Transient Foam Flow in Porous Media

by A. R. Kovscek and C. J. Radke, University of California at Berkeley, Berkeley, California

Author(s) are solely responsible for copyright and contents.

This paper was prepared for presentation at the DOE/NIPER, Symposium on Field Application of Foams for Oil Production held in Bakersfield, California, February 11-12, 1993.

This paper was selected for presentation by a Program Committee following review of information contained in an abstract submitted by the author(s). Contents of the paper, as presented, have not been reviewed and are subject to correction by the author(s). The material, as presented, does not necessarily reflect any position of the U.S. Department of Energy or the National Institute for Petroleum and Energy Research.

Abstract

Efficient application of foam as a mobility-control agent for enhanced oil recovery requires a numerical model that can describe and predict its flow through porous media. Further, quantitative information on foam-flow behavior at reservoir flow rates and pressures is required for accurate field-scale modeling.

An experimental and mechanistic-modeling study is reported for the transient flow of foam through 1.3 μm^2 (1.3 D) Boise sandstone at backpressures in excess of 5 MPa (700 psi). Total superficial velocities range from as little as 0.42 to 2.20 m/day (1.4 ft/day to 7 ft/day). Sequential pressure taps and gamma-ray densitometry measure flow resistance and in situ liquid saturations, respectively. Thus, we generate experimental pressure and saturation profiles in both the transient and steady states.

A mechanistic foam simulator is created by incorporating a foam-bubble population balance[1] with the traditional reservoir simulation equations. Since foam mobility depends heavily upon its texture[2,3], the population balance is both useful and necessary as the role of foam texture must be incorporated into any model which seeks accurate prediction of flow properties. Our model utilizes saturation-dependent kinetic expressions for lamellae generation and coalescence and also a term for trapping of lamellae.

We find good quantitative agreement between experiment and theory in both the transient and steady states.

References and illustrations at end of paper.

Introduction

Foam is an excellent fluid for achieving mobility control of gases in porous media. Further, foam is relatively cost effective because it is mainly gas with stabilization of the gas/liquid interface provided by a relatively low concentration of surfactant (of order 1 wt%) within the aqueous phase. Since the gaseous portion of foam is dispersed, gas-phase flow mobility is greatly reduced and hence gravity override and viscous fingering through high-permeability streaks may be negated. However, practical implementation of foams for mobility control in enhanced oil recovery (EOR) processes has been hindered because a general understanding and a predictive model of foam flow does not exist.

Most previous studies were Eddisionian and focused upon the steady state. Although transient flow (i.e., displacement) is the most relevant to EOR, a reliable experimental data set that includes transient pressure and in-situ saturation profiles (along the length of a core) does not exist for foam flow. The most notable attempts at modeling foam flow have focused either on predicting transient flow[4] or on predicting steady state results[3,5], but not both. Additionally, the transient work of Friedmann et al[4] was for gas frontal advance rates between roughly 10 and 1000 m/day.

In recognition of the above issues, we undertook a simultaneous experimental and simulation study of transient foam displacement. We track experimentally the propagation of foam fronts within Boise sandstone at low displacement rates. Total superficial velocities in the transient mode are restricted to a maximum of 0.5 m/day (1.6 ft/day). Under steady state conditions, the liquid flow rate is varied while holding the gas flow rate constant (and vice versa) and measuring the resulting pressure drop behavior. Finally we model these results via a new population-balance simulator.

The purpose of this paper is to describe an easily implementable mechanistic simulator for foam displacement in porous media, to verify the theoretical results by comparison to experiment, and to identify areas of the model which may require further refinement. We concentrate on oil-free systems to avoid confusing foam propagation with foam/oil interaction. Before embarking on this task, it is helpful to describe how foam is configured within the pore space and to understand the pore-level events which alter the size and shape of foam bubbles.

Pore-Level Schematic of Foam Flow

Numerous pore-level phenomena control foam flow. The texture or number density of foam bubbles per unit volume strongly controls the actual flow resistance of foam. Individual foam bubbles encounter drag because of the presence of pore walls and pore constrictions, and because the gas/liquid interfacial area of a flowing foam bubble is constantly being rearranged by viscous and capillary forces[2]. Foam bubbles do not maintain their identity during transport. They are relentlessly destroyed and remade[26] according to the nature of the porous medium. Foam texture arises through a balance between varied and complicated foam generation and destruction mechanisms[6]. Additionally, all foam bubbles present in a porous medium are not flowing. Stationary foam severely reduces the permeability of a porous medium to gas by blocking many of the available flow paths. Dual-gas tracer studies[4,7] have measured the fraction of gas trapped within a foam at steady state to be between 85 and 99%.

Radke and Gillis[7] proposed Fig. 1 as a schematic for the pore-level distribution of foam. In this picture, cross-hatched circles are unconsolidated water-wet sand grains. Wetting fluid is denoted as the dotted phase. Foam bubbles are either unshaded or darkly shaded, depending upon whether they are trapped or flowing. The largest pore channels lie at the top of the figure while the smallest lie at the bottom. This orientation of pore channels is for ease of illustration.

Since there are strong capillary forces, wetting liquid occupies the smallest pore space and clings to the surface of sand grains as wetting films. The aqueous wetting phase maintains continuity throughout the pore structure shown in Fig. 1 so that aqueous-phase relative permeability is unchanged in the presence of foam[8]. Unshaded flowing foam transports as trains of bubbles through the largest and least resistive flow channels. If we adopt a continuum approach and speak of foam as a "phase," flowing foam becomes the least wetting phase in compliance with these strong capillary forces. Because the smallest pore space is occupied solely by aqueous phase and the largest pore space carries flowing foam, foam must trap (dark shading denotes trapped foam) in the intermediate-sized pores.

Foam reduces gas mobility in two manners. First, stationary or trapped foam blocks channels that otherwise carry gas. Second, bubble trains within the flowing fraction contain lamellae that interact with pore walls and thus a greater pressure drop is required to move gas through the porous medium than in the foam-free case. These trains are in a constant state of rearrangement. Bubbles transport a distance, are destroyed, and then reformed. Snap off is one mechanism by which foam is generated[9-11]. Intermittently, liquid fills a pore throat, is displaced by gas invasion, and subsequently a foam bubble is created if the pore throat to body aspect ratio is large enough (Fig. 2). It is also believed that bubble or lamellae division can play a role in generating fine bubbles[6,12]. Foam lamellae primarily break by a "stretching squeezing"[13] mechanism in oil-free porous media. When a lamella flowing from a pore throat into a body is stretched too rapidly it becomes unstable to infinitesimal disturbances and ruptures (Fig. 3). Because high capillary pressures thin lamellae by suction at Plateau borders, flowing lamellae are especially susceptible to rupture at low wetting saturations. More thorough reviews of foam generation, coalescence, and transport on the pore level are given in references 6 and 14.

We break the remainder of this paper into three sections. We begin by discussing our experimental apparatus, procedure, and experimental results. We then lay out a mechanistic but easily implemented one-dimensional population balance method that accounts for the propagation of foam and display both transient and steady state model results for a few test cases. Because foam in porous media displays flow properties very different from its individual constituent phases, it is mandatory that we use a method that incorporates the effect of foam texture on flow resistance. Next, we discuss the extent to which the theoretical predictions match experiment. Conclusions round out the paper.

Experiment

Apparatus

Persoff et al[15] originally constructed the apparatus (displayed schematically in Fig. 4) used for the experimental foam floods. The centerpiece of the apparatus is a vertically mounted, 60-cm long, 5.1-cm diameter, 1.3-μm^2 (1.3-D) Boise sandstone core with a porosity of 0.25. Thus, one pore volume corresponds to 300 cm^3. The core is epoxy-mounted into a 316 stainless steel sleeve designed to withstand pressures up to 20 MPa (3000 psi). A Mity-mite dome-loaded backpressure regulator (Grove Valve and Regulator Company, Emeryville, CA) maintains core backpressure.

Nitrogen gas and foamer solution are injected at the top of the core to prevent unwanted buoyancy driven gas flow. The original fluid injection system was replaced by a Brooks 5850C mass flow controller (Emerson Electric, Hatfield, PA) for nitrogen flow and an ISCO 500D syringe pump (Instrumentation Specialties Company, Lincoln, NE) for metering liquid flow. At 5 MPa (700 psi) backpressure, gas Darcy velocities between 0.30 and 2.1 m/day (1 to 7 ft/day) are now possible while liquid velocities as low as 0.009 m/day (0.03 ft/day) are employed.

Liquid saturation profiles are measured by scanning gamma-ray densitometry utilizing a 47 mCi Cs-137 source collimated to a 0.32 cm (1/8 in.) diameter beam. Gamma rays are detected by a Harshaw 5.1 cm (2 in.) NaI(Tl) scintillation counter and an NB-15X plug-on preamplifier (Harshaw Chemical Co., Solon, OH). Counting is performed by a Norland IT-5300 multichannel analyzer (Norland, Corp., Ft. Atkinson, WI) equipped with a digital gain stabilizer to compensate for drift. After a simple calibration where the intensity (counts/s falling within a 662 keV peak) of the gamma-ray beam is measured at preselected points along the core at 0% (I_d) and 100% liquid saturation (I_w), the liquid content at any previously calibrated point in the core is found from the Beer-Lambert law, $S_w = [\ln(I_d/I)]/[\ln(I_d - I_w)]$, where I is the intensity measured at any unknown saturation.

Scanning of the sandstone for liquid saturation profiles is achieved by mounting the gamma-ray source and detector on a translating carriage controlled by a Slow-syn motor (Superior Electric Company, Bristol, CT) and Model DPF107 motor controller (Anaheim Automation, Anaheim, CA). Since gamma rays are a product of radioactive decay, the square root of the number of events counted equals the standard deviation of the number of events counted. More accurate determinations of liquid saturation are found by using longer counting periods, however overly long counting periods reduce the precision of individual transient measurements and overall saturation profiles. The low frontal advance rates we use during transient foam displacements (a maximum of 0.5 cm/day) make it a relatively easy task to constrain the error in individual transient saturation measurements to about 4 saturation units with no loss in resolution of the advancing foam fronts. The error in steady state saturation measurements is less than 1 saturation unit.

Pressure taps are located at the core inlet, outlet, and at 10 cm (4 in.) intervals along the core, and are sealed with Swagelok O-seal (Crawford Fitting Company, Solon, Ohio) fittings. Pressure is measured using a single Paroscientific 43 KT piezoelectric quartz-crystal pressure transducer (Paroscientific, Redmond, WA). A Scannivalve 12L7 multiplexing valve (Scannivalve, San Diego, CA) allows all pressure taps to be visited sequentially and rapidly. A scan of all pressure taps is instantaneous (approximately 30 seconds) in comparison to the frontal advance rate. An HP-9000 (Hewlett Packard Co., Mountain View ,CA) controls the apparatus and records all data.

Procedure

The foamer solution is a saline solution containing 0.83 wt% NaCl (J. T. Baker, reagent grade) with 0.83 wt% active C_{14-16} α-olefin sulfonate surfactant (Bioterg AS-40, Stepan). Water is provided by a Barnstead Fi Streem II glass still (Barnstead, Thermolyne Corp., Dubuque, Iowa). The solution surface tension is 33 mN/m measured by the Wilhelmy plate method, and has a viscosity of 1 mPa·s. Bottled nitrogen is the gas source.

The core is first flushed with copious amounts (20-40 PV) of 0.83 wt% brine at 7 MPa backpressure. Periodically, the backpressure is released and then reapplied. This treatment removes virtually all gas from the core. Because trace amounts of isopropanol or methanol can have a deleterious effect on foam production, no alcohols are used as foam breakers or as cleaning solvents on any portion of the experimental apparatus. Following the surfactant-free preflush, at least another 5 PV of foamer solution is injected to satisfy rock adsorption of surfactant. Elemental analysis of the core effluent stream for sulfur reveals that after 2 PV of foamer solution is injected, the concentration of surfactant in the inlet and effluent streams is equal.

In all runs, liquid and gas are injected directly at a constant volumetric rate and a constant mass flow rate respectively. We do not foam the gas/liquid mixture before injection. The initial injection rates are not altered until a steady state pressure drop is achieved. The progress of foam propagation through the core is tracked by frequent pressure and saturation sweeps. After steady state is reached the liquid and gas rates are varied independently to reach a series of new steady states.

Results

We report first on the transient behavior when nitrogen and foamer solution are coinjected at constant rate. In the transient mode, we wish to determine the length of time required for the system to come to steady state and to verify the existence and track the movement of foam displacement fronts within the core. Then we examine the steady state behavior as gas or liquid solution flow rate is changed in a stepwise fashion. In the steady-state mode, our objective is to determine the effect of varying fluid flow rates on pressure drop (i.e., gas mobility) and to compare with previously published results[3,15].

Figures 5 and 6 give the transient saturation and pressure profiles, respectively. Experimental data points at each time level are connected by solid lines. Elapsed time is given nondimensionally in pore volumes (PV) which is the ratio of the total volumetric flow rate (at exit pressure) multiplied by elapsed time divided by the void volume of the core. Darcy velocities relative to the exit pressure are 0.43 m/day (1.4 ft/day) and 0.058 m/day (0.19 ft/day).

Steep saturation fronts are measured, whereby aqueous saturation upstream of the front is approximately 30%, about 5 units above connate, and downstream it is 100%. From the saturation profiles it appears that foam moves through the rock in a piston-like displacement. After the front passes a location, saturation changes very little. We find this rapid desaturation in all experiments. It is evident that a very efficient displacement of the aqueous phase is occurring. Even though nitrogen and surfactant solution are injected separately, rapid foam generation and liquid desaturation still occurs very near the core inlet. Gas breakthrough is at roughly 1.0 pv and little or no change occurs in the saturation profile after breakthrough. In general, we find that desaturation is complete 1 to 2 PV for all cases.

The pressure behavior of Fig. 6 confirms the existence of a strong foam piston moving through the core. Large pressure gradients are witnessed where aqueous phase saturation is low and vice versa. Further, Fig. 4 reveals that pressure profiles cease to change in roughly 3 PV also. The large pressure gradients with foam displayed in Fig. 4 are partly a result of the mode of fluid injection. If a surfactant alternating gas (SAG) process had been used, the measured gradients would be lower. Because foam is a dispersed gaseous phase separated by thin liquid films, forcing the two fluids to flow at a constant rate raises the pressure drop substantially.

The steady state results from varying the gas and liquid flow rates independently are shown in Figs. 7 and 8. For generality, we give pressure gradient information (i.e., the ratio of pressure drop to length) rather than core pressure drops. Figure 7 reports the pressure gradient behavior when gas injection velocity is held constant while varying liquid flow rate, whereas Fig. 8 shows the results from holding liquid injection rate constant but varying gas flow rates. In Fig. 7 the pressure gradient increases linearly from roughly 0.40 MPa/m to 3.6 MPa/m (18 to 160 psi/ft) as liquid velocity is varied between between 0.012 and 0.058 m/day (0.04 and 0.19 ft/day). For comparison, the pressure drop of water flowing at 0.46 m/day in 1.3 μm^2 (1.3 D) Boise sandstone is 4.2 kPa/m (0.18 psi/ft). Figure 8 illustrates that the pressure gradient remains fixed at approximately 1.4 MPa/m (63 psi/ft) while the gas velocity is varied between 0.43 and 1.90 m/day (1.4 and 6.2 ft/day). Again, the velocities reported are Darcy velocities relative to the exit pressure.

These steady state trends compare favorably with those previously published[3,15,16]. Namely, liquid saturations for steady state foam flow are a few units above connate and the pressure gradient is independent of gas velocity. We also reconfirm that steady state saturation for strong foam flow is a few units above connate (around 30% in this instance) and sensibly independent of both liquid and gas velocity. Persoff et al[15] also found that steady state pressure gradient increased linearly with liquid velocity.

A Foam Displacement Model

Our goal, in this section, is to outline a population-balance foam displacement model which is easy to implement, fits simply into the framework of current reservoir simulators, employs a minimum of parameters, but embodies pore-level events, and reproduces saturation and pressure drop versus flow rate results in both the transient and steady states. We begin first with the requisite material balance equations and then turn to incorporating foam into a typical reservoir simulation framework. We write equations for foam coalescence, generation, and lamellae flow resistance. Finally, we show selected one-dimensional numerical results and then compare results to the experimental data.

Conservation Equations

The mass balance equations for the gas and aqueous phases are written in standard reservoir simulator form[17,18]

$$\frac{\partial(\phi\rho_g S_g)}{\partial t} + \frac{\partial(\rho_g u_g)}{\partial x} = 0 , \qquad (1)$$

and

$$\frac{\partial(\phi\rho_w S_w)}{\partial t} + \frac{\partial(\rho_w u_w)}{\partial x} = 0 . \qquad (2)$$

In Eqns. (1) and (2), ϕ is the porosity of the porous medium, the subscripts g and w refer to the gaseous

and aqueous phases respectively, S_i is the saturation of each phase i, ρ_i is the density, and u_i the Darcy velocity of each phase.

The effective resistance of the gas phase is a strong function of foam texture[3,5]. Therefore, mechanistic prediction of foam flow in porous media is impossible without a conservation equation accounting for the evolution of foam texture[1]. Rates of accumulation, trapping, convection, generation, and coalescence of foam bubbles must be incorporated into a separate balance, analogous to inclusion of polymer into a reservoir simulator. Following Patzek[1], (c.f. also, 4 and 5) we write a transient one-dimensional population balance on the average flowing bubble size

$$\frac{\partial[\phi(S_f n_f + S_t n_t)]}{\partial t} + \frac{\partial(u_f n_f)}{\partial x} = \phi\, S_g(r_g - r_c), \qquad (3)$$

where the subscripts f and t refer to flowing and trapped foam respectively, n_f is the number of bubbles per unit volume of the flowing foam (i.e., the texture), and the total gas saturation is given by $S_g = S_f + S_t$. The first term of the time derivative is the rate of accumulation of flowing foam while the second is the rate of foam trapping. The spatial term tracks the convection of foam bubbles. On the right side of Eqn. (3), we express generation and coalescence rates, r_g and r_c, on per volume of gas basis. Hence, they are multiplied by porosity and gas-phase saturation. We turn next to constructing rate equations for the generation and coalescence of foam.

Coalescence Rate

A pore-level rate expression for foam coalescence is easy to write. Figure 3 illustrates that foam lamellae or bubbles are destroyed in proportion to their flux (i.e., $v_f n_f$) into termination sites[6]. Hence, we write

$$r_c = k_{-1}(S_w)\, v_f n_f\,, \qquad (4)$$

where $k_{-1}(S_w)$ is a coalescence rate constant which varies with local aqueous-phase saturation, S_w, and correspondingly capillary pressure. Additionally, v_f is the local interstitial velocity ($v_f = u_f/\phi S_f$). Eqn. (4) teaches that higher interstitial gas velocities lead to increased foam coalescence.

The saturation dependence of $k_{-1}(S_w)$ is quite dramatic. Khatib et al[19] have shown that for strongly foaming solutions $k_{-1}(S_w)$ is small for high aqueous phase saturations but rises steeply as S_w decreases. Since rapidly stretched lamellae become very thin, they are fragile and vulnerable to breakage. Sufficient time at low aqueous phase saturations does not exist for surfactant solution to flow into a rapidly stretched lamella thereby thickening and stabilizing it[13]. In fact, the study of single foam films has shown that a single limiting capillary pressure (P_c^*) exists for film breakage[20,21] depending strongly upon surfactant formulation and concentration. When P_c^* is met or exceeded foam films spontaneously rupture. Thus, an aqueous phase saturation near or below that corresponding to P_c^* leads to a rate of foam coalescence approaching infinity[19]. Cognizant of these facts we write

$$k_{-1}(S_w) = k_{-1}^{o}\frac{(1 - S_w)}{(S_w - S_w^*)}\,, \qquad (5)$$

where S_w^* is the saturation corresponding to P_c^*. Figure 9 displays schematically the coalescence rate versus saturation dependence.

Generation Rate

In writing a rate expression for generation by capillary snap-off we must point out that the necessary conditions are the accumulation of liquid at a pore throat and a disturbance in the gas liquid interface sufficient to cause breakup and rearrangement of the invading gas thread. Figure 2 illustrates the pore-level events leading to the formation of a foam lamella by snap-off. The rate of liquid accumulation is hence controlled by the local flow of foamer solution, v_w, into the pore throat, whereas the size of the bubble generated per snap-off event depends upon v_f. These conditions translate to dependence of foam generation by snap-off in both liquid and gas velocity. Thus, we simply write

$$r_g = k_1 v_f^a v_w^b\,, \qquad (6)$$

where a and b are power indices. The generation rate constant, k_1, reflects the number of foam germination sites. As long as the concentration of surfactant in the aqueous phase remains constant and the aqueous phase saturation remains above S_w^*, we assume that k_1 has little saturation dependence. Otherwise, when S_w falls below S_w^* sufficient liquid does not accumulate at pore throats for snap-off and the generation rate falls to zero.

Some researchers have found a velocity dependence for the onset of foam generation[4,9]. For foam generation at steady liquid saturation, Friedmann et al[4] report critical velocities of several hundred meters per day in some cases. They generate foam in a core where rock adsorption of surfactant is apparently satisfied, but the initial S_w is variable and low. Recent experiments in glass beadpacks, Boise,

and Berea sandstone, however, do not confirm the existence of a critical gas velocity or pressure drop which must be exceeded for successful foam generation[15,22-25] when the porous medium is presaturated with surfactant solution and foam generation occurs in a displacement process. We choose an initial S_w of 100 % and do not write a velocity criterion for the onset of generation.

Figure 9 displays the dependence of both coalescence and generation on S_w. Intersection of the two curves is set by the limiting capillary pressure, $P_c^*(S_w^*)$, which in turn sets the steady state saturation. The intersection is a stable point. If the system is perturbed away from this point, it naturally returns. Because we have explicitly written individual equations for foam generation and coalescence, this model reflects the relentless process of foam destruction and rebirth occurring within a porous medium[26]. To mimic the steady state flow rate pressure drop trends of Figs. 7 and 8, foam texture readjusts every time a change in either gas or liquid flow occurs.

As mentioned earlier, bubble division is another mechanism which creates flowing foam. The rate of bubble or lamellae division is proportional to the flux of lamellae into division sites. Thus, the rate of foam generation by division is similar in form to Eqn. (4). The difference between the coalescence rate and the generation rate by division is the value of the rate constant. However, both rate constants share the property of being small when S_w is high. More division sites become available as S_w drops increasing the likelihood of division. If significant bubble division does occur, an apparent lower coalescence rate is realized. It is difficult to separate division and coalescence. We do not attempt to do so here[3].

Effective Viscosity

Application of Eqns. (5) and (6) demands knowledge of the velocities of the gas and aqueous phases. Since foam behaves effectively as a nonwetting phase, Darcy's law,

$$u_f = \frac{K\, k_{rf}}{\mu_f}\left(\frac{-\partial p_g}{\partial x}\right), \qquad (7)$$

is employed here to describe foam flow behavior. In Eqn. (7), u_f, K, k_{rf}, μ_f, and p_g are the gas superficial velocity, absolute permeability, gas-phase relative permeability, foam effective viscosity, and gas-phase pressure, respectively. Water-phase Darcy velocity is similarly written. Darcy's law is not strictly obeyed in Eqn. (7) because foam is in general nonNewtonian.

The effective viscosity of flowing foam in porous media is generally an order of magnitude or two larger than gas viscosity alone. Experimentally, μ_f is calculated from Eqn. (7). Modeling of foam flow, though, requires a functional form. Two properties are generally included in all models of μ_f. First, the shear thinning or velocity dependence of foam is acknowledged. The notion that effective viscosity is a function of the foam texture, or number of lamellae per unit volume, is also included. Finer textured foams compel a larger flow resistance.

Friedmann et al[4] introduced an expression for effective viscosity that directly incorporates foam texture and velocity dependence. We adopt a slightly modified version

$$\mu_f = \mu_g + \frac{\alpha\, n_f}{v_f^c}, \qquad (8)$$

where α is a constant of proportionality. According to Eqn. (8) foam viscosity increases linearly with foam texture but decreases with increasing interstitial velocity. Friedmann et al[4] report an empirical value of 0.29 for the exponent c while the theoretical value is 1/3[2,27].

Trapped Foam

The fraction of foam trapped in a porous medium controls the fraction and rate of foam able to propagate and, along with effective foam viscosity, sets the pressure gradient. The fraction of foam that is trapped, $X_t = S_t/S_g$, is a currently unknown function of pressure gradient, capillary pressure, aqueous phase saturation, and pore geometry. Conversely, the flowing foam fraction is written $X_f = S_f/S_g$. Thus far, trapped gas fraction has only been successfully measured for experimental systems at steady state[4,7]. Percolation models, though, hold much promise for determining the functional dependence of X_f[28-33]. We write the trapped fraction as a function of n_f, which in turn is set by S_w and v_f,

$$X_f = 1 - (1 - X_{f,eq})\left(\frac{A_1 A_2 n_f}{1 + A_1 n_f}\right), \qquad (9)$$

where A_1 and A_2 are bubble trapping parameters and $X_{f,eq}$ is the flowing foam fraction at steady state exclusive of inlet or end effects. Equation (9) makes X_f equal to 1 when no flowing foam is present and allows X_f to decline smoothly to its equilibrium value as foam texture becomes finer. Both Eqns. (8) and (9) embody the experimental fact that finer textured foams lead to larger flow resistances. A reduced flowing foam fraction increases flow resistance by reducing gas-phase relative permeability.

Relative Permeabilities

For simplicity, a standard Corey exponent model is adopted for relative permeability functions. Water-phase relative permeability is unaffected by the presence of foam[8], hence

$$k_{rw} = k_{rw}^{o} \bar{S}_w^{g} , \tag{10a}$$

where

$$\bar{S}_{wd} = \frac{(S_w - S_{wc})}{(1 - S_{wc})} , \tag{10b}$$

and S_{WC} is the connate aqueous phase saturation. A major portion of the gas in a foam flood is present as trapped foam and blocks gas flow. Thus, gas-phase relative permeability must be modified. The saturation of gas actually flowing, S_f, is used to evaluate relative permeability rather than the entire gas-phase saturation

$$k_{rf} = k_{rg}^{o}\left[X_f(1 - \bar{S}_w)\right]^{h} . \tag{11}$$

Thus, gas-phase relative permeability is a function of foam texture and is much smaller than the case of a free gas propagating through a porous medium at the same wetting liquid saturation.

Assumptions and parameter fitting

It is assumed that surfactant is present in equal concentration throughout the aqueous phase and that rock adsorption has been satisfied. Also assumed is that the size of trapped and flowing foam bubbles are approximately the same. This is a good assumption under conditions of coinjection of surfactant solution and gas. Foam undergoes relentless generation and coalescence. The flowing portion is in constant contact with the trapped fraction. The trapped fraction is thus dynamic. That is, some portion of foam bubbles in the trapped fraction constantly mobilize, but they are replenished by a part of the flowing foam fraction trapping. As a result, trapped and flowing foam have about the same texture and the temporal derivative in Eqn. (3) reduces to $\partial[\phi\,(n_f\,S_g)]/\partial t$. The aqueous phase is taken as incompressible, and since the gas phase is nitrogen, the ideal gas law is assumed[34]. Gravitational and capillary effects are neglected.

The usual parameters required for modeling continuum two-phase flow are absolute rock permeability and porosity, exponents and endpoints for relative permeability, and phase viscosities. We fit Eqns. (10) and (11) to the relative permeabilities reported by Persoff et al[15]. Our implementation of the population balance requires specification of generation and coalescence rate constants, the saturation (S_w^*) corresponding to P_c^*, the exponents a and b for the generation rate expression, the proportionality constant and velocity exponent for effective viscosity, and the parameters for the flowing foam fraction relationship. Table 1 lists all constants and parameters used. Table 1 shows that 10 additional parameters are needed for the population balance, whereas undispersed flow already requires 9 parameters.

Parameter values for the population balance portion of the model are determined chiefly by steady state trends. Specifically, steady state saturation, pressure drop profiles, and flowing foam fraction must be matched. Fortunately, this drastically narrows our range of parameter choices. Thus, we first choose S_w^* slightly above connate, 0.26, and $X_{f,eq}$ equal to 0.1 in accordance with previous studies[4,7].

The flow rate exponent for effective viscosity, c in Eqn. (8), is set to 1/3. This is the theoretical gas-velocity dependence[2] applicable at low rates and close to the previously reported empirical value of 0.29[4]. Next, exponents are required for the liquid and gas rates for foam generation in Eqn. (6). When the rate of coalescence (Eqn.(4)) is subtracted from the rate of generation (Eqn. (6)), the result set to zero (i.e., $r_g - r_c = 0$), and Darcy's law (Eqn. (7)) including the effective viscosity function is substituted for phase velocities, the resulting expression reflects steady-state pressure gradients. This equation only applies when bubble generation and coalescence are in equilibrium. To obtain pressure drops independent of gas velocity while liquid velocity is held constant we choose a = 1/3. Likewise, for a linear dependence between liquid velocity and pressure drop at fixed gas velocity choose b = 1.

The ratio k_1/k_{-1} sets the equilibrium bubble density (defined by the equation $r_g - r_c = 0$). We find steady state textures[3] on the order of 10^5 cm^{-3}. Equation (8) combined with the equilibrium texture now sets the value of the steady state pressure drop and consequently α. Finally, the magnitudes of k_1, k_{-1}, A_1, and A_2 are adjusted to confine the region of net texture refinement to be close to the inlet face of the porous medium. Thus, A_1 and A_2 are chosen such that $X_t = (1 - X_f)$ is 75% of its equilibrium value when n_f is 50% of its equilibrium texture. Although there are 10 parameters needed for implementation of the population balance method, steady state trends directly set 6 of them. The only liberty allowed in parameter adjustment lies in specifying the values of k_1 and k_{-1} (but not the ratio of the two) and the trapping parameters A_1 and A_2.

The preceeding procedure illustrates that only one set of transient saturation and pressure profiles along

with the accompanying steady state trends need to be determined. This is easily accomplished within one experimental run.

Equations (1) through (11) are incorporated in a standard finite difference implicit pressure explicit saturation (IMPES) simulator with standard upstream weighting of the phase mobilities and solved. The three primitive unknowns are pressure, gas-phase saturation, and bubble density. All calculations are made on a DEC 5900. Further numerical details are available elsewhere[24].

Comparison of Theory and Experiment

Figures 5 and 6 contain the model results in addition to the experimental saturation and pressure profiles. Theoretical results are presented as dashed lines. The theoretical saturation profiles track the experimental results very well. Because the dispersing action of capillary pressure has not been included in the model formulation, model fronts remain steep and sharp. The model further predicts that S_w is high at the core inlet. Aqueous saturation is around 76% at x/L equal to zero, but drops rapidly to approximately 30% by x/L equal to 0.2. Since no foam is injected, n_f is essentially zero at the inlet, effective viscosity is equal to gas viscosity, and consequently S_w is high. Minssieux[35] detected such a region of high S_w near the inlet of a sandpack. A region of net foam generation exists near the inlet by implication. Foam texture increases rapidly, but the region where rates of generation and coalescence are out of balance is finite. Additionally, the fraction of foam trapped is zero at the inlet and grows to $1-X_{f,eq}$. Unfortunately due to equipment limitations, few experimental data are available in this region.

The region of net foam generation is also witnessed in the transient pressure profiles of Fig. 6. Both the experimental and model results (dashed lines) show that pressure gradients near the inlet are not steep indicating that flow resistance is small. Steep gradients are found downstream of the inlet region. Recall that large gas flow resistance arises from a viscous resistance contributed by flowing lamellae and also from resistance contributed by stationary foam through reduction in relative permeability. Although it is not possible to decouple these two effects[36], both are necessary if one wishes to model accurately foam flow. The adjustment of viscous resistance by foam texture is essential if the nonNewtonian behavior of foam is to be mimicked. Further, the viscous contribution alone is not sufficient to create the large overall pressure drops while still maintaining a region of net generation and smaller pressure gradients near the inlet. Hence, we infer experimentally that foam texture must be coarse near the inlet and the fraction of foam flowing there large.

These inferences are born out in Fig. 10 which reports model predicted foam texture as a function of dimensionless distance and time. We cannot compare directly to experiment because no experimental method currently exists to measure bubble density in situ. At all time levels, foam bubbles are coarsely textured near the inlet, but beyond the first fifth of the core, foam texture becomes nearly constant at each time level. Figure 10 also confirms that foam moves through the column in a piston-like fashion consistent with the experimental data in Figs. 5 and 6. Further consideration of these three figures shows that the saturation, pressure, and foam texture fronts track exactly both experimentally and theoretically. High pressure gradients and fine foam textures are seen where liquid saturation is low and vice versa.

We notice one more interesting feature of Fig. 10. At times of 0.62 and 0.80 PV the bubble density downstream of the inlet region exceeds the foam texture at steady state. This effect arises because the compressibility of the gas is included. A foam bubble created upstream finds itself out of equilibrium with the local pressure (that is, smaller or more dense than the local pressure demands) when it transports downstream. Hence, the steady-state texture is overshot somewhat as finely textured flowing foam fills the initially liquid filled regions near the foam front. Coalescence forces coarsen the bubbles over time back to the equilibrium density. At steady state the foam texture decreases away from the inlet region. Essentially, the bubbles expands and hence their number density decreases as they flow downstream into lower pressure areas. No overshoot in bubble texture is found in the calculations when the gas is made incompressible.

The overshoot in bubble density also causes an overshoot in the system pressure drop. Because the foam is finely textured, its flow resistance and hence pressure drop are large. At roughly 1 PV the core pressure drop exceeds the steady state pressure drop by approximately 15 per cent, then declines and undershoots the steady state slightly, and finally reaches the steady state value. Figure 11 illustrates this effect fully by contrasting the experimental system pressure drop as a function of throughput with the theoretical. We see that the experiment also overshoots steady state pressure drop. The experimental overshoot occurs about 1 PV later than predicted, though.

This discrepancy is likely a result of assuming that trapped and flowing foam are always in equilibrium. Equation (9) is constructed so that the correct steady state pressure profile is achieved. However, pressure gradient, gas velocity, and pore-geometry are also important for bubble trapping[28-31] during transient foam displacement.

In the steady state we find excellent agreement among experiment and theoretical prediction. Figures 7 and 8 report the model pressure gradient behavior as solid lines. In Fig. 7, the model pressure gradient increases linearly and overlies the experimental points except for the slight depression at roughly 0.028 m/day. The independence of pressure drop is illustrated in Fig. 8. Unfortunately, model prediction of pressure drop (1.6 MPa/cm) is slightly greater than the experimental result (1.4 MPa/cm). This discrepancy is understood by comparing the constant liquid velocity (0.028 m/day) used in Fig. 7 to the results in Fig. 8. The only experimental point which did not fall on the model predicted line lies at 0.028 m/day. The data taken during that portion of the experiment appear to have slightly depressed pressure drops.

The steady state pressure drop trends are a result of the adjustment of foam texture as flow rates change. When gas velocity is varied under constant liquid flow rate conditions, foam texture becomes coarser, viscosity decreases, and constant pressure drop is maintained. When liquid velocity is increased while gas rates are held constant, foam texture increases linearly with v_w and hence viscosity is adjusted so that Newtonian behavior is found. Flow resistance adjusts itself because foam texture must comply with a constant capillary pressure and low aqueous phase saturation.

Conclusions

We have developed a foam displacement model based on the population-balance method that is readily incorporated into current reservoir simulators. The proposed method is not computationally intensive and results are readily obtained using standard numerical methods. Because our formulation is mechanistic, it is general. Thus, extension to CO_2 or steam foams is straightforward. In general, we find good quantitative agreement between experiment and theory in both the transient and steady states.

Direct incorporation of the role of foam texture in our population-balance foam displacement model is the key to its success. Foam texture governs foam flow in porous media. A change in the flow velocity of either wetting liquid or gas must be accomodated by a change in texture and in turn a change in flow resistance.

Specifically, we draw the following conclusions for foam flow in 1.3 μm^2 (1.3 D) Boise sandstone at 5 MPa backpressure and for total superficial velocities between 0.40 and 2.1 m/day:

1. During transient experimental foam flooding of an initially surfactant filled and saturated core, resistance to gas flow builds rapidly in time. Steady state is generally achieved in 3 PV or less.

2. Our proposed population-balance model predicts the location of saturation and pressure fronts accurately. Steady state is predicted to be achieved in about 1.5 PV.

3. In the transient and steady state modes, fine foam textures are predicted to lead to large pressure gradients and low liquid saturations, whereas coarse textures lead to lesser gradients and higher liquid saturations.

4. We reconfirm experimentally that foam pressure gradients are independent of gas velocity, and also that foam pressure gradient increases linearly with liquid velocity. We predict these experimental results exactly with our population-balance model.

5. We find both experimentally and theoretically that a region of net foam generation exists very close to the inlet face of a linear core. Unfoamed surfactant solution and nitrogen are converted rapidly into a finely textured foam in this region.

Nomenclature

A_1,A_2	bubble trapping parameters in Eqn. 9
a,b,c	velocity exponents in foam generation and effective viscosity expressions
g	wetting phase relative permeability exponent
h	nonwetting phase relative permeability exponent
k	rate constant, units depend on rate expression
k_{ri}	relative permeability
I	intensity of gamma-ray beam (counts/sec)
K	permeability (m^2)
n_f	number density of flowing foam (# of bubbles/volume of flowing foam)
p	phase pressure (Pa)
PV	total pore volumes injected
P_c	capillary pressure, p_{nw}-p_w (Pa)
r	foam generation or coalescence rate (#of bubbles/(time)(volume of gas))
S_i	phase saturation
t	time (s)
u	Darcy velocity of phase i (m/s)
v_i	interstitial phase velocity (m/s)
x	spatial variable (m)
X_i	foam fraction

Greek Letters

α	proportionality constant for effective viscosity
ϕ	porosity
μ_i	viscosity

Subscripts

1	denotes generation rate constant
-1	denotes coalescence rate constant
c	coalescence
f	flowing foam
fd	normalized flowing foam saturation
f,eq	flowing foam at equilibrium between generation and coalescence rates
g	denotes gas phase on p and μ
g	generation
nw	nonwetting phase
t	trapped foam
w	wetting phase
wd	normalized wetting phase saturation

Superscripts

o	denotes reference value of rate constant
*	value corresponds to the critical capillary pressure

Acknowledgement

P. Persoff provided invaluable assistance in setting up the experiments presented in this paper. This work was supported by the U. S. Department of Energy under contract No. DC03-76SF00098 to the Lawrence Berkeley Laboratory of the University of California.

References

1. Patzek, T. W.: "Description of Foam Flow in Porous Media by the Population Balance Method," in Surfactant Based Mobility Control Progress in Miscible-Flood Enhanced Oil Recovery;" Smith, D. H. Ed., ACS Symposium Series No. 373, 326-341 (1988).

2. Hirasaki, G. J. and Lawson: "Mechanisms of Foam Flow in Porous Media: Apparent Viscosity in Smooth Capillaries;" SPEJ (April 1985) 176-190.

3. Ettinger, R. A.and Radke, C. J: "Influence of Foam Texture on Steady Foam Flow in Berea Sandstone," SPERE (February 1992) 83-90.

4. Friedmann, F, Chen, W. H., and Gauglitz, P. A.: "Experimental and Simulation Study of High-Temperature Foam Displacement in Porous Media;" SPERE (February 1991) 37-45.

5. Falls,A. H., Hirasaki, G. J., Patzek, T. W., Gauglitz, P. A., Miller, D. D., and Ratulowski, T.: "Development of a Mechanistic Foam Simulator: The Population Balance and Generation by Snap-Off;" SPERE (August 1988) 884-892.

6. Chambers, K. T. and Radke, C. J.: "Capillary Phenomena in Foam Flow Through Porous Media," in Interfacial Phenomena in Petroleum Recovery, Morrow, N. R. Ed., Marcel Dekker Inc., New York (1991) Ch. 6 191-255.

7. Gillis, J. V.and Radke, C. J.: "A Dual Gas Tracer Technique for Determining Trapped Gas Saturation During Steady Foam Flow in Porous Media," SPE 20519, presented at 65th Annual Technical Conference, New Orleans, LA, September, 1990.

8. Bernard, G. G., Holm, L. W., and Jacobs, W. L.: "Effect of Foam on Trapped Gas Saturation and on Permeability of Porous Media to Water," SPEJ (December 1965) 295-300.

9. Ransohoff, T. C. and Radke, C. J.: "Mechanisms of Foam Generation in Glass-Bead Packs;" SPERE (May 1988) 573-585.

10. Gauglitz, P. A., St. Laurent, C. M., and Radke, C. J.: "An Experimental Investigation of Gas-Bubble Breakup in Constricted Square Capillaries," JPT (September 1987) 1137-1146.

11. Ransohoff, T. C., Gauglitz, P.A., Radke, C. J.: "Snap-Off of Gas Bubbles in Smoothly Constricted Noncircular Capillaries," AIChE Journal (May 1987) 753-765.

12. Shirley, A. I.: "Foam Formation in Porous Media, A Microscopic Visual Study," in Surfactant Based Mobility Control Progress in Miscible-Flood Enhanced Oil Recovery;" Smith, D. H. Ed., ACS Symposium Series No. 373, 234-257 (1988).

13. Jiménez, A. I. and Radke, C. J.: "Dynamic Stability of Foam Lamellae Flowing Through a Periodically Constricted Pore," in Oil-Field Chemistry: Enhanced Recovery and Production Stimulation, Borchardt, J. K.and Yen, T. F. Eds., ACS Symposium Series No. 396, 460 - 479 (1989).

14. Kovscek, A. R. and Radke, C. J.: "Fundamentals of Foam Transport in Porous Media," in Foams in the Petroleum Industry, Schramm, L. L. Ed., ACS Advances in Chemistry Series, to appear 1993.

15. Persoff, P, Radke, C. J., Pruess, K., Benson, S. M., and Witherspoon, P. A.: "A Laboratory Investigation of Foam Flow in Sandstone at Elevated Pressure;" SPERE (August 1991) 365-371.

16. De Vries, A.S.and Wit, K: "Rheology of Gas/Water Foam in the Quality Range Relevant to Steam Foam," SPERE (May, 1990) 185-92.

17. Aziz, K. and Settari, A.: Petroleum Reservoir Simulation, Applied Science Publishers LTD London (1979) 125-199.

18. Hillestad, J. G. and Mattax, C. C.: "Selecting the Numerical Solution Method," in Reservoir Simulation; Mattax, C. C. and Dalton, R. L. Eds., SPE Monograph Series Vol. 13, Ch. 6 57-61 (1990).

19. Khatib, Z. I., Hirasaki, G. J., and Falls, A. H.: "Effects of Capillary Pressure on Coalescence and Phase Mobilities in Foams Flowing Through Porous Media," SPERE (August 1988) 919-926.

20. Khristov, K, Krugljakov, P., and Exerowa, D.: "Influence of the Pressure in the Plateau-Gibbs Borders on the Drainage and the Foam;" Colloid and Polymer Sci. (257 1979) 506-511.

21. Bergeron, V and Radke, C. J.: "Equilibrium Measurements of Oscillatory Disjoining Pressure," to appear Langmuir (1993).

22. Ettinger, R. A.: Foam Flow Resistance in Berea Sandstone M.S. Thesis, University of California, Berkeley (1989).

23. Chou, S. I.: "Conditions for Generating Foam in Porous Media," SPE 22628, presented at 66th Annual Technical Conference, Dallas, TX, October, 1991.

24. Kovscek, A. R. PhD thesis, University of California, Berkeley, in preparation (1993).

25. Fagan, M. E.: The Stability of Foam and Pseudoemulsion Films and Foam Flow Through Glass Beadpacks MS Thesis, University of California, Berkeley (1992).

26. Holm, L. W.: "The Mechanisms of Gas and Liquid Flow Through Porous Media in the Presence of Foam," SPEJ (December 1968) 359-369.

27. Falls, A. H., Muster, J. J., and Ratulowski, J.: "The Apparent Viscosity of Foams in Homogeneous Beadpacks," SPERE (May 1989) 155-164.

28. Rossen, W. R. "Theory of Mobilization Pressure Gradient of Flowing Foams in Porous Media: I. Incompressible Foam;" JCIS 1990, 136(1), 1-16.

29. Rossen, W. R. "Theory of Mobilization Pressure Gradient of Flowing Foams in Porous Media: II. Effect of Compressibility;" JCIS 1990, 136(1), 17-37.

30. Rossen, W. R. "Theory of Mobilization Pressure Gradient of Flowing Foams in Porous Media: III. Asymmetric Lamella Shapes;" JCIS 1990, 136(1), 38-53.

31. Rossen, W. R.; Gauglitz, P. A. "Percolation Theory and Mobilization of Foams in Porous Media," AIChE 1990, 36(8), 1176-1188.

32. Chou, S. I. "Percolation Theory of Foam in Porous Media;" SPE/DOE 20239, presented at SPE/DOE 7th Symposium on Enhanced Oil Recovery: Tulsa, OK, April, 1990.

33. de Gennes, P. G.: "Conjectures on Foam Mobilization," Revue De L'Institut Francais Du Pe'trol (47(2) 1992) 249-254.

34. Perry, R. H. and Green, D. W. Eds.: Perry's Chemical Engineers Handbook 6th Edition, McGraw Hill Book Company, New York (1984) Ch. 3 113.

35. Minssieux, L.: "Oil Displacement by Foams in Relation to Their Physical Properties in Porous Media," JPT (January 1974) 100-108.

36. Rossen, W. R.: "Modeling Foam Mobility in Porous Media," SPE 22627, presented at 66th Annual Technical Conference, Dallas, TX, October, 1991.

Table 1: Parameter Values

Reservoir Simulation Parameters		Population Balance Method	
parameter	value	parameter	value
K	1.3 μm^2	k_1	5.13 E+5 $s^{1/3} cm^{-13/3}$
ø	0.25	k_{-1}^o	1.50 E-3 cm^{-1}
g	3.0	S_w^*	0.26
k_{rw}^o	0.70	a	1/3
h	3.0	b	1.0
k_{rg}^o	1.0	α	1.80 E-6 mPa s $s^{1/3}$ $cm^{8/3}$
Swc	0.25	c	1/3
μ_w	1.0 mPa·s	$X_{f,eq}$	0.10
μ_g	0.018 mPa·s	A_1 , A_2	4.0, 1.25

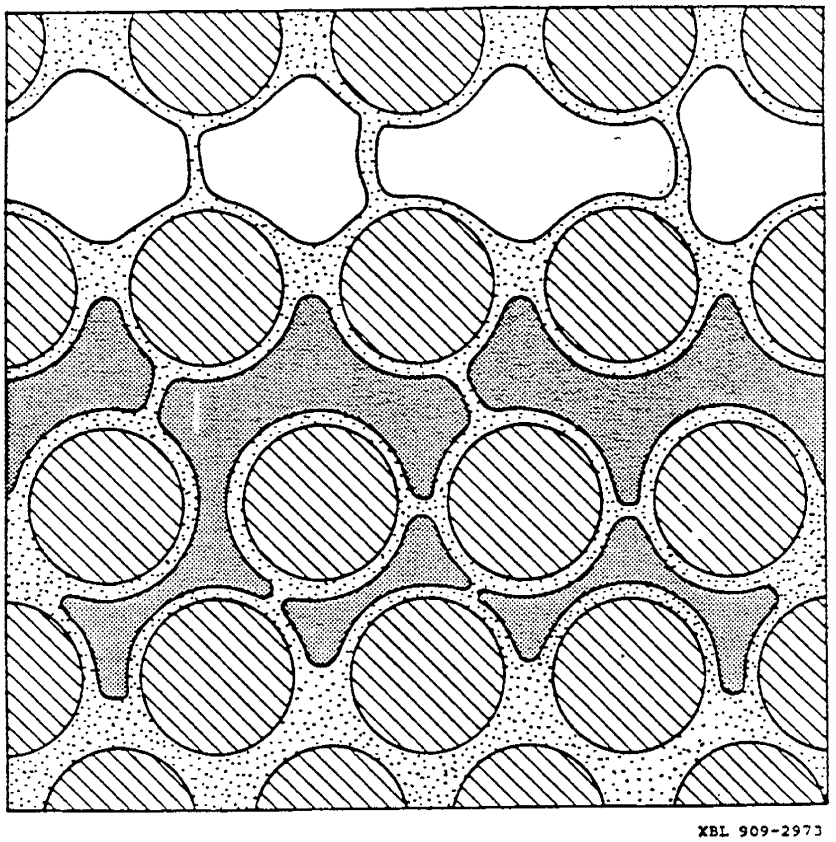

Figure 1: Pore-level schematic for a flowing foam. Flowing bubbles are unshaded and trapped gas is darkly shaded.

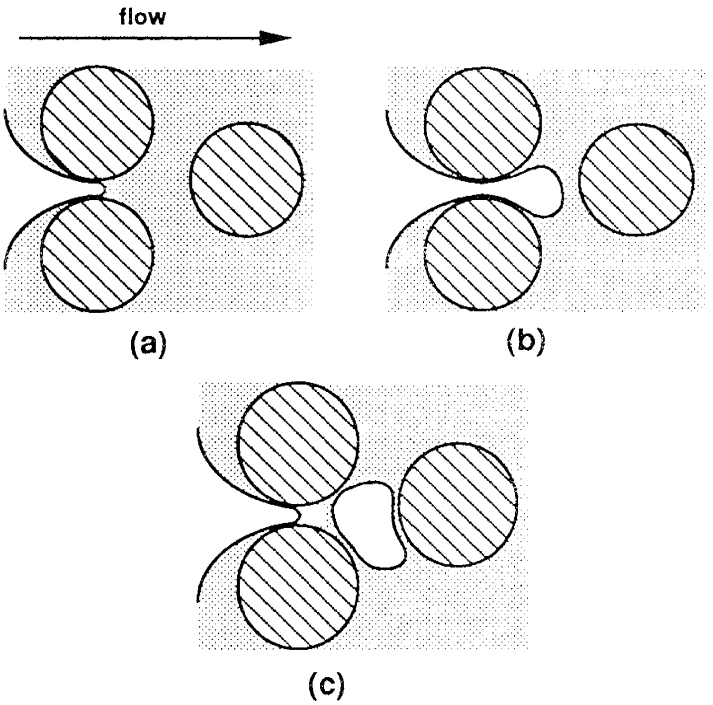

Figure 2: Schematic of snap-off mechanism. Gas is unshaded.

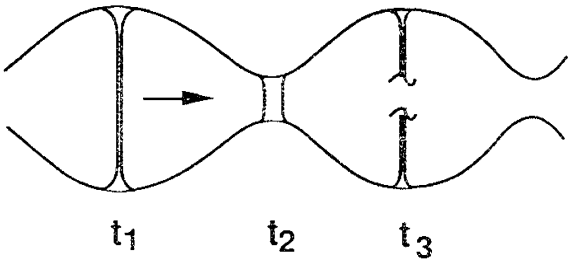

Figure 3: Foam lamella translating from left to right in a periodically constricted pore. Coalescence occurs at t_3 .

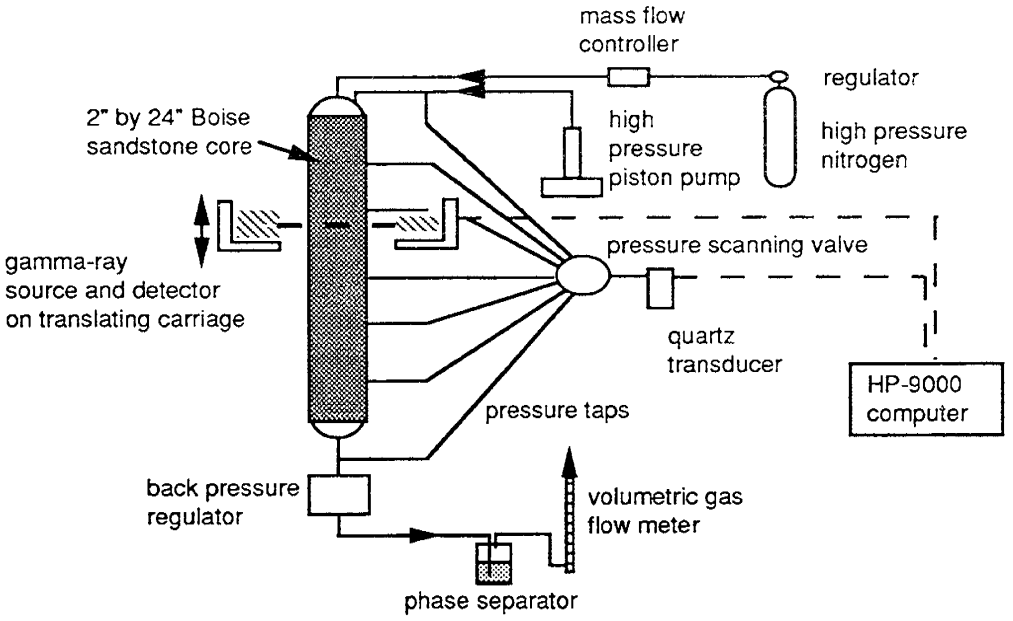

Figure 4: Apparatus for foam displacement experiments.

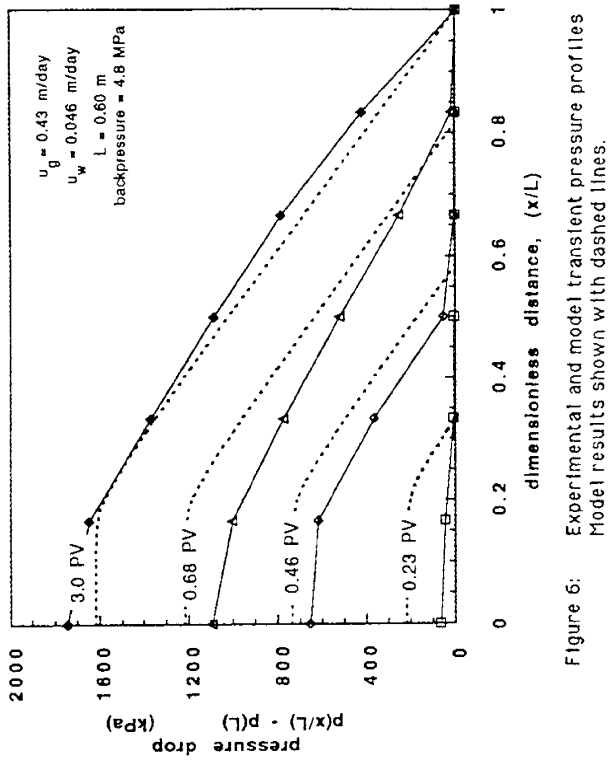

Figure 6: Experimental and model transient pressure profiles. Model results shown with dashed lines.

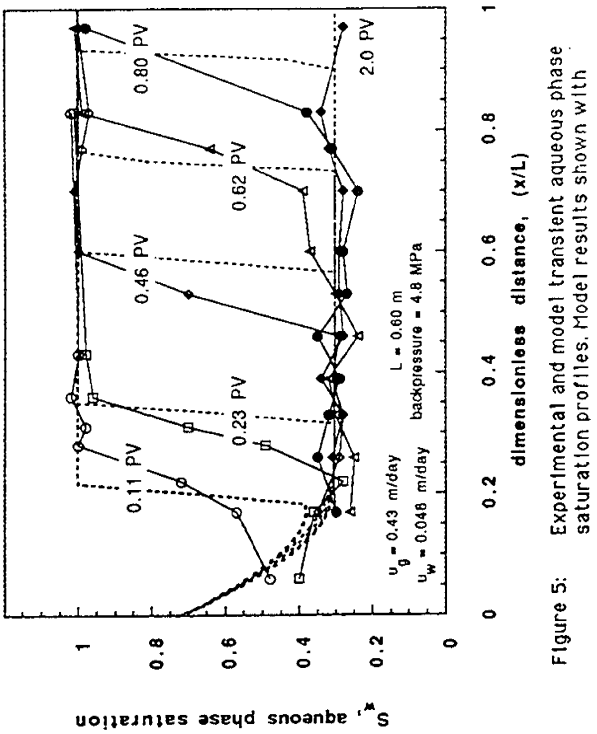

Figure 5: Experimental and model transient aqueous phase saturation profiles. Model results shown with dashed lines

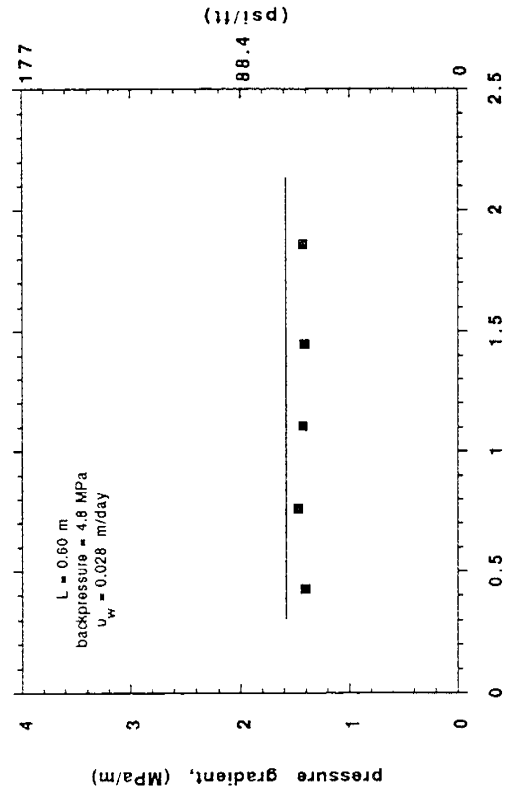

Figure 8: Experimental and model (solid line) steady state pressure gradient versus gas-phase velocity.

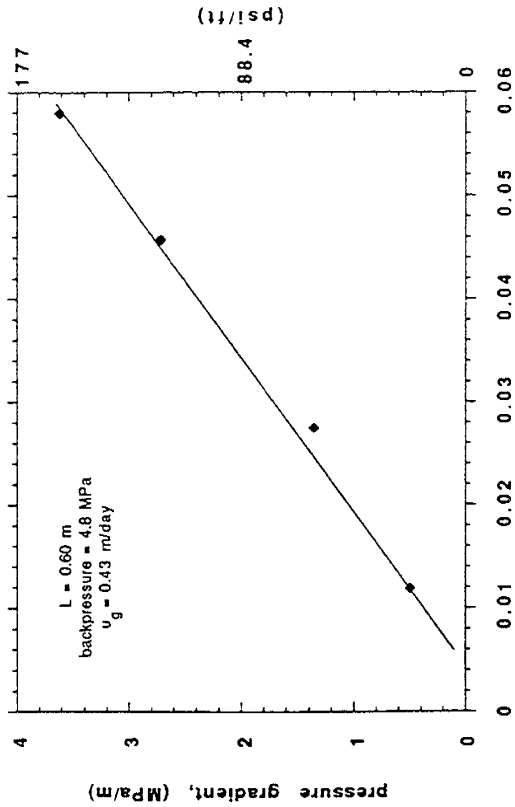

Figure 7: Experimental and model (solid line) steady state pressure gradient versus liquid velocity.

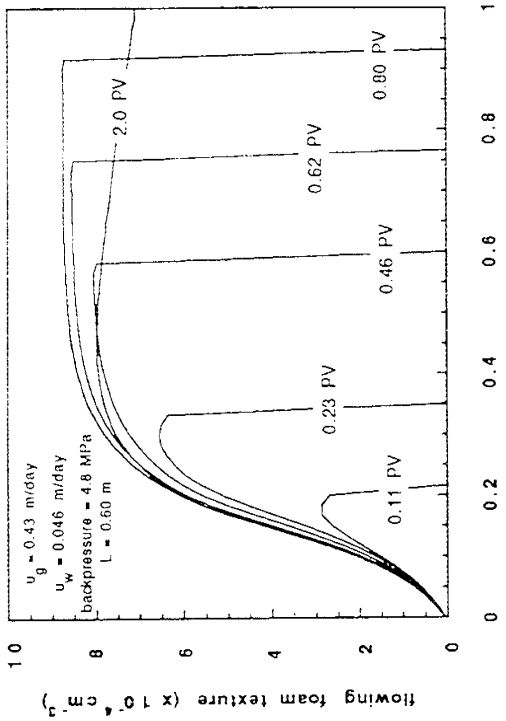

Figure 10: Model transient flowing foam textures.

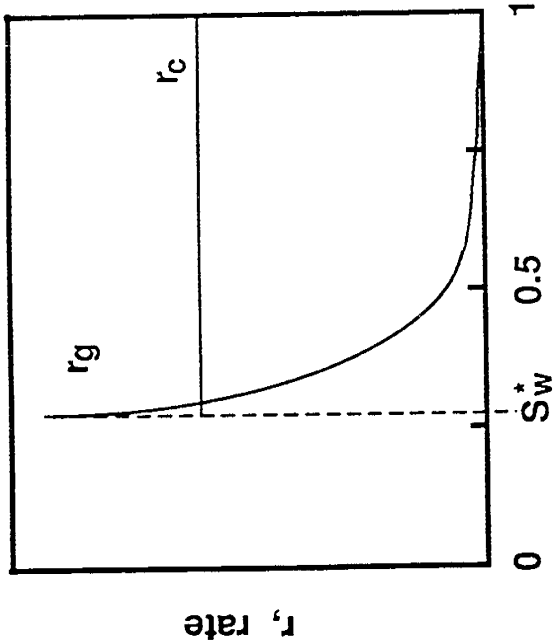

Figure 9: Generation and coalescence rates as a function of aqueous-phase saturation (schematic).

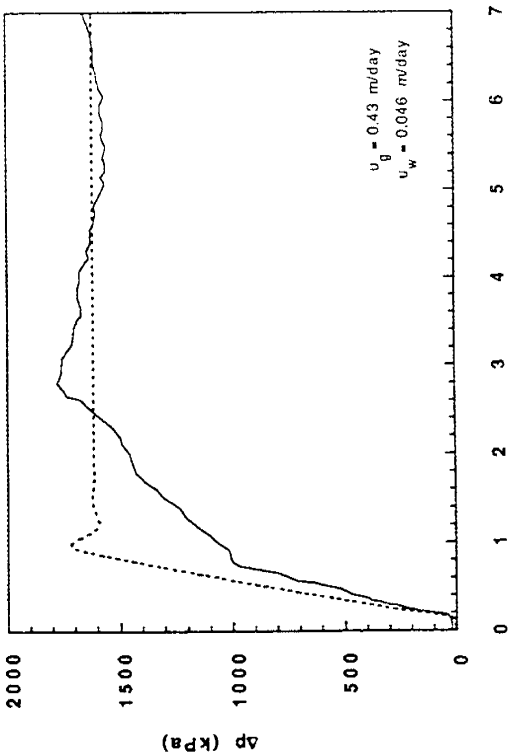

Figure 11: Experimental and model core pressure-drop history. Model results shown with dashed lines

CO_2 Foam Field Verification Pilot at EVGSAU: Phase II—Foam Injection Design and Operating Plan

by J. E. Stevens, K. J. Harpole and D. R. Zornes, Phillips Petroleum Company, and F. D. Martin, New Mexico Petroleum Recovery Research Center, Socorro, New Mexico

Originally presented as Society of Petroleum Engineers paper No. 24642 at the 67th Annual Technical Conference & Exhibition of SPE held at Washington, D.C., October 4-7, 1992. Copyrighted by Society of Petroleum Engineers, Inc., 1992.

This paper was prepared for presentation at the DOE/NIPER, Symposium on Field Application of Foams for Oil Production held in Bakersfield, California, February 11-12, 1993.

This paper was selected for presentation by a Program Committee following review of information contained in an abstract submitted by the author(s). Contents of the paper, as presented, have not been reviewed and are subject to correction by the author(s). The material, as presented, does not necessarily reflect any position of the U.S. Department of Energy or the National Institute for Petroleum and Energy Research.

ABSTRACT

The East Vacuum Grayburg San Andres Unit (EVGSAU) operated by Phillips Petroleum, is the site selected for a comprehensive evaluation of the use of foam for improving the sweep efficiency of a CO_2 flood. The four-year project is jointly funded by the EVGSAU Working Interest Owners (WIO), the U.S. Department of Energy (DOE), and the State of New Mexico. The Petroleum Recovery Research Center (PRRC), a division of the New Mexico Institute of Mining and Technology (NMIMT), is providing laboratory and research support for the project. A Joint Project Advisory Team (JPAT) composed of technical representatives from numerous major oil companies, PRRC, and DOE provides input, review and guidance for the project.

This paper is the second in a series of papers detailing various aspects of the CO_2 Foam Field Verification Pilot test at EVGSAU. An earlier paper summarized the project plans and detailed the laboratory work leading to the selection of a surfactant for the field trial. This paper presents: 1) an overview of the operating plan for the project, 2) details of the foam injection schedule and design criteria, and 3) a discussion of the data collection program and performance criteria to be used in evaluating successful application of foam for mobility control in the EVGSAU CO_2 project.

Specific items discussed in the foam injection design include the determination of surfactant volume and concentration, selection of the surfactant-alternating-gas (SAG) injection sequence for foam generation, field facilities, operations during foam injection, and contingency plans. An extensive data collection program for the project is discussed including production testing, injection well pressure and rate monitoring, injection profiles, production well logging, observation well logging program, and both gas and water phase tracer programs.

References and illustrations at end of paper.

INTRODUCTION

The EVGSAU, located about 15 miles northwest of Hobbs in Lea County is the site of the first full-scale miscible carbon dioxide injection project in the state of New Mexico[1,2]. CO_2 injection at EVGSAU began in September, 1985. The CO_2 project area covers 5000 acres developed using an 80-acre inverted nine-spot flood pattern. The total CO_2 injection rate is about 30 MMcf/D. A water-alternating-gas (WAG) ratio of 2:1 (time basis) is used in the project, resulting in about one-third of the project area being on CO_2 injection at any one time. In any given area, a WAG cycle consists of about four months of CO_2 injection followed by eight months of water injection. This results in approximately 1.5 to 2% hydrocarbon pore volume (HCPV) CO_2 injection and 3 to 4% HCPV brine injection per WAG cycle. The project is currently in the seventh WAG cycle. The tertiary oil response at EVGSAU to date has been very favorable. As shown in Figure 1, the waterflood decline established prior to CO_2 injection has been arrested, and oil production has held approximately constant near the current 9000 BOPD Unit total for the past six years.

While the overall project performance has been very encouraging, certain wells/patterns have shown anomalously high CO_2 production. This has resulted in isolated cases of poor pattern sweep efficiency, inefficient CO_2 utilization, and increased recycling costs and compression requirements. Laboratory results with mobility control foams for CO_2 flooding appeared to offer some potential for controlling the excessive CO_2 production problems at EVGSAU[3,4]. The CO_2 Foam Field Verification Pilot was designed to evaluate the application of foam mobility control technology in a field-scale CO_2 flood project. Additional background on the project planning and laboratory screening work leading to the selection of a specific foaming surfactant for application at EVGSAU was published earlier[1].

The EVGSAU produces primarily from the San Andres Formation. At EVGSAU, the San Andres can be divided into upper and lower sections by the Lovington sandstone/siltstone. The San Andres sections consist of a series of shallowing-upward carbonate sequences, each typically 20 to 30 feet thick, which have been extensively dolomitized. Total gross reservoir thickness ranges from 200 to 300 feet. A geologic study of the EVGSAU reservoir identified twelve zones which are laterally continuous across the foam pilot area (Figure 2). The location of the pattern selected for the foam pilot test is shown in Figure 3. This pattern was selected for the field trial based on the following criteria:

1) the pattern has shown excessive CO_2 breakthrough in one of the production wells (3332-032); the remainder of the wells in the pattern have shown more typical CO_2 response.

2) the reservoir geology in the pattern area is representative of most of the EVGSAU reservoir to allow results from the pilot to be scaled up to the entire Unit;

3) the injection well in the pattern (3332-001) has sufficient injectivity to reduce the chance of the well becoming pressure-limited during foam injection.

An observation well (3332-003) was drilled in the pilot pattern about 150 feet from the WAG injector, as shown in Figure 3. This well was sponge cored to provide current oil saturation information, as well as additional details on the reservoir geology in the pattern area. Zone C (shown subdivided into C1, C2, and C3 on the type log in Figure 2) is the major flow unit within the pilot area. Zones D and E show good porosity development and high oil saturation, but are less permeable and take only a small fraction of the fluid injected into this pattern. The A and B zones show little or no reservoir potential in this area, while the zones below the Lovington have good porosity and permeability, but have high water saturation in the pilot area. Falloff tests from most of the EVGSAU injection wells show an extended period of linear flow, indicating that they are most likely injecting into a fracture. However, the excessive CO_2 breakthrough problems do not appear to be simply the result of direct fracture communication between injectors and producers.

Within the foam pilot pattern area, the zones designated as C2 and C3 (Figure 2) contain intervals with very high permeability. For example, a five-foot interval in Zone C2 from the observation well core averages almost 250 millidarcies. Oil saturations obtained from the sponge core in this interval were consistently less than 5% PV, indicating they had probably been contacted by a large volume of CO_2. Injection profiles taken in the WAG injector show almost two-thirds of the injected fluids entering Zone C2 and the lower portion of Zone C3. Similarly, a production log run in well 3332-032 (Figure 8) shows 60% of the produced fluid to be coming from these same C2 and C3 zones. In contrast, Zone E, which shows high porosity and good oil saturation, is indicated to be taking less than 5% of the injected fluid. One of the primary objectives of the foam injection is to divert a larger percentage of the injected CO_2 into these lower permeability zones which are not being efficiently processed in the current WAG operation.

The production history for the foam injection pilot pattern is shown in Figure 4. Note that the pattern gas production increased sharply in early 1987 when well 3332-032, a side producer in the nine-spot pattern (shown in Figure 3, located to the southwest of the injection well), began to flow spontaneously in response to CO_2 injection. This producer had previously been open to production, however it was not being pumped because of excessive WOR during the pre-CO_2

waterflood period. Since 1987, the 3332-032 well has been capable of flowing following each CO_2 injection cycle. Although this well has not received any special monitoring during the CO_2 flood prior to initiating the foam project, production records indicate the apparent time lag between the beginning of the CO_2 injection half-cycle and the increase in gas-oil ratio (GOR) in well 3332-032 has varied from about 6 to 14 weeks. CO_2 production rates from well 3332-032 at the end of the past two CO_2 injection half-cycles have been 25-30% of the average CO_2 injection rate into the pattern injector (well 3332-001). Favorable changes in the CO_2 production response characteristics in well 3332-032 will be an important indicator of successful foam treatment in this pattern.

PROJECT DESIGN CONSIDERATIONS

This project is a cooperative industry-government effort to bring emerging technology from promising laboratory research to field application. The JPAT, composed of technical representatives from DOE, PRRC, and several WIO oil companies provided input, review, and guidance for the project design. The primary objective of the project was to achieve a successful field implementation of the CO_2 foam mobility control technology. Identification of the economic optimum surfactant concentration, slug size, foam quality, etc. for an eventual commercial expansion of the process was of secondary concern.

Surfactant System Design

Several significant issues arose during the initial project design discussions. The first was whether the objective of the foam project should be directed toward near-well fluid diversion or more in-depth mobility control throughout the pattern. Preliminary laboratory data indicated surfactant adsorption would be in the range of 600 to 1800 pounds of active surfactant adsorbed per acre-foot of bulk formation volume contacted. Based on economic considerations, it was decided to design the project primarily for near-well fluid diversion using a smaller (approximately 1% HCPV), higher surfactant concentration foam slug rather than attempt to control mobility throughout the pattern using a larger volume slug with a lower surfactant concentration.

Extensive laboratory testing was conducted prior to selecting the specific surfactant for use in the EVGSAU CO_2 foam pilot test[1,3-6]. The primary criteria considered in the surfactant selection process were: 1) the effectiveness of the surfactant in reducing CO_2 mobility in coreflood experiments, 2) the amount of surfactant lost to adsorption onto the reservoir rock, and 3) the stability or durability of the foam. Secondary criteria also considered in the selection process were surfactant cost, availability, ease of handling and transporting, and stability under field storage and injection conditions. After consideration of all of these criteria, the Chevron Chemical surfactant Chaser CD-1045® was selected. There was some difference of opinion among JPAT members as to the optimum surfactant concentration for use in this pilot test, however, based on the laboratory coreflood results, a design concentration of 2500 ppm active surfactant was selected.

The project design calls for an 80% quality foam to be injected during the first half of a CO_2 injection cycle in the normal WAG process, followed by straight CO_2 injection for the remainder of the CO_2 portion of that WAG cycle. The objective is to fit the foam injection into the normal WAG cycle rotation in the pattern as much as possible so that any changes in pattern performance due to non-foam, operational changes would be minimized. During a normal CO_2 WAG half-cycle in this pattern, the limiting injection rate of 1000 RB/D results in approximately 2% pattern HCPV of CO_2 being injected per WAG cycle. Thus, a nominal 1% HCPV foam slug was selected. This size foam slug was considered to be large enough to reduce the probability that the project would fail or yield inconclusive results due to insufficient quantity of chemical being injected (allowing for dilution, out of zone injection, surfactant adsorption, etc. being larger than anticipated). The selection of 80% foam quality was based on the successful laboratory results obtained at PRRC using this quality. Again, it was not the purpose of this field trial to attempt to economically optimize the foam process, but rather to prove the technology in a field application.

® Registered trademark of Chevron Chemical Company

Injection of an adsorption pad of sacrificial surfactant solution (also 2500 ppm active) began on April 14, 1992. At the design surfactant concentration of 2500 ppm, the average surfactant adsorption measured in coreflood tests was 835 pounds per acre-foot. The sacrificial surfactant pad is designed to satisfy this level of surfactant adsorption in the reservoir volume to be occupied by the 1% HCPV foam slug. Approximately 90,000 pounds of active surfactant will be injected in the sacrificial adsorption slug during the three month period immediately preceding injection of the foam slug. The total surfactant required for the project design (adsorption slug plus foam slug) is about 105,000 pounds of active surfactant. Thus, about 85% of the total surfactant to be injected during the project will be needed to satisfy adsorption.

Foam Injection and Monitoring

Another issue debated during project design planning was the method of injecting the foam slug, i.e., coinjection of surfactant and CO_2 vs. alternate injection of slugs of surfactant and CO_2 (SAG). Consideration was given to the degree of mixing in the tubulars vs. that occurring during flow in the formation, possible gravity segregation of fluids over the injection interval, differential surface injection pressures of CO_2 vs. surfactant solution, possible use of downhole mixers, loss of injectivity, etc. Ultimately, the JPAT decided on a SAG process with the most rapid alternation between CO_2 and surfactant that was practical to consider in a large-scale field operation. Thus, a cycle of 3 days of surfactant injection (3000 res. bbls.) followed by 12 days of CO_2 injection (12000 res. bbls.) was selected.

Based on average pattern properties, a 1% HCPV foam slug would occupy a cylindrical volume around the injection well with a radius of about 100 feet. However, considering (1) the geologic description of the pattern; (2) saturation, porosity, and permeability data obtained from the observation well sponge core (located about 150 feet from the injection well); (3) the injection profile in the foam injector; and (4) estimates of the probable geometry of a high permeability zone, based on production response and geologic data; surfactant could be expected to propagate several hundred feet away from the injection well in a high permeability zone.

Reservoir simulation of the foam pattern waterflood and CO_2 flood history is being conducted to further refine these initial estimates of foam propagation. The modeling work includes modification of a commercial miscible flood simulator to model the basic foam mobility control mechanisms, with validation of the modified simulator against the mechanistic foam model developed at PRRC. The modified commercial simulator will then be used to refine predictions of foam propagation and pattern response to foam injection. After history matching the foam pilot performance, the simulator will be used to predict long-term and commercial scale application of the foam process. Simulation modeling can also be used to help optimize the foam process for any future applications.

Several methods will be used to verify successful development of mobility control and/or fluid diversion with the surfactant foam system:

1) Injectivity response in the foam pattern injection well will be carefully monitored by measuring injection rates and pressures and by monitoring any changes in the injection profile;

2) Pressure falloff tests will be run to monitor wellbore condition (skin) and to attempt to measure changes in the in-situ fluid mobility;

3) Time sequence logging runs will be made through fiberglass casing in the observation well to monitor changes in reservoir fluid flow or fluid distribution;

4) Production characteristics of the "offending" well (3332-032) in the pattern will be closely monitored for changes in GOR and oil production response after injection of the foam slug;

5) Water phase and gas phase tracers will be injected both during the baseline cycle and the foam injection cycle to observe changes in fluid flow patterns.

OPERATING PLAN

A formal project schedule and detailed operating procedures were developed in a series of open discussions at JPAT project meetings. The final operating plan is necessarily a compromise between the desire to conduct a controlled experiment in the field and the need to mesh the foam project operations into the ongoing WAG operations of a full-field CO_2 flood project at EVGSAU. The resulting project schedule is shown as Figure 5.

The project schedule can be characterized in three phases: 1) an extensive pre-foam pattern conditioning and data gathering period, 2) the foam injection period, and 3) a production monitoring period. DOE sponsorship of the "Field Verification of CO_2 Foam" project (DOE Grant No. DE-FG21-89MC26031) covers a four-year project period. Actual field operations extend over a 3 year period with the first year dedicated to sampling, coring, surfactant selection, and foam pattern conditioning; the second year being slated for surfactant injection (with the possibility of more than one foam generation cycle, depending on project funding and reservoir response); and the third year concentrating on production monitoring and evaluation of foam performance.

Surface Facilities & Equipment

Surface facilities for foam injection are fairly simple and required no changes to the existing injection meter run. A schematic of the facilities is shown in Figure 6. In the future, since the surface facilities needed to handle the surfactant are fairly simple, it is anticipated that all of this equipment could be truck or trailer mounted to facilitate individual well treatments.

Surfactant is delivered in bulk 5500 gallon (131 bbl) lots via a tanker truck. Since enough storage capacity is needed on location to handle a new shipment without being critically low on surfactant, a standard 210-bbl fiberglass tank was selected. The tank is connected via 1-inch tubing through a strainer to a variable stroke length Bran-Lubbe injection pump. This pump was selected for its ability to change injection rate easily, as it was anticipated that the surfactant injection rate would need to be reduced during the foam generation period. Since the surfactant injection period during foam generation SAG cycles is only three days, a manual control on the pump was considered to be adequate for maintaining a steady surfactant concentration (versus automating the pump with a rate controller). The pump is connected to the existing injection line with 1/2-inch stainless steel tubing to a port downstream of the injection meter and pressure transducer. Thus, the injection meter measures only the injection water and not the combination of surfactant and water.

Each tanker truck shipment of surfactant has a quality control certificate issued by the manufacturer upon loading to document the chemical's content, activity, and specific gravity. In addition, routine quality control checks are made on the delivered product by the operator prior to injection. There was some concern that the viscous (approximately 200 cp.) surfactant would not mix adequately with the injection brine in the 35 feet of 2-inch injection line upstream of the wellhead sampling point, and an in-line mixer might be needed. However, the surfactant concentration measured on multiple samples taken at the injection wellhead during the first few weeks of injection were consistent and the samples were clear and uniform, indicating no significant problems with mixing. Based on these sampling results it was concluded that an in-line mixer was not needed.

Injection Schedule

The project schedule (Figure 5) calls for injection of the foam slug to begin in mid-July, 1992. The nominal 1% HCPV, 80% quality foam slug is to be injected using a rapid SAG (surfactant-alternating-gas) injection scheme of five SAG cycles with 12,000 res. bbls. CO_2 and 3000 res. bbls. of 2500 ppm active surfactant in injection brine in each SAG cycle. At the historical limiting injection rates of 1000 RB/D, this would be a SAG cycle of 12-days on CO_2, followed by 3-days of surfactant solution. The foam slug would then be followed by straight CO_2 injection for the remainder of the normal CO_2 half-cycle in the fieldwide WAG operation. The decision on when to switch back to the brine injection half-cycle will be dictated by the response to foam injection.

Use of the rapid SAG process for injection of the foam slug raised the concern that even without any surfactant addition or foam generation, the

change in normal WAG cycle operations might produce a change in pattern flood behavior, thus complicating interpretation of the pilot results. To reduce this possible complication, the project design was expanded to include a "baseline" WAG cycle prior to the surfactant foam injection cycle. During the baseline cycle, all operations were conducted and monitored exactly as planned for the foam injection cycle, except no surfactant was injected.

The baseline CO_2 injection cycle began on September 25, 1991 with the injection of a series of five rapid WAG cycles. Each cycle consisted of 12 days on CO_2 and 3 days on water at 1000 RB/D for each fluid. The rapid WAG was followed by straight CO_2 injection from December 10, 1991 to February 28, 1992. Following injection profiles and falloff testing, brine injection was resumed March 14, 1992 (Figure 7). Surfactant (2500 ppm active) was introduced into the injection brine beginning April 14, 1992 and continued during the final three months of the normal brine injection half-cycle. This three-month pad contained sufficient surfactant to satisfy adsorption prior to injection of the foam slug.

DATA COLLECTION PROGRAM

The CO_2 Foam Field Verification Project will focus on two main questions: 1) is a foam generated in situ which effectively reduces the mobility of injected CO_2, and 2) is the foam effective in producing an improvement in the pattern sweep efficiency and/or production performance? An effort will be made to estimate the amount of incremental oil which may ultimately be produced as a result of foam injection. This will be difficult, but it is important to assess the economic potential of foam for future applications. The following outlines the program of data collection and analyses planned for monitoring and evaluation of the foam injection project.

Injection Well Performance

Rate and pressure data are taken once a day on the foam pattern injection well (3332-001). An increase in injection pressure is probably the most important indication that foam is forming downhole. During surfactant injection, a wellhead injection pressure recorder was installed to monitor pressure continuously. Figure 7 shows the injection well performance through the baseline period and into the injection of the adsorption surfactant slug. The baseline CO_2 injection half-cycle ended when well 3332-001 was shut in for a falloff test in early March, 1992. The well went back on water injection March 14, 1992. Surface injection pressure built up to about 750 psi. This is about 150 psi above the injection pressure at the end of the baseline water injection half-cycle prior to the rapid WAG and baseline CO_2 injection. No significant change has been observed in the injection pressure vs. time behavior since the start of the sacrificial surfactant injection on April 14, 1992.

An injection profile is run in well 3332-001 at the end of each cycle of injection, with more frequent profiles run during the foam generation period, as indicated on the Project Schedule (Figure 5). The injection profiles will be used to detect any significant changes in the intervals taking injection fluids. The profile is developed from a log of temperature, tracer intensities, velocities and casing caliper. A typical injection profile for well 3332-001 is shown in Figure 8. Note that approximately 65% of the injected fluid is indicated to be entering Zone C2 and the lower portion of Zone C3. This distribution of injection fluids is consistent with the permeability distribution seen in the observation well core located 150 feet away.

Falloff tests were planned to provide data on effective formation properties and wellbore condition (skin) during the foam project. It was also hoped that falloff tests would provide a direct measurement of fluid mobility changes in the reservoir as a result of foam injection. As indicated in the project schedule, two falloffs were performed prior to foam injection and one is planned after injection of the foam slug.

Pattern Production Performance

The eight wells in the foam pattern (Figure 3) are production tested once a week. Testing began on a weekly basis in February 1991, more than a year before foam injection began. While the pattern production performance may be one of the most important criteria in evaluating success, it is also one of the most difficult to measure consistently and accurately over the life of the project. Normal operations are maintained in the

eight foam pattern producers as much as possible, however some production swings have occurred due to routine equipment change outs in some wells.

Figure 4 shows the foam pattern production history. A reduction in producing GOR vs. CO_2 injection is expected to be one of the first positive indications that the foam injection has succeeded in altering CO_2 mobility and flow patterns in the reservoir. Well 3332-032 has shown the greatest CO_2 production in this pattern and is expected to show the first changes in GOR behavior if the foam treatment is successful.

Flowing production logs are run at the end of each injection cycle in the "offending" well (3332-032), as indicated in the Project Schedule (Figure 5). The production log consists of flowing temperature, one-hour decay temperature, two-hour decay temperature, crossflow checks, radioactive tracer, flowing capacitance, and shut-in capacitance. An indication of successful foam performance would be increased production from less prolific zones in the offending well that are not now contributing very much due to the high pressure and large volume of gas produced from the high permeability zones (Zone C2 and the lower portion of Zone C3), as shown in Figure 8. Note that about 60% of the produced fluids are indicated to be coming out of these zones. The production log profile is very similar to the injection tracer survey.

Observation Well Logging

An observation well (3332-003) was drilled about 150 feet from the foam pattern injection well (Figure 3). The following log suite was run in the observation well at the time it was completed:

Open Hole:
- Compensated neutron/density log
- Induction log
- Sonic log
- Dual laterolog
- Repeat formation tester

Cased Hole:
- Compensated neutron log
- Cement evaluation log
- Induction log
- Pulsed neutron capture log

At the end of each injection cycle an induction log and a compensated neutron log are run to check for saturation changes. During the rapid WAG and CO_2 injection in the baseline cycle (prior to any surfactant injection), observation well logging runs indicated changes in water and gas saturations in response to the injection into well 3332-001 (Figure 9). As a result, the scheduled frequency of logging in the observation well was increased during the foam injection SAG period as indicated in the Project Schedule (Figure 5). It is hoped that foam injection will produce measurable changes in the timing, magnitude, and/or location of saturation changes at the observation well, which can then be related to changes in flow patterns and sweep efficiency. Figure 9 shows results of a series of logging runs made in the observation well during the baseline cycle. These logs indicate that the largest saturation changes are occurring in the same high permeability zones where the maximum fluid injection and production are seen in wells 3332-001 and 3332-032, respectively.

Interwell Tracers and Fluid Sampling

An interwell tracer program was designed to show any changes in fluid transit times from the injector to the producers as a result of foam generation. Tracers were injected in early December, 1991 after the rapid WAG portion of the baseline cycle (Figure 5). The two tracers injected were Krypton 85 (one curie) in the gas phase, and Tritium (nine curies) in the water phase. Gas samples are collected from the two side producers in the foam pattern which have shown the most rapid and severe CO_2 breakthrough problems (wells 3332-032 and 2801-001). Produced gas samples are taken daily for five weeks and twice per week thereafter. Water samples are taken from all eight pattern producers on the same frequency. Results from these tracers will be compared to a similar set of tracers to be injected after the rapid SAG portion of the foam injection cycle.

As of May 15, 1992 neither of the tracers injected in December, 1991 has been detected. An additional tracer of 0.15 curies of Cobalt 60 was injected in the water phase just prior to start of the adsorption slug of surfactant in mid-April, 1992. If surfactant does propagate through the reservoir, the difference in arrival times between the non-adsorbing radioactive tracer (Co-60) and

the surfactant may help to further quantify in-situ surfactant adsorption.

Water samples are being taken at the injection wellhead to monitor the surfactant concentration in the injection brine. Produced water samples are being taken on a weekly basis from the offending well (3332-032), specifically for the purpose of analyzing for the presence of surfactant. If surfactant is detected, then more frequent sampling will be done to monitor the produced surfactant concentration vs. time. This information will aid in predicting and combatting emulsion and foaming problems in the surface equipment. In addition, the water samples being taken from the other seven pattern production wells for tracer analysis are being saved, and would be available for analysis for surfactant content in the event that surfactant breakthrough was suspected.

CONTINGENCY PLANS

In view of the problems inherent in implementing any emerging technology in a field application, it was clear that a key element of the operating plan had to be operational flexibility. While it is not possible to anticipate and prepare for all possibilities, the JPAT members and the Operator did identify several potential problem areas.

Injectivity Reduction

It was anticipated that injectivity would be reduced, perhaps dramatically, if we were successful in generating a strong foam near the injection well. Interpretation of the test response would be much easier if a constant injection rate could be maintained throughout all phases of the project. The injection well in the foam pattern has been injecting water at the limiting rate of 1000 RB/D at a surface injection pressure of 600-750 psi (Figure 7). The maximum surface injection pressures allowed at EVGSAU are 1350 psi for water injection and 1800 psi for CO_2 injection (per New Mexico Oil Conservation Division regulations). Recent step rate tests conducted in this area of the field indicate that the formation parting pressure is above these limits. Project operations will attempt to hold the injection rate constant at 1000 RB/D, while allowing the surface injection pressure to rise to the field limits. If injectivity declines further, it will be necessary to let the injection rate decline.

Multiple injection profiles will be run during the SAG injection phase to help evaluate the injection rate and pressure response. The period of rapid SAG will continue for five cycles or until the injectivity declines to the point that the rate must be cut back to 250 RB/D. At this point the SAG injection would be terminated and immediately followed with a period of CO_2 injection until a total volume of CO_2 equal to the pre-foam CO_2 volume has been injected. Since the CO_2 injection rate would probably be reduced as a result of foam generation, it is not possible to specify an exact time period for this CO_2 injection. Injection of an equal volume of CO_2 in the WAG cycles both before and after foam generation would result in a better comparison of production response in the foam pattern.

Adsorption Slug Surfactant Breakthrough

The exact quantity of surfactant needed to satisfy adsorption is uncertain due to the fact there is a large range in the laboratory measurements of adsorption, and the flow paths in the foam pattern are not known. If the injected surfactant is confined to a small channel directed toward the offending well (EVGSAU 3332-032), then it might be possible for the large pre-foam surfactant slug to propagate to the offending producer. It was decided to inject the adsorption surfactant until either it was produced from the offending well, indicating that adsorption had been satisfied over the complete length of the high permeability flow channel, or for the three-month period needed to satisfy adsorption requirements of the 1% HCPV foam slug to follow. This would introduce enough surfactant to allow foam to be generated at depth in the reservoir.

In the event that surfactant is propagated through the reservoir and foam generation occurs in the production separators, a de-foamer will be injected downstream of the wellhead which will allow the de-foamer to work in the flowline prior to reaching the separation facilities. We do not plan to inject any de-foamer into the injection well; however, it will be available as a last resort if total injectivity is lost.

Laboratory testing is being conducted to determine if any emulsification problems could arise in the producing facilities, and an appropriate de-emulsifier will be available, if needed. The weekly water samples will aid in forecasting emulsion problems as well as determining if/when surfactant may have propagated through the reservoir to the producing well(s).

CONCLUDING REMARKS

This project is an excellent example of a joint industry-government research effort that has potential to prove up promising laboratory research in a field application. At the time of this writing (June, 1992), the baseline cycle has been completed, and the sacrificial adsorption slug of surfactant is being injected with no problems. The surfactant is mixing well and the injection equipment is performing satisfactorily. As expected, no significant changes in either injection pressure or profile have been observed as a result of the sacrificial surfactant injection which began on April 14, 1992.

The "offending" producing well in the pattern (3332-032) began flowing within two months from the time the rapid WAG CO_2 injection began (late September, 1991). Neither the water phase nor gas phase tracers injected on December 7 and 12, 1991, respectively, have been detected in fluid samples taken and analyzed as of May 15, 1992. This indicates there is probably not a direct fracture communication between the injector and producer in this pattern. Evidence from the injection well tracer log, the production log from well 3332-032 (Figure 8), and the results of the monitor logging runs in the observation well (Figure 9), all indicate that most of the fluid movement in this pattern is occurring in the high permeability zones (C2 and C3), as assumed in the foam design.

ACKNOWLEDGEMENTS

The authors would like to thank Phillips Petroleum Company for the opportunity to write this paper. A special thanks goes to Don Thorp and Joe Brown for their devotion in supervising the collection of the field data, and to Matt Gerard, Larry Hallenbeck, and Don Wier for their technical and editorial contributions. The project would not have run as smoothly as it has with out the participation and input from the various JPAT representatives listed below:

Arco - Erwin Sutanto, Sophany Thach
Chevron - Doug Jasek
DOE - Royal Watts
Exxon - Todd Reppert, Gary Teletzke
Marathon - Gwen Ginley
Mobil - Ed Shaw
PRRC - John Heller, Bill Weiss, Jyun-Syung Tsau
Texaco - Jim Ware,John Prieditis

Funding for this joint government-industry project is being provided by the U.S. Department of Energy, the State of New Mexico, and the Working Interest Owners of the EVGSAU.

REFERENCES

1. Martin, F.D., Heller, J.P., Weiss, W.W., Tsau, Jyun-Syung, Zornes, D.R., Sugg, L.A., Stevens, J.E., and Kim, J.E.: "CO_2 Foam Field Verification Pilot Test at EVGSAU Injection Project - Phase I: Project Planning and Initial Results", paper SPE 24176 presented at the 1992 SPE/DOE Enhanced Oil Recovery Symposium, Tulsa, April 22-24.

2. Brownlee, M.H. and Sugg, L.A.: "East Vacuum Grayburg-San Andres Unit CO_2 Injection Project: Development and Results to Date", Proc., 62nd Annual Technical Conference and Exhibition, Dallas (1987) 241-254.

3. Lee, H.O., Heller, J.P., & Hoefer, A.M.W.: "Change in Apparent Viscosity of CO_2 Foam with Rock Permeability", SPERE (Nov. 1991) 421-428.

4. Tsau, J.S. and Heller, J.P.: "Evaluation of Surfactants for CO_2-Foam Mobility Control", paper SPE 24013 presented at the 1992 Permian Basin Oil and Gas Recovery Conference, Midland, March 18-20.

5. Kuehne, D.L., Frazier, R.H., Cantor, J., and Horn, W.: "Evaluation of Surfactants for CO_2 Mobility Control in Dolomite Reservoirs", paper SPE 24177 presented at the 1992 SPE/DOE Enhanced Oil Recovery Symposium, Tulsa, April 22-24.

6. Prieditis, J. and Paulett, G.S.: "CO_2 Foam Mobility Tests at Reservoir Conditions in San Andres Cores", paper SPE 24178 presented at the 1992 SPE/DOE Enhanced Oil Recovery Symposium, Tulsa April 22-24.

SI METRIC CONVERSION FACTORS

bbl	x	1.589 873	E-01	= m3
cp	x	1.0*	E+00	= $mP_{\eta}s$
curie	x	3.7*	E+10	= Bq
ft	x	3.048*	E-01	= m
gal	x	3.785 412	E-03	= m3
in	x	2.54*	E+01	= mm
lbm	x	4.535924	E-01	= kg
md	x	9.869 233	E-04	= um2
psi	x	6.894 757	E+00	= kPa
qt	x	9.463 529	E-01	= dm3

*Conversion factor is exact.

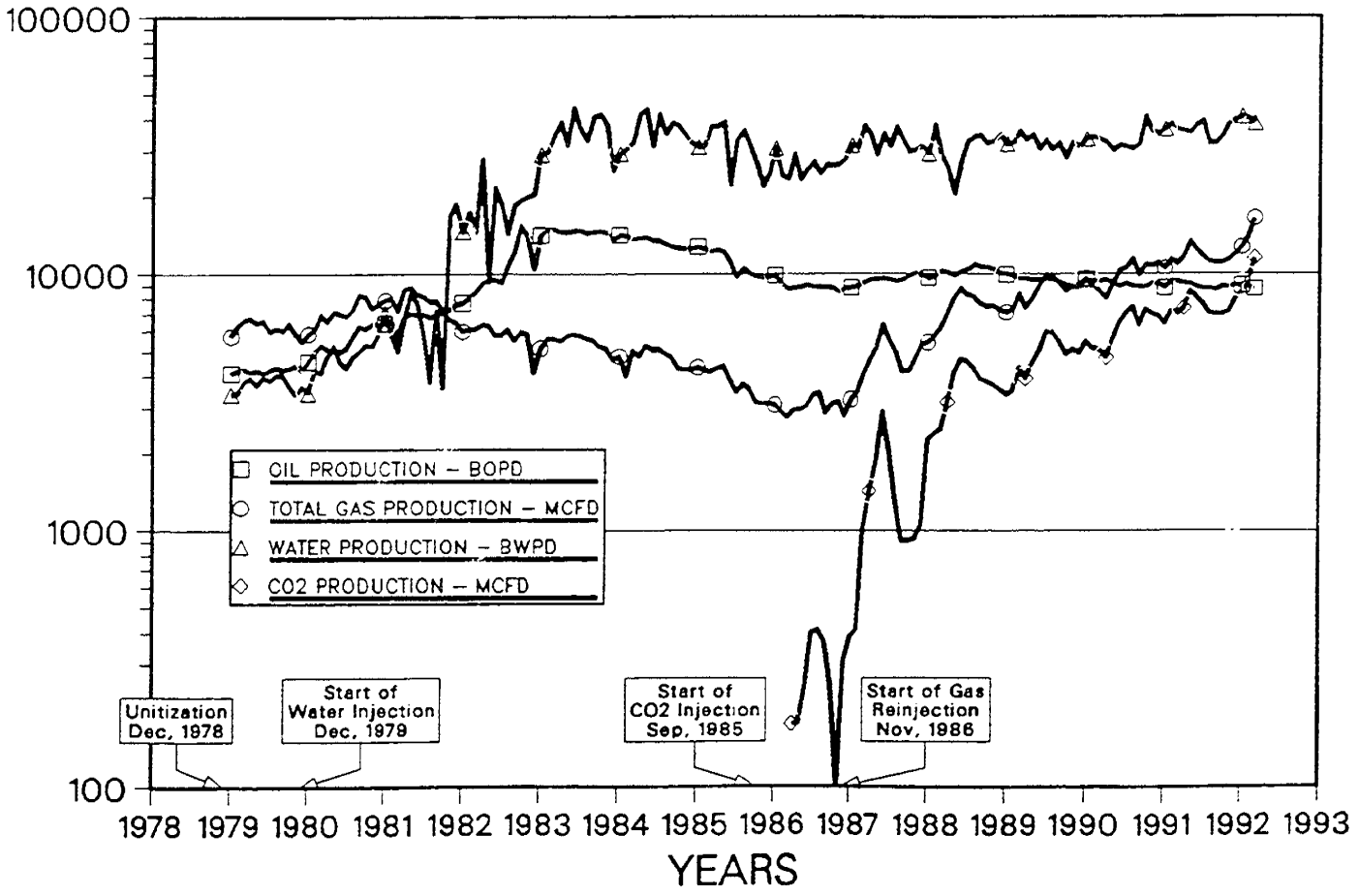

Figure 1 - EVGSAU Production History

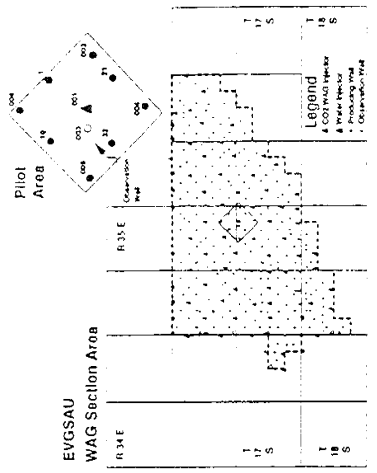

Figure 3 - Location of the Foam Pilot Pattern

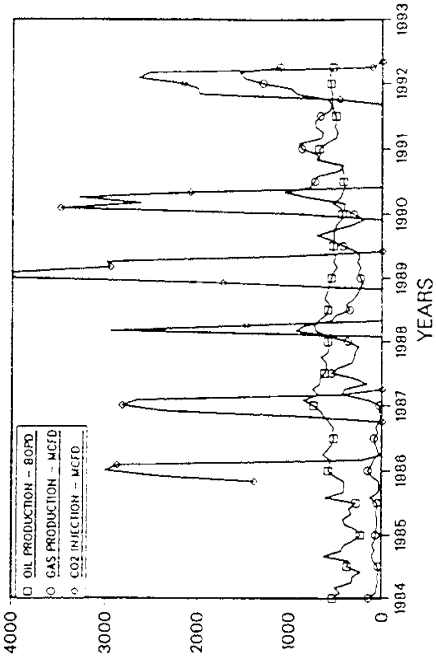

Figure 4 - Foam Pattern Performance History (8 producers/ 1 injector)

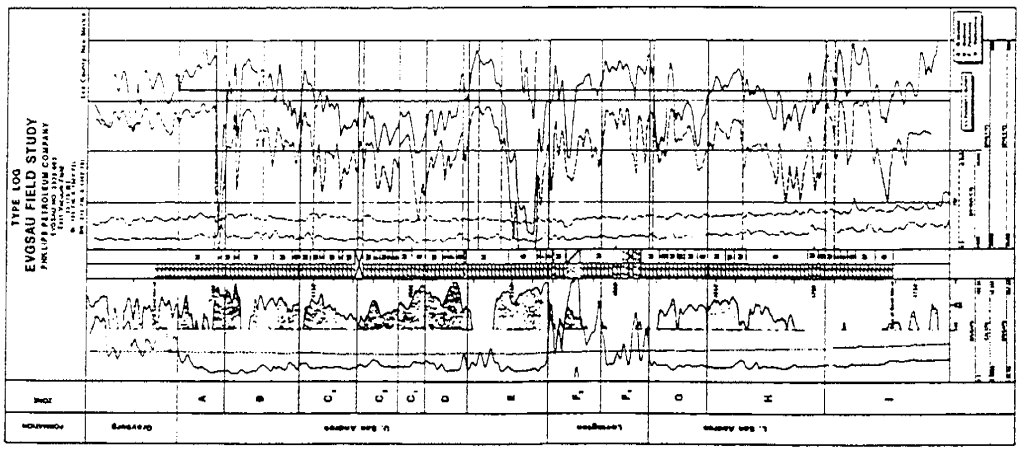

Figure 2 - Type Log Showing Geological Zonation in the EVGSAU Foam Pilot Area

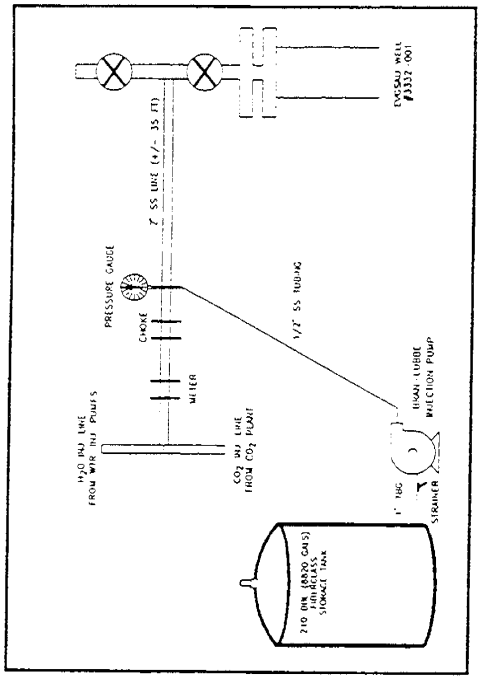

Figure 6 - EVGSAU Foam Injection Equipment Layout

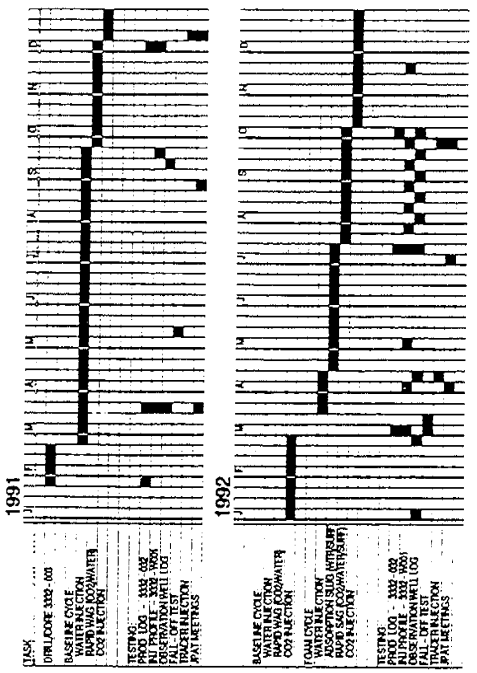

Figure 5 - EVGSAU CO_2 Foam Project Schedule

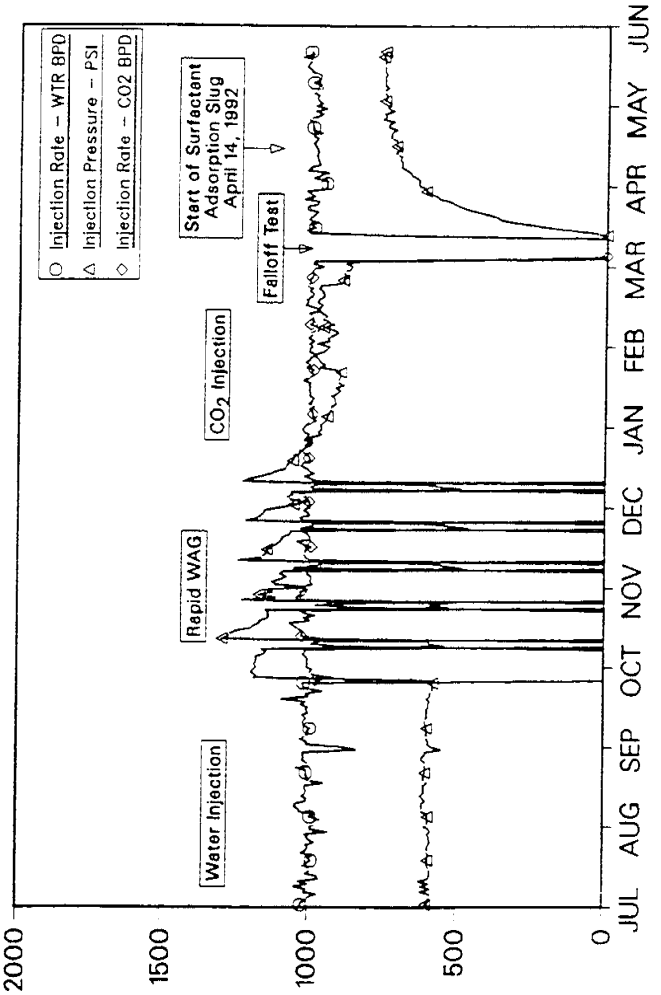

Figure 7 - Injection Well 3332-001 Pressure and Rate History

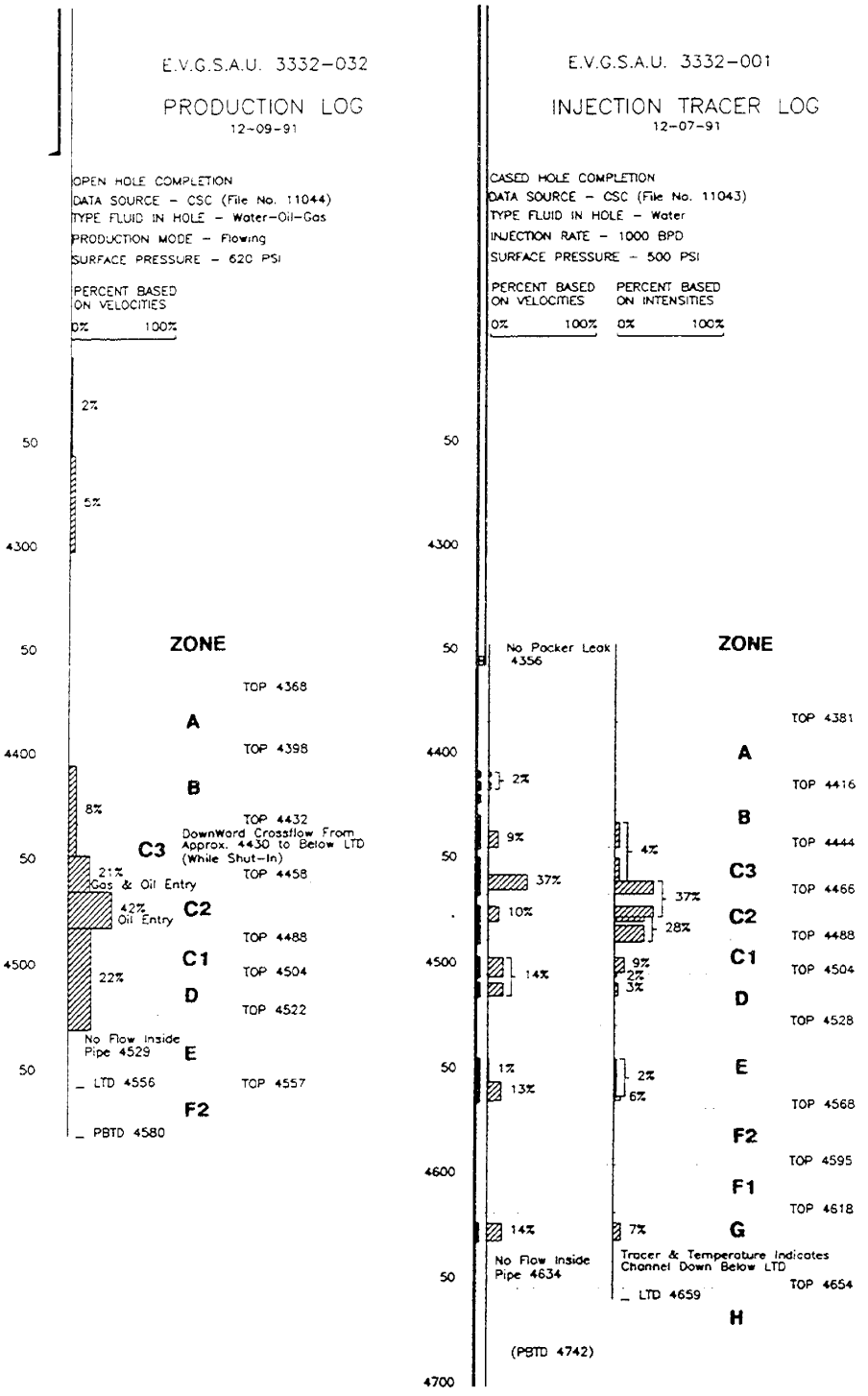

Figure 8 - Well 3332-001 Injection Profile and Well 3332-032 Production Log

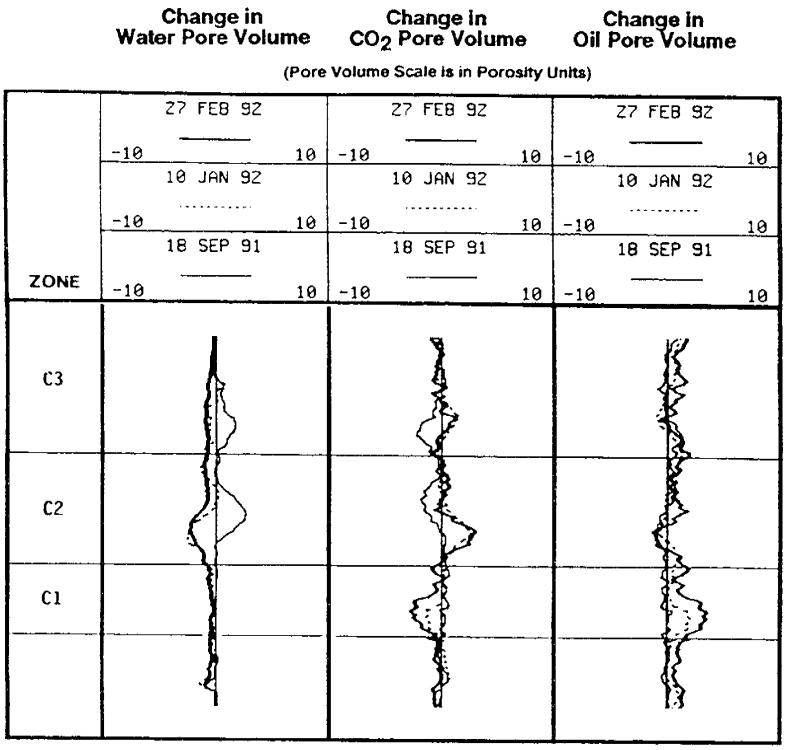

Figure 9 - Sequential Logging Runs in Observation Well 3332-003 (All Runs Relative to Base Log Run of March 20, 1991).

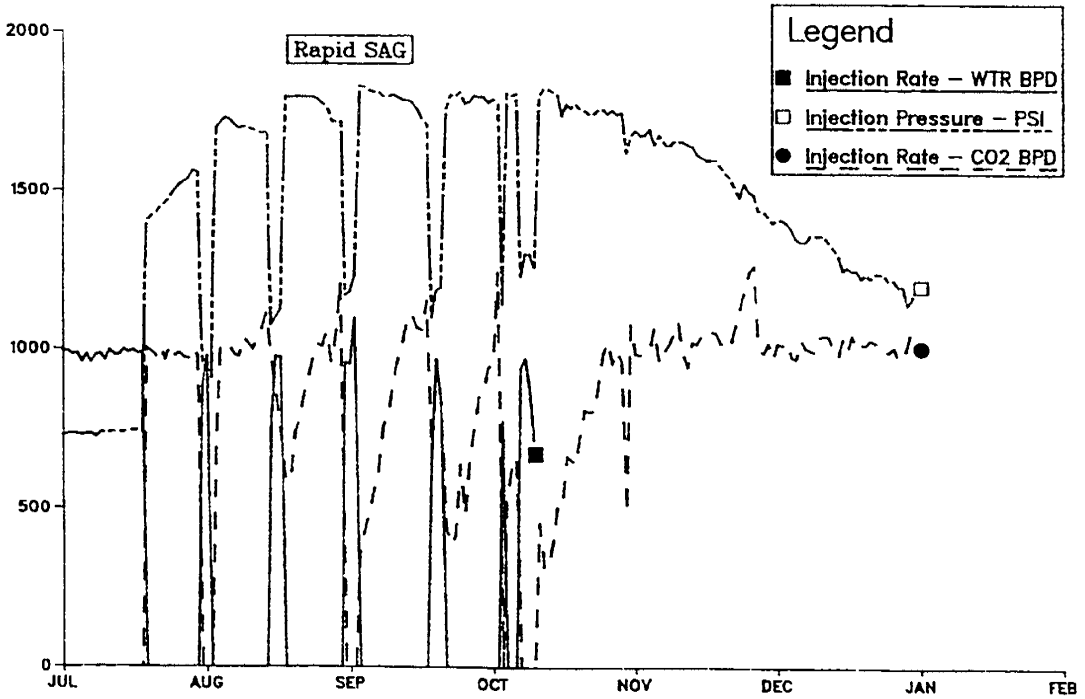

Figure 10 - Injection Well 3332-001 Pressure and Rate History During Foam Generation and Subsequent CO_2 injection. July 1992 to January 1993.

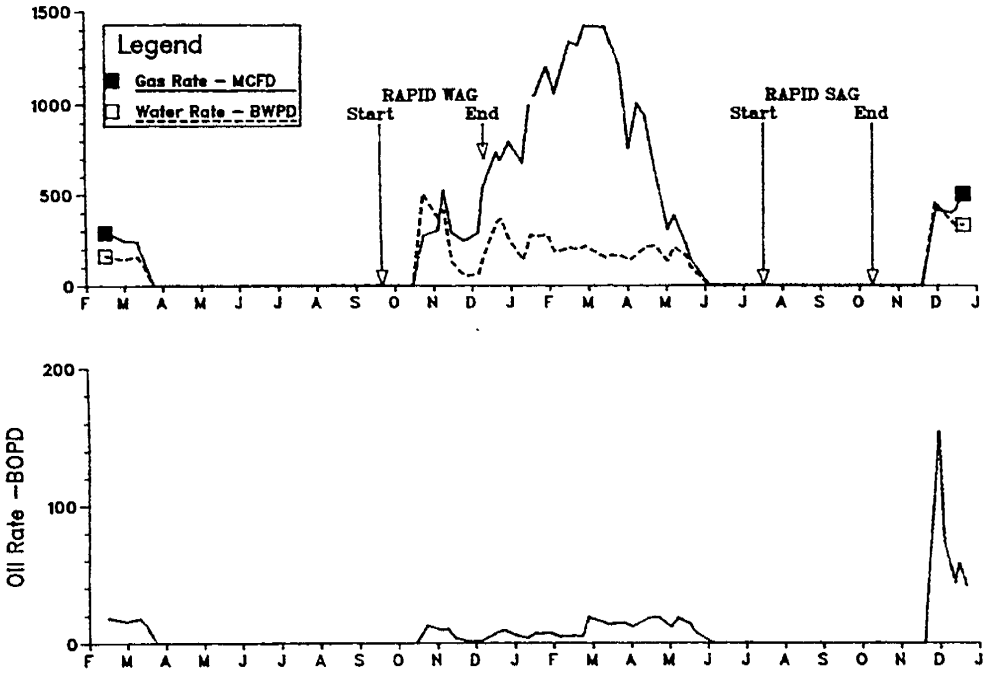

Figure 11 - Weekly Production Tests for Well 3332-032 "The Offending Well" With Rapid WAG and Rapid SAG Sequences Indicated. February 1991 to January 1993.

DOE/NIPER

Well Treatment Against Gas Coning Must Exploit Gravity Effects

by S. Ekrann and J. E. Hanssen, Rogaland Research, Stavanger, Norway

Author(s) are solely responsible for copyright and contents.

This paper was prepared for presentation at the DOE/NIPER, Symposium on Field Application of Foams for Oil Production held in Bakersfield, California, February 11-12, 1993.

This paper was selected for presentation by a Program Committee following review of information contained in an abstract submitted by the author(s). Contents of the paper, as presented, have not been reviewed and are subject to correction by the author(s). The material, as presented, does not necessarily reflect any position of the U.S. Department of Energy or the National Institute for Petroleum and Energy Research.

Abstract

The paper discusses production well treatments to reduce gas coning problems. Thin, homogeneous, horizontal reservoirs are considered. It is shown, by analytical methods and from simulations, that well treatments must rely on gravity to be effective. With strongly supercritical production rates, therefore, one expects coning problems to be difficult to remedy. With only relatively weakly supercritical rates, the ideal treatment should produce a horizontal barrier to flow, positioned somewhere above the production perforations. Such a barrier is more effective the larger its lateral penetration, and the closer it is to the perforations.

The *foam block* process achieves the required deep penetration by gravity controlled injection. A liquid foamer is injected, with a density between that of the reservoir oil and that of the reservoir gas. Under favourable circumstances the foamer will penetrate some 10's of meters into the formation in a matter of weeks, by gravity spreading along the gas-oil contact. Once oil production is resumed, reservoir gas will try to penetrate the blanket of foamer, generate foam, and thus block its own progress. Laboratory experiments demonstrating the basic feasibility of this process are briefly reported.

Introduction

Gas *coning* is the process by which gas in an overlying gas cap is drawn down against the forces of gravity into production perforations in the oil zone. The term is coined in reference to the cone-shaped gas-oil interface obtained, with vertical wells. Similarly, with an underlying aquifer, one may experience water coning.

Coning implies production of free gas and/or water in addition to the target oil. Such coproduction is generally unwanted, for a number of reasons:

- Extra processing capacity required
- Reduced oil rate
- Lift problems (water production)
- Loss of drive energy
- Loss of oil as residual[9,14]

Presented at NIPER/DOE Symposium on Field Application of Foams for Oil Production, Bakersfield Feb. 1993. Previously presented at IEA Collab. Proj. on EOR, 13th Symp./Workshop, Banff Sept. 1992.

Two complementary concepts are in use to characterize a well's tendency for coning: The *critical rate* to coning is the largest oil production rate possible in steady state without attendant production of unwanted fluids. The *time to breakthrough* is the length of the initial period from start of production until an unwanted fluid is first produced. The literature gives many alternative methods to compute critical rates for vertical[4,5,25,49] and horizontal[4,7,16,28,31] wells. Methods to compute the time to breakthrough are in shorter supply, although some results do exist, both for vertical[2,43] and horizontal[33,34] wells.

According to Høyland et al.,[25] the critical rate to coning, q_c, for a vertical well is

$$q_c \propto \Delta\rho\, h_o^2 \frac{k_h}{\mu_o} q_{cD}\,, \qquad (1)$$

where h_o is the thickness of the oil zone, and q_{cD} is a dimensionless critical rate. q_{cD} is a function of the dimensionless drainage radius, $r_{eD} = (r_e/h_o)(k_v/k_h)^{1/2}$, and also depends on the length and position of the perforated interval. An increase of r_{eD} from 0.5 to 20 reduces q_{cD} by a factor of about 10, see Ref. 25. The oil zone thickness h_o is seen by Eq. 1 to be of the major importance in determining a well's susceptibility to coning, since the critical rate increases with h_o more rapidly than does h_o^2. Also important is the density difference, $\Delta\rho$, between oil and the unwanted fluid in question, the horizontal permeability, k_h, and the oil viscosity, μ_o. Finally, the critical rate increases weakly with decreasing vertical permeability, k_v. The significance of the r_e dependence is somewhat unclear, since one needs to impose unrealistic boundary conditions at the outer boundary in order to obtain steady state, as described later.

A similar picture emerges for time to breakthrough, t_{bt}. Sobocinski and Cornelius[43] give t_{bt} for a vertical well as

$$t_{bt} \propto \frac{\mu_o h_o}{\Delta\rho k_v} t_{btD}\,, \qquad (2)$$

where t_{btD} is a dimensionless time to breakthrough, proportional to $(\Delta\rho k_h h_o^2)/(\mu_o q)$ if the production rate, q, is strongly supercritical. Thus, in this case

$$t_{bt} \propto \frac{k_h}{k_v}\frac{h_o^3}{q}\,. \qquad (3)$$

Again, the dramatic importance of the oil zone thickness is apparent, as is the advantage of a high horizontal permeability. The vertical permeability influences t_{bt} much more than it does the critical rate. For

extremely low k_v's, $k_v = 0.001\,k_h$, say, a large fraction of the original OIP may be produced prior to breakthrough, even if the production rate is strongly supercritical.[9,14] Such low effective k_v's may conceivably occur, *e.g.*, in very shaly formations.

Although the analytical results outlined above are based on simplifying assumptions, they do bring out clearly the important sensitivities. Coning tendencies for vertical wells increase with

- decreasing oil zone thickness
- decreasing horizontal permeability
- increasing oil viscosity
- decreasing density difference
- increasing vertical permeability

Most fields will experience coning problems, at least towards the end of their life, when the remaining oil zone becomes thin. The obvious remedy of strongly reducing the production rate, *e.g.*, to below the critical, is often not applicable, since low rates may be uneconomical. Any practical method to reduce coning at a given total production rate should be of considerable interest, therefore.

Horizontal wells have been shown theoretically[4,9,14,21,26,27,33] and by field experience[3,9,26,32,39] to have significantly better coning characteristics than vertical wells. In fact, this is often a major motivation for drilling horizontal wells in the first place.[3,21,30,35,41] In this paper we shall consider production well treatments to reduce coning. Indications are that horizontal wells are much harder to improve upon than are vertical wells.[12] Only vertical wells will be considered in the paper.

Extensive field experience exists on well treatments to protect against water production.[9] Over the years, many substances have been used for injection or *in-situ* generation with the aim of shutting off water. Proposed techniques include controlled-precipitation fluids,[24] circulation fluids,[42,48] foams,[38] resins,[15,22] inorganic gels,[29] as well as organic polymer and gel systems.[50] The latter substances, preferably with the ability to reduce water permeability without affecting oil permeability too much,[44] have received much attention lately, and are well covered in recent literature and by other contributors at this Symposium. Such treatments may be relatively cheap if successful: $8 /bbl extra oil has been quoted for a series of treatments using one particular technology.[46] Field experience is somewhat erratic, however, some treatments being very successful while others are unqualified failures.[44,50] Few attempts have been made to analyze the fluid flow mechanisms by which treatments work. This lack of understanding in turn makes the design of treatments difficult, and presumably contributes to the erratic field experience.

In oil zones sandwiched between an overlying gas cap and an underlying aquifer, gas coning will generally tend to be a larger problem than water coning,[9,14] essentially because of the order(s) of magnitude lower viscosity of gas. The paper will concentrate on gas coning. The fluid flow mechanisms are identical in the two cases, however. Most results should be valid also for water coning, therefore, at least qualitativly.

The paper describes a study of generic well treatments to reduce coning tendencies. A production well treatment consists of injecting into the reservoir some treatment substance. Upon resumption of oil production, the treated zone should contribute to shutting off or reducing the production of gas. We will study the consequences on production profiles of successful treatments, and not the chemical makeup of the injectants themselves. The problem is addressed analytically at first. This requires heavy idealization, but provides a framework in which to understand and analyze later simulation results. A simulation study is reported, which confirms and quantifies the analytical findings. Finally, *foam* is advocated as a treatment substance against gas coning, based on experiments, having the major advantage of being possible to place where it is most beneficial.

Analytical Considerations

Geometry

We consider the geometry illustrated in Fig. 1. A vertical well is centrally located in a circular drainage area. The oil zone is overlain by a gas cap. Capillary effects are neglected, such that there is a sharp gas-oil interface (GOC). The GOC is kept constant at the outer boundary, which is a constant pressure boundary. Oil and gas are incompressible. Thus, oil and gas are fed in through the boundary to compensate for production. This configuration allows steady-

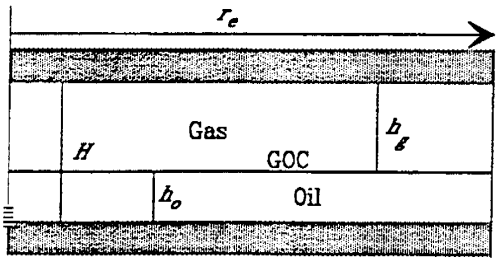

Figure 1: Lateral drive geometry

state solutions, and is frequently used to derive critical rates.[4,12,16,25,26,31,49]

Steady-State GOR Without Gravity

We shall assume in this section that gravity can be neglected, *i.e.*, the production rate is assumed to be large enough to let viscous forces dominate completely over gravity forces.

If H/r_e is sufficiently small, the GOC must remain essentially horizontal far from the well. With a hori-

zontal GOC, potential gradients are strictly horizontal, and do not vary vertically. Both phases see the same horizontal potential gradient, therefore, and we must have in steady state

$$R_{Fs} \approx R_{F\mathrm{lim}} \stackrel{def}{=} \frac{h_g \lambda_{hg}}{h_o \lambda_{ho}} . \quad (4)$$

Here, R_{Fs} is the steady-state producing gas-oil ratio, and λ_h is the (endpoint) horizontal mobility.

By Eq. 4, R_{Fs} is independent of near-well details. Thus, well treatments are expected to have no influence whatsoever on the steady-state GOR. If, *e.g.*, the near-well gas relative permeability could be reduced by orders of magnitude without influencing the oil relative permeability, the net long-term effect should only be an increased gas saturation in the treated region (to allow the local GOR to equal R_{Fs}), and an associated increased pressure drawdown.

Thus, as a tentative conclusion, a well treatment can be beneficial at most temporarily, even if the integrity of the treatment itself remains perfect, if gravity effects are absent.

With gravity effects, equality of potential gradients far from the well may no longer be assumed. A GOC which is not quite horizontal may introduce hydrostatic effects comparable in magnitude to viscous effects. Thus, the conclusion above is no longer necessarily true. The next section generalizes the discussion to include gravity.

Also, the relevance in practical situations of steady-state considerations is far from obvious. It remains to determine how temporary is "temporary". The approach to steady state is not well covered in the literature. We shall not attempt an analytical treatment, but rather rely on simulations.

Steady-State GOR With Gravity

Appendix A develops individual phase steady-state production rates in the presence of gravity effects. The geometry is as illustrated in Fig. 1, except that an underlying water zone was added for generality. In the two-phase case of interest here, results can be manipulated to yield

$$R_{Fs} = R_{F\mathrm{lim}} \frac{1 - q_c/q}{1 + R_{F\mathrm{lim}}\, q_c/q} , \quad (5)$$

and

$$q_{os} = q \left[(1 - \frac{q_c}{q})(1 + R_{F\mathrm{lim}})^{-1} + \frac{q_c}{q} \right] , \quad (6)$$

where q_{os} is the steady-state oil production rate. As can be seen, R_{Fs} approaches $R_{F\mathrm{lim}}$ as q approaches infinity, as it should.

While approximate, these expressions do suggest some conclusions. First, if $R_{F\mathrm{lim}} \gg 1$, then $q_{os} \approx q_c$ for all q, as long as $q/q_c \ll R_{F\mathrm{lim}}$. Increasing the total production rate in this range, therefore, increases the gas rate while leaving the oil rate nearly constant.

Second, in realistic situations the total fluid production rate q may be practically fixed by, *e.g.*, processing capacity. By Eq. 6, a well treatment should aim at increasing the critical rate to coning, q_c, which in turn would increase the steady-state oil production rate, q_{os}, for a given q. Suppose that we are able to increase the critical rate by a factor of α. The resulting incremental steady-state oil rate becomes

$$\begin{aligned} \Delta q_{os} &\stackrel{def}{=} q_{os}(q_c = \alpha\, q_c^{\mathrm{orig}}) - q_{os}(q_c = q_c^{\mathrm{orig}}) \\ &= q_c^{\mathrm{orig}} (\alpha - 1)\left(1 - (1 + R_{F\mathrm{lim}})^{-1}\right) , \end{aligned} \quad (7)$$

where q_c^{orig} is the original (untreated) critical rate, and where we have assumed that the production is supercritical even after treatment. The incremental oil rate is proportional to q_c^{orig}, and does not depend on q. Thus, well treatments must be expected to be most effective, in absolute terms, in situations where oil production is not too bad from the outset, *i.e.*, where q_c^{orig} is not too low compared to the given total rate, q. This qualitatively agrees with the previous discussion, which concluded that no steady-state benefits should be expected from well treatments in the complete absence of gravity effects.

Simulations

A suite of simulations was carried out using ECLIPSE,[8] a commercial finite difference reservoir simulator. Two sets of reservoir data were used. The first set of data describes a situation similar to that used for the analytical considerations above, to facilitate comparisons. The second set is more realistic, *i.e.*, with compressible gas and a closed outer boundary.

In each case we compare two classes of well treatment. One class has a treated zone which surrounds the production perforations, and extends but a few meters into the reservoir. This is the type of geometry one expects to obtain naturally by injecting through the production perforations, when no particular control over the injection process is exercised. In the simulations, we let the relative permeability to gas be reduced by a factor of 10^3 in the treated zone, while the relative permeability to oil is unaltered. We shall refer to this as (near-well) treatment, and to treated wells. Our base case treatment has a 10 m thick treated zone with 4.5 m radius, see Fig. 2.

The second class of treatment has a thin horizontal, impermeable (to both phases) barrier somewhere above the production perforations. This barrier may extend an appreciable distance into the reservoir. To obtain a treated zone of such a shape, the injection must obviously be controlled in some way. This is a point to which we will return later. Our base case barrier has a radius of 49.5 m and is positioned 10 m above the bottom of the reservoir, *i.e.*, in the middle of the oil zone, see Fig. 3.

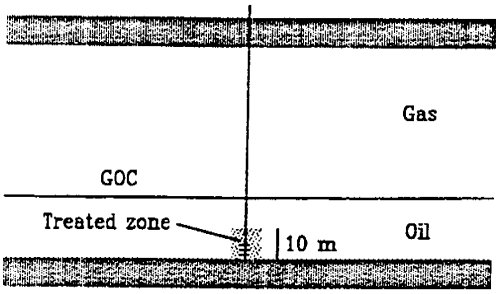

Figure 2: Base case near-well treatment geometry

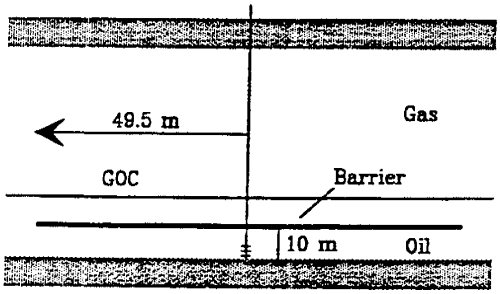

Figure 3: Base case barrier geometry

Incompressible Fluids, Constant Pressure Boundary

A horizontal reservoir is considered, with a single production well positioned in the centre of a circular drainage area, as illustrated in Fig. 1. The well is completed from the bottom of the reservoir. Fluids are (near) incompressible, and the lateral boundary is (approximately) a constant pressure boundary. Capillary effects are absent. Relative permeabilities are rectilinear. Other base case reservoir and fluid data are given in Table 1.

Drainage radius, r_e, (m)	999.5	
Well radius (m)	0.1	
Horizontal permeability (D)	10	
Porosity	0.3	
k_v/k_h	1	
Completion interval (m)	5	
Fluid production rate (Rm^3/d)	1500	
	Oil	Gas
Viscosity (cp)	1	0.01
Endpoint rel. perm.	1	1
Residual saturation	0	0
Zone thickness (m)	20	50
Density (kg/m^3)	500	499.9
	800	300

Table 1: Base case reservoir and fluid data

Simulations were carried out with 65 gridblocks radially and 18 gridblocks vertically. Vertical gridblock dimensions were 2.5 m (8 bottom blocks) and 5 m (10 top blocks). Radial gridblock dimensions were, from the well block outwards, 10 x 1 m, 10 x 2 m, 10 x 4 m, 9 x 10 m, 10 x 20 m, and 16 x 40 m.

The total fluid (oil + gas) production rate was fixed during each simulation. If only oil is produced, 100 % of the OOIP will have been produced after about 12500 days, at the $1500\,m^3/d$ production rate.

The effect of well treatments was investigated in the absence ($\rho_o = 500\,kg/m^3$, $\rho_g = 499.9\,kg/m^3$) and presence ($\rho_o = 800\,kg/m^3$, $\rho_g = 300\,kg/m^3$) of gravity effects. Equal densities are not realistic, and are chosen here for simplicity. Identical results would have been obtained by increasing the production rate sufficiently, or by decreasing the permeability.

Figs. 4 and 5 show the oil production rate and the cumulative oil production, respectivly, in the negligible gravity case. Results are shown for an untreated well, and with the base case near-well treatment and the base case barrier.

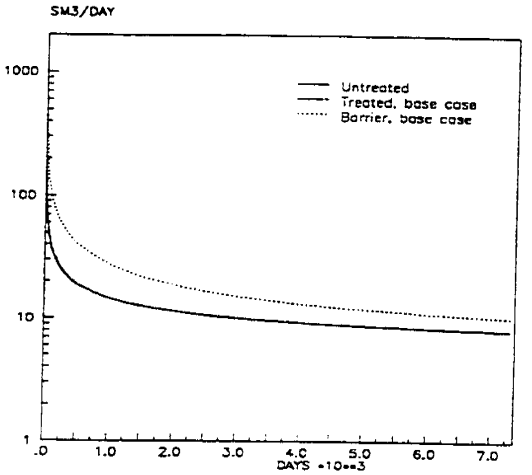

Figure 4: Oil rate. Equal densities

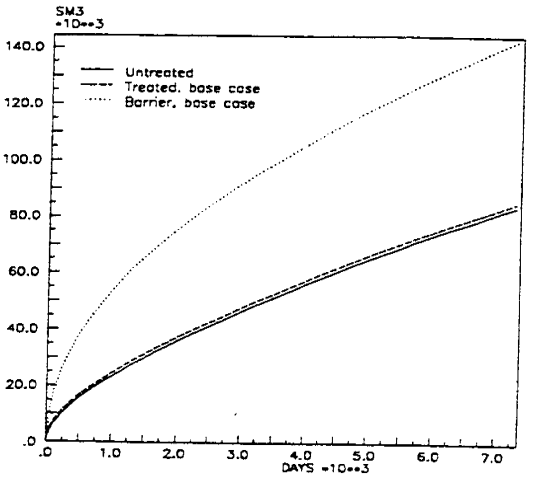

Figure 5: Cumulative oil production. Equal densities

A production rate of $1500\,m^3/d$ corresponds to a steady-state oil rate of 6 m^3/d, compare Eq. 4, for all three wells. Steady state can be seen not to have been

obtained after 7000 days. Even so, there is hardly a difference between the oil production rates of the treated and untreated wells, except in a short initial period. The barrier makes an appreciable difference, however. The barrier extends 49.5 m into the formation, as opposed to the 4.5 m radius of the near-well treatment. This, it would appear, is sufficient to delay gas production noticeably. Even the barrier case has less than 1 % of the OOIP produced after 6000 days, however.

Fig. 6 shows the pressure drawdown, $p_e - p_w$, vs. time. The treated well has a stabilized drawdown about 100 times larger than the untreated/barrier wells. This large drawdown is obtained in the first few days. As anticipated, it is caused by a very high gas saturation in the entire treated zone.

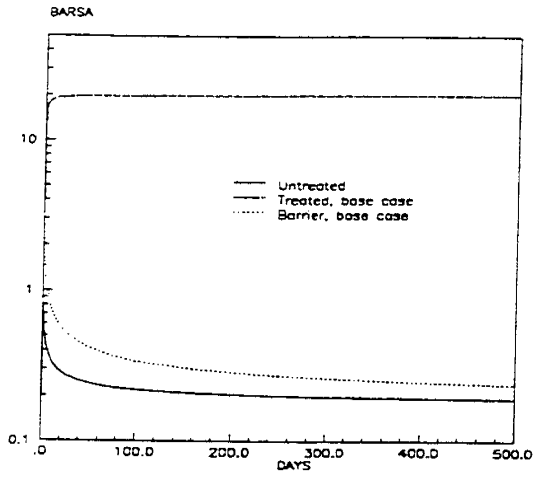

Figure 6: Pressure drawdown. Equal densities

The simulations were repeated with $k_v/k_h = 10^{-3}$. Fig. 7 shows the cumulative oil production for the untreated and treated wells. Again, the difference is insignificant. The production is much higher in this case, however, due to the delayed production of gas, compare Eq. 3. At 6000 days, the oil rates are about $130\,\mathrm{m^3/d}$, an order of magnitude larger than the steady-state rate. The late time pressure drawdown is now about a factor 40 larger for the treated well, again caused by increased gas saturation in the treated zone.

Steady state is not achieved in these simulations. Even so, our previous conclusions based on steady-state considerations turn out to hold true. Transient effects will not save the day for near-well treatments, if gravity is negligible. Even in production situations where steady state is never even approached, the difference in oil rate between treated and untreated wells quickly disappears, resulting in an insignificant increase in the cumulative oil produced with a treated well. The main effect of a near-well treatment is increased drawdown.

Next, we turn on gravity by letting $\rho_o = 800\,\mathrm{kg/m^3}$ and $\rho_g = 300\,\mathrm{kg/m^3}$. With other data unchanged

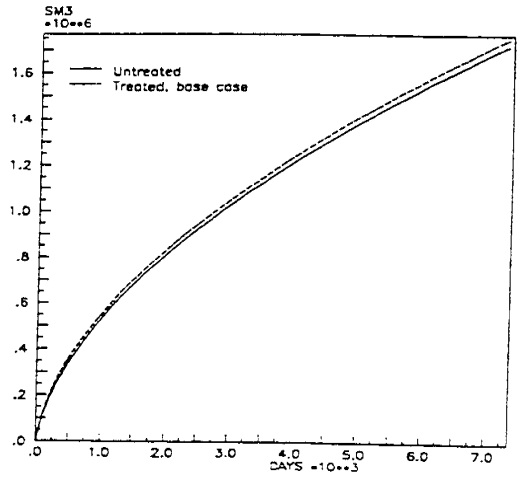

Figure 7: Cumulative oil production. Equal densities. $k_v/k_h = 10^{-3}$

($k_v/k_h = 1$), $q_c \approx 750\,\mathrm{m^3/d}$, from Høyland et al.[25] With $q = 1500\,\mathrm{m^3/d}$, the steady-state oil production rate becomes $q_{os} = 753\,\mathrm{m^3/d}$ by Eq. 6, for the untreated well. This is two orders of magnitude larger than the corresponding gravity-free rate.

Fig. 8 shows the actual oil production rate for the untreated well, for our base case near-well treatement and for the base case barrier. In addition, results for a 0.5 m radius near-well treatment is shown, as well as for a 4.5 m radius barrier positioned 2.5 m above the bottom of the reservoir. The well is completed only in the lowermost 2.5 m in the latter case.

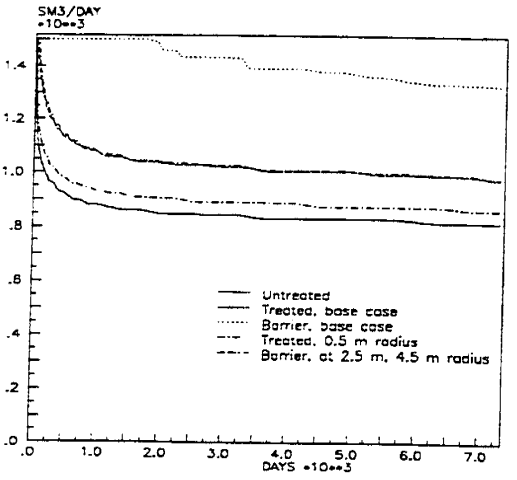

Figure 8: Oil rate. Unequal densities

Except for the base case barrier, all wells seem to be near steady state at 2000 days, say. The untreated steady-state oil rate is close to that estimated above. Even the 0.5 m radius near-well treatment increases the steady-state oil rate by some 50 $\mathrm{m^3/d}$. Our base case 4.5 m radius treatment increases the steady-state oil rate by some $160\,\mathrm{m^3/d}$, while the base case barrier

increases the rate by some 500 m^3/d.

It is also interesting to note that the 4.5 m radius barrier results in almost exactly the same production profile as the base case near-well treatment. This is actually a striking illustration of the mechanism by which the near-well treatment works. Consider Fig. 9, showing the stabilized gas saturation in the vicinity of the well. The gas saturation is very high in the treated zone, except in the lowermost layer of gridblocks. With a high gas saturation, the permeability to both oil and gas is low. Thus, the treated zone acts to effectivly plug the perforations above 2.5 m. Also, it acts as a barrier, positioned at 2.5 m, and with a 4.5 m radius. It is not surprising, therefore, that production profiles match so well.

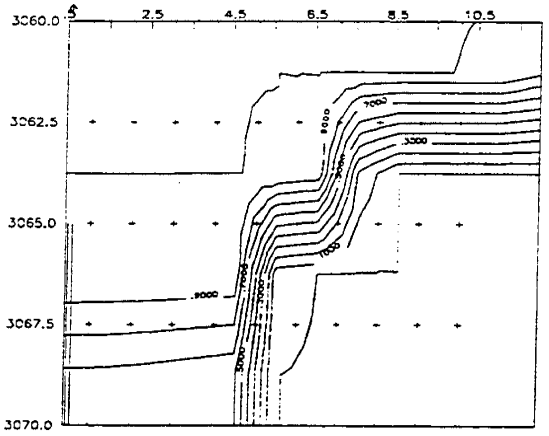

Figure 9: Stabilized gas saturation for base case near-well treatment. Unequal densities. Gridblock corner points shown

In the 0.5 m radius treatment case, the effective reduction of the length of the perforated interval presumably accounts for the improvement by itself, the lateral penetration of the barrier being too small to provide extra protection. Thus, a very small radius treatment like this is at best equivalent to a recompletion.

It can be seen from Fig. 9 that there is an appreciable gas saturation even in the lowermost layer of gridblocks, which should imply a larger pressure drawdown than in the true barrier case. This is indeed so, as shown in Fig. 10. The increased drawdown for the untreated well (compare Fig. 6) is caused by hydrostatic effects.

A reduction of k_v/k_h to 0.1 delays breakthrough of gas to after 7000 days even for the untreated well in this case.

Fig. 11 shows the oil rates when the total production rate has been increased threefold to 4500 m^3/d. The pattern is very similar to that of Fig. 8. Steady-state oil rates are seen to have increased only slightly. Thus, the increased production is almost entirely made up of gas, as predicted by Eq. 6.

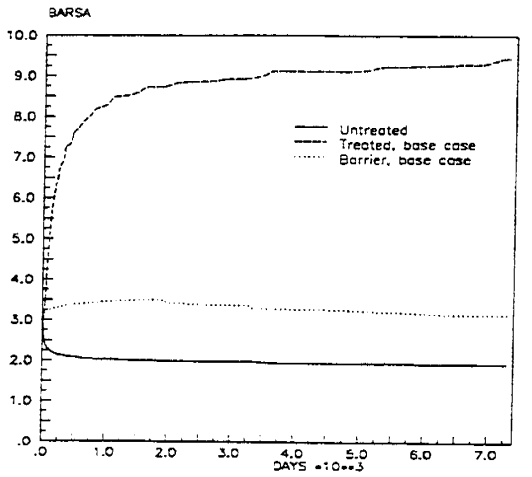

Figure 10: Pressure drawdown. Unequal densities

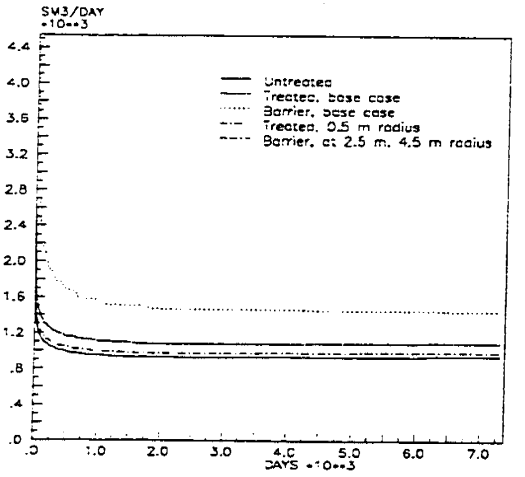

Figure 11: Oil rate. Unequal densities. Total rate 4500 m^3/d

Compressible Gas, Closed Reservoir

In real life, unfortunately, there is no such thing as a constant pressure boundary to feed oil into the reservoir. We have repeated the simulations, therefore, in a closed reservoir where the drive energy is provided by gas compressibility. Other data are as in the previous case, see Table 1, except that the drainage radius is reduced to $r_e = 499.5$ m, which is a somewhat more realistic value, in offshore environments.

Simulations were carried out with 56 gridblocks radially and 30 gridblocks vertically in this case. Vertical gridblock dimensions were 1 m (20 bottom blocks) and 5 m (10 top blocks). Radial gridblock dimensions were, from the well block outwards, 10 x 1 m, 10 x 2 m, 10 x 4 m, 9 x 10 m, and 17 x 20 m.

Two cases were studied, both with gas formation volume factors varying almost linearly with pressure, and with no gas dissolving in the oil. Oil is incompressible in both cases, with a density of 800 kg/m^3.

In the first case, the gas density is 133 kg/m^3 initially and 67 kg/m^3 after 20 years of production. Fig. 12 shows the oil production rates, for the untreated well and for two near-well treatments and two barriers, all at our standard 1500 Rm^3/d total production rate. The staircase-like appearance of these curves at late times is a numerical artifact, each "step" corresponding to the passing of the GOC to a new layer of gridblocks.

The 4.5 m barrier and base case near-well treatment still exhibit very similar production profiles, confirming previous observations. The near-well treatment

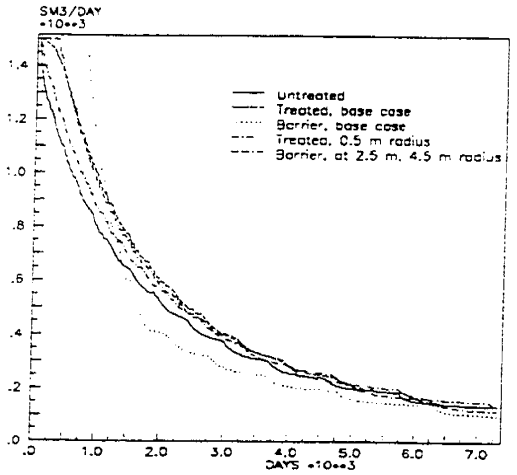

Figure 12: Oil rate. Closed reservoir, compressible gas

actually performs slightly better than the barrier in this case. This is presumably caused by the gridding used. The gas saturation now effectively shuts off oil in all but the lowermost 1 m of the reservoir, see Fig. 13, which by our reasoning should correspond to a barrier positioned 1 m above the bottom, and not the 2.5 m of the actual barrier.

The fact that only the lowermost numerical layer is effectively open to oil flow, even when its thickness is reduced from 2.5 m to 1 m, makes one suspect that the solution is not converged. If the correct solution has only a very thin channel open, the reduction in productivity may be very large. This point has not been pursued.

There is one dramatic difference between the patterns exhibited by Figs. 12 and 8. While the base case barrier initially shows superior performance even with compressible gas, the oil rate reduces rapidly after breakthrough, to drop below that of the untreated well at some 1300 days. There is still much producible oil left in the reservoir at this point, as seen in Fig. 14. Total mobile oil initially present is 4.7 10^6 Rm^3. The effect is caused by the global GOC moving downwards with time, as gas expands, eventually to slip under the barrier. This is clearly seen on saturation plots (not shown). If the barrier could be made to move downwards with the GOC, dramatic improvements of

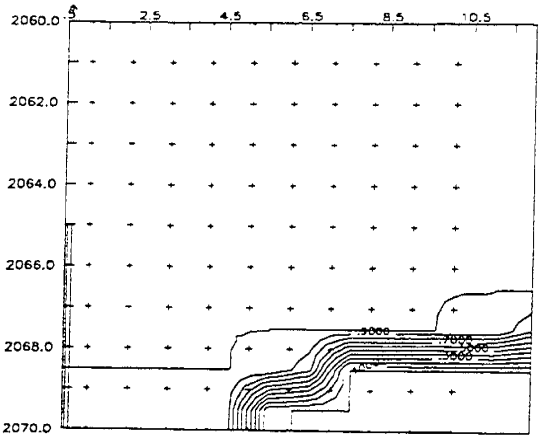

Figure 13: Stabilized gas saturations for base case near-well treatment. Closed reservoir, compressible gas. Gridblock corner points shown

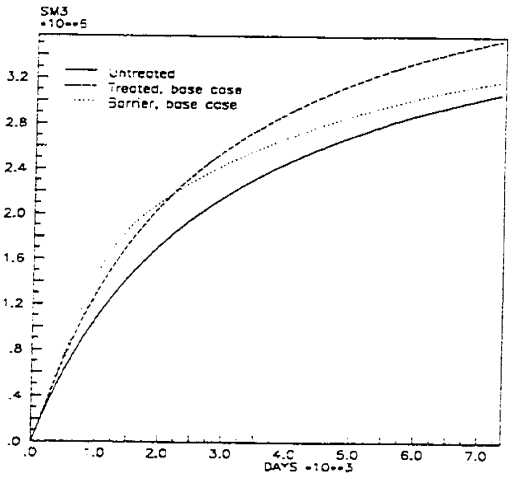

Figure 14: Cumulative oil production. Closed reservoir, compressible gas

late time performance should be expected. To demonstrate this effect, the simulation above was repeated, except that the barrier was moved to a position 5 m above the bottom of the reservoir after 1900 days. A dramatic improvement ensues, see Fig. 15.

To demonstrate the importance of gravity effects, even in the compressible case, the simulations above were repeated with a gas having initially the same density as oil, and dropping to 400 kg/m^3 after 20 years of production. Fig. 16 shows oil production rates. ECLIPSE could not be persuaded to simulate the base case barrier well further than 3750 days, for some unknown reason.

Initially, gravity effects are weak and the oil rate decreases very rapidly, compare Fig. 4. As gas is produced, however, reservoir pressure and therefore gas density decreases. As gravity effects become significant, the oil rate increases. At late times the pattern

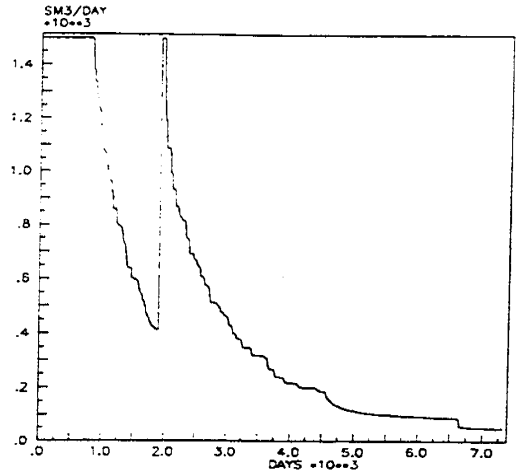

Figure 15: Oil rate with base case barrier, moved at 1900 days. Closed reservoir, compressible gas

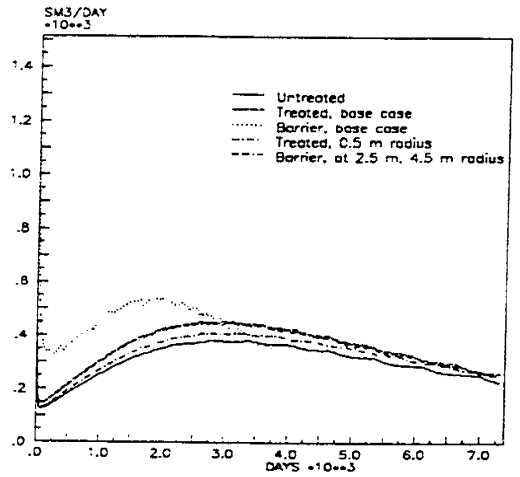

Figure 16: Oil rate. Closed reservoir, compressible but denser gas

becomes similar to that in the previous case, except that oil rates are now higher since there is more oil left in the reservoir.

Remark

Reasoning above concentrated on long-term effects, both for convenience and in order to facilitate comparison with the analytical results. Well treatments cannot be expected to retain their integrity for anything approaching the lifetime of a field. The reasoning may seem somewhat off the point, therefore. The simulations show, however, that the near-well saturation distribution establishes quickly for treated wells, and that the relative performance of the different wells is similar in the transient period to that in steady state. We maintain, therefore, that the conclusions are valid even for relatively short-lived treatments.

Foam as a Gas-Coning Barrier

We have established that well treatments to effectively reduce gas production must exploit gravity effects. Successful treatments produce horizontal barrieres to gas flow, positioned somewhere above the production perforations. It has been shown[12,45] that a barrier is more effective the larger its radius and the smaller its vertical distance from the perforations.

A foam confined inside a porous medium has the ability to reduce the effective permeability to gas by orders of magnitude, without affecting too much the relative permeability of its constituent liquid phase.[23] A hydrocarbon foam or, if both liquid phases are affected similarly, an oil-tolerant aqueous foam, would thus have properties similar to those of our previously fictitious treatment substance. This gas-blocking ability makes foam a candidate for near-well treatment, and foam injection has indeed been successful in reducing the gas-oil ratio in producing wells.[1]

Even a perfect near-well treatment has limitations, however, as demonstrated previously. The ideal treatment produces a large-radius barrier. This could in principle be obtained by extending a near-well treatment, *i.e.*, by increasing the volume of injectant. However, besides requiring an excessive volume of injectant, the bulk of which would go where it is not needed, the high apparent viscosity of flowing foam is not favourable to deep penetration. Pressures gradients during steady-state flow of strong foams in $\approx 1\,\mathrm{D}$ sandstone have been measured at 10–600 bar/m for velocities in the range 1–7 m/d.[36,37,47] Consequently, injection pressures may exceed pump capacity or fracture the formation at a relatively shallow penetration.

A novel concept has been patented which attempts to remedy these problems.[13] Instead of injecting foam, the injectant is a foaming-agent solution with a density between that of the reservoir oil and that of the reservoir gas. After injection, the well is shut in for a period of time. If injected in the oil zone, the injectant will rise by buoyancy to find the GOC, and spread along it to form a thin circular blanket of foamer. Appendices B and C give methods to estimate the timing of these events. Under favourable circumstances, the injectant can penetrate 40 m into the formation by such gravity spreading in a matter of weeks. A substantially deeper penetration would seem to be difficult to obtain in practice, since the time to reach a certain radius r is proportional to r^4.

With the foamer in place, once oil production is started, gas will try to penetrate the blanket of foamer, generate foam, and thus block its own further progress. The initial foam barrier thus generated has the major disadvantage of being positioned at the GOC. In this position, the barrier will influence the critical rate to gas coning only if it has an appreciable thickness, such that gas has to travel vertically at its rim.[12] A layer of foamer will always be present below the barrier due to drainage of liquid from the foam, causing any gas breaking through the barrier to generate more foam below it. This "latent barrier"

may be further enhanced by using an excess of injectant. At the barrier edges, gas underride will induce foamer to trickle down by gravity, causing new generation of foam below the rim of the original barrier. The end result is conjectured to be a barrier of the shape illustrated in Fig. 17. This geometry should be equivalent to the flat barriers used in the simulations, provided "earlobes" extend vertically to the position of the equivalent flat barrier, since the critical phenomenon is gas slipping underneath the barrier at its rim.[12]

The presence of a mobile layer of foamer provides the foam barrier with the ability to move, or actually regenerate, at a lower position as the global GOC moves downward. This is a highly desirable property, compare Fig. 15.

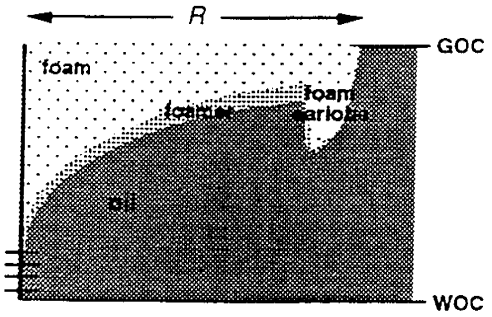

Figure 17: Conceptual shape of deep penetration foam block

This method, termed the *foam-block* process, has been studied in our laboratory for several years. In partially scaled radial physical flow models, each step of the process described has been verified for model systems,[17] except for "earlobe" formation which so far has only been inferred from the observed reduction in gas coning with a partially penetrating barrier. Other main goals of our effort have been to determine whether foams can maintain reliable gas blockage in the presence of oil at reservoir conditions,[18,19] and identify chemicals that provide this while simultaneously satisfying the density requirements.[19] Some new results are shown in Figs. 18–20.

Fig. 18 shows placement of a hydrocarbon-based foamer solution in a physical sector model. A low injection rate was chosen so that gravity dominated the placement, and a 0.1 pore volume slug penetrated two-thirds of the model radius in 150 hours. The previously described procedure of faster injection followed by gravity spreading was used for aqueous model fluids in an earlier study,[17] which also describes the general design of these models.

The effect of foam barriers on gas coning performance, also from sector model experiments, is shown in Fig. 19. The graph labeled "weak foam" is that actually generated from the slug placed in Fig. 18, which at the time of the experiment represented the maximum performance achievable with hydrocarbon foams. The graph labeled "strong foam" refers to an

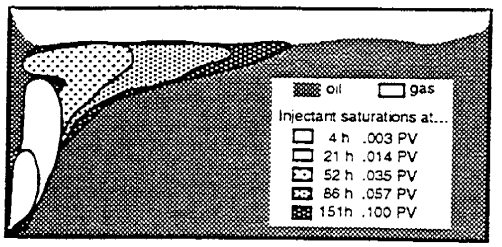

Figure 18: Placement of a 2 % solution of a proprietary nonaqueous foamer in n-decane ($\rho = 730\,\mathrm{kg/m^3}$, $\mu = 0.70\,\mathrm{cp}$) in a sector model of $k = 5.5\,\mathrm{D}$, initially saturated with a white oil ($\rho = 775\,\mathrm{kg/m^3}$, $\mu = 1.52\,\mathrm{cp}$). Injection is from left to right through the lower wellbore perforation. Digitized from photographs

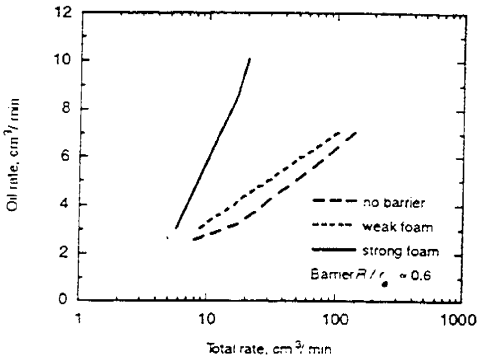

Figure 19: Experimental results from gas coning in sector models with and without foam barriers. Sector model experiments were performed at room temperature and atmospheric back pressure

aqueous foam studied earlier.[17] Through the active collaboration of selected surfactant makers, hydrocarbon foamers have been developed that match the gas-blockage performance of good aqueous systems, as demonstrated by the data depicted in Fig. 20. The custom test method by which these data were obtained is described elsewhere.[18–20]

A field trial of the foam-block process is currently being planned.

Conclusions

We have studied two generic types of well treatments to reduce gas coning. Type 1 reduces the relative permeability to gas by a factor of 10^3 in the near-well region, while leaving the relative permeability to oil unaltered. Type 2 has an impermeable horizontal barrier, positioned somewhere above the perforations. The base case type 1 treatment had a radius of 4.5 m, and the base case barrier a radius of 49.5 m.

The investigation was carried out for thin, horizontal, homogeneous reservoirs, using both analytical methods and reservoir simulation. The following conclusions emerged:

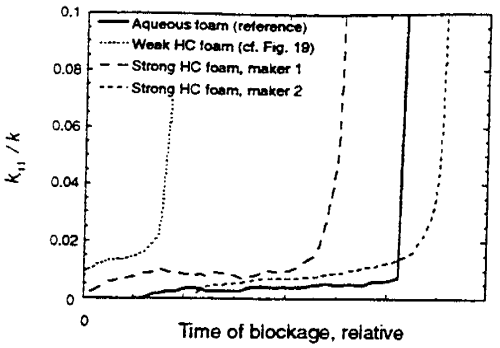

Figure 20: Foam performance by gas-blockage testing, expressed as gas permeability reduction factor vs. time. Surfactants at 1.0% concentration tested in 5.5 D, 2 m long bead packs at $\approx$ 7 bar back pressure, and an average pressure gradient of $\approx$ 1 bar/m, 70 °C

- Well treatments are more effective the more important are gravity effects
  - Well treatments are practically useless in the negligible gravity limit
  - Treatments are most beneficial, in absolute terms, if the production rate is only weakly supercritical
- Type 1 treatments increase drawdown, because of a rapidly established high gas saturation in the treated zone. This effect appears to be most dramatic in the negligible gravity limit
- A successful type 1 treatment works by essentially the same mechanism as a barrier type treatment. The top portion of the treated zone obtains a particularly high gas saturation, and acts as a barrier to both oil and gas flow
- Barriers are more effective the larger their radius and the closer they are positioned to the perforations
- The *foam block* process is a promising candidate to produce the sought-after barrier geometry, in high permeability reservoirs

Nomenclature

Symbols

F_{wo} = water-oil ratio, reservoir conditions
g = acceleration of gravity
h = thickness of zone
H = thickness of reservoir
k = absolute permeability
k_r = relative permeability
p = pressure
q = production rate
q_c = critical oil rate to coning
r = radial coordinate
r_e = drainage radius
R = radius of injectant disc
R_F = gas-oil ratio, reservoir conditions
$R_{F\mathrm{lim}}$ = gas-oil ratio in steady state, in the negligible gravity limit
t_{bt} = time to breakthrough
u = Darcy velocity
v_{rise} = rise velocity of injectant
V = volume of injectant
z = vertical coordinate
$\Delta\rho$ = density difference
λ = mobility, $\lambda = k\,k_r/\mu$
μ = viscosity
ϕ = porosity
ϕ_e = effective porosity
Ψ = potential

Subscripts

D = dimensionless
f = foam
g = gas
h = horizontal
i = injectant
o = oil
s = steady-state
v = vertical
w = water

Superscripts

g = at critical rate for gas coning
w = at critical rate for water coning

Acknowledgement

The work on which this paper is based was partly performed under contract with Statoil, Norske Shell, and SPOR. We are grateful for their permission to publish. The simulations reported were expertly carried out by Vidar Haugse. Additional funding for preparation of the paper was provided by the foam subprogram of RUTH.

References

[1] Bain, G.F., *et al.*: "Foam Treatment of Producing Wells to Increase Oil Production at Prudhoe Bay," paper SPE/DOE 24191 presented at the 1992 SPE/DOE Symposium on Enhanced Oil Recovery, Tulsa.

[2] Bournazel, C. and Jeanson, B.: "Fast Water-Coning Evaluation Method," paper SPE 3628 presented at the 1971 SPE Annual Technical Conference and Exhibition, New Orleans, Oct. 3–6.

[3] Broman, W.M., Stagg, T.O., and Rosenweig, J.J.: "Horizontal Well Performance at Prudhoe

Bay," paper SPE 20961 presented at Europec 90, The Hague, Oct. 22–24.

[4] Chaperon, I.: "Theoretical Study of Coning Toward Horizontal and Vertical Wells in Anisotropic Formations: Subcritical and Critical Rates," paper SPE 15377 presented at the 1986 SPE Annual Technical Conference and Exhibition, New Orleans, Oct. 5–8.

[5] Chierici, G.L., Ciucci, G.M., and Pizzi, G.: "A Systematic Study of Gas and Water Coning By Potentiometric Models," *JPT* (Aug. 1964) 923–29.

[6] Coats, K.H., Nielsen, R.L., Terhune, M.H., and Weber, A.G.: " Simulation of Three-Dimensional, Two-Phase Flow in Oil and Gas Reservoirs," *SPEJ* (Dec. 1967) 377–388.

[7] Dikken, B.J.: "Pressure Drop in Horizontal Wells and Its Effect on Their Production Performance," paper SPE 19824 presented at the 1989 SPE Annual Technical Conference and Exhibition, San Antonio, Oct. 8–11. Abridged version in *JPT* (Nov. 1990) 1426–33.

[8] "ECLIPSE 100, Reference Manual, Version 92A," Intera Information Technologies Ltd., 1992.

[9] Ekrann, S.: "Production from Thin Oil Zones," Technical Report No. T-6/87. Rogaland Research, Stavanger, Sept. 1987.

[10] Ekrann, S.: "An Analysis of Gravity-Segregated Piston-Like Displacement in Stratified Reservoirs," *SPERE* (Feb. 1992) 143–148.

[11] Ekrann, S.: "Cross-Sectional Displacement," *Recent Advances in Improved Oil Recovery Methods for North Sea Sandstone Reservoirs*, S.M. Skjæveland and J. Kleppe (eds.), Norwegian Petroleum Directorate, Stavanger, 1992.

[12] Ekrann, S.: "On the Protection Against Coning Provided by Horizontal Barriers of Limited Lateral Extent," *Proc.*, Vol. 3, Sixth European Symposium on Improved Oil Recovery, Stavanger (1991), 169–178.

[13] Ekrann, S. and Hanssen, J.E.: "A Method for Establishing Effective Barriers to Production of Undesired Fluids in the Recovery of Oil," US Patent No. 4903771 (1990).

[14] Ekrann, S. and Skjæveland, S.M.: "Thin Oil Zones," *Recent Advances in Improved Oil Recovery Methods for North Sea Sandstone Reservoirs*, S.M. Skjæveland and J. Kleppe (eds.), Norwegian Petroleum Directorate, Stavanger, 1992.

[15] Falk, D.O.: "Selectively Plugging Subterranean Formations with a Hydrocarbon Soluble Fluid," US Patent No. 4482015 (1984).

[16] Giger, F.M.: "Analytic 2-D Models of Water Cresting Before Breakthrough for Horizontal Wells," paper SPE 15378 presented at the 1986 SPE Annual Technical Conference and Exhibition, New Orleans, Oct. 5–8.

[17] Hanssen, J.E., *et al.*: "Foam Barriers Against Gas Coning in Thin Oil Zones," *Proc.*, Fifth European Symposium on Improved Oil Recovery, Budapest (1989) 737–746.

[18] Hanssen, J.E. and Dalland, M.: "Foams for Effective Gas Blockage in the Presence of Crude Oil at Reservoir Temperature," paper SPE/DOE 20193 presented at the 1990 SPE/DOE Symposium on Enhanced Oil Recovery, Tulsa.

[19] Hanssen, J.E. and Dalland, M.: "Foam Barriers for Thin Oil Rims: Gas Blockage at Reservoir Conditions," *Proc.*, Vol. 1, Sixth European Symposium on Improved Oil Recovery, Stavanger (1991), 95–104.

[20] Hanssen, J.E.: "Gas-Blocking Foams in Porous Media I: Experimental Observations and Parametric Study," submitted for journal publication (1992).

[21] Haug, B.T., Ferguson, W.I., and Kydland, T.: "Horizontal Wells in the Water Zone: The Most Effective Way of Tapping Oil From Thin Oil Zones?," paper SPE 22929 presented at the 1991 SPE Annual Technical Conference and Exhibition, Dallas, Oct. 6–9.

[22] Hess, P.H.: "One-Step Furfuryl Alcohol Method for Formation Plugging," *JPT* (Oct. 1980) 1834–1842.

[23] Holm, L.W.: "Mechanism of Gas and Liquid Flow Through Porous Media in the Presence of Foam," *SPEJ* (June 1968) 359–369.

[24] Howard, G.C.: "Plugging Formations with Hot Solutions," US Patent No. 2779415 (1975).

[25] Høyland, L.A., Papatzacos, P. and Skjæveland, S.M.: "Critical Rate for Water Coning: Correlation and Analytical Solution," *SPERE* (Nov. 1989) 495–502.

[26] Joshi, S.D.: *Horizontal Well Technology*, Penn-Well Publishing Company, Tulsa, 1991.

[27] Karcher, B.J.: "Some Practical Formulas To Predict Horizontal Well Behavior," paper SPE 15430 presented at the 1986 SPE Annual Technical Conference and Exhibition, New Orleans, Oct. 5–8.

[28] Kidder, R.E.: "Flow of Immiscible Fluids in Porous Media: Exact Solution of a Free Boundary Value Problem," *J. Appl. Phys.* (1956) **27**, No. 8, 867–69.

[29] Krumrine, P.H. and Boyce, S.D.: "Profile Modification and Water Control with Silica Based Systems," paper SPE 13578 presented at the 1985 SPE International Symposium on Oilfield and Geothermal Chemistry, Phoenix.

[30] Lien, S.C., Havig, S.O., and Kydland, T.: "Experience From the Ongoing Long-Term Test With a Horizontal Well in the Troll Oil Zone," paper SPE 20715 presented at the 1990 SPE Annual Technical Conference and Exhibition, New Orleans, Sept. 23–26.

[31] McCarthy, J.F.: "Applications of the Hodograph Method to Cresting Problems," poster

presented at the 3rd European Conference on the Mathematics of Oil Recovery, Delft, June 17–19, 1992.

[32] Murphy, P.J.: "Performance of Horizontal Wells in the Helder Field," paper SPE 18340 presented at Europec 88, London, Oct. 16–19.

[33] Ozkan, E. and Raghavan, R.: "A Breakthrough Time Correlation for Coning Toward Horizontal Wells," paper SPE 20964 presented at Europec 90, The Hague, Oct. 22–24.

[34] Papatzacos, P., Herring, T.R., Martinsen, R., and Skjæveland, S.M.: "Cone Breakthrough Time for Horizontal Wells," *SPERE* (Aug. 1991) 311–318.

[35] Patel, R.S. and Broomhall, R.W.:" Use of Horizontal Wells in Vertical Miscible Floods, Pembina Nisku. Alberta, Canada," paper SPE/DOE 24124 presented at the SPE/DOE Eight Symposium on Enhanced Oil Recovery, Tulsa, April 22–24, 1992.

[36] Persoff, P.J., *et al.*: "A Laboratory Investigation of Foam Flow in Sandstone at Elevated Pressure," *SPEJ* (Aug. 1991) 365–372.

[37] Radke, R.J. and Ettinger, R.A.: "The Influence of Texture on Steady Foam Flow in Berea Sandstone," *SPERE* (April 1992) 83–90.

[38] Raza, S.H., Froning, H.R., and Shelton, J.L.: "Method for Combating Water Production in Oil Wells," US Patent No. 3547199 (1968).

[39] Reiss, L.H.: "Horizontal Wells' Production After Five Years," paper SPE 14338 presented at the 1985 SPE Annual Technical Conference and Exhibition, Las Vegas, Sept. 22–25.

[40] Roberts, L.J. and Hulbert, G.: "A Numerical and Analytical Study of Off-Shore Oil Rim Depletion During Tertiary Gas Injection," *Proc.*, Vol. 2, Sixth European Symposium on Improved Oil Recovery,

[41] Sherrard, D.W., Brice, B.W., and MacDonald, D.G.: "Application of Horizontal Wells at Prudhoe Bay," paper SPE 15376 presented at the 1986 SPE Annual Technical Conference and Exhibition, New Orleans, Oct. 5–8.

[42] Smith, C.R. and Pirson, S.J.: "Water Coning Control in Oil Wells by Fluid Injection," *SPEJ* (Dec. 1963), 314–325.

[43] Sobocinski, D.P. and Cornelius, A.J.: "A Correlation for Predicting Water Coning Time," *JPT* (May 1965) 594–600.

[44] Sparlin, D.D.: "An Evaluation of Polyacrylamides for Reducing Water Production," *JPT* (Aug. 1976) 906–914.

[45] Strickland, R.F.: "An Analysis of Artificial Barriers for Controlling Water Coning," MS thesis, Texas A&M University, College Station, (1974).

[46] Sydansk, R.D. and Moore, P.E.:"Responses in Wyoming's Big Horn Basin Resulting from Application of Acrylamide Polymer/Cr(III) Carboxylate Gels," paper presented at Sixth University of Wyoming Enhanced Oil Recovery Symposium, Casper, WY (1990).

[47] de Vries, A.S. and Wit, K.: "Rheology of Gas/Water Foam in the Quality Range Relevant to Steam Foam," *SPEJ* (May 1990) 185–192.

[48] West, T.S.: "A Gravel Pack Completion for Exclusion of Gas and Water," *Trans.* AIME (1951), **192**, 183–190.

[49] Wheatley, M.J.: "An Approximate Theory of Oil-Water Coning," paper SPE 14210 presented at the 1985 SPE Annual Technical Conference and Exhibition, Las Vegas, Sept. 22–25.

[50] White, J.L., Goddard, J.E., and Phillips, H.M.: "Use of Polymers to Control Water Production in Oil Wells," *JPT* (Feb. 1973) 143–150.

Appendix A. Steady-State GOR and WOR

Expressions for steady-state gas, oil and water rates in the presence of gravity effects were developed by Ekrann,[9] and later employed by Roberts and Hulbert[40] in their study of tertiary gas injection. The development is repeated here for convenience.

The geometry considered is the one illustrated in Fig. 1, except that an underlying aquifer of thickness h_w is added for generality. On the assumption that H/r_e is sufficiently small and k_v/k_h is sufficiently large, vertical potential gradients can be neglected at the lateral boundary, and

$$\partial_r \Psi_w = \partial_r \Psi_o + \Delta\rho_{wo}\, g\, \partial_r h_w\,, \qquad (8)$$

$$\partial_r \Psi_g = \partial_r \Psi_o + \Delta\rho_{og}\, g\, \partial_r h_g\,. \qquad (9)$$

Individual phase steady-state production rates are

$$q_{gs} = 2\pi r_e\, h_g \lambda_{hg}\, \partial_r \Psi_g\,, \qquad (10)$$

$$q_{os} = 2\pi r_e\, h_o \lambda_{ho}\, \partial_r \Psi_o\,, \qquad (11)$$

$$q_{ws} = 2\pi r_e\, h_w \lambda_{hw}\, \partial_r \Psi_w\,, \qquad (12)$$

where variables are to be taken at $r = r_e$.

Suppose for definiteness that the well is completed in the oil zone, and that $q_{cg} < q_{cw}$. At $q = q_{cg}$, $q_{gs} = 0$, and Eqs. 10 and 9 combine to yield

$$0 = \partial_r \Psi_o^g + \Delta\rho_{og}\, g\, \partial_r h_g^g \qquad (13)$$

Also, $q_{os} = q_{cg}$, and Eq. 11 reads

$$q_{cg} = 2\pi r_e\, h_o\, \lambda_{ho}\, \partial_r \Psi_o^g\,, \qquad (14)$$

In these equations, variables $\partial_r \Psi_o$ and $\partial_r h_g$ have been superscripted to indicate that they are taken at the critical rate to gas coning, q_{cg}.

Steady-state slopes, $\partial_r h_g$ and $\partial_r h_w$, will increase in magnitude with the total production rate, q. We shall make the essential approximation that a slope does not change once the oil production rate exceeds the critical rate to coning for the phase in question.

(e.g., such that $\partial_r h_g = \partial_r h_g^q$ for $q \geq q_{cg}$. While not exact, this approximation is expected to be reasonably accurate, since the geometry does not allow substantial increase in slope once breakthrough has occurred.

With this approximation, the previous equations (Eqs. 8 and 12 not needed) can be combined to yield

$$q_{gs} = R_{Flm}\,(q_{os} - q_{cg})\,, \tag{15}$$

valid for $q, q_{os} \geq q_{cg}$.

In keeping with our present definition of critical rates, q_{cw} is taken to be the critical *oil* rate to water coning (whereas Refs. 9 and 40 take q_{cw} to be the critical *total* rate). Thus, at $q_{os} = q_{cw}$,

$$0 = \partial_r \Psi_o^w + \Delta\rho_{wo}\, g\, \partial_r h_w^w\,, \tag{16}$$

$$q_{cw} = 2\pi r_e\, h_o\, \lambda_{ho} \partial_r \Psi_o^w\,. \tag{17}$$

Mimicking the previous development,

$$q_{ws} = F_{w\,olm}\,(q_{os} - q_{cw})\,, \tag{18}$$

for $q_{os} \geq q_{cw}$.

With

$$q = q_{os} \qquad q \leq q_{cg}\,, \tag{19}$$

$$q = q_{os} + q_{gs} \qquad q_{cg} \leq q_{os} \leq q_{cw}\,, \tag{20}$$

$$q = q_{os} + q_{gs} + q_{ws} \qquad q_{cw} \leq q_{os}\,, \tag{21}$$

Eqs. 15 and 18 determine individual phase steady-state rates as functions of the total rate, critical rates, and limiting ratios. Results are approximate.

Appendix B. Rise Velocity

In a porous medium, consider a blob of injectant immersed in a resident fluid, as illustrated in Fig. 21. We assume a sharp interface between injectant and

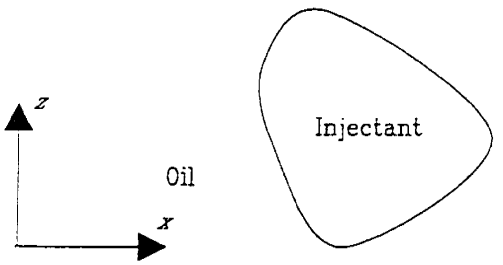

Figure 21: Buoyant injectant blob

resident fluid, on either side of which only one of the fluids is mobile. For definiteness, let the resident fluid be oil, and let the density difference, $\Delta\rho_{oi}$, between oil and injectant be positive. The injectant will then tend to move upwards by buoyancy. We shall estimate the rise velocity.

We neglect horizontal pressure gradients both in the oil and in the injectant, i.e., $p_o(x,z) = p_o(z)$ and $p_i(x,z) = p_i(z)$. This also implies $p_o(z) = p_i(z)$, by continuity of pressure at the fluid interface.

If, in addition, we neglect vertical viscous pressure gradients in the oil, things simplfy tremendously. A hydrostatic pressure distribution ensues,

$$p_o(z) = p_0 - \rho_o\, g\, z\,, \tag{22}$$

where p_0 is some reference pressure.

Then

$$\partial_z \Psi_i = -\Delta\rho_{oi}\, g\,. \tag{23}$$

and, by Darcy's law,

$$u_{vi} = -\lambda_{vi}\, \partial_z \Psi_i = \lambda_{vi}\, \Delta\rho_{oi}\, g\,. \tag{24}$$

The rise velocity of the injectant becomes

$$v_{\rm rise} = \frac{u_{vi}}{o_e}\,, \tag{25}$$

with

$$o_e = o\,(1 - S_r)\,, \tag{26}$$

and S_r being the residual saturation of original fluids (oil + water + gas) after injectant flooding. Combining Eqs. 24 and 25, we obtain

$$v_{\rm rise} = \frac{\Delta\rho_{oi}\, g\, \lambda_{vi}}{o_e}\,. \tag{27}$$

The previous development neglected viscous pressure gradients, except vertically in the injectant. The final answer is optimistic, therefore. The neglect of horizontal pressure losses is equivalent to the well-known vertical equilibrium (VE) approximation.[6,10,11] The additional neglect of vertical viscous pressure losses in the oil is thought to be an acceptable approximation, due to the large cross-section open to oil flow.

With $\Delta\rho_{oi} = 100\,\mathrm{kg/m^3}$, $k_v = 0.1\,\mathrm{D}$, $k_{ri} = 0.9$, $\mu_i = 1\,\mathrm{cp}$, and $\phi_e = 0.2$, we have $v_{\rm rise} = 3.8\,\mathrm{cm/d}$ from Eq. 27. If injected through the production perforations, and required to rise through a 10 m thick oil zone, say, this injectant would need 260 days. This is not tolerable. One needs at least a 10-fold increase in vertical permeability to reduce rise times to interesting levels, or a corresponding decrease in injectant viscosity. A more promising strategy would seem to be to inject through separate perforations in the gas zone, close to the GOC, in which case one is helped by a larger density difference ($\Delta\rho_{ig}$) and a shorter distance to the GOC.

Appendix C. Gravity Spreading

Once the injectant has reached the gas-oil interface, it starts spreading by gravity, much like an oil slick on water. The spreading is rapid initially, to slow down as spreading progresses. We shall model this process by assuming the original gas-oil interface to be a fixed impermeable boundary. In reality, gravity spreading of the injectant would induce some flow in the oil, too. Since gas mobility is one or two orders of magnitude larger than that of oil, however, one would expect oil movement to be minor.

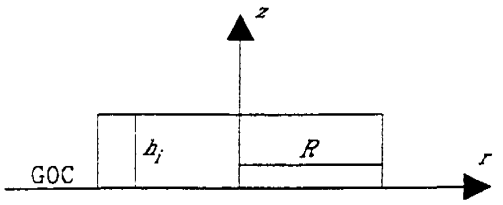

Figure 22: Injectant geometry for gravity spreading

For a rough computation, we assume the injectant distribution to always have a rectangular cross-section, as illustrated in Fig. 22. As in the previous development, we neglect all viscous pressure gradients in the gas, as well as vertical viscous pressure gradients in the injectant. We shall take

$$\Delta\Psi_i = \Delta\rho_{ig}\, g\, h_i\,, \tag{28}$$

as a representative pressure (potential) drop between the origin and the perimeter of the injectant disc. By mass conservation,

$$2\,\pi\, r\, h_i\, \overline{u}_{hi}(r) = -\phi_e\, \pi\, r^2\, \frac{dh_i}{dt}\,. \tag{29}$$

Here, $\overline{u}_{hi}(r)$ is the height-averaged horizontal injectant Darcy velocity,

$$\overline{u}_{hi}(r) = \frac{1}{h_i}\int_0^{h_i} u_{hi}(r,z)\,dz\,, \tag{30}$$

with u_{hi} being the local velocity. Eq. 29 is constructed by requiring all injectant slumping down in a cylinder with height h_i and radius r to leave horizontally through the vertical boundary of that cylinder.

With Darcy's law,

$$\begin{aligned}\int_0^R \overline{u}_{hi}(r)\,dr &= \int_0^R \left[\frac{1}{h_i}\int_0^{h_i} u_{hi}(r,z)\,dz\right] dr \\ &= -\frac{\lambda_{hi}}{h_i}\int_0^R\int_0^{h_i} \partial_r\Psi_i\, dz\, dr \\ &= \lambda_{hi}\,\Delta\overline{\Psi}_i\,,\end{aligned} \tag{31}$$

where $\Delta\overline{\Psi}_i$ is the average potential drop. We let $\Delta\overline{\Psi}_i = \Delta\rho_{ig}\, g\, h_i$. Integrating Eq. 29 and using Eq. 31,

$$\frac{R^2}{h_i^2}\,\frac{dh_i}{dt} = -\frac{4\,\lambda_{hi}\,\Delta\rho_{ig}\,g}{\phi_e}\,. \tag{32}$$

Let the total volume of injectant be V, i.e., $V = \pi\, R^2\, h_i\, \phi_e$, which allows h_i to be expressed as a function of R. After substitution into Eq. 32,

$$R^3\,\frac{dR}{dt} = \frac{2}{\pi}\,\frac{\lambda_{hi}\,\Delta\rho_{ig}\,g\,V}{\phi_e^2}\,, \tag{33}$$

which has the solution

$$R(t) = \left[\frac{8\,\lambda_{hi}\,\Delta\rho_{ig}\,g\,V}{\pi\,\phi_e^2}\right]^{1/4} t^{1/4}\,. \tag{34}$$

In Eq. 34 we have assumed for convenience that $R(0) = 0$. Since the front velocity dR/dt is seen to be very large initially, only to decay dramatically as R increases, exact initial conditions are not important. The time to reach a certain radius will be dominated by the final stages of the process.

The development producing Eq. 34 has other questionable points. The basic assumption of a rectangular injectant cross-section is expected to be acceptable only if the injectant is less mobile than the gas. This should generally be the case. More importantly, the accuracy of the substitution $\Delta\overline{\Psi}_i \rightarrow \Delta\rho_{ig}\, g\, h_i$ is not obvious. The solution is not very sensitive to such assumptions, in terms of the radius reached after a given time, because of the 1/4 power dependence. In terms of the time to reach a certain radius, however, the solution is much more sensitive. The solution should be used with caution in the latter mode.

With $\Delta\rho_{ig} = 500\,\mathrm{kg/m^3}$, $k_h = 5\,\mathrm{D}$, $k_{ri} = 0.9$, $\mu_i = 1\,\mathrm{cp}$, $\phi_e = 0.2$, and $V = 1{,}000\ \mathrm{m^3}$, 3 weeks suffice to produce a penetration of $R = 40\,\mathrm{m}$. This relatively deep penetration relies on a high permeability reservoir, and even on a rather large volume of injectant. With $k_h = 500\,\mathrm{mD}$ and $V = 100\,\mathrm{m^3}$, a penetration of 12.6 m ensues after 3 weeks.

CO_2 Foam Field Trial at North Ward-Estes

by S. I. Chou, S. L. Vasecek and D. L. Pisio, Chevron Oil Field Research Company, La Habra, California, and D. E. Jasek and J. A. Goodgame, Chevron USA Inc., Midland, Texas

Originally presented as Society of Petroleum Engineers paper No. 24643 at the 67th Annual Technical Conference & Exhibition of SPE held n Washington, D.C., October 4-7, 1992. Copyrighted by Society of Petroleum Engineers, Inc., 1992.

This paper was prepared for presentation at the DOE/NIPER, Symposium on Field Application of Foams for Oil Production held in Bakersfield, California, February 11-12, 1993.

This paper was selected for presentation by a Program Committee following review of information contained in an abstract submitted by the author(s). Contents of the paper, as presented, have not been reviewed and are subject to correction by the author(s). The material, as presented, does not necessarily reflect any position of the U.S. Department of Energy or the National Institute for Petroleum and Energy Research.

ABSTRACT

A CO_2 foam field trial was conducted in the North Ward-Estes field in Texas to evaluate the effectiveness of foam in improving CO_2 sweep efficiency. This paper describes the design, results, and analysis of foam treatment with emphasis on the design methodology of applying foam in grossly heterogeneous reservoirs, characterized by uneven areal and vertical sweep in most patterns.

Over a period of nearly two years, foam was emplaced into an injector four times by alternately injecting CO_2 and surfactant solution, and followed by continuous CO_2 injection after each emplacement. Foam was generated in situ, which reduced CO_2 injectivity by 40 to 85%. Gas production in the problem producer decreased dramatically, while gas and oil production in other offset producers increased, indicating areal diversion. Vertical diversion also occurred, as evidenced by significant increase in oil production in the problem producer, where tertiary oil response had peaked prior to the foam treatment.

The field test shows that a properly designed foam treatment can significantly improve the CO_2 sweep efficiency and be economically successful. The methodology developed in the design and analysis of the foam test may be applied to other conformance improvement processes.

INTRODUCTION

The North Ward-Estes (NWE) field is located in Ward and Winkler counties, Texas. Primary production began in 1929, waterflood began in 1955, and CO_2 flood started in 1989. The oil-in-place for the CO_2 project area at the beginning of CO_2 flood was estimated at 77 million barrels, or 54% of original oil-in-place. The CO_2 project area, covering 3,840 acres, was developed in 20-acre patterns within six sections.

The producing formation in this area is Yates, which consists of A, BC, D, E, F, Stray, J1, and J2 sands, separated by dense dolomite. The sands vary from fine-grained sandstone to siltstone, containing various amounts of clays. Fig. 1 is a type log of this formation. Rock permeability varies greatly between and within sands, with a Dykstra-Parsons coefficient of about 0.85. Table 1 summarizes NWE reservoir properties. Additional information about the NWE CO_2 flood has been documented previously[1].

Poor sweep efficiency has been a concern since the start of the CO_2 flood. Poor sweep was manifested by fast CO_2 breakthrough and low tertiary oil production. In some areas, CO_2 breakthrough occurred in less than a month, with tertiary oil response peaking in less than three months. Several methods were considered to improve the CO_2 conformance. Mechanical treatments were impractical in NWE because most wells were completed as open holes, "shot" with nitroglycerine, and hydraulically fractured. Drilling new wells would be risky and expensive. Foam treatment was the most promising alternative because foam can selectively retard gas flow. A field trial was conducted to evaluate its potential in this reservoir. This paper describes the design methodology, lab study, results, and analysis of the foam field trial.

PROJECT DESIGN

Objective of Foam Treatments

In past studies, foam has been considered mainly for in-depth mobility control purposes. This was not a viable objective in NWE because high CO_2 mobility was not the culprit for poor sweep. Lab and field injectivity studies[1] showed that the CO_2 mobility was only marginally higher than the water mobility and that the mobility of a 1:1 WAG was about half of the water mobility. Furthermore, it may not be possible

References and illustrations at end of paper.

to propagate foam deep into the reservoir, and the cost of an in-depth foam treatment, even if confined to one or two sands, would be prohibitively high.

Accordingly, foam was considered as a near-wellbore treatment, and the objective was to divert CO_2 from thief zones to other unswept zones. For this purpose, as in other near-wellbore conformance treatments, foam application must be done on a highly selective basis. Foam treatments in the wrong well will not improve the sweep efficiency, and may actually decrease oil production.

Selection of Test Pattern

As noted above, the NWE reservoir is a highly stratified formation. It was natural to assume that poor sweep efficiency was due to poor vertical conformance, caused by large permeability variations between sands. Therefore, the original targets for foam treatments were cased-hole injectors with poor injection profiles.

After analyzing available injection profiles in the CO_2 flood area, however, we found no correlation between profile and rock permeability distribution. This is illustrated in Fig. 2, which plots the percentage of fluid injected into each sand versus the percent KH (permeability times pay thickness) of each sand for six cased-hole wells. Similarly, there was no correlation between total KH and injection rate of each well. The lack of correlation between profile and KH distribution suggested that either the profile did not properly describe fluid entry into the reservoir or the KH distribution was misleading due to 35 years of waterflood with poor-quality water, or both. In any case, the injection profile cannot be used as a criterion for selecting foam candidate wells, nor for evaluating foam performance. This is not surprising, considering that most of the injectors are "shot" holes and nearly all have been hydraulically fractured. Therefore, poor injection profile was eliminated as a criterion for selecting foam candidates.

The question, then, was how to identify reservoir patterns with poor sweep efficiency due to high-permeability thief zones. The existence of a predominant thief zone may be inferred by high injectivity at the injector and high CO_2 production rate at an offset producer. It was easier to find the problem producer first, and then identify the responsible injector. Fig. 3 compares the 3-month average of producing GOR (gas-oil-ratio) and CO_2 production rates in Section 7 prior to the first foam treatment. In this plot, poor sweep efficiency is manifested by high gas production rate and high GOR. Well 1020 stood out as the number one problem producer. Its CO_2 production rate exceeded 900 MCFPD (thousand standard cubic feet/day) with a GOR exceeding 1000 MCF/bbl by January 1990. The 3-month average CO_2 production rate per well in Section 7 was 89 MCFPD, and the average GOR was 5.4 MCF/bbl at that time.

Upon examining the injection schedules of the four offset injectors to well 1020, we determined that both 82WC and 117WC could be responsible for the high CO_2 production at 1020. Fig. 4 shows well locations in that region. Well 82WC was then placed on water, while 117WC remained on CO_2 injection. Gas production at 1020 immediately dropped off. Subsequently, when 82WC was switched to CO_2, gas production at 1020 increased within a few days. This behavior indicated that 82WC was the problem injector. Not surprisingly, 82WC had an injection rate two to three times that of nearby injectors.

Another major criterion used for selecting foam candidates was that the injector was currently operating at a pressure substantially below the formation parting pressure. This was necessary because plugging off the thief zone would merely improve CO_2 distribution in the reservoir on a relative basis; to divert CO_2, i.e. to decrease CO_2 flow in the thief zone and increase CO_2 flow in unswept or less swept zones, the injection pressure must also be increased. If an injector was operating very close to the parting pressure, the injection pressure during foam treatments could not be increased significantly without extending the fracture and possibly negating the effect of foam treatments.

Two additional criteria were (1) that the injector was located in a pattern with significant potential for additional tertiary response, and (2) that the existing tertiary response had already peaked at the problem producer (to avoid premature plugging of productive intervals). Well 82WC appeared to satisfy all these requirements and was chosen for the first foam field test.

Laboratory Study

Given the objective of using foam to block off thief zones, a lab program was initiated to develop a suitable foam formulation. The main emphasis was on foam resistance factor (RF) and foam durability in NWE cores. Foam RF was defined as the ratio of the normalized pressure drop (pressure divided by flow rate) during foam injection to that during single-phase water flow. Chaser CD1040, an alpha-olefin sulfonate, exhibited higher RF than others and was selected for further study. The effects of surfactant concentration, foam quality, flow rate, and rock permeability on foam RF were also measured because they influence the design of the foam emplacement program.

Fig. 5 shows the performance of 80% quality (80% CO_2 fractional flow) foams generated in NWE cores with 0.2% and 0.5% surfactant concentrations. In this study, a 1"-diameter by 4.3"-long butted core was presaturated with 0.2% surfactant. Surfactant and CO_2 were then co-injected at 20 ft/day, followed by CO_2 injection. Foam was generated without delay, and the foam RF exceeded 15 and 23 for the 0.2% and 0.5% concentrations, respectively. In these short-core experiments, steady state was not reached during the co-injection period and the RFs were still rising slowly. Foam was quite durable to CO_2 injection, as indicated by the gradual decline of RF: after 12 pore volumes of CO_2 injection (PVINJ), foam still retained 21% of its original RF.

Fig. 6 illustrates foam durability under constant-pressure conditions. Here, CO_2 was injected at a constant pressure gradient of 130 psi/ft after 60% quality foams with 0.2% and 0.5% surfactant concentrations were generated in NWE cores, respectively. The inverse RF is plotted versus the cumulative pore volume of CO_2 injected. For both foams, over 70 pore volumes of CO_2 were injected before the RF dropped below one. This suggests that a CO_2 volume of roughly 70 times the foam volume emplaced can be injected before foam disintegrates. This number may

be used as a preliminary estimate of how long foam may last in the field.

The effect of rock permeability on foam RF was studied. Because only a limited number of NWE cores were available, all with similar permeabilities, Rangely cores were included in this study. As shown in Fig. 7, foam RF increased sharply with increasing permeability. Thus, stronger foams tend to be generated in higher-permeability rocks, retarding CO_2 flow by a greater extent, than in lower-permeability rocks.

Fig. 8 shows that foam RF also decreased with increasing flow rate. This characteristic enables foam to propagate farther from a nonfractured well, where fluid velocity and pressure gradient are high near the wellbore. It is of lesser value to foam applications in a hydraulically fractured well, where fluid velocity exiting the fracture face varies little and foam penetration into the rock matrix is largely limited by foam volume.

Prefoam Tests

Step rate and falloff tests were conducted in 82WC prior to foam treatment. The step rate test indicated a formation parting pressure of about 1,750 psi, which is comparable to that of other wells in the region. Two falloff tests were performed: one when the well was on water, and one during CO_2 injection. Pressure falloff data may be used to determine the fracture length and the average matrix permeability.

The complete falloff data were too complex to match closely any known type curve. This could be due to a number of factors: that 82WC has been "shot" and hydraulically fractured, that some of the sands may not be connected to the fracture, strong interference from well 1020, and nonuniform fluid saturations during the CO_2 falloff test. General diagnostics revealed a large wellbore storage, partial bilinear flow, extended linear flow, very brief pseudo-radial flow, and strong interference afterwards. A fracture half-length of 220 ft was calculated from the water injection falloff data, which was more amenable to analysis than the CO_2 falloff data. This number was used in the subsequent calculation of surfactant requirements.

A fast WAG (1 day CO_2 and 1 day water) was conducted before foam to compare injection rates and pressure with those encountered during foam emplacement. Extended baseline injection for the purpose of evaluating production response was deemed useless because reservoir saturations were rapidly changing during early stages of the CO_2 flood. Likewise, a tracer program was not conducted because CO_2 already served as a tracer in identifying communication between wells.

Foam Emplacement Program

Several parameters need to be specified in designing a foam treatment program: quantity of surfactant to be injected, prefoam surfactant slug size, surfactant concentration, foam quality, and injection schedule. The preferred foam emplacement method, either alternate injection of surfactant and CO_2 (SAG) or co-injection of both fluids, needs to be specified. Injection rates and pressure during foam emplacement and the subsequent CO_2 chase need to be considered. Finally, the conditions under which foam treatments would be repeated or terminated need to be determined. The following paragraphs describe our methodology.

The amount of surfactant to be injected is perhaps the most important variable. While foam preferentially enters high-permeability rocks, it increasingly enters lower-permeability rocks as more foam is generated in the higher-permeability rocks. Continued foam injection beyond a certain point may result in a foam distribution in the formation that is less than optimum and may eventually plug the injector. Indeed, in the only two published gas foam tests in unfractured wells, the Painter N_2 foam[2] and the Rock Creek CO_2 foam[3] tests, foam appeared to plug up both injectors. On the other hand, a foam treatment that is too small will not last long and needs to be repeated often, thereby increasing the operational costs.

Plugging by foam is less likely in a fractured well because most of the surfactant injected will exit the fracture face and extend the foam depth. Thus, the amount of surfactant needed is proportional to the fracture surface area and the depth of foam penetration desired. Previous experience in Rangely[4] suggested that an average foam depth of 1.5 ft was adequate. Given the fracture area, foam depth, rock porosity, average water saturation and surfactant concentration within the foam bank, and surfactant adsorption loss, one can estimate the amount of surfactant needed. In the present case, this was about 5,000 lbs.

The prefoam surfactant slug should be sufficiently large to saturate the desired foam region with surfactant solution so that foam can be generated in situ without delay[5] during the subsequent SAG injection. Surfactant adsorption loss should be accounted for in this stage. The prefoam slug is particularly important in a fractured well, where fluid velocity exiting the fracture face is low (about 2 ft/day in the present case). The amount of surfactant in this slug was calculated by equating the average surfactant concentration within the desired foam region to a minimum value (0.1% here, as explained below). The size of this slug can be substantially reduced after the first foam treatment because adsorption loss will have been satisfied.

The minimum effective surfactant concentration depends largely on rock and surfactant characteristics. Lab study showed that foams generated with a surfactant concentration between 0.2% and 0.5% were adequate, whereas foam RF dropped off sharply and foam generation was greatly delayed below a concentration of about 0.1%. Thus, 0.1% was the minimum surfactant concentration, and the surfactant concentration was maintained between 0.1% and 0.5% throughout the field test.

The 60% foam had slightly higher RF than the 80% foam. The difference should be insignificant in a near-wellbore treatment, where foam quality is nonuniform and steady state is not reached because of the small foam volume. Lab study showed that foam durability was roughly independent of foam quality, as long as the amount of surfactant in the foam was the same. Therefore, an average foam quality between 50% and 80% was maintained during the SAG injection period.

There has been some concern about whether foam emplacement method - simultaneous or alternate injection of CO_2 and surfactant - affects foam properties. Lab study showed that the two methods generated

similar foams in cores presaturated with surfactant solution; if not presaturated with surfactant, SAG generally generated foam sooner than simultaneous injection. To our knowledge, neither method has demonstrated superiority in the field. Because it is easier and less costly to conduct SAG than simultaneous injection, SAG was used in this test. The SAG injection schedule (1 day surfactant - 1 day CO_2, 1 day surfactant - 2 day CO_2, etc.) may have some near-term impact on foam injectivity. In general, a longer cycle propagates the foam somewhat deeper in the reservoir but with lower RF. Because foam propagation in a hydraulically fractured injector is practically limited by foam volume, a shorter cycle is preferred here. Thus, the shortest cycle consistent with the operators' schedule (1 day surfactant - 1 day CO_2) was used during the SAG injection periods.

In a fractured well, the injector bottomhole pressure (BHP) during SAG injection should be kept below the formation parting pressure. If BHP data are not available at all times, the injection rate should be kept below a certain limit, which can be estimated from the step-rate test data and foam RF. The BHP during CO_2 chase should be kept below that during SAG to prevent premature foam degradation. A maximum rate should also be set in this period because the local pressure gradient is proportional to the injection rate, and foam durability decreases with increasing local pressure gradient. However, it is desirable to inject CO_2 at a pressure higher than the prefoam injection pressure to increase CO_2 flow rates in the formation. Therefore, the CO_2 injection pressure was set 50 to 100 psi below that during SAG, and the CO_2 injection rate was kept below 600 MCFPD.

Foam treatment may be repeated when CO_2 injection pressure falls to the prefoam level (1250 to 1350 psi) at the maximum CO_2 injection rate. When the cumulative CO_2 injected reaches the target CO_2 injection volume - 40% hydrocarbon pore volume in the pattern, for example - further foam treatments would not be performed and the test injector may be switched to water injection.

Table 3 summarizes the treatment dates and amount of surfactant, water, and CO_2 used in each of the four foam treatments. Much less surfactant was used in the second foam treatment than the first one to determine whether foam could be regenerated with a much smaller volume of surfactant than was previously used.

Surface Facility

The basic facility needed to conduct SAG injection is simple. During surfactant injection, a concentrated surfactant solution was pumped from a stock tank into the water line at a rate proportional to the water flow rate. This can be accomplished by using a PID (proportional-integral-differential) controller with the water flow rate as input. A more elaborate setup was needed to conduct SAG injection at constant BHP. First, capillary tubing filled with helium was installed in the wellbore. The helium pressure, measured at the wellhead and approximately equal to the BHP, was fed into another PID controller that regulated either CO_2 flow rate or water flow rate through an adjustable choke valve. The BHP control apparatus was installed prior to the third foam treatment. Surface injection rates and pressure were measured and recorded throughout the field test.

RESULTS AND ANALYSIS

Injector Response

Fig. 9 shows the injector BHP, surface pressure, and injection rate during the first foam treatment. The BHP data were recorded on four separate occasions, whereas the surface data were measured continuously since February 1990.

The prefoam BHP during CO_2 injection was 1400 psi at an injection rate of 850 BPD. The BHP during the prefoam fast WAG varied between 1300 and 1680 psi at 700 BPD. During SAG injection, the average BHP was 1650 psi at about 200 BPD, indicating a reduction in CO_2 injection indices (injection rate divided by incremental BHP) by as much as 85%. The BHP gradually declined during the CO_2 chase and reached prefoam levels after three months of CO_2 chase.

Pressure surveys conducted during SAG injection indicated that BHP was significantly higher than calculated using surface pressure and an assumed hydrostatic gradient in the well. Also, BHP dropped substantially during the CO_2 chase while surface pressure increased slightly. Thus, there was no correlation between surface and bottomhole pressures during CO_2 injection under field operating conditions. Consequently, capillary tubing was installed to allow continuous monitoring of BHP in later foam treatments.

Fig. 10 presents injection data from the second, third, and fourth foam treatments. In the second foam treatment, foam was regenerated with a much smaller volume of surfactant, about one-fourth of that used in the first treatment. However, it lasted only one and a half months based on the BHP behavior. This result is consistent with lab data in which foam durability is roughly proportional to the amount of surfactant in foam.

The third foam treatment started on October 19, 1990. The BHP was maintained at 1500 psi during SAG injection and at 1400 psi after foam. Injection rates varied between 100 BPD during SAG and 300 BPD during the CO_2 chase. The best foam durability was observed with this treatment, wherein the CO_2 injectivity did not return to the prefoam level until six months later. Significantly, the injection pressure was well-controlled throughout this period.

The fourth foam treatment commenced on June 26, 1991. During SAG injection, the PID controller was not functioning properly and caused much fluctuation in the injection rates and pressure. The average CO_2 rate was about 250 BPD at 1500 psi. The CO_2 injection rate also fluctuated greatly after foam, and exceeded 500 BPD on several occasions. This may have degraded the foam because the BHP dropped to 1350 psi only a month into the CO_2 chase. Since then, CO_2 was injected at a target rate from 150 to 350 BPD. The capillary tubing was pulled, and no further BHP data were collected after August 1991. The CO_2 chase ended and water injection began on January 28, 1992.

In sum, the results show that (1) foam was generated without delay in this fractured well; (2) foam reduced CO_2 injectivity by 40% to 85% during SAG injection; and (3) foam lasted up to six months.

Production Response of Individual Wells

Fig. 11 shows production data from well 1020, the problem producer. The data were taken from individual tests at the separator. Oil production dropped below 1 BPD for two months prior to the first foam treatment. Gas breakthrough occurred in May 1989, within a month after CO_2 injection began in 82WC. The gas production rate exceeded 900 MCFPD, and the well was converted from pumping to flowing just before the first foam treatment.

Soon after the first foam injection, the gas production rate dropped sharply. It increased during the subsequent CO_2 chase, and started to drop as soon as the next foam injection began. This behavior suggests that foam blocked the thief zones between 1020 and 82WC.

Oil production at well 1020 rose from below 1 BPD to a high of 15 BPD during the first foam injection, declined during the CO_2 chase and the second foam, but increased significantly since the third foam. It reached a high of 80 BPD in May 1991, but dropped to approximately 15 BPD after June 1991. Response to the fourth foam injection appeared to be slower than before. The CO_2 production rate rose in October 1991, followed by an oil rate increase in November 1991. The slower response could be a result of tertiary oil being produced from increasingly tighter sands as the CO_2 flood matures. The increased oil production in 1020 suggests that foam also diverted CO_2 to lower-permeability zones toward well 1020.

Soon after 82WC was switched from CO_2 to water injection in late January 1992, water production at well 1020 nearly tripled while gas and oil production decreased substantially. This behavior again demonstrated the existence of a predominant thief zone between 82WC and 1020.

Fig. 12 shows the production behavior of well 96, which was in sharp contrast to well 1020. CO_2 had not broken through by the time foam treatment started. The gas production rate increased dramatically during the first foam injection and reached 400 MCFPD after the third foam. By then, well 96 had comparable gas production rate to well 1020. Concurrent with rising gas production, oil production increased from less than 1 to over 15 BPD during the first foam treatment and continued to rise through the second and third foam treatments to over 100 BPD in March 1991. It dropped back to around 15 BPD by September 1991 but started to rise again in November 1991.

After 82WC was switched to water injection, water production at well 96 increased substantially, indicating close communication between 82WC and 96. Interestingly, oil and gas production also increased, probably because of increased injection support at 82WC (500 BPD water versus 350 BPD CO_2 before). Throughout the foam treatment period, the rise and fall of oil and gas production rates at well 96 were closely synchronized, suggesting that the oil produced was likely due to diverted CO_2.

Production data from well 75 are shown in Fig. 13. Prior to the first foam treatment, oil production was declining while gas production was rising. Following the first foam treatment, gas production decreased substantially while oil production continued to decline. However, oil and gas production increased significantly after the third foam treatment. The response to the fourth foam treatment was slower than previous ones, similar to those observed in wells 1020 and 96. After 82WC was switched to water injection, water production increased while gas and oil production decreased.

At well 80, it appears that both oil and gas production had already peaked before the first foam treatment (see Fig. 14). After the first foam treatment, gas production rate increased to between 100 and 300 MCFPD, and water production rate decreased to between 200 and 300 BPD. The average oil production rate was 20 BPD before foam, 30 to 40 BPD after the first foam treatment, then declined and later rebounded after the fourth foam treatment. In comparison with the other three offset producers, the variations in production rates since the start of foam treatments were minimal, suggesting that well 80 was least affected by foam in the pattern.

Changes in sweep efficiency may be analyzed by comparing the producing GOR and cumulative oil produced since the start of the CO_2 flood. The analysis is shown in Fig. 15 for the four offset producers. For well 1020, significant reductions in GOR were evident after the first and second foam treatments. For the other three offsets, GOR was reduced at various times but the reduction appears to be most pronounced after the fourth foam. However, because of the time required to propagate the diverted CO_2 front toward the offset producers, it is not possible to attribute GOR responses to a specific foam treatment.

In fact, because of the complex reservoir structure involved, one cannot be sure that all the responses noted above are truly due to foam. However, other producers in the region showed much less fluctuation in production rates (somewhat analogous to that shown in Fig. 14 for well 80). In addition, water production rates in those wells decreased by an average of 40%, whereas in the three offsets to 82WC (except well 80) water production rates decreased by 60 to 80%. This behavior was consistent with the greatly reduced water injection at 82WC. Finally, the sharp decrease in gas production at well 1020 and increase at well 96, together with the increased injection pressure in 82WC, indicates that foam diverted CO_2 areally in the pattern.

Pattern-to-Pattern Comparisons

The previous analysis of the production history at each offset producer gives a strong indication that CO_2 diversion occurred and that incremental oil was produced. The following analysis provides a quantitative measure of the improvement in CO_2 sweep efficiency.

Monthly allocated production data were used in this analysis. Fig. 16 shows the monthly average producing GOR in the 82WC pattern in comparison with that of the surrounding eight patterns. The average GOR in the 82WC pattern was 71 MCF/bbl before foam, well above the average of surrounding patterns. It sharply declined to 8 MCF/bbl six months after the first foam treatment and remained lower than that of the surrounding patterns for some time. The current GOR in 82WC and other patterns are comparable. A reduced GOR is a good indication of

improved sweep in gas floods.

Fig. 17 shows cumulative oil produced per well since the start of the CO_2 flood versus cumulative CO_2 injected in 82WC and its surrounding patterns. This figure illustrates CO_2 utilization. Before the foam treatment started, the cumulative CO_2 utilization was 64 (MCF/bbl) in 82WC and 34 in the surrounding patterns. The average CO_2 utilization in the period between the first foam treatment and the end of the fourth CO_2 chase was 22 in 82WC and 20 in the surrounding patterns, showing a threefold increase in CO_2 utilization due to foam. The improvement is even greater if one focuses on the period after the third foam treatment (where oil production in the 82WC pattern increased significantly) and considers the final water injection period as part of the foam treatment program. Thus, the average CO_2 utilization in the 82WC pattern was 15 between the third foam treatment and April 1992, compared to 18 in the surrounding patterns over the same period. Again, improved CO_2 utilization indicates improved CO_2 sweep efficiency in a highly heterogeneous reservoir.

While foam (followed by CO_2) practically eliminates water injection, CO_2 injection is not necessarily more than that with a 1:1 WAG. As shown in Fig. 18, the cumulative CO_2 injected in 82WC was twice as high as the average of surrounding injectors before foam. Since the first foam treatment, the cumulative CO_2 injected was 316 MMCF in 82WC and averaged 322 MMCF in the surrounding patterns. This is particularly noteworthy because higher injection pressures were achieved with foam. Further, if the 1:1 WAG at 82WC had been continued, the cumulative CO_2 injected would have been three times as much as that used with foam. Therefore, foam can effectively reduce CO_2 cycling through the thief zone where WAG cannot.

Economics

Economic analysis of a single, nonisolated pattern test is difficult because of the uncertainty in allocating oil production from the offset producers. Nonetheless, the following gives some idea of the economics of injector foam treatments.

A CO_2 flood becomes uneconomic when the producing GOR exceeds a certain limit, above which the cost of injecting and processing CO_2 exceeds the value of the oil produced. Given the average cost of CO_2 at \$0.8/MCF and oil price at \$20/bbl, the limiting GOR was calculated to be 25 (MCF/bbl). Because well 1020 had a GOR greater than 1,000 before foam, far exceeding the economic limit, it should be plugged if CO_2 injection was to continue at 82WC. Alternatively, 82WC could be switched to water injection while keeping 1020 on production. While there are many other scenarios, only these two cases are compared with foam here.

In the waterflood case, oil production can be estimated from the waterflood baseline prior to the CO_2 flood, and water injection can be extrapolated from water injection rates before foam. In the WAG case, oil production was assumed to be one-fourth of the oil produced from wells 96, 80, and 75. This number represents an upper limit for the WAG case because a significant portion of the oil produced in these offsets was likely due to foam and would not be available had WAG been continued at 82WC. The same number plus the entire oil production from well 1020 was allocated to the foam case. This is a conservative estimate because incremental oil from the other three offsets was not counted at all. The CO_2 injection for WAG was extrapolated from the 2-month average CO_2 injection rate before foam, and the total water injected was half of that assumed for the waterflood.

The results are summarized in Table 3: (1) continuing WAG at 82WC would have incurred a loss of over \$400,000, (2) switching 82WC to 100% water injection would have barely broken even, and (3) foam treatment resulted in a gain of \$248,300. We caution, however, these numbers are for comparisons only, and they do not include such costs as capital depreciation, interest, or royalty. The significant point is that the cost of surfactant in a foam treatment is minimal compared to the cost of CO_2. Thus, the key to achieving economic success in foam applications is to reduce CO_2 cycling as much as possible. In other words, a strong foam using more surfactant is much preferred to a weak foam using less surfactant.

CONCLUSIONS

Based on the results of the four foam treatments in 82WC, the following conclusions can be made:

1. Strong foams were generated in situ under North Ward-Estes conditions, which reduced CO_2 injectivity by 40 to 85%.

2. Foam reduced CO_2 injectivity for one to six months. The duration of injectivity reduction depended on the amount of surfactant injected and the CO_2 injection pressure and rate after foam.

3. Foam apparently diverted CO_2 from the thief zone to unswept regions, as indicated by the sharp decline in the CO_2 production at the problem producer and increased CO_2 production at other offset producers.

4. Incremental oil may have been produced as a result of CO_2 diversion vertically (toward well 1020) and areally (toward wells 96, 80 and 75).

5. Foam can dramatically improve CO_2 utilization in reservoirs containing large thief zones.

6. The economics of near-wellbore foam treatments strongly depend on the ability of foam to reduce CO_2 channeling through thief zones.

ACKNOWLEDGMENTS

J.C. Tsiao conducted all laboratory experiments and helped in the analysis of lab and falloff test data. B. Gael and R. Guice were involved in the design and pattern selection process. R. D. Portalski and D.L. Shay assisted in the operation and construction of wellsite equipment. B. Wilcox, M. Harkins, D. Savage, M. Cornelius, T.A. Darr-Van Reet, and D.J. Smith helped collect field data. Discussions with J.H. Bae have been helpful.

REFERENCES

1. Winzinger et al., "Design of a Major CO_2 Flood, North Ward-Estes Field, Ward County, Texas," SPE 19654 presented at the 64th Annual Technical Conference and Exhibition of SPE, San Antonio, TX, Oct. 8-11, 1989.

2. Kuehne, D.L., Ehman, D.I., Emanuel, A.S., and Magnani, C.F., "Design and Evaluation of a Nitrogen Foam Field Trial," SPE/DOE 17381 presented at the sixth SPE/DOE Enhanced Oil Recovery Symposium, Tulsa, OK, April 17-20, 1988.

3. Heller, J.P., Boone, D.A., and Watts, R.J., "Field Test of CO_2 Mobility Control," SPE 14395 presented at the 60th Annual Technical Conference and Exhibition of SPE, Las Vegas, NV, Sept. 22-25, 1985.

4. Jonas, T.M., Chou, S.I., and Vasicek, S.L., "Evaluation of a CO_2 Foam Field Trial - Rangely Weber Sand Unit," SPE 20468 presented at the 65th Annual Technical Conference and Exhibition of SPE, New Orleans, LA, Sept. 23-26, 1990.

5. Chou, S.I., "Conditions for Generating Foam in Porous Media," SPE 20239, Presented at the SPE Annual Technical Conference and Exhibition of SPE, Dallas, TX, Oct. 6-9, 1991.

TABLE 1 - NWE RESERVOIR PROPERTIES

Lithology	Sandstone /Dolomite
Depth (ft)	2600
Average Net Pay (ft)	60
Average Porosity	0.18
Average Permeability (md)	15
Dykstra-Parsons Coeff.	0.85
Reservoir Temp. (°F)	83
Reservoir Pressure (psi)	1100
Oil Gravity (°API)	37
Oil Viscosity (cp)	1.4

TABLE 2 - FOAM FIELD TRIAL SUMMARY

	First	Second	Third	Fourth
PREFOAM SLUG	90/03/02	90/07/28	90/10/19	91/06/21
Volume, bbls	2300	1100	1700	1700
Surfactant, lbs	3700	800	1300	2300
Conc., %	0.43	0.21	0.21	0.39
SAG	90/03/06	90/07/31	90/10/25	91/06/28
CO_2 Volume, bbls	8300	2200	4600	2900
Water Volume, bbls	2100	2300	5500	2700
Surfactant, lbs	1700	1600	5100	2700
Conc., %	0.21	0.19	0.26	0.28
Total Surfactant, lbs	5500	2400	6400	5000
CO_2 CHASE	90/04/27	90/08/24	90/11/21	91/07/21
Duration, Days	93	44	200	130

TABLE 3 - ECONOMICS ANALYSIS[1]

	WAG	WATER	FOAM
Oil Produced, bbl	14,400	3,000	27,400
	$288,000	$58,000	$548,000
CO_2 Injected, MCF	847,000	0	316,000
	$677,600	$0	$252,800
Water Injected, bbl	257,000	514,000	88,000
	$25,700	$51,400	$8,800
Other Expenses[2]	-	-	$38,100
Gain (Loss)	($415,300)	$6,600	$248,300

[1] CO_2 cost: $1.1/MCF-purchased CO_2 (60%), $0.35/MCF-recycled (40%). Oil price: $20/bbl. Water processing cost: $0.1/bbl.

[2] Surfactant cost: $0.94/lb, $18,100 total. Equipment depreciation, data acquisition, and other expenses: $20,000.

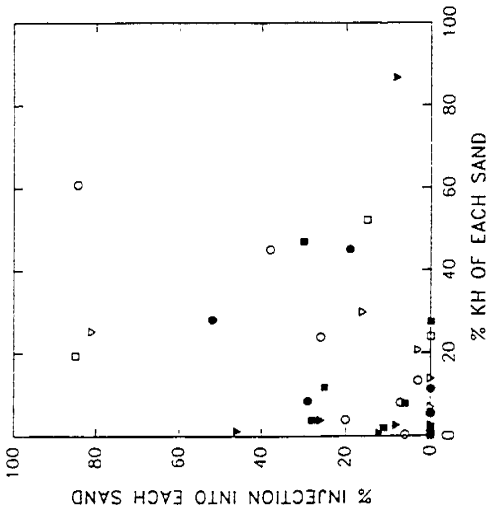

Fig. 2 - Correlation between injection profile and KH distribution. Each symbol represents a cased-hole injector in Section 7.

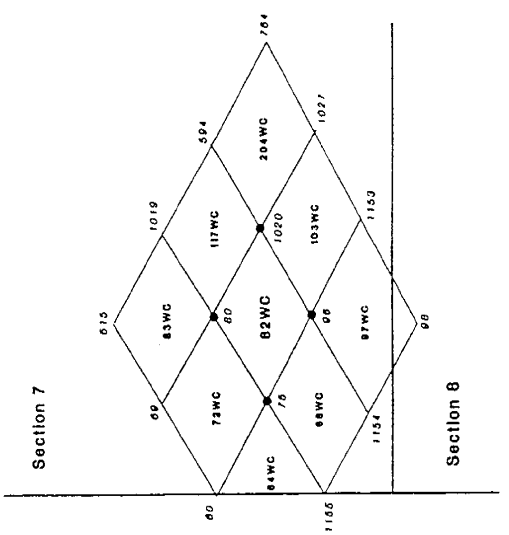

Fig. 4 - Well locations around 82WC, Section 7, North Ward-Estes.

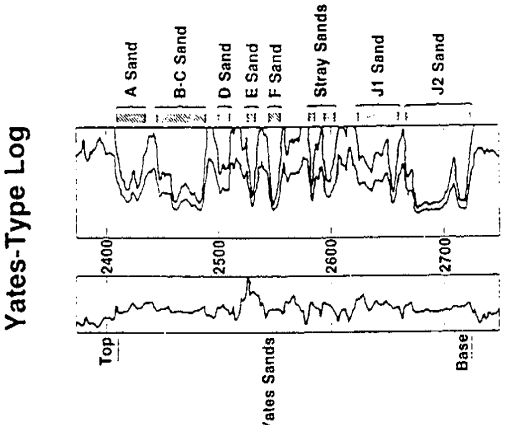

Fig. 1 - Type log of the Yates formation.

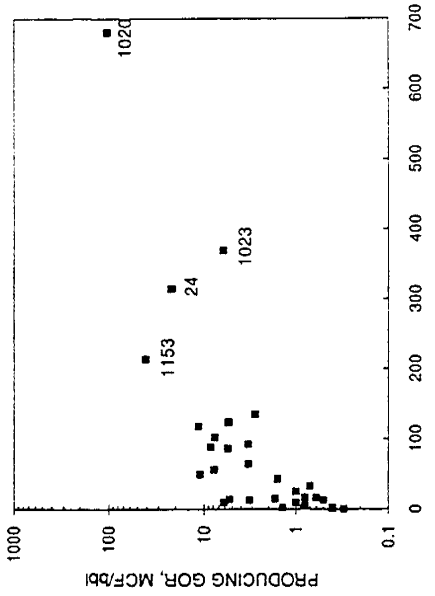

Fig. 3 - Identifying problem producers - comparing GOR and gas production rate of Section 7 producers before foam.

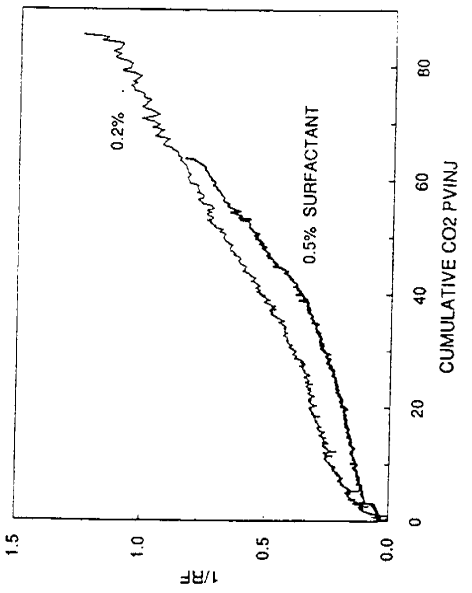

Fig. 6 - Foam durability in NWE cores - CO_2 displacing foam at 130 psi/ft.

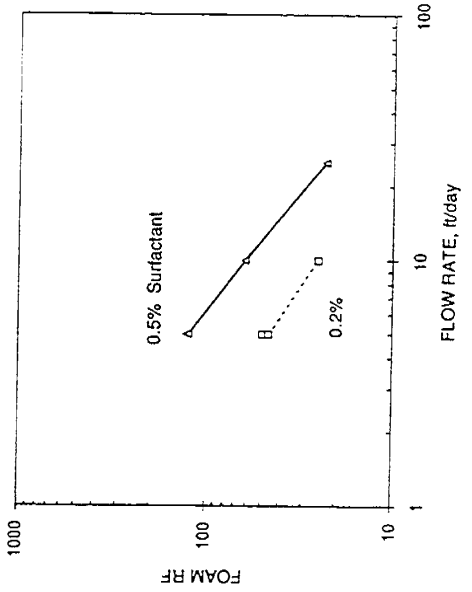

Fig. 8 - The effect of flow rate on foam resistance factor.

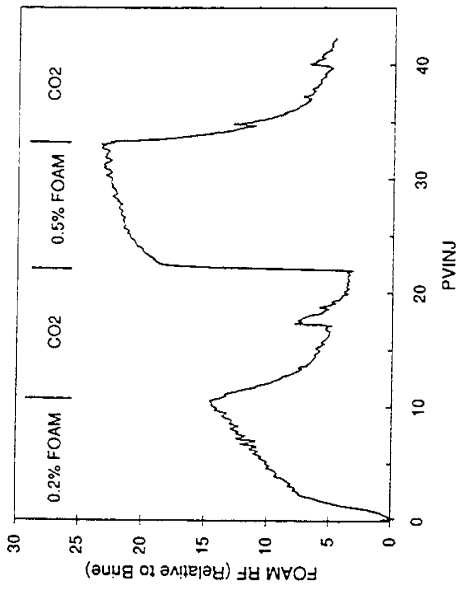

Fig. 5 - Foam generation followed by CO_2 chase in NWE cores.

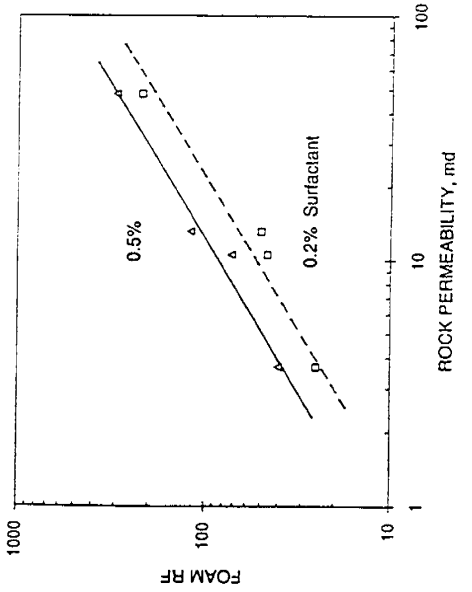

Fig. 7 - The effect of rock permeability on foam resistance factor.

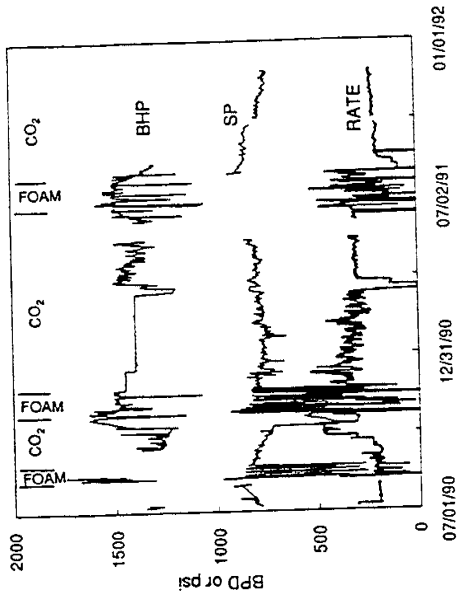

Fig. 10 - Injection rate and pressure during the 2nd, 3rd, and 4th foam treatments.

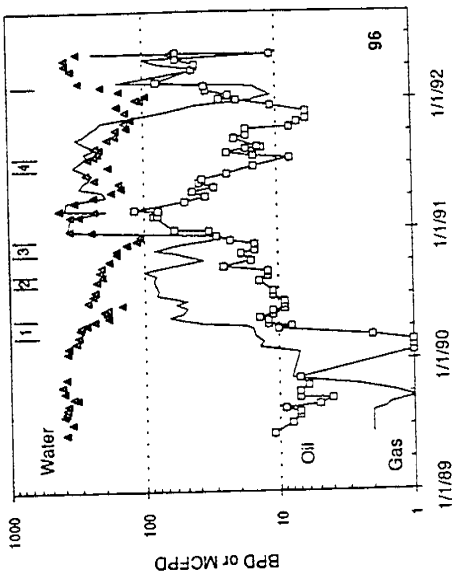

Fig. 12 - Production behavior of Well 96.

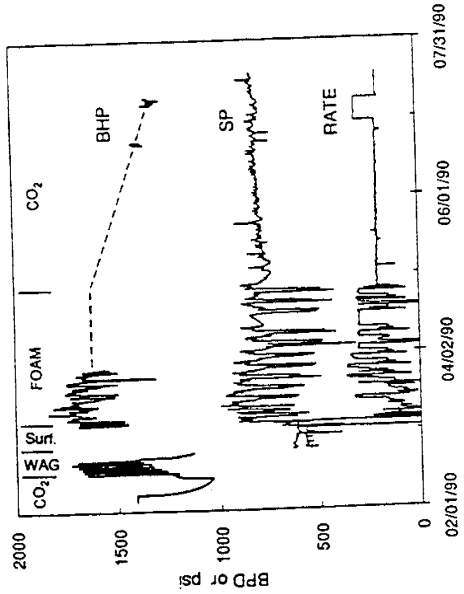

Fig. 9 - Injection rate and pressure during the 1st foam treatment.

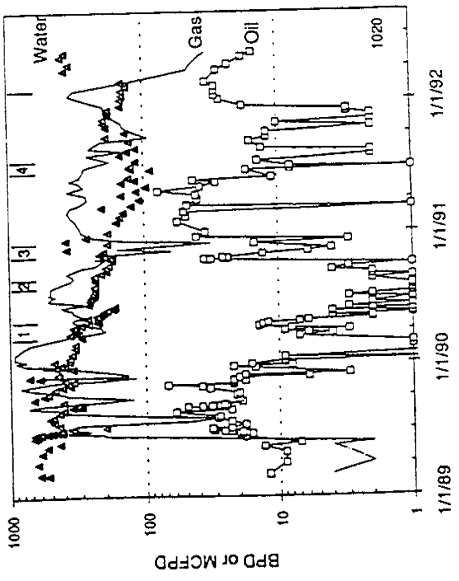

Fig. 11 - Production behavior of Well 1020.

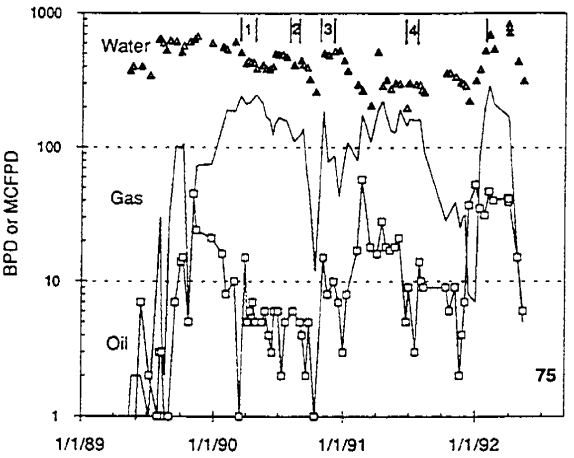

Fig. 13 - Production behavior of Well 75.

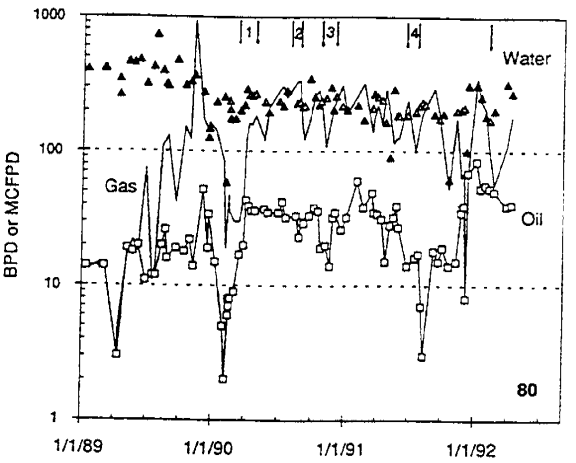

Fig. 14 - Production behavior of Well 80.

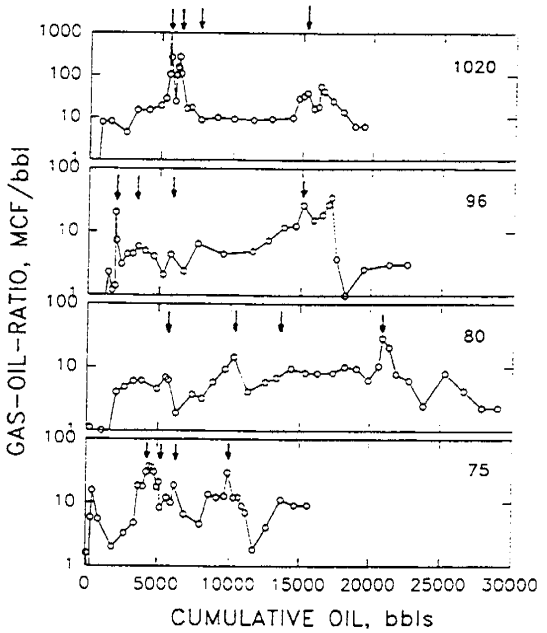

Fig. 15 - GOR and cumulative oil from the four offset producers to 82WC.

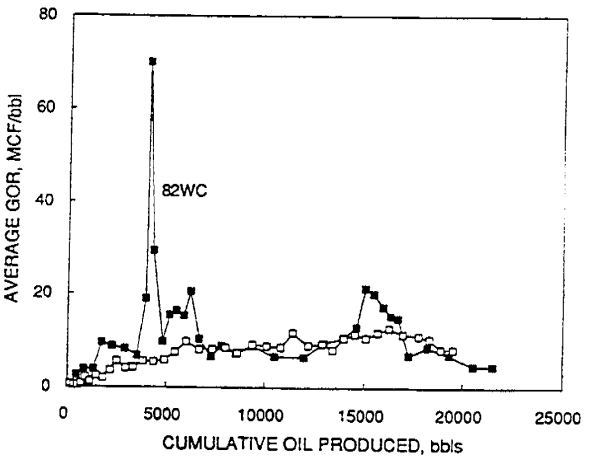

Fig. 16 - GOR and cumulative oil in 82WC and the surrounding patterns.

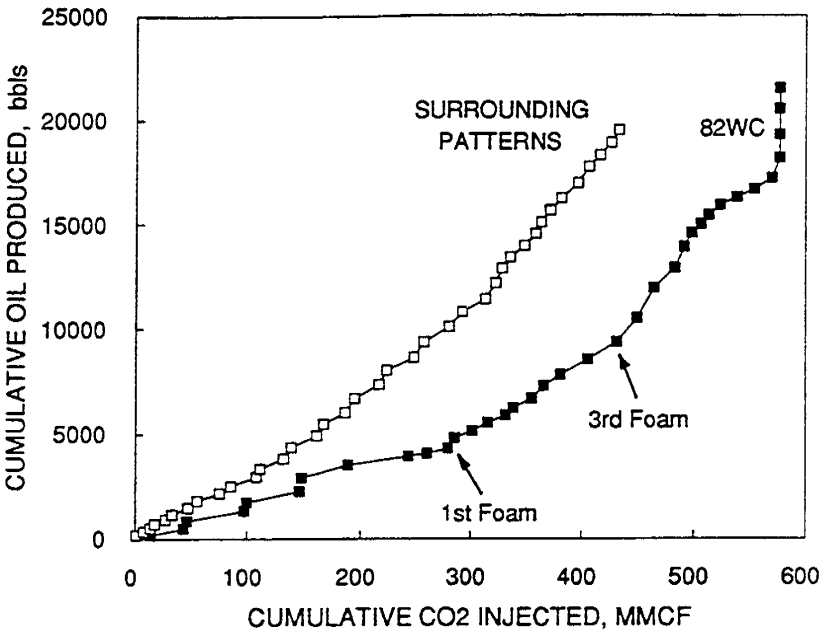

Fig. 17 - CO_2 utilization in 82WC and the surrounding patterns.

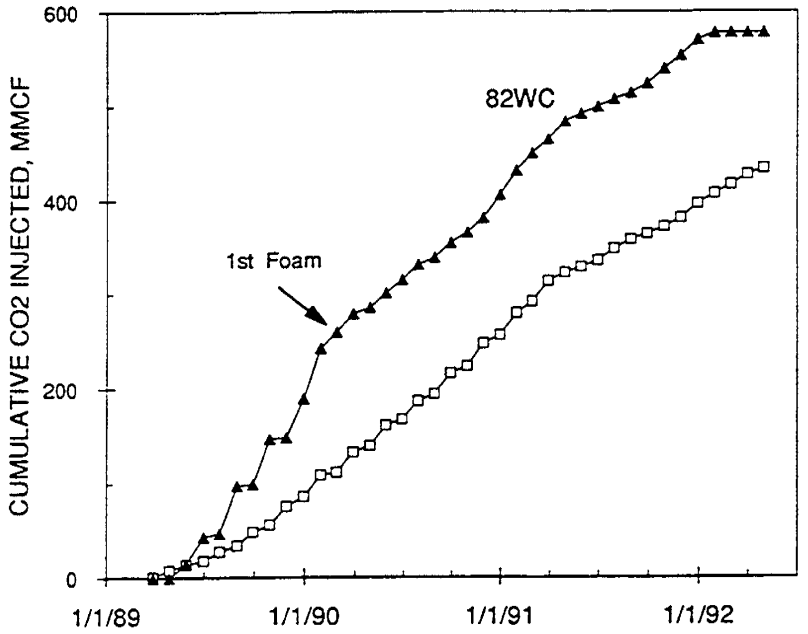

Fig. 18 - Cumulative CO_2 injected in 82WC and the surrounding patterns.

No. FS13

DOE/NIPER

Two Field Tests of CO_2-Foam

by J. P. Heller, New Mexico Petroleum Recovery Research Center, Socorro, New Mexico, and R. J. Watts, U.S. DOE, Morgantown, West Virginia

Author(s) are solely responsible for copyright and contents.

This paper was prepared for presentation at the DOE/NIPER, Symposium on Field Application of Foams for Oil Production held in Bakersfield, California, February 11-12, 1993.

This paper was selected for presentation by a Program Committee following review of information contained in an abstract submitted by the author(s). Contents of the paper, as presented, have not been reviewed and are subject to correction by the author(s). The material, as presented, does not necessarily reflect any position of the U.S. Department of Energy or the National Institute for Petroleum and Energy Research.

ABSTRACT

This manuscript describes and compares two different oilfield tests of the injection of CO_2-foam. Although there were numerous differences between these field trials, important similarities are also evident. The tests differed in the formation type, temperature and depth of the formation of interest, thickness of pay interval, the area affected by the test, type of surfactant used, the manner in which the mixture of surfactant solution and dense CO_2 were injected, and the magnitude of the industry interest and data-gathering effort. On the other hand, the tests have each demonstrated that CO_2-foam can be injected into an oilfield, and that the injectivity is decreased as a result. This outcome is evidently caused by the desired mechanism — the lowering of mobility of the injected fluid. The smaller of these tests, in West Virginia, was concluded five years ago. It was in a region of an oil field that contained very little remaining producible oil after a number of different production methods had been used to their respective economic limits. The other test, in a portion of a currently productive oilfield in the Permian Basin of eastern New Mexico, is currently underway. Each of the topics referred to in the above list is recounted in some detail in the following pages, and a number of conclusions are drawn regarding them.

INTRODUCTION

The field trials of CO_2-foam to be described in this paper were stimulated by early considerations that the special properties of foam could make it especially useful as an injection fluid in reservoirs. These considerations included patents by Bond and Holbrook[1] in 1958 and Craig and Lummus[2] in 1965, and technical investigations and reports by Bernard and Holm[3] in 1964 and by Holm[4] in 1968. While the continuous phase in the foam referred to in these early works was a water-based surfactant solution, the discontinuous but volumetrically major phase was air, nitrogen or natural gas. In 1970, L.W. Holm[5] described a field test of an air foam at 440 feet depth in the Siggins Field in Illinois. Air was injected both along with and after injection of an ammonium lauryl sulfate surfactant. Although these tests succeeded in reducing the water production from surrounding wells, they also reduced oil recovery. The decrease in water-oil ratio did not provide a sufficient economic motive for repetition of the tests. It had been hoped that foam could be used to reduce or block gas flow in higher permeability strata, while permitting oil to be recovered from other horizons in the field. Although this expectation remains, the views of reservoir engineers have also been modified and expanded since that time. In addition to the desire to reduce flow through the high permeability regions of the rock, the general goal of increased displacement efficiency has also been advanced.

In contrast to the early foams considered above or the steam foams used in heavy-oil reservoirs, the two tests to be described in this paper do not use air or nitrogen, but rather involve the use of dense carbon dioxide as the discontinuous, nonpolar phase in the foam. While air and nitrogen are compressed to high pressure under reservoir conditions, they remain gases of relatively low density. The properties of CO_2, on the other hand, are such that under reservoir conditions it is compressed into either a liquified or a dense-gas state. Although these technical designations suggest a considerable difference between the two forms of high-pressure CO_2, both of them are liquid-like, with the ability to dissolve many

hydrocarbons and hydrocarbon-based chemicals and polymers. The major factor that determines the solvent power of CO_2 is its density: even at temperatures above the 88°F critical point, CO_2 can be brought to a density that makes it completely miscible with hydrocarbons up to C_{14}, and capable of dissolving appreciable quantities of heavier components of crude oils. There is a relationship between reservoir depth and pressure required for a miscible CO_2 flood.[6]

It is this solvent power that gives CO_2 floods the possibility of very high efficiency. Because dense CO_2 is a solvent, one might foresee that if the solubility of the surfactants used in foam floods were large enough, they could be leached out of the water solution into the CO_2. For most of the surfactants used in experiments with CO_2-foam, however, only their solubility in water or brine is significant. It is of interest to note that in some of the earlier, low-pressure laboratory foam experiments, dense CO_2 was successfully simulated with isooctane, a light hydrocarbon.

Foam was often described as a Bingham fluid, or by some more complex rheological model. Despite this, Holm[7] stated clearly in a different 1968 paper that when foam was flowed through porous rock it did not stay together as a body, but that the bubbles were continually broken and reformed. Further, the works of Hirasaki and Lawson[8] in 1983, and of Kuntamukkula and Heller[9] in 1987, have shown that flow resistance depends greatly on the scale of the measurement. Even in the flow of foam through pipes, scale-independent rheological parameters cannot be found: as shown by Kraynik,[10] foam flows differently from ordinary, macroscopically continuous fluids even in this environment. Inside of small 3-dimensional porespace, the difference can be expected to be accentuated. In cores and larger samples of porous rock, one can measure the mobility as the ratio of the superficial or Darcy velocity to the pressure gradient. The lowered mobility of foam is evidence of lamellae or bubble films within the pores of the rock. Unfortunately, the population and strength of these lamellae cannot yet be predicted on the basis of macroscopic measurements of the surfactant properties, or of its concentration in the aqueous solution, or of the volumetric abundances of gas and liquid in the rock.

Extensive laboratory measurements have been made, much of it summarized by Yang and Reed[11] in 1989 and by Lee et al.[12] in 1990, so that much is known experimentally about the macroscopic behavior of a population of lamellae in reservoir rock, and the effect of various parameters on the mobility. In addition, theoretical work has been published by Zhou et al.[13] and others of Rossen's students, by Falls et al.[14] and by Friedmann and Jensen.[15] There is general agreement that foam mobility is dependent on the population density of the lamellae in the porespace and that, by several mechanisms, continual changes take place in this population as flow occurs through the rock. It is also agreed that the steady-state concentration of lamellae, and therefore the mobility of the foam, is the outcome of several, simultaneous dynamic processes. Although there have been numerical simulation schemes built upon models of these population-changing processes, detailed consensus is still lacking regarding the importance of the different mechanisms and of the natural heterogeneity of the rock.

Despite the existence of such unresolved questions, it is natural that there has been the desire to 'try it out' in oil field situations. Simultaneously there has been a natural reluctance to risk a large amount of capital or oil reserves. The two field tests to be described were both under control of the regular field operators, with financial support from the U.S. Department of Energy and additional technical support from the New Mexico Petroleum Recovery Research Center.

DESCRIPTIONS OF THE PROJECTS

Rock Creek

In both of the tests to be discussed, continuous or WAG CO_2 floods preceded the tests of CO_2-foam. In both of them, it had become apparent that additional mobility control measures were required, in order to increase the oil recovery. From this point onward, the situations in these two tests diverged. The earlier of the tests, a description of which is given first, was considerably smaller in area and in scope. This test took place in the Rock Creek field of Roane County, West Virginia. This oil field had been produced since 1906, and was near the end of its economic life in 1984, when the CO_2-foam test was started. As noted in Table I, the producing horizon, the Big Injun Sand, is a 25 foot thick, low permeability sandstone (about 21.6 md) with high clay content and porosity of 21.7%, about 2000 feet below the surface. The oil is paraffinic, with a viscosity of 3.2 cp. The location of the field is shown in Figure 1, and a more detailed map of the test site in Figure 2. The area utilized in this test was a small region near one of the side injectors in the two ten-acre five-spots that had been subjected to a conventional CO_2 flood and subsequent waterflooding in addition to primary production and to gas recycling. The early exploitation history of the Rock Creek field, including the CO_2 project, has been described by San Filippo and Guckert.[16]

In the years from 1977 to 1983 a test of continuous CO_2 injection had been performed, with the assistance of the DOE, in the area of the two fivespots shown in Figure 2 consisting of the injection wells PI-1 through PI-6 and the central producers LWS-1 and LWS-4. In this test, the area had first been pressurized by water injection into the above-mentioned pattern wells, as well as into the surrounding "backup water injection" wells also shown in Fig. 2. When the predetermined Minimum Miscibility Pressure (MMP) was reached, CO_2 injection was started into the six wells of the five spot, while water injection into the surrounding wells was maintained.

During this time the additional injectors PI-7 and PI-8, and the observation well OB-1, were also drilled. The injection of CO_2 continued for two years, interrupted three times during the period, for CO_2 supply and operational reasons. Oil production climbed in response to the CO_2 injection in the last half of 1979. It remained high through most of 1980 and climbed still higher during the first part of 1981, after injection was started in the two new wells. Following this rise, however, there was a fairly precipitous decrease. Production of CO_2 had started only a few months following the start of CO_2 injection, and also continued throughout the period of oil production, rising to a high level throughout 1981. As oil production decreased in that year, it became apparent that the productivity of the flood was decreasing, and injection of CO_2 was halted in January of 1982. The production of both oil and CO_2 then decreased rapidly, and water injection was also halted at the end of 1982.

During the latter part of the CO_2 flood, the two new injectors, and two observation wells OB-1 and OB-2 had been drilled. The first three of these wells opened a "mini-pilot" region in the southeastern corner of the existing patterns, as OB-1 was produced. They were partly responsible for the increased oil production in the latter half of 1981. Whereas OB-1 was nearly halfway between PI-6 and the producer LWS-1, the second observation well OB-2 was only 75 feet from PI-2, and was primarily drilled to help determine the effect of the CO_2 flood. OB-2 was cored and its oil content at various levels was measured. These cores showed evidence that while the CO_2 flood had reduced the oil saturation to about 4% in the topmost ten feet of the pay, it had not been so effective in the lower half of the formation, where the oil saturation after the flood averaged about 19%.

It was shown by this short test that injected CO_2 could displace some Rock Creek oil that could not be recovered by waterflood. On the other hand, the sweep efficiency was low, and the economics were poor even before major CO_2 breakthrough, owing mostly to the fact no CO_2 recovery program was attempted, and that only food-grade CO_2 was available, brought in by truck over mountain roads to tanks at the site.

Because the quantity of CO_2 which could be used in the test was limited, a full-scale program to seek additional oil production by CO_2-foam from Rock Creek's two five-spot patterns was not planned. Instead, it was hoped that useful test results could be obtained in the "mini-pilot" area outlined on Fig. 2, defined by PI-6 through PI-8. Injection of CO_2-foam would be into these three wells, with production from OB-1. To enable the progress of the fronts of CO_2 and foam to be followed as they moved away from PI-7 toward OB-1, the additional observation well OB-3 was drilled. Extensive plans were also drawn up to measure the flow velocity past OB-1, and to take small fluid samples from it for other analyses.

Unfortunately, circumstances forced these initial plans to be abandoned. Preliminary tests on the prospective injectors revealed that substantial quantities of fluid injected into PI-7 were leaking out of the Big Injun formation. With the discovery of this condition, and the operator's judgement that the well could not be repaired economically, the decision was made to perform the CO_2-foam test in a different portion of the field. The new injection site was PI-2, with major production at LWS-4, 465 feet away. So that fluid composition observations could be made in a reasonable time, four perforations were shot though the fiberglass casing of OB-2, which was only 75 feet away in the same direction, two at the depth of 2065 feet and two at 2075.

In previous operations the well PI-2 had been used for the injection of both water and CO_2 (but not simultaneously). Available injection water is low in mineral content (about 500 ppm dissolved solids) and is obtained from a shallow well. Cold liquid CO_2 was pumped into the injection system from the pressurized and insulated tanks at the site, and passed through a heater that raised its temperature to about 65°F (18°C) and the pressure to 1000 psi (6.9 Mpa). Injection plant pressures for both water and CO_2 could be maintained at a desired level by use of pressure-controlled by-pass valves. The rates of flow of CO_2 and of water were measured separately, by calibrated turbine meters.

Only minor modifications of this injection system were needed for the mobility control test. Admixture of surfactant into the injection water stream was accomplished by means of a high-pressure chemical feed pump that sent the output directly into the pipe carrying water to PI-2. The feed pump was operated at such a stroke setting that, at the nominal water injection rate of 100 bbl/day, the concentration of surfactant would be as specified. This surfactant mixing system was to be used during both injection of the surfactant pad, and later while both CO_2 and surfactant solution were being injected simultaneously to form the CO_2-foam.

To safeguard against corrosion during the simultaneous injection period, the surfactant solution and the CO_2 were brought from the injection plant through separate conductors and mixed only at the wellhead. A two-inch fiberglass tubing carried them down the wellbore in two-phase flow (calculated to be turbulent at total rates above about 30 BPD) to an isolated cased and perforated region below a packer set just below the top of the Big Injun.

The injection program consisted of a short period of fresh water injection (which also contained a slug of ammonium thiocyanate as a tracer) at about 150 BPD, followed by a "CO_2 pad" of water containing Alipal CD-128 at a concentration of 0.1% active. Some feed pump difficulty led to irregular flow rates when surfactant was first added, but these problems were overcome and a pad of 2644 barrels of surfactant solution was injected into PI-2 by November, 1984. At this point the

operator commenced simultaneous injection of CO_2 and an 0.05% solution of Alipal in water. The volumetric fraction of CO_2 in the mixture was 80%. Unfortunately this injection was also intermittent, and was even interrupted by a three month shutdown during which PI-2 underwent extensive well work. Altogether, however, a total volume of almost 8000 barrels of CO_2-foam were injected into PI-2. Although the foam injection rate could not be maintained at over 100 BPD, and was sometimes much less, these sharp decreases were apparently due to the deteriorating condition of the well casing that led to a developing casing seal leak and the need for workover. Despite this, there were extended periods in which the simultaneous injection was successfully accomplished, and the individual rates of CO_2 and surfactant solution maintained.

The CO_2-foam test in Rock Creek had two major goals. The first was to determine whether the oil remaining in this area could be displaced by a slug of thickened CO_2 to form a mobile oil, and be detected at a nearby observation well. A second goal was to test the injectivity of CO_2-foam as liquid CO_2 and dilute surfactant solution were pumped simultaneously down fiberglass tubing into the injection well. It had been realized at the start of the project, of course, that not enough CO_2 was available, and the test could not last long enough, to reach the designated producer LWS-4 with any of the injected fluids. Instead, a relatively small production rate (8-10 BPD) was maintained at the closer-by OB-2 in the hope that we could then observe in daily samples the changes in composition of the fluids passing by it.

Unfortunately, the first of these goals was unsuccessful; the samples collected from OB-2 showed no sign of either the NH_4CN tracer, the surfactant, or oil. Several reasons for this may be cited, among which might be: the total fluid injected was only marginally sufficient to fill a cylindrical region of a hypothetically uniform reservoir out to 75 feet radial distance, the perforations in OB-2 may well have been accidently located in lower permeability zones, the fraction of remaining oil may have been too small to form an oil bank to be displaced by foam, or the rate of adsorption may have been greater than that predicted from our laboratory experiments (which indeed were not well developed at that time).

The second goal, however, was quite successful. It did prove possible to inject surfactant solution and CO_2 simultaneously. Some control problems were experienced when this was first attempted; it was difficult to maintain the desired "quality" (or flowing ratio) with precision, except as averaged over several days. Such difficulties are to be expected because of the markedly different compressibilities of the two fluids. On the other hand, maintenance of the ratio "on the average" should certainly be quite acceptable. A major reason why simultaneous injection could be satisfactory in Rock Creek, however, is the relatively narrow pay zone, that provided only a short distance in which gravitational segregation of the injected fluids could occur.

A second project success is that the CO_2-foam did lower the mobility ratio of the flood in about the ratio specified. The evidence for this was in the increased surface pressure required for injection after several weeks of injection. Laboratory measurements of the Alipal foam used in the field test had shown a mobility about 0.5 relative to that of a water/CO_2 mixture of the same proportions. Although under the intermittent flooding circumstances described above it was difficult to arrive at a precise figure, it is apparent that the injectivity index was indeed somewhat less than one half. Further details of the CO_2-foam project are also available.[17,18]

East Vacuum

The second of the CO_2-foam tests that are the subjects of this paper is currently being conducted in the East Vacuum field, 15 miles northwest of Hobbs, in Lea County of New Mexico. The WAG section of the field, and the pattern selected for the CO_2-foam test, are shown in Figure 3. The primary goal of the project is to evaluate the use of CO_2-foam for field-scale application. The project includes objectives to: 1) conduct reservoir studies, laboratory tests, simulation runs and field tests to evaluate the use of foam for both mobility control and fluid diversion, and 2) evaluate the concept of CO_2-foam in the field by using a reservoir where CO_2 flooding is ongoing, characterizing the reservoir, modeling the process, and verifying the effectiveness.

Referring to Table I, the reservoir rock in this field is a dolomitic limestone, known as the San Andres formation. It consists of more than half a dozen pay zones distributed over about 250 feet at an average depth from surface of 4450 feet. The permeability in these zones varies from one or two to 400 md, and the porosity from 6% to 16.5%. The oilfield was unitized in 1978 into the East Vacuum Grayburg San Andres Unit (EVGSAU), and waterflood was initiated in 1979. CO_2-WAG injection was then started in 1985, and has arrested the decline of oil production that was becoming evident at that time. The field is divided into three sections for a staggered, 2:1 CO_2-WAG injection schedule, with water injected into the central wells of the nine-spot patterns in each section for eight months, and CO_2 for four. Early history of the East Vacuum development, including the design of the CO_2 flood, have been recorded by Brownlee and Sugg.[19]

In any given area, a WAG cycle consists of about four months of CO_2 injection followed by eight months of water injection. This results in approximately 1.5 To 2% hydrocarbon pore volume (HCPV) CO_2 injection and 3 to 4% HCPV brine injection per WAG cycle. The project is currently in the seventh WAG cycle. The tertiary oil response at EVGSAU to date has been very favorable. As shown in Fig. 4, the waterflood decline established prior to CO_2 injection has been arrested, and oil production for the unit has held approximately constant near the current 9000 BOPD over the past six years.

While the overall project performance of the WAG CO_2 program has been very encouraging, certain wells/patterns have shown anomalously high CO_2 production. This has resulted in isolated cases of poor pattern sweep efficiency, inefficient CO_2 utilization, and increased recycling costs and compression requirements. The CO_2 Foam Field Verification Pilot was designed to evaluate the application of foam mobility control technology for controlling the excessive CO_2 production problems in a field-scale CO_2 flood project.

During the first year of the project, the Petroleum Recovery Research Center (PRRC) identified the East Vacuum Grayburg/San Andres Unit (EVGSAU), operated by Phillips Petroleum Company (PPCo), as an appropriate site for the proposed work. Representatives from the PRRC and PPCo prepared an initial site-specific plan for the proposed work at the EVGSAU, which was approved by the EVGSAU Working Interest Owners (WIO) in June 1990. A Joint Project Advisory Team (JPAT), representing several of the EVGSAU WIO companies, serves as a technical steering committee that acts in an advisory capacity.

A typical one of the 80 acre, inverted nine-spot patterns was chosen for the CO_2-foam test. Several different criteria were considered for this selection: that the pattern had shown excessive CO_2 breakthrough in one of its production wells, that the reservoir geology was typical of the field, and that the pattern injector had sufficient injectivity to allow some margin for decrease of mobility of the injected fluids. All of the above conditions were met in the chosen pattern. The injection well is designated 3332-001 on Fig. 3, and the "offending well" with higher CO_2 production, # 032, lies to the southwest of the injector.

An observation well was drilled to improve reservoir characterization in the pattern area, to serve as an observation well, and to provide core material for laboratory tests. The location of the observation well (3332-003) in the pilot pattern, about 150 feet from the WAG injector, is shown in Fig. 3. This well was sponge cored to provide current oil saturation information, as well as additional details on the reservoir geology in the pattern area. As noted above, the permeability variation over the reservoir interval is quite large.

The EVGSAU produces primarily from the San Andres Formation. At EVGSAU, the San Andres can be divided into upper and lower sections by the Lovington sandstone/siltstone. The San Andres sections consist of a series of shallowing-upward carbonate sequences, each typically 20 to 30 feet thick, which have been extensively dolomitized. Total gross reservoir thickness ranges from 200 to 300 feet. A geologic study of the EVGSAU reservoir identified twelve zones which are laterally continuous across the foam pilot area (Fig. 5). Zone C (shown subdivided into C1, C2, and C3 on the type log in Fig. 3) is the major flow unit within the pilot area. Zones D and E show good porosity development and high oil saturation, but are less permeable and take only a small fraction of the fluid injected into this pattern. The A and B zones show little or no reservoir potential in this area, while the zones below the Lovington have good porosity and permeability, but have high water saturation in the pilot area. Falloff tests from most of the EVGSAU injection wells show an extended period of linear flow behavior, which is interpreted as fracture flow in the reservoir. However, the excessive CO_2 breakthrough problems do not appear to be simply the result of direct fracture communication between injectors and producers.

Within the foam pilot pattern area, the zones designated as C2 and C3 (Fig. 5) contain intervals with very high permeability. For example, a five-foot interval in Zone C2 from the observation well core averages almost 250 millidarcies. Oil saturations obtained from the sponge core in this interval were consistently less than 5% PV, indicating they had probably been contacted by a large volume of CO_2. Injection profiles taken in the WAG injector show almost two-thirds of the injected fluids entering Zone C2 and the lower portion of Zone C3. In contrast, Zone E, which shows high porosity and good oil saturation, is indicated to be taking less than 5% of the injected fluid. One of the primary objectives of the foam injection is to divert a larger percentage of the injected CO_2 into these lower permeability zones which are not being efficiently flooded in the current WAG operation.

In the design of the CO_2-foam test it became apparent that the extent of the project would be limited not by the available CO_2, as in Rock Creek, but by the surfactant quantity. Preliminary laboratory data indicated surfactant adsorption would be in the range of 600 to 1800 pounds of active surfactant adsorbed per acre-foot of bulk formation volume contacted. Based on economic considerations, it was decided to design the project primarily for near-well fluid diversion using a smaller (approximately 1% HCPV), higher surfactant concentration foam slug rather than attempt to control mobility throughout the pattern using a larger volume slug with a lower surfactant concentration.

All members of the JPAT also agreed after discussion that because of the large overall interval, there was little hope of a uniform distribution of CO_2 and surfactant solution in the different pay zones, if simultaneous injection was used. In consequence, a rapid "Surfactant-Alternated-with-Gas" (SAG) was planned. After consultation with the operator's field engineers, it was decided that two-week cycles were practical, consisting of about 11 days of CO_2 injection, followed by 3 days of brine/surfactant injection. During the year previous to the initiation of the actual foam injection, the effect of alternations were simulated by "rapid WAG" cycles.

For both tests, the choice of surfactant was of great importance, and the choices were made according to similar criteria. These were primarily 1) that laboratory tests showed

the mobility of CO_2-foam formed with the surfactant in question to be significantly lower than the combined mobility of a surfactant-free mixture of water and CO_2 in the same ratio, 2) that the adsorption of surfactant on the reservoir rock was not so large as to render the project too costly, 3) that the surfactant could remain chemically stable in the reservoir environment, and 4) that the lamellae formed between bubbles of dense CO_2, by solutions of this surfactant in the available water, would be relatively stable. In support of the CO_2-foam tests at both Rock Creek and at East Vacuum, laboratory tests were conducted to determine whether the proposed surfactants would be satisfactory.

Although the criteria were similar for the two tests in the two cases, they were not identical. The differences resulted not only from contrast between the fields, but also to the new knowledge that has been obtained, and the new instruments and experimental methods that were developed in the intervening years. Generally, it has also been possible to examine each of the above criteria more critically and extensively in the tests conducted for the EVGSAU field work. An important element of this latter has been the result of the wide interest and ownership of the East Vacuum lease. Important parts of the tests were consequently performed in various industrial laboratories, as well as in those of the PRRC. Principal among these laboratory tests were those conducted by PPCo in Bartlesville, and by the Chevron laboratories in Richmond, California.

Amongst these laboratories, tests were made on about six different surfactants for the various important properties mentioned above, although not all samples were tested at each laboratory or for each property. From an evaluation of all the results collected for this project, surfactant cost data, and other factors such as surfactant handleability, a consensus of the JPAT representatives favored the selection of Chevron Chaser CD-1045® for the field test at EVGSAU. While there was some difference of opinion regarding optimum surfactant concentration, the JPAT representatives agreed that 2500 ppm CD-1045® should be used for both a pre-foam pad to satisfy surfactant adsorption in the reservoir as well as for the surfactant solution used during (SAG) cycles of the field test.

Prior to the injection of surfactant or CO_2-foam, an extensive "baseline" test period of about a year's duration was scheduled. During this time, the regular schedule of injection into the designated pattern was modified. The planned eight months of brine injection was shortened by a month and a half, and two months of rapid WAG injection was interposed prior to the next four months of CO_2. This provided not only assurance that field operators could successfully interchange injection fluids on such a tight schedule, but also that appropriate pressure records would exist for comparison purposes.

Surface facilities for foam injection are fairly simple and required no changes to the existing injection meter run. The CO_2 is brought in by high-pressure line from the CO_2 plant at the field. A schematic of the facilities is shown in Fig. 6. In the future, since the surface facilities needed to handle the surfactant are fairly simple, it is anticipated that all of this equipment could be truck- or trailer-mounted to facilitate individual well treatments.

Surfactant is delivered in bulk 5500 gallon (131 bbl) lots via a tanker truck. Since enough storage capacity is needed on location to handle a new shipment without being critically low on surfactant, a standard 210-bbl fiberglass tank was selected. The tank is connected via 1-inch tubing through a strainer to a variable stroke length Bran-Lubbe injection pump. This pump was selected for its ability to change injection rate easily, as it was anticipated that the surfactant injection rate might need to be reduced during the foam generation period. Since the surfactant injection period during foam generation SAG cycles is only three days, a manual control on the pump was considered to be adequate for maintaining a steady surfactant concentration (versus automating the pump with a rate controller). The pump is connected to the existing injection line with 1/2-inch stainless steel tubing to a port downstream of the injection meter and pressure transducer. Thus, the injection meter measures only the injection water and not the combination of surfactant and water.

Each tanker truck shipment of surfactant had a quality control certificate issued by the manufacturer upon loading to document the chemical's content, activity, and specific gravity. In addition, routine quality control checks were made on the delivered product by the operator prior to injection. There was some concern that the viscous (approximately 200 cp.) surfactant would not mix adequately with the injection brine in the 35 feet of 2-inch injection line upstream of the wellhead sampling point, and an in-line mixer might be needed. However, the surfactant concentration measured on multiple samples taken at the injection wellhead during the first few weeks of injection were consistent and the samples were clear and uniform, indicating no significant problems with mixing. Based on these sampling results it was concluded that an in-line mixer was not needed.

The surfactant pad or adsorption slug injection was initiated in April 1992, and continued until June 15 of the same year. This was followed by five cycles of rapid SAG, during the later of which the injection pressure has climbed high enough to slow CO_2 injection, although not intolerably. At this writing, the precise future of the course to be taken is in some doubt, but it is apparent that again the first objective, of lowering the injectivity with the apparent propagation of foam into the formation, is being accomplished. A second result that seems to be developing is a reduced amount of direct CO_2 conductivity to the offending well, and a corresponding rise in the oil production.

As in the case of the Rock Creek field, it is difficult to compute a precise value for the injectivity decrease due to CO_2-foam. The difficulty is greater because of the changing pressures during the injection of foam during the rapid SAG periods. It is apparent, though, that the mobility has been decreased; it is to be hoped that as more data is collected it may become possible to determine the changed injectivity more exactly. Further details on the EVGSAU CO_2-foam project can be found in recent SPE papers[20-22] and DOE reports,[23,24] and more will be forthcoming.

CONCLUSIONS

Although the engineering attention accorded to the EVGSAU test has greatly exceeded that which was given to the Rock Creek test, both tests have confirmed that it is feasible to inject foam into a reservoir, and to propagate it away from the injector. Neither has answered the long-term question of whether foam can increase sweep efficiency. This latter question seems unanswerable by a test of such limited duration and extent as these two, and must be left for future, larger-scale and longer-term projects.

A further unanswered question has not been mentioned in this paper; it asks "Under what conditions can Selective Mobility Reduction (SMR) be achieved, in which the mobility of CO_2-foam in higher permeability rock in a formation will be less than proportional to its mobility in lower permeability regions." This question is the topic of active discussion, and a further investigation is just now being initiated.

ACKNOWLEDGEMENTS

The cooperation of Dave Martin and Jyun-Syung Tsau of the Petroleum Recovery Research Center is acknowledged for consultations during preparation of this paper. The authors are also grateful to many unwitting collaborators such as Jim Stevens and others of Phillips Petroleum Company, and to Paul King and Dan Boone of Pennzoil, for having taken much of the data and for performing the field work represented in this paper.

REFERENCES

1. Bond, D.C. and Holbrook, O.C.: "Gas Drive Recovery Process," U.S. Patent No. 2,866,507 (1958).

2. Craig, F.F. and Lummus, J.L.: "Oil Recovery by Foam Drive," U.S. Patent #3,185,634 (May 25, 1965).

3. Bernard, G.G. and Holm, L.W.: "Effect of Foam on Permeability of Porous Media to Gas," *SPEJ* (Sept. 1964) **4**, 267-74.

4. Holm, L.W.: "The Mechanism of Gas and Liquid Flow Through Porous Media in the Presence of Foam," *SPEJ* (Dec. 1968) **8**, 359-69.

5. Holm, L.W.: "Foam Injection Test in the Siggins Field, Illinois," *JPT* (Dec. 1970) **22**, 1499-1506.

6. Heller, J.P. and Taber, J.J.: "Influence of Reservoir Depth on Enhanced Oil Recovery by CO_2 Flooding," paper SPE 15001 presented at the 1986 Permian Basin Oil and Gas Recovery Conference, Midland, TX, March 13-14.

7. Holm, L.W.: "The Mechanism of Gas and Liquid Flow Through Porous Media in the Presence of Foam," *SPEJ* (Dec. 1968) **8**, 359-69.

8. Hirasaki, G.J. and Lawson, J.B.: "Mechanism of Foam Flow in Porous Media—Apparent Viscosity in Smooth Capillaries," *SPEJ* (1985) **25**, 176-90; SPE 12129, 1983.

9. Heller, J.P. and Kuntamukkula, M.S.: "Critical Review of Foam Rheology Literature," *I&EC Res.* (1987) **26**, 318-25.

10. Kraynik, A.M.: "Aqueous Foam Rheology," paper B-10 presented at 54th Annual Meeting of Society of Rheology, Evanston, IL, Oct. 24-28, 1982.

11. Yang, S.H. and Reed, R.L.: "Mobility Control Using CO_2 Foams," paper SPE 19689 presented at the 64th Annual Technical Conference of the Society of Petroleum Engineers, San Antonio, TX, Oct. 8-11, 1989.

12. Lee, H.O., Heller, J.P., and Hoefer, A.M.W.: "Change in Apparent Viscosity of CO_2-Foam with Rock Permeability," *SPERE* (1991) 421-428; paper SPE 20194 presented at the SPE/DOE Seventh Symposium on Enhanced Oil Recovery, Tulsa, April 22-25, 1990.

13. Zhou, Z. and Rossen, W.R.: "Applying Fractional Flow Theory to Foam Processes at the 'Limiting Capillary Pressure'," paper SPE/DOE 24180 presented at the Eighth SPE/DOE Symposium on EOR, Tulsa, April 22-24, 1992.

14. Falls, A.H., Gauglitz, P.A., and Hirasaki, G.J.: "Development of a Mechanistic Foam Simulator: The Population Balance and Generation by Snap-Off," paper SPE/DOE 14961 presented at the 1986 SPE/DOE Symposium on EOR.

15. Friedmann, F. and Jensen, J.A.: "Some Parameters Influencing the Formation and Propagation of Foams in Porous Media," paper SPE 15087 presented at the 1986

California Regional Meeting of the Society of Petroleum Engineers.

16. San Filippo, G.P. and Guckert, L.G.: "Development of a Pilot CO_2 Flood in the Rock Creek-Big Injun Field, Roane County, WV," presented at the ERDA Symposium (Aug.-Sept. 1977) C/3, 1-15; paper SPE 6626 presented at the Eastern Regional Meeting, Pittsburgh, Oct. 27-28, 1977.

17. Heller, J.P., Boone, D.A., and Watts, R.J.: "Field Test of CO_2 Mobility Control at Rock Creek," paper SPE 14395 presented at the 1985 SPE Conference, Las Vegas, September 22-25.

18. Heller, J.P.: "Mobility Control for CO_2 Injection," Final Report, U.S.Department of Energy, MC/16426-19, August 1986.

19. Brownlee, M.H. and Sugg, L.A.: "East Vacuum Grayburg-San Andres Unit CO_2 Injection Project: Development and Results to Date," *Proc.*, 62nd Annual Technical Conference and Exhibition, SPE 16721 (1987) 241-254.

20. Martin, F.D., Heller, J.P., Weiss, W.W., Tsau, Jyun-Syung, Zornes, D.R., Sugg, L.A., Stevens, J.E., and Kim, J.E.: "CO_2 Foam Field Verification Pilot Test at EVGSAU Injection Project - Phase I: Project Planning and Initial Results," paper SPE 24176 presented at the 1992 SPE/DOE Enhanced Oil Recovery Symposium, Tulsa, April 22-24.

21. Stevens, J.E., Harpole, K.J., Zornes, D.R., and Martin, F.D.: "CO_2 Foam Field Verification Pilot Test at EVGSAU Phase II: Foam Injection Design and Operating Plan," paper SPE 24642 presented at the 67th Annual Technical Conference and Exhibition, Washington, D.C., October 4-7, 1992.

22. Tsau, J.S. and Heller, J.P.: "Evaluation of Surfactants for CO_2-Foam Mobility Control," paper SPE 24013 presented at the 1992 Permian Basin Oil and Gas Recovery Conference, Midland, March 18-20.

23. Martin, F.D., Heller, J.P., and Weiss, W.W.: "Field Verification of CO_2-Foam," Annual Report to U.S. Department of Energy, No. DOE/MC/26031-4 (May 1991).

24. Martin, F.D., Heller, J.P., and Weiss, W.W.: "Field Verification of CO_2-Foam," 2nd Annual Report to U.S. Department of Energy, No. DOE/MC/26031-6 (May 1992).

TABLE I

	Rock Creek	EVGSAU
Formation Type	Sandstone	Dolomite Limestone
Depth (ft)	2000	4450
Reservoir Temperature °F	73	102
Average Reservoir Pressure (psi)	1500	2100
Average Net Pay (ft)	25	71
Gross Thickness (ft)	35	250
ϕ (%)	21.7	11/7
k (md)	21.5	11
Oil Gravity (°API)	43	38
CO_2 Area (acres)	20	5000
Area of Foam Test (acres)	2.5	134

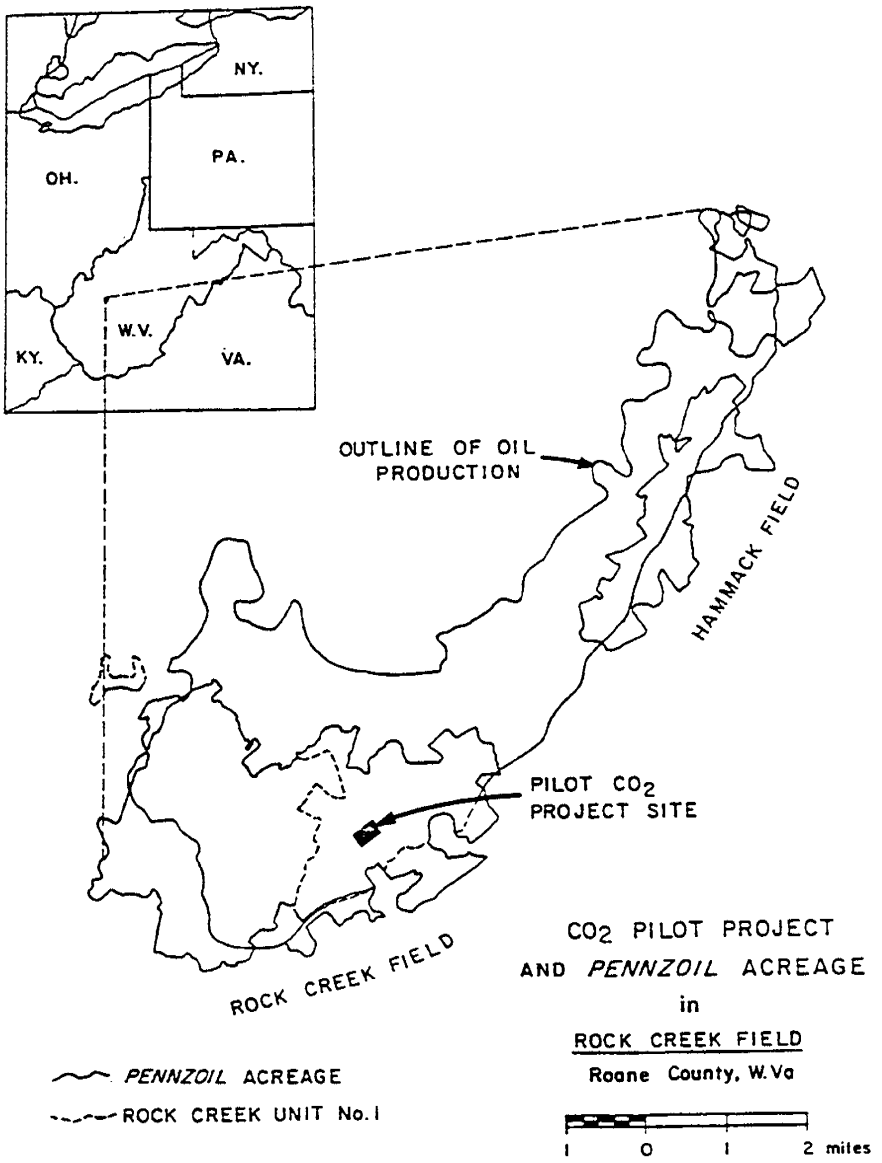

Figure 1. Location of Rock Creek Field in West Virginia.

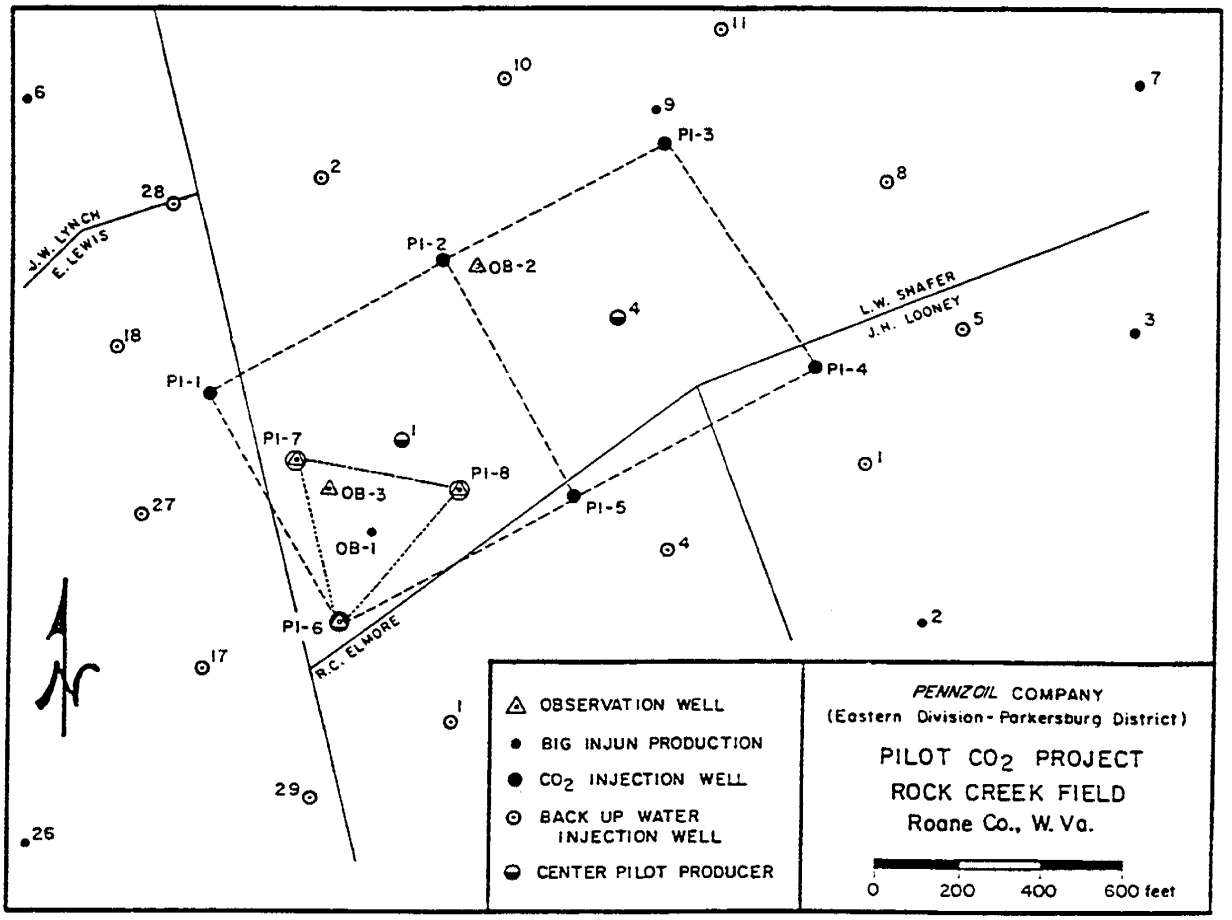

Figure 2. CO_2 and CO_2-foam patterns in Rock Creek Field.

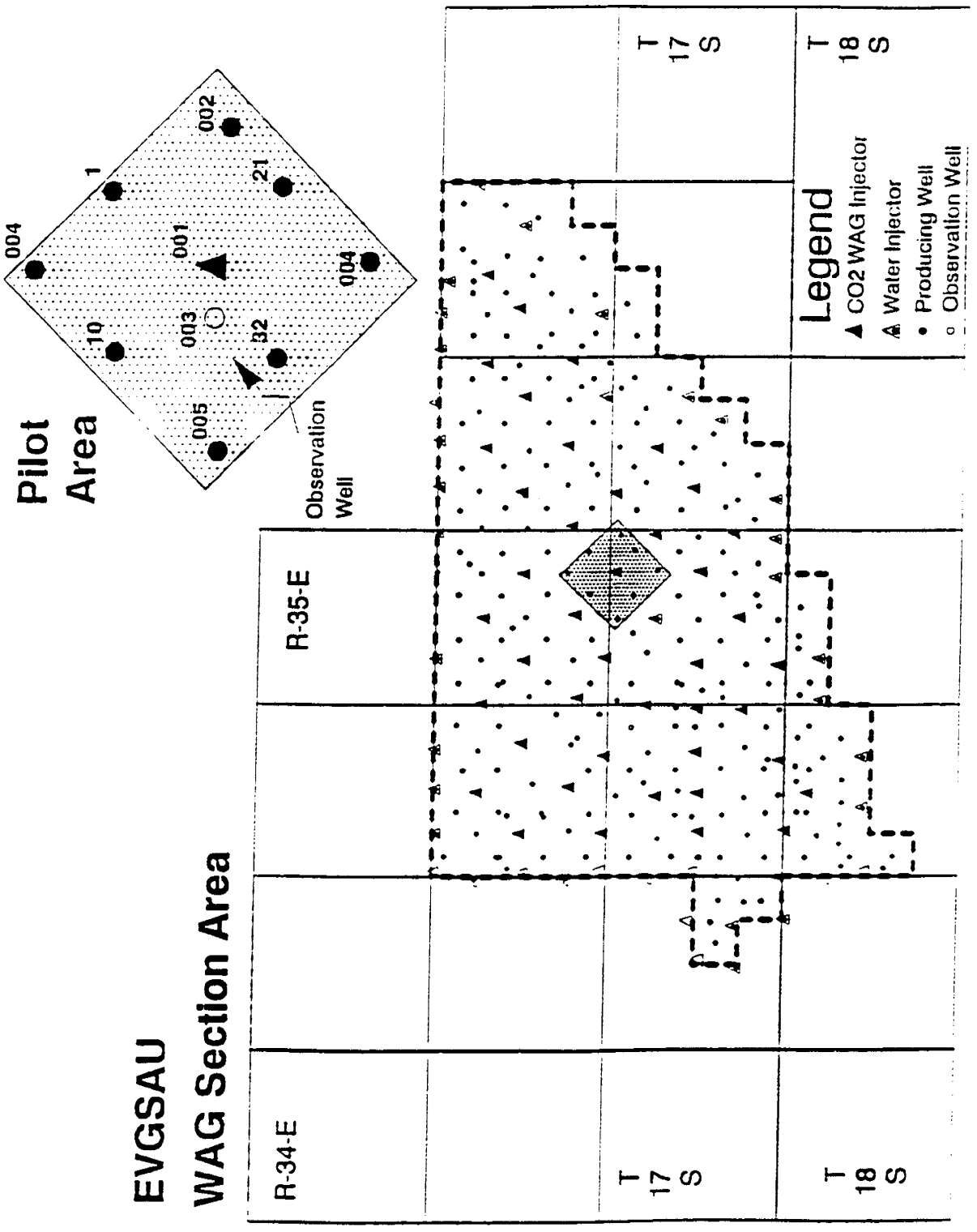

Figure 3. Flooding Patterns in East Vacuum Field.

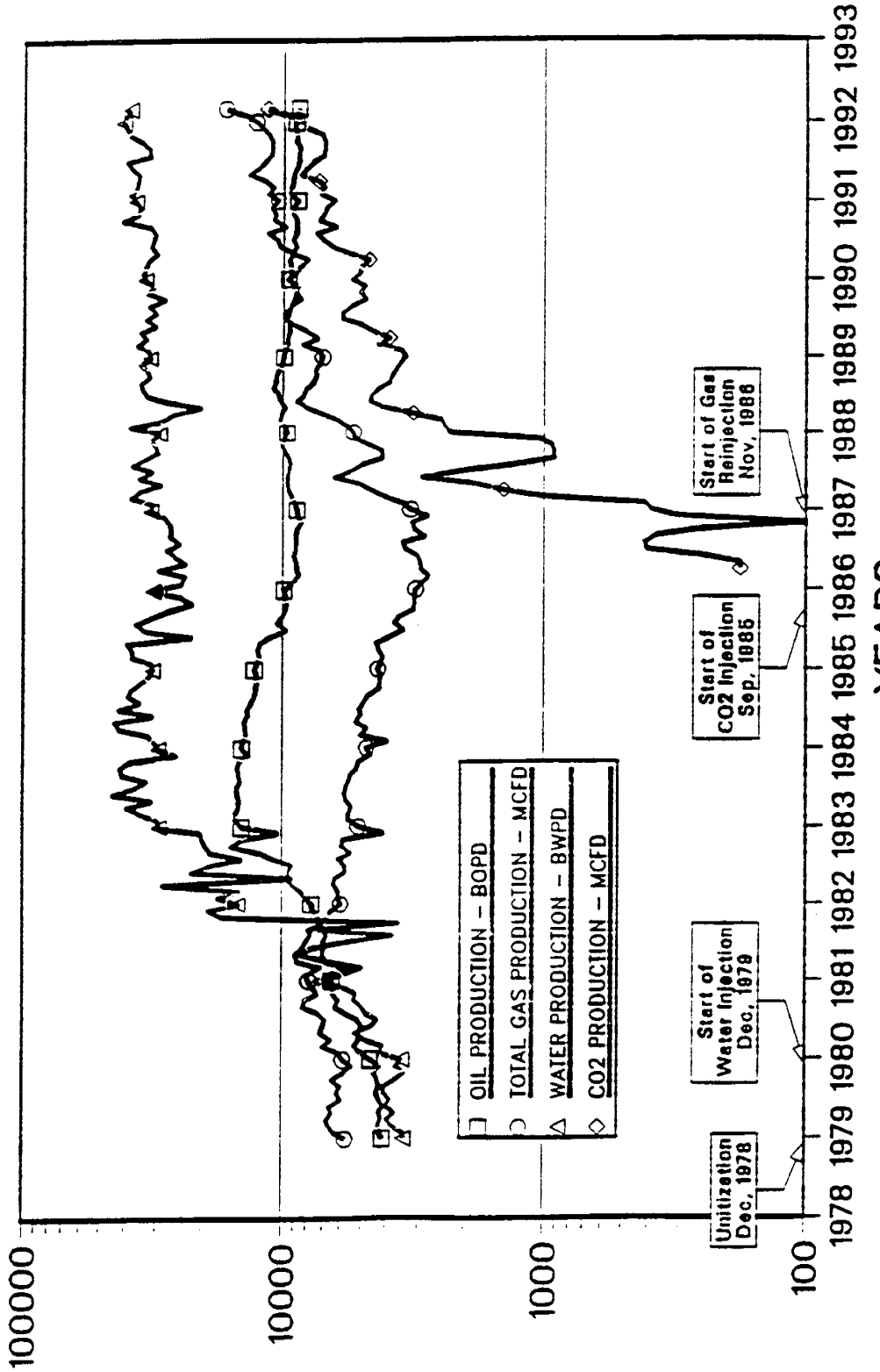

Figure 4. Production History of EVGSAU.

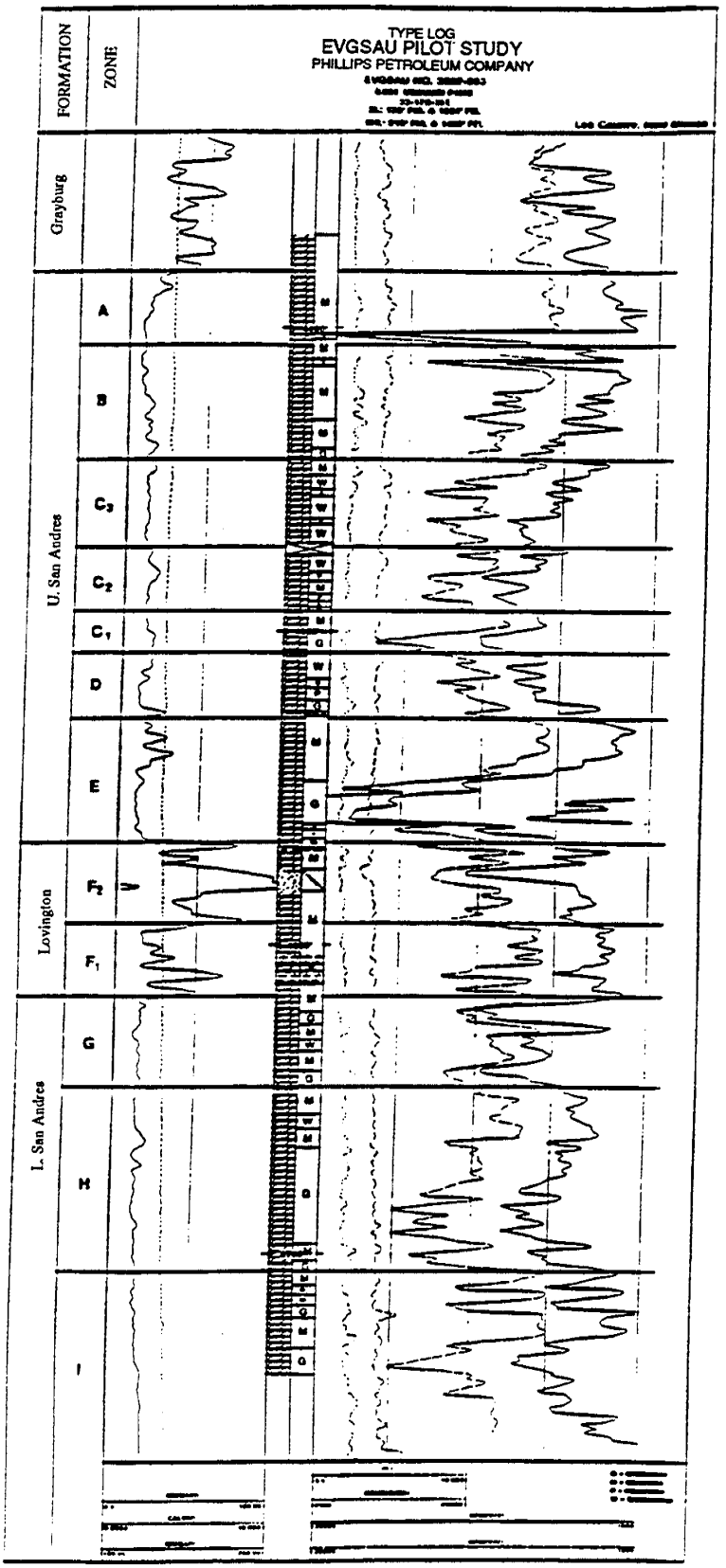

Figure 5. Type log in East Vacuum Field.

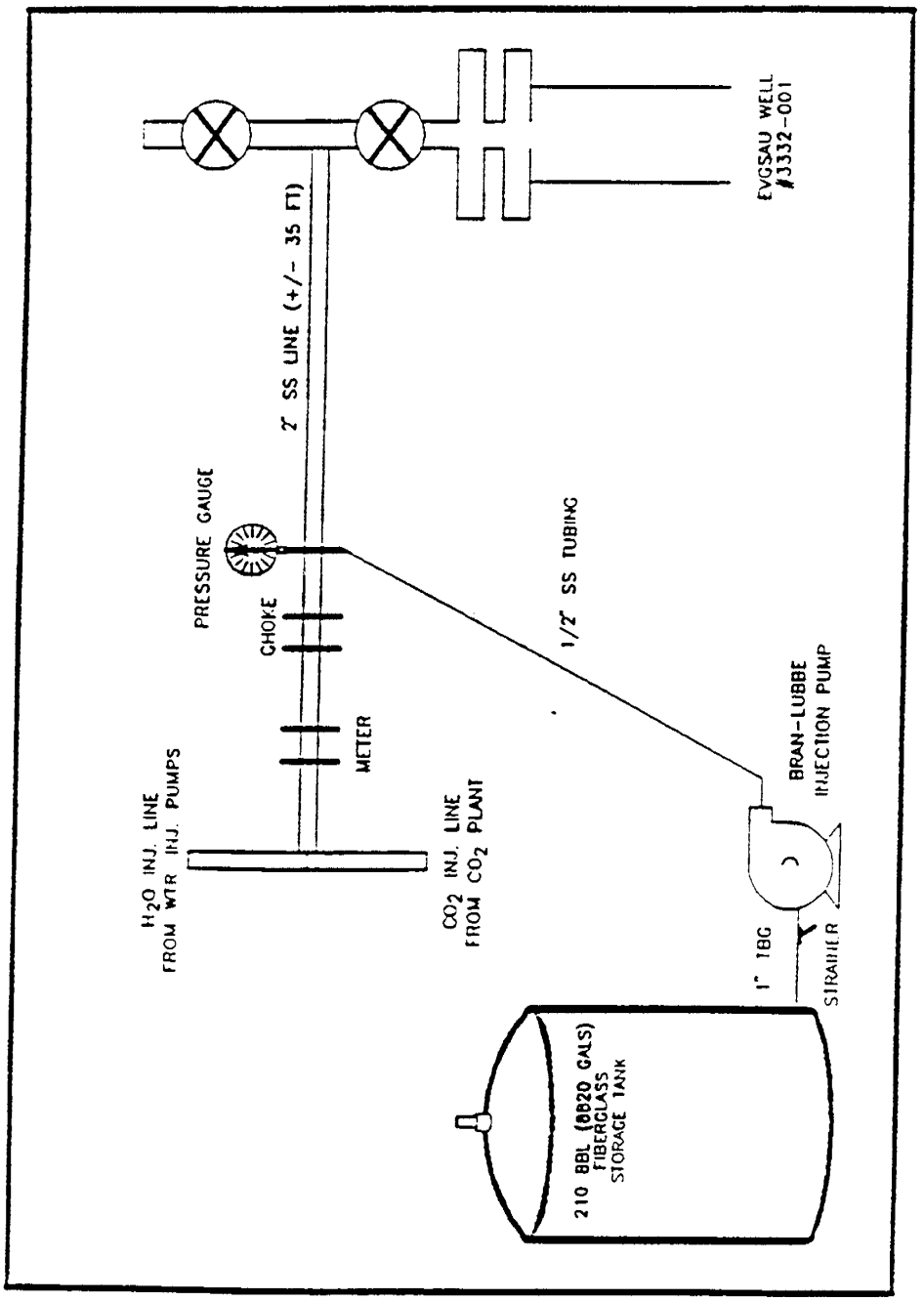

Figure 6. Surfactant Addition Facilities, EVGSAU injector.

GAS FOAM APPLICATION SESSION
DISCUSSION

Co-Chairmen: Jerry Casteel, U.S. DOE
Mark Hoefner, Mobil R&D

Speakers: Rick Gdanski, Halliburton Services
Bill Rossen, University of Texas, Austin
Anthony Kovscek, University of California, Berkeley
Jim Stevens, Phillips Petroleum Company
Jan Hanssen, Rogaland Research, Stavanger, Norway
Sang Chou, Chevron Oil Field Research Company
John Heller, New Mexico Petroleum Recovery Research Center

Paper FS7—Design Considerations for Foam Diversion of Acid Stimulation Treatments

Question for Rick Gdanski from John Heller, New Mexico Petroleum Recovery Research Center

Can you comment on the quality of foam used in acid stimulation treatments?

Response by Rick Gdanski

Since, in our case, the hydrostatic gradient and the gas compression newly balanced the pressure loss in the tubing due to friction, the foam quality at the perforation was essentially the same as the surface foam quality.

Question for Rick Gdanski from Maura Puerto, Exxon Production Research

What is the ionic strength of the surfactant used to generate foam?

Response by Rick Gdanski

Since charged surfactants are not very effective in foaming the acids, only nonionic surfactants are used in the foam stimulation application. Most service companies use a single dominant nonionic surfactant for foaming the acid. These surfactants are usually epoxylated alcohol and have a very high cloud point.

Paper FS9—A Comprehensive Description of Transient Foam Flow in Porous Media

Question for Anthony Kovscek from Bill Brigham, Stanford University

The basic model (foam flow in porous media) you have presented does not confirm the standard fractional flow theory and to me it appears that according to this model the distance traveled by a slug is directly proportional to the volume of the injected slug. In other words, if you inject twice as much, it goes twice as far. Am I correct?

Response by Anthony Kovscek

I agree.

Question for Anthony Kovscek from Bill Brigham

In your slides showing saturation vs. distance as function of time (comparing experimental results with the predicted values), it appears that you have some material balance errors. Can you comment on it?

Response by Anthony Kovscek

The predicted values are correct and there is no material balance errors in it. The seeming anomaly is due to the nature of the experimental set-up and data collection system. The set-up is such that we scan saturation at 30 second intervals from the top. Since it is very likely that one scan may take a little longer (or shorter) time than others, the measured cumulative material balance may not agree.

Question for Anthony Kovscek from Bill Rossen, University of Texas, Austin

The experimental results you showed that best fit your model indicate that the pressure gradient is independent of gas rate. This observation is consistent with the 'critical capillary pressure' model. However, in real porous media things are much more complex due to the changing nature of the foam texture. Could you explain how you reproduced the results? In other words, can you clarify why your pressure gradients are independent of flow rates?

Response by Anthony Kovscek

There are two reasons why the results are reproducible. Since it is a steady-state experiment, we maintained identical water saturation from run to run. As a consequence, the water relative permeability remained the same in all runs. The other reason is that we have accounted for the effect of viscosity of foam in our measurements. These two considerations partly explain the reproducibility of the results.

Comment by Clay Radke, University of California, Berkeley

Let me answer your question differently. Our model directly accounts for the critical (limiting) capillary pressure. Once you get S_w^*, you are at P_c^* and the coalescence becomes infinite. This is the main reason for reproducibility of the results. We cannot reproduce steady-state data without accounting for P_c^*.

Paper FS10—CO_2 Foam Field Verification Pilot at EVGSAU: Phase II - Foam Injection Design and Operating Plan

Question for Jim Stevens, Phillips Petroleum Company, from Tad Patzek, University of California, Berkeley

You have stated in your presentation that you did not see much permeability reduction in the upper zone (due to foam). As I see it, you did not get enough surfactant into the upper zone simply because you have injected surfactant first followed by gas. Since the surfactant solution is a denser fluid, it has a natural tendency to underride and occupy the lower zone in preference to the upper zone. Can you comment on it?

Response by Jim Stevens

Our wells are perforated over the entire zone and all our perforations take fluids. Therefore, we assume all zones have surfactant in them.

Question for Jim Stevens from Tad Patzek

Are not these zones in communication?

Response by Jim Stevens

No, we don't believe so. This is a very layered and tight reservoir, so we are positive that every layer has surfactant in it. Our injection profiles indicated that CO_2 has invaded every zone, so we are reasonably sure that foam is present everywhere. Since the upper zone is more permeable, we anticipated having a stronger foam in the high-permeability channel.

Question for Jim Stevens from Tad Patzek

Your geological description of the reservoir indicate the upper most zone is the thickest. Even if you have injected surfactant into this zone, it is likely that the surfactant drains quickly to the bottom zone because of high permeability and unavailable for foam generation. Any comment?

Response by Jim Stevens

In my geological description, I did not represent the top zone properly. The upper most zone, which we call the 'C' zone, in reality consists of 3 zones—C_1, C_2 and C_3. Even though all of the 3 zones have high permeability, the bottom part of the C_2 zone has much higher permeability compared to C_1 or C_3 zones. Surfactant may drain from the top layer due to gravity, but it is unlikely due to the differing permeability of the 3 zones in the top layer.

Question for Jim Stevens from Shane Mohammadi, UNOCAL

What is the ratio of vertical to horizontal permeability in the C-zone?

Response by Jim Stevens

I am not sure.

Comment by Shane Mohammadi

I want to make a quick comment. You mentioned that you have a pressure limitation in your injection well. You may have reached that limit and as a result were unable to get a satisfactory volumetric distribution away from the well. This may have affected your ability to generate foam.

Response by Jim Stevens

When we experienced the injection problem, we did away with the 3 days-12 days cycle and did a rapid WAG rapid SAG cycle, and saw a pressure increase during the SAG cycle.

Question for Jim Stevens from Shane Mohammadi

Let us carry this argument further and assume you are comparing the history of WAG and SAG over a 5-year period. It is likely you will be putting significantly less surfactant in the SAG process than in the WAG process. Is that correct?

Response by Jim Stevens

I wouldn't say the difference will be significant.

Question for Jim Stevens from Shane Mohammadi

Had there not been a pressure limitation on the injection equipment, you would more likely force the fluid into the formation and the difference may not be significant. However, you are not forcing it and every month due to this additional backpressure, you may not be able to inject volumetrically the same amount in both processes. Am I correct?

Response by Jim Stevens

Yes, we saw a slight reduction in the volume of CO_2 injection during the SAG process. Let me explain. After a rapid WAG, we injected 52,000 barrels of CO_2 over a 3-month period. After our SAG process, we want to inject the same amount of CO_2. Since our object is to inject the same volume of CO_2 in the SAG as in WAG, we did not stick to the 3-month cycle. We were not able to inject the volume in one cycle but able to do so in 2 cycles. The reduced injection was only for a period of 5 days.

Comment by Shane Mohammadi

I understand what you are trying to do. Down the line you would definitely need to simulate the process to compare the benefits of doing a SAG as opposed to a WAG. Let me make another suggestion. It is very easy to determine the adsorption in the field, if you use a simulator that can simulate near wellbore effect. The way you do that is to compare WAG with 2 or 3 SAG cycles. In the first SAG cycle, you expect to see a lower pressure increase as compared to the first cycle and a gradual increase during subsequent cycles. The amount of pressure increase depends upon the amount of surfactant adsorbed by the rock in a particular cycle. After the first 2 cycles, you are

likely to satisfy the appetite of rock for surfactant and are able to generate a larger pressure increase for the same volume of surfactant injected.

Question for Jim Stevens from Eric Waninger, Chevron Chemical Company

I am curious about the mechanism that causes CO_2-foam to propagate so much further into the reservoir compared to the steam-foam. In the thermal side, factors such as minimum pressure gradient and minimum velocity determines how far into the reservoir the foam will propagate and stall. Can you enlighten me?

Response by Jim Stevens

Good question! I have no answer for that. Perhaps some foam expert in the audience can answer that question.

Comment by Bill Brigham, Stanford University

The reason for this difference is that in steam-foam operations when you inject steam into the reservoir, a good portion of it condenses and hence the vapor volume in the reservoir is not the same as the volume you injected. In the gas-foam situation, the volume remains the same. Another thing you have to bear in mind is that in the calculation you assume radial flow and in actuality such is not the case. The gas goes into specific channels and specific areas and the calculated flow may not subscribe to actual flow.

Question for Jim Stevens from Maura Puerto, Exxon Production Research

Did you encounter any asphaltene depositional problems?

Response by Jim Stevens

We did encounter asphaltene deposition in a few of our production wells. It is a very minor problem compared to the calcium sulfate and calcium carbonate scaling problem. We are acidizing the production wells 3 times a week.

Paper FS11—Well Treatment Against Gas Coning Must Exploit Gravity Effects

Question for Jan Hanssen from Clay Radke, University of California, Berkeley

The gas inside the foam is essentially in contact with the gas in the reservoir separated only by a very thin film. This gas will escape rather quickly by diffusion and you cannot stop that. How do you stabilize the foam?

Response by Jan Hanssen

The foam is stabilized by the porous media. In our physical model it lasted for over a month.

Comment by Clay Radke

No, I disagree. In the pores, the foam is separated from the gas by a very thin film, probably less than 100 Angstrom thick. Diffusion across such a thin film is a rapid process—almost instantaneous.

Response by Jan Hanssen

I am not saying diffusion is unlikely. What I am saying is diffusion across the foam film is not likely to be instantaneous as you claim. It is likely to be a relatively slow process.

Paper FS12—CO_2 Foam Field Trial at North Ward-Estes

Question for Sang Chou, Chevron Oil Field Research, from John Heller, New Mexico Petroleum Recovery Research Center

Your surface pressure was shown to be 800 psi or so. Would you exceed the fracture pressure had your surface pressure been higher?

Response by Sang Chou

No, but we tried to calculate the fracture pressure from the surface pressure. However, we were unable to do so because surface pressure does not give a gradient to estimate the bottomhole pressure.

Question for Sang Chou from John Heller

What was your maximum bottomhole pressure?

Response by Sang Chou

The maximum bottomhole pressure we experienced was about 1,800 psi which is slightly higher than the fracture pressure of 1,750 psi.

Question for Sang Chou from Tad Patzek, University of California, Berkeley

You have done some economics of the trial. Did you make any attempt to scale the economics or extrapolate the economics to a larger scale such as fieldwide to try to determine the benefit of a large scale operation?

Response by Sang Chou

That is a very good question. That is one of the reasons why we need to be aware of the stages of profit. For these tests, the injection treatments for wellbore improvement were very selective. This is because after the analysis of data for a single treatment we concluded we cannot treat another 3 or 4 wells without shutting the surrounding producers. If you do that, it will affect the profitability. This is true not only for those 3 or 4 wells, but also for the entire field.

APPENDIX
LIST OF SYMPOSIUM ATTENDEES

Adamache, Ion
Adamache Petro Eng. Ltd.
Apt. 908
330 26 Ave. SW
Calgary, Alberta
Canada T2S 2T3

Bain, George F.
Chevron Chemical Company
5001 California Ave.
Bakersfield, CA 93309

Beattie, Craig I.
Imperial Oil Resources Ltd.
3535 Research Road, N.W.
Calgary, Alberta
Canada T2L 2K8

Bird, Gordon
Alberta Research Council
P.O. Box 8330, Postal Station F
Edmonton, Alberta, Canada T6H
5X2

Boberg, Thomas
311 Electra
Houston, TX 77024

Brigham, William E.
Petroleum Eng. Dept.
Stanford University
350 Mitchell Bldg.
Stanford, CA 94035-2220

Busby, Joel
Mobil
P.O. Box 633
Midland, TX 79707

Carson, Jacquiline D.
Chevron Chemical Co.
601 Bollinger Canyon Rd.
San Ramon, CA 94583

Castanier, Louis M.
Petroleum Eng. Dept.
Stanford University
350 Mitchell Bldg.
Stanford, CA 94035-2220

Casteel, Jerry F.
DOE/BPO
P.O. Box 1398
Bartlesville, OK 74005

Chou, S. I.
Chevron Oil Field Research
P.O. Box 446
La Habra, CA 90633-0446

Cooke, Ralph W.
Enhanced Petroleum Tech. Inc.
P.O. Box 212
Bakersfield, CA 93302

Dalland, Mariann
Rogaland Research
P.O. Box 2503 Ulandhaug
N-4004 Stavanger, Norway

De Paz, Miriam Lopez
Lagoven S.A.
P.O. Box 172
Maracaibo, Venezuela

Djabbarah, Nizar
Mobil R&D
P.O. Box 819047
Dallas, TX 75381

Eson, Rod
Enhanced Petroleum Tech. Inc.
P.O. Box 212
Bakersfield, CA 93302

Evans, E. M. (Gene)
Mobil Oil Corporation
P.O. Box 633
Midland, TX 79702-0633

Flor, Gutierrez, Secretary
Empresa Nacional Del Petroleo
New York Office, Suite 5151
One World Trade Center
New York, NY 10048-0497

Forst, Harry F.
Chevron Chemical Company
P.O. Box 2449, Suite 400
Houston, TX 77252-2449

Gangle, Francis J.
DOE
P.O. Box 11
Tupman, CA 93278

Gdanski, Rick
Haliburton Services
605 Fielderest
Duncan, OK 73533

Giangiacomo, Leo
FD Services, Inc.
907 N. Poplar, Suite 100
Casper, Wyoming 82601

Gonzales, Sandy K.
ARCO Oil & Gas Company
P.O. Box 147
Bakersfield, CA 93302

Handy, Lyman
University of Southern California
Petroleum Engineering Program
Chemical Engineering Dept.
HEDCO 316-University Park
Los Angeles, CA 90089-1211

Hanssen, Jan Erik
Rogaland Research
P.O. Box 2503 Ulandhaug
N-4004 Stavanger, Norway

Heller, John
Petroleum Recovery Research Center
Socorro, New Mexico 87801

Hendricks, Marvin L.
Dept. of Energy
907 N. Poplar, Suite 150
Casper, WY 82601

Henry, Richard
Amoco Research Center
Box 3385
Tulsa, OK 74102

Herrmann, Daniel
FD Services Inc.
907 N. Poplar, Suite 100
Casper, WY 82601

Hoang, Viet T.
Chevron Research and Technology
6001 Bollinger Canyon Rd.
San Ramon, CA 94583

Hoeffner, Mark
MEPTEC
Box 819047 (zip 75381)
13777 Midway Rd.
Dallas, TX 74243

Honstein, Glen
Bechtel Petroleum Op., Inc.
P.O. Box 116
Tupman, CA 93276

Hosein, Aleem
Tritoc Ltd.
Pointe-a-Pierre
Trinidad

LIST OF SYMPOSIUM ATTENDEES—Continued

Hutchison, David A.
Shell Western E&P
5060 California Avenue
Bakersfield, CA 93309

Idol, Keith
Exxon Production Research Co.
P.O. Box 2189
Houston, TX 77252-2189

Isaacs, Eddy
Alberta Research Council
P.O. Box 8330, Postal Station F
Edmonton, Alberta
Canada T6H 5X2

Joubert, Geovanny
Lagoven S.A.
P.O. Box 254
Maturin, Monagas, Venezuela

Kovscek, Anthony R.
University of CA/Berkeley
201G Gilman Hall
Berkeley, CA 94720

Kuehne, Don
Chevron Research & Technology
100 Chevron Way
Richmond, CA 94802-0627

Leong, John K.
UNOCAL
1800 30th Street, Suite 200
Bakersfield, CA 93301

Lim, Frank H.
Union Pacific Resources
P.O. Box 7
Fort Worth, TX 76101

Mahmood, Syed
NIPER
P.O. Box 2128
Bartlesville, OK 74005

Martin, Jim
Bechtel Petroleum Op., Inc.
P.O. Box 116
Tupman, CA 93276

Mendez, Zuleyka
INTEVEP S.A.
Los Teques, Edo. Miranda
Apdo. 76343
Caracas 1070A, Venezuela

Milter, Jess
Improved Recovery Group
Rogaland Research
P.O. Box 2503 Ulandhaug
N-400 Stavanger, Norway

Mohammadi, Shane
UNOCAL
P.O. Box 76
Brea, CA 92621

Olsen, David K.
NIPER
Box 2128
Bartlesville, OK 74005

Osterloh, Terry
Texaco EPTD
P.O. Box 770070
Houston, TX 77215-0070

Papir, Joe
Chevron Chemical Co.
6001 Bollinger Canyon Rd.
San Ramon, CA 94583

Patzek, Tadeusz
University of California, Berkeley
Chemical Eng. Dept.
Berkeley, CA 94720

Prieditis, John
Texaco Inc. EPTD
3901 Briarpark
Houston, TX 77042

Puerto, Maura C.
Exxon Production Research
P.O. Box 2189 (zip 77252-2189)
2015 Briarstem
Houston, TX 77077

Radke, Clayton J.
University of CA/Berkeley
Chemical Engineering Dept.
Berkeley, CA 94720

Reid, Thomas B.
DOE/BPO
P.O. Box 1398
Bartlesville, OK 74005

Reppert, Todd
Exxon Production Research
3120 Buffalo Speedway
Houston, TX 77098

Rossen, William
The University of Texas at Austin
Dept. of Petroleum Engineering
Austin, TX 78712-1061

Sarathi, Partha
NIPER
P.O. Box 2128
Bartlesville, OK 74005

Schramm, Laurier L.
Petroleum Recovery Institute
100, 3512-33 Street N.W.
Calgary, Alberta, Canada T2L 2A6

Smith, Michael
Chevron Petroleum Technology Co.
1300 S. Beach Blvd.
La Habra, CA 90631

Soroko, Daryl
Saskoil
1777 Victoria Ave.
P.O. Box 1550
Regina SK, Canada S4P 3C4

Stevens, Jim
Phillips Petroleum Co.
E&P
North America Division
4001 Penbrook
Odessa, TX 79762

Stowe, G. R. III
Drilling Representative
Chevron U.S.A. Inc.
6004 Ambergrove Street
Bakersfield, CA 93313

Strycker, Arden
NIPER
P.O. Box 2128
Bartlesville, OK 74005

Sugiauto, Steve
Saskoil
1777 Victoria Avenue
P.O. Box 1550
Regina SK, Canada S4P 3C4

Talley, Larry D.
Exxon Research & Engineering Co.
P.O. Box 4255
Baytown, TX 77522-4255

Teletzke, Gary
Exxon Production Research
P.O. Box 2189
Houston, TX 77252-2189

LIST OF SYMPOSIUM ATTENDEES—Continued

Waninger, Eric
Chevron Chemical
P.O. Box 1392
Bakersfield, CA 93302

Welch, Robert A.
NIPER
P.O. Box 2128
Bartlesville, OK 74005

Weyland, Ginny
DOE
Box 11
Tupman, CA 93278

Williams, Richard L.
Santa Fe Energy Resources
5201 Truxtun Avenue, Suite 100
Bakersfield, CA 93309

Yortsos, Yanis C.
USC, Dept. of Chemical Engineering
HEDCO 316, University Park
Los Angeles, CA 90089-1211